

DOE/BC/14126-17
(DE91002201)

**MULTICOMPONENT, MULTIPHASE FLOW IN POROUS
MEDIA WITH TEMPERATURE VARIATION -- SUPRI TR 71**

By
J.S. Wingard
F.M. Orr, Jr.

October 1990

Performed Under Contract No. FG19-87BC14126

Stanford University
Petroleum Research Institute
Stanford, California



**Bartlesville Project Office
U. S. DEPARTMENT OF ENERGY
Bartlesville, Oklahoma**

DISCLAIMER

This report was prepared as an account of work sponsored by an agency of the United States Government. Neither the United States Government nor any agency thereof, nor any of their employees, makes any warranty, express or implied, or assumes any legal liability or responsibility for the accuracy, completeness, or usefulness of any information, apparatus, product, or process disclosed, or represents that its use would not infringe privately owned rights. Reference herein to any specific commercial product, process, or service by trade name, trademark, manufacturer, or otherwise does not necessarily constitute or imply its endorsement, recommendation, or favoring by the United States Government or any agency thereof. The views and opinions of authors expressed herein do not necessarily state or reflect those of the United States Government or any agency thereof.

Available to DOE and DOE contractors from the Office of Scientific and Technical Information, P.O. Box 62, Oak Ridge, Tennessee 37831; prices available from (615)576-8401, FTS 626-8401.

Available to the public from the National Technical Information Service, U.S. Department of Commerce, 5285 Port Royal Rd., Springfield, Virginia 22161.

Price: Printed Copy A12
Microfiche A01

MULTICOMPONENT, MULTIPHASE FLOW IN POROUS
MEDIA WITH TEMPERATURE VARIATION

SUPRI TR 71

By
J. S. Wingard
F. M. Orr, Jr.

October 1990

Work Performed Under Contract No. FG19-87BC14126

Prepared for
U.S. Department of Energy
Assistant Secretary for Fossil Energy

Thomas B. Reid, Project Manager
Bartlesville Project Office
P.O. Box 1398
Bartlesville, OK 74005

Prepared by
Stanford University
Petroleum Research Institute
Stanford, CA 94305-4042

TABLE OF CONTENTS

LIST OF FIGURES	v
LIST OF TABLES	viii
ACKNOWLEDGEMENTS	ix
ABSTRACT	x
1. INTRODUCTION	1
1.1 Problem Description	1
1.2 Problem Applications	2
1.3 Solution Description	2
1.3.1 The Reservoir as a Chromatograph	3
1.3.2 Method of Characteristics	3
1.4 What about Simulation?	5
What lies ahead?	6
2. MATHEMATICAL MODEL	8
2.1 Conservation Equations	8
2.2 Method of Characteristics	10
2.2.1 Calculation of Component and Enthalpy Velocities	12
Coherence and the Eigenvalue Problem	14
What is Coherence?	14
Formulation of the Eigenvalue Problem	14
2.3 Evaluation of the Derivatives in the Eigenvalue Matrix	16
2.3.1 Fluid Property Calculation	17
2.3.2 Calculating the Derivatives for the Eigenvalue Problem	18
2.4 Shock Calculations	19
3. SOLUTION PROCEDURES	22
3.1 Path Selection	22
3.2 Shock Calculations	26
4. EXAMPLE SOLUTIONS	31
4.1 Single Component with Temperature Variation	31
4.1.1 Problem Formulation	31
Single-Phase Regions	32
Two-Phase Region	33
Connecting the Single and Two-Phase Regions	35
Summary	41
4.2 Two Component — Three-Phase Systems	42
4.2.1 Problem Formulation	42
4.2.2 Example Cases	45
Base Case	45
4.2.3 Types of Displacement Patterns	52
Type 2 Displacement	58
Type 3 Displacement	66
Type 4 Displacement	71
4.2.4 Solution Procedure	72
4.2.5 Temperature Profile in the Steam-Oil Region	77
4.2.6 Solutions with Viscous Oils	84
Summary	98

4.3	Three Component — Three-Phase Systems	100
4.3.1	Problem Formulation	100
4.3.2	Path Topology	103
4.3.3	Solution Problems	107
5.	CONCLUSIONS AND RECOMMENDATIONS	109
5.1	General Conclusions and Limitations	109
5.1.1	Conclusions	109
5.1.2	Observations	110
5.1.3	Limitations	110
5.2	Specific Applications	111
5.2.1	Single Component with Temperature Variation	111
5.2.2	Two-Component, Three-Phase Immiscible System	112
5.2.3	Three-Component, Three-Phase System with Temperature Variation	113
5.3	Future Recommendations	113
6.	NOMENCLATURE	115
7.	REFERENCES	118
	APPENDIX A: FLUID PROPERTIES	122
A.1	Steam-Oil-Water Problem	122
A.2	CO ₂ -Oil-Water Problem	123
A.2.1	Flash Calculations	123
A.2.2	Fluid Properties	142
	APPENDIX B: ENTHALPY BALANCE ACROSS A DISCONTINUITY	144
	APPENDIX C: COMPLEX EIGENVALUES	145
	APPENDIX D: EXCEL SPREADSHEETS	148
D.1	Cell Formulas	148
D.2	Changes in Injection Temperature	148
D.3	Changes in Initial Temperature	193
D.4	Changes in Matrix Heat Capacity	226
	APPENDIX E: COMPUTER PROGRAMS	247

LIST OF FIGURES

2.1	One-to-one mapping from the space of independent variables, x and t to the space of dependent variables, C_1 and C_2	10
2.2	Mapping from the space of independent variables, x and t to the space of dependent variables, C_1 and C_2	11
2.3	Map of constant state region from a region in $x-t$ space to a single point in C_1, C_2 space.	12
2.4	Shock position at time t and $t + \Delta t$	19
3.1	Illegal composition path for a ternary displacement as the path moves from initial conditions to injection conditions.	23
3.2	Legal path switch at an equal eigenvalue point for a ternary displacement as the path moves from injection conditions to initial conditions.	25
3.3	Legal path switch for a ternary displacement as the path moves from injection conditions to initial conditions.	26
3.4	Illegal path switch for a ternary displacement as the path moves from injection conditions to initial conditions.....	27
3.5	Tangent construction for Buckley-Leverett shock front that illustrates how the tangent construction matches shock and wave velocities.	29
4.1	Solution line in hodograph space for steam injected into liquid water at constant pressure.	32
4.2	Trailing shock conditions for steam-water problem.	36
4.3	Wave and shock velocities for trailing shock in steam-water displacement.	37
4.4	Saturation profile after 1.0 pore volumes of steam injection into water at injection temperatures from 500 K—1000 K.	39
4.5	Saturation profile after 1.0 pore volumes steam injection into water at initial temperatures from 300 K—450 K.	40
4.6	Saturation profile after 1.0 pore volumes steam injection into water where the matrix heat capacity varies from 25.0 (kJ/kg-K) to 0.2 (kJ/kg-K).	40
4.7	Hypothetical solution to the two-component, three-phase problem showing the different flow regions.	42
4.8	Plot of eigenvalues along a constant temperature path in the water-oil region.	44
4.9	Composition path for the injection of 100% steam at 650 K into 94.5% oil and 6.5% water at 390.19 K.	47
4.10	Eigenvalues crossing the three-phase to water-oil boundary at 80% oil saturation.	48
4.11	Saturation profile for the injection of 1.0 pore volumes of 100% steam at 650 K into 94.5% oil and 6.5% water at 390.19 K.	50
4.12	Temperature profile for the injection of 1.0 pore volumes of 100% steam at 650 K into 94.5% oil and 6.5% water at 390.19 K.	51
4.13	Flow velocity profile for the injection of 1.0 pore volumes of 100% steam at 650 K into 94.5% oil and 6.5% water at 390.19 K.	52
4.14	Composition path that moves between two arbitrary points in the three-phase region.	53
4.15	Type 2 composition path that moves between two arbitrary points in the three-phase region.	54
4.16	Type 3 composition path that moves between two arbitrary points in the three-phase region.	55
4.17	Type 3 composition path that moves between two arbitrary points in the three-phase region.	56
4.18	Possible self-sharpening wave in the three-phase region.	57

4.19	Limiting case self-sharpening wave in the three-phase region.	58
4.20	Adjusted Type 1 composition path that moves between two arbitrary points in the three-phase region.	59
4.21	Adjusted Type 2 composition path that moves between two arbitrary points in the three-phase region.	60
4.22	Adjusted Type 3 composition path that moves between two arbitrary points in the three-phase region.	61
4.23	Composition path for the injection of 100% steam at 650 K into 92.4% oil and 7.6% water at 412.09 K.	62
4.24	Temperature profile for the injection of 1.0 pore volumes of 100% steam at 650 K into 92.4% oil and 7.6% water at 412.09 K.	63
4.25	Flow velocity profile for the injection of 1.0 pore volumes of 100% steam at 650 K into 92.4% oil and 7.6% water at 412.09 K.	64
4.26	Saturation profile for the injection of 1.0 pore volumes of 100% steam at 650 K into 92.4% oil and 7.6% water at 412.09 K.	65
4.27	Composition path for the injection of 100% steam at 650 K into 91.6% oil and 8.4% water at 428.62 K.	67
4.28	Saturation profile for the injection of 100% steam at 650 K into 91.6% oil and 8.4% water at 428.62 K.	68
4.29	Temperature profile for the injection of 100% steam at 650 K into 91.6% oil and 8.4% water at 428.62 K.	69
4.30	Flow velocity profile for the injection of 100% steam at 650 K into 9.16% oil and 8.4% water at 428.62 K.	70
4.31	Three-phase region of the steam-oil-water displacements showing the regions where the fath path eigenvalues and water saturation permit a jump into the water-oil region.	71
4.32	Composition path for the injection of 100% steam at 650 K into 88.1% oil and 11.9% water at 433.79 K.	73
4.33	Saturation profile for the injection of 1.0 pore volumes of 100% steam at 650 K into 88.1% oil and 11.9% water at 433.79 K.	74
4.34	Temperature profile for the injection of 1.0 pore volumes of 100% steam at 650 K into 88.1% oil and 11.9% water at 433.79 K.	75
4.35	Flow velocity profile for the injection of 1.0 pore volumes of 100% steam at 650 K into 88.1% oil and 11.9% water at 433.79 K.	76
4.36	Composition path for the injection of 100% steam at 650 K into 94.8% oil and 5.24% water at 402.13 K with a temperature wave in the steam-oil region.	78
4.37	Temperature profile for the injection of 1.0 pore volumes of 100% steam at 650 K into 94.8% oil and 5.24% water at 402.13 K with a temperature wave in the steam-oil region.	80
4.38	Flow velocity profile for the injection of 1.0 pore volumes of 100% steam at 650 K into 94.8% oil and 5.24% water at 402.13 K with a temperature wave in the steam-oil region.	81
4.39	Saturation profile for the injection of 1.0 pore volumes of 100% steam at 650 K into 94.8% oil and 5.24% water at 402.13 K with a temperature wave in the steam-oil region.	82
4.40	Saturation profiles in the steam-oil region for the injection of 1.0 pore volumes of 100% steam at 650 K into reservoirs with porosities from 0.05 to 0.5.	83
4.41	Temperature profiles in the steam-oil region for the injection of 1.0 pore volumes of 100% steam at 650 K into reservoirs with porosities from 0.05 to 0.5.	84
4.42	Viscosities for water, steam, and three different oils as a function of temperature from 275 K to 1000 K.	85
4.43	Composition path for the injection of 100% steam at 650 K into 99.9% Heavy Oil #1 and 0.1% water at 458.95 K.	86

4.44	Saturation profile for the injection of 100% steam at 650 K into 99.9% Heavy Oil #1 and 0.1% water at 458.95 K.	88
4.45	Temperature profile for the injection of 100% steam at 650 K into 99.9% Heavy Oil #1 and 0.1% water at 458.95 K.	90
4.46	Flow velocity profile for the injection of 100% steam at 650 K into 99.9% Heavy Oil #1 and 0.1% water at 458.95 K.	91
4.47	Composition path for the injection of 100% steam at 650 K into 88.1% Heavy Oil #2 and 11.9% water at 433.79 K.	92
4.48	Saturation profile for the injection of 100% steam at 650 K into 88.1% Heavy Oil #2 and 11.9% water at 433.79 K.	93
4.49	Temperature profile for the injection of 100% steam at 650 K into 88.1% Heavy Oil #2 and 11.9% water at 433.79 K.	94
4.50	Flow velocity profile for the injection of 100% steam at 650 K into 88.1% Heavy Oil #2 and 11.9% water at 433.79 K.	95
4.51	Phase diagram for a system of CO ₂ -Oil-Water at temperatures below the saturation temperature of water.	101
4.52	Phase diagram for a system of CO ₂ -Oil-Water at temperatures below the saturation temperature of water.	102
4.53	Four distinct flow regions in the CO ₂ -Oil-Water system.	104
4.54	Composition paths for the CO ₂ -Oil-Water system at a constant temperature.	105
A.1	Isothermal ternary phase diagram showing the five regions and the 15 composition points.	123
A.2	Isothermal slice of the complete ternary phase diagram for the CO ₂ -Oil-Water system at 300 K.	124
A.3	Isothermal slice of the complete ternary phase diagram for the CO ₂ -Oil-Water system at 350 K.	126
A.4	Isothermal slice of the complete ternary phase diagram for the CO ₂ -Oil-Water system at 375 K.	128
A.5	Isothermal slice of the complete ternary phase diagram for the CO ₂ -Oil-Water system at 400 K.	130
A.6	Isothermal slice of the complete ternary phase diagram for the CO ₂ -Oil-Water system at 425 K.	132
A.7	Isothermal slice of the complete ternary phase diagram for the CO ₂ -Oil-Water system at 450 K.	134
A.8	Isothermal slice of the complete ternary phase diagram for the CO ₂ -Oil-Water system at 460 K.	136
A.9	Isothermal slice of the complete ternary phase diagram for the CO ₂ -Oil-Water system at 470 K.	138
A.10	Isothermal slice of the complete ternary phase diagram for the CO ₂ -Oil-Water system at 475 K.	126
A.11	Stacked ternary phase diagrams for the CO ₂ -Oil-Water system from 300-600 K.	142
C.1	Region of complex eigenvalues using Stone's model II with $\alpha_g = 1.0$, $\alpha_w = 3.0$, $\alpha_{ow} = 2.0$, and $\alpha_{lg} = 2.0$	146
C.2	Region of complex eigenvalues using Stone's model II with $\alpha_g = 1.0$, $\alpha_w = 2.0$, $\alpha_{ow} = 2.0$, and $\alpha_{lg} = 2.0$	147
E.1	Basic Flow Chart for the tracepath Program that performs the path integration for the steam-oil-water problem.	248
E.2	Basic Flow Chart for the jump Program that calculates the shock conditions for the steam-oil-water problem.	250

LIST OF TABLES

4.1	Base conditions for the generation of steam-water profiles at 2.0 MPa.	38
4.2	Three phase relative permeability parameters for Stone's model II.	45
4.3	Composition path for the injection of 100% steam at 650 K into 94.5% oil and 6.5% water at 390.19 K.	46
4.4	Abbreviations used to describe the different flow regions.	46
4.5	The four different three-phase wave profiles for the displacement of oil and water by steam and water.	53
4.6	Type 2 composition path for injection of 100% steam at 650 K into 92.4% oil and 7.6% water at 412.09 K.	66
4.7	Type 3 composition path for injection of 100% steam at 650 K into 91.6% oil and 8.4% water at 428.62 K.	66
4.8	Type 4 composition path for injection of 100% steam at 650 K into 88.1% oil and 11.9% water at 433.79 K.	72
4.9	Composition path for the injection of 100% steam at 650 K into 94.8% oil and 52.4% water at 402.13 K with a temperature wave in the steam-oil region.	78
4.10	Comparison of composition paths for solutions with and without a temperature variation in the steam-oil region.	79
4.11	Composition path for the injection of 100% steam at 650 K into 99.9% Heavy Oil #1 and 0.01% water at 458.95 K.	87
4.12	Composition path for the injection of 100% steam at 650 K into 88.1% Heavy Oil #2 and 11.9% water at 433.79 K.	89
4.13	Non-tie line path in the vapor-liquid region of the CO ₂ -oil-water system.	106
4.14	Typical composition path in the liquid-liquid region of the CO ₂ -oil-water system.	107
A.1	Input data for CO ₂ -oil-water phase diagram at 300 K.	125
A.2	Input data for CO ₂ -oil-water phase diagram at 350 K.	127
A.3	Input data for CO ₂ -oil-water phase diagram at 375 K.	129
A.4	Input data for CO ₂ -oil-water phase diagram at 400 K.	131
A.5	Input data for CO ₂ -oil-water phase diagram at 425 K.	133
A.6	Input data for CO ₂ -oil-water phase diagram at 450 K.	135
A.7	Input data for CO ₂ -oil-water phase diagram at 460 K.	137
A.8	Input data for CO ₂ -oil-water phase diagram at 470 K.	139
A.9	Input data for CO ₂ -oil-water phase diagram at 475 K.	141

ACKNOWLEDGEMENTS

Financial support during the course of this study was provided by Stanford University Petroleum Research Institute and Department of Energy Contract #DE-AC19-87BC14126.

ABSTRACT

Recovery of hydrocarbons from porous media is an ongoing concern. Advanced techniques augment conventional recovery methods by injecting fluids that favorably interact with the oil. These fluids interact with the oil by energy transfer, in the case of steam injection, or by mass transfer, as in a miscible gas flood. Often both thermal and compositional considerations are important. An understanding of these injection methods requires knowledge of how temperature variations, phase equilibrium and multiphase flow in porous media interact.

The material balance for each component and energy balance are cast as a system of non-strictly hyperbolic partial differential equations. This system of equations is solved using the method of characteristics. The model takes into account the phase behavior by using the Peng-Robinson equation of state to partition the individual components into different phases. Temperature effects are accounted for by the energy balance. Flow effects are modelled by using fractional flow curves and a Stone's three phase relative permeability model.

Three major problems are studied in this dissertation. Each new problem adds an level of interaction to the solution before. The first problem eliminates the phase behavior aspect of the problem by studying the flow of a single component as it undergoes an isothermal phase change. The second problem couples the effects of temperature and flow behavior by including a second component that is immiscible with the original component. Finally, phase behavior is added by using a set of three partially miscible components that partition into two or three separate phases.

Solutions for these equations are formed by spreading waves that propagate in space and time with a constant velocity. The spreading wave regions are connected by jump discontinuities or zones of constant state. The solutions are presented for the three example systems in the form of saturation or composition profiles and solution paths in the composition space. An analysis of the effect of varying some of the important parameters are also presented for each displacement system.

1. INTRODUCTION

Multiphase, multicomponent flow in porous media occurs in every stage of hydrocarbon recovery, from primary drainage to the most exotic enhanced recovery process. Many times this flow includes temperature variations. The purpose of this study is to present a semi-analytical model that accounts for the interaction between the phase behavior, temperature variation, and fluid flow properties so that a wide variety of cases can be analyzed using this technique.

This chapter begins with a description of the problem and its application to hydrocarbon recovery. The interactions between temperature, phase behavior and flow properties are discussed. A review of the past efforts using the method of characteristics to solve the differential equations describing conservation laws is contained in the next section. Most of the examples apply to fluid flow in porous media; however, other systems are also mentioned. The reasons for using a semi-analytical model rather than full scale numerical simulations are also covered. Finally, the chapter concludes by describing how the model used in this study expands on the existing models by including temperature gradients.

1.1 PROBLEM DESCRIPTION

In any displacement process where there are temperature changes, three major effects interact. These effects are the temperature gradient, the phase behavior, and the flow properties of the fluids and porous medium. These three contributions interact in a complex fashion. The first to be mentioned is the local temperature. The introduction of temperature gradients has a profound effect on the displacement profiles because an increase in temperature directly affects flow properties by reducing the viscosity of the fluids and possibly changing relative permeabilities.

Temperature differences also change the phase compositions by shifting the phase equilibrium. Less volatile components that remain in the liquid phases at lower temperatures move to the vapor phase as the temperature increases. The mass transfer between phases stipulates the degree to which components partition into the mobile phases that are transported downstream.

Phase behavior is the second player in the displacement game. Miscible EOR processes depend on the mass transfer between the injected fluids and the oil to change the flow properties of the hydrocarbons in a favorable way. When CO₂ is injected into an oil bearing zone, the CO₂ is able to extract significant amounts of intermediate and heavy hydrocarbons into the CO₂ rich phase Rathmell *et. al.* (1971).

Simon and Graue (1965) showed that addition of CO₂ to crude oils can swell the crude to almost twice its original volume for light crude oils. They also reported that the viscosities of the CO₂-crude mixtures are lower than those of the dead oil. The changes in saturation and viscosity are the result of mass transfer between the injected CO₂ and the hydrocarbon phases.

The solution equilibrium is effected by the temperature and pressure of the system. When the temperature increases, the amount of CO₂ that can dissolve into the oil is reduced. When effects of thermal gradients are included in the system, the amount of CO₂ that dissolves varies over the length of the displacement, adding to the interplay between the chemical equilibrium and the temperature effects.

Finally, phase behavior changes the heat capacities of the different phases by changing their compositions (Walas 1985). The ability of the various phases to store enthalpy depends on the density of the phase and the heat capacity. These factors determine how the enthalpy partitions between the different flowing phases as well as the matrix. These factors all combine to determine the temperature profile of the displacement.

The third factor in the displacement process is the flow properties of the different phases and the porous medium. The flow properties are usually quantified by fractional flows. These fractional flows

tell which phases move with higher velocities and which are slower or immobile. In general, fractional flows are nonlinear functions of the phase saturations and viscosities and are the most important factor determining composition and saturation profiles.

Temperature changes have a dramatic effect on the fractional flow relationships. Temperature is a major factor determining the viscosities of the liquid phases which are directly related to the fractional flows. The reduction in viscosity of the hydrocarbon phases is much more dramatic than for water, and is the basis for all thermal recovery processes (Prats 1982). The vapor phase viscosity, on the other hand, shows only a small temperature effect. Below the critical temperature, the viscosity of gases increases proportionally to the square root of the absolute temperature (Reid *et al.* 1977).

Variations in composition also change the viscosity of the hydrocarbon phases. A primary benefit of CO₂ miscibility is the reduction of the crude oil viscosity. Correlations relating the composition to the viscosity have been developed for general hydrocarbon systems by Lohrenz *et al.* (1964) and Lawal (1986). Specific correlations for CO₂-heavy oil mixtures are given by a number of authors. Emanuel (1985) presents a correlation for predicting the viscosities of crude oil-CO₂ mixtures. In his paper Emanuel extends a formula by Loeb (1973) to a ternary mixture of CO₂, light (C₆⁻) and heavy (C₇⁺) pseudocomponents. A set of equations was presented by Chung *et al.* (1986) that is suitable for use in numerical simulations. These equations relate crude API gravity to the properties of CO₂ crude mixtures.

The interaction of the temperature gradients, chemical equilibrium and fractional flow relationships is a web of causes and effects that has been impossible to separate. The purpose of this dissertation is to develop a semi-analytical model in which the interactions of these three factors is taken into account.

1.2 PROBLEM APPLICATIONS

The motivation for the study of this problem was to examine the region ahead of an oxygen enriched combustion process. When an inert gas such as nitrogen is removed from the injection air, large amounts of CO₂ and steam are produced by the burning reactions. These high temperature products are able to move ahead of the combustion front into the cold reservoir. This process not only transports the heat contained in the product gases downstream but also moves components that can significantly change the properties of the hydrocarbons.

As the combined CO₂ and steam move ahead into the reservoir, many things transpire. First, the hot gases heat the oil and the surrounding formation. Second, as the steam condenses, a water phase forms that changes the flow characteristics via the saturations. Third, as the CO₂ cools to reservoir temperatures it dissolves in the crude oil changing the density and viscosity of the oil.

The examination of the interactions of the flue gases from the combustion and the original oil is not the only application of multicomponent, multiphase flow with temperature variations. A steam drive can be characterized primarily as an energy transport process. The major benefit from steam injection is the increased oil mobility due to viscosity reduction at higher temperatures. Water injected in the form of steam releases some of its enthalpy to the surrounding oil and matrix. This transfer causes the steam to condense and become a hot waterflood ahead of the steam front. Transport properties in the steam-oil region are very different from the water-oil regions.

1.3 SOLUTION DESCRIPTION

This section describes the fundamental processes that control how solutions to the model behave. The underlying assumption that is made is that the porous media behaves much like a chromatograph. The difference is that components are partitioned by fractional flow considerations rather than by adsorption onto a stationary column.

1.3.1 The Reservoir as a Chromatograph

The flow properties of fluids that form during a displacement are determined by the local composition and enthalpy conditions. The local composition is imposed by the flow conditions upstream. The species present in the most mobile phase move ahead of those components that remain in a less mobile phase. This component separation resembles the adsorptive separation used in multicomponent chromatography. Chromatography separates components by adsorption onto a stationary column. For the case of multicomponent displacements in porous media, the components are separated by partitioning into different phases that travel at different velocities.

The model used in this study is essentially the theory of multicomponent chromatography applied to multiphase flow systems (Helfferich 1981). For different species the fractional flow relationships for multiphase flow are applied in place of adsorption isotherms. The same models used in chromatography can be used, after small adaptations, to describe the flow of multicomponent, multiphase mixtures in porous media.

Simplifying assumptions reduce the material and enthalpy balance equations to a system of quasi-linear hyperbolic equations. The solution of these equations is found by the method of characteristics.

1.3.2 Method of Characteristics

Use of the method of characteristics to study multiphase flow in porous media dates from the work of Buckley and Leverett (1942) who solved a linear displacement of oil by an immiscible aqueous phase. The authors used a graphical solution where the multivalued saturation velocities were resolved by the use of an "equal area" technique. This matching of areas is essentially the application of the Rankine-Hugoniot conditions at the point of discontinuity. Although the authors did not explicitly use characteristics to arrive at the saturation profiles, Scheidegger (1957) discussed how the method of characteristics could be applied to this problem.

Welge (1961) quantified the effects of phase behavior on a condensing gas drive. By using a technique similar to the method of characteristics, the author developed sets of equations based on material balances that allowed for the calculation of composition paths. It was also shown that along tie lines, where the phase compositions are fixed, the calculations reduce to the Buckley-Leverett equations.

Temperature effects were introduced by Fayers (1962). The method of characteristics was applied to the problem of hot water injected into an oil filled reservoir. The temperature dependence of the fractional flows appears through the viscosity terms. Densities and heat capacities of the rock and fluids were assumed independent of temperature. One of the important observations made by Fayers was that where there was a discontinuity in temperature, a coincident saturation shock must also be present. This observation was later proved by Hovdan (1986) using Reimann invariants.

Reimann invariants were applied by Rhee *et al.* (1970) to solve the hyperbolic equations of multicomponent chromatography. The flow model contained one mobile phase and mass transfer was described using a Langmuir isotherm. Reimann invariants were also used by Hovdan (1986) to solve the hot waterflood problem of Fayers. The entropy condition of Lax (1957) was used to find the physically correct jump conditions.

An isothermal problem similar to the hot waterflood was presented by Temple (1982) for a three component, two phase system of polymer, water and oil. In this paper, viscosity of the aqueous phase was a function of the polymer concentration rather than temperature. Polymer was not allowed to exist in the oil phase and the fractional flows of water and polymer were general nonconvex¹ functions of saturations.

¹Nonconvex implies that there is a point of inflection in the fractional flow curve. This inflection point separates the curve into a convex portion and a concave portion of the fractional flow function.

The blending of the theories of multicomponent chromatography with the description of multiphase flow was first advanced by Helfferich (1981). In his paper the coherence criterion,² which had been used in chromatography for many years, was applied to general systems of multiphase flow. Helfferich calculated the velocities of individual components using the method of characteristics in an approach similar to the way saturation velocities are calculated in the Buckley-Leverett problem. Coherence is applied by setting all these velocities equal, which turns the system of material balance equations into an eigenvalue problem.

The set of eigenvalues represent the coherent velocities that satisfy the material balance relationships. The associated eigenvectors delineate the paths in composition space that the characteristics associated with a particular eigenvalue may follow. A solution profile is constructed by marching along these characteristics from injection to initial conditions.

The integrations of the eigenvectors from the injection to initial condition are the "composition paths." For a multicomponent system there can be many of these paths which emanate from an individual point in composition space. Application of the physical constraint that the faster compositions must reside downstream of slower ones results in a unique and physically correct solution.

The model used by Helfferich was broadened by Dumoré (1984) to include volume change on mixing. As a result the flow velocity was added as a dependent variable along with the overall composition. This changed the form of the eigenvalue problem from that described by Helfferich to a general eigenvalue problem. Eigenvalues still represented the set of coherent velocities, and the eigenvectors were the directions in the space of dependent variables that characteristics can propagate.

Monroe (1986) extended the model of Dumoré to four component systems and used this model to examine the effect of methane on the minimum miscibility pressures of quaternary CO₂ hydrocarbon systems. Solutions to the four component system required a trial and error procedure to find the unique solution satisfying a given set of initial and injection conditions. The trial and error procedure was necessary because of the existence of an intermediate or "cross-over" tie line. The difficulty stems from the fact that this tie line does not extend through either the initial or injection compositions.

Karankas (1986) used the method of characteristics to solve a combination of the problems given by Fayers (1962) and Temple (1982). The model described the coinjection of hot water and a chemical additive into a viscous oil. The viscosities of the oil and water phases were assumed to be functions of temperature along with the adsorption of the additive onto the matrix. The effect of the additive was to lower the residual oil saturation, changing the relative permeability relationships. Heat capacities for all components and the porous medium were assumed constant.

This method has been used recently by Pande (1988) to describe the effects of viscous crossflow in a two-layered system. By assuming that crossflow equalizes the pressure differences caused by having a different viscosity profile in each layer, a hyperbolic system of equations results which can be analyzed by the method of characteristics. The displacement with miscible two and three component cases are covered. In this work the effects of volume change on mixing are neglected.

The model developed in this dissertation primarily extends the works of Dumoré and Monroe by relaxing the assumption of constant temperature. The work adds to the earlier temperature studies by allowing phase densities, viscosities, heat capacities and phase compositions to be functions of the local temperature. Past efforts, with the exception of the general works by Helfferich and Dumoré and recently Monroe (1985), have also been limited to three total components and two phases. This dissertation expands the system to a four component, three-phase system.

The method of characteristics maps the independent variables of distance and time in terms of the dependent variables; composition, temperature and flow velocity. The space of dependent variables is

²The coherence criterion is discussed in more detail in §2.2.2.

often called hodograph and the transformation from the independent variables of space and time to composition space is known as the hodograph transformation Courant and Friedrichs (1984). In this model, the term hodograph space is taken to mean the composition space, which includes the dependent variables temperature and flow velocity as well as the overall composition.

The idea of "coherence" is applied by setting the velocities of all the components as well as the characteristic velocity of the enthalpy equal. Application of the coherence criterion results in a general eigenvalue problem, where the eigenvalues represent the permissible coherent velocities and the eigenvectors indicate the direction in hodograph space along which solutions may propagate. The solution in terms of the hodograph variables is obtained by integrating along these coherent paths from an injection condition to an initial condition.

When the initial conditions are specified for all space, the problem reduces to the Riemann problem. The Riemann problem is a solution to the more general Cauchy problem which is given by,

$$\partial_t C(x,t) + \partial_x \mathcal{F}(C(x,t)) = 0 \quad (1.1)$$

The Riemann problem restricts the system of equations given in Eq. 1.1 to the following initial conditions,

$$C(x,0) = \begin{cases} C^- & \text{for } x < 0 \\ C^+ & \text{for } x > 0 \end{cases} \quad (1.2)$$

where:

C = Vector of compositions, temperature and flow velocity
($C_1, C_2, \dots, C_{n_c-1}, T, u$)

\mathcal{F} = The fractional flow relationships

C^+ = Initial conditions to the right of the origin

C^- = Initial conditions to the left of the origin

Solution of this problem tells how an initial discontinuity is resolved into regions of constant state, simple waves and shocks (Dafermos 1983). The constant state regions are bounded by either simple waves or by jump discontinuities, also known as shocks. Since these shocks involve sets of conservation laws, they are known as Rankine-Hugoniot conditions (Jeffrey 1976).

Solution of these balance equations yields a number of possible paths at each point; however, only one of these paths makes physical sense. The route from the injection conditions to the initial state is subject to a velocity constraint: *the slower velocities as given by the eigenvalue must lie upstream of the faster velocities*. The selection of the correct path using the velocity constraint is the key to obtaining a physically correct solution. Once the proper path is found, the composition, temperature, and saturation profiles are found by relating the composition and temperature at a point to the solution path's eigenvalue.

1.4 What about Simulation?

The development of sophisticated compositional and thermal simulators in the recent past raises an important question: Why not simply use a finite difference simulation to solve these problems? This question has a number of answers.

Numerical simulation of multiphase flow in porous media is rapidly becoming the reservoir engineer's most used tool. These sophisticated programs solve reservoir engineering problems whose solu-

tions were unattainable only a few years ago. The use of simulation models has become the standard for present day reservoir engineering.

The use of simulation models does not require an understanding of the physical principles that govern multicomponent multiphase flow in porous media. Complete reliance on reservoir simulation programs as "black boxes" to design oil recovery projects carries with it a danger of eliminating the need to understand completely the physical interactions that control oil recovery processes. Study of analytical models permits the reservoir engineer to become more familiar with the physical interactions controlling displacement processes and, in addition, gain insight into the behavior of simulations.

A second use for semi-analytical models is verification of their numerical counterparts. General models are often too complicated and costly to apply to all types of recovery schemes. Specialized models are developed that apply to a particular crude oil system or reservoir. An individual model can incorporate features of a formation's lithology or geometry, model the phase behavior of a particular crude oil with an injected solvent, or oxygen requirements of a particular in situ combustion process.

The third motive for studying the analytical solution is identification of the important mechanisms that control the displacements in porous media. Study of analytical models illustrates what factors a numerical model must consider to retain the essential features of the governing differential equations. For example, an analytical model can provide insights into how the many components of a crude oil may be combined into fewer pseudocomponents for compositional simulators and still retain the phase behavior features of the fully compositional system.

What lies ahead?

The next chapter will begin by developing the eigenvalue problem from the mass and conservation laws. Relationships for the velocities of the dependent variables are obtained and the eigenvalue problem formulated by setting these velocities equal. The chapter continues by describing how the physically correct solution can be filtered out from among the many possible solution paths using the velocity constraint. Discontinuities in the form of shocks and "self-sharpening" waves are the most difficult parts of the correct solution, and their properties are covered at the end of the chapter.

Chapter 3 discusses the solution procedure, that is taking the eigenvalue problem and recovering composition, saturation and temperature profiles for specific problems. The chapter opens with a discussion on the basic ideas used to construct these profiles. Rules for the integration along the characteristics are covered along with the rules for handling the jump conditions.

Chapter 4 contains three examples of how the model is applied to particular displacement problems. The first of these cases is the injection of steam into a liquid water filled system. Features of this process include temperature effects and fractional flow in a two-phase region. Because this system contains a single component the effects of phase equilibrium are eliminated. The temperature and fractional flow effects are coupled at the discontinuities that carry the solution into and out of the two-phase region.

The steam-water system is extended in the second example by the addition of an oil component. The oil and water phases are assumed immiscible, so phase behavior still has no effect. The new feature is the interaction of temperature and fractional flow properties. This interaction creates temperature profiles in the steam-oil and water-oil regions that are not seen in the single component case.

The third case considered is a three component case with temperature variation. The components are CO₂, water, and a heavy oil. The components also form three phases, an aqueous phase that contains little CO₂ or oil, a CO₂ rich phase that can contain a large amount of water vapor at high temperatures, and an oleic phase that can have significant amounts of water and/or CO₂ depending on the local temperature. This system contains all the features and interactions mentioned earlier. The interaction of the oleic phase with the other two phases is significant, while the CO₂ rich phase and the aqueous phase hardly interact.

The conclusions and recommendations for future work are discussed in Chapter 5. General statements about the use of the method of characteristics to solve displacement problems are included along with specific comments regarding the interaction of temperature variations, phase behavior and flow properties of the systems detailed in Chapter 4.

2. MATHEMATICAL MODEL

This chapter covers the development of the mathematical model. The model begins with the basic conservation equations for mass and total energy. Simplifying assumptions reduce the equations to a system of hyperbolic partial differential equations. The eigenvalue problem is formulated from by a first using the method of characteristics to find the characteristic velocity for each equation and then restricting the solutions to where all the characteristic velocities are equal.

The calculation of the elements in the eigenvalue matrix by finite difference is discussed. Included here are the two and three phase relative permeability models used to calculate fractional flows. Finally the chapter concludes with a discussion of the jump conditions. At discontinuities, the conservation equations are transformed from differential form into a system of algebraic equations.

2.1 CONSERVATION EQUATIONS

The model proposed in this study is an extension of the multiphase, multicomponent flow model proposed by Dumoré *et al.* For a system of n_c components partitioning into n_p phases, if dispersion is neglected, a material balance on the moles of the i^{th} component is,

$$\frac{\partial}{\partial t} \sum_{j=1}^{n_p} \phi X_{ij} \rho_j S_j + \sum_{j=1}^{n_p} \nabla \cdot \rho_j X_{ij} \bar{u}_j = 0 \quad i = 1 \dots n_c \quad (2.1)$$

In addition to the mass of each component, total energy is also conserved. Heat is transported by the flowing phases just as the components are, and the resulting equation, that expresses the conservation of energy is,

$$\frac{\partial}{\partial t} \sum_{j=1}^{n_p} \phi H_j \rho_j S_j + (1 - \phi) \rho_m H_m + \sum_{j=1}^{n_p} \nabla \cdot \rho_j H_j \bar{u}_j = 0 \quad (2.2)$$

where

- n_p = Number of phases.
- n_c = Number of components.
- ρ_j = Molar density of phase j . ($\text{kg} \text{---} \text{mol}/\text{m}^3$)
- ρ_m = Density of the matrix. (kg/m^3)
- S_j = Saturation of phase j .
- X_{ij} = Mole fraction of component i in phase j .
- H_j = Specific Molar Enthalpy of phase j . ($\text{kJ}/\text{kg} \text{---} \text{mol} \cdot \text{m}^3$)
- H_m = Specific Enthalpy of the matrix. ($\text{kJ}/\text{kg} \cdot \text{m}^3$)
- \bar{u}_j = Phase velocity of phase j . (Pore Volumes/Time)
- ϕ = Porosity.

Writing the total energy balance equation in this manner makes Eq. 2.2 have the same form as the n_c material balance equations. In essence, this model treats heat as another component.

The balance equations are simplified by using the following definitions,

$$G_i \equiv \sum_{j=1}^{n_c} \rho_j X_{ij} S_j \quad (2.3)$$

$$F_i \equiv \frac{u}{\phi} \sum_{j=1}^{n_c} \rho_j X_{ij} f_j \quad (2.4)$$

$$\Gamma \equiv \frac{u}{\phi} \sum_{j=1}^{n_c} \rho_j H_j S_j + \left(\frac{1-\phi}{\phi} \right) \rho_M C_{PM} T \quad (2.5)$$

$$\Theta \equiv \frac{u}{\phi} \sum_{j=1}^{n_c} \rho_j H_j f_j \quad (2.6)$$

where

$$f_j \equiv \bar{u}_j \cdot \frac{\phi}{u} = \text{Fractional flow of phase } j.$$

$$C_{pm} \equiv \frac{H_m}{T} = \text{Heat capacity of the matrix. (kJ/kg} \cdot \text{K)}$$

Applying the definitions in Eqs. 2.3-2.6 to Eqs. 2.1 and 2.2 gives the model's basic conservation equations.

$$\frac{\partial G_i}{\partial t} + \frac{\partial F_i}{\partial x} = 0 \quad i = 1 \dots n_c \quad (2.7)$$

$$\frac{\partial \Gamma}{\partial t} + \frac{\partial \Theta}{\partial x} = 0 \quad (2.8)$$

The term G_i represents the local overall concentration of component i , similar to the local concentration term in the familiar Buckley-Leverett (1942) equation. The term F_i represents the flux of component i . The Γ term is the energy analog to the local concentration term in the material balance. It differs from the mass terms in that the matrix is also allowed to accumulate heat from the fluids and vice versa. The $\rho_M C_{PM} T$ term in the definition of Γ accounts for the heat stored in the matrix. Finally, the Θ term accounts for the heat flux in the system. Since the matrix is immobile, there is no term for flux due to the matrix.

The model is based on the following assumptions that maintain the hyperbolic nature of the equations. These assumptions are excellent approximations when the flow rates are high compared to the diffusive terms such as thermal conduction, capillary pressure or dispersion.

- Flow is one-dimensional.
- Pressure is constant over the length of the displacement. This assumption is made with respect to the thermodynamic equilibrium. While there must be a pressure gradient in order for flow to occur, the solutions are independent of the pressure gradient once the injection velocity is set.

The assumption of constant pressure also allows the use of the enthalpy of the phase in the accumulation term. While it is not correct to say that enthalpy can be accumulated, because the system is at constant pressure and constant total volume, there is no PV work term to consider. Under these conditions, it is correct to consider the total energy and enthalpy balances as identical.

- Porosity is constant.
- Mass and heat transfer are instantaneous.
- Mass transfer by dispersion and diffusion is neglected.
- Heat transfer by conduction and radiation is neglected.
- Heat capacity of the porous medium is constant over the temperature range of interest.

Because Eqs. 2.7 and 2.8 retain their hyperbolic character, the method of characteristics can be used to solve these coupled equations. If solutions are sought for which a given mixture composition moves at a single velocity, the set of $n_c + 1$ balance equations is reduced to a general eigenvalue problem where component velocities are given by the eigenvalues and characteristic directions by the associated eigenvectors.

2.2 METHOD OF CHARACTERISTICS

In its most basic form, the method of characteristics is a mapping of the solution in the space of the independent variables, x and t to the space of dependent variables, C_i , T , and u . Consider a system of equations with independent variables, x and t , and dependent variables, C_1 and C_2 . When the Jacobian is not singular,

$$\frac{\partial(C_1, C_2)}{\partial(x, t)} \neq 0 \quad (2.9)$$

there exists a transformation from any point in the space of independent variables to a unique point in the space of dependent variables. The mapping is illustrated in Fig. 2.1.

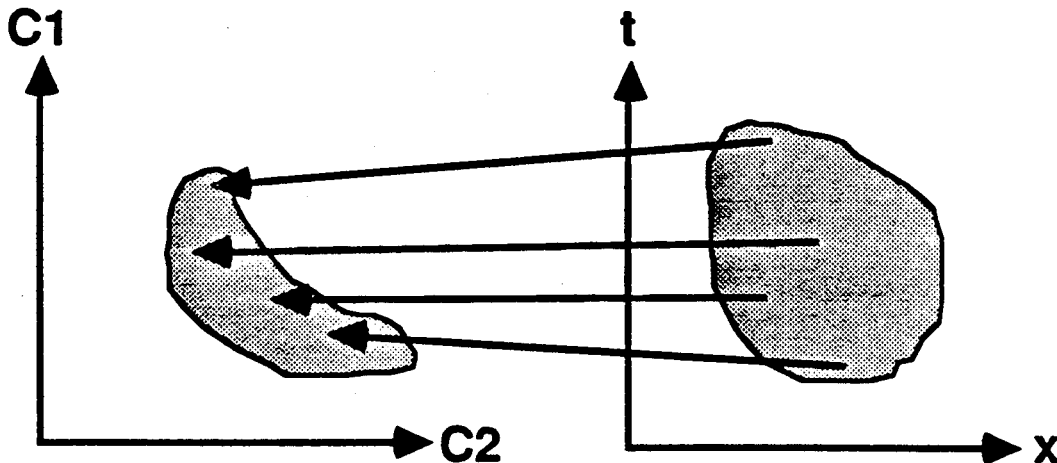


Figure 2.1: One-to-one mapping from the space of independent variables, x and t to the space of dependent variables, C_1 and C_2 . Jacobian of rank 2.

This type of mapping violates the coherence condition placed on the valid solutions. When the Jacobian given in Eq. 2.9 is not singular then all components travel independently of other components. There is no set of compositions that travels together under these conditions. The assumption of coherence and the restriction of the boundary and initial conditions to constant values eliminates this situation from consideration in this dissertation.

Compositions may travel with the same velocity if the Jacobian given by Eq. 2.9 is singular. The Jacobian can be singular if the rank of the Jacobian matrix is either one or zero. When the Jacobian has a rank of one, mapping from a region in $x-t$ space results in a single curve in the space of dependent variables. This mapping is illustrated in Fig. 2.2. A rank one Jacobian implies that the two flow equations are not independent, that is,

$$C_1 = \mathcal{F}(C_2) \tag{2.10}$$

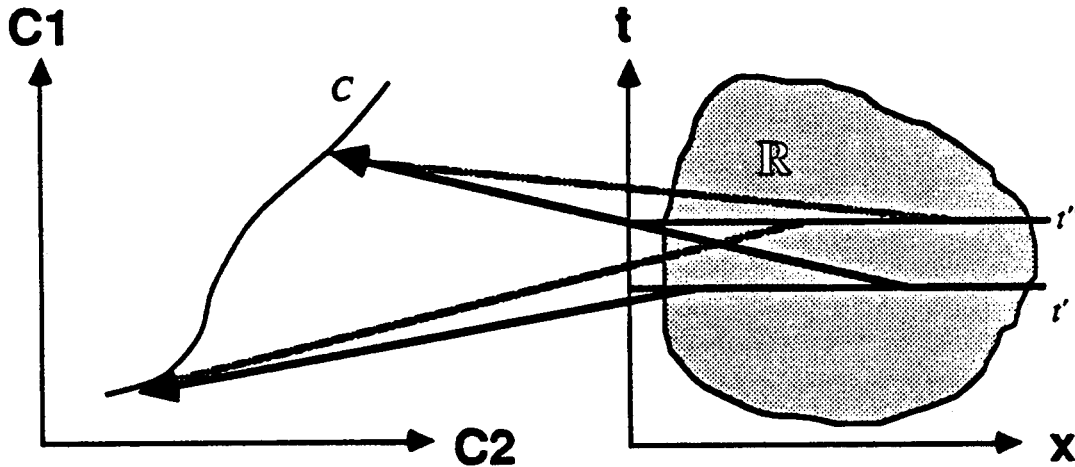


Figure 2.2: Mapping from the space of independent variables, x and t to the space of dependent variables, C_1 and C_2 . Jacobian is rank 1.

Only composition points that lie on the curve C are allowed over the region R . At time t' the compositions along curve C are the local compositions at the positions indicated by the tails of the arrows. At some later time, t'' , the new mapping must result in the same set of compositions given by curve C . Although the position of a given composition point will change, the makeup of the composition points does not change. This is the concept of coherence.

Finally, the Jacobian given by Eq. 2.9 can be of rank zero. Fig. 2.3 shows a region of $x-t$ space mapped onto a single point in composition space. Because a single composition is spread over a finite region of time and space, this mapping describes a region of constant state. The composition given by point A will exist at a position x' from time t_0 to t_1 . Similarly, at time t' , the composition profile will have a value A from x_0 to x_1 .

It has been shown by Lax (1957) that the solution to the Reimann problem consists of regions of constant state bounded by regions of simple waves. The ordering of these waves follows the physical rule that the faster compositions must lie ahead of the slower compositions. The calculation of the component velocities is key to obtaining a physically correct solution.

2.2.1 Calculation of Component and Enthalpy Velocities

The first step in the development of the eigenvalue problem is to calculate the wave velocities for all the components and the wave velocity for the enthalpy. These velocities are the slopes of the characteristic curves in the $x-t$ plane.

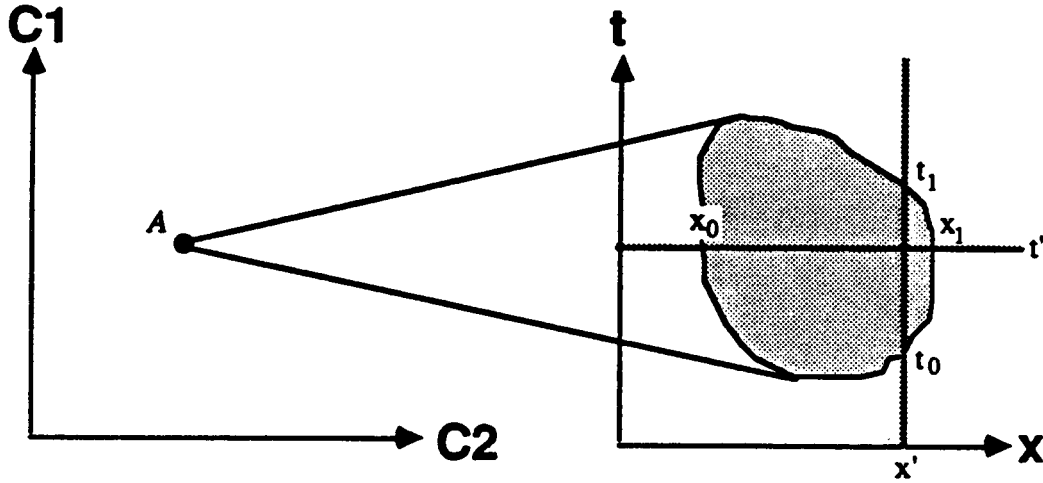


Figure 2.3: Map of constant state region from a region in $x-t$ space to a single point in C_1, C_2 space. Jacobian is of rank 0.

Let η be a dummy variable that is a function of the independent variables, x and t . Writing the basic conservation equations (Eqs. 2.7 and 2.8) in terms of the dummy variable gives,

$$\frac{dG_i}{d\eta} \frac{\partial \eta}{\partial t} + \frac{dF_i}{d\eta} \frac{\partial \eta}{\partial x} = 0 \quad i = 1 \dots n_c \quad (2.11)$$

and

$$\frac{d\Gamma}{d\eta} \frac{\partial \eta}{\partial t} + \frac{d\Theta}{d\eta} \frac{\partial \eta}{\partial x} = 0 \quad (2.12)$$

Here the derivatives with respect to η are ordinary derivatives since the solution is mapped onto a single variable.

The method of characteristics seeks solutions along characteristic lines, that is, where the value of the characteristic variable, η , is constant.

$$d\eta = dt \frac{\partial \eta}{\partial t} + dx \frac{\partial \eta}{\partial x} = 0 \quad (2.13)$$

For the i^{th} component, Eq.2.11 and Eq.2.13 form a set of linear algebraic equations with the characteristic curve parameters, $d\eta/dt$ and $d\eta/dx$ as the unknowns. A non-trivial solution exists if and only if the determinant of the coefficient matrix is zero.

$$\det \begin{bmatrix} \frac{dG_i}{d\eta} & \frac{dF_i}{d\eta} \\ \frac{d\eta}{dt} & \frac{d\eta}{dx} \end{bmatrix} = 0 \quad (2.14)$$

A similar relationship holds for all the other $n_c - 1$ components and the heat, where Γ replaces G_i and Θ substitutes for F_i .

The characteristic or wave velocity of component i is calculated by expanding the determinant of the coefficient matrix Eqn. 2.14). Writing the determinant of Eq. 2.14 and solving for dx/dt gives,

$$u_{C_i} = \frac{dx}{dt} = \frac{(\partial F_i / \partial \eta)}{(\partial G_i / \partial \eta)} \quad (2.15)$$

a similar equation for the velocity of the enthalpy is,

$$u_H = \frac{dx}{dt} = \frac{(\partial \Theta / \partial \eta)}{(\partial \Gamma / \partial \eta)} \quad (2.16)$$

For each of the n_c components there is a characteristic velocity described by Eq. 2.15. In addition to these n_c component velocities, the total energy balance as shown in Eq. 2.16, gives a characteristic velocity associated with the enthalpy, u_H , for a total of $n_c + 1$ different wave velocities. The coherence condition is applied by setting these $n_c + 1$ velocities equal.

Expanding the terms in the velocity equations (Eqs. 2.15 and 2.16) in terms of the hodograph variables C_j , T , and u , yields;

$$\frac{dG_i}{d\eta} = \sum_{k=1}^{n_c-1} \frac{\partial G_i}{\partial C_k} \frac{\partial C_k}{\partial \eta} + \frac{\partial G_i}{\partial T} \frac{\partial T}{\partial \eta} \quad i = 1 \dots n_c \quad (2.17)$$

$$\frac{d\Gamma}{d\eta} = \sum_{k=1}^{n_c-1} \frac{\partial \Gamma}{\partial C_k} \frac{\partial C_k}{\partial \eta} + \frac{\partial \Gamma}{\partial T} \frac{\partial T}{\partial \eta} \quad (2.18)$$

$$\frac{dF_i}{d\eta} = \sum_{k=1}^{n_c-1} \frac{\partial F_i}{\partial C_k} \frac{\partial C_k}{\partial \eta} + \frac{\partial F_i}{\partial T} \frac{\partial T}{\partial \eta} + \frac{\partial F_i}{\partial u} \frac{\partial u}{\partial \eta} \quad i = 1 \dots n_c \quad (2.19)$$

$$\frac{d\Theta}{d\eta} = \sum_{k=1}^{n_c-1} \frac{\partial \Theta}{\partial C_k} \frac{\partial C_k}{\partial \eta} + \frac{\partial \Theta}{\partial T} \frac{\partial T}{\partial \eta} + \frac{\partial \Theta}{\partial u} \frac{\partial u}{\partial \eta} \quad (2.20)$$

Substitution of the expressions in Eqs. 2.17 and 2.19 into Eq. 2.15 for the i^{th} component yields,

$$\sum_{k=1}^{n_c-1} \frac{\partial F_i}{\partial C_k} \frac{\partial C_k}{\partial \eta} + \frac{\partial F_i}{\partial T} \frac{\partial T}{\partial \eta} + \frac{\partial F_i}{\partial u} \frac{\partial u}{\partial \eta} = u_{C_i} \left(\frac{\partial G_i}{\partial C_k} \frac{\partial C_k}{\partial \eta} + \frac{\partial G_i}{\partial T} \frac{\partial T}{\partial \eta} \right) \quad (2.21)$$

a similar substitution using Eqs. 2.18 and 2.20 into Eq. 2.16 gives, for the velocity of the enthalpy wave,

$$\sum_{k=1}^{n_c-1} \frac{\partial \Theta}{\partial C_k} \frac{\partial C_k}{\partial \eta} + \frac{\partial \Theta}{\partial T} \frac{\partial T}{\partial \eta} + \frac{\partial \Theta}{\partial u} \frac{\partial u}{\partial \eta} = u_H \left(\sum_{k=1}^{n_c-1} \frac{\partial \Gamma}{\partial C_k} \frac{\partial C_k}{\partial \eta} + \frac{\partial \Gamma}{\partial T} \frac{\partial T}{\partial \eta} \right) \quad (2.22)$$

There are η equations like Eq. 2.21, one for each component, and Eq. 2.22 for the enthalpy velocity giving $n_c + 1$ separate velocities. The coherence condition states that the only solutions that are stable

have all $n_c + 1$ velocities equal. Solutions where these component velocities are equal are found by solving the general eigenvalue problem described in the next section.

Coherence and the Eigenvalue Problem

The idea of coherence has been used for many years in the field of multicomponent chromatography and has recently been used by to describe the flow of multicomponent, multiphase mixtures in porous media. This section discusses the basis for the coherence criteria and how it formulates the system of characteristic equations into an eigenvalue problem.

What is Coherence?

One of the major assumption of the model is that physically correct solutions to the hyperbolic conservation equations are formed from regions of constant state surrounded by coherent waves. The term coherent was applied by Helfferich (1981) to mean that the only propagationally stable solutions were those where, at any given point in the displacement, all the waves associated with each conserved quantity moved at the same velocity.

The mathematical equivalent of coherence takes $n_c + 1$ independent flow equations and couples them by requiring certain sets of compositions to flow together. This eliminates n_c of the component velocities and creates the eigenvalue problem.

Physically, coherence is simply a statement of velocity. Given fixed initial and injection conditions, any set of components that exists at a particular location must all have travelled the same distance, Δx , over the same amount of time, Δt . The only way these compositions could arrive together is if they all travel with the same velocity.

Sillen (1950) and later Lax (1957) proved that if the solution to the Reimann problem is unique then it is a function of x/t only. The two independent variables can be reduced to a single parameter, $\eta = x/t$. This is equivalent to the mapping illustrated earlier in Fig. 2.2. For the Reimann problem, the entire $x-t$ space is mapped into regions of simple waves when the Jacobian is rank one or into regions of constant state if the Jacobian is of rank zero.

Coherence has been used by a number of authors to describe fluid flow in porous media (Fayers 1961 and 1987, Rhee *et al.* 1970, Monroe 1986, Gorell 1988, and Pande 1988). These authors all solve an eigenvalue problem to determine the composition routes and wave velocities. The velocity constraint is used to isolate the physically correct solution from among the many possible answers.

Formulation of the Eigenvalue Problem

The $n_c + 1$ velocities calculated from Eqs. 2.15 and 2.16 represent the rates at which different conserved quantities move through the flow system. Imposing the coherence condition confines the solutions to regions in hodograph space where all these $n_c + 1$ velocities have the same value. This assumption leads to the formulation of the eigenvalue problem.

The first step is to write the component velocities as functions of the dummy variable, η ,

$$u = \frac{(\partial F_1 / \partial \eta)}{(\partial G_1 / \partial \eta)} = \frac{(\partial F_2 / \partial \eta)}{(\partial G_2 / \partial \eta)} = \dots = \frac{(\partial F_{n_c} / \partial \eta)}{(\partial G_{n_c} / \partial \eta)} = \frac{(\partial \Theta / \partial \eta)}{(\partial \Theta / \partial \eta)} \quad (2.23)$$

Using Eqs. 2.17 and 2.19 in Eq. 2.23 gives for the velocity of component i ,

$$\sum_{k=1}^{n_c-1} \frac{\partial F_i}{\partial C_k} \frac{\partial C_k}{\partial \eta} + \frac{\partial F_i}{\partial T} \frac{\partial T}{\partial \eta} + \frac{\partial F_i}{\partial u} \frac{\partial u}{\partial \eta} = u_{C_i} \left(\sum_{k=1}^{n_c-1} \frac{\partial G_i}{\partial C_k} \frac{\partial C_k}{\partial \eta} + \frac{\partial G_i}{\partial T} \frac{\partial T}{\partial \eta} \right) \quad (2.24)$$

and a similar substitution of Eqs. 2.18 and 2.20 into Eq. 2.23 yields the velocity of the enthalpy wave,

$$\sum_{k=1}^{n_c-1} \frac{\partial \Theta}{\partial C_k} \frac{\partial C_k}{\partial \eta} + \frac{\partial \Theta}{\partial T} \frac{\partial T}{\partial \eta} + \frac{\partial \Theta}{\partial u} \frac{\partial u}{\partial \eta} = u_H \left(\sum_{k=1}^{n_c-1} \frac{\partial \Gamma}{\partial C_k} \frac{\partial C_k}{\partial \eta} + \frac{\partial \Gamma}{\partial T} \frac{\partial T}{\partial \eta} \right) \quad (2.25)$$

This gives n_c equations in the form of Eq. 2.24 and one equation from Eq. 2.25, for a total of $n_c + 1$ velocities. Coherence requires that the velocities for all components and the enthalpy be equal. The system of $n_c + 1$ equations, written in matrix form is given in Eq. 2.26, where a single value, λ , has replaced the $n_c + 1$ velocities ($u_{C_1}, u_{C_2}, \dots, u_{C_{n_c}}, u_H$).

$$\begin{bmatrix} \frac{\partial F_1}{\partial C_1} & \frac{\partial F_1}{\partial C_2} & \dots & \frac{\partial F_1}{\partial C_{n_c-1}} & \frac{\partial F_1}{\partial T} & \frac{\partial F_1}{\partial u} \\ \frac{\partial F_2}{\partial C_1} & \frac{\partial F_2}{\partial C_2} & \dots & \frac{\partial F_2}{\partial C_{n_c-1}} & \frac{\partial F_2}{\partial T} & \frac{\partial F_2}{\partial u} \\ \vdots & \vdots & \dots & \vdots & \vdots & \vdots \\ \vdots & \vdots & \dots & \vdots & \vdots & \vdots \\ \frac{\partial F_{n_c}}{\partial C_1} & \frac{\partial F_{n_c}}{\partial C_2} & \dots & \frac{\partial F_{n_c}}{\partial C_{n_c-1}} & \frac{\partial F_{n_c}}{\partial T} & \frac{\partial F_{n_c}}{\partial u} \\ \frac{\partial \Theta}{\partial C_1} & \frac{\partial \Theta}{\partial C_2} & \dots & \frac{\partial \Theta}{\partial C_{n_c-1}} & \frac{\partial \Theta}{\partial T} & \frac{\partial \Theta}{\partial u} \end{bmatrix} \begin{bmatrix} \frac{dC_1}{d\eta} \\ \frac{dC_2}{d\eta} \\ \vdots \\ \vdots \\ \frac{dT}{d\eta} \\ \frac{du}{d\eta} \end{bmatrix}$$

$$\lambda \begin{bmatrix} \frac{\partial G_1}{\partial C_1} & \frac{\partial G_1}{\partial C_2} & \dots & \frac{\partial G_1}{\partial C_{n_c-1}} & \frac{\partial G_1}{\partial T} & 0 \\ \frac{\partial G_2}{\partial C_1} & \frac{\partial G_2}{\partial C_2} & \dots & \frac{\partial G_2}{\partial C_{n_c-1}} & \frac{\partial G_2}{\partial T} & 0 \\ \vdots & \vdots & \dots & \vdots & \vdots & \vdots \\ \vdots & \vdots & \dots & \vdots & \vdots & \vdots \\ \frac{\partial G_{n_c}}{\partial C_1} & \frac{\partial G_{n_c}}{\partial C_2} & \dots & \frac{\partial G_{n_c}}{\partial C_{n_c-1}} & \frac{\partial G_{n_c}}{\partial T} & 0 \\ \frac{\partial \Gamma}{\partial C_1} & \frac{\partial \Gamma}{\partial C_2} & \dots & \frac{\partial \Gamma}{\partial C_{n_c-1}} & \frac{\partial \Gamma}{\partial T} & 0 \end{bmatrix} \begin{bmatrix} \frac{dC_1}{d\eta} \\ \frac{dC_2}{d\eta} \\ \vdots \\ \vdots \\ \frac{dT}{d\eta} \\ \frac{du}{d\eta} \end{bmatrix} \quad (2.26)$$

Eq. 2.26 will, in general contain $n_c + 1$ eigenvalues. When the conservation equations are hyperbolic, all the eigenvalues are real (Jeffrey 1976), and represent $n_c + 1$ different coherent velocities.¹ Recent studies have shown that during three phase flow, regions of the composition space are *elliptic*. Because the final column in the \bar{G} matrix is zero, one of the eigenvalues is infinite. The infinite eigenvalue represents the rate which flow velocity changes propagate through the system (Monroe 1986). Therefore, there remain n_c real, finite velocities for any given composition and temperature.

At certain singular points, two of the n_c eigenvalues can be equal. Systems that exhibit this property are called *nonstrictly* hyperbolic. These equal eigenvalue points are important in the construction of the solution, for at these points, the solution path is free to switch, with no jump in velocity, from one of the characteristics to the other characteristic with the equal eigenvalue. In essence, these points represent a zone of constant state with a length of zero.

Along with the velocities as represented by the eigenvalues, the associated eigenvectors describe the characteristic curve in hodograph space for each of the eigenvalues. These eigenvectors tell what set of compositions and temperature can lie directly ahead of and behind the current composition and still satisfy the material and energy balances.

2.3 EVALUATION OF THE DERIVATIVES IN THE EIGENVALUE MATRIX

The derivatives in the eigenvalue matrix (Eq. 2.26) relate how the saturation and flux terms for each component vary when the overall composition, temperature and flow velocity at a particular location change. Evaluation of these derivatives requires that the properties of all the existing phases be known for a given overall composition and temperature. These properties are:

1. The molar density of each phase.
2. The composition of each phase.
3. The saturation of each phase.
4. The enthalpy of each phase.
5. The viscosity of each phase.
6. The relative permeability of each phase.

With the exception of the viscosity and the relative permeability, all other properties can be obtained directly from an equation of state. The viscosity is usually given in the form of empirical curves or a correlation relating the phase composition, temperature and pressure to the viscosity of the phase. Relative permeabilities of the existing phases depend not only on the fluid properties, but on the wetting condition of the matrix as well as the saturation of the coexisting phases. In general the relative permeabilities of the wetting and gaseous phases are functions of the wetting and gaseous phase saturations, respectively. The remaining phases are given as functions of the two phase relative permeabilities between the intermediate phase and both the wetting and gaseous phases.

¹Recent studies have shown that during three phase flow, regions of the composition space are *elliptic*. These elliptic regions have complex eigenvalues and can change the nature of the conservation equations. A brief explanation of the elliptic regions is presented in Appendix D.

2.3.1 Fluid Property Calculation

The method for calculation of the fluid properties depends on the particular system involved. When phase behavior is not included in the problem, correlations relating the viscosity specific volume and enthalpy of the components against temperature are all that are needed to calculate the derivatives in the eigenvalue matrix. When phase behavior is included as part of the solution, a flash calculation is required. This calculation is usually done by calculating component fugacities using an equation of state. Once the individual phase compositions are found, the physical properties are calculated from the composition, temperature and pressure. Appendix B gives the details on how the fluid properties were obtained for each of the examples presented in Chapter 4.

Relative permeabilities of the wetting and gaseous phases are calculated using a power law

$$k_{rg} = \sigma_g \left(\frac{S_g}{1 - S_{or} - S_{wc}} \right)^{\alpha_g} \quad (2.27)$$

and

$$k_{rw} = \sigma_w \left(\frac{S_w - S_{wc}}{1 - S_{or} - S_{wc}} \right)^{\alpha_w} \quad (2.28)$$

where:

- k_{rg} = gaseous phase relative permeability
- k_{rw} = wetting phase relative permeability (usually water)
- σ_g = end point (maximum) relative permeability of the gaseous phase
- σ_w = end point (maximum) relative permeability of the wetting phase
- S_g = gaseous phase saturation
- S_w = wetting phase saturation
- S_{wc} = connate wetting phase saturation
- S_{or} = residual intermediate phase saturation
- α_g = gaseous phase exponent
- α_w = wetting phase exponent

These equations are used for both the two and three phase relative permeabilities. When three phases are present, the relative permeability of the intermediate phase, usually oil, requires further calculations.

This dissertation uses two models to calculate the relative permeability of the intermediate phase. Both models combine two phase relative permeability values to calculate the three phase relative permeability. One set of the two phase relationships between the intermediate and wetting phases, oil and water. In this model the oil phase relative permeability in the absence of a free gas phase is given by,

$$k_{row} = \sigma_{ow} \left(\frac{S_o - S_{wc}}{1 - S_{or} - S_{wc}} \right)^{\alpha_{ow}} \quad (2.29)$$

where:

- k_{row} = Oil relative permeability in the oil-water system
- σ_{ow} = end point (maximum) relative permeability of the intermediate phase
- S_o = intermediate phase saturation, $S_o = 1 - S_w - S_g$
- α_{ow} = oil-water exponent

The second relative permeability relationship is the gas-liquid relationship. This relative permeability relationship is taken at the irreducible water saturation, which is included in the saturation of the intermediate phase.

$$k_{rig} = \alpha_{lg} \left(\frac{1 - S_g - S_{wc}}{1 - S_{or} - S_{wc}} \right)^{\alpha_{lg}} \quad (2.30)$$

where:

- k_{rig} = Oil relative permeability in the liquid-gas system
- σ_{lg} = end point (maximum) relative permeability of the intermediate phase
- S_l = liquid phase saturation, $S_l = 1 - S_g$
- α_{lg} = liquid-gas exponent

Eqs. 2.29 and 2.30 are combined to give the oil phase relative permeability. The model for the intermediate phase permeability is taken from Stone (1970) as given by Aziz and Setarri (1979),

$$k_{ro} = \frac{(k_{rov} + k_{rw}) (k_{rig} + k_{rg})}{k_{rov}} \quad (2.31)$$

where:

- k_{rocw} = intermediate phase relative permeability at irreducible water saturation

Once all the fluid properties are calculated for each phase, G, F, Γ , and are calculated using the definitions given in Eqs. 2.3-2.6.

2.3.2 Calculating the Derivatives for the Eigenvalue Problem

The relationships between the overall composition and temperature to the quantities needed for evaluation of the eigenvalue matrix are very complex. Even when calculating fluid properties using an equation of state, evaluation of the derivatives is a costly procedure. Simple forward or backward differences are the easiest to calculate and provide excellent approximations to the true derivatives. Monroe (1986) used this technique to calculate his composition paths.

The primary variables, G, F, Γ , and Θ are calculated at the current "composition" point² using a flash calculation to obtain the fluid properties. Another flash is performed at a perturbed composition point by adding a small amount to the mole fraction of one of the components and decreasing the mole fraction of another. A new flash is performed and new values for the four primary variables are calculated. For example, to calculate $(\partial F_1 / \partial C_2)$ the following difference is used,³

$$\frac{\partial F_1}{\partial C_2} = \frac{F_1(C_1, C_2 + \Delta C_2, \dots, C_{nc} - \Delta C_2, T, u) - F_1(C_1, C_2, \dots, C_{nc}, T, u)}{\Delta C_2} \quad (2.32)$$

²The term composition point means the position in hodograph space. It includes temperature as well as overall composition.

³The results of the eigenvalue problem do not depend on the choice of component from which that ΔC_2 is subtracted. As long as the choice is consistent, the resulting eigenvalues and eigenvectors do not change.

There are $n_c - 1$ compositional derivatives plus a temperature derivative to calculate, meaning that at every time the eigenvalue problem is solved, n_c flash calculations must be performed.⁴ The change in composition at the perturbed points is done on a mole fraction basis so only $n_c - 1$ of the compositions are independent. This requires that the same mole fraction be subtracted from the C_{nc} term in the forward difference. Temperature does not have this restriction so the perturbed point is found by changing the temperature value only. The derivatives of F and Θ with respect to u are simple and are calculated analytically.

Near phase boundaries, the changes in saturation and phase properties can be dramatic. In these regions simple forward differences may not accurately represent the true derivative. Equations of state used to represent the phase behavior of the fluid systems contain the information required to construct the derivatives in the eigenvalue matrix (Eq. 2.26) (Nutakki, *et al.* 1985).

The need for more accurate representation of the derivatives is only necessary near phase boundaries. In regions removed from these boundaries, the simple forward differences give excellent results. When the solution path travels between regions where the number of phases changes, discontinuities in composition exist which skip over regions near the phase boundaries. This physical feature often causes the solution path to be far enough from the phase boundaries that the simple forward differences are accurate.

The eigenvalues and the associated eigenvectors are found using an algorithm presented by Moler and Stewart (1973) as implemented in the IMSL routine EIGZCF. The algorithm uses Householder transformations to reduce the \bar{F} matrix to an upper Hessenberg and the \bar{G} matrix to upper triangular form. These transformed matrices are diagonalized to find the eigenvalues by successive QZ diagonalizations.

2.4 SHOCK CALCULATIONS

When the integration along the characteristics must violate the velocity constraint, it is necessary to introduce discontinuities or shocks into the solution. When conservation laws are applied across the shocks, the relationships between the speed of the shock and the conditions upstream and downstream of the discontinuity are known as Rankine-Hugoniot conditions.

The Rankine-Hugoniot conditions are found by applying a material or heat balance across the discontinuity. Consider a shock traveling with a velocity, λ as illustrated in Figure 2.4 (from Monroe 1985).

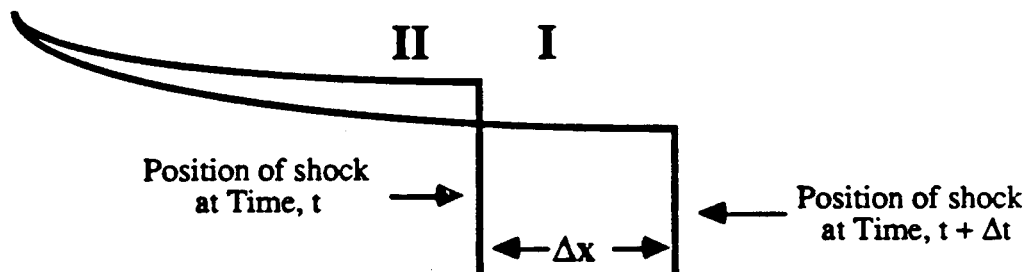


Figure 2.4: Shock position at time t and $t + \Delta t$. After Monroe (1985).

⁴While this may seem like many flash calculations, because the ΔC 's are small, the flash calculation can be provided with an excellent initial guess and the number of iterations is kept low.

Using an approach outlined by Dumoré, the shock velocity is given by the material balances,

$$\Lambda = \frac{1}{\phi} \left(\frac{u^+ F^+ - u^- F^-}{G^+ - G^-} \right) \quad (2.33)$$

Where the superscripts (+) and (-) refer to the downstream and upstream sides of the shock, respectively. The same arguments apply to the heat accumulation in a moving shock. The heat balance across the shock is given by,

$$\Lambda = \frac{1}{\phi} \left(\frac{u^+ \Theta^+ - u^- \Theta^-}{\Gamma^+ - \Gamma^-} \right) \quad (2.34)$$

These balances are the Rankine-Hugoniot conditions.

Shocks are described completely by three states, the upstream conditions, the downstream conditions, and the shock velocity. Table 2.1 indicates that $2n_c + 5$ variables are needed to describe fully a discontinuity. The problem is to relate the conditions on one side of the shock to the shock velocity and the conditions on the other side of the discontinuity.

Table 2.1: Unknowns describing a discontinuity in a system with n_c components.

	Upstream	Downstream
Components	n_c	n_c
Temperature	1	1
Flow Velocity	1	1
TOTALS	$\frac{\quad}{n_c + 2}$	$\frac{\quad}{n_c + 2}$

+ $\Lambda = 2n_c + 5$ Variables

These states are related through Rankine-Hugoniot conditions. For a system of n_c components the material and energy balances are given by equating $n_c + 1$ equations like Eq. 2.33 and one given by Eq. 2.34,

$$\phi \Lambda = \frac{u^+ F_1^+ - u^- F_1^-}{G_1^+ - G_1^-} = \frac{u^+ F_2^+ - u^- F_2^-}{G_2^+ - G_2^-} = \dots = \frac{u^+ F_{n_c}^+ - u^- F_{n_c}^-}{G_{n_c}^+ - G_{n_c}^-} = \frac{u^+ \Theta^+ - u^- \Theta^-}{\Gamma^+ - \Gamma^-} \quad (2.35)$$

By eliminating Λ from this set of equations, we are left with n_c independent equations relating the conditions on the upstream side of the shock to the downstream conditions. One of these equalities is used to relate the unknown flow velocity the flow velocity on the opposite side of the shock. Constraints on the mole fraction summations and total saturation provide two additional equations. This leaves $n_c + 3$ variables that remain to be set.

Setting the conditions on one side of the shock fixes $n_c + 1$ of the remaining variables, leaving a single degree of freedom. Physical considerations usually require that the shock velocity, Λ to be equal to

one of the wave velocities adjacent to the discontinuity.⁵ This eliminates the final degree of freedom, fixing the shock conditions.

The model described in this chapter can be applied to a wide variety of multiphase, multicomponent flow problems. It includes the effects of phase behavior, temperature gradients and flow properties in a manner that is only available in complex reservoir simulation programs. Chapter 3 lays the groundwork for application of the model to specific problems. The chapter covers the details of the solution path construction and provides guidelines for how a particular solution is obtained. Details on the formation and behavior of discontinuities and how they relate to the solution paths is discussed.

Chapter 4 provides specific examples on three displacement systems. These three systems are distinguished by the number of phases and components present. Isothermal solutions and solutions with temperature variation are discussed where appropriate. Saturation or composition profiles illustrate the behavior of the different systems. Each system is studied for the effects of varying one or more relevant parameters such as injection temperature, matrix heat capacity or oil viscosity.

Chapter 5 summarizes the general features and limitations of the model. Difficulties and the methods used to overcome potential pitfalls are stressed. Results for each specific system studied in Chapter 4 are presented. Finally, some ideas for future study and application of the model are mentioned.

⁵This matching of the wave velocity and shock velocity results in a shock that is known as an intermediate discontinuity. These intermediate discontinuities are the multidimensional equivalent of the Buckley-Leverett "tangent" shock. These shock classifications are discussed fully in §3.2.

3. SOLUTION PROCEDURES

The solution procedure for the different examples used in this dissertation indicate how the general formulation given in Eq. 2.26 is adapted to different conditions. By using information on how the system is physically constrained to behave, the general formula is modified to conform to the specific problem at hand. This simplification often brings hidden features of the particular system to the surface. In this way the model helps to isolate the reasons behind the behavior of the simplified systems.

A good example of this is provided by the example problem detailed in §4.1. Briefly, when high temperature steam is injected into a system initially filled with liquid water, a two-phase region forms where the steam and water coexist. Application of the phase rule constrains the flow to be isothermal wherever one component exists in two phases simultaneously. Keeping this restriction in mind and reducing the general formula to a two by two system with saturation and flow velocity as the independent variables reveals that the steam-water system behaves exactly like an immiscible Buckley-Leverett system.

This chapter covers the application of the concepts and equations described in Chapter 2 to specific displacement systems. The chapter begins with the basic rules that are common to all problem formulations. The rules for integrating along the composition paths are explained along with a physical interpretation of the different types of path switches. The chapter concludes with the conditions governing the shocks and discontinuities that are expected in these types of problems.

Many of the concepts and basic solution methods used in Chapter 2 are common to the different problems that this model can describe. First, the dependent variables are chosen. These quantities should be changing in the region of interest. Often the problem will be broken into different regions where different dependent variables change. For example, in the steam-water problem described later in §4.1, the two-phase region uses vapor saturation as the hodograph variable while in the single-phase region, the temperature is chosen as the dependent variable.

The accumulation and flux derivatives in the general eigenvalue problem (Eq. 2.26) are written with respect to the dependent variables. This means that the problem formulation may be different for the various regions within a single problem. The eigenvalue problem is solved for the velocities (eigenvalues) and the directional derivatives (eigenvectors) in the space of the dependent variables. The solution is integrated along the eigenvectors, from the injection to the initial condition, such that the associated eigenvalue increases as the integration moves downstream towards the initial conditions.

3.1 PATH SELECTION

The velocity constraint limits the choice of integration path by requiring the solution to have increasing velocity as the integration proceeds from the injection to the initial conditions in hodograph (dependent variable) space. The following rules control the way the integration from the injection to initial conditions may proceed.

Rule I: The solution must lie along a path

The eigenvectors indicate which compositions may lie directly ahead and directly behind any point in the composition space. To veer off a composition path, as in Figure 3.1, violates the conservation equations (Eqs. 2.1 and 2.2).

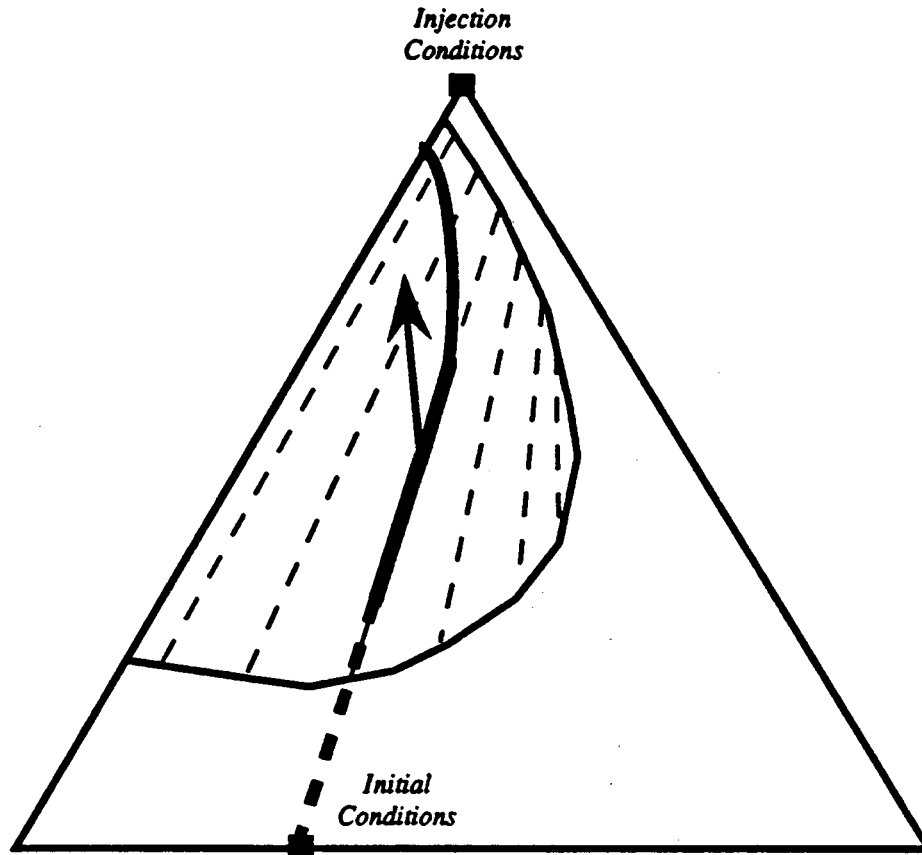


Figure 3.1: Illegal composition path for a ternary displacement as the path moves from initial conditions to injection conditions.

Rule II: While travelling exclusively along a path, the velocity may increase or decrease regardless of the direction of integration.

As long as the solution remains exclusively along a composition path, the change in velocity along that path determines the type of simple wave that the path represents. Increasing velocity as the solution moves downstream is in accordance with the velocity rule, and these types of simple waves are known as spreading waves. The continuous part of the saturation profile in the Buckley-Leverett solution is an example of a spreading wave. The wave is known as a spreading wave because the body of the wave is associated with steadily increasing velocities. As time passes, the conditions at the leading edge of the wave separate from their neighbors. This spreading occurs over the length of the wave causing it to grow larger and larger.

The opposite of a spreading wave is a "self-sharpening" wave. These waves are created when the velocity decreases as the integration moves downstream. The portion of the composition path that is self-sharpening resolves into a jump discontinuity, and its velocity is calculated by applying the material balance relationships as if the wave were a genuine shock. An example of this kind of wave is the Buckley-Leverett saturation front.

Between these two cases is an "indifferent" wave that neither spreads or sharpens. When the eigenvalue remains constant along a composition path, the compositions just ahead and just behind travel at the same velocity as the current composition point and remain the same distance from the composition point as time increases. This is equivalent to saying that the two characteristics are parallel.

Mathematically an indifferent wave is equivalent to,

$$\bar{t}^k \cdot \nabla_c \lambda^k = 0 \quad (3.1)$$

where \bar{t}^k is the directional derivative of the k^{th} characteristic and $\nabla_c \lambda^k$ is the gradient of the k^{th} characteristic velocity in composition space. Jeffrey (1976) showed that these types of waves can only occur in linear or semilinear equations. Where the coefficient matrix, in our case the fractional flow relationships, is strictly non-linear this kind of wave does not appear.

Waves that are only slightly spreading or only slightly sharpening are found in some of the problems that have been analyzed previously. Many times the composition paths that travel along non-tieline paths have eigenvalues that show a only a slight change along the solution route. Monroe (1986) found these types of slightly spreading waves in his solutions for CO_2 -hydrocarbon systems.

Rule III: Path switches may take place at points where two of the eigenvalues are equal.

The hyperbolic system of equations derived in this model has a number of singular points where two of the eigenvalues are equal. The composition path may switch from one path to the other at these points.

Figure 3.2 gives an example for a ternary system. The eigenvalues are plotted along a tie-line in a two-phase region. The dark line indicates the velocities of compositions that are all on the path as it moves from the injection condition to the initial composition. When the path comes to the equal eigenvalue point, labelled E, the path switches from the eigenvalues of the tie-line path to those velocities along non tie-line path.

Rule IV: Switches from a slow path to a faster path are allowed.

The path switch at the equal eigenvalue point is a smooth transition from one path to the other. Path switches may also be discontinuous. These switches from a slower path to a faster path are permitted as long as the change does not violate the velocity constraint. This means that as the integration moves from the injection to the initial conditions, the only legal switches are from a slower path to a fast path. Figure 3.3 is an example of a legal path switch.

The switch from a slow path to a fast path indicates that a point in composition space has two velocities. This is mathematically equivalent to a region in $x-t$ space that is mapped onto a single point in the composition space. These regions have a single composition point that is constant over a finite interval in time and distance; for this reason they are known as regions of constant state. This condition is true when the transformation Jacobian given by Eq. 2.9 is of rank zero.

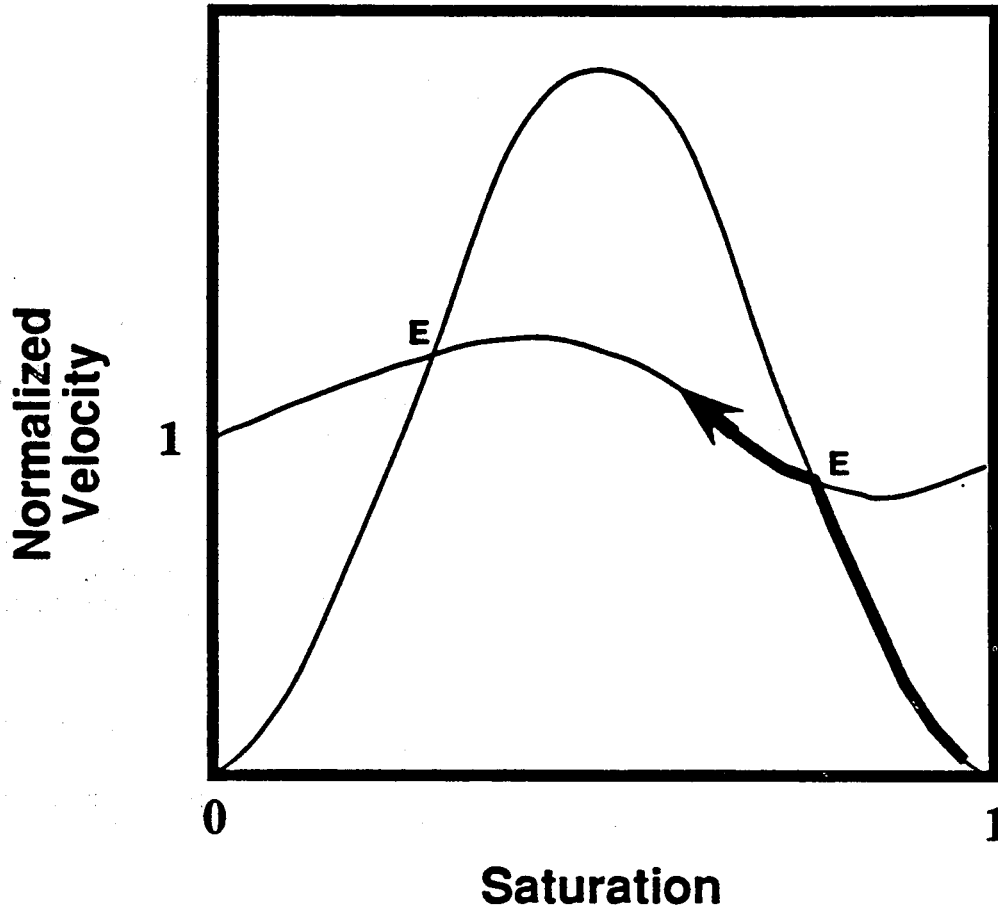


Figure 3.2: Legal path switch at an equal eigenvalue point for a ternary displacement as the path moves from injection conditions to initial conditions.

Rule V: **Switches from a fast path to a slower path are not allowed.**

Path switches that violate the velocity constraint are *not* allowed. Figure 3.4 shows an example of an illegal path switch that violates the velocity constraint. This kind of switch is similar to the zone of constant state. In both cases the switch indicates that a given composition point has two coherent velocities. However the difference in the illegal switch is that the slower velocities on the non-tie-line path lie downstream of the faster tie-line velocities. This is physically not possible since all the waves began at the same position in $x-t$ space. Solutions that require this type of switch are not physically realizable.

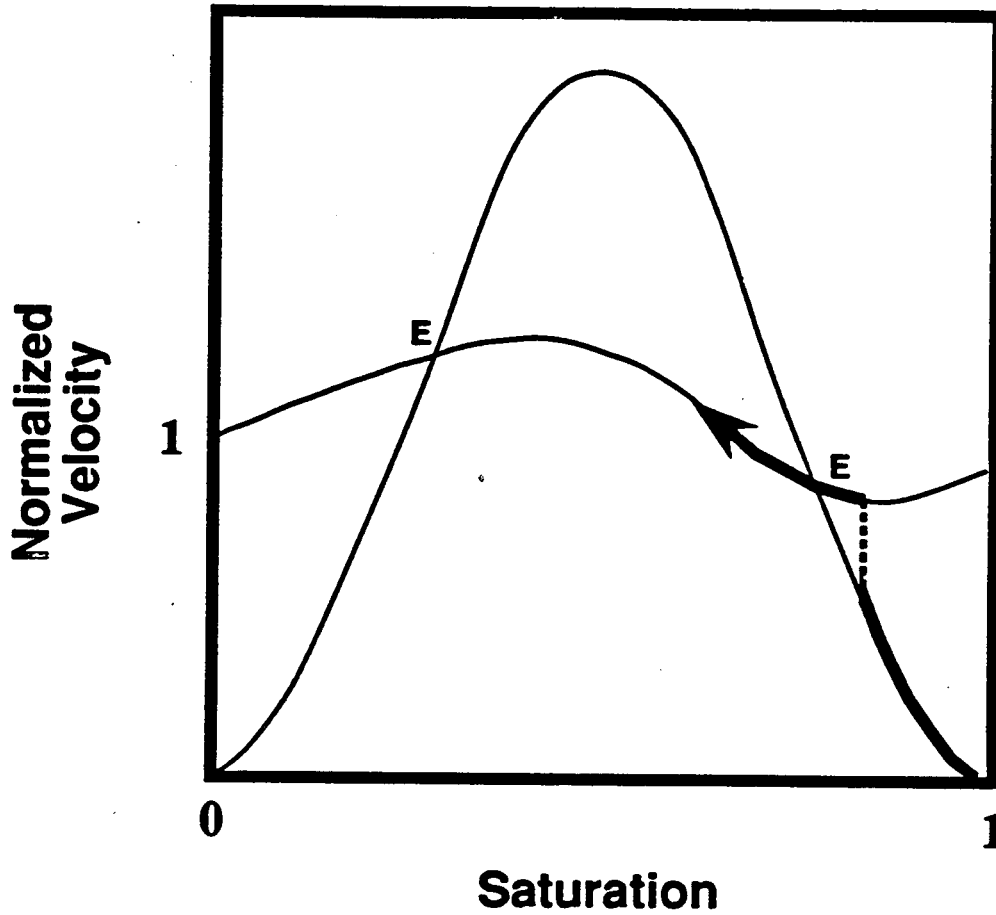


Figure 3.3: Legal path switch for a ternary displacement as the path moves from injection conditions to initial conditions.

3.2 Shock Calculations

Discontinuities in the form of shocks and/or “self-sharpening” waves appear whenever the velocity rule would be violated. Under these conditions, the differential equation along a characteristic becomes an algebraic equation relating conditions on each side of the discontinuity. These algebraic equations are the Rankine-Hugoniot conditions that relate the hodograph variables on either side of the shock to the shock velocity.

Consider a discontinuity that propagates with a velocity, L^k . Since the system of equations is hyperbolic, there are $n_c + 1$ distinct eigenvalues ordered such that $\lambda_1 < \lambda_2 < \dots < \lambda_{n_c+1}$ on each side of the shock. The conditions for the shock to be admissible are provided by Lax (1957) and are,

$$\lambda_k^+ \leq \Lambda_k \leq \lambda_k^- \quad (3.2)$$

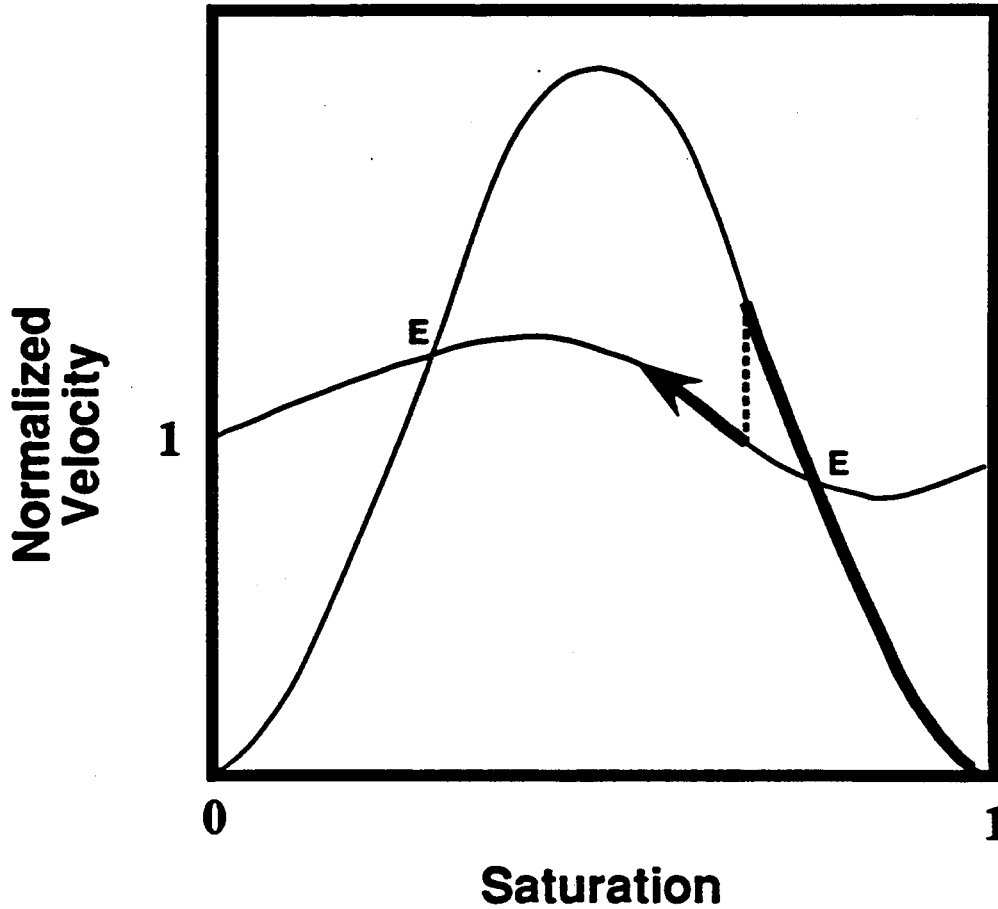


Figure 3.4: Illegal path switch for a ternary displacement as the path moves from injection conditions to initial conditions.

$$\lambda_j^+ < \Lambda_k \quad \lambda_j^- < \Lambda_k \quad \text{when } j < k, \quad (3.3)$$

$$\Lambda_k < \lambda_j^+ \quad \Lambda_k < \lambda_j^- \quad \text{when } j > k \quad (3.4)$$

where the superscripts (+) and (-) represent the conditions on the downstream and upstream side of the shock, respectively. Shocks that adhere to these relationships are said to satisfy the Lax Entropy Conditions. Keyfitz and Kranzer (1980) extended the Lax conditions to include systems which are non-strictly hyperbolic.

Shocks are distinguished by the relationship of the shock velocity to the wave velocities immediately surrounding the discontinuity (Eq. 3.2). The three types of shocks are: contact discontinuity, intermediate discontinuity or semi-shock, and evolutionary or genuine shock (Jeffrey 1976). When the shock velocity matches the wave velocities on both sides of the discontinuity the inequalities in Eq. 3.2 are changed to equalities. These shocks are called *contact discontinuities*.

Contact discontinuities are found in problems where the one of the characteristic families is essentially linear (Keyfitz and Kranzer 1980). The fractional flow relationships for multiphase flow are, in general, nonlinear functions of the dependent variables so this type of shock does not appear in any of the solutions that are presented in this dissertation.

An *intermediate discontinuity* or *semi-shock* has a velocity that matches the wave velocity on only one side of the jump. One, but not both of the inequalities in Eq. 3.2 are changed to equalities, so either,

$$\lambda_k^- = \Lambda_k > \lambda_k^+ \quad (3.5)$$

or

$$\lambda_k^- > \Lambda_k = \lambda_k^+ \quad (3.6)$$

These discontinuities are often referred to as contact discontinuities by many authors (Lax, 1957, Keyfitz and Kranzer, 1980, and Temple 1982). Other authors call these discontinuities "tangent" shocks (Welge 1961 and Monroe 1986). Where the wave velocity and shock velocity match, the shock is the limit of the spreading wave on that side of the shock. In this dissertation these shocks will be referred to as either **upstream intermediate discontinuity (UID)** if Eq. 3.5 holds, or **downstream intermediate discontinuities (DID)** when Eq. 3.6 is true.

Equation 3.5 is the condition that controls the front in the Buckley-Leverett problem. Figure 3.5 shows how the tangent construction represents the matching of the shock and wave, or characteristic velocities. The tangent connecting the downstream side of the shock to the upstream side represents the Rankine-Hugoniot material balance across the shock. The slope of the tangent line is equal to the shock velocity, Λ .

The wave velocity in the Buckley-Leverett case is given by the velocity of the saturation, $\partial f_w / \partial S_w$. This represents the eigenvalue on the upstream side of the shock, λ^- . When the slope of the fractional flow curve and the material balance (tangent) line are equal, then Eq. 3.5 holds.

A *genuine* or *evolutionary* shock has a velocity that does not match the wave velocity on either side of the discontinuity. Both of the inequalities in Eq. 3.2 hold for the genuine shock. These discontinuities are found in solutions where the jump condition is bounded by regions of constant state on both sides of the shock (Monroe 1986 and Pande 1988). Monroe refers to these discontinuities as "non-tangent" shocks. Many times these shocks are the result of arriving on an exit tie-line path at a point where an immediate jump to the exit conditions is indicated. The inclusion of genuine discontinuities into the physical solution represents the most difficult aspect of solution path construction. The difficulty arises from the realization that not all the information required is immediately available. Many times the shock velocity and/or the conditions on the upstream and downstream sides of the shocks are not known *a priori*.

The nature of the region adjacent to the shock can provide a starting place for the shock calculation. A region of continuous variation usually means that the shock is an intermediate discontinuity with a region of constant state on the other side of the shock. In this case a multidimensional tangent construction (Welge 1952) can be used to locate the position of the shock if the constant state conditions are known.

On the other hand, when a genuine shock is needed, the conditions surrounding the discontinuity are unknown points on unconnected composition paths. The situation is illustrated in Fig. 3.6.

Points 1 and 2 are on the path that connects to the injection conditions and points A—C are on a path that intersects the initial conditions. The narrow dot-dashed lines represent some of the possible jumps from the injection path to the initial path. These lines represent only a small number of the possible jumps. Only one of these lines represents the actual shock that satisfies the velocity constraint.

Locating the one shock from among all the possibilities is a most difficult task. Often this task becomes the heart of the solution construction problem.

Chapter 4 covers the application of the techniques described in this chapter to different displacement systems. These solutions range from a simple steam-water displacement to a complex system where phase behavior, temperature effects and flow properties interact to control the flow process.

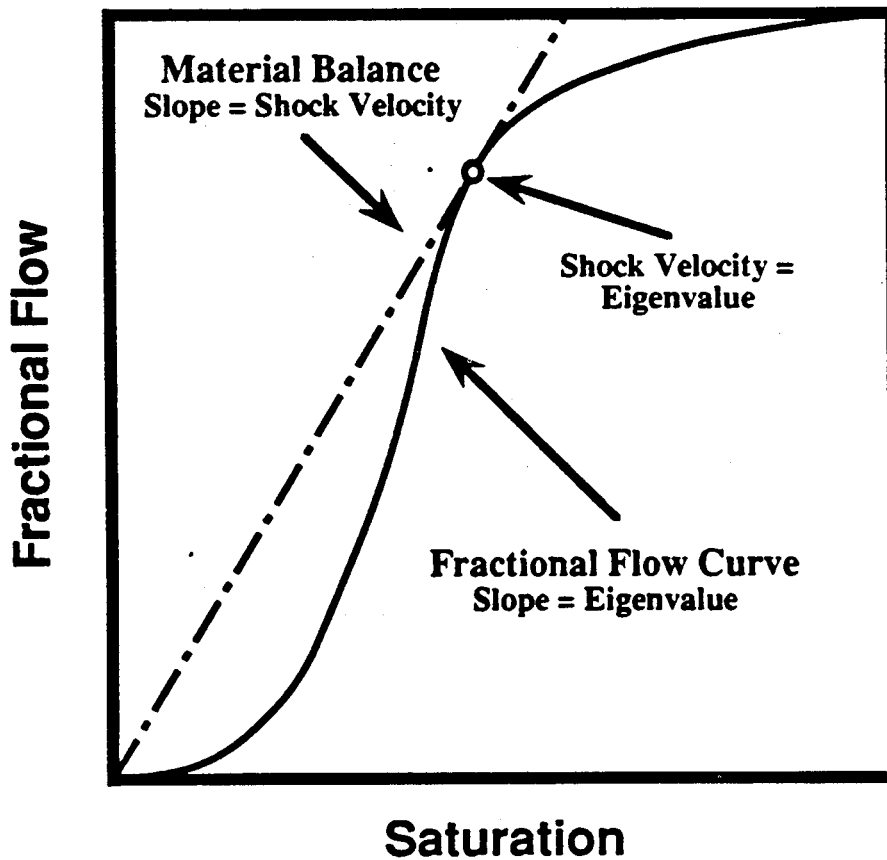


Figure 3.5: Tangent construction for Buckley-Leverett shock front that illustrates how the tangent construction matches shock and wave velocities.

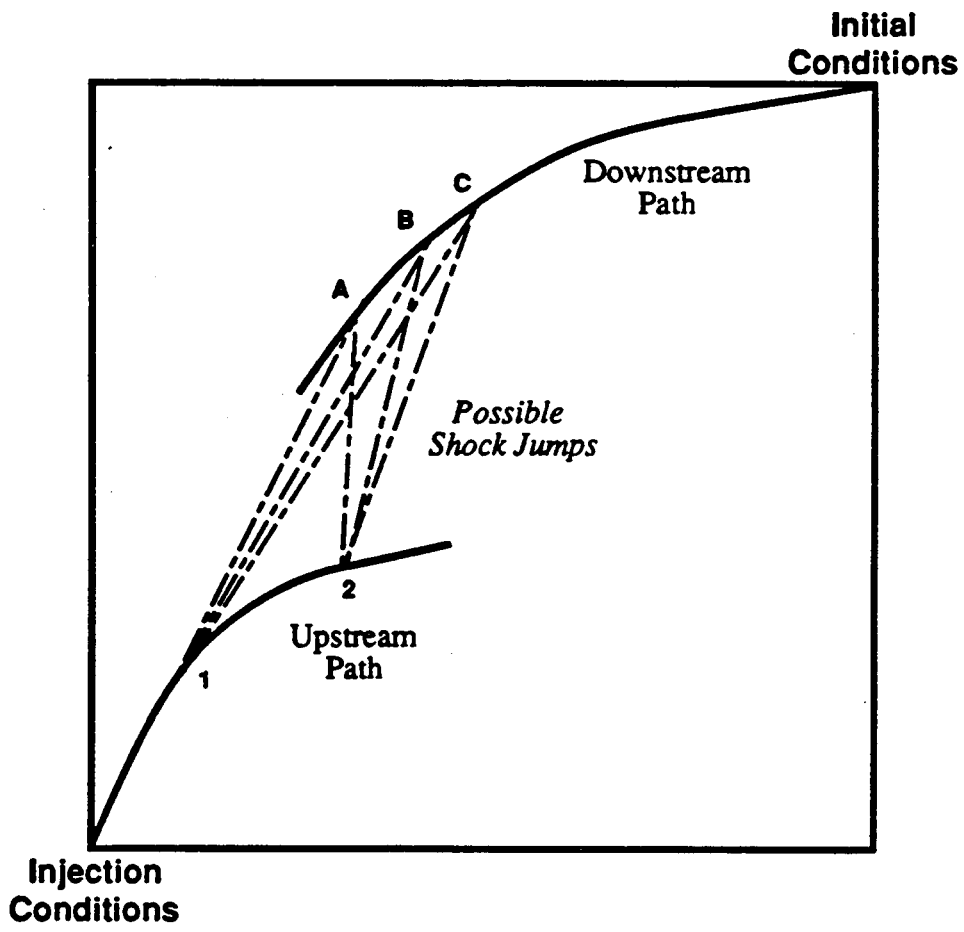


Figure 3.6: Hypothetical shock locations for a three component system.

4. EXAMPLE SOLUTIONS

The solution procedures discussed in Chapter 3 are applied to specific displacement problems. Three different classes of problems are covered in this chapter. In general, the problems are classified by the number of components and the total number of phases. The greater these numbers, the more complex the problem. The progression of problems begins with a single component, two-phase system with temperature variation. This problem is simple in concept, but reveals very interesting results concerning the behavior of these systems.

The second problem adds an immiscible component to the single component problem. This addition adds a new flowing phase to the single component problem. The second phase can lead to the formation of temperature profiles that are not found in the single component case. The new phase also changes the nature of the flow in the isothermal region from that of two-phase to three-phase flow.

The third and final problem extends the two-phase problem by adding the effect of phase behavior. The steam-oil-water system in the second problem is extended by adding a third component that is partially miscible in both the aqueous and oleic phases. The temperature changes the phase behavior by moving the water component from a less mobile liquid phase at low temperatures to the highly mobile vapor phase at high temperatures. The solubility of the third component, represented by CO_2 , in the oleic phase is also affected by the temperature variations.

4.1 SINGLE COMPONENT WITH TEMPERATURE VARIATION

4.1.1 Problem Formulation

The injection of steam into liquid water represents a simple type of problem that can be studied using the method of characteristics. By eliminating the compositional variations, the behavior of the temperature waves, especially in the single-phase region can be observed.

The method of characteristics maps from the space of independent variables, x and t , into a space that is representative of the quantities that can be measured. In this problem the hodograph variables are vapor saturation, temperature and local flow velocity.

These three variables are not independent. The Gibbs phase rule relates the degrees of freedom to the number of components and the number of coexisting phases. When a single component exists in two phases the phase rule indicates that there is only one degree of freedom. Fixing the pressure also sets the temperature at the saturation temperature corresponding to that pressure. This restriction changes the nature of the problem by forbidding the solution from most of the hodograph space.

Figure 4.1 illustrates where the solution can exist in hodograph space. The allowable solution consists of three straight lines. Above the saturation temperature, the liquid saturation is set at zero and the temperature varies from the injection temperature down to the saturation temperature. The horizontal line represents the two-phase region. When a single component exists in two-phase equilibrium at a constant pressure, the temperature is fixed at the saturation temperature. Finally in the liquid region, the saturation is set at zero and the temperature varies down from the saturation value to the initial value.

Note that flow velocity, which is the third dimension of the hodograph space, is not shown. This is because the flow velocity is not physically related to the temperature and saturation variables. This changes the picture only slightly, changing the three lines into a three dimensional curve in full hodograph space.

The mathematical model for this situation consists of one mass balance and the enthalpy balance. The solution is divided into three distinct regions represented by the three straight lines in Figure 4.1.

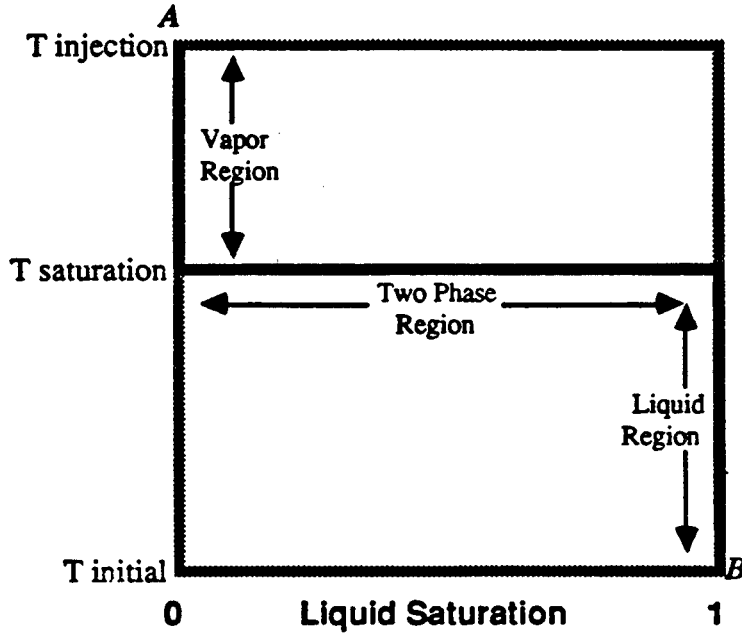


Figure 4.1: Solution line in hodograph space for steam injected into liquid water at constant pressure.

The two-phase region lies between the single-phase regions providing a transition from steam to liquid water. This means that as the solution traverses the hodograph space from point A to B, the eigenvalues must increase.

Single-Phase Regions

In the single-phase region saturations are fixed, leaving the temperature and the flow velocity as the hodograph variables. The eigenvalue problem for this set of equations is shown below.

$$\begin{bmatrix} \frac{\partial F}{\partial T} & \frac{\partial F}{\partial u} \\ \frac{\partial \Theta}{\partial T} & \frac{\partial \Theta}{\partial u} \end{bmatrix} \begin{bmatrix} \frac{dT}{d\eta} \\ \frac{du}{d\eta} \end{bmatrix} - \lambda \begin{bmatrix} \frac{\partial G}{\partial T} & 0 \\ \frac{\partial T}{\partial T} & 0 \end{bmatrix} \begin{bmatrix} \frac{dT}{d\eta} \\ \frac{du}{d\eta} \end{bmatrix} \quad (4.1)$$

Since the matrix is two by two, the solution for the two eigenvalues is a quadratic equation. As in the general case (Eq. 2.26) one of the eigenvalues is infinite and the finite value is given by,

$$\lambda' = \frac{\frac{\partial \Theta}{\partial T} \frac{\partial F}{\partial u} - \frac{\partial \Theta}{\partial u} \frac{\partial F}{\partial T}}{\frac{\partial T}{\partial T} \frac{\partial F}{\partial v} - \frac{\partial \Theta}{\partial u} \frac{\partial G}{\partial T}} \quad (4.2)$$

The associated eigenvector is found by setting one of the components to a predefined value and solving for the other component. Either the mass or enthalpy equation can be used to find the value of this component. Fixing the value of $(\partial T / \partial \eta)$, gives for the velocity change,

$$\frac{\partial u}{\partial \eta} = \frac{\frac{\partial T}{\partial \eta} \left(\lambda \frac{\partial G}{\partial T} - \frac{\partial F}{\partial T} \right)}{(\partial F / \partial u)} \quad (4.3)$$

In the single-phase region, the evaluation of the derivatives in the eigenvalue matrix is simplified because the saturation and fractional flow terms are either one or zero and drop out of the equations. These derivatives are,

$$\begin{aligned} \frac{\partial G}{\partial T} &= \frac{\partial \rho}{\partial T} & \frac{\partial T}{\partial T} &= H \frac{\partial \rho}{\partial T} + \left(\frac{1-\phi}{\phi} \right) \rho_m C p_m \\ \frac{\partial F}{\partial T} &= \frac{1}{\phi} \left[u' \frac{\partial \rho}{\partial T} + \rho \frac{\partial u'}{\partial T} \right] & \frac{\partial \Theta}{\partial T} &= \frac{1}{\phi} \left[u' \rho \frac{\partial H}{\partial T} + \rho H \frac{\partial u'}{\partial T} \right] \end{aligned}$$

and

$$\frac{\partial F}{\partial u} = \frac{F}{u'} \quad \frac{\partial \Theta}{\partial u} = \frac{\Theta}{u'} \quad (4.4)$$

Substituting these values into Eq. 4.2, and remembering that in the single-phase region $Q = F \times H$ gives for the eigenvalue,

$$\lambda' = \frac{u'}{\phi} \left[\frac{\rho \frac{\partial H}{\partial T}}{\rho \frac{\partial H}{\partial T} + \left(\frac{1-\phi}{\phi} \right) \rho_m C p_m} \right] \quad (4.5)$$

Eq. 4.5 represents what can be thought of as a "fractional" heat capacity. Every unit of enthalpy that exists at a point in the single-phase region partitions into the fluid phase or the matrix. Eq. 4.5 represents the fraction of the enthalpy that the fluid phase takes over the total enthalpy available.

Enthalpy carried along with the fluids must heat the matrix to its temperature before the wave can proceed beyond its location. The ability of the matrix to store enthalpy acts to slow the temperature wave. As the matrix heat capacity decreases, or the porosity increases, a larger fraction of the enthalpy accumulation remains in the mobile phase and the velocity of the temperature wave increases, approaching the flow velocity at a matrix heat capacity of zero.

The temperature profile jumps from the injection temperature in the single-phase region to the saturation temperature in the two-phase region. This initial discontinuity is prevented from spreading in the single-phase region by the nature of the single phase flow. The enthalpy can only be carried downstream by the flowing fluid. The matrix thermal conductivity is neglected and the matrix is stationary. Therefore, only one velocity, the velocity of the flowing fluid, carries the enthalpy downstream. The lack of a second flowing phase creates the temperature shock in the single-phase region.

Two-Phase Region

Temperature is constant in the two-phase region, so a hodograph variable other than temperature is needed in this region. The logical choice is one of the phase saturations; in this case the vapor phase saturation is chosen.

The eigenvalue problem is similar to Eq. 4.1, except that saturation replaces temperature as the hodograph variable. Derivatives with respect to temperature become derivatives taken with respect to vapor saturation.

$$\begin{bmatrix} \frac{\partial F}{\partial S_v} & \frac{\partial F}{\partial u} \\ \frac{\partial \Theta}{\partial S_v} & \frac{\partial \Theta}{\partial u} \end{bmatrix} \begin{bmatrix} \frac{dS_v}{d\eta} \\ \frac{du}{d\eta} \end{bmatrix} - \lambda \begin{bmatrix} \frac{\partial G}{\partial S_v} & 0 \\ \frac{\partial \Gamma}{\partial S_v} & 0 \end{bmatrix} \begin{bmatrix} \frac{dS_v}{d\eta} \\ \frac{du}{d\eta} \end{bmatrix} \quad (4.6)$$

The eigenvalue and eigenvector are calculated in the same manner as in the single-phase regions

$$\lambda^{II} = \frac{\frac{\partial \Theta}{\partial S_v} \frac{\partial F}{\partial u} - \frac{\partial \Theta}{\partial u} \frac{\partial F}{\partial S_v}}{\frac{\partial \Gamma}{\partial S_v} \frac{\partial F}{\partial u} - \frac{\partial \Theta}{\partial v} \frac{\partial G}{\partial S_v}} \quad (4.7)$$

and

$$\frac{\partial u}{\partial \eta} = \frac{\frac{\partial S_v}{\partial \eta} \left(\lambda \frac{\partial G}{\partial \Gamma} - \frac{\partial F}{\partial \Gamma} \right)}{\frac{\partial F}{\partial u}} \quad (4.8)$$

Considerable simplification of the expression for the two-phase velocity is possible because the temperature and fluid properties in the two-phase region are constant. The only changes are the phase saturations and the fractional flows. Using the definitions in Eqs. 2.3-2.6 when the number of phases is two, $n_c = 2$, gives,

$$\frac{\partial G}{\partial S_v} = \rho_v - \rho_l \quad \frac{\partial \Gamma}{\partial S_v} = H_v \rho_v - H_l \rho_l \quad (4.9)$$

$$\frac{\partial F}{\partial S_v} = \frac{u^{II}}{\phi} (\rho_v - \rho_l) \frac{\partial f_v}{\partial S_v} \quad \frac{\partial \Theta}{\partial S_v} = \frac{u^{II}}{\phi} (\rho_v H_v - \rho_l H_l) \frac{\partial f_v}{\partial S_v} \quad (4.10)$$

and

$$\frac{\partial F}{\partial v} = \frac{F}{u^{II}} \quad \frac{\partial \Theta}{\partial v} = \frac{\Theta}{u^{II}} \quad (4.11)$$

Substituting these expressions into Eq. 4.7 gives a very simple expression for λ^{II}

$$\lambda^{II} = \frac{\frac{u^{II}}{\phi} \left[\frac{F}{u^{II}} (\rho_v H_v - \rho_l H_l) - \frac{\Theta}{u^{II}} (\rho_v - \rho_l) \right] \frac{\partial f_v}{\partial S_v}}{\left[\frac{F}{u^{II}} (\rho_v H_v - \rho_l H_l) - \frac{\Theta}{u^{II}} (\rho_v - \rho_l) \right]} = \frac{u^{II}}{\phi} \left(\frac{\partial f_v}{\partial S_v} \right) \quad (4.12)$$

The saturation velocity in this case is the same as the Buckley-Leverett velocity calculated in the two component, immiscible case. The derivative of the fractional flow curve gives the wave velocity in the two-phase region. This analysis makes sense. In the two-phase region, because the system is assumed to be at constant pressure, then it must also be at constant temperature. The steam, water, and matrix coexist with no energy or mass transfer between the phases. The displacement behaves as an isothermal, immiscible displacement.

The velocity component of the eigenvector is calculated using the same equation as in the single-phase case. Writing the analog to Eq. 4.3 in terms of the saturation derivatives gives

$$\frac{\partial u}{\partial \eta} = \frac{\partial S_v}{\partial \eta} \lambda \frac{\partial G}{\partial S_v} - \frac{\partial F}{\partial S_v} \quad (4.13)$$

Because the densities of the phases remain constant in this region, the change in overall velocity must be zero. This is similar to marching along a tie-line in the immiscible case. This is made apparent by evaluating the derivatives of Eq. 4.13 in the two-phase region. Substitution of the two-phase derivatives into Eq. 4.13 gives

$$\frac{\partial u}{\partial \eta} = \frac{\partial S_v \frac{\partial f_v}{\partial S_v} (\rho_v - \rho_l) - \frac{\partial f_v}{\partial S_v} (\rho_v - \rho_l)}{\frac{\partial F}{\partial u}} = 0 \quad (4.14)$$

The phase rule confines the two-phase region to be at a constant temperature. This also requires the phase densities to be constant. The flow velocity responds to variations in phase density, so in the two-phase region the flow velocity is constant.

Connecting the Single and Two-Phase Regions

The three regions must be physically connected through a set of shocks. These jumps must occur when the coefficients of the eigenvalue matrix are discontinuous (Jeffrey 1976). Changes in densities and fractional flows at a phase boundaries are the sources of these transition shocks. The problem is to find a pair of shocks that carry the solution into and out of the two-phase region.

The shock solution we seek is described in §3.2 as an intermediate discontinuity. The shock velocity matches the wave velocity on only one side of the jump. The correct solution is an intermediate discontinuity where the shock velocity matches the wave velocity in the two-phase region. Monroe calls this type of shock a "tangent" shock. Mathematically, the equations are,

$$\Lambda = \frac{1}{\phi} \frac{u'' F'' - u' F'}{G'' - G'} = \lambda'' = \frac{u''}{\phi} \left(\frac{\partial f_v}{\partial S_v} \right) \quad (4.15)$$

The reason that the velocities must match on the two-phase side of the shock is that in the single-phase region no spreading of the temperature profile can occur. In order to match the shock and wave velocities at the discontinuity, the shock must be the limit of a continuous variation. In the single-phase region, there are no fractional flow effects to partition the enthalpy into a more or less mobile phase. The assumption of local temperature equilibrium requires that the matrix and the fluids be at the same temperature. Since the matrix is immobile, the temperature of the fluid must equal the matrix temperature before it can move downstream. Therefore, the upstream side of the trailing shock must be at the injection temperature and the downstream side of the leading shock must be at the initial temperature.

The solution procedure is iterative. The unknowns for this calculation are the conditions on the two-phase side of the shock. The unknowns are the saturation and flow velocity u^{II} . The trailing shock conditions are calculated first. A diagram of the known conditions in the system is given in Figure 4.2.

The first step is to guess a saturation value on the upstream side of the shock. The primary quantities, G , F , Γ and Θ are calculated on both sides of the estimated shock. The two-phase flow velocity, u^{II} , can then be calculated by equating the Rankine-Hugoniot conditions for the mass and the enthalpy and solving for u^{II} . The jump balance is given by,

$$\frac{u^{II}F^{II} - u^IF^I}{G^{II} - G^I} = \frac{u^{II}\Theta^{II} - u^I\Theta^I}{\Gamma^{II} - \Gamma^I} \quad (4.16)$$

Trailing Shock Conditions

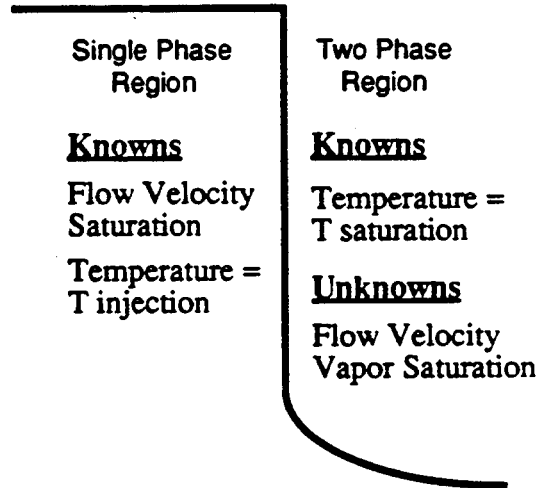


Figure 4.2: Trailing shock conditions for steam-water problem.

Solving for the velocity ratio yields,

$$\frac{u^{II}}{u^I} = \frac{F^I(\Gamma^{II} - \Gamma^I) - \Theta^I(G^{II} - G^I)}{F^{II}F^I(\Gamma^{II} - \Gamma^I) - \Theta^{II}(G^{II} - G^I)} \quad (4.17)$$

Once the two-phase flow velocity is known, the shock velocity can be calculated using the Rankine-Hugoniot conditions for either the mass or enthalpy across the shock. The equation for the mass balance is given by,

$$\Lambda_w = \left(\frac{1}{\phi}\right) \frac{u^{II}F^{II} - u^IF^I}{G^{II} - G^I} \quad (4.18)$$

and the enthalpy balance yields,

$$\Lambda_H = \left(\frac{1}{\phi} \right) \frac{u''\Theta'' - u'\Theta'}{\Gamma'' - \Gamma'} \quad (4.19)$$

either of these equations can be used to calculate the shock velocity. These two balance equations are coupled by the two-phase flow velocity calculation represented by Eq. 4.17.

The last velocity needed is the wave velocity in the two-phase region. Eq. 4.7 is used to calculate the wave velocity. The correct solution is where the shock and wave velocities are equal. A plot of the shock and wave velocities against saturations shows how sensitive the solution is to changes in saturation.

From Figure 4.3, the saturation guess can be adjusted depending on the difference between the two velocity values. The saturation is regulated down if the shock velocity exceeds the wave velocity and is increased if the opposite is true.

The calculation for the leading shock is similar to the trailing shock with one exception. The flow velocity on the *single-phase* side of the shock is the unknown, along with the saturation on the two-phase side. The flow velocity on the two-phase side of the shock is equal to the flow velocity calculated at the trailing shock since there is no change in the two-phase region.

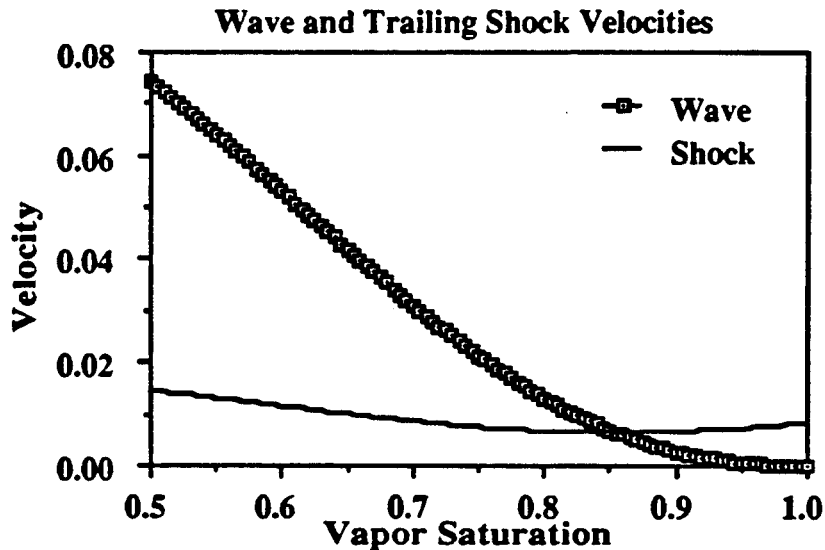


Figure 4.3: Wave and shock velocities for trailing shock in steam-water displacement

After the shock conditions are found, the saturation profile in the two-phase region is constructed by relating the wave velocity calculated by Eq. 4.7 to the saturation value. The wave velocity tells how far a given saturation has moved in after a given number of pore volumes have been injected. The wave velocity is multiplied by the injection amount to give the position of the saturations between the two shock values.

An EXCEL spreadsheet was developed to automate the calculation for a given set of injection and initial conditions. Details of the spreadsheet contents along with the calculations for the examples are found in Appendix D.

Three parameters were studied for their effect on the saturation profile and location of the trailing and leading shocks. The three variables are: the injection temperature of the steam, the initial temperature of the water, and the heat capacity of the surrounding matrix.

Table 4.1 shows the conditions that are common for all three examples. For all cases the saturation temperature, fluid densities and enthalpies were found by curve fitting a fifth order polynomial in temperature to the values given in Reynolds (1979) for water at 2.0 MPa [290.16 psia]. Viscosities at the saturation pressure were estimated from equations given by Reid (1977). The injection velocity was set at one pore volume of steam per dimensionless time unit.

Pressure		2.0 MPa
Injection Velocity		1.0 (m/day)
Saturation Temperature	T_{sat}	485.57 K
Irreducible Water Saturation	S_{wi}	0.0
Steam Phase Exponent	n_g	1.0
Water Phase Exponent	n_w	3.0
Fluid Properties at Saturation Temperature		
Steam Viscosity	μ_g	0.0217 (mPa·sec)
Water Viscosity	μ_w	0.1303 (mPa·sec)
Steam Density	ρ_g	9.970241 (kg/m ³)
Water Density	ρ_w	850.4723 (kg/m ³)
Steam Enthalpy	H_g	2808.52 (kJ/kg)
Water Enthalpy	H_w	901.41 (kJ/kg)
Matrix Properties		
Density	ρ_m	2650.0 (kg/m ³)
Heat Capacity	C_{pm}	0.047 (kJ/kg — K)
Porosity	ϕ	0.100

Table 4.1: Base conditions for the generation of steam-water profiles at 2.0 MPa

The first example looks at the effects of changing the temperature of the injected steam. Figure 4.4 shows five saturation profiles after the injection of 1.0 pore volume of steam.

The major difference between the five profiles is the position of the leading and trailing shocks as the injection temperature increases. At the leading shock, the shock height remains constant, while the velocity increases with increasing injection temperature. The conditions ahead of the leading shock are constant for all the profiles. This causes the saturation change across the discontinuity to be the same for all the cases. The reason that the position of the shock changes is the reduced flow velocity in the two-phase region at higher temperatures. Physically, the lower velocity corresponds to the decreased heat content at higher temperatures.

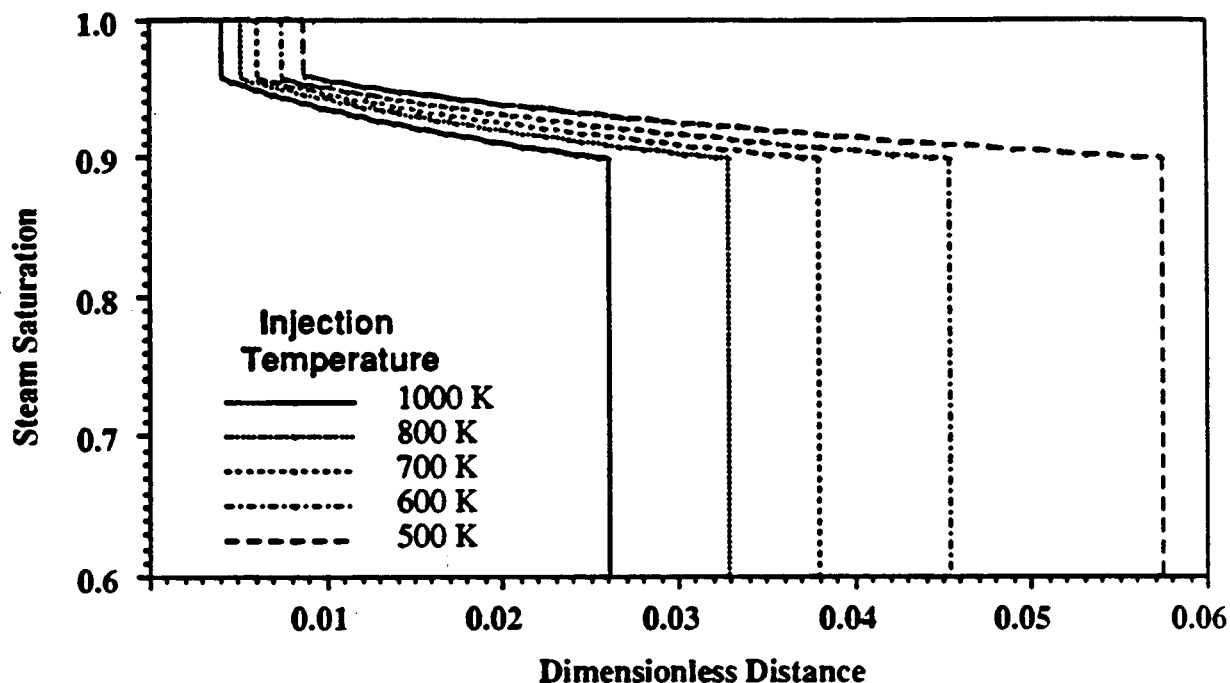


Figure 4.4: Saturation profile after 1.0 pore volumes of steam injection into water at injection temperatures from 500 K — 1000 K.

The behavior of the trailing shock is explained by looking at the heat balance across the trailing shock. As the injection temperature is increased, the enthalpy difference across the shock increases. To compensate for the increased heat crossing the discontinuity at the higher injection temperature, the shock velocity decreases. This result is seen in Figure 4.4.

The second parameter studied was the initial temperature. It causes much smaller and more predictable changes in the saturation profiles than the initial temperature. Figure 4.5 illustrates the change in location of the leading shock as the initial temperature changes from 300 K to 450 K. The initial temperature only changes the location and height of the leading shock. The hyperbolic nature of the equations means that the conditions downstream do not affect the upstream values. The trailing shock would behave the same regardless of the temperature or saturations downstream of the two-phase region.

The reason for the faster shocks at higher initial temperatures is simply a heating effect. The fluid from the two-phase region must heat the matrix and surroundings from the initial temperature to the saturation temperature before the leading shock can propagate downstream. If the initial temperature is close to the saturation temperature, little enthalpy is needed and the shock has a high velocity and a low height. When the initial temperature is far below the saturation temperature, much more enthalpy is needed and the shock travels slowly. This also requires a larger transfer of enthalpy via condensation, hence a greater shock height.

The third parameter examined was the matrix heat capacity. Figure 4.6 shows how the saturation profile is modified by the matrix heat capacity. As the heat capacity of the matrix is decreased from a value of 25.0 (kJ/kg-K) to zero, the positions of the leading and trailing shocks are affected while the saturation profile remains unchanged. The explanation for the insensitivity of the two-phase region is clear. Recall that the two-phase region is at constant temperature, therefore no heat transfer can take place

from the fluids to the matrix or vice versa. This takes the thermal properties of the matrix out of the equations representing the two-phase region.

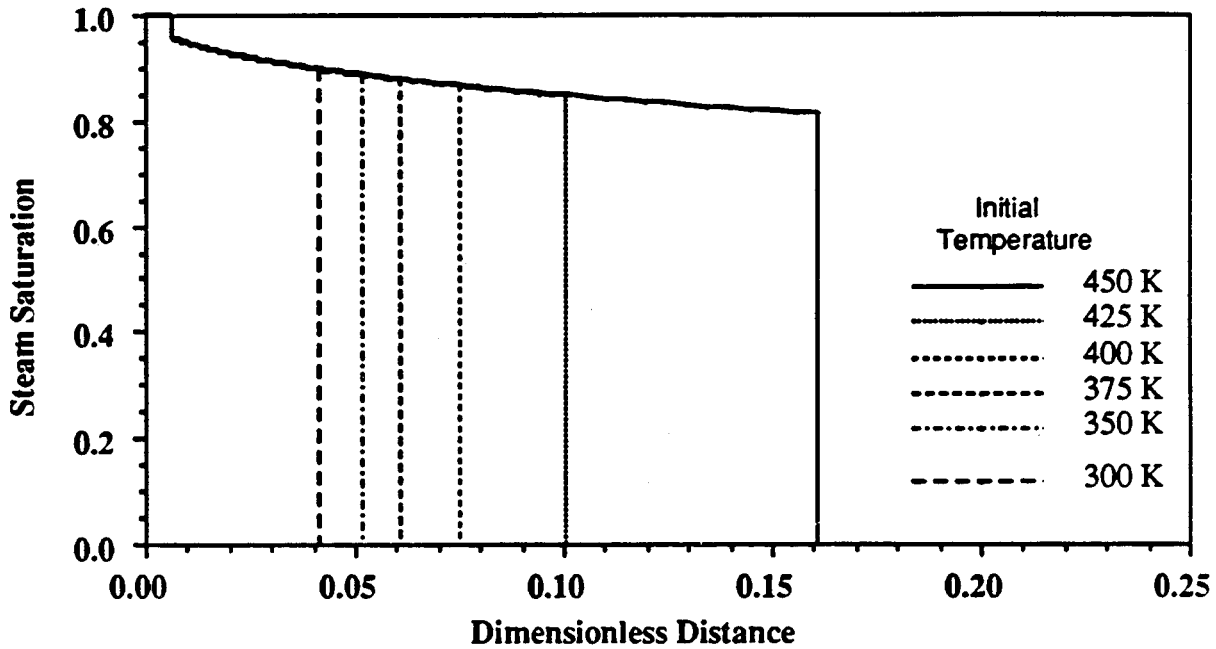


Figure 4.5: Saturation profile after 1.0 pore volumes steam injection into water at initial temperatures from 300 K-450 K.

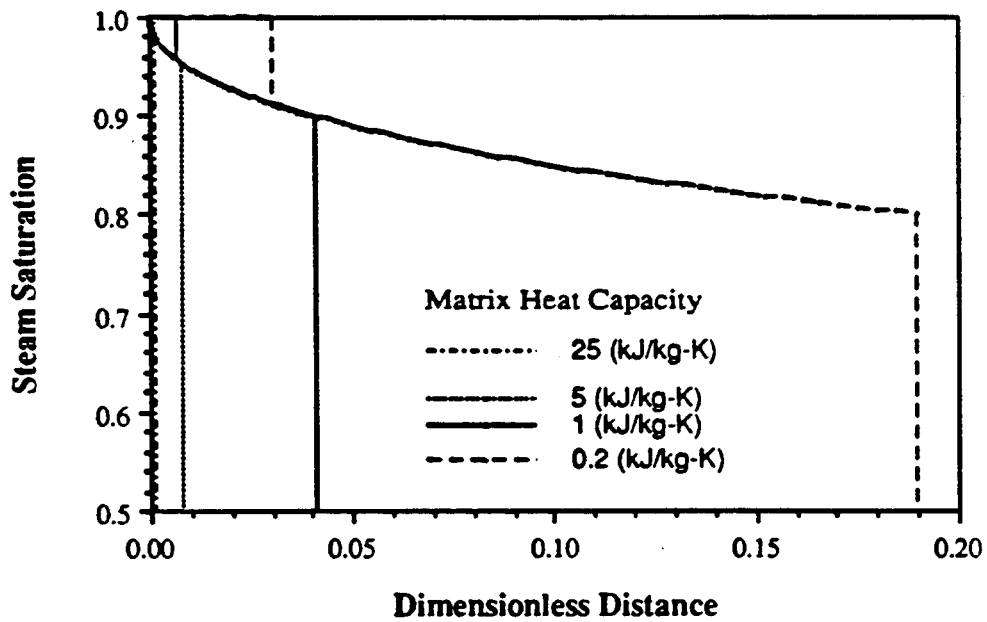


Figure 4.6: Saturation profile after 1.0 pore volumes steam injection into water where the matrix heat capacity varies from 25.0 (kJ/kg-K) to 0.2 (kJ/kg-K).

The velocities of both the trailing and leading shocks increase as the matrix heat capacity decreases. The explanation is essentially identical to that for the initial temperature variation. Lower heat capacity means that less enthalpy is stored per degree of temperature. Less enthalpy is therefore required to raise the matrix from the initial temperature to the saturation temperature and subsequently from the saturation temperature to the injection temperature.

Summary

The displacements in the single component case are characterized by the following features:

1. The displacement has a central, two-phase, isothermal region. This region is flanked by single-phase regions containing only vapor towards the injection end and liquid at the leading end.
2. The single-phase regions are regions of constant state. The temperature of the trailing region is at the injection temperature and the leading region is at the initial temperature. This is due to the single-phase flow in these regions.
3. The behavior of the two-phase region is identical to a two component, immiscible displacement. Saturation velocity in this region is given by the derivative of the fractional flow curve and the shocks that carry the system into and out of the two-phase region are intermediate discontinuities or tangent shocks.
4. The conditions downstream have no effect on the features of the saturation profile upstream. This means that the initial temperature only effects the leading shock, while the injection temperature can modify the entire saturation profile.

The nature of the single-phase regions can be altered by the addition of a second, immiscible component. These two phases can flow at different velocities creating temperature profiles in the leading and trailing regions. The solution to this problem is described in the next section.

4.2 TWO COMPONENT — THREE-PHASE SYSTEMS

4.2.1 Problem Formulation

The second example system examined in this dissertation is an extension of the steam-water problem described in the previous section. A second component, referred to as the oil component, is added to the system. The oil is totally immiscible with both aqueous phases. This has the effect of adding a second phase to the single-phase region and a third phase to the two-phase region of the steam-water problem described in the previous section. Since the oil component forms its own phase, separate from the water component, the presence of the oil has no effect on the phase behavior of the water. The only change the oil makes is on the flow properties of the fluids.

The addition of the oil component to the steam-water system results in two significant changes. The first of these differences concerns the two-phase oil-water and steam-oil regions. The addition of a second flowing phase can create a temperature profile in these regions. In the single phase case, there was no separation of the enthalpy due to the single phase flow.

Second, a three-phase region replaces the isothermal two-phase region in the previous problem. The region is still at constant temperature because there is no mass transfer in this region, but the effect of the three phase relative permeability problem is added. The solutions in this region are the three phase analog to the Buckley-Leverett problem. Figure 4.7 presents a hypothetical saturation profile for this problem. Each region is treated separately and is connected through a series of shocks to form the complete solution.

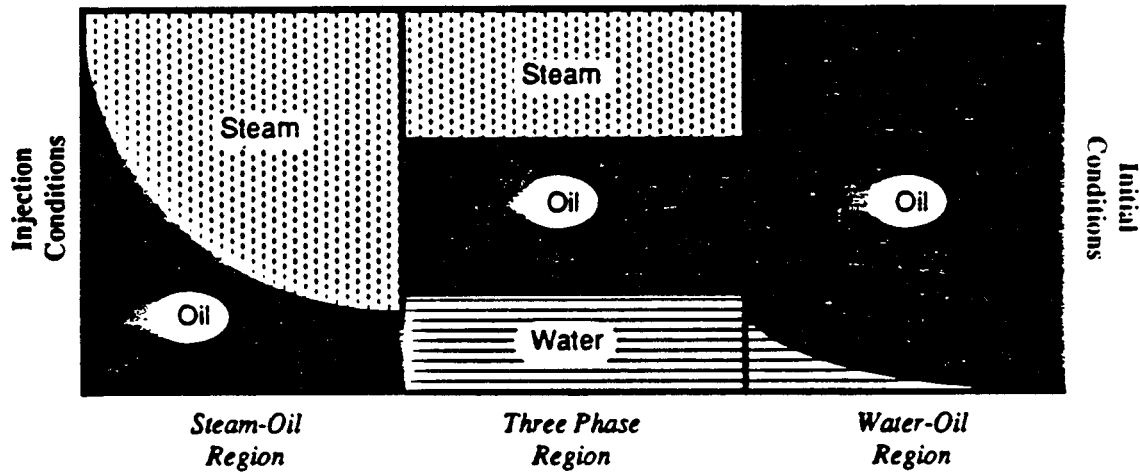


Figure 4.7: Hypothetical solution to the two-component, three-phase problem showing the different flow regions.

Adding a second component changes the formulation of the eigenvalue problem from a simple 2x2 to a 3x3 system. The formulations for the two-phase and three-phase regions still have different hodograph variables. In the two-phase regions the hodograph variables are the saturation of one of the phases, the temperature and the flow velocity. In the example problems the saturation of the water component was chosen as the hodograph variable. For the steam oil region Eq. 2.26 reduces to where the subscript w refers to the water component, subscript o represents the oleic component, and subscript v refers to the vapor phase. Since the matrix system is 3x3 the exercise of solving for the eigenvalues and eigenvectors analytically is more complex and will not be done for these systems.

$$\begin{bmatrix} \frac{\partial F_w}{\partial S_v} & \frac{\partial F_w}{\partial T} & \frac{\partial F_w}{\partial u} \\ \frac{\partial F_o}{\partial S_v} & \frac{\partial F_o}{\partial T} & \frac{\partial F_o}{\partial u} \\ \frac{\partial \Theta}{\partial S_v} & \frac{\partial \Theta}{\partial T} & \frac{\partial \Theta}{\partial u} \end{bmatrix} \begin{bmatrix} \frac{dS_v}{d\eta} \\ \frac{dT}{d\eta} \\ \frac{du}{d\eta} \end{bmatrix} - \lambda \begin{bmatrix} \frac{\partial G_w}{\partial S_v} & \frac{\partial G_w}{\partial T} & 0 \\ \frac{\partial G_o}{\partial S_v} & \frac{\partial G_o}{\partial T} & 0 \\ \frac{\partial \Gamma}{\partial S_v} & \frac{\partial \Gamma}{\partial T} & 0 \end{bmatrix} \begin{bmatrix} \frac{dS_v}{d\eta} \\ \frac{dT}{d\eta} \\ \frac{du}{d\eta} \end{bmatrix} = 0 \quad (4.20)$$

The matrix formulation in the liquid water-oil region is similar to the steam-oil system. The saturation of the vapor phase is replaced by the saturation of the liquid water phase and the following system results, where S_w represents the liquid water phase saturation.

$$\begin{bmatrix} \frac{\partial F_w}{\partial S_w} & \frac{\partial F_w}{\partial T} & \frac{\partial F_w}{\partial u} \\ \frac{\partial F_o}{\partial S_w} & \frac{\partial F_o}{\partial T} & \frac{\partial F_o}{\partial u} \\ \frac{\partial \Theta}{\partial S_w} & \frac{\partial \Theta}{\partial T} & \frac{\partial \Theta}{\partial u} \end{bmatrix} \begin{bmatrix} \frac{dS_w}{d\eta} \\ \frac{dT}{d\eta} \\ \frac{du}{d\eta} \end{bmatrix} - \lambda \begin{bmatrix} \frac{\partial G_w}{\partial S_w} & \frac{\partial G_w}{\partial T} & 0 \\ \frac{\partial G_o}{\partial S_w} & \frac{\partial G_o}{\partial T} & 0 \\ \frac{\partial \Gamma}{\partial S_w} & \frac{\partial \Gamma}{\partial T} & 0 \end{bmatrix} \begin{bmatrix} \frac{dS_w}{d\eta} \\ \frac{dT}{d\eta} \\ \frac{du}{d\eta} \end{bmatrix} = 0 \quad (4.21)$$

The eigenvalues and eigenvectors in these two regions behave in a similar manner. One of the eigenvectors has a zero component in the temperature direction, ($\partial T / \partial \eta = 0$). This result is expected; in order to move between any two composition points at the same temperature, an isothermal path must be provided. The magnitude of the eigenvalue along this path is the familiar Buckley-Leverett, ($\partial f / \partial S$) curve. Figure 4.8 demonstrates how the eigenvalues typically vary along a constant temperature path in the water-oil region.

The isothermal path resembles the Buckley-Leverett fractional flow derivative plot. It is large at intermediate saturations but trails off to zero at the saturation end points. The eigenvalue of the non-isothermal path does not show the large variations evident along the isothermal path. However at the points labelled E, the eigenvalues are equal and a continuous path switch may take place at this point according to Rule III as given in §3.1.

In addition the isothermal path also has a zero component for the change in the flow velocity. As in the case for the steam-water problem, this result is directly related to the fact that the phase densities are assumed to be functions of temperature only. Along the non-isothermal path all hodograph variables change.

In the three-phase region, the Gibbs phase rule still demands that the region be at constant temperature. The hodograph variables are chosen to be the steam saturation, the water saturation and the flow velocity. As in the steam-water problem, the flow velocity in this region turns out to be constant. The matrix formulation for this region is given by

$$\begin{bmatrix} \frac{\partial F_w}{\partial S_v} & \frac{\partial F_w}{\partial S_w} & \frac{\partial F_w}{\partial u} \\ \frac{\partial F_o}{\partial S_v} & \frac{\partial F_o}{\partial S_w} & \frac{\partial F_o}{\partial u} \\ \frac{\partial \Theta}{\partial S_v} & \frac{\partial \Theta}{\partial S_w} & \frac{\partial \Theta}{\partial u} \end{bmatrix} \begin{bmatrix} \frac{dS_v}{d\eta} \\ \frac{dS_w}{d\eta} \\ \frac{du}{d\eta} \end{bmatrix} - \lambda \begin{bmatrix} \frac{\partial G_w}{\partial S_v} & \frac{\partial G_w}{\partial S_w} & 0 \\ \frac{\partial G_o}{\partial S_v} & \frac{\partial G_o}{\partial S_w} & 0 \\ \frac{\partial \Gamma}{\partial S_v} & \frac{\partial \Gamma}{\partial S_w} & 0 \end{bmatrix} \begin{bmatrix} \frac{dS_v}{d\eta} \\ \frac{dS_w}{d\eta} \\ \frac{du}{d\eta} \end{bmatrix} = 0 \quad (4.22)$$

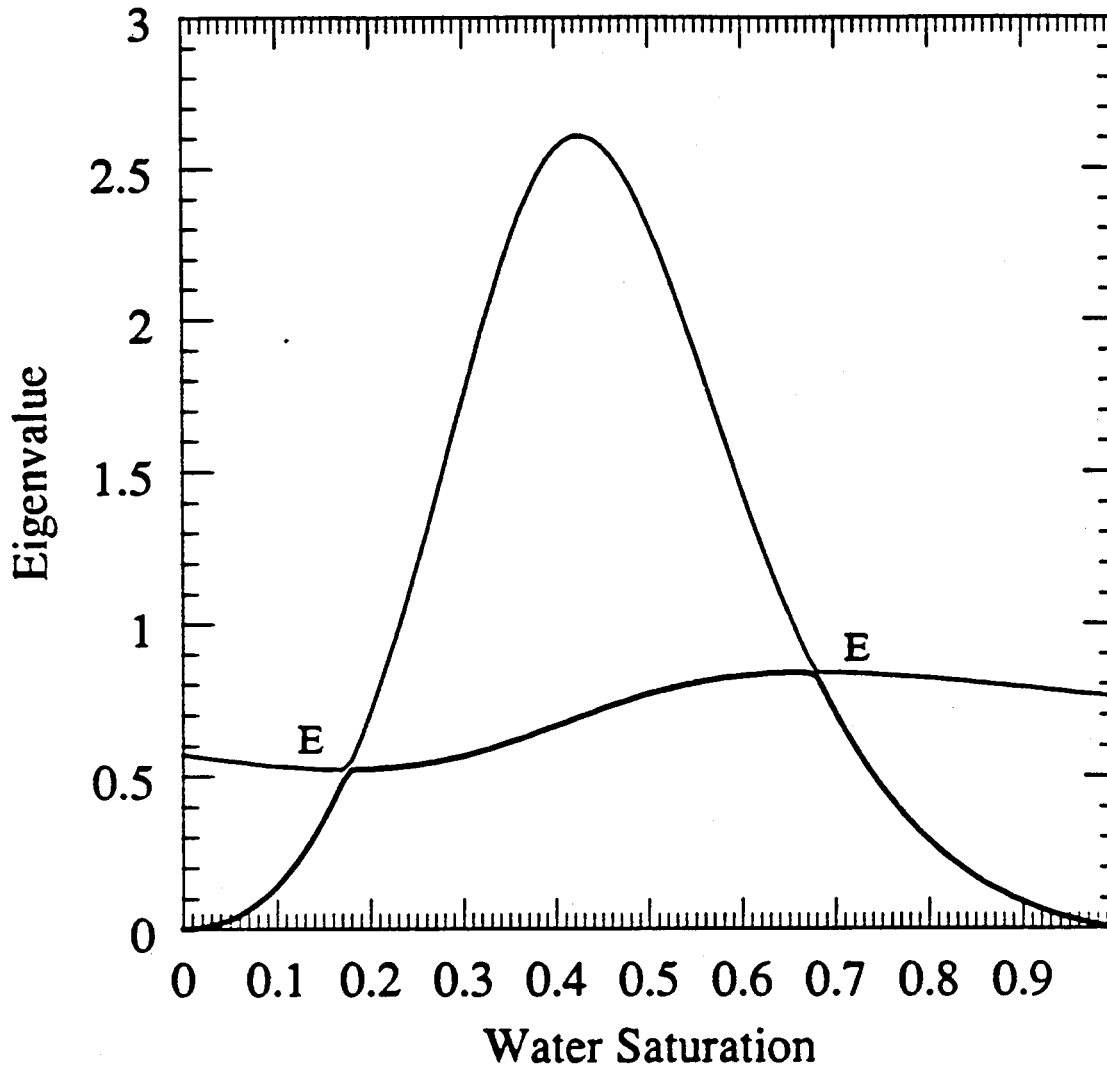


Figure 4.8: Plot of eigenvalues along a constant temperature path in the water-oil region.

This region requires that the three phase relative permeability relationships discussed in §2.3.1 be used to calculate the relative permeability of the oil phase. For most of the examples used in this section, the three phase relative permeability model of Stone (1970), given in Eq. 2.31, is used to calculate the relative permeability of the oil phase.

The three systems presented are joined to form the solution of the injection of steam into a reservoir filled with oil or oil and water at a lower temperature. The solution is traced from the injection conditions in the steam-oil region, through the three-phase region where steam, oil and water flow simultaneously and into the leading region where oil and water may be flowing.

4.2.2 Example Cases

The solution for the injection of steam into a reservoir initially filled with oil or oil and water at a lower temperature is presented in this section. The procedure for constructing a solution path from injection conditions to initial conditions is detailed. An example solution used as a base case is presented along with the discussion on the solution procedures.

Four basic wave patterns are seen in these displacement systems. The four cases and how they are obtained as variations of the base case are discussed following the base case presentation. The effect of the different displacement types on the saturation and temperature profiles is examined.

The four types of displacement may also be changed by selection of a different path through the injection conditions. Solutions with temperature variations in the steam-oil region, near the injection conditions, are presented and compared to displacements with no temperature profile in the steam-oil region.

Finally, the effect of oil viscosity on the displacement patterns is of concern to the displacement of heavy oils by steam injection. These effects are studied by changing the equation used to represent the oil viscosity. Two "heavy" oils are used, one which has a higher viscosity than the base case oil at all temperatures, and a second that is more viscous at reservoir temperatures, but also has a stronger dependence on temperature and so has a comparable viscosity at injection temperatures.

Base Case

The base case presented in this section outlines the procedures used to construct a solution from the given fluid properties, relative permeability model and boundary conditions. The equations used to calculate the fluid properties in this model are presented in Appendix A. The densities and viscosities of all the phases are assumed to be functions of temperature only. The oleic phase and the two aqueous phases do not interact by mass transfer. The conditions for the problem are identical to the steam-water problem presented in §4.1 in Table 4.1.

The relative permeability model used is Stone's Model II, given by Eqs. 2.27—2.31. The parameters used in these example solutions are listed in Table 4.2.

Gas Exponent	$\alpha_g = 1.00$
Water Exponent	$\alpha_w = 3.00$
Liquid-Gas Exponent	$\alpha_{lg} = 2.00$
Water-Oil Exponent	$\alpha_{ow} = 2.00$
End point Gas Permeability	$\sigma_g = 1.00$
End point relative permeability of the liquid phase in the liquid-gas system	$\sigma_{lg} = 1.00$
End point relative permeability of the oil phase in the oil-water system	$\sigma_{ow} = 1.00$

Table 4.2: Three phase relative permeability parameters for Stone's model II.

The construction of the solution begins at the injection conditions. The injection conditions for the base case is given as Point A in Table 4.3 and the composition path is shown in Figure 4.9. For the first leg of the solution the slow path is integrated from the injection conditions up to an arbitrary composition point, Point B. This choice is reasonable because far upstream the compositions must have

very small wave velocities. At Point B, an upstream intermediate discontinuity (tangent shock) carries the solution into the three-phase region. The choice of this composition is up to the designer of the solution; for a specific displacement, the choice will depend on the initial and injection conditions, and an iterative solution will be required.

Label	Composition Point				Flow Velocity	Wave Velocity	Type of Flow Region
	Saturations			T (K)			
	Steam	Oil	Water				
A	1.00000	0.00000	0.00000	650.00	1.00000	0.000000	INJ → SPW
B	0.92000	0.08000	0.00000	650.00	1.00000	0.010777	SPW → UID
C	0.41924	0.39087	0.18989	485.57	0.7058	0.010777	UID → ZCS
D	0.4924	0.39087	0.18989	485.57	0.7058	0.064505	ZCS → UID
E	0.00000	0.96566	0.03434	390.19	0.419	0.093985	UID → INI
F	0.00000	0.96566	0.03434	390.19	0.0419		INI

Table 4.3 Composition path for the injection of 100% steam at 650 K into 94.5% oil and 6.5% water at 390.19 K.

Abbreviation	Flow Region
INJ	Injection Conditions
INI	Initial Conditions
EEP	Equal Eigenvalue Point
ZCS	Zone of Constant State
SPW	Spreading Wave
SSW	Self-Sharpening Wave
UID	Upstream Intermediate Discontinuity
DID	Downstream Intermediate Discontinuity

Table 4.4: Abbreviations used to describe the different flow regions.

There is only one composition point in the three-phase region that satisfies material balances and also the condition that the shock is an upstream intermediate discontinuity. A discontinuity which satisfies the Rankine-Hugoniot conditions is completely described by fixing two of the three shock parameters, the upstream composition, the downstream composition, and the shock velocity (Jeffrey 1976). The constraint that the shock is an upstream intermediate discontinuity fixes both the upstream conditions, B, and the shock velocity, A. This means that the downstream conditions are uniquely determined.

The point in the three-phase region that is downstream of the intermediate discontinuity is given by Point C in Table 4.3 and Figure 4.9. The dashed line in Figure 4.9 represents the upstream intermediate discontinuity that takes the solution from Point B in the steam-oil region to C in the three-phase region. Point C is referred to as the "three phase landing" point and Point B is the "jumping point".

In the three-phase region the solution must switch from the slow path to the fast path. With the relative permeability model used in the base case, there are no points in the three-phase region that have equal eigenvalue points. These systems are called *strictly hyperbolic* systems. The only way to switch paths in strictly hyperbolic regions is with a path switch described by Rule IV of §3.1.

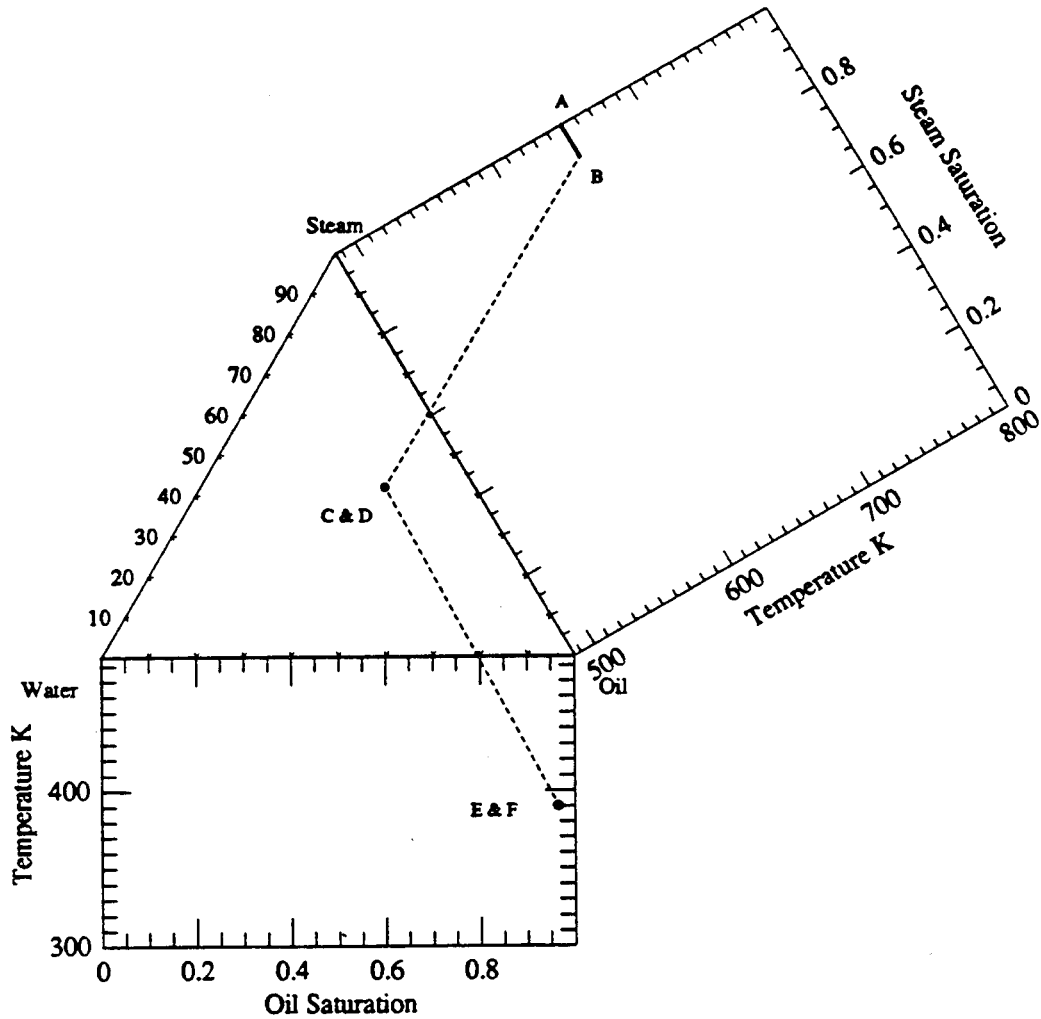


Figure 4.9: Composition path for the injection of 100% steam at 650 K into 94.5% oil and 6.5% water at 390.19 K.

Point C has two eigenvalues, both of which are larger than the shock velocity. An immediate jump to the large eigenvalue at C satisfies Rule IV. This jump moves the solution directly onto the fast path at composition C. The path switch creates a zone of constant state at Point C between the positions of the upstream intermediate discontinuity and the composition point on the fast path, Point D in Table 4.3.

The final part of the solution is to jump from Point D directly to the initial conditions. This shock is also an upstream intermediate discontinuity. The arguments used to verify that the three phase landing Point, C, is unique also apply to downstream side of this jump. The initial conditions are represented by Point E. Using the Rankine-Hugoniot conditions and the value of the large eigenvalue at Point D, the initial conditions are located somewhere in the steam-water region. Table 4.3 and Figure 4.9 show the finished solution paths for the base problem.

The need to jump directly to the initial conditions is made evident by looking at the eigenvalues in the water-oil region. At the boundary between the three-phase region and the water-oil region one of the eigenvalues is continuous¹ across the phase boundary while the other eigenvalue has a discontinuity at the phase transition. Figure 4.10 gives an example of this transition at the saturation temperature.

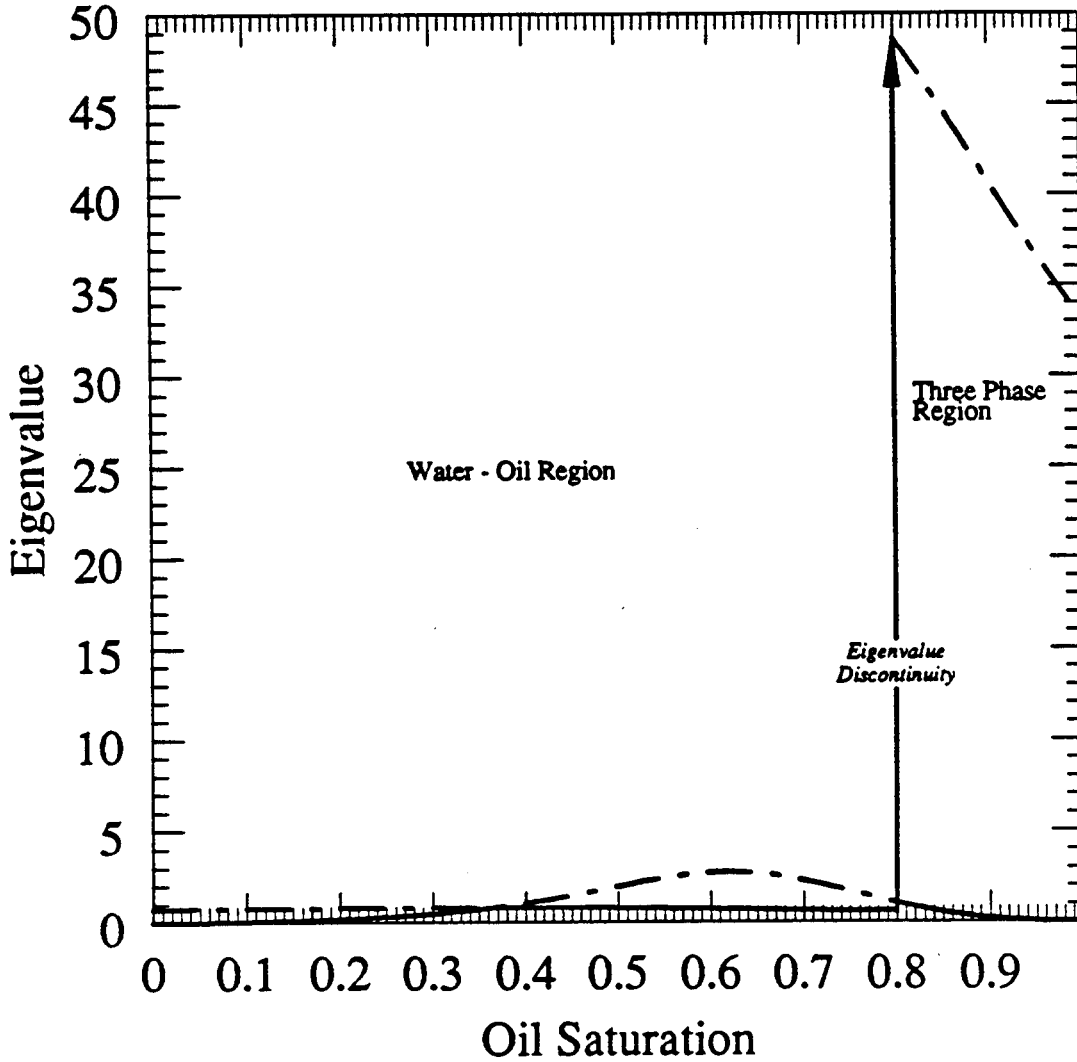


Figure 4.10: Eigenvalues crossing the three phase to water-oil boundary at 80% oil saturation.

¹This continuation of the eigenvalue across the phase boundary is a consequence of having smooth three-phase relative permeability functions that reduce to the appropriate two phase relationships as the saturation of one of the phases goes to zero. If this is not true, then both the eigenvalues would be discontinuous across the phase boundary.

As the solution moves downstream along the fast path in the three-phase region, the velocity is discontinuous at the phase boundary. This jump in the wave velocity requires that the solution have a discontinuity as it moves across this boundary (Jeffrey 1976).

Having shown that a shock is required to go from the three-phase to the water-oil region, it remains to establish the exact landing point in the water-oil region. For the base oil, the landing points in the water-oil region have slower velocities than their corresponding jumping points in the three-phase region. This is primarily due to the low local flow velocity once the steam has condensed into the liquid phase. There can be no solution path in the water-oil region that is faster than the three phase jumping point. This, coupled with the fact that the water-oil region is downstream of the three-phase region leads to the conclusion that there is only one point downstream of the three-phase region. This point must be the initial conditions.

The saturation, temperature and flow velocity profiles after 1.0 pore volumes of steam have been injected are given in Figures 4.11—4.13. Four features about the solution are important to note.

1. When a specific set of initial condition is required, a trial and error procedure similar to that of Monroe is needed. The initial condition may be adjusted by changing the location of the initial jumping off composition, Point B, or by introducing spreading waves into the three-phase region. The introduction of the spreading waves changes the upstream composition point (Point D) of the leading shock, thereby changing the initial conditions that can be reached by the solution path.
2. The velocity profile mimics the temperature profile exactly. The flow velocity must follow the temperature profile because changes in phase densities, which are functions of temperature only, directly determine the flow velocity.
3. There are no regions where the temperature varies smoothly. All temperature changes are in the forms of shocks that carry the solution from the injection temperature to the saturation temperature and then finally, to the initial temperature.
4. In the three-phase region, the saturations of all three phases remain constant. This zone of constant state over the entire three-phase region is a feature of the specific displacement type used to construct the solution. This represents one limit of the "wave patterns"² that can exist in the three-phase region. Three other wave patterns are made possible by adding a spreading wave to the region ahead, behind, or on both sides of the zone of constant state. These variations are discussed in the next section.

The example presented has no compositional variation in the three-phase region. This represents only one limiting case of the types of displacement profiles that are seen in the steam-oil-water displacements. The next section describes the different wave patterns and explains how they are constructed. An example solution is presented for the three other wave patterns and a discussion of how each type of pattern effects the resulting initial conditions is also included.

²The term "wave pattern" is used to describe a progression of wave regimes from the injection end to the initial conditions. For example in the previous example the wave pattern was a spreading wave in the steam-oil region followed by an upstream intermediate discontinuity into the three-phase region. This was followed by a zone of constant state and another upstream intermediate discontinuity to the initial conditions.

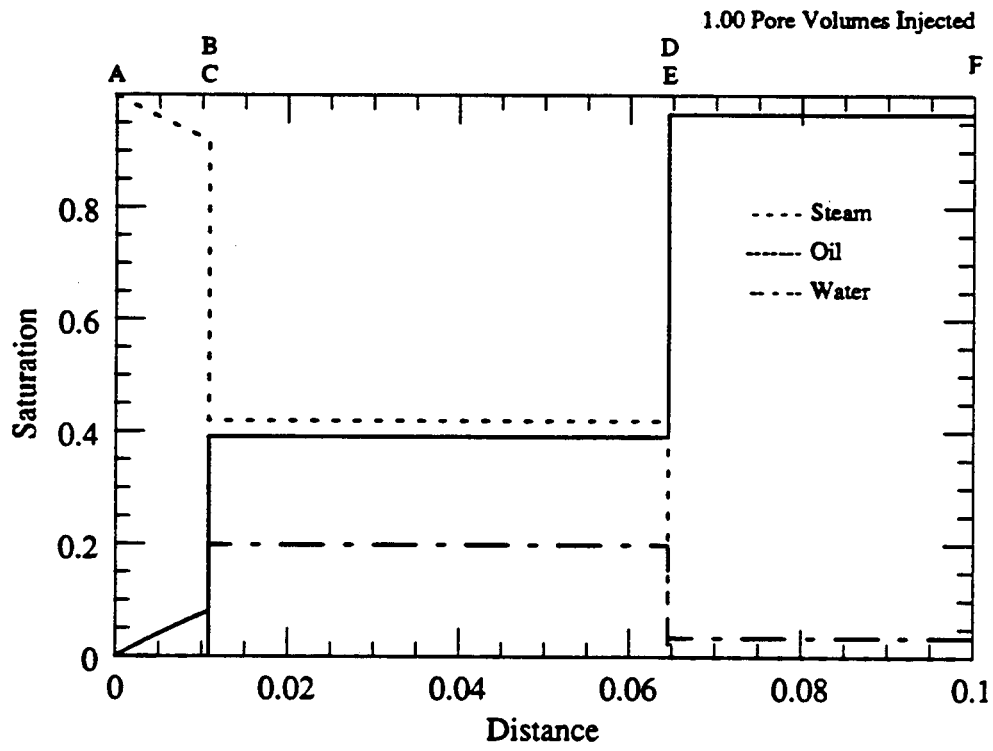


Figure 4.11: Saturation profile for the injection of 1.0 pore volumes of 100% steam at 650 K into 94.5% oil and 6.5% water at 390.19 K.

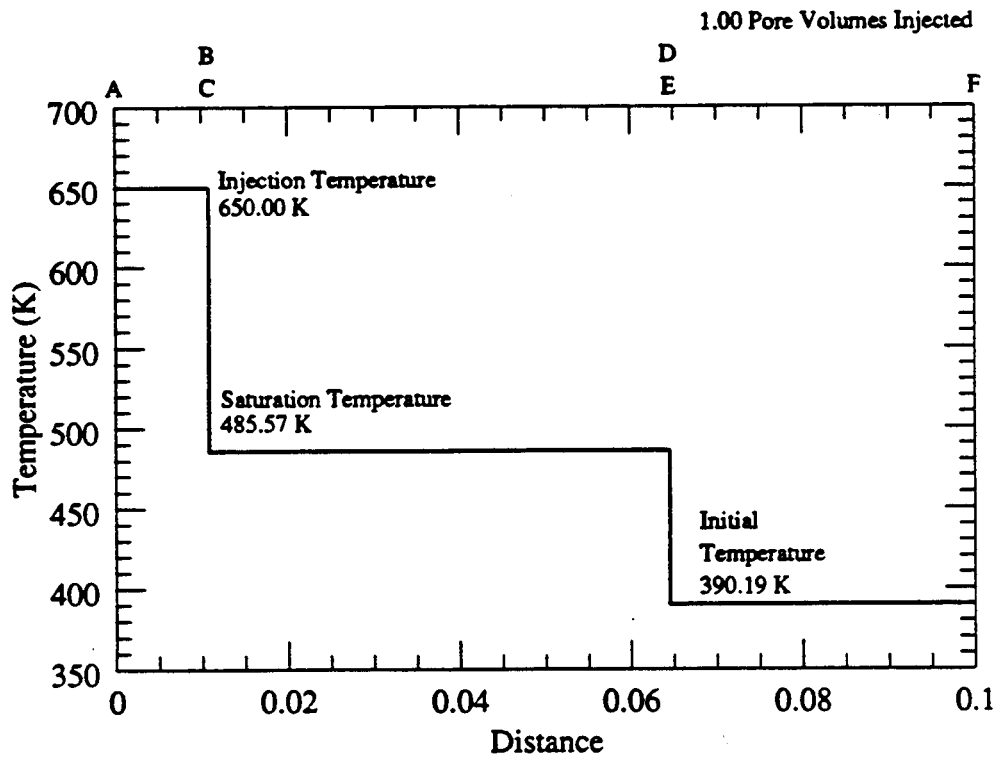


Figure 4.12: Temperature profile for the injection of 1.0 pore volumes of 100% steam at 650 K into 94.5% oil and 6.5% water at 390.19 K.

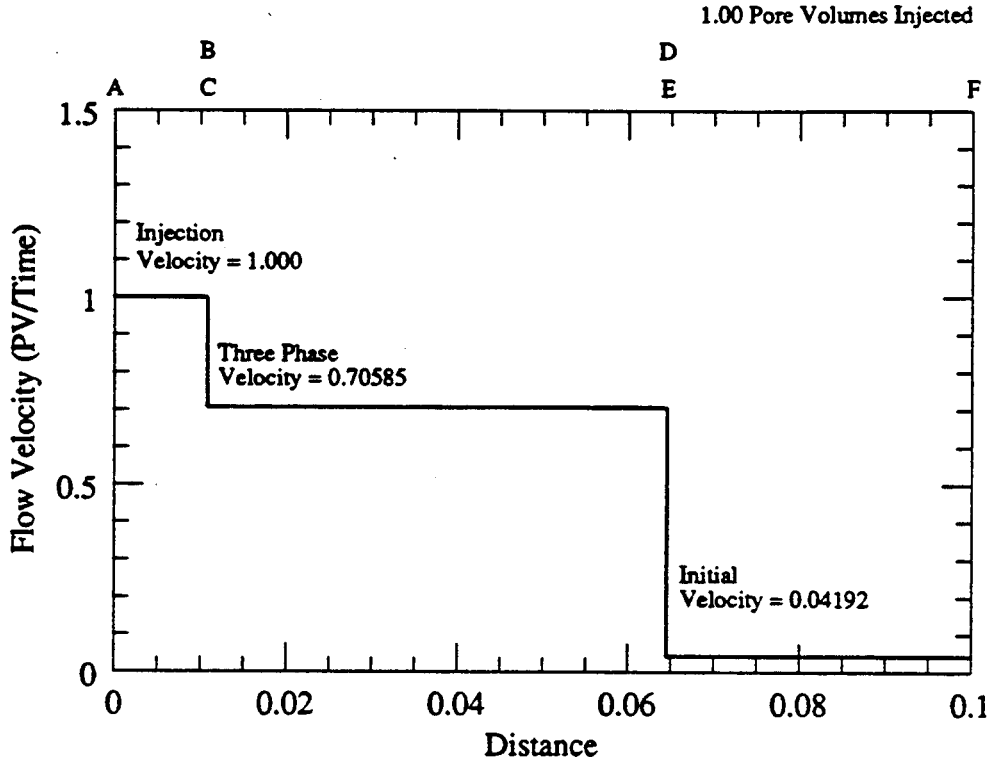


Figure 4.13: Flow velocity profile for the injection of 1.0 pore volumes of 100% steam at 650 K into 94.5% oil and 6.5% water at 390.19 K.

4.2.3 Types of Displacement Patterns

This section discusses the four different wave patterns. Profiles are presented for three new patterns that initially follow the same composition path as the previous case in the steam-oil region. These different cases are distinguished by the type of wave that exists downstream and upstream of the central zone of constant state.

In the three-phase region the object is to move from the slow eigenvalue at the landing point to the fast path at some other point in the three-phase region. This is illustrated by Figure 4.14. The Point U is the landing point from the steam oil region and point D is the jumping point to the water-oil region downstream. The slower path moving through Point U is illustrated by the dashed curve and the solid line represents the fast path that intersects Point D. The paths intersect at Point I. This divides the three-phase region into three sections:

1. A central zone of constant state as the path switches from the slow path to the fast path at Point I.
2. A trailing wave that follows the slow path from Point U to Point I.
3. A leading wave that follows the fast path from Point I to the downstream Point D.

The four displacement types are distinguished by the kind of waves that are upstream and downstream of the central zone of constant state. These four types are listed in Table 4.5.

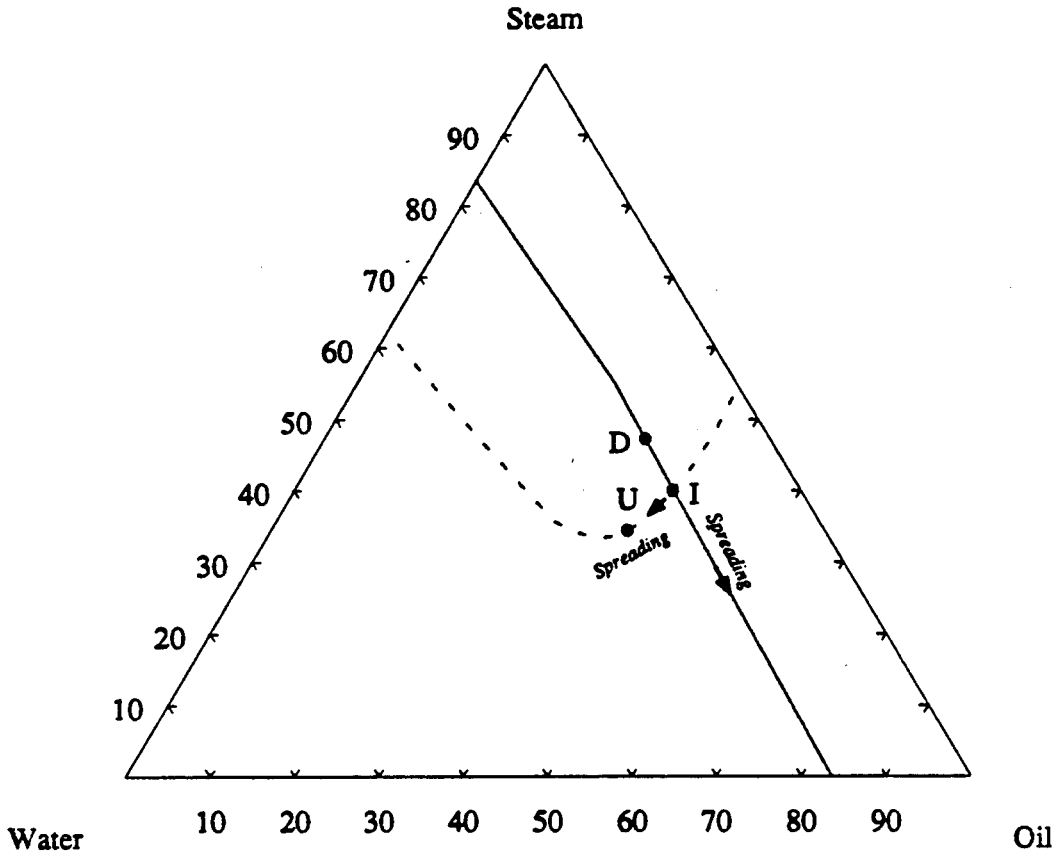


Figure 4.14: Composition path that moves between two arbitrary points in the three-phase region.

Displacement		
Type	U — I*	I — D
1	Self Sharpening	Self Sharpening
2	Spreading	Self-Sharpening
3	Self-Sharpening	Spreading
4	Spreading	Spreading

*U—>I represents the composition path from the upstream landing point to the point of intersection where the composition path switches from the slow path to the fast path and I—>D is the portion of the solution that travels along the fast path.

Table 4.5: The four different three-phase wave profiles for the displacement of oil and water by steam and water.

The example solution has a self-sharpening wave both upstream and downstream of the central zone of constant state, this corresponds to a Type 1 displacement.

A spreading wave is created when the path eigenvalue increases as the integration proceeds downstream. The spreading wave at the trailing end (from U to I) follows the slow path. This wave is found in the Type 2 wave pattern illustrated in Figure 4.15 and the Type 4 wave patterns as shown in Figure 4.16. The slow path parallels the contours of constant vapor flow. A integration along the slow path in the spreading direction increases the water saturation and decreases the oil saturation while leaving the saturation of the vapor phase relatively unchanged. The extent of this spreading wave is limited by a maximum velocity on the slow path.

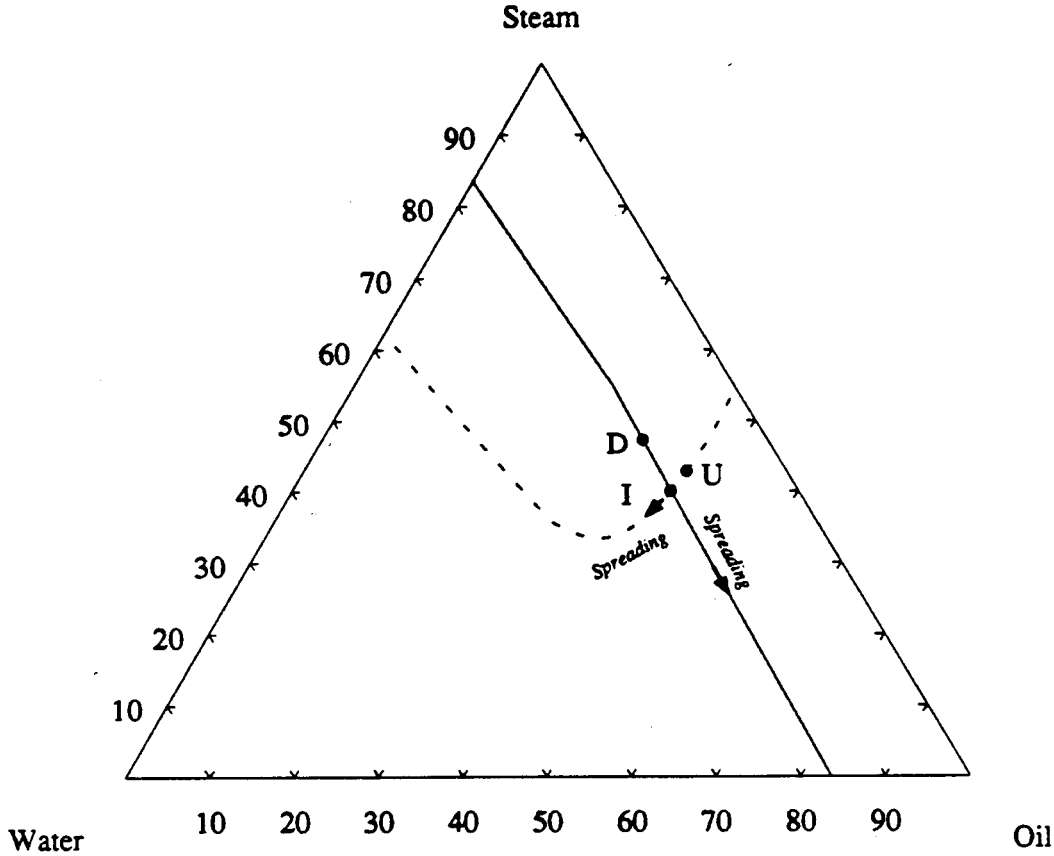


Figure 4.15: Type 2 composition path that moves between two arbitrary points in the three-phase region.

A spreading wave can also exist downstream of the central zone of constant state. This wave is found in the Type 3 and Type 4 wave patterns. The Type 3 composition path is shown in Figure 4.17. The eigenvalues along the fast path change much more rapidly than along the slow path. The fast path nearly parallels lines of constant water saturation. These conditions cause the profiles ahead of the zone of constant state to be spread out to a much greater extent near the initial end of the displacement.

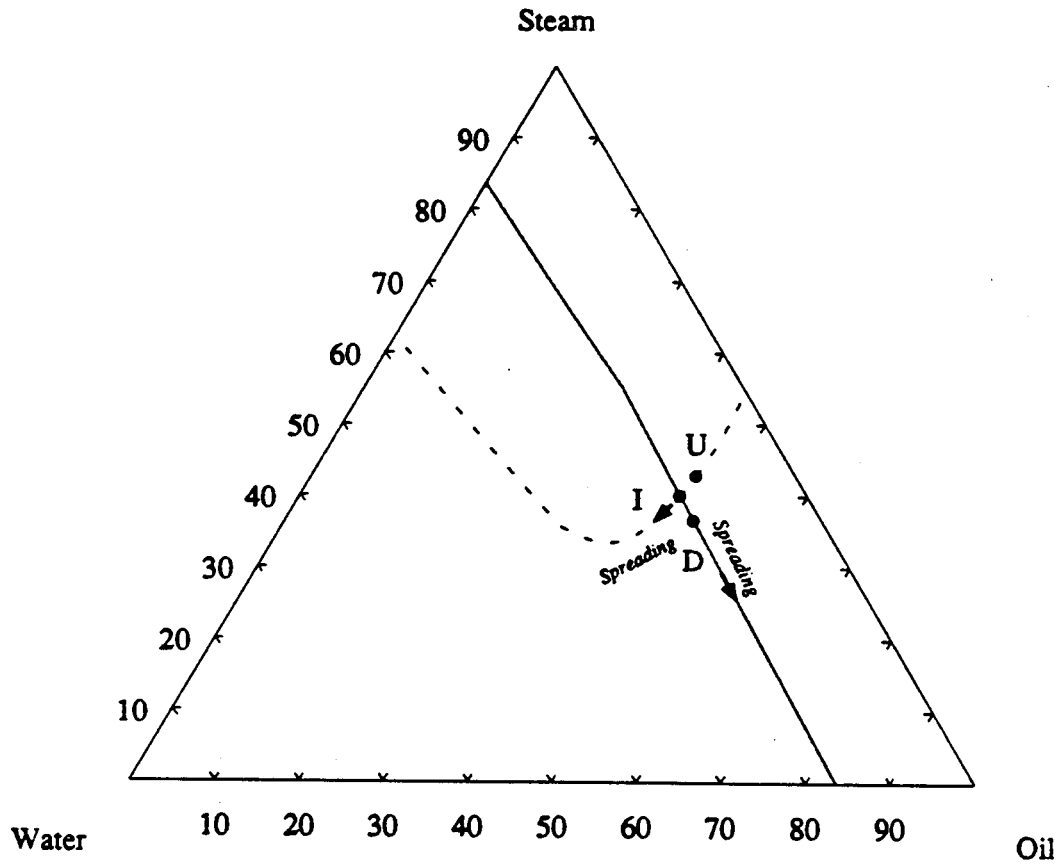


Figure 4.16: Type 4 composition path that moves between two arbitrary points in the three-phase region.

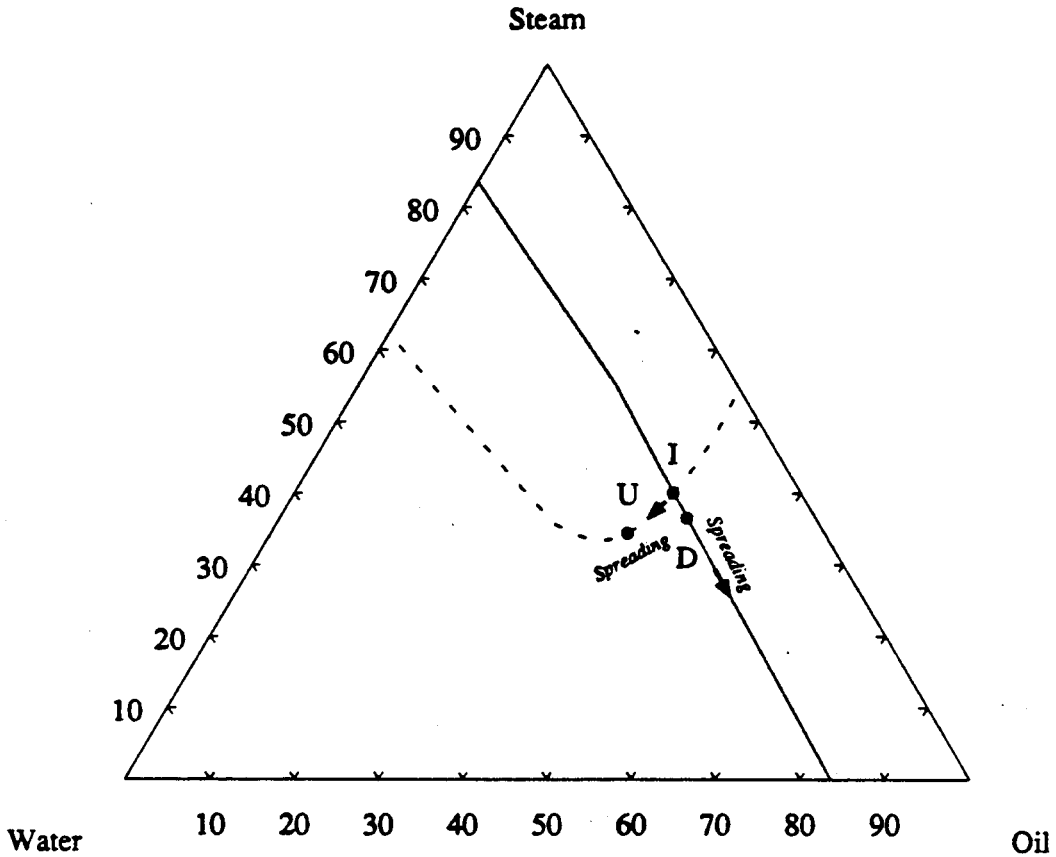


Figure 4.17: Type 3 composition path that moves between two arbitrary points in the three-phase region.

The opposite of the spreading wave is a self-sharpening wave. These waves appear when the eigenvalues decrease as the integration moves downstream. The construction of the self-sharpening waves changes from a continuous integration and becomes a shock calculation. A self-sharpening wave represents the limit of a continuous variation along a composition path. This makes the resolution of the self-sharpening wave an intermediate discontinuity.

The trailing self-sharpening wave is restricted to a narrow region just downstream of the phase transition shock. The reasons for this are tied to the velocity constraint. First, and most evident, the self-sharpening wave velocity must be larger than or equal to the velocity of the upstream intermediate discontinuity initially brings the solution into the three-phase region, or,

$$\lambda_1^+ = \Lambda_{mid} \leq \Lambda_{ss} \leq \lambda_1^- \quad (4.23)$$

where:

λ_1^+ = Small eigenvalue in the upstream region

λ_1^- = Small eigenvalue in the downstream region

Λ_{uid} = Velocity of the upstream intermediate discontinuity between the upstream and downstream region

Λ_{ss} = Velocity of the discontinuity created by the self-sharpening wave

If the self sharpening wave velocity were to be less than the velocity of the upstream intermediate discontinuity, then a condition downstream, the self-sharpening wave, would have a lower velocity than the upstream condition, the upstream intermediate discontinuity. This is clearly prohibited by the velocity constraint.

When the solution contains a self-sharpening wave, the eigenvalues along the slow path decrease in a smooth fashion between the landing Point U and the intersection Point I. It is known that the shock velocity formed by a self-sharpening wave is intermediate between the endpoints of the path which forms the wave (Jeffrey 1976). That is,

$$\lambda_1^I \leq \Lambda_{ss} \leq \lambda_1^U \tag{4.24}$$

Since the downstream point, composition I, has a slow path velocity that is less than the velocity of the landing point, I, all self-sharpening wave velocities must be less than the velocity of the small eigenvalue at the landing point, Composition U. This eliminates all self sharpening waves with velocities that satisfy the following inequality,

$$\lambda_1^+ = \Lambda_{uid} < \lambda_1^- < \Lambda_{ss} \tag{4.25}$$

This only leaves self-sharpening waves that fall in the zone of constant state that usually couples the eigenvalues λ_1^+ and λ_1^- . This type of self sharpening wave is illustrated in Figure 4.18.

There is a zone of constant state that couples the phase shock velocity to the slow eigenvalue in the three-phase region at U. The limiting case of the self-sharpening wave is when the zone of constant state vanishes. This condition is equivalent to an immediate jump from the steam-oil region to the large eigenvalue at I. The original discontinuity and the self-sharpening wave are added together to give one large shock as illustrated in Figure 4.19. This is the type of shock that was presented in the first example solution in §4.2.2.

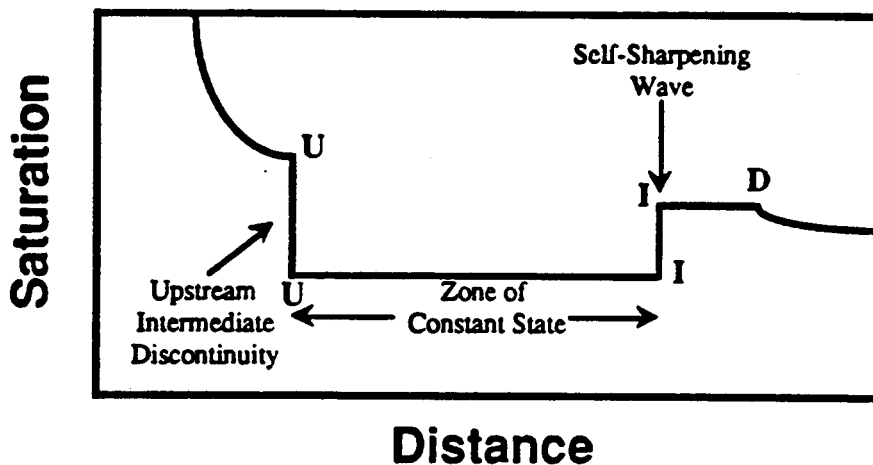


Figure 4.18: Possible self-sharpening wave in the three-phase region.

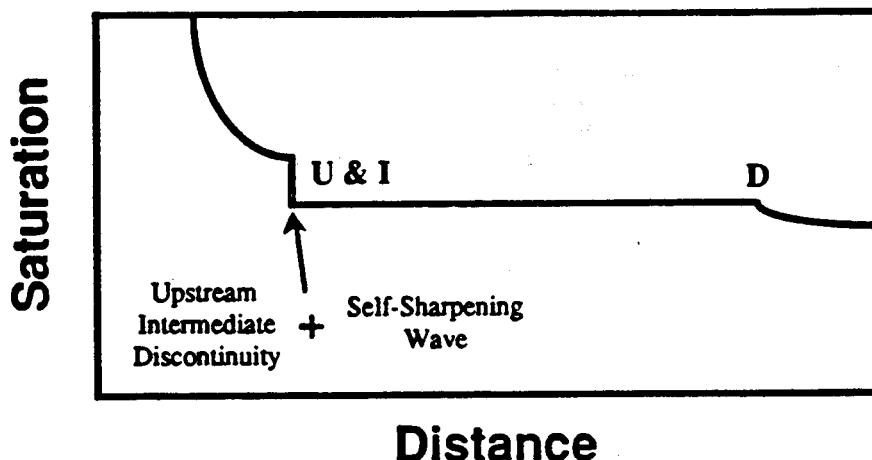


Figure 4.19: Limiting case self-sharpening wave in the three-phase region.

For cases where the two liquid phases have a comparable viscosities, the self-sharpening waves do not move downstream of the limiting case. This has the effect of switching directly to the fast path at the three phase landing point, Point U. The three different wave patterns that contain a self-sharpening wave will be presented as the limiting case examples. The "heavy" oil solutions, on the other hand, contain examples of self sharpening waves that do move ahead of the trailing upstream intermediate discontinuity.

The same situation can theoretically occur where the a self sharpening wave can be called for from the intersection Point I to the downstream jumping point, Point D. These kinds of adjustments are not found in these displacements. The zone of constant state that acted as a buffer between the phase change shock and the self-sharpening wave does not exist. Only the limiting case, where the downstream jumping point, D, is equivalent to the intersection point, I, is found in these types of displacements.

The self-sharpening waves are resolved by locating an additional upstream intermediate discontinuity or a downstream intermediate discontinuity that takes the solution from the landing point, U, to a new point of intersection, I'. The new landing point, I', will not be the same as the original intersection point, I, on the path defining the self-sharpening wave. The fractional flow relationship across a discontinuity such as a self-sharpening wave is different that the continuous flow variation described by the path from U to I. The limiting self-sharpening waves at either of the end points, U or D, are adjusted by moving Point U or D to the new point of intersection, I. This adjustment for the Type 1 displacement is illustrated in Figure 4.20. The construction of the self-sharpening waves requires that displacement types 1—3 be changed from composition paths illustrated in Figures 4.14—4.17 to those shown in Figures 4.20—4.22. The Type 4 wave pattern has spreading waves on both legs of the path in the three-phase region and satisfies the velocity constraint without adjustment.

Type 2 Displacement

The Type 2 displacement has a spreading wave on the upstream side of the three-phase region. This is done by moving along the slow path in the direction of increasing eigenvalues before jumping into the water-oil region. The composition path followed for the Type 2 wave pattern is given by Figure 4.23. The portion of the path in the steam-oil region is the same as the base case. This means that Point C is also identical to the base case. From Point C a zone of constant state takes the solution to Point D, where the eigenvalue matches the slow path.

The Type 2 temperature profile as shown in Figure 4.24 is similar to the Type 1 temperature profile given in Figure 4.12. Both profiles have a constant temperatures at the injection temperature until the trailing shock drops the temperature to the three phase saturation temperature. The difference between the Type 2 and Type 1 temperature profiles is only seen at the leading shock.

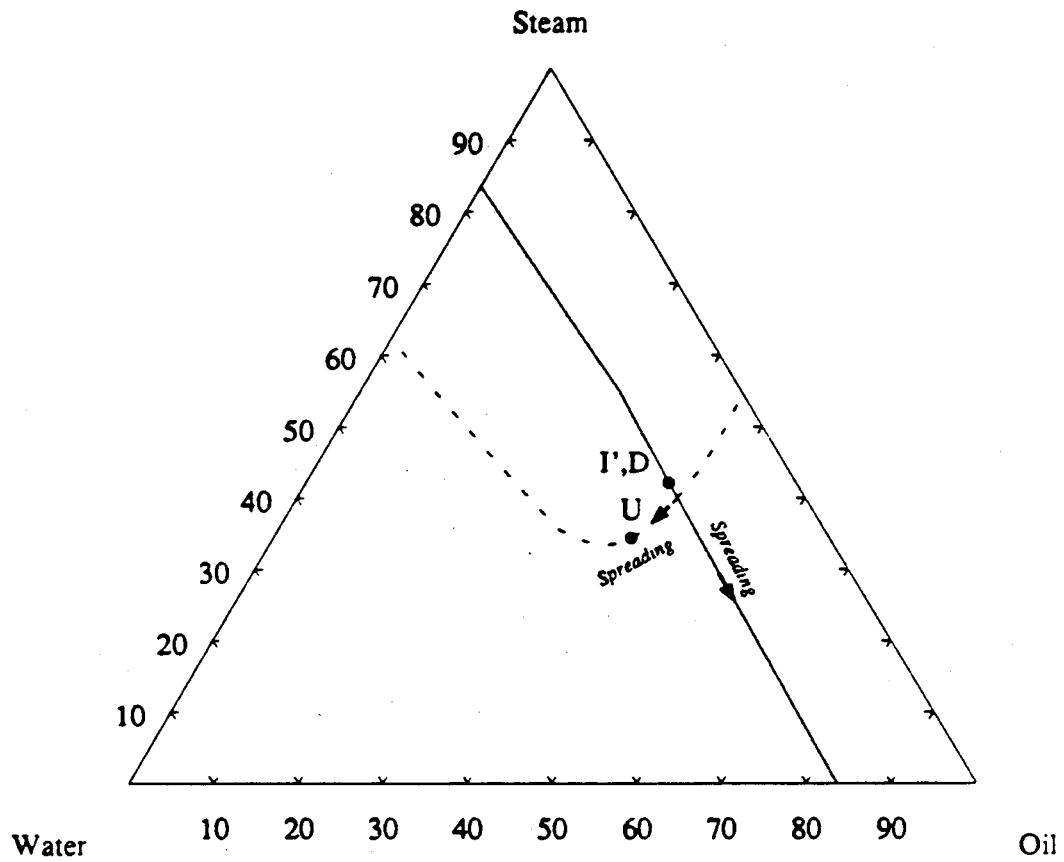


Figure 4.20: Adjusted Type 1 composition path that moves between two arbitrary points in the three-phase region.

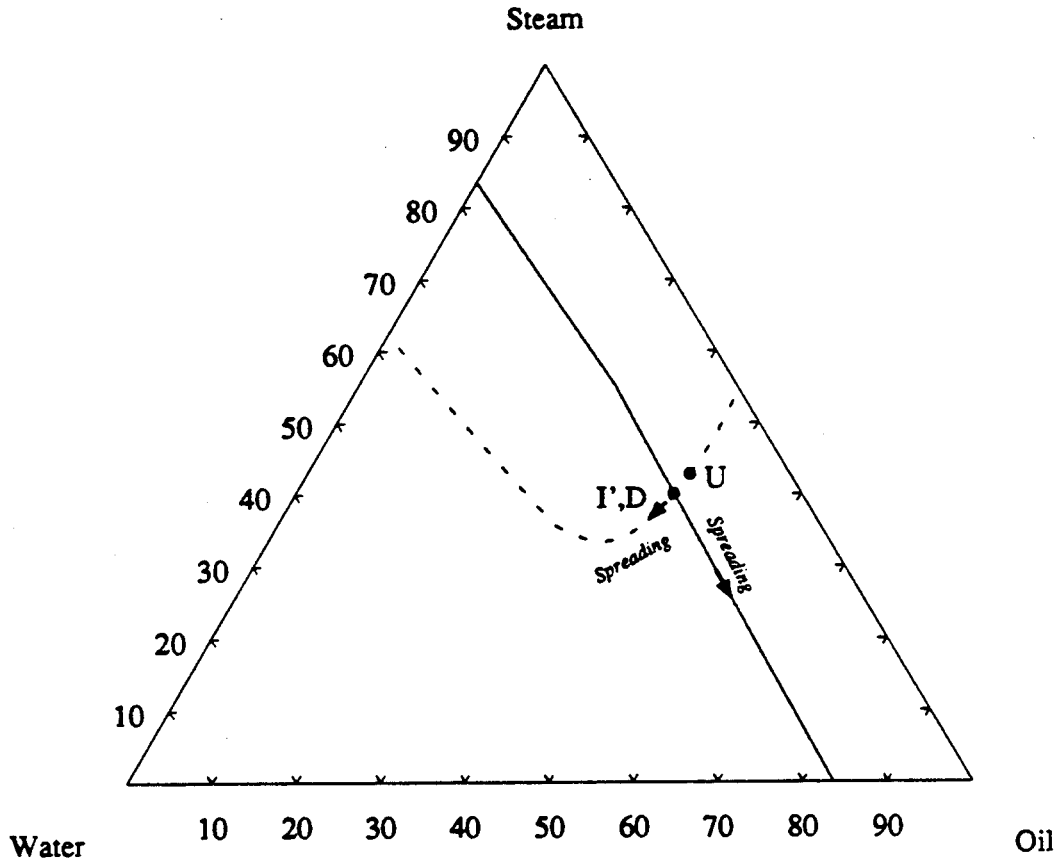


Figure 4.21: Adjusted Type 2 composition path that moves between two arbitrary points in the three-phase region.

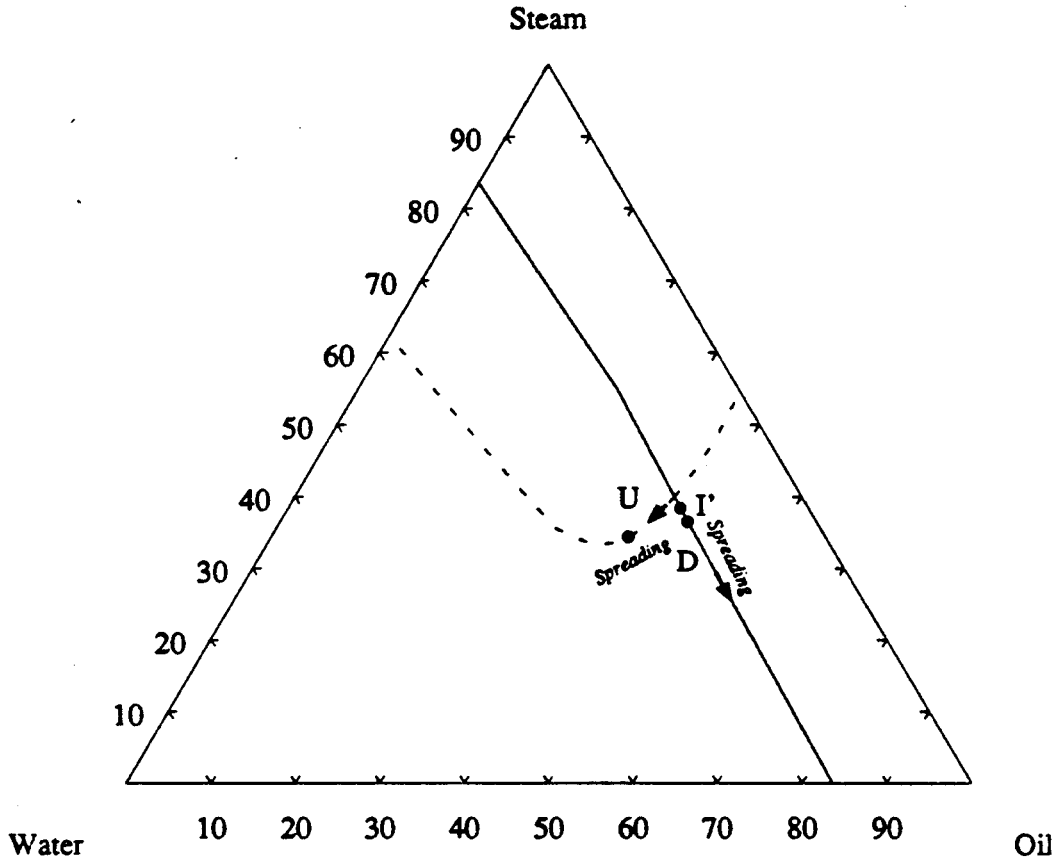


Figure 4.22: Adjusted Type 3 composition path that moves between two arbitrary points in the three-phase region.

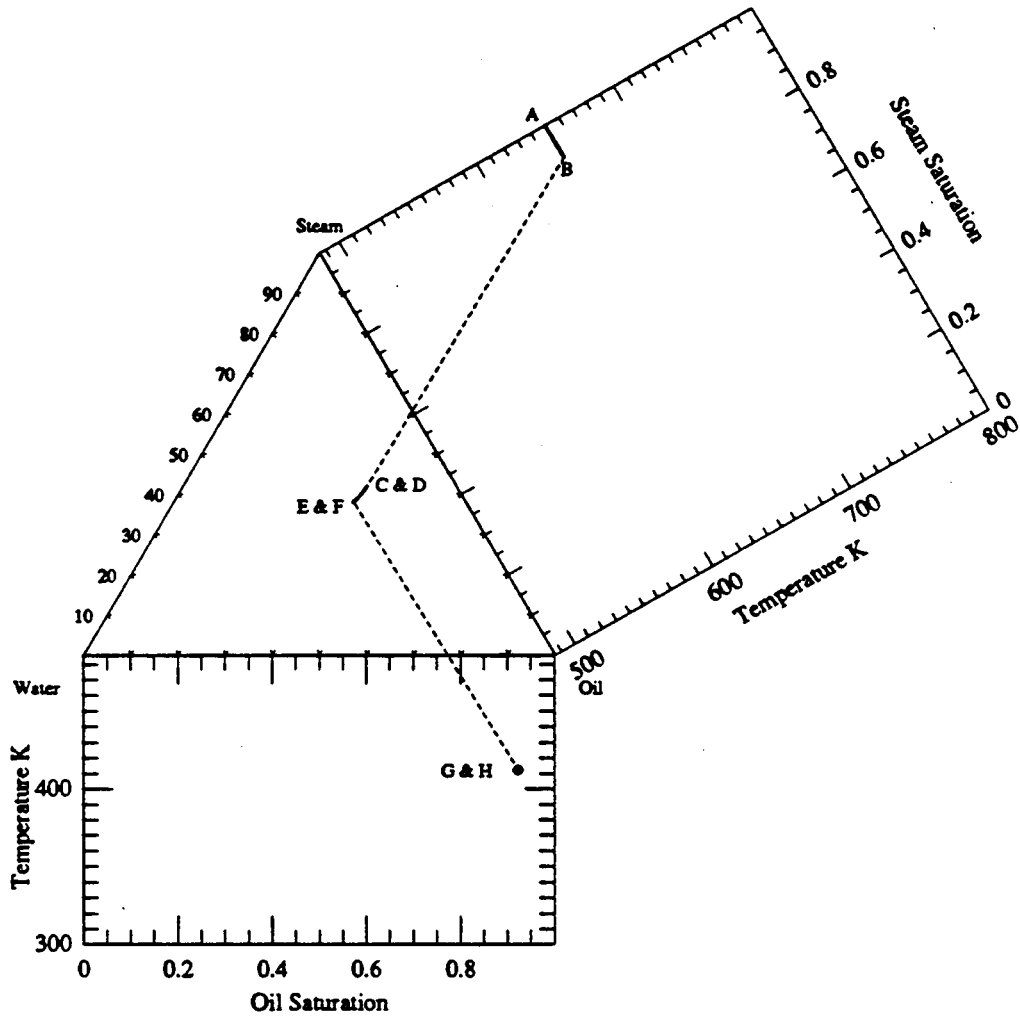


Figure 4.23: Composition path for the injection of 100% steam at 650 K into 92.4% oil and 7.6% water at 412.09 K.

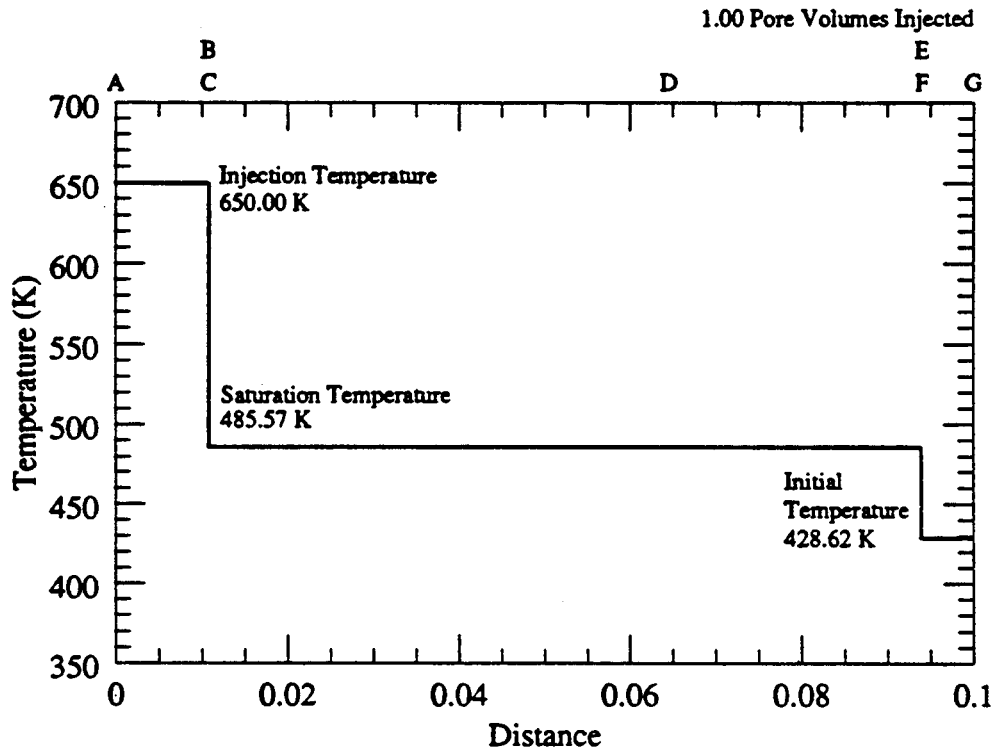


Figure 4.24: Temperature profile for the injection of 1.0 pore volumes of 100% steam at 650 K into 92.4% oil and 7.6% water at 412.09 K.

The Type 2 temperature profile has a leading shock with a higher velocity and initial conditions at a higher temperature. These two conditions are coupled by the heat balance across the shock. The higher temperature at the initial conditions require that less heat crosses the leading shock in the Type 2 displacement. Less heat crosses because the temperature difference is less in the Type 2 conditions. The result of the smaller heat content crossing the shock is that the shock travels with a higher velocity.

The flow velocity in the Type 2 displacement is shown in Figure 4.25. As in the Type 1 profile, the changes in velocity are a direct result of density changes associated with the volume change of the water component as it condenses across both the leading and trailing shocks. The slightly higher velocity in the Type 2 case is the result of the slightly higher density of the liquid water at 412.09 K than at the 390.19 K in the Type 1 profile.

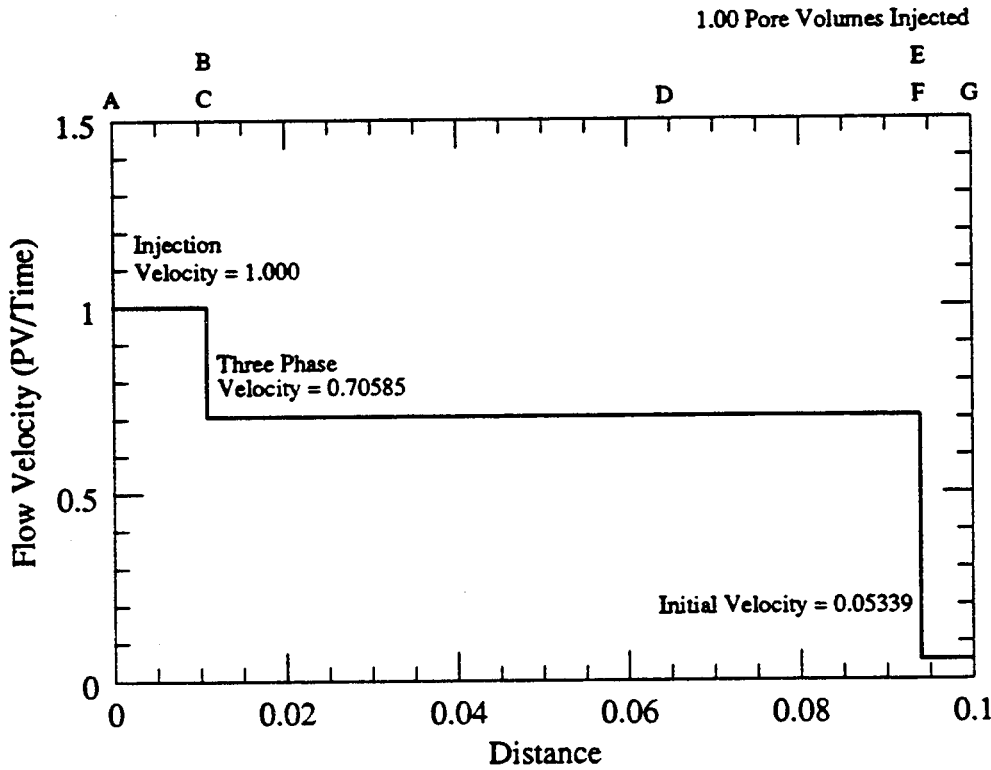


Figure 4.25: Flow velocity profile for the injection of 1.0 pore volumes of 100% steam at 650 K into 92.4% oil and 7.6% water at 412.09 K.

The important differences are shown when the saturation profiles are compared. The saturation profile in the Type 2 displacement is illustrated in Figure 4.26. Comparing this saturation profile to the saturation profile of the Type 1 shown in Figure 4.11 shows that in the Type 2 saturation profile has a spreading wave that leads the central zone of constant state. This wave extends from Point D to Point D in Figure 4.26.

The solution path in composition space is shown in Figure 4.23. The solution path departs from the Type 1 solution path by integrating along the slow path from Point D to Point E. The eigenvalues along this path increase, creating the spreading wave. The path roughly follows the contours of constant vapor fractional flow,

$$\frac{\partial f_v}{\partial \eta_1} = 0 \tag{4.26}$$

where η_1 is the distance along the slow path.

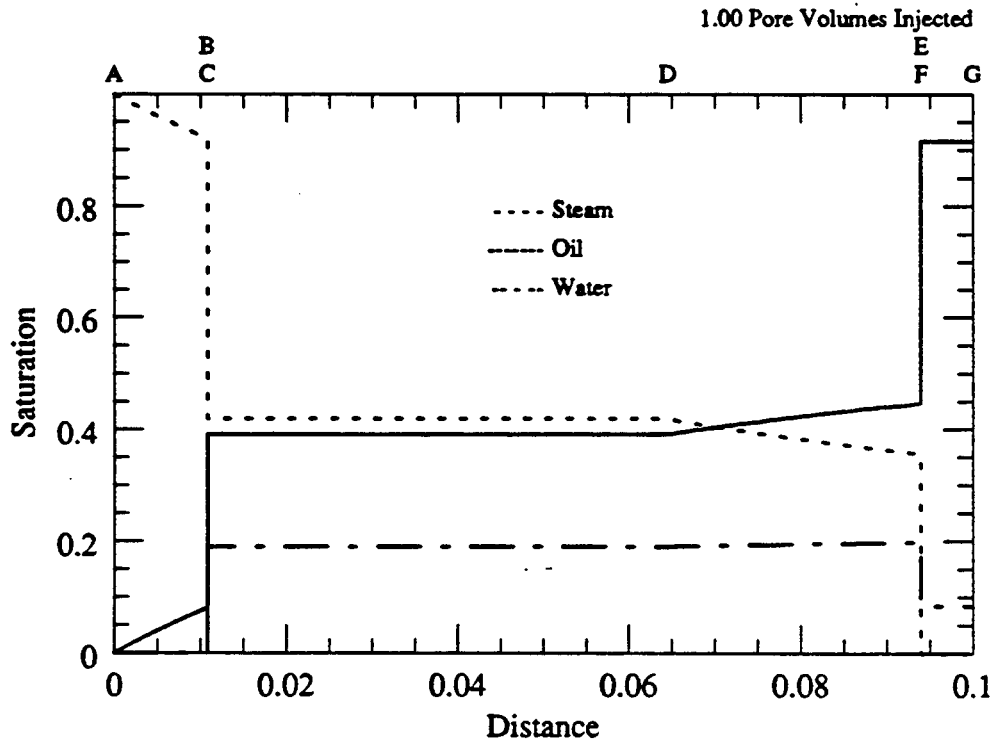


Figure 4.26: Saturation profile for the injection of 1.0 pore volumes of 100% steam at 650 K into 92.4% oil and 7.6% water at 412.09 K.

At Point E, a path switches to the fast path and creates a zone of constant state ahead of the spreading wave. Point E is also the jumping point to the initial conditions via an upstream intermediate discontinuity. Because the large eigenvalue at Point E is higher than the jumping point in the base case, the initial temperature will also be higher than in the base case.

The spreading wave along the slow path changes the water saturation of the jumping point to a much larger extent than did integration along the fast path. This increase in water saturation at the initial conditions also increases the water saturation of the jumping point from the fast path. Physically the slow path represents the fractional flow relationship of the changing oil and water saturations at the trailing edge of the three phase region. In this region, the more mobile vapor phase has already moved ahead of these compositions and reached a steady value leaving only the oil and water saturations to change.

This increase in water saturation is shown along the example solution path. When the water saturation is higher at Point E, the resulting water saturation of the initial conditions, Point F is also

higher. This increase in water saturation is accomplished by adding the spreading wave to the upstream end of the three-phase region.

Label	Composition Point					Wave Velocity	Type of Flow Region
	Saturations			T (K)	Flow Velocity		
	Steam	Oil	Water				
A	1.00000	0.00000	0.00000	650.00	1.00000	0.000000	INJ → SPW
B	0.92000	0.08000	0.00000	650.00	1.00000	0.010777	SPW → UID
C	0.41924	0.39087	0.18989	485.57	0.7058	0.010777	UID → ZCS
D	0.41924	0.39087	0.18989	485.57	0.7058	0.064505	ZCS → SPW
E	0.35572	0.44658	0.19770	485.57	0.7058	0.093985	SPW → UID
F	0.00000	0.91566	0.08434	428.62	0.0534	0.093985	UID → INI
G	0.00000	0.91566	0.08434	428.62	0.0534		INI

Table 4.6: Type 2 composition path for injection of 100% steam at 650 K into 92.4% oil and 7.6% water at 412.09 K.

Type 3 Displacement

The Type 3 displacement attaches a spreading wave to the downstream portion of the three-phase region. Table 4.7 and Figure 4.27 outline the solution path for this displacement pattern. The resulting hodograph profiles are shown in Figures 4.28—4.30. The solution jumps immediately to the fast path from the three phase landing point as in the Type 1 wave pattern. Instead of immediately jumping to the initial conditions as with the Type 1 case, an integration along the fast path adds a spreading wave downstream of the zone of constant state before jumping to the initial conditions. This has the effect of increasing the oil saturation at the expense of the steam saturation. Another change is in the speed of the leading phase transition shock. As the integration proceeds along the fast path the eigenvalues must necessarily increase. Since the velocity of the phase transition shock matches the eigenvalue of the upstream conditions, this velocity must also increase.

The integration along the fast path from D to E is the new feature of the Type 3 displacement. This wave is highly spread over the zone preceding the leading phase transition shock. The reason is that the increase in the wave velocity along the fast path is much larger than along the slow path seen in the Type 2 wave pattern. As the vapor saturation decreases, the derivative of the water phase fractional flow curve, (df_w / dS_w) , increases, causing the eigenvalues along the fast path to rise rapidly. The end effect of an integration along this path is to force a change the initial conditions by significantly raising the initial temperature without appreciably affecting the initial water saturation.

Label	Composition Point					Wave Velocity	Type of Flow Region
	Saturations			T (K)	Flow Velocity		
	Steam	Oil	Water				
A	1.00000	0.00000	0.00000	650.00	1.00000	0.000000	INJ → SPW
B	0.92000	0.08000	0.00000	650.00	1.00000	0.010777	SPW → UID
C	0.41924	0.39087	0.18989	485.57	0.7058	0.010777	UID → ZCS
D	0.41924	0.39087	0.18989	485.57	0.7058	0.064505	ZCS → SPW
E	0.35572	0.44658	0.19770	485.57	0.7058	0.093985	SPW → UID
F	0.00000	0.91566	0.08434	428.62	0.0534	0.093985	UID → INI
G	0.00000	0.91566	0.08434	428.62	0.0534		INI

Table 4.7: Type 3 composition path for injection of 100% steam at 650 K into 91.6% oil and 8.4% water at 428.62 K.

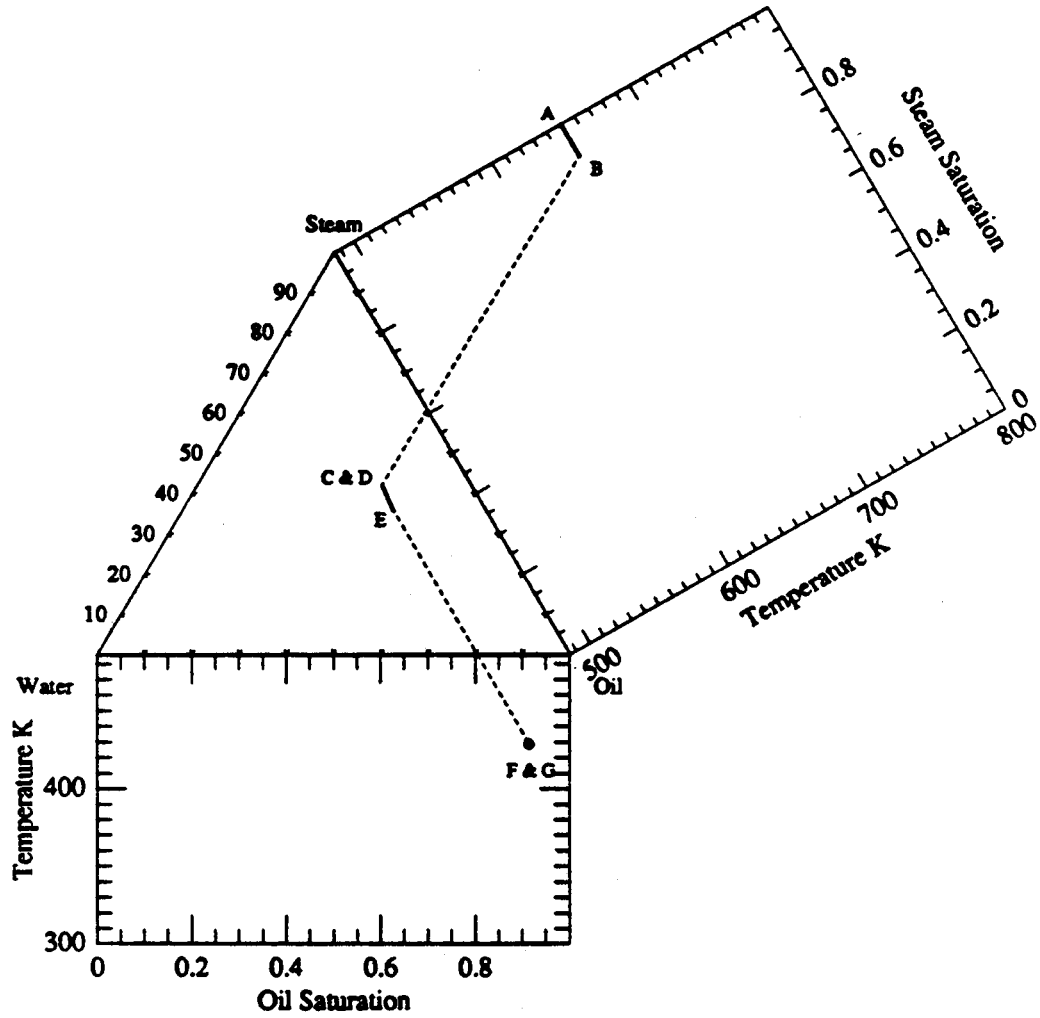


Figure 4.27: Composition path for the injection of 100% steam at 650 K into 91.6% oil and 8.4% water at 428.62 K.

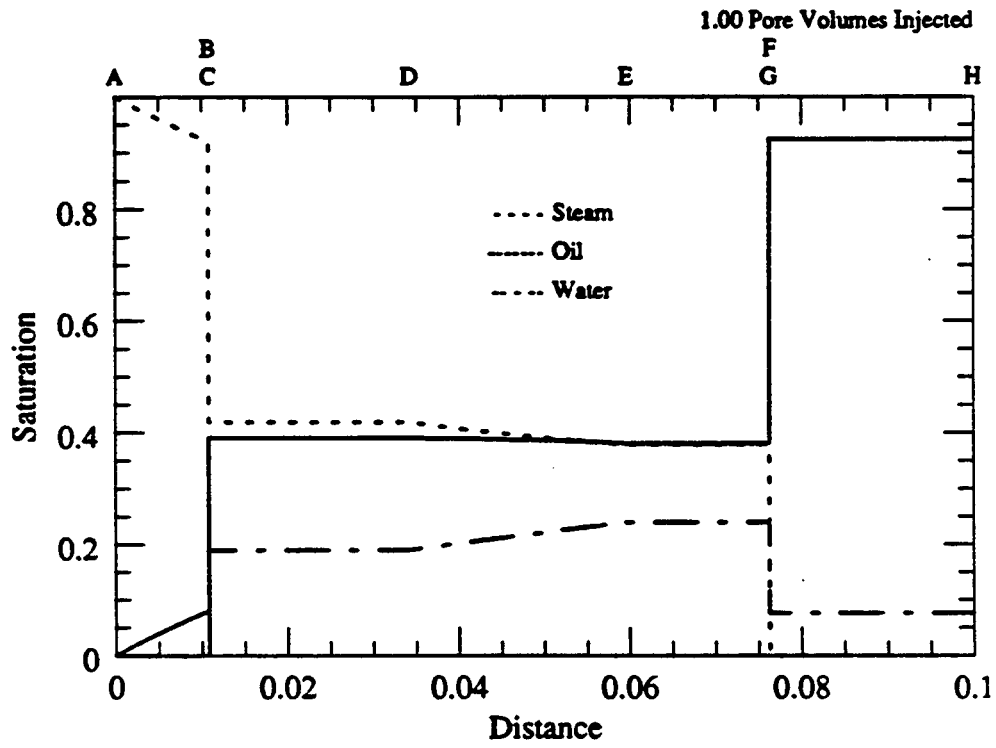


Figure 4.28: Saturation profile for the injection of 100% steam at 650 K into 91.6% oil and 8.4% water at 428.62 K.

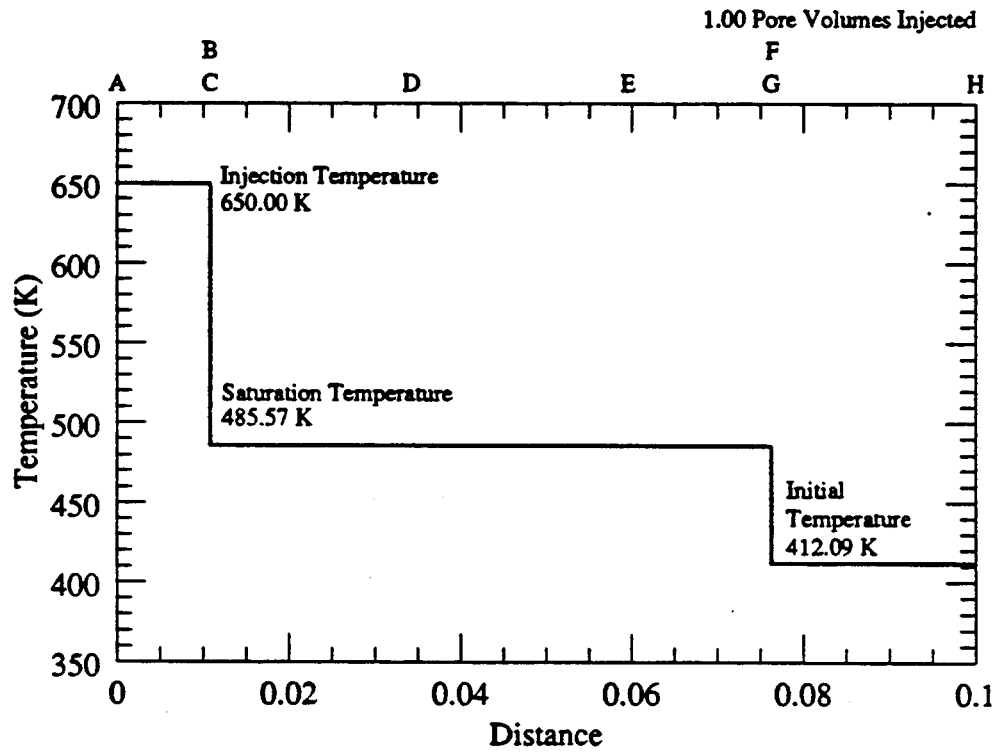


Figure 4.29: Temperature profile for the injection of 100% steam at 650 K into 91.6% oil and 8.4% water at 428.62 K.

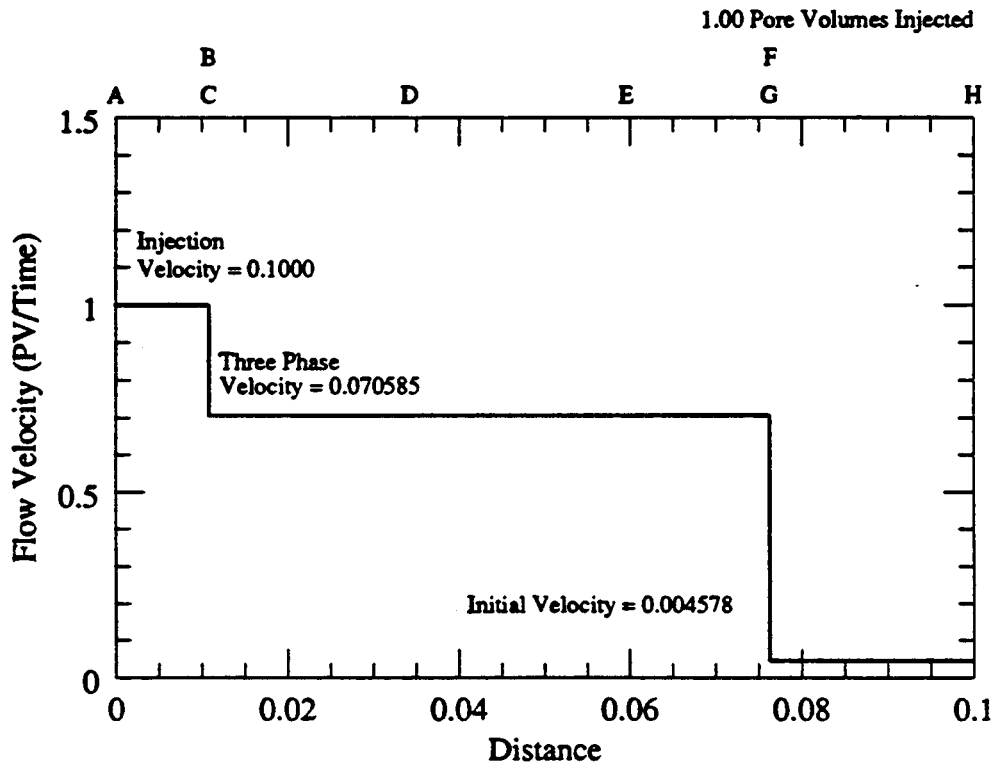


Figure 4.30: Flow velocity profile for the injection of 100% steam at 650 K into 91.6% oil and 8.4% water at 428.62 K.

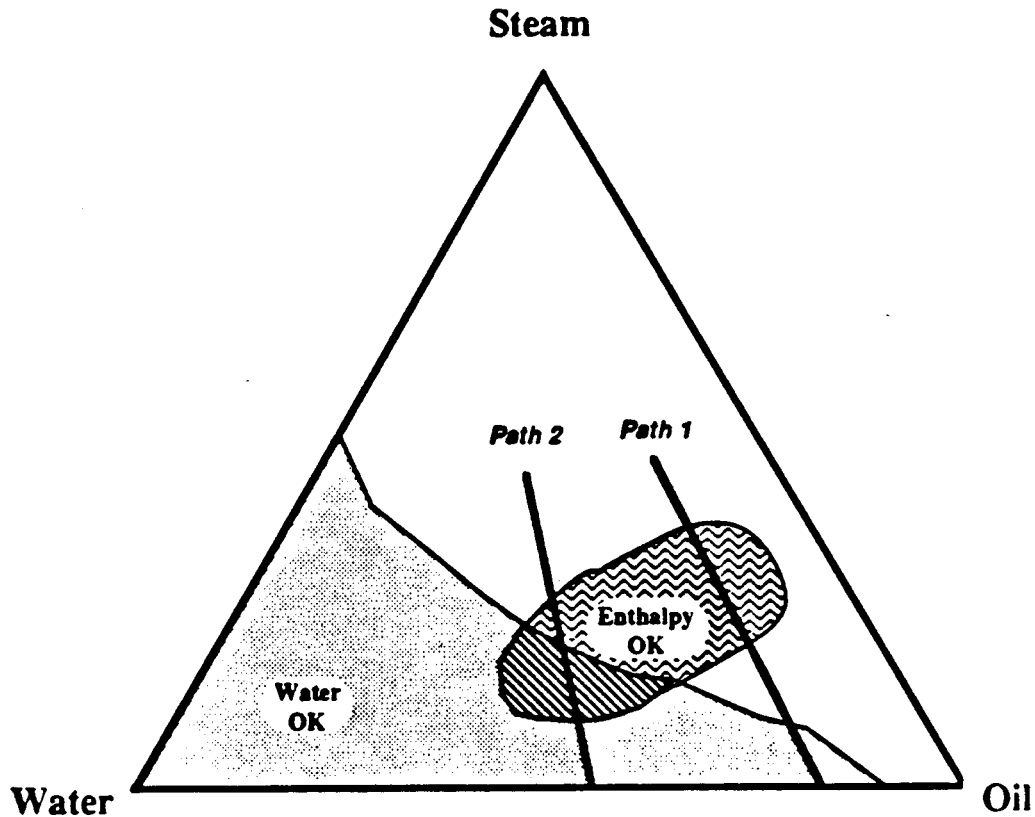


Figure 4.31: Three-phase region of the steam-oil-water displacements showing the regions where the fast path eigenvalues and water saturation permit a jump into the water-oil region.

The jumping condition from the fast path to the water-oil region is controlled by two factors; these are the enthalpy and water balances across the shock. Because the wave velocity changes rapidly, there is a small region along the fast composition path that can jump into the allowable hodograph space in the water oil region. In the three phase space there is a region where the eigenvalues are in the allowable range to satisfy the enthalpy balance. Another region has a large enough water saturation so that the steam and water are mobile enough to cross the phase change shock and form a liquid water phase. Only paths that cross the intersection of these two regions can jump into the water-oil region. These regions are illustrated in Figure 4.31. If the fast path is chosen as Path 1, there is no composition point along that path that satisfies both the enthalpy requirement and the water saturation for a jump into the water-oil region. Path 2 on the other hand does cross into the intersecting region and a solution for the phase transition shock can be found.

Type 4 Displacement

The Type 4 displacement is a combination of the Type 2 and Type 3 systems. A spreading wave is located before and after the zone of constant state. The Type 4 wave pattern has the fastest leading shock and hence requires the highest initial temperatures and water saturations. The composition path for the Type 4 wave pattern is illustrated in Figure 4.32 and listed in Table 4.8.

The saturation, temperature and flow velocity profiles in Figures 4.33—4.35 show the profiles that result from following the composition path in Figure 4.32. The oil saturation in the three-phase region remains essentially constant over the entire region. An interesting feature of this path is that the oil saturation decreases along the path D → E upstream of the zone of constant state, then increases along F → G before jumping to the water-oil region.

The water bank has a lower saturation at the upstream end of the three-phase region and slowly increases over the length of the three-phase region. This is due to the spreading waves that follow increasing water saturation in the three-phase region.

Label	Composition Point				Flow Velocity	Wave Velocity	Type of Flow Region
	Saturations			T (K)			
	Steam	Oil	Water				
A	1.00000	0.00000	0.00000	650.00	1.00000	0.000000	INJ → SPW
B	0.92000	0.08000	0.00000	650.00	1.00000	0.010777	SPW → UID
C	0.41924	0.39087	0.18989	485.57	0.7058	0.010777	UID → ZCS
D	0.41924	0.39087	0.18989	485.57	0.7058	0.034233	ZCS → SPW
E	0.37839	0.38132	0.24029	485.57	0.7058	0.059471	SPW → ZCS
F	0.37839	0.38132	0.24029	485.57	0.7058	0.076318	ZCS → SPW
G	0.34243	0.39977	0.25780	485.57	0.7058	0.098756	SPW → UID
H	0.00000	0.88119	0.11881	433.79	0.0539	0.098756	UID → INI
I	0.00000	0.88119	0.11881	433.79	0.0539		INI

Table 4.8: Type 4 composition path for injection of 100% steam at 650 K into 88.1% oil and 11.9% water at 433.79 K.

This section has presented example solutions for four different wave patterns seen in the steam-oil-water displacements. All the cases presented were limiting case examples where the velocity of the self-sharpening waves were matched to the tangent shocks that occurred at the phase transitions. Many other possible solutions exist, all matching a given set of injection conditions to a specific set of initial conditions. The self-sharpening waves were calculated assuming that they were all upstream intermediate discontinuities. Other solutions could involve one or two downstream intermediate discontinuities in place of the either upstream intermediate discontinuity. The effect of varying the injection conditions or the relative permeability model has not been discussed, but the techniques described in the following section could be used to construct such solutions.

4.2.4 Solution Procedure

The complete solution to the steam-oil-water problem is obtained using the following steps:

1. Select the injection conditions. This requires choosing the injection composition, injection temperature and injection velocity.
2. Integrate along the slow path until some point, B, is reached. Point B can be completely arbitrary with one exception that is noted in the next step.
3. Calculate the composition point in the three-phase region that is reached by crossing an upstream intermediate discontinuity from Point B, in the steam-oil region, into the three-phase region. This requires that the shock velocity as given by Eq. 2.35 be equal to the small eigenvalue at Point B. The landing point in the three-phase region, C, is unique.

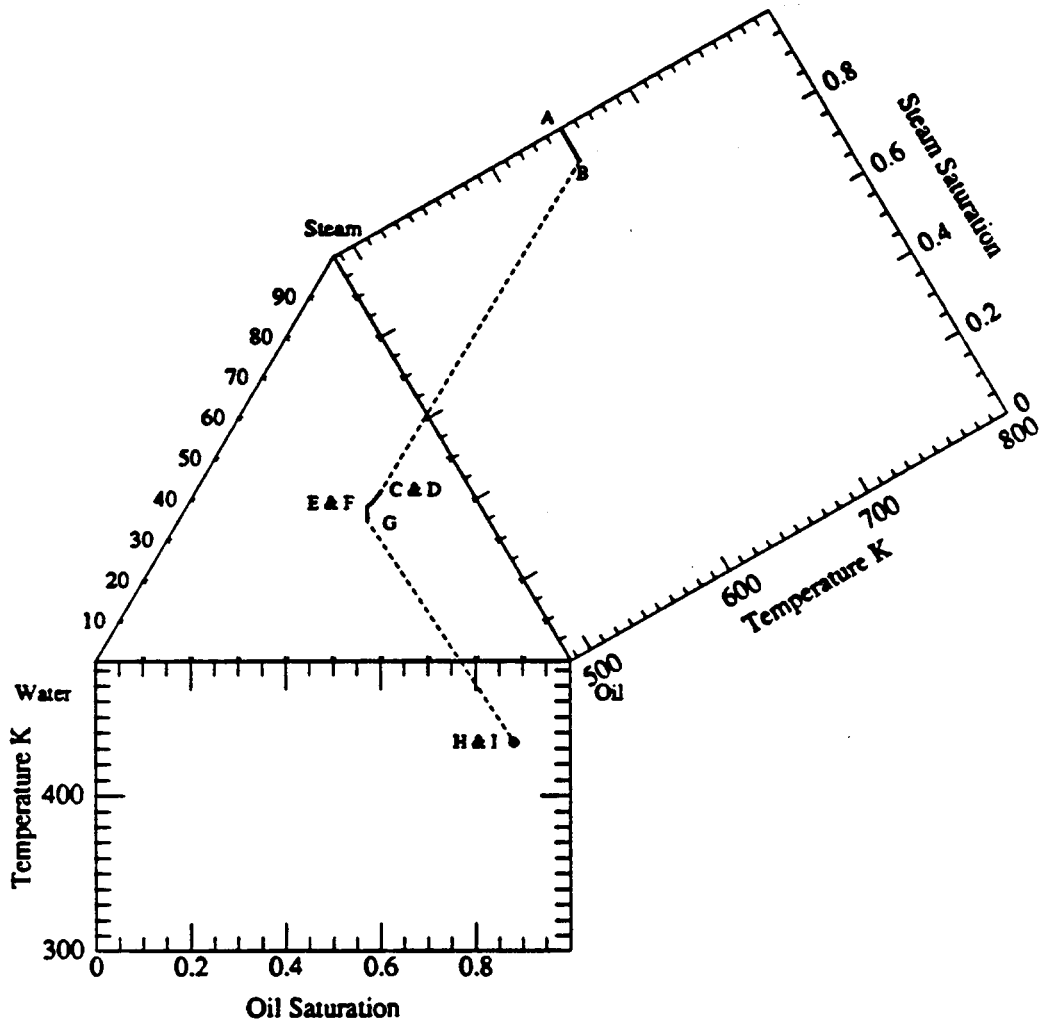


Figure 4.32: Composition path for the injection of 100% steam at 650 K into 88.1% oil and 11.9% water at 433.79 K.

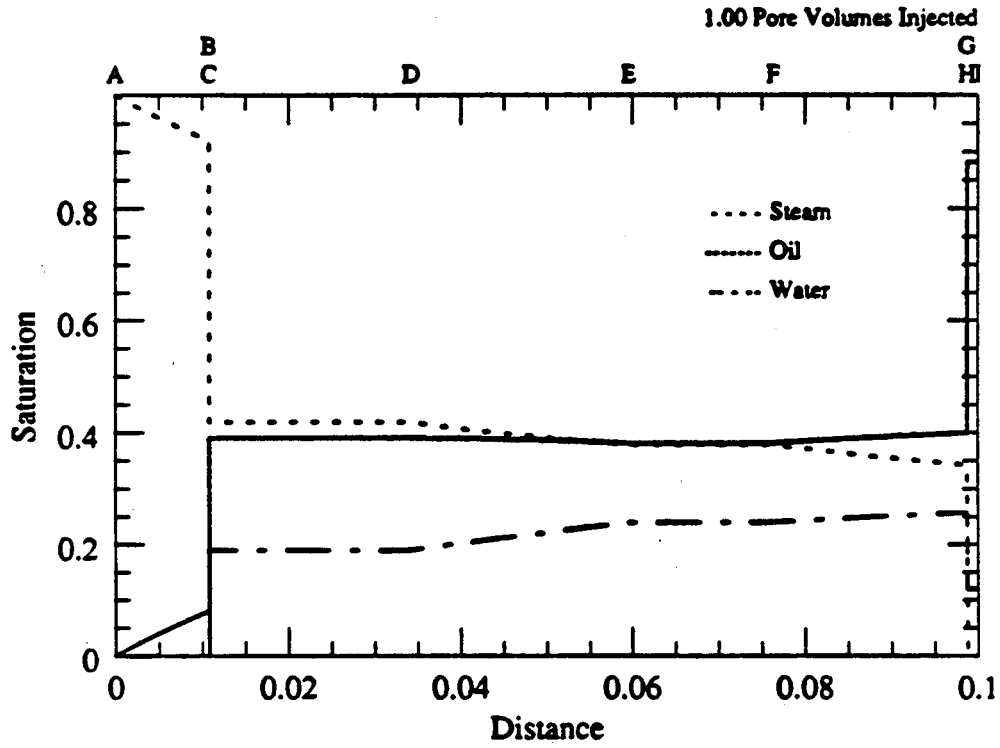


Figure 4.33: Saturation profile for the injection of 1.0 pore volumes of 100% steam at 650 K into 88.1% oil and 11.9% water at 433.79 K.

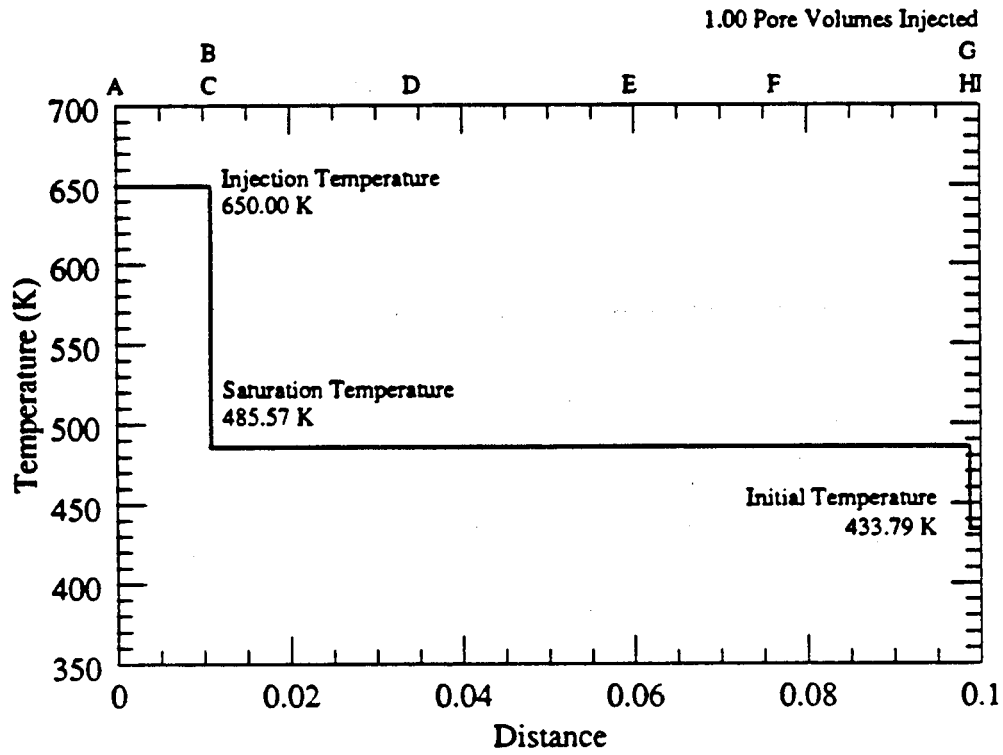


Figure 4.34: Temperature profile for the injection of 1.0 pore volumes of 100% steam at 650 K into 88.1% oil and 11.9% water at 433.79 K.

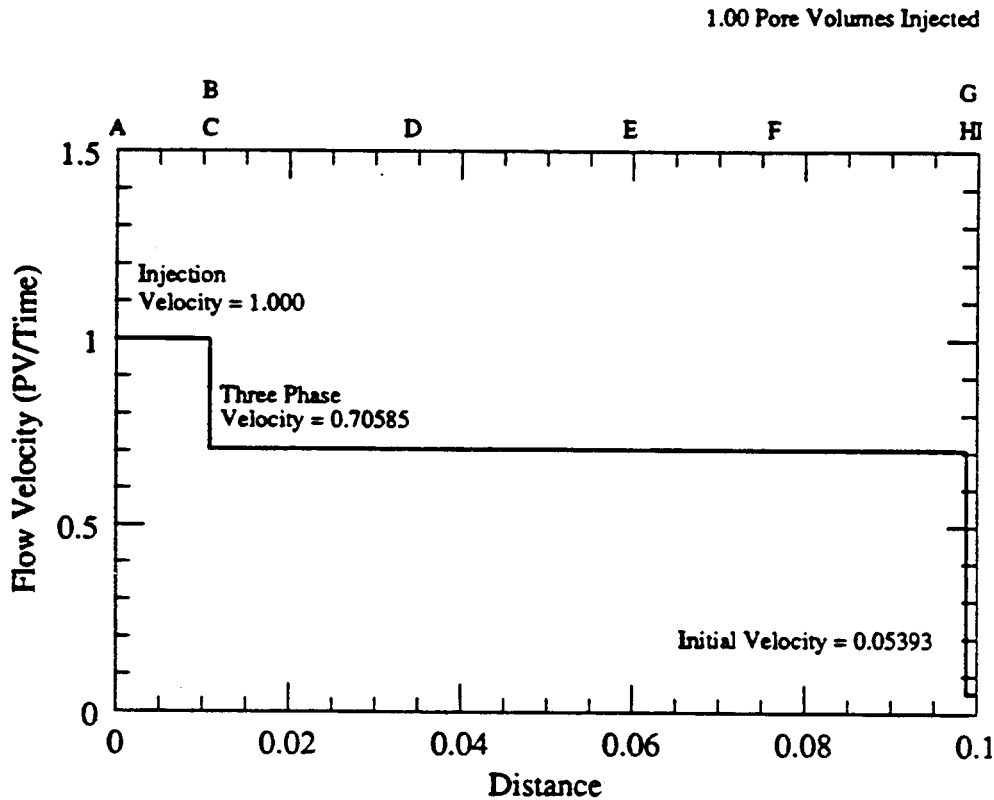


Figure 4.35: Flow velocity profile for the injection of 1.0 pore volumes of 100% steam at 650 K into 88.1% oil and 11.9% water at 433.79 K.

If the velocity of Point B is too small, there will be no solution for Composition C in the allowable hodograph space. This is indicated by having one or more of the saturation values be less than zero or greater than one at the landing point. If this happens, the selected point, B, is not a valid jumping point and another composition point further along the injection path (A \rightarrow B) must be chosen.

4. Integrate along the slow path from C to a new point in the three-phase region, Composition D. Composition D will be the point of intersection between the slow path and fast path. At this composition, the solution switches paths from the slow to the fast path, creating a zone of constant state at Point D.

The velocities must increase as the integration moves from C \rightarrow D. If the velocities decrease, a self-sharpening wave is indicated. A point must be chosen on a spreading portion of the path as the upstream set of conditions. If the eigenvalues immediately decrease in the desired direction, then the landing point must be at the upstream conditions. This is the limiting case presented in the example solutions. The self-sharpening wave is calculated by matching the shock velocity to the eigenvalue on either the upstream or downstream side of the shock. This has the effect of slightly shifting the intersection point to the fast path because of fractional flow considerations. This adjustment is indicative of the Type 1 and Type 3 wave patterns discussed in Table 4.5.

5. Integrate from Point D to another composition point, E, on the fast path. This large eigenvalue point cannot be so large that a material balance, or more importantly a heat balance, carries the shock solution out of the allowable hodograph space.

The limitation on self-sharpening waves also applies as the integration travels from D to E. The self-sharpening wave is resolved by jumping to the water-oil region directly from Point D. The self-sharpening wave along the fast path is usually not seen because this takes the solution away from the region where the solution can jump into the water-oil region. This kind of adjustment creates Type 1 or Type 2 displacements as mentioned in Table 4.5.

6. Point E is the jumping point into the water-oil region. Calculate the point in the water-oil region that satisfies the material balances and also matches the shock velocity to the large eigenvalue at Composition E. The landing point in the water-oil region, F, is the initial condition.

The nature of the eigenvalues in the water-oil region prevent the development of spreading waves in this region. All the eigenvalues in the water-oil region are slower than their three phase counterparts which necessarily lie upstream of the initial conditions. This situation often occurs in compressible gas dynamics where the leading shock travels faster than all the wave velocities in the region of initial conditions.

The initial temperature has a significant effect on the resulting velocity of the leading shock. The higher is the initial temperature, the less heat that must cross the shock and the faster its velocity must be. The Type 1 displacement has the minimum slowest leading shock for a given initial steam-oil jumping point (Point B). This type of displacement pattern therefore, is a result of approaching the lower limit on the initial temperature and flow velocity at the initial conditions for a given initial jumping point, Point B.

The spreading directions on both the fast and especially the slow path in the three-phase region have increasing water saturations. This increase of the water saturation at the initial conditions results in an increase in water saturation on the upstream side of the leading shock.

So far all the cases presented have followed the same path in the steam-oil region and have jumped into the three phase region from the same composition point. When the integration is allowed to continue farther along the slow path in the steam-oil region, a composition point is reached where the eigenvalues are equal. At this point, a path switch in accordance with Rule III, illustrated in Figure 3.2, takes the solution from the isothermal path onto a path with temperature variations. Following this variable temperature path results in a temperature profile in the initial steam-oil region upstream of the trailing upstream intermediate discontinuity. The portion of the slow path that changes temperature is an example of a slightly spreading wave where the eigenvalues do not change significantly from the equal eigenvalue point to the saturation temperature. An example solution following this type of path is given in the next section.

4.2.5 Temperature Profile in the Steam-Oil Region

Solutions with temperature profiles in the steam-oil region are presented in this section. By continuing along the injection path past the equal eigenvalue point, the solution follows a path that decreases in temperature as the eigenvalues increase. This forms a spreading wave where the saturations, temperature and flow velocity are continuously changing upstream of the trailing upstream intermediate discontinuity.

The composition path for the Type 1 displacement with a temperature profile in the steam-oil region is illustrated by Figure 4.36 and outlined in Table 4.9. The new solution path, (Figure 4.36) compared with the the solution path in the original Type 1 displacement, (Figure 4.9) appears very different on a first examination. The original solution path in the steam oil region is very short and the path in the new solution is much different.

Label	Composition Point			T (K)	Flow Velocity	Wave Velocity	Type of Flow Region
	Saturations						
	Steam	Oil	Water				
A	1.00000	0.00000	0.00000	650.00	1.00000	0.000000	INJ → SPW
B	0.91681	0.09319	0.00000	650.00	1.00000	0.011266	EEP
C	0.74335	0.25665	0.00000	525.00	0.7712	0.011916	SPW → UID
D	0.39946	0.39680	0.20373	485.57	0.6948	0.040644	UID → ZCS
E	0.39946	0.39680	0.20373	485.57	0.6948	0.069397	ZCS → UID
F	0.00000	0.94757	0.52424	402.13	0.0434	0.069397	UID → INI
G	0.00000	0.94757	0.52424	402.13	0.0434		INI

Table 4.9: Composition path for the injection of 100% steam at 650 K into 94.8% oil and 52.4% water at 402.13 K with a temperature wave in the steam-oil region.

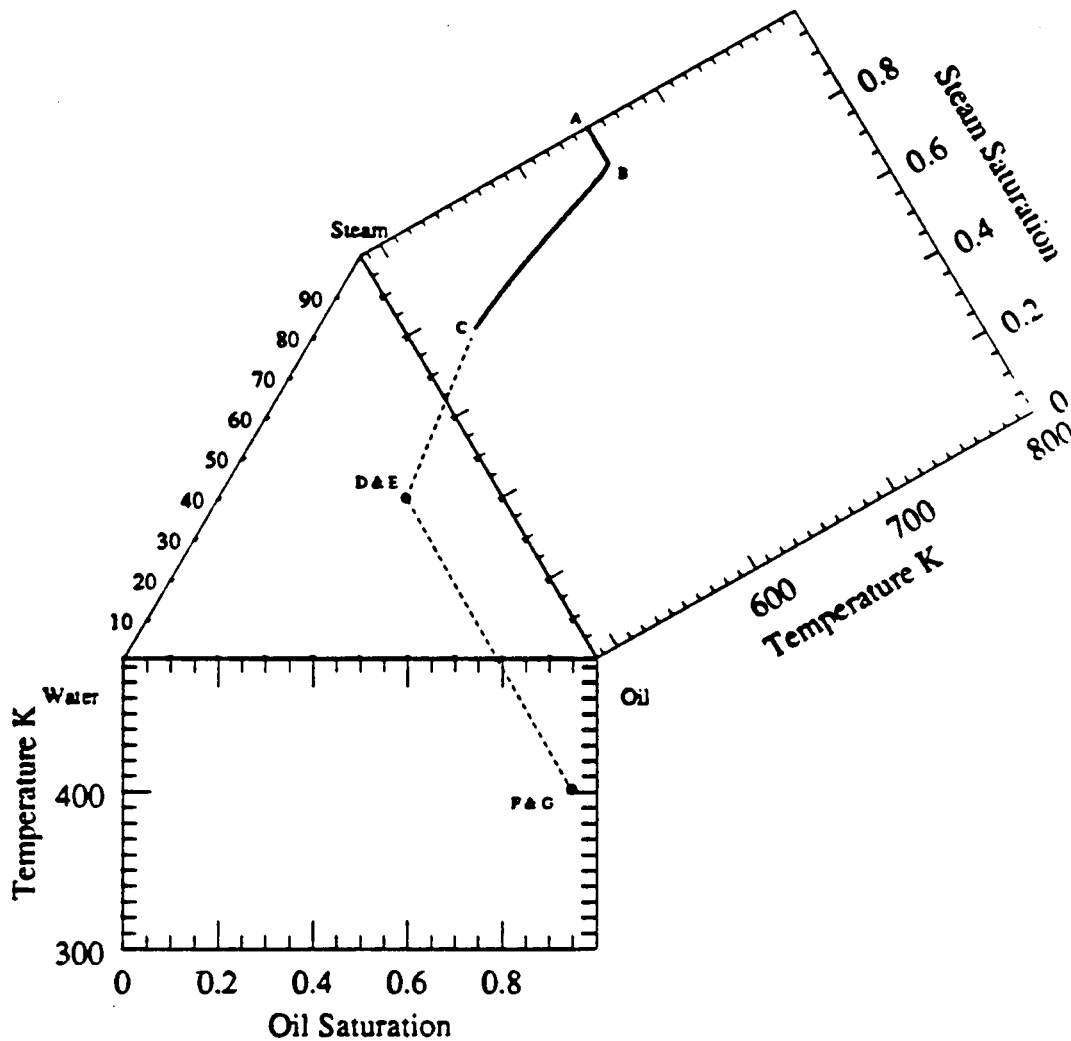


Figure 4.36: Composition path for the injection of 100% steam at 650 K into 94.8% oil and 5.24% water at 402.13 K with a temperature wave in the steam-oil region.

The key points to compare are the two landing points in the three phase region; see Table 4.10.

The landing point the the three-phase region in the original case is given by Point C1 and the landing point for the case with an initial temperature variation is Point D2. The variation between these points is very small. This leads to two important conclusions.

1. A small change in the three phase landing point can have a large effect on the solution path in the steam-oil region.
2. The effect of a temperature variation in the steam-oil region has a small effect on the saturation and temperature profiles downstream of the steam-oil region.

Label	Composition Point				Flow Velocity	Wave Velocity	Type of Flow Region
	Saturations			T (K)			
	Steam	Oil	Water				
Original Type 1 Composition Path							
A1	1.00000	0.00000	0.00000	650.00	1.0000	0.000000	INJ → SPW
B1	0.92000	0.08000	0.00000	650.00	1.0000	0.010777	SPW → UID
C1	0.41924	0.39087	0.18989	485.57	0.7058	0.010777	UID → ZCS
Original Type 1 Composition Path							
A2	1.00000	0.00000	0.00000	650.00	1.0000	0.000000	INJ → SPW
B2	0.91681	0.09319	0.00000	650.00	1.0000	0.011266	EEP
C2	0.74335	0.25665	0.00000	525.00	0.7712	0.011916	SPW → UID
D2	0.39946	0.39680	0.20373	485.57	0.6948	0.040644	UID → ZCS

Table 4.10: Comparison of composition paths for solutions with and without a temperature variation in the steam-oil region.

The reason that the temperature profile in the steam-oil region does not have a significant effect on the conditions in the three-phase region is seen clearly in the temperature and flow velocity profiles for the solution path in Figure 4.36. The temperature profile is shown in Figure 4.37. The portion of the temperature profile from Point B to Point C is the initial temperature variation. The temperature profile in the steam-oil region appears not as a continuous variation followed by a discontinuity, but as only a discontinuity from the injection temperature to the saturation temperature. This is because the eigenvalues along the spreading wave portion of the solution path do not significantly change along the solution from Point B to Point C.

The spreading wave in the steam-oil region is an excellent example of a slightly spreading wave. The eigenvalues from B to C increase only by 0.1%. Because the wave from B to C is slightly spreading, the combination of A → D in this example behaves almost exactly like the path A → C in the base case. Table 4.10 compares the three phase landing points for the base case and the solution that includes an initial temperature variation.

The reason for the steep profile is the high volumetric heat capacity of the matrix relative to the steam and oil. The stationary matrix is the reservoir for most of the heat that is input by the injected steam. This locks the majority of the heat into a stationary phase, and the little heat remaining in the fluids cannot flow downstream very rapidly. Higher porosity or lower matrix heat capacity spreads the initial wave out over a longer portion of the steam-oil region. This also moves the location of the equal eigenvalue point further downstream for a given amount of steam injected. Figures 4.40 and 4.41 demonstrate how the composition path in the steam-oil region changes as a function of the porosity. The effect of porosity is not linear, but closely follows the form found in the definition of the local heat content in Eq. 2.5.

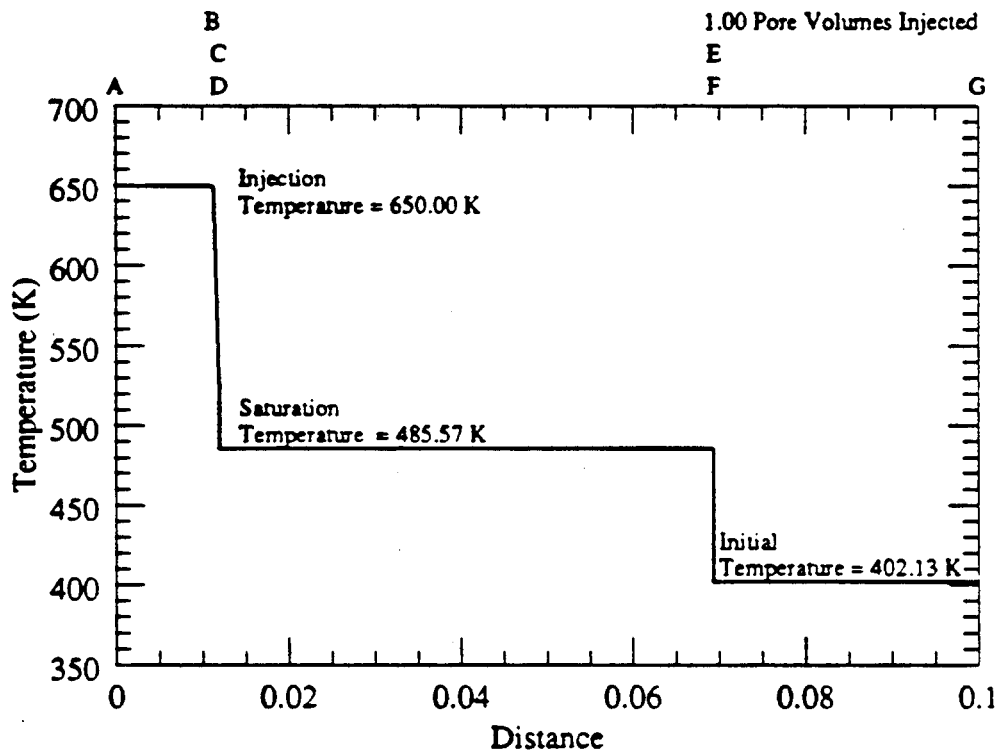


Figure 4.37: Temperature profile for the injection of 1.0 pore volumes of 100% steam at 650 K into 94.8% oil and 5.24% water at 402.13 K with a temperature wave in the steam-oil region.

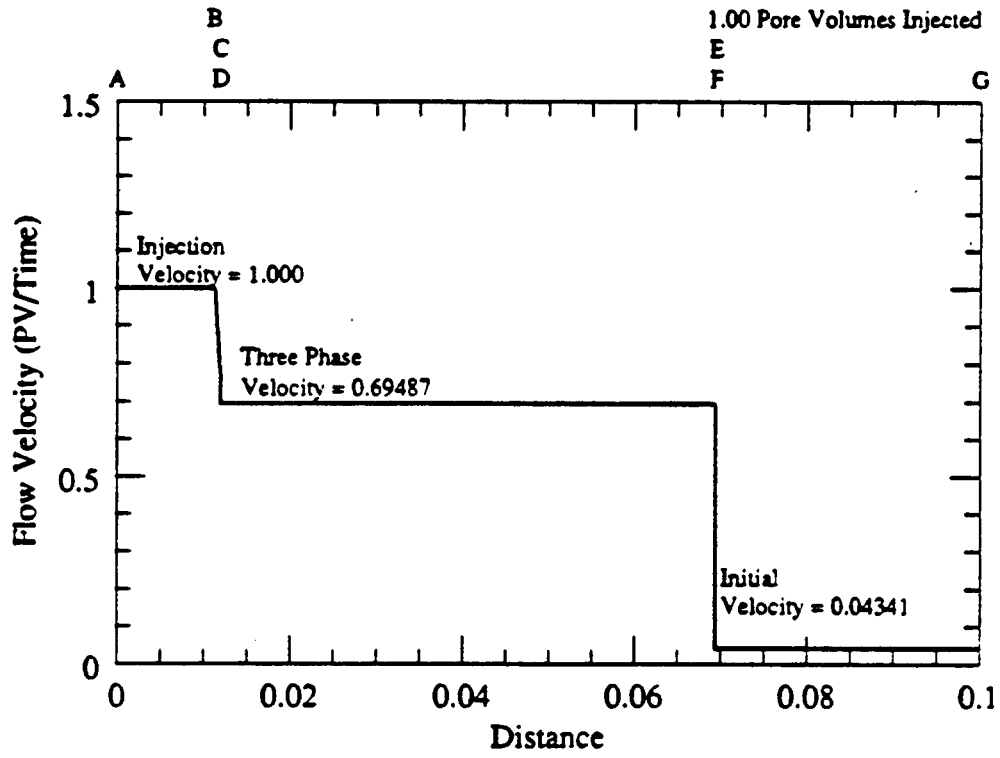


Figure 4.38: Flow velocity profile for the injection of 1.0 pore volumes of 100% steam at 650 K into 94.8% oil and 5.24% water at 402.13 K with a temperature wave in the steam-oil region.

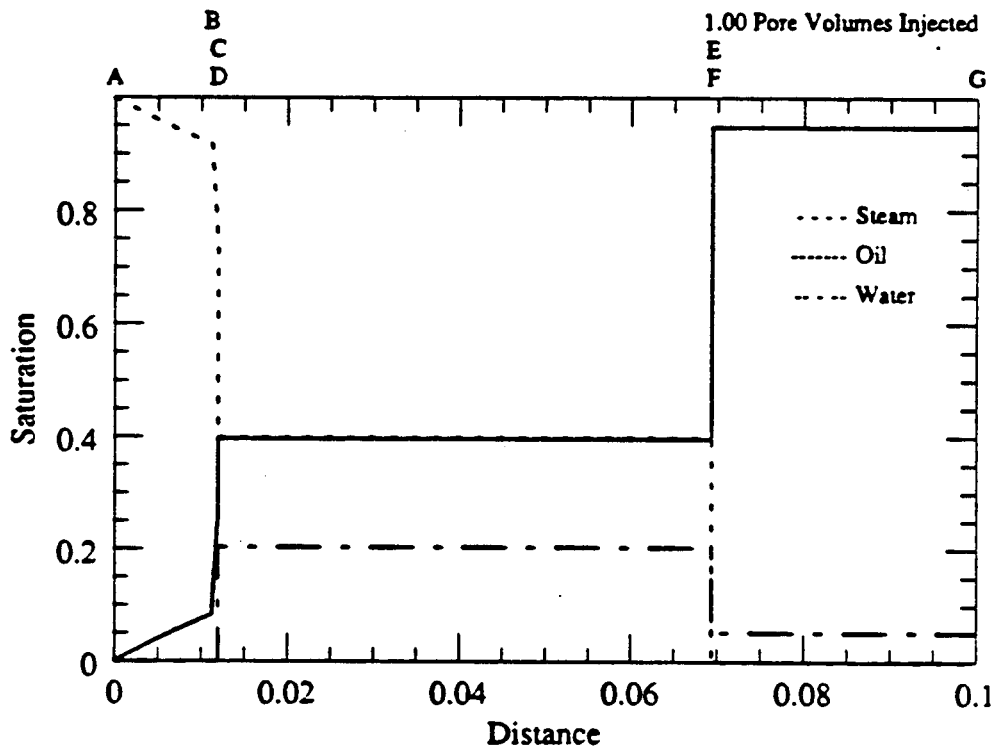


Figure 4.39: Saturation profile for the injection of 1.0 pore volumes of 100% steam at 650 K into 94.8% oil and 5.24% water at 402.13 K with a temperature wave in the steam-oil region.

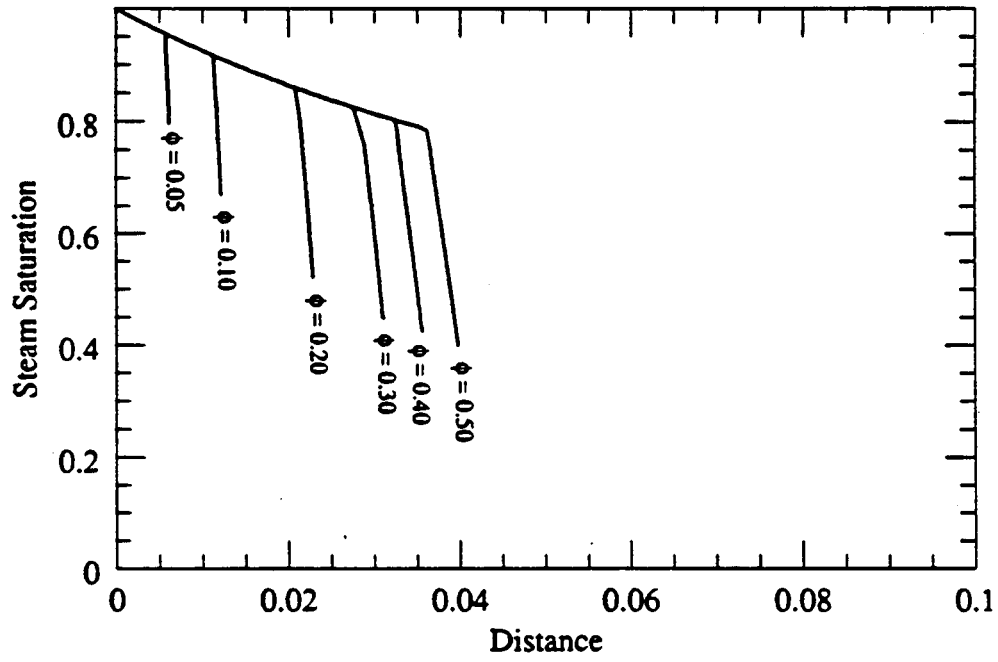


Figure 4.40: Saturation profiles in the steam-oil region for the injection of 1.0 pore volumes of 100% steam at 650 K into reservoirs with porosities from 0.05 to 0.5.

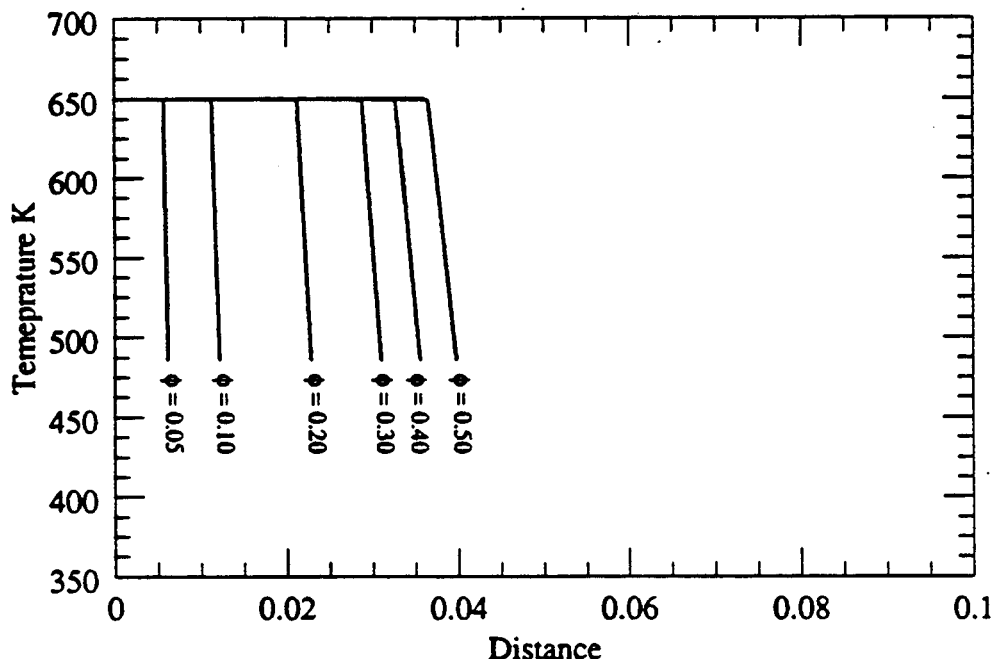


Figure 4.41: Temperature profiles in the steam-oil region for the injection of 1.0 pore volumes of 100% steam at 650 K into reservoirs with porosities from 0.05 to 0.5.

In the three-phase region, the effect of the thermal properties is not seen. This is identical to the heat capacity effect in the steam-water problem in §4.1. The thermal properties of the matrix did not effect the saturation profile in the two-phase, isothermal region. This is also the case in the three-phase region for this system. Because there is no enthalpy transfer in the three-phase region, the thermal properties of the matrix such as density, heat capacity and porosity do not affect the solutions.

4.2.6 Solutions with Viscous Oils

Steam injection is extensively used in the recovery of heavy oils. The solutions for two "heavy" oils are presented in this section. The oils are modified by increasing the viscosity from the base case. Heavy Oil #1 has a viscosity that is 200 times higher than the base case oil for the entire temperature range. Heavy Oil #2 has a higher viscosity at the initial conditions but a greater dependence on the temperature. This stronger temperature effect lowers the viscosity to near that of the base oil at injection conditions. Figure 4.42 shows the viscosities of the base case oil, the two heavy oils and the two water phases against the temperature. The discontinuity in the steam-water curve occurs at the saturation temperature of 485.57 K at 2.0 MPa.

Composition points demarking the boundaries of the different flow regions are given in Table 4.11 and the composition path is shown in Figure 4.43. The composition path shown in Figure 4.43 is much more detailed than for the composition paths for the lighter oil (see Figures 4.9, 4.23, 4.27, and 4.32). In the steam-oil region, there is a portion of the path that follows along the isothermal portion of the path from Point A to Point B. At Point B there is an equal eigenvalue point where the solution continues along the slow path. After Point B, continuing along the slow path to Point C lowers the temperature from the injection value of 650 K to 588 K.

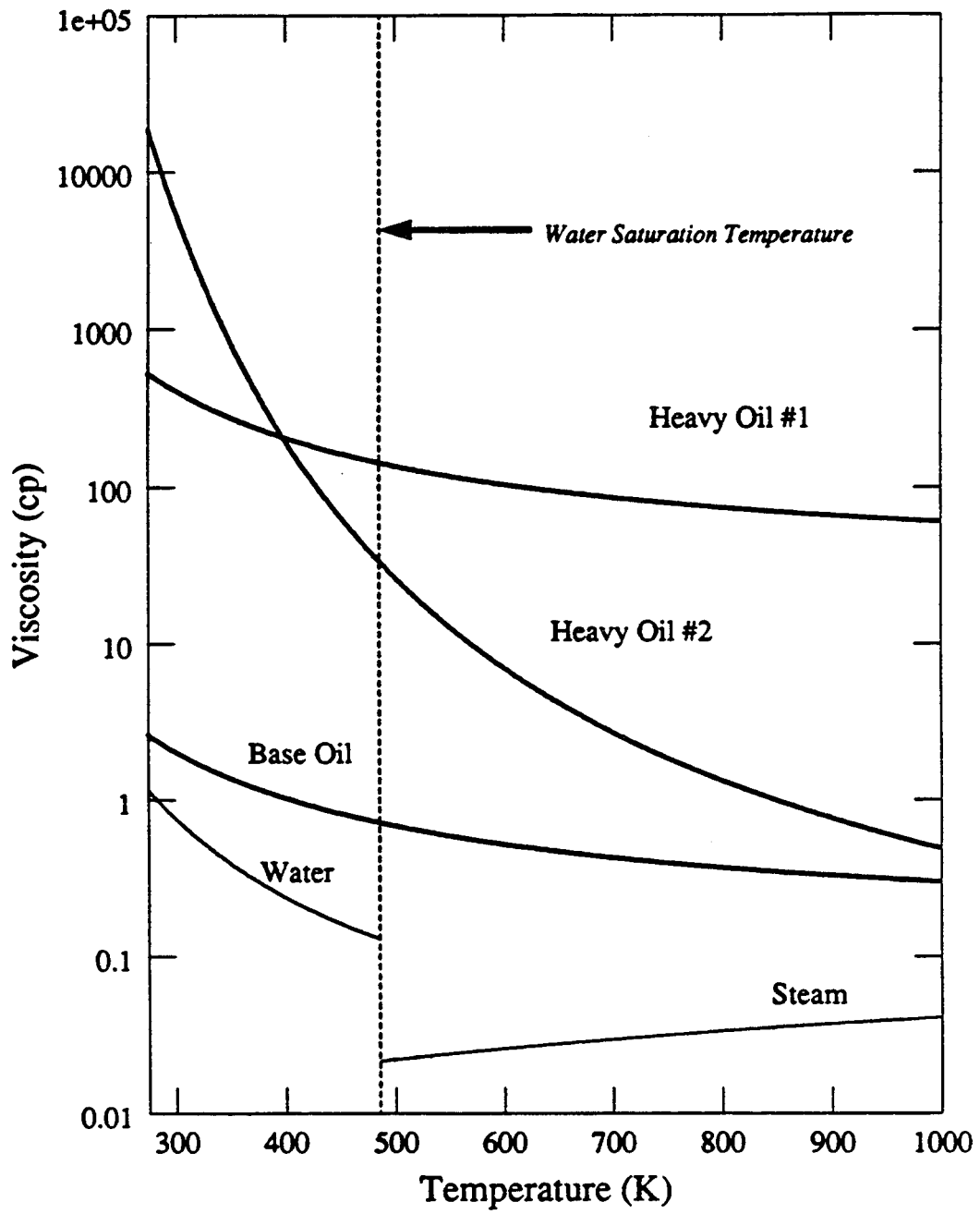


Figure 4.42: Viscosities for water, steam, and three different oils as a function of temperature from 275 K to 1000 K.

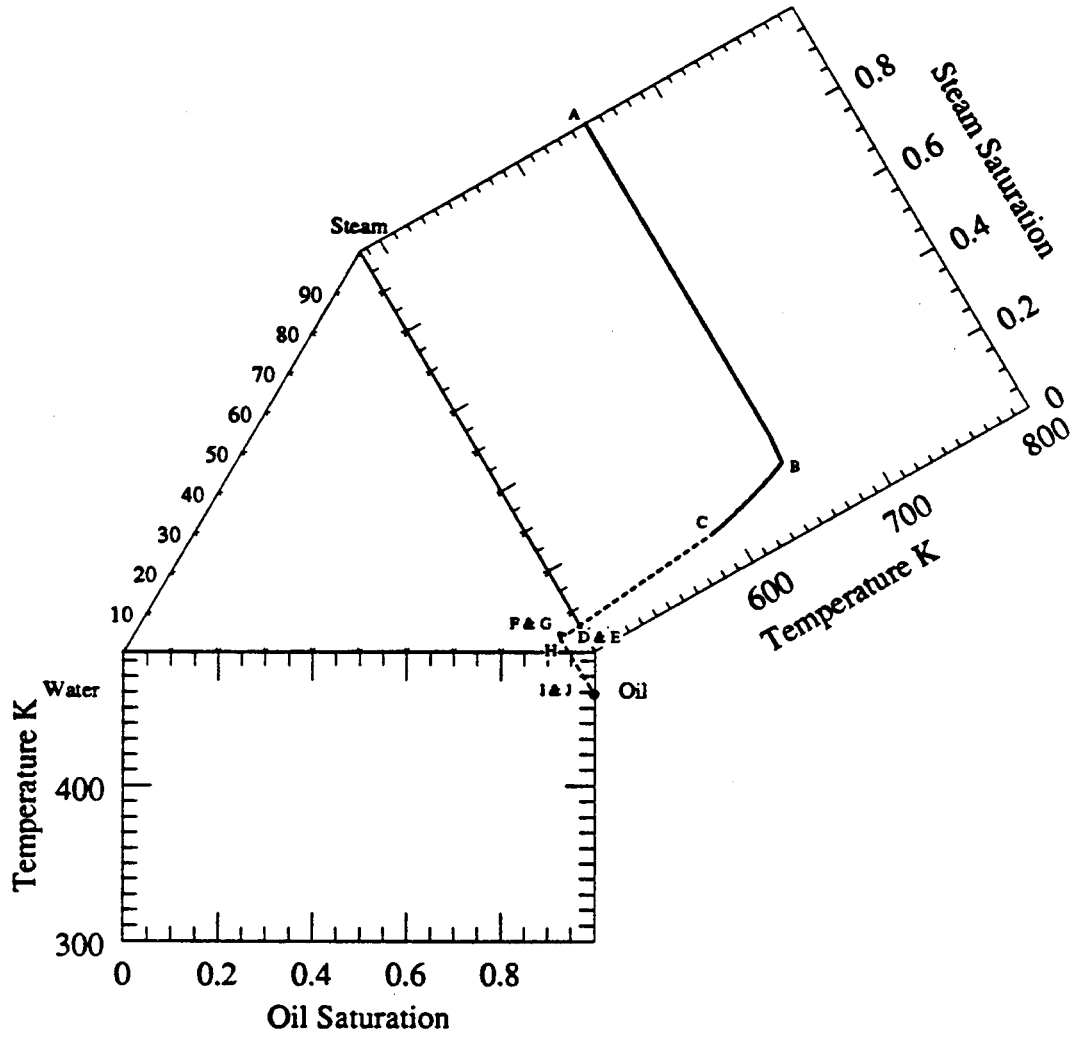


Figure 4.43: Composition path for the injection of 100% steam at 650 K into 99.9% Heavy Oil #1 and 0.1% water at 458.95 K.

Another difference is that the location of the equal eigenvalue point, represented by Point B on Figure 4.43 and Table 4.11, has a much lower steam saturation than with the light oils (see Table 4.9 for example). This result is expected. The less favorable mobility ratio causes the steam to quickly override or channel through the heavier oil. For a given injection volume of steam, the steam saturation near the injection end will be much lower than in the case of the lighter oil. The steam will be "spread" over a larger volume of the system, reducing the local saturation.

Label	Composition Point				Flow Velocity	Wave Velocity	Type of Flow Region
	Saturations			T (K)			
	Steam	Oil	Water				
A	1.00000	0.00000	0.00000	650.00	1.00000	0.000000	INJ → SPW
B	0.22000	0.78000	0.00000	650.00	1.00000	0.00565	SPW → UID
C	0.09651	0.90349	0.00000	588.00	0.88813	0.006054	UID → ZCS
D	0.043058	0.915853	0.04109	485.57	0.69682	0.006054	ZCS → SPW
E	0.043058	0.915853	0.04109	485.57	0.69682	0.012700	SPW → ZCS
F	0.047199	0.899429	0.053372	485.57	0.69682	0.016852	ZCS → SPW
G	0.047199	0.899429	0.053372	485.57	0.69682	0.053628	SPW → UID
H	0.027784	0.914043	0.058173	485.57	0.69682	0.156870	UID → INI
I	0.00000	0.998536	0.001464	458.95	0.01836	0.156870	UID → INI
J	0.00000	0.998536	0.001464	458.95	0.01836		INI

Table 4.11: Composition path for the injection of 100% steam at 650 K into 99.9% Heavy Oil #1 and 0.01% water at 458.95 K.

In the three phase region, the heavy oil solution shows the Type 4 wave pattern discussed in Table 4.5. There is a spreading wave from Point E to Point H that trails the central zone of constant state. Another spreading wave precedes the central zone of constant state, given by the path from Point G to Point H. The major difference from the light oil cases is that the composition changes along these two waves are very small. The changes in the hodograph variables along the spreading waves are more restrictive in the heavy oil solutions. Only a small corner of the three phase region has flow characteristics that permit passage from the steam-oil region through the three phase region and into the water-oil region.

The upstream spreading wave, Point E to Point F, follows the slow path in the three phase region. The direction of the slow path causes a change in the oil saturation. Due to high oil viscosity, small changes in the oil saturation rapidly bring the composition to that of the central zone of constant state.

The downstream spreading wave, Point G to Point H, follows the fast path. This path closely parallels the lines of constant oil saturation. The fast path is spread over a longer region for the same reasons that the trailing spreading wave is shortened. The changes in water and steam saturation have less effect on the fractional flows as the saturations of the steam and water change. This causes the spreading wave to take a longer time reaching the conditions at the leading shock than for the base case.

The leading shock must be downstream of the initial spreading wave and must have enough water flowing across the shock. These two requirements tend to push the leading shock further and further downstream. As the the temperature at the initial conditions increase, the velocity of the leading shock must also increase. This leads to faster leading shocks for the displacement of Heavy Oil #1.

The saturation profile for the case of Heavy Oil #1, shown in Figure 4.44, is also very different from the light oil counterpart, Figure 4.33. In the case of the heavy oil, the initial steam-oil region, from Point A to Point C, is much shorter and the saturation changes much greater than in the light oil case. The shape and size of the steam oil region verifies the observation made concerning the steam

override with the heavy oils. With the high mobility ratio the steam quickly flows downstream, causing the shorter initial steam-oil region, and spreads out over a larger portion of the reservoir, causing a larger three phase region.³

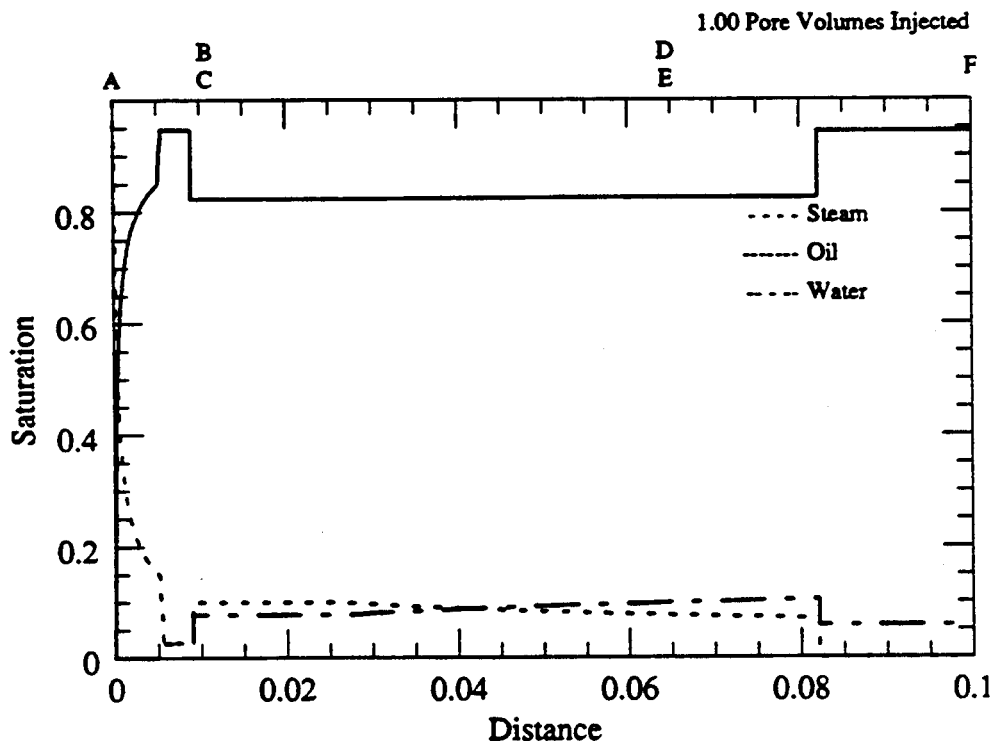


Figure 4.44: Saturation profile for the injection of 100% steam at 650 K into 99.9% Heavy Oil #1 and 0.1% water at 458.95 K.

On the other hand, the temperature profile, illustrated in Figure 4.45, and the flow velocity profile shown in Figure 4.46 show the same behavior as the case of the light oils. The major difference is in the location of the leading and trailing temperature shocks. The leading shock has a higher velocity in the case of the heavy oil and the trailing shock a slower velocity. Again, the high shock velocity is attributable to the high mobility steam bypassing the steam-oil region and spreading over the three phase region.

As in the case of the light oils, the non-isothermal portion of the steam oil region, from Point B to Composition C in Figure 4.45 appears as an extension of the actual phase change shock between Point C and Point D. The portion of the solution path that follows along the non-isothermal section in the steam-oil region is always seen in these solutions. The reason is that the wave velocity at the point where the two eigenvalues are equal is too small to satisfy the material and primarily the heat balance across the shock. The minimum velocity of an intermediate discontinuity is faster than the equal eigenvalue point. In order to satisfy the heat balance, the system must cool towards the saturation temperature before a suitable heat balance across the trailing shock is possible.

³Note the X-axis scale change between the figures given in the light oils 4.11, 4.26, 4.28, and 4.33 to that in Figure 4.44.

The viscosity of Heavy Oil #2 is more dependent on the temperature than the base oil or Heavy Oil #1. The composition path for a displacement of Heavy Oil #2 with the same injection and initial conditions as the light oil, Type 4 displacement shown in Figures 4.32—4.35 and outlined in Table 4.8 is presented in Figures 4.47—4.50 and Table 4.12.

Label	Composition Point				Flow Velocity	Wave Velocity	Type of Flow Region
	Saturations			T (K)			
	Steam	Oil	Water				
A	1.00000	0.00000	0.00000	650.00	1.00000	0.000000	INJ → SPW
B	0.65350	0.34650	0.00000	650.00	1.00000	0.008822	SPW → UID
C	0.11901	0.88099	0.00000	526.00	0.77235	0.009613	UID → ZCS
D	0.052518	0.88117	0.06632	485.57	0.69358	0.009613	ZCS → SPW
E	0.05251	0.88117	0.06632	485.57	0.69358	0.027298	SPW → ZCS
F	0.05264	0.87995	0.06741	485.57	0.69358	0.028005	ZCS → SPW
G	0.13794	0.70626	0.15580	485.57	0.69358	0.028005	SPW → UID
H	0.13794	0.70626	0.15580	485.57	0.69358	0.086357	UID → INI
I	0.13657	0.70645	0.15698	458.95	0.69358	0.088938	UID → INI
J	0.00000	0.94420	0.05579	433.89	0.02667	0.088938	INI
K	0.00000	0.94420	0.05579	433.89	0.02667	0.119812	UID → ZCS
L	0.00000	0.91321	0.08679	433.89	0.02667	0.197647	SPW → UID
M	0.00000	0.88123	0.11876	433.89	0.02667	0.197647	UID → INI
N	0.00000	0.88123	0.11876	433.89	0.02667		INI

Table 4.12: Composition path for the injection of 100% steam at 650 K into 88.1% Heavy Oil #2 and 11.9% water at 433.79 K.

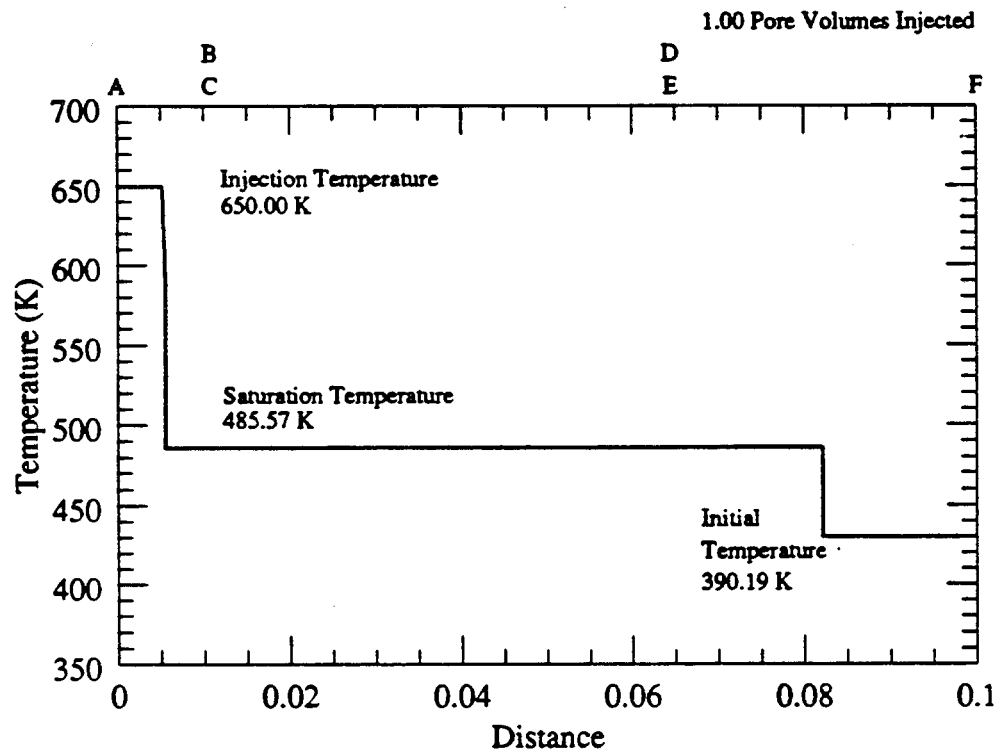


Figure 4.45: Temperature profile for the injection of 100% steam at 650 K into 99.9% Heavy Oil #1 and 0.1% water at 458.95 K.

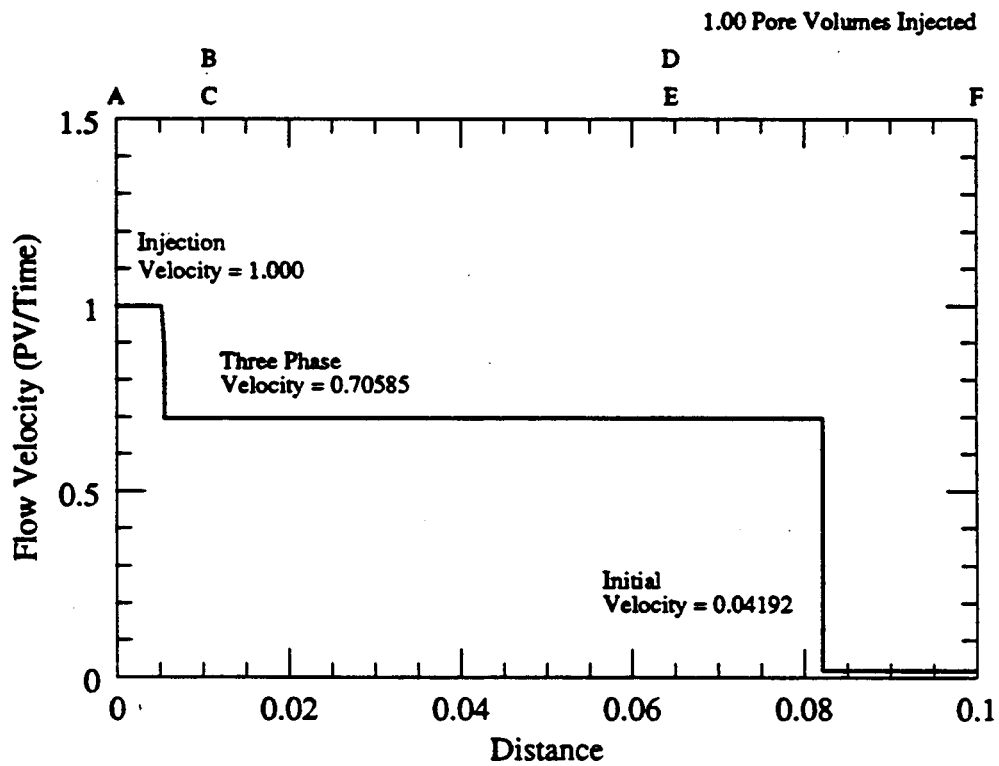


Figure 4.46: Flow velocity profile for the injection of 100% steam at 650 K into 99.9% Heavy Oil #1 and 0.1% water at 458.95 K.

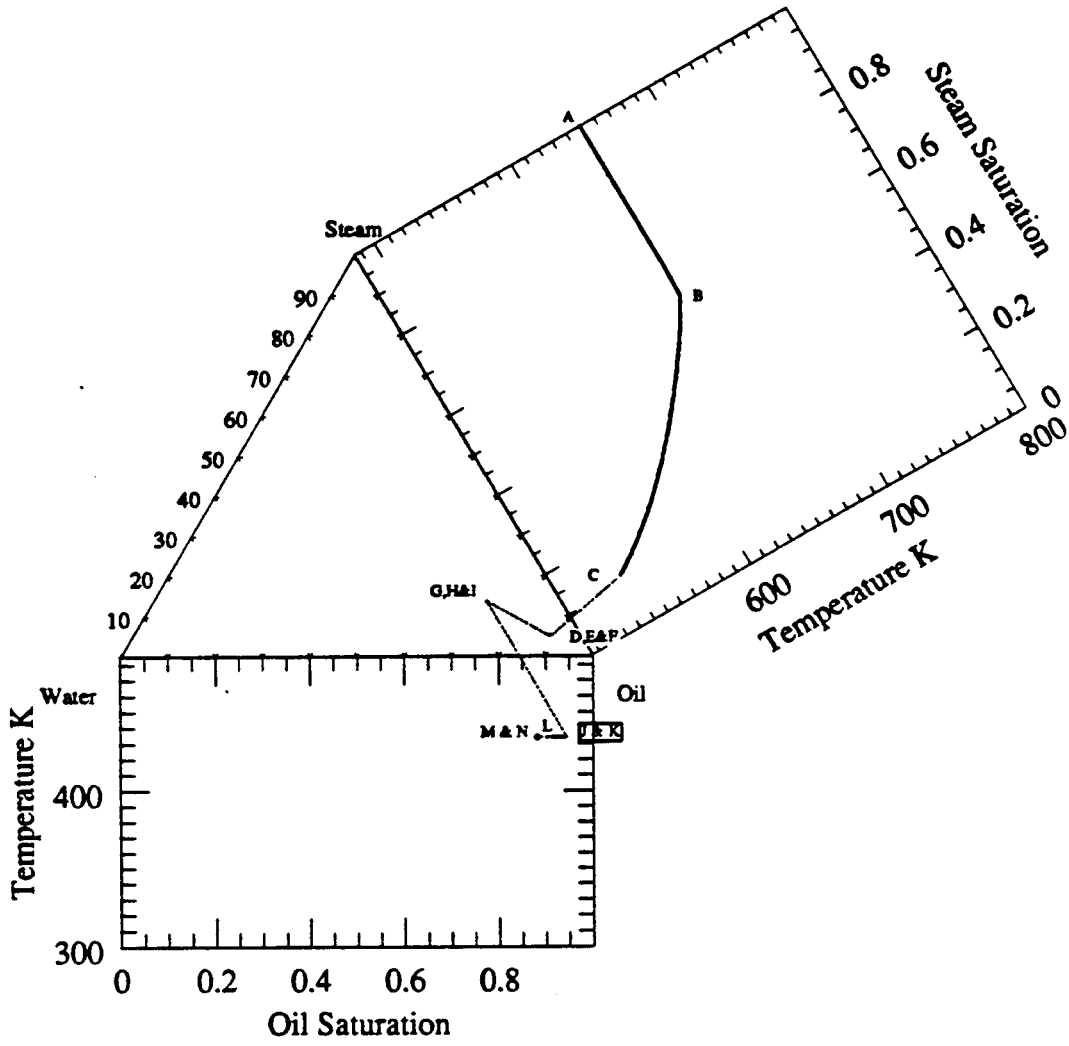


Figure 4.47: Composition path for the injection of 100% steam at 650 K into 88.1% Heavy Oil #2 and 11.9% water at 433.79 K.

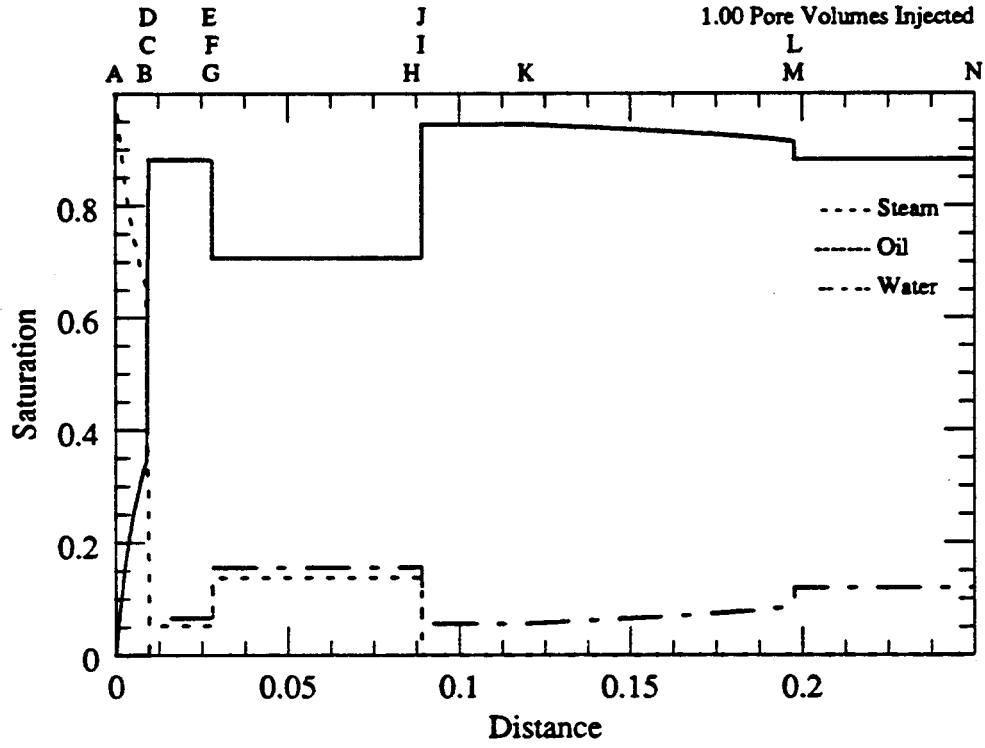


Figure 4.48: Saturation profile for the injection of 100% steam at 650 K into 88.1% Heavy Oil #2 and 11.9% water at 433.79 K.

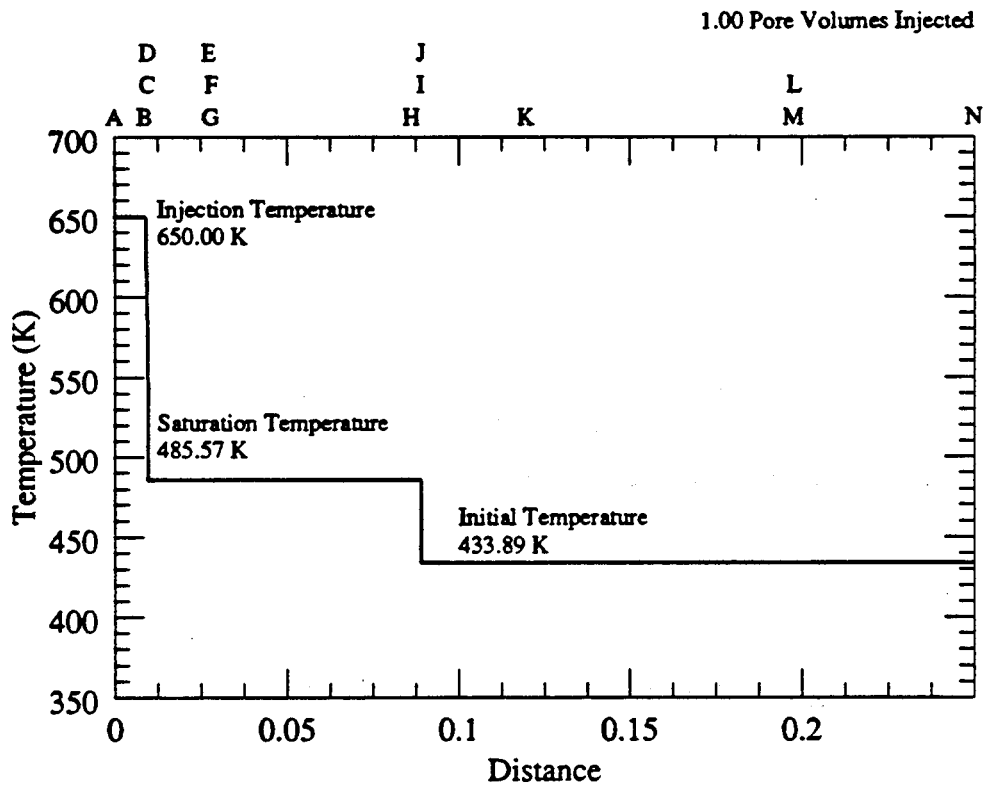


Figure 4.49: Temperature profile for the injection of 100% steam at 650 K into 88.1% Heavy Oil #2 and 11.9% water at 433.79 K.

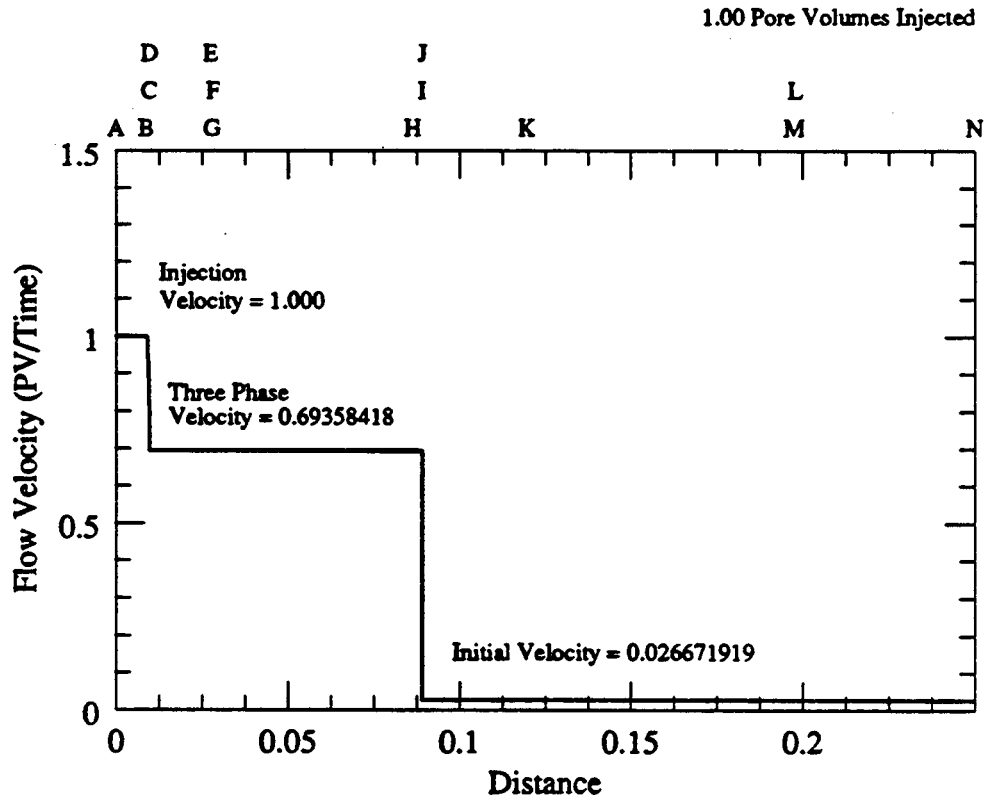


Figure 4.50: Flow velocity profile for the injection of 100% steam at 650 K into 88.1% Heavy Oil #2 and 11.9% water at 433.79 K.

The most direct comparison between the heavy oil and light oil case can be made by comparing the saturation profiles of the light oil case, Figure 4.33, and the heavy oil case, Figure 4.48. Beginning at the injection conditions and working downstream there is an immediate difference in the initial steam-oil region. Looking at Figure 4.48, the solution follows the slow path from the injection conditions at Composition A to the equal eigenvalue point, B. From Point B to Composition C, the solution continues along the slow path. This region is characterized by a slightly spreading wave carrying the solution from the injection temperature toward the saturation temperature. This path also changes steam saturation at the same time the temperature is changing. The rapidly changing oil viscosity helps to lengthen the section of the solution that travels along the non-isothermal path, from Point B to Point C. The increased oil viscosity also raises the oil saturation for a given velocity or temperature along the path from B to C.

The shape of the steam-oil region resembles the steam-oil region of the Heavy Oil #1 displacement, Figure 4.44. The same analysis that applied in the case of Heavy Oil #1 also applies in this case. The high mobility steam rapidly moves downstream of the two phase region and spreads over the central three phase region that exists between Point D and Point I in Figure 4.48.

At Point C, an upstream intermediate discontinuity carries the solution into the three-phase region at Point D. There are two restrictions that apply to the choice of the jumping point, C. If the eigenvalue at Point C is too low, there will be no solution in the three-phase region that satisfies the material and energy balances across the shock. A larger temperature jump across a shock results in a slower shock velocity; for some very slow shock velocities, the temperature jump is so large that the resulting tem-

perature must be less than the saturation temperature. In these cases there is no solution in the three-phase region.

The trailing phase transition shock is much slower than in the profiles with the base oil; as shown in Figures 4.11, 4.26, 4.28, and 4.33. The equal eigenvalue point represents the point where the Buckley-Leverett saturation velocity, $(\partial f_v / \partial S_v)$, is equal to the change in fractional increase in enthalpy transport. This is given by,

$$\frac{\partial f_v}{\partial S_v} = \frac{\partial}{\partial S_v} \left(\sum_{i=1}^{n_r} H_i f_i \right) \quad (4.27)$$

The velocity of the non-isothermal path is relatively independent of the oil viscosity. At a given oil saturation, the velocity of the isothermal path decreases as the oil viscosity increases. Therefore, to reach a given velocity, the oil saturation must be increased dramatically.

In the three-phase region, a zone of constant state, that extends from Point D to Point E, couples the shock velocity to the slow eigenvalue at the three-phase landing Point D. The solution must be able to follow the slow path at the trailing end of the three-phase region. Were the velocity on the slow path, as represented by the smaller eigenvalue, to be less than the shock velocity, this would restrict the solution to only fast paths in the three-phase region. The problem with this is that in order to move between two arbitrary points in the three-phase region, the solution must first travel along the slow path. (See the discussion on page 52).

After the zone of constant state a spreading wave carries the solution from E to Composition F. The change in composition along this portion of the solution is barely noticeable. Without this small change, the solution cannot reach the desired initial temperature. As the length of the spreading wave from E to F increases, lower and lower initial temperatures result for a fixed initial water saturation.

Continuing along the slow path past Composition F, the eigenvalues will eventually reach a maximum value and begin to decline. The velocity constraint sets a limit on the distance that the integration along the slow path can continue without introducing a discontinuity in the form of a self-sharpening wave. This self-sharpening wave is found by selecting a point on the slow path before the small eigenvalue reaches its maximum value. This selected point is at Composition F.

At Point F an upstream intermediate discontinuity carries the solution to Composition G. The shock is necessary to keep the initial conditions in the allowable hodograph space. For the solutions that switch to a fast path before the shock, the velocity of the fast path or the oil saturation on the path is too large. When the oil saturation is too large, the shock solution results in a composition with a negative water saturation. Thus, when the eigenvalue is too fast, the solution results in a initial temperature that is not realizable due to physical considerations, *e.g. below the freezing temperature of water.*

The shock from F to G carries the solution to the other side of the maximum point, much like the a leading Buckley-Leverett shock carries the solution past the saturation where $(\partial f_w / \partial S_w)$ is a maximum, to the initial conditions. On this side of the maximum point, the velocity of the fast path and the oil saturation are lower and give solutions that remain in the allowable hodograph space. The distance between the endpoints of the shock depends on how close the jumping point is to the maximum velocity point. The closer the jumping point, the closer the landing point is on the other side, and the closer the shock velocity is to the maximum. Because the self-sharpening wave is an upstream intermediate discontinuity, the shock velocity matches the eigenvalue of the upstream point, Composition F, and closely matches the eigenvalue of the downstream point.

At Point G, a second zone of constant state, often referred to as the "central" zone of constant state, couples the shock velocity to the wave velocity at H. The zone of constant state represents the path

switch from the slow path at G to the fast path at H. There must be a path switch at this point due to the behavior of the compositions that form a self-sharpening wave. Jeffrey (1976) showed that the velocity of the discontinuity formed by a self-sharpening wave must be intermediate between the eigenvalues of the upstream and downstream composition points. Since we have a self-sharpening wave, the small eigenvalue at the downstream composition (Point H) must be slower than the shock velocity. This requires that the solution, on arriving at Composition H switch to the fast path.

A spreading wave is attached ahead of the zone of constant state. This spreading wave is also small and does not noticeably change the composition point. Along the path from H to I, the spreading wave takes the solution to an upstream intermediate discontinuity that carries the solution out of the three-phase region into the water-oil region. The eigenvalues along the fast path change very rapidly and the eigenvalue along this path must remain in a narrow range if the downstream temperature is to remain below the saturation temperature. As the solution turns out, the length of the integration along this path is short and the eigenvalues change very little.

Comparing the three phase regions of Figure 4.33 and Figure 4.48 shows a striking difference in the shape of the saturation profiles in this region. The spreading wave in the heavy oil displacements are very small, both in real and hodograph space. The leading spreading wave, from Point H to Point I in Figure 4.48 has a wave velocity of 0.086357 at the trailing edge of the wave and only 0.088938 at the leading edge of the wave. This means that 387.5 pore volumes of steam would need to be injected before this wave occupied one pore volume of displacement space. In contrast, the leading spreading wave in the base oil case, Point F to Point G in Figure 4.33 has a wave velocity of 0.076318 at the trailing edge and a velocity of 0.098756 at the leading edge. This requires only 44.6 pore volumes of injected steam for this wave to occupy the same single pore volume.

The physical interpretation for the narrow spreading waves in the heavy oil case is founded in the three phase relative permeability model. In the region of three-phase space, where all phases can flow, the fractional flow derivatives, $(\partial f_o / \partial S_o)$ and $(\partial f_o / \partial S_w)$, are small and do not change much with saturation. In other words, because the oil is more viscous, it remains relatively immobile over a larger range of saturations than in the lighter oil case.

The upstream intermediate discontinuity at I takes the solution into the water-oil region, Point J. At Point J there is a path switch to the fast path in the water-oil region. This path switch follows Rule IV and is illustrated in Figure 3.3 This path switch takes the solution to Point K. The solution then travels along the fast path, forming a spreading wave between Point K to Point L. Finally, a leading upstream intermediate discontinuity carries the solution from the fast path at Point L to the initial conditions at Point M. This region of the solution resembles a traditional Buckley-Leverett displacement system with an unfavorable mobility ratio. The saturation profile is long and stretched out and the leading shock is small.

The water-oil region in the heavy oil case can be compared to the same region in the light oil displacement as shown in Figure 4.33 from Point H to Point I. There wave pattern is much more complex in the heavy oil case than the light oil case. As mentioned in §4.2.3, the eigenvalues in the water-oil region are all slower than those in the three phase region. This forces the leading phase change shock to jump directly to the initial conditions from the three-phase region. The highly adverse mobility ratio in the heavy oil case shown in Figure 4.48 does not have this restriction.

The eigenvalue on the fast past in the water-oil region is proportional to the derivative of the fractional flow of water with respect to the water phase saturation. This is the traditional Buckley-Leverett saturation velocity. In the nomenclature of this dissertation this can be written as,

$$\lambda_3 \propto \frac{\partial f_w}{\partial S_w} \tag{4.28}$$

When the mobility ratio is close to unity this derivative is small, but when the mobility ratio is high the derivative is also large. For the case of Heavy Oil #2 the derivative is large enough to exist downstream of the leading phase change shock, between Point I and Point J.

The wave velocity on the fast path in the water-oil region reaches a maximum value before reaching the initial conditions. This is similar to the situation that created the self-sharpening wave between Compositions F and G in the three-phase region. The final portion of the solution is obtained by calculating an isothermal upstream intermediate discontinuity with downstream conditions that match the desired initial conditions. This shock was found at composition L. Between K and L, a spreading wave along the fast path moves the solution between the desired points.

Comparing the temperature profiles shown in Figure 4.34 and the profile for the heavy oil case given in Figure 4.49 show the same basic pattern. The only differences are in the location of the phase change shocks. There is a portion of the path that remains at the injection conditions until the temperature shocks to the three-phase saturation temperature, 485.57 K, and remains at that temperature throughout the three-phase region. The temperature jumps from the three-phase saturation temperature to the initial conditions at the leading phase change shock.

In the heavy oil case, the steam cannot build up any saturation near the injection conditions because of its high mobility relative to the heavier oil phase. This causes the trailing phase change shock to be slower in the heavy oil solution. The leading phase change shock is only slightly faster in the light oil case. The difference in shock velocity is due primarily to the slower flow velocity on the two-phase side of the shock in the heavy oil case. The heavy oil case actually has less steam condensing across the shock, but the volume lost is a greater portion of the water phase in the heavy oil case. This volume change compensates for the increased energy transfer in the light oil case.

A closer examination of the solution paths in the steam-oil region reveals a subtle difference between the light oil solution and the heavy oil case. In the light oil case, the temperature remains at the injection temperature from the injection conditions to the trailing phase change shock at Point B. In the heavy oil case, the path follows the isothermal slow path at the injection temperature between Point A and Point B. At Point B a path switch at the equal eigenvalue point takes the solution along the non-isothermal path between Point B and Point C. This portion of the path behaves much like the solutions described in §4.2.5. The non-isothermal portion of the path is a "slightly" spreading wave and behaves much like the extension of the trailing phase change shock that is shown between Point C and Point D.

The velocity profile for the heavy oil case is shown in Figure 4.50. As in the other solutions, the velocity profile mimics the shape of the temperature profile. The heavy oil solution follows this pattern. Again density changes due to temperature changes are the cause of the flow velocity variations and in the heavy oil case this relationship is maintained.

Summary

The steam-oil-water displacements presented in this section were calculated by applying the model to a different hodograph space in three separate regions. A central three-phase isothermal region is ahead of a trailing steam-oil region. A water-oil region, representing the initial conditions is ahead of the three-phase region.

The three regions are connected by a pair of phase transition shocks. These shocks have coincident temperature and saturation changes. Both shocks are intermediate discontinuities.

The trailing region is a steam-oil region. The solution path in this region follows along the slow path until reaching a phase transition shock. This shock separates the two-phase steam-oil region from the central three-phase region. The shock is an intermediate discontinuity with a velocity that matches the small eigenvalue on the upstream side of the shock.

The solution path follows along the eigenvector associated with the small eigenvalue for the entire steam-oil region. At some point along this path, an equal eigenvalue point changes the nature of the slow path from an isothermal path to a path that also has a temperature gradient.

Downstream of the equal eigenvalue point, the wave becomes a slightly spreading wave. For this reason, the portion of the path with a temperature change behaves like an addition to the phase transition shock. As a result, the saturation profiles downstream of the trailing phase transition shock are not effected by the temperature profile in the steam-oil region.

In the central three-phase region, the solution proceeds along the slow path until a path switch carries the solution onto the fast path. This path switch is seen as a central zone of constant state. The solution then travels along the fast path until the phase transition shock into the water-oil region.

Four wave patterns describe the displacements in the three-phase regions. These patterns are distinguished by the waves that precede and follow the central zone of constant state. Each of the two waves may either be a spreading or a self-sharpening wave, creating the four wave patterns.

The leading region is a water-oil region that remains at the initial conditions until a phase transition shock carries the solution into the three-phase region. The low flow velocity reduces the wave velocities in the water-oil region below the wave velocities in the three phase region, so an immediate jump to the initial conditions is required.

The effect of increasing oil viscosity changes the patterns in all three of the displacement regions. In the steam-oil region an increasing oil viscosity dramatically reduces the steam saturation on the upstream side of the phase transition shock. A related effect is to reduce the velocity of the phase transition shock and the equal eigenvalue point. This reduction is greater for the equal eigenvalue point. At very high mobility ratios no shocks between the steam-oil region and the three phase region are possible without a reduction in temperature, below the injection temperature.

In the three-phase region, compositions do not exhibit a large variation. The increased oil viscosity causes the oil phase to be virtually immobile in the three-phase region. The trailing spreading waves are shortened and the leading spreading waves are lengthened as compared to the less viscous oil.

When the trailing spreading wave changes into a self-sharpening wave at very high oil viscosities, this new self-sharpening wave creates an oil bank at the trailing end of the three-phase region. Physically this bank is formed as the mobile water and vapor phases move ahead of the immobile oil phase.

The water-oil region is effected by the increase in mobility ratio. The increased oil viscosity compared to the water phase increases the fractional flow derivative, $(\partial f_w / \partial S_w)$, and hence, the isothermal wave increases velocity until it is greater than the waves in the three-phase region. This results in spreading and self-sharpening waves in the water-oil region.

Two different displacement systems that include temperature variations have been examined by the method of characteristics. These systems have included the effects of temperature and flow properties. The final and most intricate effect is that of phase behavior. A third component that is partially miscible with the oil phase is introduced into the system. The next section discusses a displacement of oil and water by CO₂ and water at an elevated temperature. This represents a system that includes the interaction of phase behavior, temperature and flow properties in one series of displacements.

4.3 THREE COMPONENT - THREE PHASE SYSTEMS

The final example solution combines the effects of phase behavior, temperature variations and flow properties over the entire extent of the system. This problem is considerably more general than the previous systems. In this system, there is no natural temperature plateau that was present in the oil-water systems. Since the three components are allowed to exist in all three phases, the only phase restriction is that in the three phase region, for a given temperature, the compositions of the three separate phases are fixed.

The section begins with a description of the problem and the formulation of the general eigenvalue problem, given by Eq. 2.26, to this specific system. Preliminary results for a specific system are given along with the path topology. Final solution profiles and composition paths are not presented due to computational difficulties. The majority of the problems stem from the calculation of the phase transition shocks. The section concludes with a discussion of the problems trying to find solutions for a system where phase behavior, temperature variations and flow properties are always interacting over the length of the displacement system.

4.3.1 Problem Formulation

The system examined in this section is the injection of CO₂ and water into a reservoir filled with a heavy oil. The third system examined adds the effects of phase behavior to the interactions of temperature and flow properties studied in the previous sections. The phase behavior for this system is complex. The system has three distinct phases at low temperatures:

1. A vapor phase that contains mostly CO₂, but can also contain water vapor and trace amounts of the oil component. As the temperature is increased, the concentration of water in the vapor phase increases until the vapor temperature of the water component is reached. At this temperature, the system becomes a two-phase system. A vapor phase containing CO₂ and water coexisting with a liquid phase containing oil, water and small amounts of CO₂.
2. An oleic or upper liquid phase. This phase contains mostly the oil component. At lower temperatures the CO₂ is able to dissolve into the oil and at higher temperatures significant amounts of the water are present in the hydrocarbon phase.
3. An aqueous phase that is almost pure water. Small amounts of CO₂ are also present in the water phase, but no oil enters the aqueous phase.

A typical phase diagram for the system at lower temperatures is shown in Figure 4.51.

At higher temperatures, the water moves into the vapor phase until the saturation temperature of the water is reached. Above this temperature, the three phase triangle disappears and the vapor-upper liquid region extends across the entire diagram. The phase diagram for these conditions is shown in Figure 4.52.

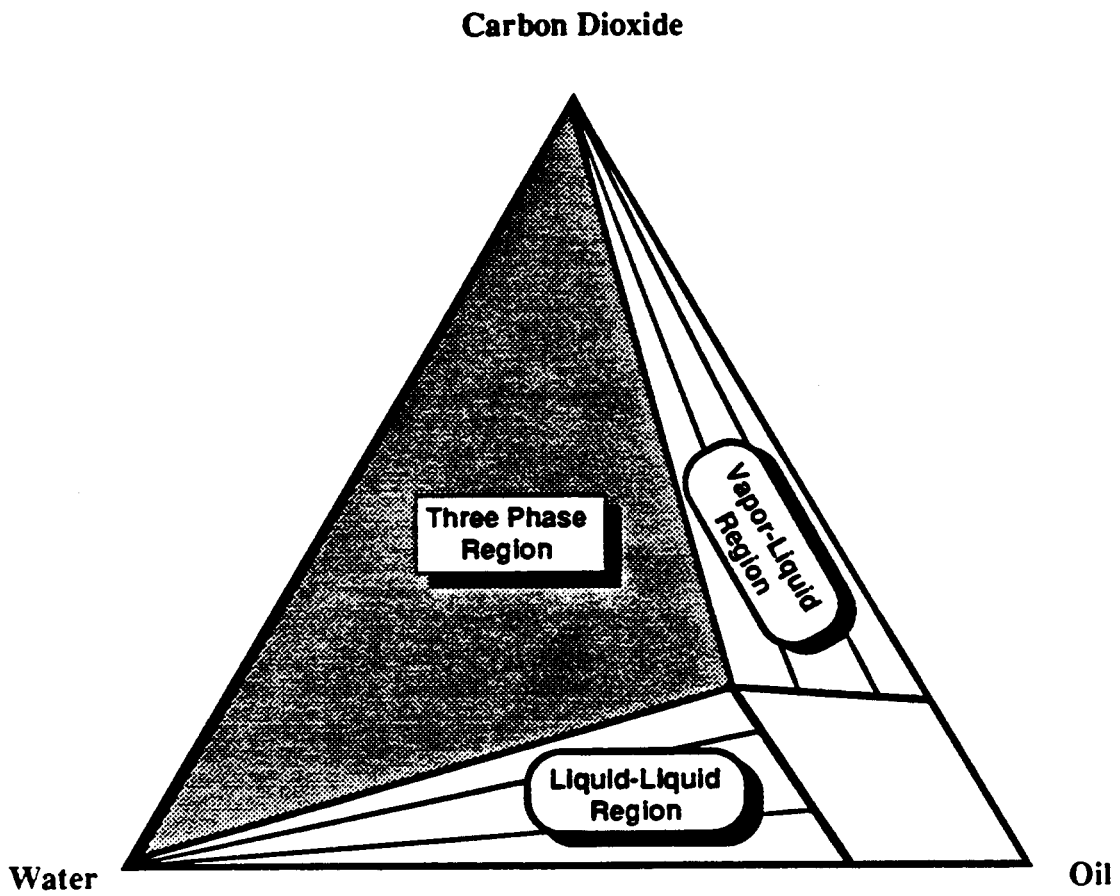


Figure 4.51: Phase diagram for a system of CO₂-oil-water at temperatures below the saturation temperature of water.

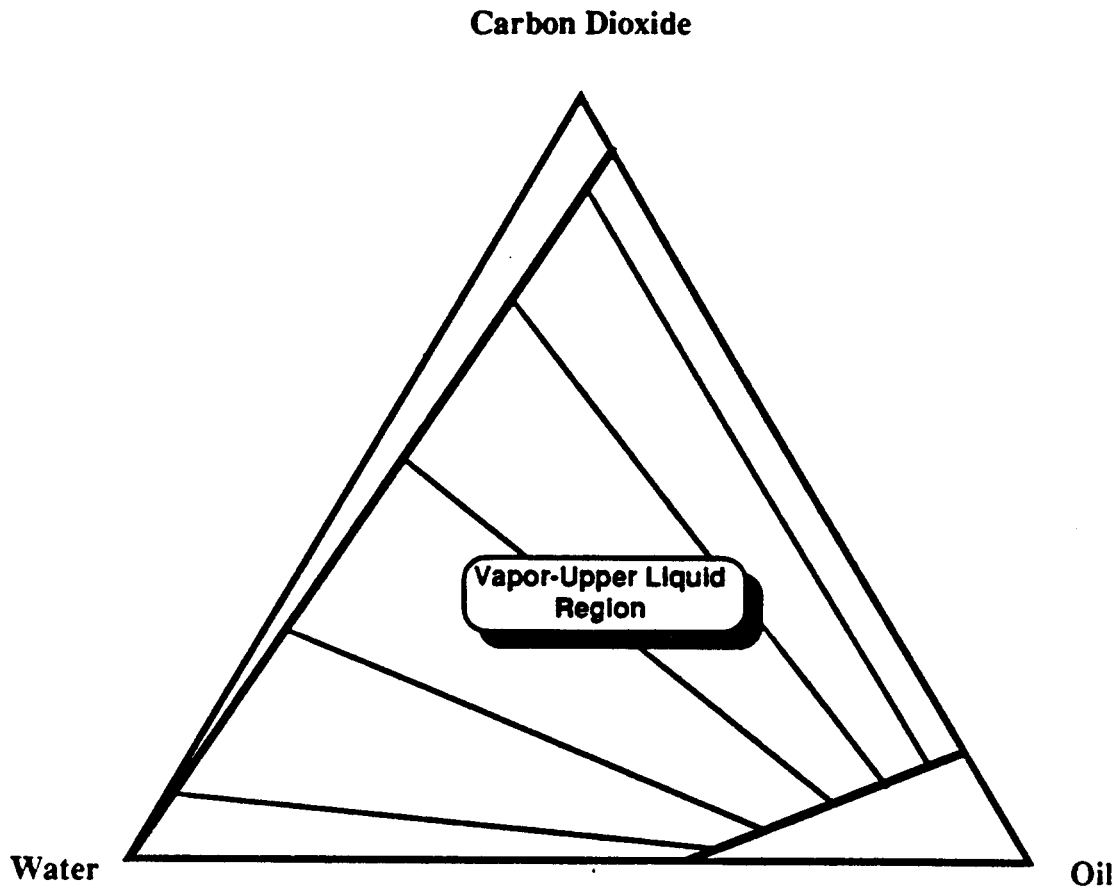


Figure 4.52: Phase diagram for a system of CO₂-oil-water at temperatures below the saturation temperature of water.

The saturations of the phases cannot be used for the hodograph variables due to the phase behavior. When the components are free to transfer between phases, the amount of each component in a given phase changes over the length of the displacement. The hodograph variables for this system are mole fractions of the CO₂ and the oil, the temperature and the flow velocity. The general eigenvalue problem described by Eq. 2.26 reduces to a 4x4 system given by,

$$\begin{bmatrix} \frac{\partial F_{CO_2}}{\partial C_{CO_2}} & \frac{\partial F_{CO_2}}{\partial C_{oil}} & \frac{\partial F_{CO_2}}{\partial T} & \frac{\partial F_{CO_2}}{\partial u} \\ \frac{\partial F_{oil}}{\partial C_{CO_2}} & \frac{\partial F_{oil}}{\partial C_{oil}} & \frac{\partial F_{oil}}{\partial T} & \frac{\partial F_{oil}}{\partial u} \\ \frac{\partial F_{H_2O}}{\partial C_{CO_2}} & \frac{\partial F_{H_2O}}{\partial C_{oil}} & \frac{\partial F_{H_2O}}{\partial T} & \frac{\partial F_{H_2O}}{\partial u} \\ \frac{\partial C_{CO_2}}{\partial \Theta} & \frac{\partial C_{oil}}{\partial \Theta} & \frac{\partial T}{\partial \Theta} & \frac{\partial u}{\partial \Theta} \\ \frac{\partial C_{CO_2}}{\partial C_{CO_2}} & \frac{\partial C_{oil}}{\partial C_{oil}} & \frac{\partial T}{\partial T} & \frac{\partial u}{\partial u} \end{bmatrix} \begin{bmatrix} \frac{dC_{CO_2}}{d\eta} \\ \frac{dC_{oil}}{d\eta} \\ \frac{dC_{oil}}{d\eta} \\ \frac{d\eta}{d\eta} \\ \frac{du}{d\eta} \end{bmatrix} - \lambda \begin{bmatrix} \frac{\partial G_{CO_2}}{\partial C_{CO_2}} & \frac{\partial G_{CO_2}}{\partial C_{oil}} & \frac{\partial G_{CO_2}}{\partial T} & 0 \\ \frac{\partial G_{oil}}{\partial C_{CO_2}} & \frac{\partial G_{oil}}{\partial C_{oil}} & \frac{\partial G_{oil}}{\partial T} & 0 \\ \frac{\partial G_{H_2O}}{\partial C_{CO_2}} & \frac{\partial G_{H_2O}}{\partial C_{oil}} & \frac{\partial G_{H_2O}}{\partial T} & 0 \\ \frac{\partial C_{CO_2}}{\partial T} & \frac{\partial C_{oil}}{\partial T} & \frac{\partial T}{\partial T} & 0 \\ \frac{\partial C_{CO_2}}{\partial C_{CO_2}} & \frac{\partial C_{oil}}{\partial C_{oil}} & \frac{\partial T}{\partial T} & 0 \end{bmatrix} \begin{bmatrix} \frac{dC_{CO_2}}{d\eta} \\ \frac{dC_{oil}}{d\eta} \\ \frac{d\eta}{d\eta} \\ \frac{d\eta}{d\eta} \\ \frac{du}{d\eta} \end{bmatrix} = 0 \tag{4.29}$$

There are three eigenvalues and three corresponding eigenvectors representing the different composition path choices for a given composition point. At all times, at least one of the composition paths remains in the constant temperature plane. However since the heat of mixing is taken into account, the other two eigenvectors do not remain in the temperature plane.

The next section describes the topology of the composition paths in both the two and three phase regions for the CO₂-oil-water system.

4.3.2 Path Topology

At a given temperature, the phase space can be divided into four distinct regions. The regions are illustrated in Figure 4.53. These four regions are:

Region 1 A vapor-upper liquid region. This region appears along the CO₂-oil edge of the diagram. This region is small at low temperatures, but expands as the temperature increases. At high temperatures, the region expands and becomes a band that crosses the entire phase (see Figure 4.52).

Region 2 A two-phase liquid-liquid region. This region extends from the oil-water edge of the phase space to the towards the CO₂ apex until it reaches the three phase boundary. This region is relatively small even at low temperatures. Increasing temperature moves the edge of the three-phase region towards the oil-water edge of the phase space, reducing the area of this two-phase region.

The next two regions are subsection of the three phase region. The size, shape and path topology in these two regions is primarily determined by the three-phase relative permeability model. The three-phase region is large at low temperatures and becomes smaller as the temperature is increased.

Region 3 A three phase region where all three phases are able to flow simultaneously. This region begins at the 100% oleic corner of the three-phase region and extends towards the vapor-aqueous line.

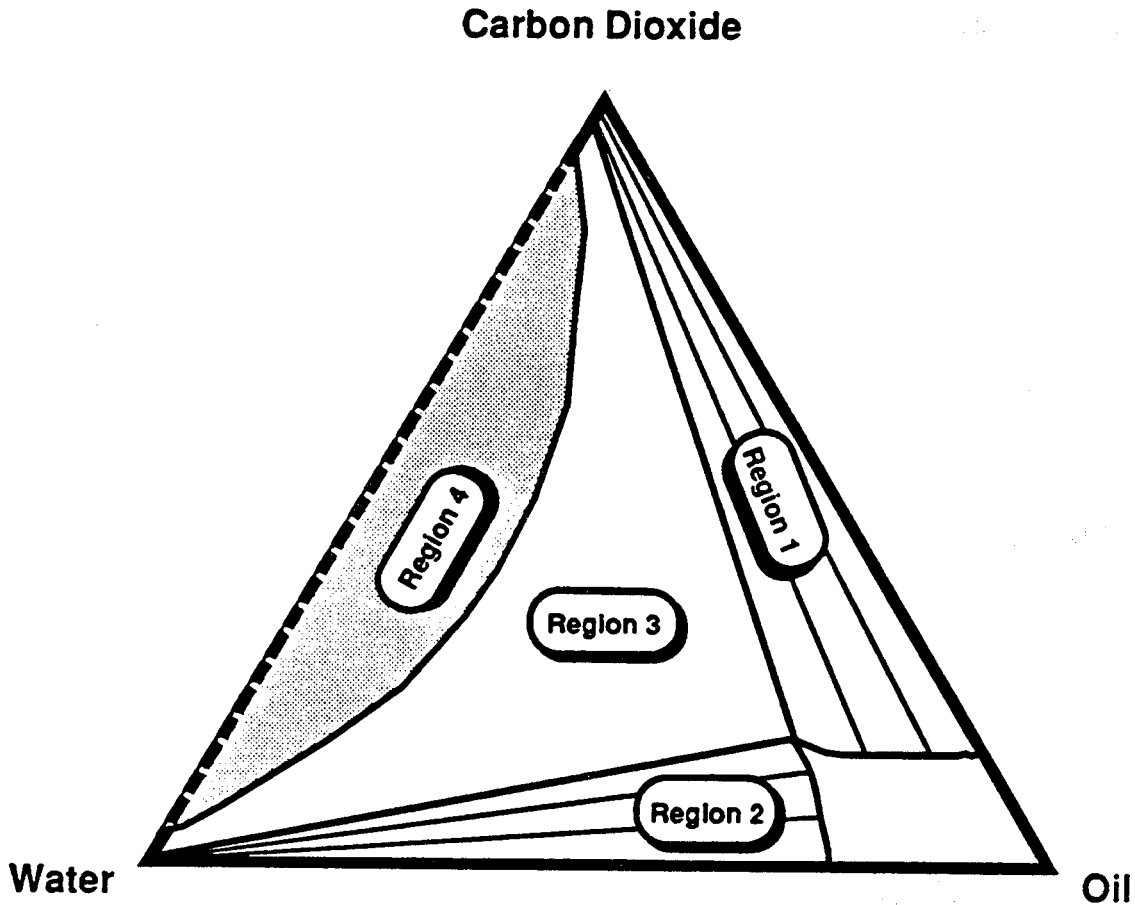


Figure 4.53: Four distinct flow regions in the CO₂-oil-water system.

Region 4 A region where the fractional flow of the oleic phase is zero. For Stone's model II the shape of this region is shown as the shaded region in Figure 4.53. The size of this region depends only on the relative permeability relationships. As long as the relative permeabilities are assumed to be independent of temperature, then the size and shape of the region is also independent of the temperature.

The *gradient* of the fractional flow as the zero oil isoperm line is approached is dependent on the temperature. As the temperature is increased, the derivative of the fractional flow is decreased. When the temperature is increased the viscosity of the oleic phase is reduced relative to the other two phases. The more favorable mobility ratio causes the fractional flow gradient to be reduced.

The composition paths in each of the four regions have a different topologies due to the different flow behavior in the different regions. In all the regions, there is one composition path that is the "temperature" path. This path closely parallels the temperature axis in the hodograph space. Integration along this path results in a temperature change with little change in composition. For most of the hodograph space, this path is the slow path.

The two remaining paths differ in direction, depending on the region of the phase space. These paths are shown in Figure 4.54. The faster of the two paths are shown by the dashed lines and the slower path by the solid lines. The tie line paths in the two two-phase regions are slow for the portions of the

tieline where the saturation of the phase approaches zero or one. In the vapor-liquid region (Region 1), the portion of the tie-line path that is slow is very small and is difficult to show on the diagrams.

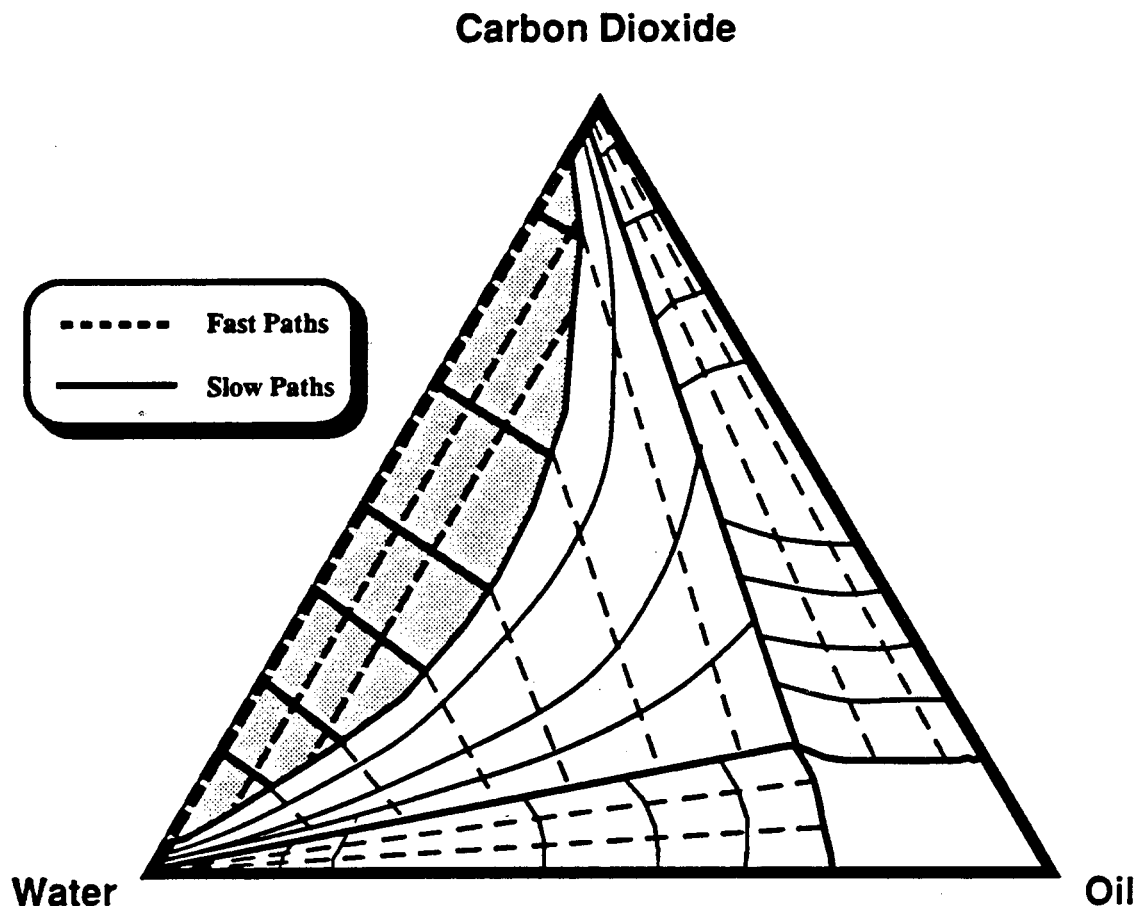


Figure 4.54: Composition paths for the CO₂-oil-water system at a constant temperature.

The liquid-liquid tie lines (Region 2) have the same situation, but the regions where the tie line paths are slow are larger than the vapor-liquid tie lines. This is due to the lower mobility contrast on the liquid-liquid tie lines. The actual portion of the tie lines that are on the slow path depends on the particular relatively permeability model used.

In region 1, the vapor-oleic region, one path is constrained to follow along the tie lines in the region. The velocity of this path is proportional to the Buckley-Leverett velocity, $(\partial f_v / \partial S_v)$. As mentioned, for the majority of region 1, the tie line path is the fast path.

The third path in this region corresponds to the non-tie line path in the isothermal case. The eigenvector that corresponds to this path has a small change in temperature in addition to the composition change. This change in temperature is primarily due to the enthalpy of mixing. Unlike the tie line path, the composition of the two phases changes along this path. The heat capacity of the phases is a function of composition. This means that the total energy stored per degree of temperature changes with the total energy remaining constant, resulting in a small change in temperature along this non-tie line path.

The amount of temperature change along this path is relatively small for the CO₂-oil-water system. A typical integration along the non-tie line path will have a composition change, ΔC_{H_2O} , of 0.1 and a corresponding temperature change, ΔT , that is approximately 3 degrees Kelvin. A typical path is given by 12 points in Table 4.13.

CO ₂	Oil	Water	Temperature	Flow Velocity
<i>Mole Fraction</i>			<i>Kelvin</i>	<i>PV/Time</i>
0.300000	0.680000	0.020000	325.00	1.000000
0.290389	0.667473	0.042137	324.34	0.998431
0.281579	0.654384	0.064037	323.69	0.996837
0.273422	0.640803	0.085776	323.03	0.995220
0.265831	0.626795	0.107374	322.38	0.993582
0.258745	0.612415	0.128840	321.72	0.991921
0.252117	0.597713	0.150170	321.07	0.990238
0.245910	0.582732	0.171358	320.41	0.988534
0.240087	0.567508	0.192405	319.76	0.986809
0.234630	0.552085	0.213285	319.10	0.985062
0.229510	0.536490	0.234000	318.45	0.983293
0.227974	0.531580	0.240447	318.24	0.982735

Table 4.13: Non-tie line path in the vapor-liquid region of the CO₂-oil-water system.

Region 2 is the liquid-liquid region. This region has two paths that are qualitatively similar to the two paths in the vapor-liquid region. A tie line path with an eigenvalue proportional to the fractional flow derivative is the fast path for the central portion of the tie lines. The fractional flow derivative approaches zero as the saturation of the phases approach zero and one. At the ends of the tie lines, the tie line path is the slow path.

The non-tie line path in the liquid-liquid region behaves much like the same paths in the vapor-liquid region. The enthalpy of mixing terms have a lesser effect than along the vapor-liquid paths. This causes the temperature deviation to be smaller than along the paths in the vapor-liquid region. An example of a typical path is shown in Table 4.14.

Region 3 has three phases, vapor, oleic, and aqueous, flowing simultaneously. The phase rule shows that for three components to partition into three phases at a constant pressure and temperature, the compositions of the phases cannot change. As the overall composition point changes in the three-phase region, only the *amounts* of each phase can change, while the composition of each phase remains constant.

CO ₂	Oil	Water	Temperature	Flow Velocity
<i>Mole Fraction</i>			<i>Kelvin</i>	<i>PV/Time</i>
0.300000	0.680000	0.020000	325.00	1.000000
0.290389	0.667473	0.042137	324.34	0.998431
0.281579	0.654384	0.064037	323.69	0.996837
0.273422	0.640803	0.085776	323.03	0.995220
0.265831	0.626795	0.107374	322.38	0.993582
0.258745	0.612415	0.128840	321.72	0.991921
0.252117	0.597713	0.150170	321.07	0.990238
0.245910	0.582732	0.171358	320.41	0.988534
0.240087	0.567508	0.192405	319.76	0.986809
0.234630	0.552085	0.213285	319.10	0.985062
0.229510	0.536490	0.234000	318.45	0.983293
0.227974	0.531580	0.240447	318.24	0.982735

Table 4.14: Typical composition path in the liquid-liquid region of the CO₂-oil-water system.

Both the slow and fast paths in this region are isothermal. The composition of the three phases remains constant over the entire region so there is no enthalpy of mixing effect on the composition paths. The slow paths in this region parallel the contour of zero fractional flow of the oil phase near the boundary of regions 3 and 4. These paths fan out toward the liquid-liquid boundary of the three-phase region until they parallel the boundary.⁴ The eigenvalues along this path increase towards the aqueous apex of the three-phase region.

The fast paths parallel the vapor-liquid boundary of the three-phase region. These paths do not change direction to a great extent over region 3. The eigenvalues increase as you move along the fast paths away from the boundary between regions 3 and 4 and towards the liquid-liquid boundary.

4.3.3 Solution Problems

The major difficulty to obtaining a full solution to the CO₂-oil-water system is the construction of the discontinuities. There are three major problems that make the calculation of the discontinuities especially difficult. These are:

1. There are no tie line extensions that constrain the the location of the leading and trailing shocks.
2. There is no clear temperature plateau on one side of the discontinuities.
3. The material and enthalpy balances are extremely sensitive to the conditions on the unknown side of the discontinuity.

Each of these reasons make it much more difficult to isolate the physically correct shock from the many possible constructions.

⁴Because the liquid-liquid boundary is also a tie line it must also be a path.

When shocking from the single-phase into a two-phase region, it has been shown that the composition on the two-phase side of the shock must lie on the tie line extension that passes through the single-phase point (Dumoré 1984). In the case where temperature is also a variable, an enthalpy balance across the discontinuity is not a linear combination of the total on the single-phase side of the shock. A mathematical description of the enthalpy balance across the discontinuity is discussed in Appendix C.

A second effect that prevents any tie line considerations is the enthalpy of mixing. The overall heat capacity is different on the single-phase side of the shock than on the two-phase side. The compositional dependence of the phase heat capacities is especially important when the latent heat of the aqueous phase is considered.

The second difficulty is that there is no clear temperature plateau on one side of the shock. In the case of the steam-oil-water system, the three-phase region was constrained to a constant temperature. This physical constraint on the three-phase side of the discontinuity makes the shock construction much easier because temperature is not variable on that side of the discontinuity.

The addition of the third component that forms a partially miscible system allows the three-phase region exist over a wide range of temperatures. This fact, combined with the consideration of the compositional effects make the construction of the shocks in this system much more difficult.

The final reason that these shocks are especially difficult to construct is that the domain of convergence is very small. For the CO₂-oil-water system the range of initial guesses that converges to a composition point that satisfies the material balances, the enthalpy balance, and also be tangent to one of the characteristic paths has proven to be the most difficult part of the solution.⁵

This concludes the presentation of the results for the three different example systems. The final section will discuss the conclusions and limitations of the model as applied to flow problems with temperature variations. The general conclusions about the model itself, apart from a specific problem or system, and the limitations are discussed first. The conclusions that apply to the three specific solutions are presented in turn, and finally, further applications of the method of characteristics are outlined.

⁵In fact NO solutions have been found that are able to connect a typical boundary condition to a point in either the two-phase or three-phase region. This is primarily a failure of the enthalpy balance to converge in a reasonable temperature range.

5. CONCLUSIONS AND RECOMMENDATIONS

This chapter is divided into three main sections. The first section presents general conclusions and observations about the model as a whole. The applications and limitations of the model are emphasized.

The second section summarizes the results obtained from applying the model to the three specific types of displacement problems discussed in Chapter 4. Each of the three systems present different approaches and results. Practical application of each of the systems will be mentioned in these sections.

Finally, the third section will mention additional topics that need to be examined. Specifically, improvements on the solution technique and applications to flow problems not yet mentioned are discussed in this section.

5.1 GENERAL CONCLUSIONS AND LIMITATIONS

The section is divided into three subsections. The first are the conclusions. These are statements about the method of characteristics as applied to multiphase multicomponent flow in porous media. The second section are "observations." These are statements that seem to be *generally* true, but could not be proven or have some exceptions in the many solutions presented in this dissertation. The final subsection discusses the two major limitations that must be considered when applying the model to other problems.

5.1.1 Conclusions

A semi-analytical model capable of describing the complex interactions between the system temperature, phase behavior and flow properties has been presented. This model is an extension of the model presented by Dumoré (1984) to include the interaction of system temperature with the phase behavior and flow properties. The solutions presented in this dissertation lead to the following general conclusions:

1. The mathematical model presented by Dumoré can be extended to include temperature variations. The temperature of the system is found by treating the overall enthalpy as though it were another component that is transported in the flowing phases. Dispersive effects of conduction and heat gains or losses from the system are neglected.
2. The solutions to the model system are piecewise continuous in the weak sense. Specifically the solutions consist of waves that propagate with constant velocities. These waves are separated by zones of constant state or by jump discontinuities.
3. Temperature shocks are always accompanied by discontinuities in the other hodograph variables. These shocks are primarily the result of increasing or decreasing the number of phases.
4. The reverse of this is not true. Saturation or composition shocks are seen that do not have a coincident change in temperature.
5. Phase boundaries are always crossed by shocks. This is due to the discontinuities in the eigenvalues as the path crosses the phase boundaries. This discontinuity is present because of the discontinuity in the fractional flow derivative as the path travels from a two phase to a three phase region.
6. In all cases there is at least one wave that moves in an isothermal plane. This is necessary for the limiting case of an isothermal injection to be possible.

5.1.2 Observations

After studying many different displacement systems using the method of characteristics, a number of patterns and rules of thumb have emerged. These ideas are observations that have not been rigorously proven. They represent concepts that are useful to keep in mind as possible solutions are being constructed.

1. The solution always begins on the slowest path at the injection conditions.
2. The solution follows along the continuous composition path whenever possible. The discontinuities are only introduced when a continuous solution is not possible.
3. All the central shocks i.e., those that do not include the initial or injection conditions on one side of the shock, are intermediate discontinuities. Genuine shocks only appear when an earlier tangent shock has constrained the composition path to land on a tie-line extension of the initial or injection conditions. In order to travel from the landing point to the boundary condition, the solution must cross a shock that does not match the wave velocity on either side of the shock. This is often the case when the boundary conditions are in the single phase region and there are no composition paths on that side of the shock.
4. At an equal eigenvalue point, where a path switch may take place, the solution leaves the point along the *same* eigenvector as the one on which it entered. For example, when the solution arrives at an equal eigenvalue point along the slow path, it also departs the equal eigenvalue point along the slow path. This is not a hard and fast rule, there are occasions where the solution leaves along a different path than the one it entered. The large majority of solutions however, do follow this maxim.
5. There is an ordering to the kinds of waves that are seen in the solutions. Continuously varying waves occur if they are possible. Discontinuities are only seen where necessary. The crossing of a phase boundary or a self-sharpening wave are examples where the discontinuities must be introduced into the solution. The discontinuities also have a ranking. Genuine shocks are only seen when an intermediate discontinuity is not possible.

As the solution travels along a continuous variation, there must be some trigger that prevents it from continuing any further. This trigger is usually a match between the characteristic velocity of the spreading wave and an intermediate discontinuity that is forced by the downstream conditions.

5.1.3 Limitations

There are a number of limitations that go along with every model. Some of these limits are not very restrictive, while others present major obstacles that need to be overcome. This section will discuss some of these limitations, both large and small, and attempt to suggest methods for dealing with some of the major restrictions.

The less restrictive limitations are inherent in the assumptions that are made in building the model. These are:

1. The system is restricted to one-dimensional displacements. The application of a method of characteristics to problems with more than two independent variables is the subject of considerable study by the mathematical community. The application of the concepts to flow problems in porous media has yet to be explored, but this restriction could be lifted.
2. The system is restricted to constant pressure.

3. The system is adiabatic and enthalpy losses outside the system are neglected. This could be a severe limitation for practical reservoir applications if the injection rate is slow or the pay formation is not thick.

There are a number of major limitations that are inherent in the model. These are limitations that severely limit the kinds of systems that can be solved by the model. The restrictions are primarily placed on the total number of components and/or phases the system can have.

One of the important considerations is the integration of a flash routine into the calculation of the eigenvalue problem. Flash programs for the calculation of two phase systems are well established and robust. This is not true for systems that exhibit more than two phases. Three phase flash routines are not well behaved especially over a wide range of temperatures. In order to use the existing equations of state, a relatively quick and robust flash routine is needed that can internally determine the number and compositions of the phases over a wide range of temperatures.

The greatest hurdle to overcome is the calculation of the discontinuities that are present in all solutions. The solution of the Riemann problem described in Chapter 2 is not unique. The introduction of a physical limitation, such as the velocity constraint, should give the one physically correct solution to the problem. However, as more components are included in the system, the complexity of the solutions increases dramatically. In the case of the viscous oil presented in §4.2.6, solutions that in theory satisfied the velocity constraint but did not appear to be physically correct were rejected. Other solutions that also satisfied the velocity constraint and appeared to be physically consistent were later found. With each new component, a new dimension is added to the hodograph space, and the level of complexity increases dramatically. Practically, the number of components, including the enthalpy, is limited to a range from 3 to 5.

5.2 SPECIFIC APPLICATIONS

This section presents the conclusions that pertain to a particular displacement system. Results for the steam-water, steam-oil-water and three phase-three component systems are discussed.

5.2.1 Single Component with Temperature Variation

The system where a single component partitions into a vapor and liquid phase at the saturation represents one type of system that can be represented by the model. The following observations are made about the single component, two phase system:

1. The effects of temperature and flow behavior are separated by the physical requirement that the two-phase region exists *only* at the saturation temperature.
2. In the single-phase region, no separation of the local enthalpy content is possible due to the nature of the single phase flow. This prevents the formation of a temperature profile in the single-phase regions. In the trailing region, the temperature remains constant at the injection temperature. In the leading region, the temperature is at the initial temperature.
3. In the two-phase region, the system behaves as an two-phase immiscible displacement. Fractional flow considerations completely determine the saturation profile in the two-phase region.
4. The single-phase regions are coupled to the two-phase region by a trailing downstream intermediate discontinuity (tangent shock) and a leading upstream intermediate discontinuity. The velocity of the shock is dominated by the temperature change across the shock. The greater the temperature change, the lower the shock velocity.

5. Changes in certain parameters only affect the conditions *downstream* of the change. This means that changes in the injection conditions alter the entire displacement profile, but changes in the initial temperature only effect the leading shock. This has only been demonstrated for this case, but the result is due to the nature of the hyperbolic equations and should be true for all the cases presented.
6. The velocity of the trailing shock reaches a maximum and then decreases as the injection temperature is decreased. This is due to the competing nature of the mass and enthalpy changes across the trailing shock.
7. The initial temperature only affects the velocity of the leading shock. As the initial temperature increases, the difference in temperature across the shock decreases. The smaller temperature change across the shock causes the shock velocity to increase.
8. The ability of the matrix to store heat is proportional to the quantity

$$\left(\frac{1-\phi}{\phi}\right)(\rho_m C p_m) \quad (5.1)$$

As matrix becomes less porous, more dense, or has a larger heat capacity, the velocity of the leading and trailing shocks is reduced. The change in velocity is much greater for the leading shock so the net effect is to decrease the size of the two-phase region.

5.2.2 Two-Component, Three-Phase Immiscible System

1. The injection of high temperature steam into a cold immiscible oil phase (with some small initial water saturation also present) can be modeled using these techniques.
2. The solution is divided into three regions. A leading liquid water-oil region, a central three-phase region where steam, oil and water flow simultaneously. A two-phase steam-oil region trails the three-phase region.
3. The three regions are connected by a pair of phase transition shocks. These shocks have a coincident change in temperature and saturations. These shocks are intermediate discontinuities with the matching eigenvalue on either the upstream or the downstream side of the shock.
4. The extent of the possible landing points in the three-phase region is very small. Greatly changing the steam-oil jumping point has only a small effect on the eventual landing point in the three-phase region. The opposite is also true, when searching for a point in the three-phase region that jumps into the steam-oil region, only a small part of the phase space will give an acceptable solution. Changing the three point greatly effects the landing point in the steam-oil region.
5. The central three-phase region is a strictly hyperbolic region where a path switch from the slow to the fast path creates a central zone of constant state.
6. The three-phase region can contain a spreading wave ahead or trailing the central zone of constant state. A self-sharpening wave can also exist between the trailing phase transitions shock and the central zone of constant state.
7. The steam-oil region follows the slow path until an intermediate discontinuity takes the solution into the three-phase region.

8. Increasing oil viscosity causes the highly mobile vapor phase to spread over the system to a much larger extent. This results in the vapor saturations being much lower than in the case of the less viscous oils.
9. The increased oil viscosity causes the formation of an oil bank at the trailing edge of the three-phase region.
10. Increased oil viscosity causes the saturation change across the phase transition shocks to be smaller than with less viscous oils.
11. The fast path follows lines of constant water saturation in the case with high oil viscosity. This is in contrast to the base case, where the fast path parallels lines of constant oil saturation.
12. Spreading waves in the leading-water oil region are possible when the oil viscosity increases.

5.2.3 Three-Component, Three-Phase System with Temperature Variations

The three component system adds the effects of phase behavior to the model. At lower temperatures, the mass transfer of CO₂ into the oleic phase alters the flowing properties of the phase by decreasing its density and viscosity. At higher temperatures, the increased temperature itself is responsible for reducing the viscosity of the oleic phase. The solutions presented for this section again represent only a small fraction of the possible systems and effects that can be studied using the method of characteristics. Some of the most important results are:

1. In the three-phase region, two paths remain in an isothermal plane and the third path follows a path that is only in the temperature direction.
2. In the two phase region, one path remains in the isothermal plane and two paths show a change in temperature. The isothermal path is the tie-line path and both nontie-line paths have a change in temperature. This temperature change is due to the enthalpy change of mixing. Along a tie-line, no mixing occurs and there is no enthalpy change because of mass transfer. Along the non-tie line paths the enthalpy of mixing changes the amount of enthalpy available as the components transfer phases influences the change in temperature.

5.3 FUTURE RECOMMENDATIONS

The solutions presented in this dissertation represent a fraction of the possible applications of the method of characteristics. Some of the projects mentioned here are direct extensions of the systems studied in chapter 4. Other ideas are ideas that stem from practical considerations in reservoir engineering. Some final ideas represent systems that have a potential for study by the method of characteristics.

The solutions presented in this dissertation are only a part of a complete description to multiphase, multicomponent systems with temperature variations. Some of the immediate extensions that deserve attention are:

1. The effect of relative permeability models on the wave patterns for the three phase systems. The three phase relative permeability models represent the greatest uncertainty incorporated into the model. An application of this model could be to use three-phase slim tube displacement data to formulate, adjust and verify three phase relative permeability models.
2. The effect of adding a second oil component. This new component represents the light, volatile components which partition into the vapor phase at high temperatures or are extracted into a CO₂-rich phase. This addition would be a more accurate description of lighter oils that are traditionally candidates for miscible floods.

3. The application of the model to one-dimensional flow in radial coordinates. Conceptually, this problem only requires the rewriting of the conservation equations into a cylindrical coordinate system. Practically, however, it changes the nature of the differential equations by grouping one of the dependent variables (the length) into the definitions of the primary variables (G , F , Γ , and Θ). This makes the coefficients of the \bar{G} and \bar{F} matrices functions of the independent variables, changing the nature differential equations from *reducible* to *irreducible*.

The application of a mathematical model to "practical" problems is always an important aspect of model development. The model by itself can be an aid to the understanding of how different phenomena interact in a multiphase, multicomponent system with temperature variations. However, these results are likely to remain in the academic arena unless a simple, practical use for the ideas is found. As an important area for future study, I feel that a concentration of effort on the application of the model to laboratory or field problems would have the greatest benefit in the long run.

Some suggestions for practical problems that could be tackled by the method of characteristics are:

- **Verifying and fine tuning three phase relative permeability models or equations of state.**

For the presentation in this dissertation, the task was to find the saturation or composition profiles of a displacement system given the phase behavior and relative permeability of the different components and phases. A good application of the model would be to study the reverse problem. In most actual circumstances, the composition profiles are the known data. The unknowns are the phase behavior and/or relative permeability models that apply to the fluids. For example, by taking periodic fluid samples, an observation well in a field that is undergoing a miscible flood can supply the compositions of the fluids that pass the well at different points in time. This information can be assimilated to give the velocities and compositions as different fronts pass the observation well.

The task is to determine, given an initial reservoir composition and an injection history, what is the phase behavior and/or relative permeability model that results in the observed set of compositions and front velocities? Since the model has the ability to change directly both these factors and examine the results in a straightforward manner, it would be ideally suited for studying this problem.

The major difficulty would be constructing the initial solution path. Once that is completed, parameter studies are straightforward. The effect of slightly changing the phase behavior or relative permeabilities is small. Because the composition path and shock values are the given data rather than the unknowns, the construction of the initial solution route is made much easier than if only the boundary conditions were specified.

6. NOMENCLATURE

Roman Symbols

C_i	Concentration of component i , $kgmol/m^3$
C_{pj}	Specific Heat of phase j , $J/kgmol K$
C_{pm}	Specific Heat of matrix, $J/kg K$
f_j	Fractional flow of phase j
F_i	Overall flux of component i , $kgmol/m^2 day$
G_i	Overall local concentration of component i , $kgmol/m^3$
H_j	Enthalpy of phase j , $J/kgmol$
H_m	Enthalpy of matrix, J/kg
k_r	Relative permeability
k_{rg}	Relative permeability of vapor phase
k_{rlg}	Two phase liquid relative permeability in liquid-vapor system used in three phase relative permeability relations
k_{ro}	Relative permeability of oil phase
k_{rocw}	Intermediate phase relative permeability at irreducible water saturation
k_{row}	Two phase oil relative permeability in oil-water system used in three phase relative permeability relations
k_{rw}	Relative permeability of aqueous phase
n_c	Total Number of Components
n_p	Total Number of Phases
S_j	Saturation of phase j
S_l	Liquid phase saturation
S_o	Intermediate phase saturation
S_{or}	Irreducible intermediate phase saturation
S_v	Saturation of non wetting (vapor) phase
S_w	Saturation of wetting (aqueous) phase

S_{wc}	Connate wetting phase saturation
t	time, <i>day</i>
T	Temperature, <i>K</i>
\bar{u}	Local flow velocity, <i>day</i>
u_{C_i}	Characteristic velocity of component <i>i</i>
u_H	Characteristic velocity of the enthalpy
χ	distance, <i>m</i>
X_{ij}	Mole Fraction of component <i>i</i> in phase <i>j</i>

Greek Symbols

α_g	Gaseous phase Corey exponent
α_{lg}	Corey exponent for liquid-gas system used in three phase relative permeability relations
α_{ow}	Corey exponent for oil-water system used in three phase relative permeability relations
α_w	Water phase Corey exponent
Γ	Local enthalpy concentration, <i>J/m³</i>
η	Characteristic dummy variable
Θ	Local enthalpy flux, <i>J/m² day</i>
Λ	Shock Velocity, <i>m/day</i>
Λ_i	Shock Velocity calculated using a material balance on component <i>i</i> , <i>m/day</i>
Λ^k	The velocity of a <i>kth</i> discontinuity
Λ_{ss}	Velocity of a discontinuity created by a self-sharpening wave <i>m/day</i>
Λ_{uid}	Velocity of a discontinuity created by an upstream intermediate discontinuity, <i>m/day</i>
λ	Characteristic velocity, <i>m/day</i>
λ^I	Characteristic velocity in the single phase region, <i>m/day</i>
λ^{II}	Characteristic velocity in the two phase region, <i>m/day</i>
λ^{III}	Characteristic velocity in the three phase region, <i>m/day</i>
λ^-	Characteristic velocity downstream of a discontinuity, <i>m/day</i>

λ^+	Characteristic velocity upstream of a discontinuity, <i>m/day</i>
λ_1	Characteristic velocity along the slowest path, <i>m/day</i>
λ_2	Characteristic velocity along an intermediate path, <i>m/day</i>
λ_3	Characteristic velocity along the fastest path, <i>m/day</i>
μ_j	Viscosity of phase <i>j</i> , <i>Pa·sec</i>
ρ_j	Molar density of phase <i>j</i> , <i>kgmol/m³</i>
ρ_m	Mass density of matrix, <i>kg/m³</i>
σ_g	End point relative permeability for non-wetting phase
σ_{lg}	End Point relative permeability for intermediate phase in the liquid-gas system
σ_{ow}	End Point relative permeability for intermediate phase in the oil-water system
σ_w	End point relative permeability for wetting phase
ϕ	Porosity of matrix

7. REFERENCES

1. Aris, R. and Admundson, N.R.: *Mathematical Methods in Chemical Engineering: Volume 2, First Order Partial Differential Equations with Applications*, Prentice-Hall, Englewood Cliffs, NJ (1973).
2. Aziz, K. and Setarri, A.: *Petroleum Reservoir Simulation*, Applied Science Publishers Ltd., London (1979).
3. Baker, L.E.: "Three-Phase Relative Permeability Correlations", SPE 17369, presented at the Sixth Symposium on Enhanced Oil Recovery, Tulsa, OK, April 17-20, 1988.
4. Bell, J.B., Trangenstein, J.A. and Shubin, G.: "Conservation Laws of Mixed Type Describing Three-Phase Flow In Porous Media", *SIAM Journal of Applied Mathematics*, 46(6):1000-1017 (December 1986).
5. Buckley, S.E. and Leverett M.C.: "Mechanism of Fluid Displacement in Sands", *Transactions of the AIME*, 146:107 (1942).
6. Chung, F.T.H., Jones, R.A. and Nguyen, H.T.: "Measurements and Correlations of the Physical Properties of CO₂-Heavy Oil Mixtures", SPE 15080, presented at the 56th California Regional Meeting, Ventura, CA, April, 1986.
7. Courant, R. and Friedrichs, K.O.: *Supersonic Flow and Shock Waves*, Springer-Verlag, New York (1948).
8. Dafermos, C.M.: "Hyperbolic Systems of Conservation Laws", In J.M Ball, editor: *Systems of Nonlinear Partial Differential Equations*, pages 25-71, D. Reidel Publishing Company, Dordrecht, Holland (1983).
9. Daripa, P., Glimm, J., Lindquist, B., and Maesumi, M.: *On the Simulation of Heterogenous Petroleum Reservoirs*, Technical Report DOE/ER/03077-279, Courant Mathematics and Computing Laboratory, New York, New York (April 1987).
10. de Pedrosa, T., Escobar, E., and Rivas, O.: *Research Program on Heavy Oil Recovery by CO₂ - Task 31 of Annex IV*, Technical Report, INTEVEP, S.A., Los Teques, Edo. Miranda, Venezuela (March 1986).
11. Dumoré, J.M., Hagoort, J., and Risseeuw, A.S.: "A Analytical Model for One Dimensional Three Component and Vaporizing Gas Drives", *SPEJ*, 24:169-179 (1984).
12. Emanuel, A.S.: "A Mixing Rule Method for Calculating the Viscosity of CO₂ and Low-Gravity Reservoir Oil", SPE 14229, presented at the 60th Annual Technical Conference and Exhibition, Las Vegas, NV, 1985.
13. Fayers, F.J.: "Extensions of Stone's Model I and Conditions for Real Characteristics in Three-Phase Flow", SPE 16965, presented at the 62nd Annual Technical Conference and Exhibition, Dallas, TX, September 27, 1987.
13. Fayers, F.J.: "Some Theoretical Results Concerning the Displacement of a Viscous Oil by a Hot Fluid in a Porous Medium", *Journal of Fluid Mechanics*, 13:65-76 (1962).
14. Glimm, J.: *The Interaction of Nonlinear Hyperbolic Waves: A Conference Report*, Conference Report, Courant Institute, New York University, New York, New York (1987).

15. Gorell, S.B.: "Modeling the Effects of Trapping and Water Alternate Gas Injection on Tertiary Miscible Displacements", SPE 17340, presented at the Sixth Symposium on Enhanced Oil Recovery, Tulsa, OK, April 17-20, 1988.
16. Hattori, H.: "The Riemann Problem for a van der Waals Fluid with Entropy Rate Admissibility Criterion—Nonisothermal Case", *Journal of Differential Equations*, 65:158-174 (1986).
17. Helfferich, F.G.: "General Theory of Multicomponent, Multiphase Displacement in Porous Media", *SPEJ*, 21:51-62 (1981).
18. Hirasaki, G.J.: "Application of the Theory of Multicomponent, Multiphase Displacement to Three-Component, Two-Phase Surfactant Flooding", *SPEJ*, 21:191-204 (1981).
19. Holden, H.: "On the Riemann Problem for a Prototype of a Mixed Type Conservation Law", *Communications on Pure and Applied Mathematics*, 40:229-264 (1987).
20. Holm, L.W. and Josendal, V.A.: "Effect of Oil Composition on Miscible-Type Displacement by Carbon Dioxide", *SPEJ*, 22:87-98 (1982).
21. Holm, L.W. and Josendal, V.A.: "Mechanisms of Oil Displacement by Carbon Dioxide", *JPT*, 16:1427-1436 (December 1982).
22. Hovdan, M.: "Vanninjeksjon - Inkompressibel Analytisk løsning med Temperatureffekter" (1986).
23. Hutchinson, C.A., Jr. and Braun, P.H.: "Phase Relations of Miscible Displacement and Oil Recovery", *A. I. Ch. E. Journal*, 7:64-72 (1961).
24. Jeffrey, A.: "The Propagation of Weak Discontinuities in Quasilinear Hyperbolic Systems with Discontinuous Coefficients Part I - Fundamental Theory", *Applicable Analysis*, 3:79-100 (1973).
24. Jeffrey, A.: *Quasilinear Hyperbolic Systems and Waves*, Pitman Publishing, London (1976).
25. Jossi, J.A., Stiel, L.I., and Thodos, G.: "The Viscosity of Pure Substances in the Dense Gaseous and Liquid Phases", *A.I.Ch.E. Journal*, 8(1):59-62 (1962).
26. Karakas, M., Saneie, S., and Yortsos, Y.: "Displacement of a Viscous Oil by the Combined Injection of Hot Water and Chemical Additive", *SPE Reservoir Engineering*, 1:391-402 (July 1986).
27. Keyfitz, B.L. and Kranzer, H.C.: "A System of Non-Strictly Hyperbolic Conservation Laws Arising in Elasticity Theory", *Archive for Rational Mechanics and Analysis*, 72:220-241 (1980).
28. Lawal, A.S.: "Prediction of Vapor and Liquid Viscosities From the Lawal-Lake-Silberberg Equation of State", SPE 15677, presented at the Fifth Symposium on Enhanced Oil Recovery, Tulsa, OK, April, 1986.
29. Lax, P.D.: "Hyperbolic Systems of Conservation Laws: Part II", *Communications in Pure and Applied Mathematics*, 10:537-566 (1957).
30. Leach, M.P. and Yellig, W.F.: "Compositional Model Studies - CO₂ Oil-Displacement Mechanisms", *SPEJ*, 21:89-97 (1981).
31. Little, J.E. and Kennedy, H.T.: "A Correlation of the Viscosity of Hydrocarbon Systems with Pressure, Temperature, and Composition", *SPEJ*, 57-161 (June 1968).

32. Leob, V.M.: *A Model for the Viscosity of Liquid-Liquid Mixtures*, PhD thesis, University of Rochester (1973).
33. Lohrenz, J., Bray, B.C., and Clark, C.R.: "Calculation Viscosities of Reservoir Fluids from their Composition", *JPT*, 6:1171-1176 (1964).
34. Metcalf, R.S. and Yarborough, L.: "The Effect of Phase Equilibria on the CO_2 Displacement Mechanism", *SPEJ*, 19:242-252 (1979).
35. Moler, C.B. and Stewart, G.W.: "An Algorithm for Generalized Matrix Eigenvalue Problems", *SIAM Journal of Numerical Analysis*, 10:241-256 (1973).
36. Monroe, W.W.: *The Effect of Dissolved Methane on Composition Paths in Quaternary CO_2 - Hydrocarbon Systems*, Master's thesis, Stanford University, Stanford, CA (September 1986).
37. Monroe, W.W., Silva, M.K., Larsen, L.L., and Orr, F.M., Jr.: "Composition Paths in Four-Component Systems: The Effect of Dissolved Methane on CO_2 Flood Performance in One Dimension", *SPE* 16172, presented at the 62nd Annual Technical Conference and Exhibition, Dallas, TX, September 27-30, 1987.
38. Nilson, R.H. and Romero, L.A.: "Self-Similar Condensing Flows in Porous Media", *International Journal of Heat and Mass Transfer*, 23:1461-1470 (1980).
39. Nutakki, R.: *Phase Behavior Calculations for Systems Containing Hydrocarbons and Water*, PhD thesis, Stanford University, Stanford, CA (September 1988).
40. Nutakki, R., Wong, T., Firoozabadi, A., and Aziz, K.: *Development of General Purpose Simulators Part 1: Vapor-Liquid Equilibrium Calculations Using Three Equations of State and Accelerated Successive Substitution*, Technical Report, Stanford University, Department of Petroleum Engineering (1985).
41. Orr, F.M., Jr.: *Simulation of the One-Dimensional Convection of Four-Phase, Four-Component Mixtures*, Topical Report DOE/ET/12082-8, New Mexico Petroleum Recovery Research Center, Socorro, NM (October 1980).
42. Pande, K.K.: *An Analytical Method of Describing Crossflow in Layered Systems using the Method of Characteristics*, PhD thesis, Stanford University, Department of Petroleum Engineering (1988).
43. Peng, D. and Robinson, D.: "A New Two-Constant Equation of State", *Industrial and Engineering Chemistry Fundamentals*, 15(1):59-64 (1976).
44. Prats, M.: *Thermal Recovery*, Society of Petroleum Engineers, Dallas, TX (1982).
45. Rathmell, J.J., Stalkup, F.I., and Hassinger, R.C.: "A Laboratory Investigation of Miscible Displacement by Carbon Dioxide", *Proceeding of the 46th Annual Conference* (October 3-6 1971).
46. Rauch, J. and Reed, M.C.: "Propagation of Singularities in Non-Strictly Hyperbolic Semilinear Systems: Examples", *Communications on Pure and Applied Mathematics*, 35:555-565 (1982).
47. Reid, R.C., Prausnitz, J.M., and Sherwood, T.K.: *The Properties of Gases and Liquids*, McGraw Hill, New York, third edition (1977).
48. Reynolds, W.C.: *Thermodynamic Properties in SI*, Department of Mechanical Engineering at Stanford University, Stanford, CA (1979).

49. Rhee, H.K., Aris, R., and Amundson, N.R., "On the Theory of Multicomponent Chromatography", *Philosophical Transactions of the Royal Society of London, Series A*, 267:419-455 (1970).
50. Schaeffer, D.G. and Shearer, M.: "The Classification of 2x2 Systems of Non-Strictly Hyperbolic Conservation Laws, With Applications to Oil Recovery", *Communications on Pure and Applied Mathematics*, 40:1 (1987).
51. Scheidegger, A.E.: *Physics of Flow Through Porous Media*, MacMillian, London (1957).
52. Schmidt, G. and Wenzel, H.: "A Modified Van der Waals Type Equation of State" *Chemical Engineering Science*, 35:1503-12 (1980).
53. Sillen, L.G.: *Arkive Kemi Mineral Geology*, 2:477 (1950).
54. Silva, M.K., Larsen, L.L., and Orr, F.M., Jr.: *CO₂ Hydrocarbon Phase Behavior in Model Systems, Part 1: CO₂-C₁-C₄-C₁₀*, Technical Report 85-31, New Mexico Petroleum Recovery Research Center (1985).
55. Simon, R. and Graue, D.J.: "Generalized Correlation for Predicting Solubility, Swelling and Viscosity Behavior of CO₂-Crude Oil Systems", *JPT*, 1:102-106 (January 1965).
56. Slobod, R.L. and Koch, H.A., Jr.: "High-Pressure Gas Injection-Mechanism of Recovery Increase", *Oil and Gas Journal*, 84 (1953).
57. Stone, H.L.: "Probability Model for Estimating Three-Phase Relative Permeability", *JPT*, 22:214-218 (February 1970).
58. Stone, H.L. and Crump, J.S.: "The Effect of Gas Composition upon Oil Recovery by Gas Drive", *Trans. AIME*, 146:91 (1956).
59. Temple, B.: "Global Solution of the Cauchy Problem for a Class of 2 x 2 Nonstrictly Hyperbolic Conservation Laws", *Advances in Applied Mathematics*, 3:335-375 (1982).
60. Torabzadeh, S.J. and Handy, L.L.: "The Effect of Temperature and Interfacial Tension on Water/Oil Relative Permeabilities of Consolidated Sands", SPE 12689, presented at the SPE/DOE Fourth Symposium on Enhanced Oil Recovery, Tulsa, OK, April 15-18, 1984.
61. Vargaftik, N.B.: *Handbook of Physical Properties of Liquids and Gases, Pure Substances and Mixtures*, Hemisphere Publishing Corporation, Washington, 2nd edition (1975).
62. Walas, S.M.: *Phase Equilibria in Chemical Engineering*, Butterworth Publishers, Boston (1985).
63. Welge, H.J.: "The Linear Displacement of Oil from Porous Media by Enriched Gas", *JPT*, 3:787-796 (1961).
64. Welge, H.J.: "A Simplified Method for Computing Oil Recovery by Gas and Water Drive", *Trans. AIME*, 146:91 (1952).
65. Yellig, W.F. and Metcalfe, R.S.: "Determination and Prediction of CO₂ Minimum Miscibility Pressures", *JPT*, 32:160-168 (1980).
66. Zapata, V.J. and Lake, L.W.: "A Theoretical Analysis of Viscous Crossflow", SPE 10111, presented at the 56th Annual Conference, San Antonio, Texas, October 5-7, 1981.

**APPENDIX A
FLUID PROPERTIES**

A.1 STEAM-OIL-WATER PROBLEM

The fluid properties for this section were calculated using equations from various sources. The density and enthalpy equations for the water were obtained by fitting a 3rd order polynomial through data obtained from Reynolds (1979) at 2.0 MPa. These results of the curve fit are for the liquid phase,

$$\rho_w = [6.94310^{-4} \quad 2.198 \cdot 10^{-6}t - 6.401 \cdot 10^{-9}t^2 + 8.066 \cdot 10^{-12}t^3]^{-1} \quad (\text{A.1})$$

$$H_w = -1.340536 \cdot 10^6 + 6.0412 \cdot 10^3 t - 5.7 t^2 + 5.699 \cdot 10^{-3} t^3 \quad (\text{A.2})$$

and for the vapor phase

$$\rho_s = [-0.078 + 4.622 \cdot 10^{-4}t - 2.343 \cdot 10^{-7}t^2 + 7.958 \cdot 10^{-11}t^3]^{-1} \quad (\text{A.3})$$

$$H_s = 1.3119117 \cdot 10^6 + 3.7801 \cdot 10^3 t - 1.9t^2 + 7.881 \cdot 10^{-4}t^3 \quad (\text{A.4})$$

The equations for the oil component were taken from a Reid et al. (1977) using the values for n-C₂₀H₄₂. The equations are,

$$\rho_o = 1132.59 = 0.750946 t + 3.37391 \cdot 10^{-4} t^2 \quad (\text{A.5})$$

$$H_o = 2.088845 \cdot 10^5 - 79.9557 t + 3.4318t^2 - 1.3171 \cdot 10^{-3} t^3 + 2.7371 \cdot 10^{-7} t^4 \quad (\text{A.6})$$

The viscosity equations were taken from the ISCOM commercial simulator supplied by the Computer Modelling Group. The curve for the viscosity of the water vapor is from the internal viscosity tables from the ISCOM simulator. The 0% salinity brine data is used for the liquid water viscosity. The curve for the base oil is the equation used by ISCOM to model the viscosity of n-C₂₀H₄₂.

$$\mu_w = 0.00752e^{(1384.86/t)} \quad (\text{A.7})$$

$$\mu_s = 0.0032 + 3.8 \cdot 10^{-5} t + 3.925 \cdot 10^{-13} t^2 - 3.009 \cdot 10^{-16} t^3 \quad (\text{A.8})$$

$$\mu_{\text{base oil}} = 0.132683e^{(821.29/t)} \quad (\text{A.9})$$

$$\mu_{\text{heavy oil \#1}} = 26.5366e^{(821.29/t)} \quad (\text{A.10})$$

$$\mu_{\text{heavy oil \#2}} = 0.009e^{(4000.0/t)} \quad (\text{A.11})$$

A.2 CO₂-OIL-WATER PROBLEM

A.2.1 Flash Calculations

Flash calculations for the problem described in §4.3 require a three phase flash routine that is robust and relatively quick. Such a routine using existing equations of state is not readily available. An alternative solution is to input phase diagrams at varying temperatures and interpolate points that lie between the input values.

The flash routine is essentially the one used by Orr (1980). For the system studied in this dissertation, an isothermal phase diagram is divided into five regions as illustrated in Figure A.1. The regions are described by entering 15 values for the boundaries of the single phase regions.

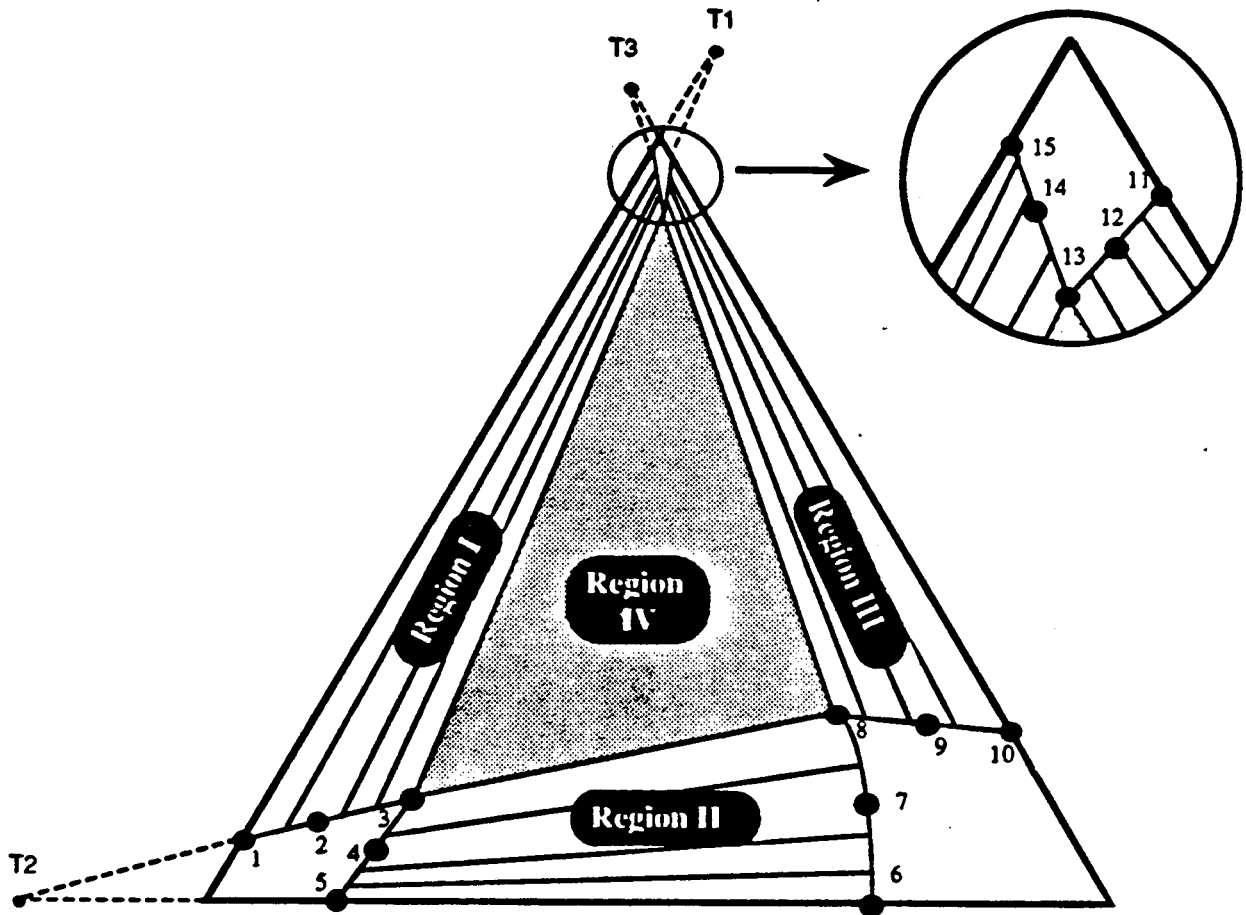


Figure A.1: Isothermal ternary phase diagram showing the five regions and the 15 composition points.

The bubble and dew point curves for each region are found by fitting a quadratic equation through the three points representing the boundary. The flash routine assumes that the tie line extensions for the two-phase regions (region I, II, and III) meet at a common point for each (T_I , T_{II} , and T_{III}).

The flash calculations are done by performing a linear interpolation between the 15 points on the two phase diagrams surrounding the flash temperature. Once a new set of points is found, the phase boundaries and the tie line extension points are calculated at the new temperature. This new phase dia-

gram is stored for future use. When one of the existing phase diagrams is at the current temperature no calculation of the phase boundaries is needed. The final flash is carried out using the procedure described by Orr on the interpolated phase diagram.

The flash routine uses a set of 9 phase diagrams ranging from 300 K-475K. All the diagrams were constructed by using a three phase flash routine developed by Nutakki (1988) to find the boundaries of the three phase region. Additional two phase flashes in regions II and III help to locate points 3-13 on the phase diagrams. A plot of the phase diagrams and the listing of the 15 composition points used to construct these diagrams are shown in Figures A.2—A.10 and Tables A.1—A.9.

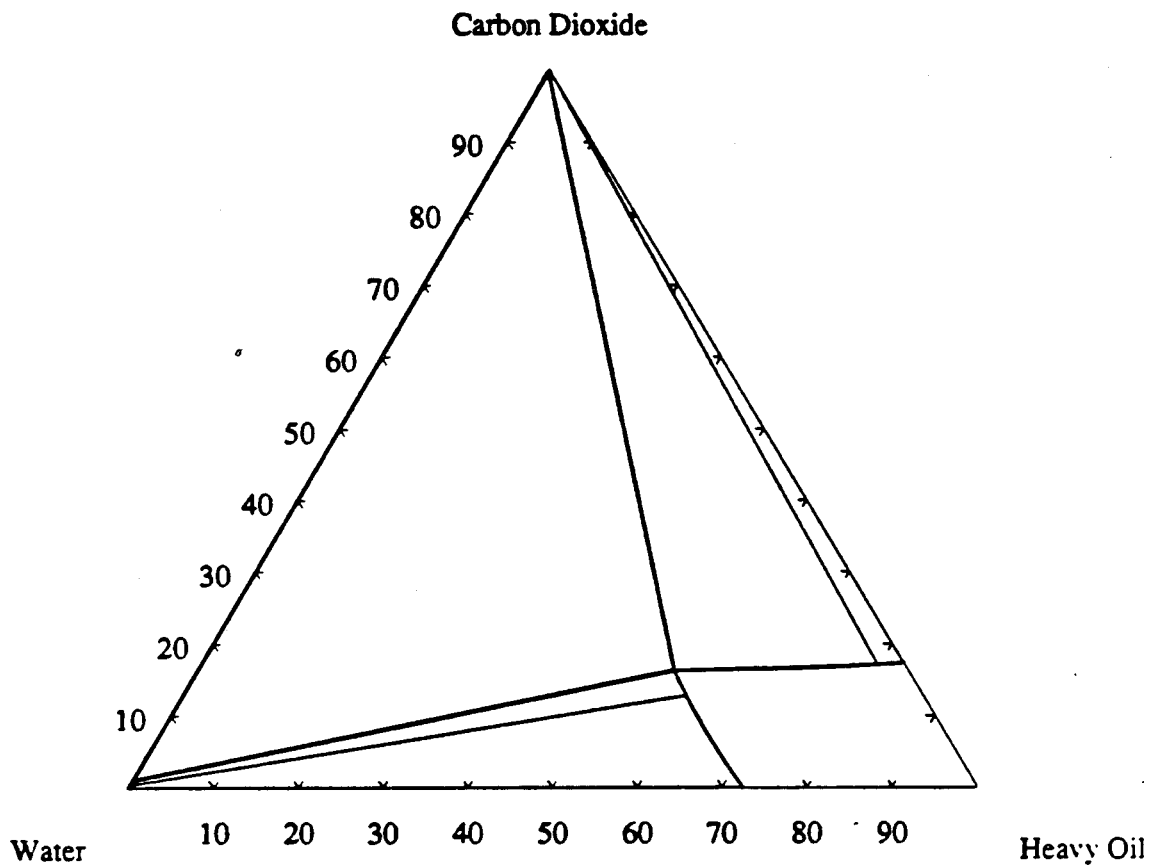


Figure A.2 Isothermal slice of the complete ternary phase diagram for the CO₂-oil-water system at 300 K.

Data	Composition		
Point	CO2	Oil	Water
1	0.01000000	0.00000000	0.99000000
2	0.01008750	0.00000005	0.98991995
3	0.01017500	0.00000010	0.98982490
4	0.00417500	0.00000007	0.99582493
5	0.00000000	0.00000060	0.99999940
6	0.00000000	0.72500000	0.27500000
7	0.12796600	0.59411400	0.27792000
8	0.16270100	0.59411400	0.27431800
9	0.17009000	0.79758700	0.03232300
10	0.17500000	0.82500000	0.00000000
11	0.99995900	0.00000250	0.00003850
12	0.99975900	0.00000200	0.00023900
13	0.99793200	0.00000100	0.00206700
14	0.99893200	0.00000050	0.00106750
15	0.99943200	0.00000000	0.00056800

Table A.1: Input data for CO₂-oil-water phase diagram at 300K

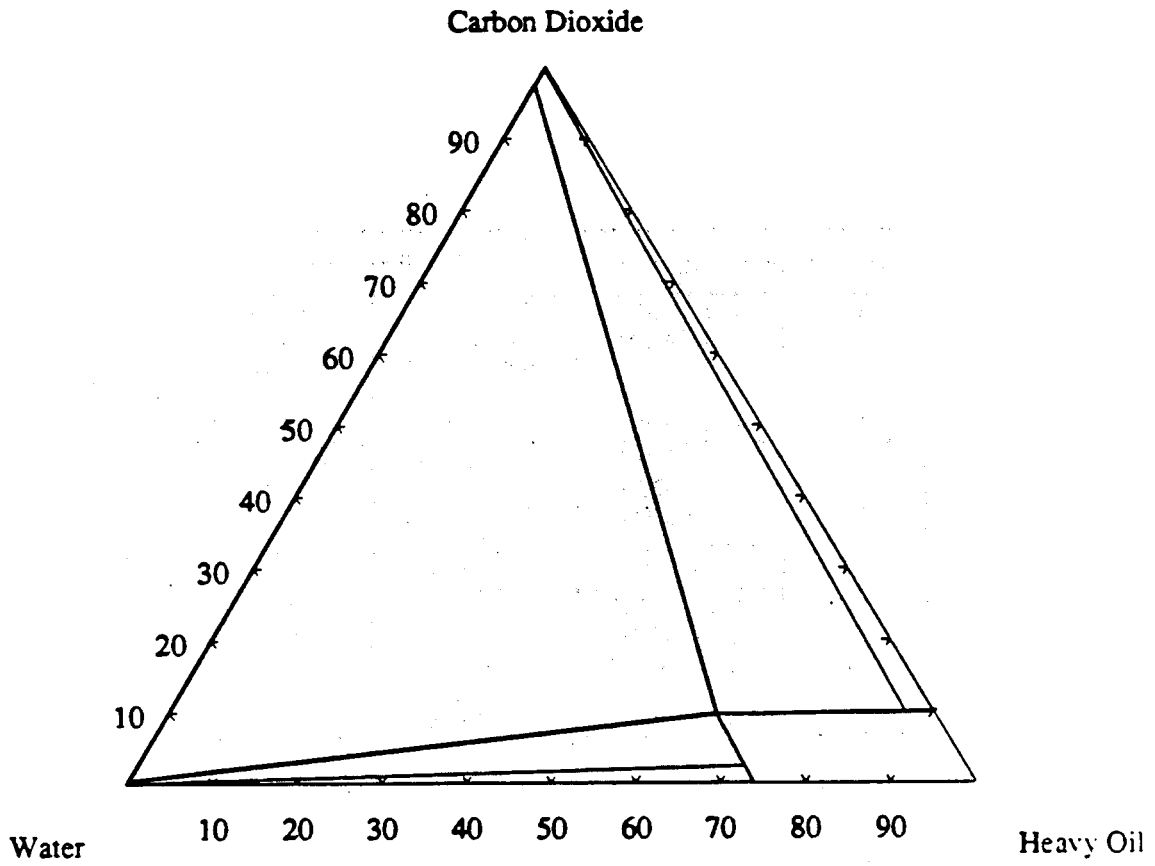


Figure A.3: Isothermal slice of the complete ternary phase diagram for the CO₂-oil-water system at 350 K.

Data Point	Composition		
	CO2	Oil	Water
1	0.00300000	0.00000000	0.99900000
2	0.00340550	0.00000005	0.99899195
3	0.00381100	0.00000010	0.99618899
4	0.00093300	0.00000003	0.99906697
5	0.00000000	0.00000003	0.99999997
6	0.00000000	0.73880000	0.26120000
7	0.02369800	0.71636400	0.25993800
8	0.09623000	0.64769400	0.25607600
9	0.10202200	0.86517700	0.03280100
10	0.10100000	0.89900000	0.00000000
11	0.99992322	0.00007678	0.00000000
12	0.99664200	0.00007400	0.00328400
13	0.97424200	0.00005500	0.02570300
14	0.97434200	0.00005100	0.02560700
15	0.97440200	0.00000000	0.2559800

Table A.2: Input data for CO2-oil-water phase diagram at 350K

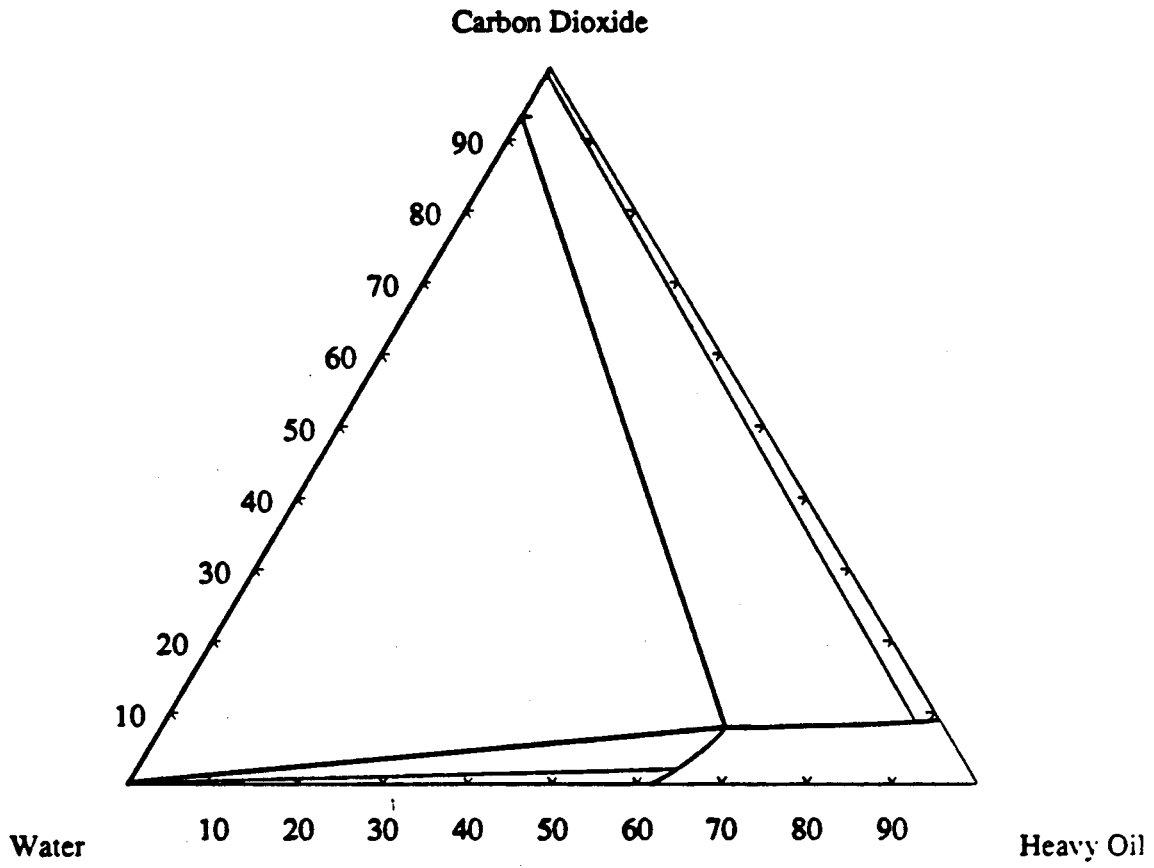


Figure A.4 Isothermal slice of the complete ternary phase diagram for the CO₂-oil-water system at 375 K.

Data Point	Composition		
	CO2	Oil	Water
1	0.02000000	0.00000000	0.99800000
2	0.00241100	0.00000005	0.99858895
3	0.00282200	0.00000010	0.99717790
4	0.00193350	0.00000003	0.99806647
5	0.00000000	0.00000003	0.99999997
6	0.00000000	0.61780000	0.38220000
7	0.02106600	0.63760000	0.34133400
8	0.07809400	0.66556200	0.25634400
9	0.08546900	0.88474700	0.02978400
10	0.08893300	0.91106700	0.00000000
11	0.99969800	0.00030200	0.00000000
12	0.99184200	0.00029500	0.00786300
13	0.93248500	0.00022200	0.06729300
14	0.93249900	0.00009200	0.06740900
15	0.93250400	0.00000000	0.06749600

Table A.3: Input data for CO₂-oil-water phase diagram at 375K

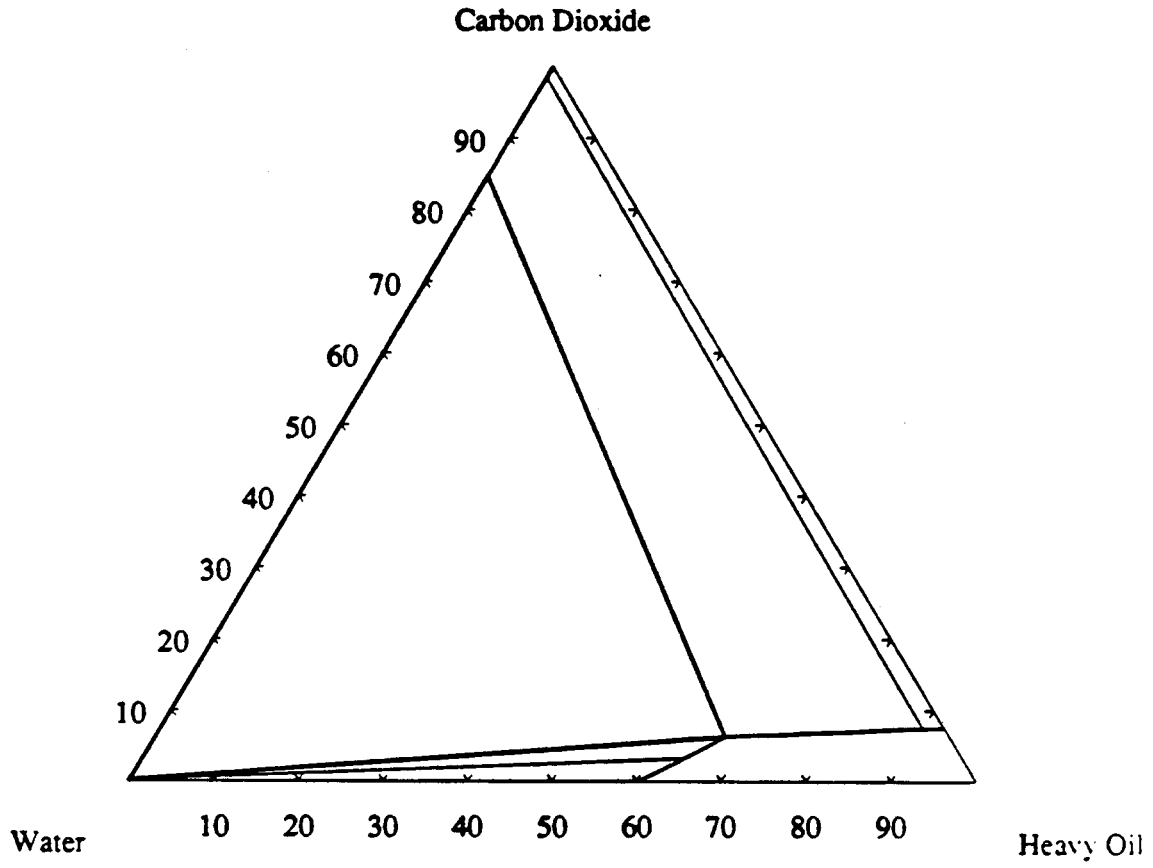


Figure A.5 Isothermal slice of the complete ternary phase diagram for the CO₂-oil-water system at 400 K.

Data Point	Composition		
	CO2	Oil	Water
1	0.00200000	0.00000000	0.99800000
2	0.00209650	0.00000005	0.99890345
3	0.00219300	0.00000010	0.99780690
4	0.00193100	0.00000003	0.99806897
5	0.00000000	0.00000003	0.99999997
6	0.00000000	0.60232100	0.39767900
7	0.03262700	0.64173600	0.32563700
8	0.06255600	0.67354600	0.26389800
9	0.07422800	0.90110200	0.02467000
10	0.07532200	0.92467800	0.00000000
11	0.99900100	0.00099900	0.00000000
12	0.98459700	0.00097200	0.01443100
13	0.84687900	0.00071500	0.15240600
14	0.84691400	0.0035500	0.15273100
15	0.84726800	0.00000000	0.15273200

Table A.4: Input data for CO₂-oil-water phase diagram at 400K

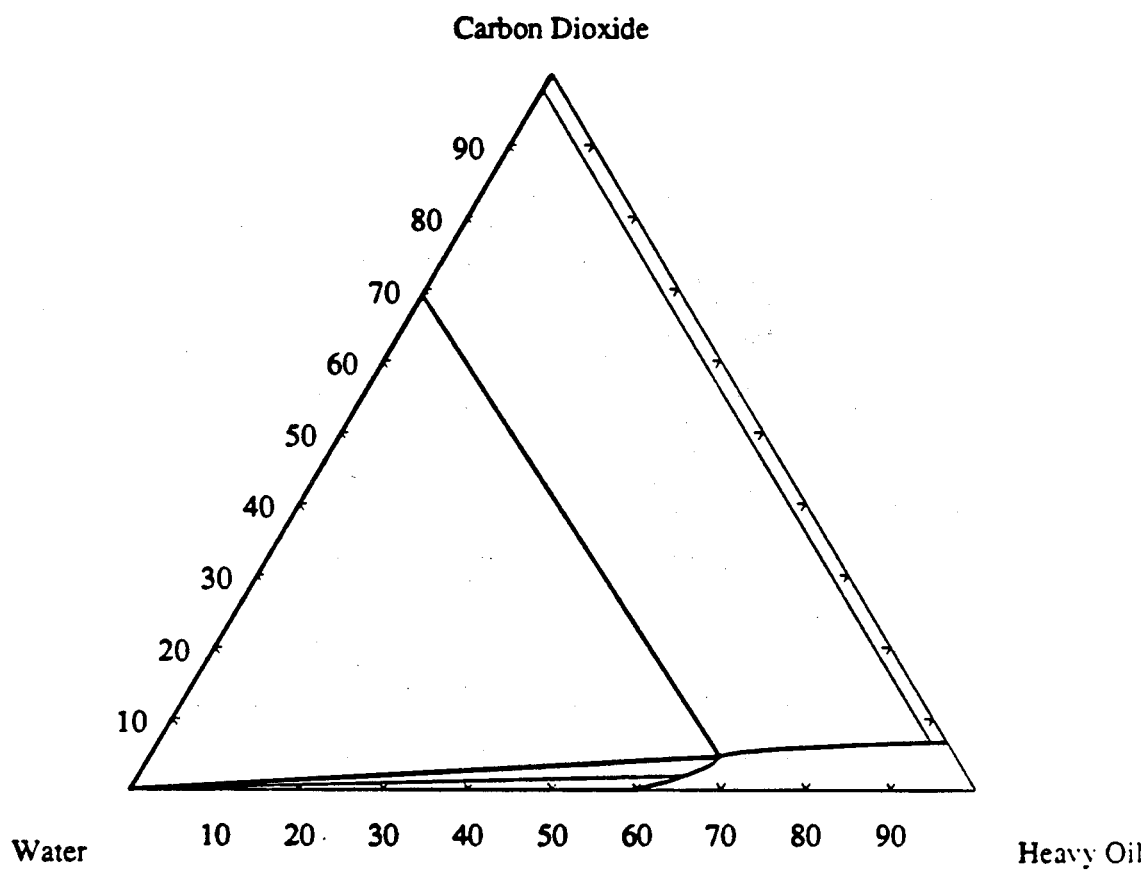


Figure A.6 Isothermal slice of the complete ternary phase diagram for the CO₂-oil-water system at 425 K.

Data Point	Composition		
	CO2	Oil	Water
1	0.00160000	0.00000000	0.99840000
2	0.00165800	0.00000002	0.99834198
3	0.00171600	0.00000010	0.99828390
4	0.00126200	0.00000003	0.99873797
5	0.00000000	0.00000003	0.99999997
6	0.00000000	0.59676200	0.40323800
7	0.02000000	0.64838000	0.33162000
8	0.04661500	0.67525500	0.27813000
9	0.06641100	0.91472800	0.01886100
10	0.06713700	0.98286300	0.00000000
11	0.99832050	0.00167950	0.00000000
12	0.97606400	0.00262800	0.02130800
13	0.69094600	0.00193500	0.30711900
14	0.69782100	0.00040300	0.30177600
15	0.69822500	0.00000000	0.30177500

Table A.5: Input data for CO₂-oil-water phase diagram at 425K

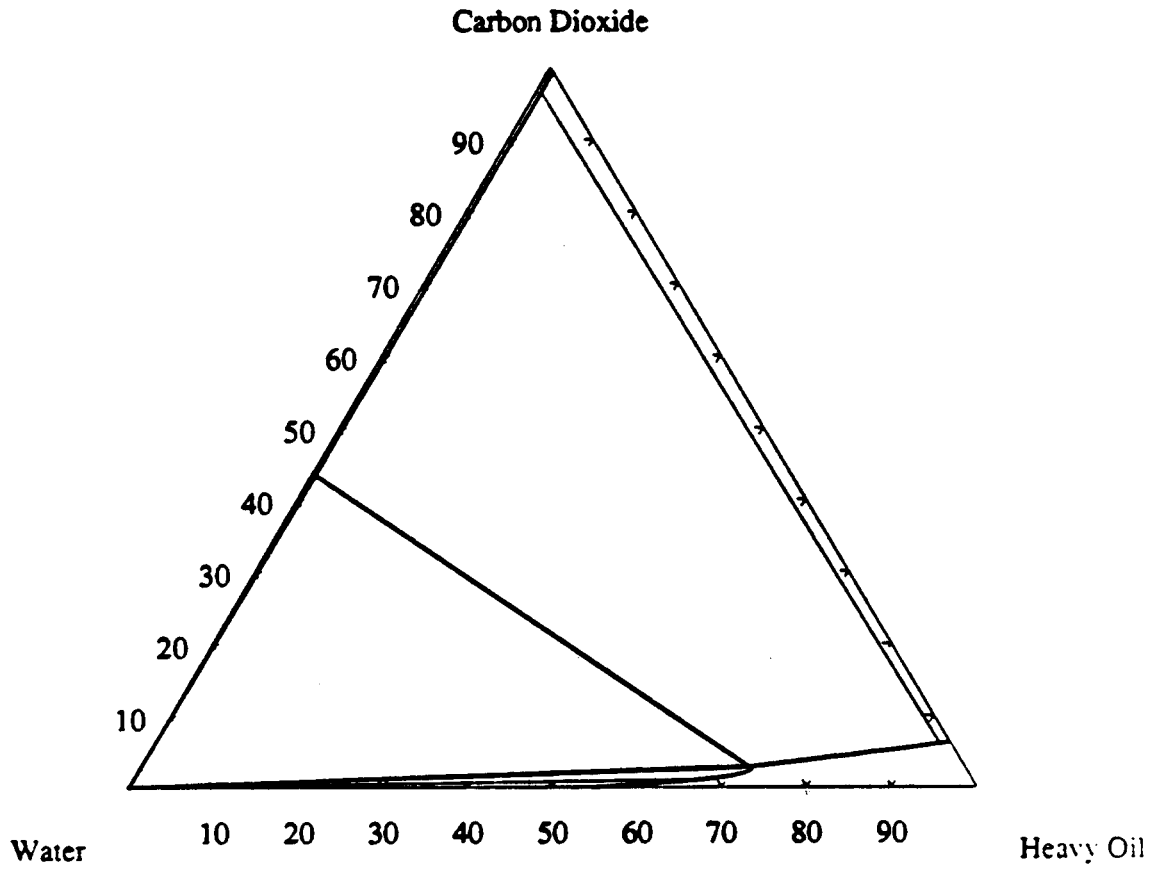


Figure A.7 Isothermal slice of the complete ternary phase diagram for the CO₂-oil-water system at 450 K.

Data Point	Composition		
	CO2	Oil	Water
1	0.00100000	0.00000000	0.99900000
2	0.00106650	0.00000002	0.99893348
3	0.00113300	0.00000010	0.99886690
4	0.00089980	0.00000003	0.99910017
5	0.00000000	0.00000003	0.99999997
6	0.00000000	0.55435000	0.44565000
7	0.10000000	0.66564000	0.32436000
8	0.02791900	0.71998800	0.25209300
9	0.06084800	0.92685900	0.01228300
10	0.06273000	0.93727000	0.00000000
11	0.99369200	0.00630800	0.00000000
12	0.96517000	0.00628500	0.02854500
13	0.43347800	0.00486200	0.56166000
14	0.43485670	0.00243100	0.56271230
15	0.43623530	0.00000000	0.56376470

Table A.6: Input data for CO₂-oil-water phase diagram at 450K

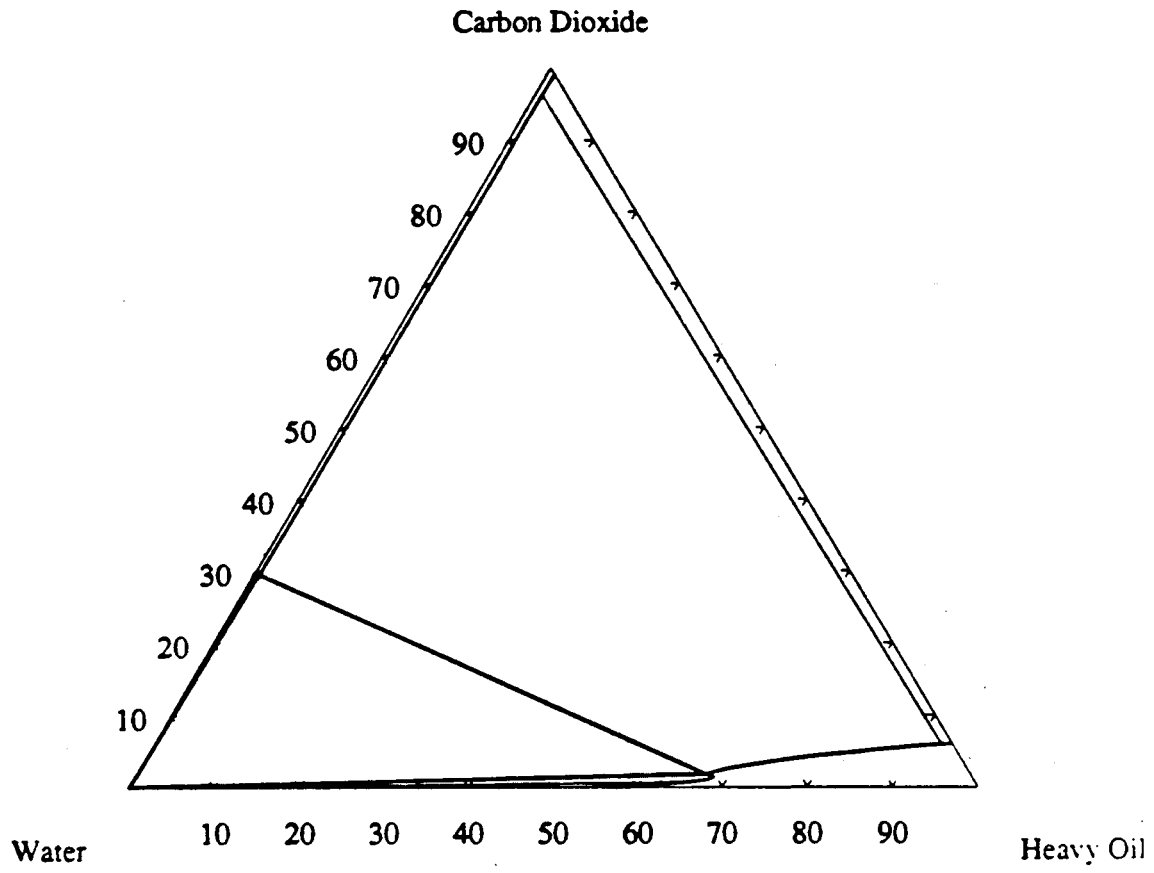


Figure A.8 Isothermal slice of the complete ternary phase diagram for the CO₂-oil-water system at 460 K.

Data Point	Composition		
	CO2	Oil	Water
1	0.00069000	0.00000000	0.99931000
2	0.00074350	0.00000002	0.99256498
3	0.00079700	0.00000010	0.99920290
4	0.00038470	0.00000003	0.99961527
5	0.00000000	0.00000003	0.99999997
6	0.00000000	0.57335000	0.42665000
7	0.00710000	0.65621000	0.33669000
8	0.01855500	0.67200400	0.30944100
9	0.05921500	0.92862000	0.01216500
10	0.06028200	0.93971300	0.00000500
11	0.99129640	0.00870360	0.00000000
12	0.96280000	0.00860000	0.02860000
13	0.29577900	0.00618200	0.69803900
14	0.29581000	0.00301200	0.70117800
15	0.29583200	0.00000000	0.70416800

Table A.7: Input data for CO₂-oil-water phase diagram at 460K

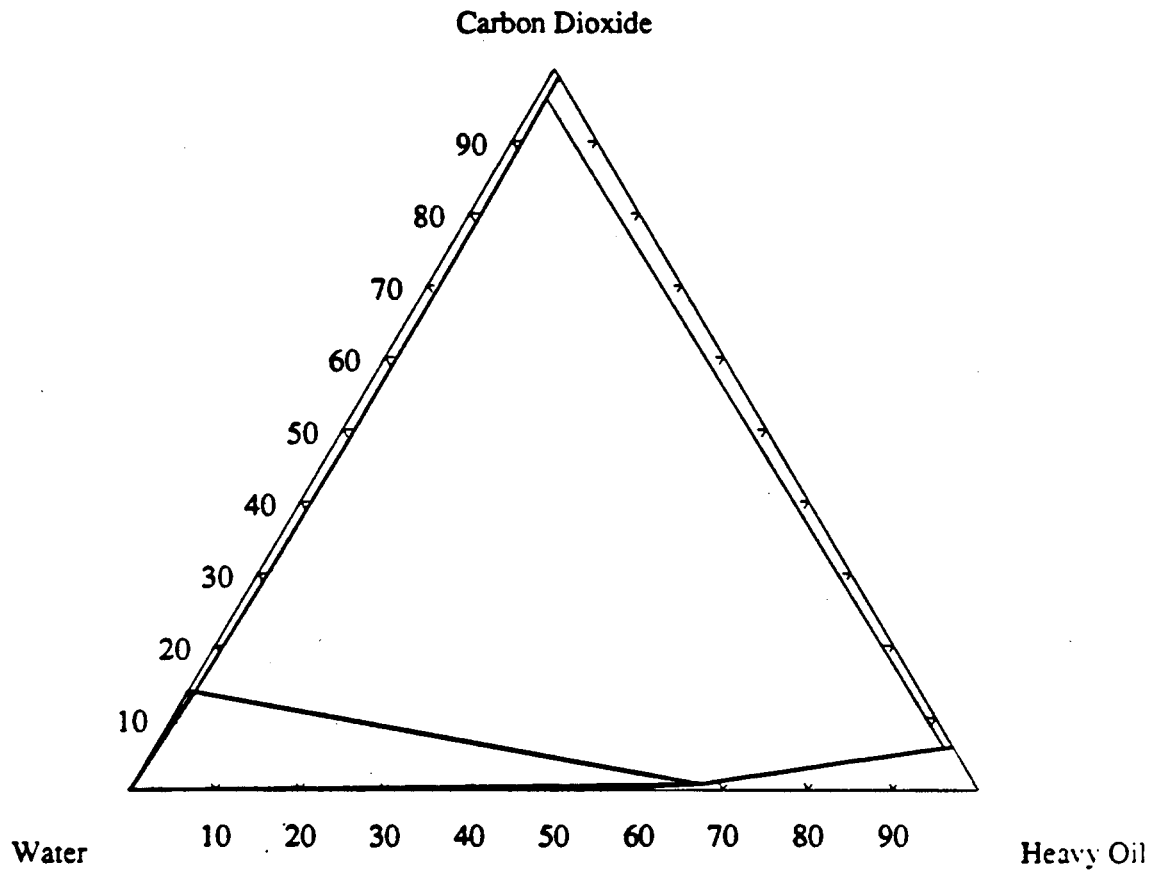


Figure A.9 Isothermal slice of the complete ternary phase diagram for the CO₂-oil-water system at 470 K.

Data	Composition		
Point	CO2	Oil	Water
1	0.00030000	0.00000000	0.99970000
2	0.00034050	0.00000002	0.99965948
3	0.00038100	0.00000010	0.99961900
4	0.00023200	0.00000003	0.99976797
5	0.00000000	0.00000003	0.99999997
6	0.00000000	0.49994000	0.50006000
7	0.00400000	0.58750000	0.40850000
8	0.00841300	0.67054100	0.32104600
9	0.05772300	0.93155300	0.01072400
10	0.05937300	0.94062700	0.00000000
11	0.99893600	0.01106400	0.00000000
12	0.95835500	0.01159400	0.03005100
13	0.13530800	0.00826400	0.85642800
14	0.13536000	0.00543600	0.85920400
15	0.13538900	0.00000000	0.86461100

Table A.8: Input data for CO₂-oil-water phase diagram at 470K

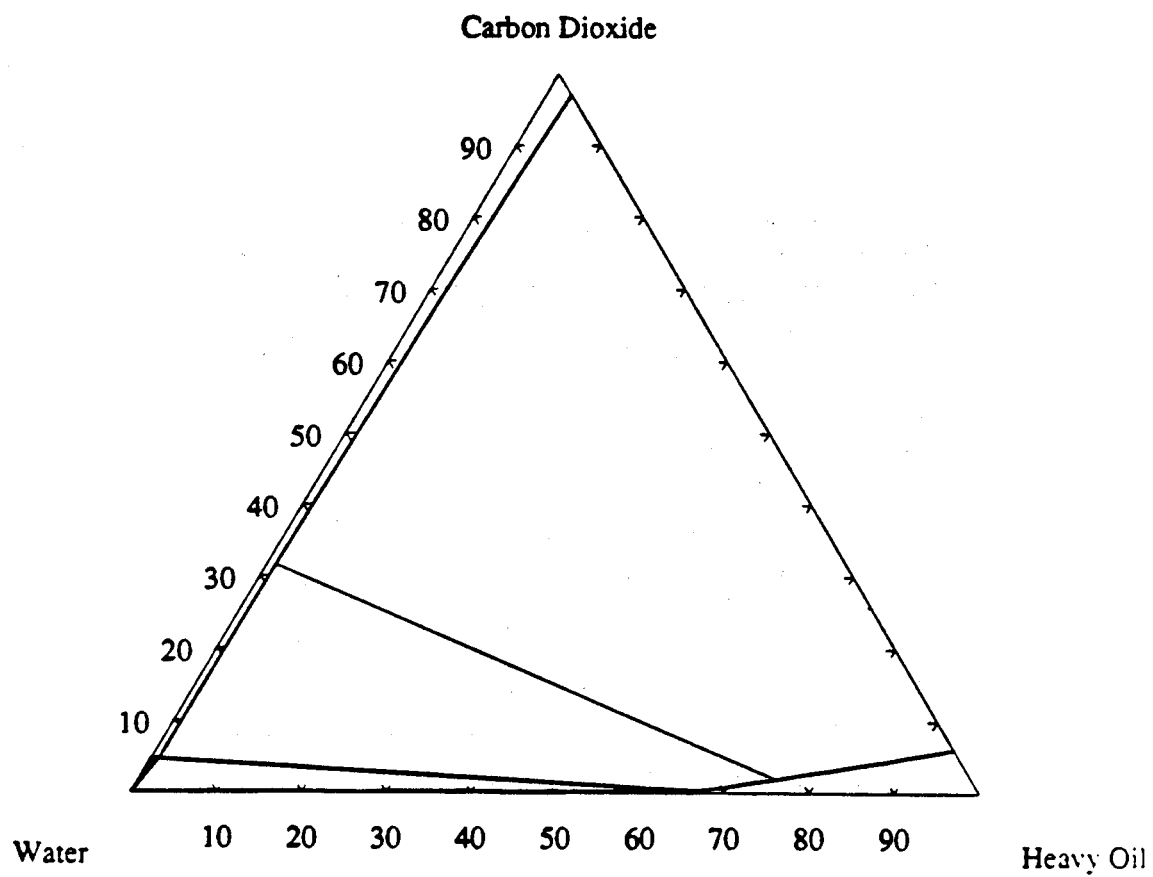


Figure A.10 Isothermal slice of the complete ternary phase diagram for the CO₂-oil-water system at 475 K.

Data Point	Composition		
	CO2	Oil	Water
1	0.00008600	0.00000000	0.99991400
2	0.00011050	0.00000002	0.99988948
3	0.00013500	0.00000010	0.99986490
4	0.00007500	0.00000003	0.99992497
5	0.00000000	0.00000001	0.99999999
6	0.00000000	0.43540000	0.56460000
7	0.00173000	0.60839300	0.38987700
8	0.00287500	0.66879200	0.32833300
9	0.01927700	0.75207100	0.22865200
10	0.06062700	0.93937300	0.00000000
11	0.96995600	0.03004400	0.00000000
12	0.31565800	0.01068700	0.67365500
13	0.04636200	0.00948100	0.94415700
14	0.04636100	0.00474050	0.94889850
15	0.04636000	0.00000000	0.95364000

Table A.9: Input data for CO₂-oil-water phase diagram at 475K

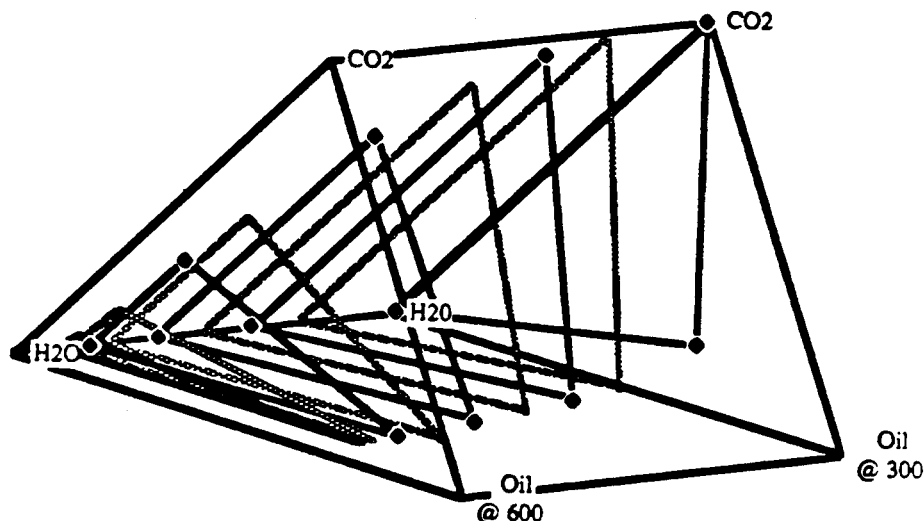


Figure A.11: Stacked ternary phase diagrams for the CO₂-oil-water system from 300-600 K.

A.2.2 Fluid Properties

The flash calculation only gives the composition of each phase. The properties of the existing phases are found by applying the Schmidt-Wenzel equation of state to the phases found by the flash calculation. The Schmidt-Wenzel equation gives improved density calculations compared to the more familiar Peng-Robinson equation of state. The density, saturations and specific molar enthalpies of all the phases are calculated from the phase composition, temperature and pressure.

The viscosity correlations commonly used for calculating viscosities of hydrocarbon mixtures are not very accurate for heavy oils. Specific correlations for mixtures of CO₂ and heavy oils have been presented, but none of these correlations take into account a water component. The formula used is an adaptation of the one given by Loeb and is valid when high viscosity contrasts between components are present. The mixing rule is given by,

$$\ln \mu_{mix} = \sum_{i=1}^{n_s} X_i \ln \mu_i \quad (A.12)$$

The equations used to model the pure component viscosities of the water and oil phases are the same as in the steam-oil-water case. The CO₂ viscosities are taken from Vargaftik (1975) at a pressure of 17.23 MPa [250 psia]. The equations used for the pure components are:

$$\mu_{CO_2,v} = -0.14658 + 0.0017199\sqrt{t} \quad (A.13)$$

$$\mu_{CO_2,l} = 0.0441259e^{(578.08/t)} \quad (A.14)$$

$$\mu_{oil,v} = 0.80 + 0.0035\sqrt{t} \quad (A.15)$$

$$\mu_{oil,l} = 0.132836e^{(821.29/t)} \quad (A.16)$$

$$\mu_{H_2O,v} = 0.0032 + 3.8 \cdot 10^{-5} t + \frac{3.925 \cdot 10^{-13} t^2}{3.009 \cdot 10^{-16} t^3} \quad (\text{A.17})$$

$$\mu_{H_2O,l} = 0.00752e^{(1384.86/t)} \quad (\text{A.18})$$

APPENDIX B ENTHALPY BALANCE ACROSS A DISCONTINUITY

The transition from the single phase to the two-phase region must occur via a shock as well as the transition from a two-phase to a three-phase region. This is because the velocities as given by the eigenvalues are discontinuous at the phase boundary. The material balance tells us that shocks entering or exiting a two phase region from a single phase boundary condition $\{x_m\}$ lie along the tie-line extension that passes through the single phase composition (Dumore *et al.* 1984).

Applying the same procedure to the enthalpy balance indicates how the temperature changes as the solution jumps from the single phase to the two phase region. Consider a system with a single phase on the downstream side of a shock and two phases on the upstream side. The two phases will be gas and oil. Since there can be no enthalpy accumulation inside the shock, the enthalpy on the downstream side must equal the enthalpy on the two-phase side of the shock. Writing an enthalpy balance yields,

$$\begin{aligned} \rho_o^- S_o^- H_o^- + \rho_g^- S_g^- H_g^- + \left(\frac{1-\phi}{\phi}\right) \rho_m H_m^- - \rho^+ H^+ - \left(\frac{1-\phi}{\phi}\right) \rho_m H_m^+ = \\ \frac{u^-}{\phi} [\rho_o^- f_o^- H_o^- + \rho_g^- f_g^- H_g^-] - \frac{u^+}{\phi} \rho^+ H^+ \end{aligned} \quad (B.1)$$

where superscript (+) refers to the downstream side of the shock, superscript (-) refers to the upstream side, and the subscripts *o* and *g* refer to the oil and gas phases, respectively.

Equation B.1 can be rearranged and solved for the upstream enthalpy content, $\rho^+ H^+$ to give,

$$\begin{aligned} \frac{1}{\left(1 - \frac{u^+}{\phi}\right)} \left\{ \left[S_o^- - \frac{U^-}{\phi} f_o^- \right] \rho_o^- H_o^- + \left[S_g^- - \frac{u^-}{\phi} f_g^- \right] \rho_g^- H_g^- + \right. \\ \left. \left(\frac{1-\phi}{\phi} \right) \rho_m C_{pm} (T^- - T^+) \right\} = \rho^+ H^+ \end{aligned} \quad (B.2)$$

The final term on the left side of Eq. B.2 represents the extra contribution of the matrix. As the porosity goes to unity or the heat capacity of the matrix goes to zero, the enthalpy balance is similar to the component balances. The enthalpy in the two phase region is found from linear combination of the single phase enthalpy.

When the matrix is allowed to take up or release enthalpy across a shock, the speed of the shock is slowed or increased depending on the relationship of the upstream to downstream conditions. The flash that calculates the conditions on the two phase side of the shock is not a strictly isenthalpic flash. The total enthalpy of the flashed fluids *plus the matrix* must remain constant during the flash. The deviation from the traditional isenthalpic flash is quantified by the $\rho_m C_{pm} \Delta T$ term in Eq. B.2.

APPENDIX C COMPLEX EIGENVALUES

Complex eigenvalues have been observed by Fayers (1987) and later, Gorell (1988) in the phase space where three phase flow is present. The complex eigenvalues indicate that the problem is no longer hyperbolic, but *elliptic*. Fayers reports that the elliptic regions cover only a small area of the three phase space. The complex regions are shown to occur when the oil viscosity is close to that of the aqueous phase. When the oil viscosity is much greater, no elliptic regions appear.

Gorell noted the existence of complex eigenvalues in regions where trapping occurs. The complex eigenvalues were attributed to the assumption that only oil is trapped, which is not always physically correct. The paths in this region were integrated using only the real parts of the eigenvalues and eigenvectors.

Glimm (1986) argues that the elliptic region introduces a linear instability which is stabilized by the non-linear considerations. A solution that is forced to begin in the elliptic region will exit the region via a shock. The solution will not return unless the boundary conditions are force the solution to return. He further argues that a solution not in the elliptic region will not enter the region unless the initial conditions are in the elliptic region.

Bell *et.al.* (1986) conducted a numerical study of the elliptic region. By adjusting the fractional flow relationships in a three phase immiscible system, they maximized the elliptic region in the saturation space. One dimensional finite difference simulations were conducted with boundary conditions that were in various locations surrounding and within the elliptic region. The results indicate that unless one of the boundary conditions was inside the elliptic region, the solution path avoided this region altogether. This even occurred when the initial and injection conditions were located near, but on opposite sides of the elliptic region.

Figures C.1 and C.2 indicate the regions in three phase space where complex eigenvalues were found for two different relative permeability models and two sets of permeability exponents. The complex regions are confined to regions near the zero oil isoperm. The solutions presented in this model avoid these elliptic regions altogether.

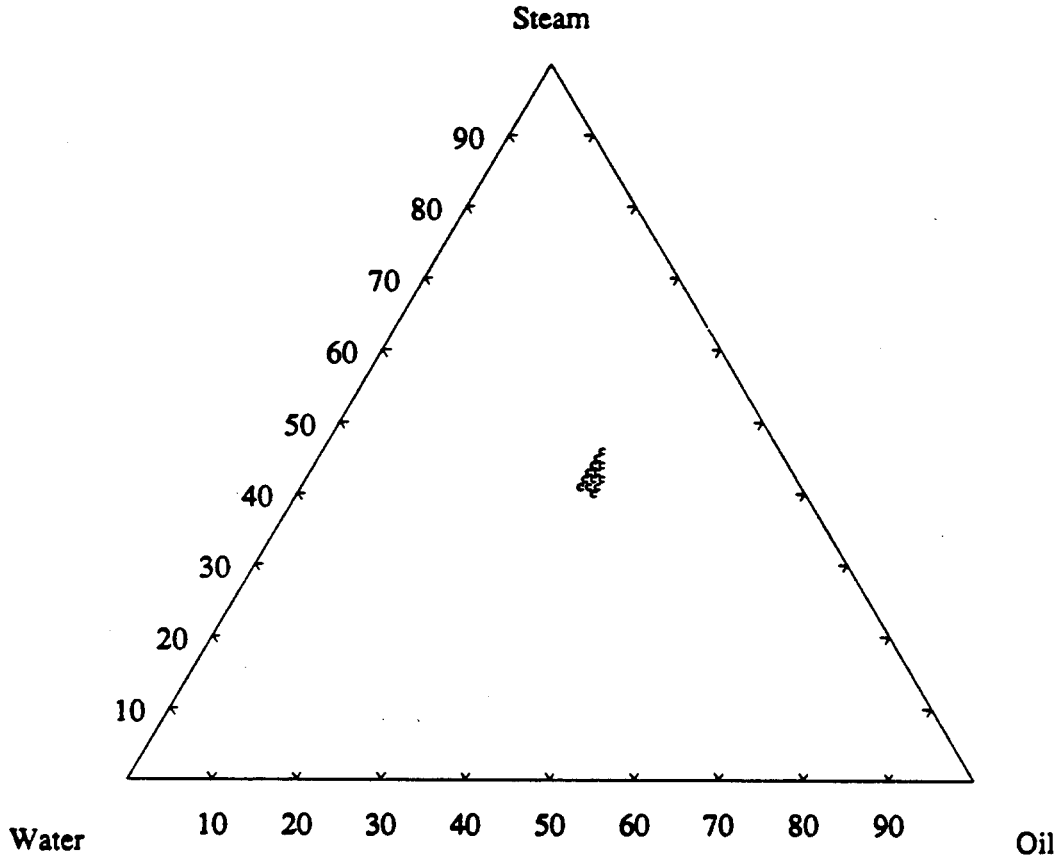


Figure C.1: Region of complex eigenvalues using Stone's model II with $\alpha_g = 1.0$, $\alpha_w = 3.0$, $\alpha_{ow} = 2.0$, and $\alpha_{ig} = 2.0$.

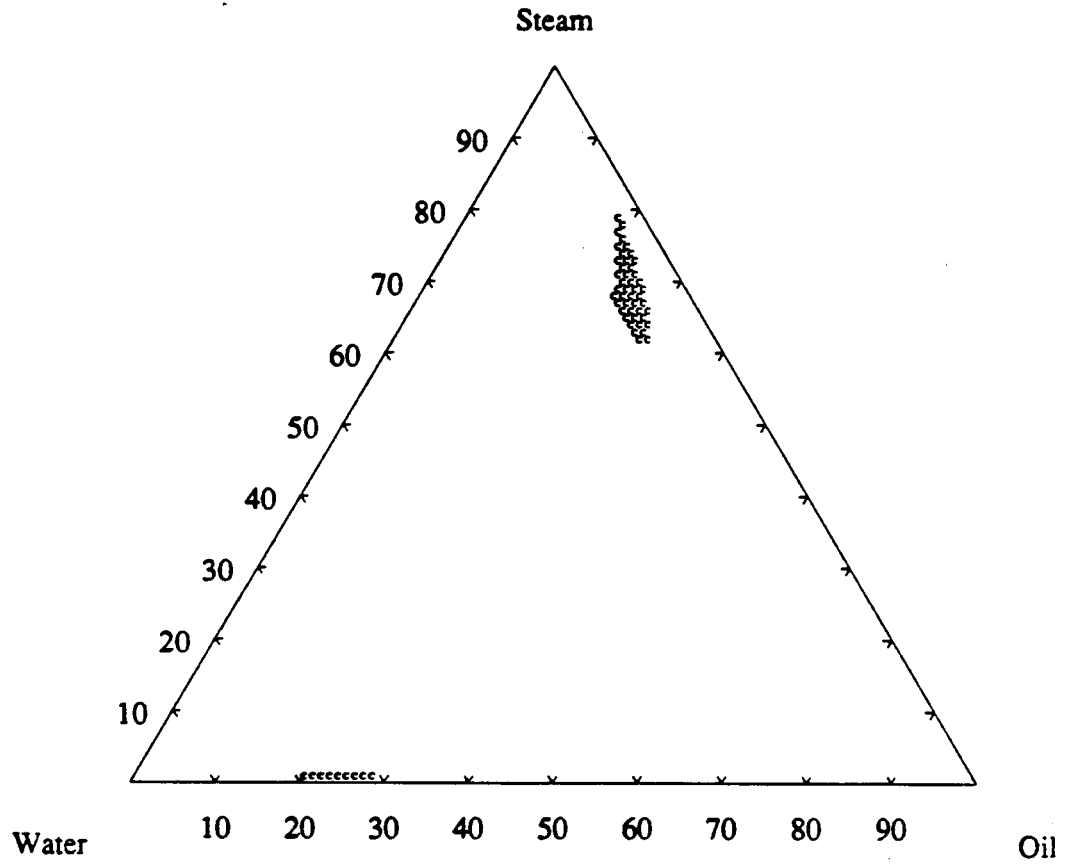


Figure C.2: Region of complex eigenvalues using Stone's model II with $\alpha_g = 1.0$, $\alpha_w = 2.0$, $\alpha_{ow} = 2.0$, and $\alpha_{lg} = 2.0$.

APPENDIX D EXCEL SPREADSHEETS

This appendix contains the EXCEL spreadsheets used to calculate the steam-water profiles found in §4.1. The spreadsheet is divided into four sections. The upper section, rows 1--25 contain the important information on the system. The matrix properties and boundary conditions are entered in this section. Results of the shock velocities and heights are reported in this area of the worksheet.

The second section calculates the saturation profiles using the relationship given by Eq. 4.7. The saturation profile is divided into fifty equally spaced points between the saturations at the trailing and leading shocks.

The third and fourth sections contain details on the calculation of the trailing and leading shocks, respectively. The calculation is done by 25 bisections over a user specified interval. The final value of the objective function, $\lambda'' - \Lambda_S$, is reported under the shock conditions.

D.1 Cell Formulas

This section of the appendix contains a cell by cell listing of the four different areas of the spreadsheet. This information should be enough to reconstruct the worksheet from scratch. The initial area is the input and output area. This area is used to enter the parameters and read the resulting conditions for the trailing and leading shocks.

Numbers appear in the cells that are used as inputs to the spreadsheet. The cells with formulas are either calculated input conditions or results.

D.2 Changes in Injection Temperature

These worksheets examine the effect of injection temperature on the saturation profiles. The injection temperature is entered in cell B22. The section contains 11 worksheets with the injection temperature ranging from 500-1000 K, in 50 K intervals.

Spreadsheet for Calculation of Stream-Water Saturation Profiles

Injection Temperature
500 °K

Initial Temperature
350 °K

Matrix Heat Capacity
1.0000 (kJ/kg)

MATRIX PROPERTIES

Porosity	Cp Matrix	Density	Rho * Cp
0.10	1.00	2650.00	2650.0000
Nw	Ng	Swi	Denom
3.00	1.00	0.00	1.000000

SATURATION CONDITIONS

Tsaturation = 485.57

	Volumes (m3/kg)	Enthalpies (kJ/kg)	Densities (kg/m3)	Viscosities (cp)	Saturation Step
Liquid	0.001176	901.41	850.4723	0.1303	0.0014361706
Vapor	0.100298	2808.52	9.970241	0.0217	

BOUNDARY CONDITIONS

	Temperature	Velocity	Heat Capacity	Wave Velocity	Density	Enthalpy
Injection	500	1.000000	2.46	0.009878	9.571897	2844.22
Initial	350	0.016526	4.15	0.023956	975.3174	319.98
	G	F	Gamma	Theta		
Injection	500	9.57	9.57	1195224.62	27224.62	
Initial	350	975.32	975.32	8659580.72	312080.72	

SHOCK CONDITIONS

	Initial Guess		Vapor Saturation	Objective Function	Two-Phase Wave Velocity	Upstream Flow Velocity	Shock Velocity	Vapor Frac Flow
Trailing	Sv-Hi	Sv-Low	0.9584	-2.6786E-09	0.0088	0.962144	0.0088	1.0000
Leading	1	0.5	0.8866	6.5987E-09	0.0725	0.016526	0.0725	0.9997
	dKrv/dSv	dKrl/dSl	Total Mobility	dFv/dSv	G	F'	Gamma	Theta'
Trailing	1.0000	0.0052	44.2669	0.0009	44.8986	9.9807	1.1640E+07	28010.7980
Leading	1.0000	0.0386	40.9610	0.0075	105.2538	10.1997	1.1693E+07	28203.2809

MATERIAL BALANCES

	Inside Mass	Initial	Injected	Produced	Balance	Error
Mass	90.985248	97.531740	9.571897	16.118375	0.0000	0.0000%
Enthalpy	888032.5527	865958.0720	27224.6208	5157.5354	-7.3953	0.0008%

Spreadsheet for Calculation of Stream-Water Saturation Profiles

Injection Temperature 500 °K		Initial Temperature 350 °K			Matrix Heat Capacity 1.0000 (kJ/kg)			
SATURATION PROFILE								
Vapor Saturation	Vapor Frac Flow	dKr/dSv	dKr/dSI	Total Mobility	dFv/dSv	lambda	Mass Inside	Enthalpy Inside
1.0000						0.000000		
1.0000						0.008769		
0.9584	0.999988	1.0000	0.0052	44.266945	0.000911	0.008769	0.083936	104808.566620
0.9570	0.999986	1.0000	0.0055	44.200674	0.000977	0.009404	0.028915	7397.278781
0.9556	0.999985	1.0000	0.0059	44.134406	0.001046	0.010063	0.030784	7672.567338
0.9541	0.999983	1.0000	0.0063	44.068143	0.001117	0.010746	0.032717	7949.554259
0.9527	0.999982	1.0000	0.0067	44.001884	0.001190	0.011453	0.034713	8228.251909
0.9513	0.999980	1.0000	0.0071	43.935630	0.001266	0.012184	0.036775	8508.672747
0.9498	0.999978	1.0000	0.0076	43.869380	0.001345	0.012938	0.038902	8790.829326
0.9484	0.999976	1.0000	0.0080	43.803135	0.001426	0.013718	0.041095	9074.734290
0.9470	0.999974	1.0000	0.0084	43.736895	0.001509	0.014521	0.043355	9360.400382
0.9455	0.999972	1.0000	0.0089	43.670660	0.001595	0.015349	0.045682	9647.840437
0.9441	0.999969	1.0000	0.0094	43.604431	0.001684	0.016202	0.048077	9937.067389
0.9426	0.999967	1.0000	0.0099	43.538206	0.001775	0.017080	0.050540	10228.094268
0.9412	0.999964	1.0000	0.0104	43.471987	0.001869	0.017983	0.053072	10520.934203
0.9398	0.999961	1.0000	0.0109	43.405774	0.001966	0.018911	0.055674	10815.600422
0.9383	0.999958	1.0000	0.0114	43.339566	0.002065	0.019865	0.058346	11112.106251
0.9369	0.999955	1.0000	0.0119	43.273364	0.002166	0.020844	0.061088	11410.465119
0.9355	0.999952	1.0000	0.0125	43.207168	0.002271	0.021848	0.063902	11710.690554
0.9340	0.999949	1.0000	0.0131	43.140979	0.002378	0.022879	0.066789	12012.796189
0.9326	0.999945	1.0000	0.0136	43.074795	0.002488	0.023935	0.069748	12316.795758
0.9312	0.999942	1.0000	0.0142	43.008618	0.002600	0.025018	0.072780	12622.703100
0.9297	0.999938	1.0000	0.0148	42.942448	0.002715	0.026126	0.075887	12930.532159
0.9283	0.999934	1.0000	0.0154	42.876284	0.002833	0.027262	0.079068	13240.296983
0.9268	0.999930	1.0000	0.0161	42.810127	0.002954	0.028424	0.082324	13552.011728
0.9254	0.999925	1.0000	0.0167	42.743977	0.003078	0.029612	0.085657	13865.690659
0.9240	0.999921	1.0000	0.0173	42.677834	0.003204	0.030828	0.089066	14181.348146
0.9225	0.999916	1.0000	0.0180	42.611698	0.003333	0.032071	0.092553	14498.998671
0.9211	0.999911	1.0000	0.0187	42.545569	0.003465	0.033341	0.096118	14818.656826
0.9197	0.999906	1.0000	0.0194	42.479449	0.003600	0.034638	0.099762	15140.337312
0.9182	0.999901	1.0000	0.0201	42.413335	0.003738	0.035963	0.103485	15464.054946
0.9168	0.999896	1.0000	0.0208	42.347230	0.003878	0.037316	0.107288	15789.824653
0.9154	0.999890	1.0000	0.0215	42.281132	0.004022	0.038697	0.111172	16117.661477
0.9139	0.999884	1.0000	0.0222	42.215043	0.004168	0.040106	0.115138	16447.580574
0.9125	0.999878	1.0000	0.0230	42.148961	0.004318	0.041544	0.119187	16779.597216
0.9110	0.999872	1.0000	0.0237	42.082888	0.004470	0.043009	0.123318	17113.726793
0.9096	0.999865	1.0000	0.0245	42.016823	0.004625	0.044504	0.127533	17449.984812
0.9082	0.999858	1.0000	0.0253	41.950767	0.004784	0.046027	0.131833	17788.386900
0.9067	0.999851	1.0000	0.0261	41.884720	0.004945	0.047580	0.136219	18128.948803
0.9053	0.999844	1.0000	0.0269	41.818682	0.005110	0.049161	0.140690	18471.686388
0.9039	0.999837	1.0000	0.0277	41.752652	0.005277	0.050772	0.145249	18816.615644
0.9024	0.999829	1.0000	0.0286	41.686632	0.005447	0.052413	0.149895	19163.752683
0.9010	0.999821	1.0000	0.0294	41.620621	0.005621	0.054083	0.154630	19513.113741
0.8996	0.999813	1.0000	0.0303	41.554619	0.005798	0.055783	0.159454	19864.715179
0.8981	0.999804	1.0000	0.0311	41.488627	0.005978	0.057513	0.164368	20218.573485
0.8967	0.999796	1.0000	0.0320	41.422645	0.006161	0.059274	0.169373	20574.705272
0.8953	0.999787	1.0000	0.0329	41.356672	0.006347	0.061065	0.174469	20933.127283
0.8938	0.999777	1.0000	0.0338	41.290709	0.006536	0.062887	0.179659	21293.856390
0.8924	0.999768	1.0000	0.0347	41.224757	0.006729	0.064740	0.184941	21656.909596
0.8909	0.999758	1.0000	0.0357	41.158814	0.006924	0.066623	0.190318	22022.304035
0.8895	0.999748	1.0000	0.0366	41.092882	0.007124	0.068538	0.195790	22390.056973
0.8881	0.999738	1.0000	0.0376	41.026961	0.007326	0.070485	0.201358	22760.185811
0.8866	0.999727	1.0000	0.0386	40.961050	0.007531	0.072463	0.207023	23132.708085
0.0000						0.072463		
0.0000						1.000000		

Spreadsheet for Calculation of Stream-Water Saturation Profiles

Injection Temperature 500 °K Initial Temperature 350 °K Matrix Heat Capacity 1.0000 (kJ/kg)

TRAILING SHOCK CALCULATIONS

Saturation	OF	Wave V	Flow V	Shock V	f _v	dK _{rv} /dS _v	dK _{rl} /dS _l
0.7500	3.24E-01	0.392300	0.855597	0.068408	0.996549	1.0000	0.1875
0.875	7.17E-02	0.088368	0.948036	0.016666	0.999629	1.0000	0.0469
0.9375	1.12E-02	0.020416	0.961412	0.009179	0.999957	1.0000	0.0117
0.96875	-3.97E-03	0.004887	0.961990	0.008855	0.999995	1.0000	0.0029
0.953125	2.45E-03	0.011240	0.962100	0.008794	0.999982	1.0000	0.0066
0.9609375	-1.05E-03	0.007721	0.962135	0.008774	0.999990	1.0000	0.0046
0.95703125	6.23E-04	0.009394	0.962141	0.008771	0.999986	1.0000	0.0055
0.958984375	-2.34E-04	0.008536	0.962144	0.008769	0.999988	1.0000	0.0050
0.9580078125	1.90E-04	0.008959	0.962144	0.008769	0.999987	1.0000	0.0053
0.9584960938	-2.28E-05	0.008746	0.962144	0.008769	0.999988	1.0000	0.0052
0.9582519531	8.34E-05	0.008852	0.962144	0.008769	0.999987	1.0000	0.0052
0.9583740234	3.02E-05	0.008799	0.962144	0.008769	0.999987	1.0000	0.0052
0.9584350586	3.66E-06	0.008773	0.962144	0.008769	0.999988	1.0000	0.0052
0.9584655762	-9.59E-06	0.008759	0.962144	0.008769	0.999988	1.0000	0.0052
0.9584503174	-2.97E-06	0.008766	0.962144	0.008769	0.999988	1.0000	0.0052
0.958442688	3.44E-07	0.008769	0.962144	0.008769	0.999988	1.0000	0.0052
0.9584465027	-1.31E-06	0.008768	0.962144	0.008769	0.999988	1.0000	0.0052
0.9584445953	-4.85E-07	0.008768	0.962144	0.008769	0.999988	1.0000	0.0052
0.9584436417	-7.06E-08	0.008769	0.962144	0.008769	0.999988	1.0000	0.0052
0.9584431648	1.36E-07	0.008769	0.962144	0.008769	0.999988	1.0000	0.0052
0.9584434032	3.29E-08	0.008769	0.962144	0.008769	0.999988	1.0000	0.0052
0.9584435225	-1.89E-08	0.008769	0.962144	0.008769	0.999988	1.0000	0.0052
0.9584434628	7.03E-09	0.008769	0.962144	0.008769	0.999988	1.0000	0.0052
0.9584434927	-5.91E-09	0.008769	0.962144	0.008769	0.999988	1.0000	0.0052
0.9584434777	5.57E-10	0.008769	0.962144	0.008769	0.999988	1.0000	0.0052
0.9584434852	-2.68E-09	0.008769	0.962144	0.008769	0.999988	1.0000	0.0052

Saturation	Total Mob	dF _v /dS _v	G	F	Gamma	Theta	High	Low
0.75	34.759228	0.045851	220.095758	12.870589	1.1794E+07	30550.407113	1	0.5
0.875	40.427490	0.009321	115.033000	10.281953	1.1701E+07	28275.535543	1	0.75
0.9375	43.300978	0.002124	62.501620	10.006619	1.1655E+07	28033.574650	1	0.875
0.96875	44.742642	0.000508	36.235931	9.974642	1.1632E+07	28005.473055	1	0.9375
0.953125	44.021547	0.001168	49.368776	9.985337	1.1643E+07	28014.871837	0.96875	0.9375
0.9609375	44.382039	0.000802	42.802353	9.978906	1.1638E+07	28009.220503	0.96875	0.953125
0.95703125	44.201778	0.000976	46.085564	9.981821	1.1641E+07	28011.782338	0.9609375	0.953125
0.958984375	44.291905	0.000887	44.443959	9.980292	1.1639E+07	28010.438726	0.9609375	0.95703125
0.9580078125	44.246841	0.000931	45.264762	9.981039	1.1640E+07	28011.094453	0.958984375	0.95703125
0.9584960938	44.269373	0.000909	44.854360	9.980661	1.1640E+07	28010.762620	0.958984375	0.9580078125
0.9582519531	44.258107	0.000920	45.059561	9.980849	1.1640E+07	28010.927538	0.95849609375	0.9580078125
0.9583740234	44.263740	0.000915	44.956960	9.980754	1.1640E+07	28010.844830	0.95849609375	0.95825195313
0.9584350586	44.266556	0.000912	44.905660	9.980708	1.1640E+07	28010.803663	0.95849609375	0.95837402344
0.9584655762	44.267964	0.000910	44.880010	9.980684	1.1640E+07	28010.783126	0.95849609375	0.95843505859
0.9584503174	44.267260	0.000911	44.892835	9.980696	1.1640E+07	28010.793391	0.95846557617	0.95843505859
0.958442688	44.266908	0.000911	44.899248	9.980702	1.1640E+07	28010.798526	0.95845031738	0.95843505859
0.9584465027	44.267084	0.000911	44.896041	9.980699	1.1640E+07	28010.795958	0.95845031738	0.95844268799
0.9584445953	44.266996	0.000911	44.897645	9.980700	1.1640E+07	28010.797242	0.95844650269	0.95844268799
0.9584436417	44.266952	0.000911	44.898446	9.980701	1.1640E+07	28010.797884	0.95844459534	0.95844268799
0.9584431648	44.266930	0.000911	44.898847	9.980701	1.1640E+07	28010.798205	0.95844364166	0.95844268799
0.9584434032	44.266941	0.000911	44.898647	9.980701	1.1640E+07	28010.798044	0.95844364166	0.95844316483
0.9584435225	44.266947	0.000911	44.898546	9.980701	1.1640E+07	28010.797964	0.95844364166	0.95844340324
0.9584434628	44.266944	0.000911	44.898596	9.980701	1.1640E+07	28010.798004	0.95844352245	0.95844340324
0.9584434927	44.266945	0.000911	44.898571	9.980701	1.1640E+07	28010.797984	0.95844352245	0.95844346285
0.9584434777	44.266945	0.000911	44.898584	9.980701	1.1640E+07	28010.797994	0.95844349265	0.95844346285
0.9584434852	44.266945	0.000911	44.898578	9.980701	1.1640E+07	28010.797989	0.95844349265	0.95844347775

Spreadsheet for Calculation of Stream-Water Saturation Profiles

Injection Temperature 500 °K Initial Temperature 350 °K Matrix Heat Capacity 1.0000 (kJ/kg)

LEADING SHOCK CALCULATIONS

Saturation	OF	Wave V	Flow V	Shock V	f _v	dKr _v /dS _v	dKr _v /dSI
0.7500	3.66E-01	0.441153	0.018531	0.075340	0.996549	1.0000	0.1875
0.875	1.72E-02	0.089683	0.016536	0.072477	0.999629	1.0000	0.0469
0.9375	-5.22E-02	0.020432	0.016673	0.072674	0.999957	1.0000	0.0117
0.90625	-2.44E-02	0.048117	0.016551	0.072498	0.999849	1.0000	0.0264
0.890625	-5.42E-03	0.067045	0.016527	0.072465	0.999756	1.0000	0.0359
0.8828125	5.42E-03	0.077884	0.016527	0.072465	0.999697	1.0000	0.0412
0.88671875	-1.16E-04	0.072347	0.016526	0.072463	0.999728	1.0000	0.0385
0.884765625	2.62E-03	0.075086	0.016527	0.072464	0.999713	1.0000	0.0398
0.8857421875	1.25E-03	0.073709	0.016526	0.072463	0.999720	1.0000	0.0392
0.8862304688	5.63E-04	0.073026	0.016526	0.072463	0.999724	1.0000	0.0388
0.8864746094	2.23E-04	0.072686	0.016526	0.072463	0.999726	1.0000	0.0387
0.8865966797	5.32E-05	0.072516	0.016526	0.072463	0.999727	1.0000	0.0386
0.8866577148	-3.16E-05	0.072432	0.016526	0.072463	0.999727	1.0000	0.0385
0.8866271973	1.08E-05	0.072474	0.016526	0.072463	0.999727	1.0000	0.0386
0.8866424561	-1.04E-05	0.072453	0.016526	0.072463	0.999727	1.0000	0.0385
0.8866348267	1.82E-07	0.072463	0.016526	0.072463	0.999727	1.0000	0.0386
0.8866386414	-5.11E-06	0.072458	0.016526	0.072463	0.999727	1.0000	0.0386
0.886636734	-2.47E-06	0.072461	0.016526	0.072463	0.999727	1.0000	0.0386
0.8866357803	-1.14E-06	0.072462	0.016526	0.072463	0.999727	1.0000	0.0386
0.8866353035	-4.80E-07	0.072463	0.016526	0.072463	0.999727	1.0000	0.0386
0.8866350651	-1.49E-07	0.072463	0.016526	0.072463	0.999727	1.0000	0.0386
0.8866349459	1.69E-08	0.072463	0.016526	0.072463	0.999727	1.0000	0.0386
0.8866350055	-6.58E-08	0.072463	0.016526	0.072463	0.999727	1.0000	0.0386
0.8866349757	-2.44E-08	0.072463	0.016526	0.072463	0.999727	1.0000	0.0386
0.8866349608	-3.75E-09	0.072463	0.016526	0.072463	0.999727	1.0000	0.0386
0.8866349533	6.60E-09	0.072463	0.016526	0.072463	0.999727	1.0000	0.0386

Saturation	Total Mob	dP _v /dS _v	G	F	Gamma	Theta	High	Low
0.75	34.759228	0.045851	220.095758	12.870589	1.1794E+07	30550.407113	1	0.5
0.875	40.427490	0.009321	115.033000	10.281953	1.1701E+07	28275.535543	1	0.75
0.9375	43.300978	0.002124	62.501620	10.006619	1.1655E+07	28033.574650	1	0.875
0.90625	41.862126	0.005001	88.767310	10.097238	1.1678E+07	28113.209409	0.9375	0.875
0.890625	41.144193	0.006968	101.900155	10.175426	1.1690E+07	28181.920650	0.90625	0.875
0.8828125	40.785677	0.008095	108.466577	10.224828	1.1695E+07	28225.334700	0.890625	0.875
0.88671875	40.964895	0.007519	105.183366	10.199203	1.1693E+07	28202.815133	0.890625	0.8828125
0.884765625	40.875276	0.007804	106.824972	10.211779	1.1694E+07	28213.867353	0.88671875	0.8828125
0.8857421875	40.920083	0.007661	106.004169	10.205432	1.1693E+07	28208.289909	0.88671875	0.884765625
0.8862304688	40.942489	0.007590	105.593767	10.202303	1.1693E+07	28205.539756	0.88671875	0.8857421875
0.8864746094	40.953692	0.007555	105.388567	10.200749	1.1693E+07	28204.174262	0.88671875	0.8862304688
0.8865966797	40.959294	0.007537	105.285966	10.199975	1.1693E+07	28203.493903	0.88671875	0.88647460938
0.8866577148	40.962095	0.007528	105.234666	10.199589	1.1693E+07	28203.154319	0.88671875	0.88659667969
0.8866271973	40.960694	0.007533	105.260316	10.199782	1.1693E+07	28203.324062	0.88665771484	0.88659667969
0.8866424561	40.961394	0.007530	105.247491	10.199685	1.1693E+07	28203.239178	0.88665771484	0.88662719727
0.8866348267	40.961044	0.007531	105.253904	10.199733	1.1693E+07	28203.281617	0.88664245605	0.88662719727
0.8866386414	40.961219	0.007531	105.250698	10.199709	1.1693E+07	28203.260397	0.88664245605	0.88663482666
0.886636734	40.961132	0.007531	105.252301	10.199721	1.1693E+07	28203.271006	0.88663864136	0.88663482666
0.8866357803	40.961088	0.007531	105.253102	10.199727	1.1693E+07	28203.276312	0.88663673401	0.88663482666
0.8866353035	40.961066	0.007531	105.253503	10.199730	1.1693E+07	28203.278964	0.88663578033	0.88663482666
0.8866350651	40.961055	0.007531	105.253703	10.199732	1.1693E+07	28203.280290	0.8866353035	0.88663482666
0.8866349459	40.961050	0.007531	105.253804	10.199733	1.1693E+07	28203.280954	0.88663506508	0.88663482666
0.8866350055	40.961052	0.007531	105.253753	10.199732	1.1693E+07	28203.280622	0.88663506508	0.88663494587
0.8866349757	40.961051	0.007531	105.253779	10.199732	1.1693E+07	28203.280788	0.88663500547	0.88663494587
0.8866349608	40.961050	0.007531	105.253791	10.199733	1.1693E+07	28203.280871	0.88663497567	0.88663494587
0.8866349533	40.961050	0.007531	105.253797	10.199733	1.1693E+07	28203.280912	0.88663496077	0.88663494587

Spreadsheet for Calculation of Stream-Water Saturation Profiles

Injection Temperature
550 °K

Initial Temperature
350 °K

Matrix Heat Capacity
1.0000 (kJ/kg)

MATRIX PROPERTIES

Porosity	Cp Matrix	Density	Rho * Cp
0.10	1.00	2650.00	2650.0000
Nw	Ng	Swl	Denom
3.00	1.00	0.00	1.000000

SATURATION CONDITIONS

Tsaturation = 485.57

	Volumes (m3/kg)	Enthalpies (kJ/kg)	Densities (kg/m3)	Viscosities (cp)	Saturation Step
Liquid	0.001176	901.41	850.4723	0.1303	0.0014037937
Vapor	0.100298	2808.52	9.970241	0.0217	

BOUNDARY CONDITIONS

	Temperature	Velocity	Heat Capacity	Wave Velocity	Density	Enthalpy
Injection	550	1.000000	2.40	0.008466	8.433526	2965.67
Initial	350	0.014566	4.15	0.021115	975.3174	319.98
	G	F	Gamma	Theta		
Injection	550	8.43	8.43	13142511.08	25011.08	
Initial	350	975.32	975.32	8659580.72	312080.72	

SHOCK CONDITIONS

	Initial Guess		Vapor Saturation	Objective Function	Two-Phase Wave Velocity	Upstream Flow Velocity	Shock Velocity	Vapor Frac Flow
	Sv-Hi	Sv-Low						
Trailing	1	0.5	0.9568	-3.0692E-10	0.0084	0.848043	0.0084	1.0000
Leading	1	0.5	0.8866	5.8161E-09	0.0639	0.014566	0.0639	0.9997
	dKrv/dSv	dKrl/dSl	Total Mobility	dFv/dSv	G	F'	Gamma	Theta'
Trailing	1.0000	0.0056	44.1922	0.0010	46.2592	9.9820	1.1641E+07	28011.9321
Leading	1.0000	0.0386	40.9610	0.0075	105.2538	10.1997	1.1693E+07	28203.2809

MATERIAL BALANCES

	Inside	Initial	Injected	Produced	Balance	Error
Mass	91.758372	97.531740	8.433526	14.206881	0.0000	0.0000%
Enthalpy	886429.7368	865958.0720	25011.0798	4545.8983	-6.4834	0.0007%

Spreadsheet for Calculation of Stream-Water Saturation Profiles

Injection Temperature 550 °K		Initial Temperature 350 °K			Matrix Heat Capacity 1.0000 (kJ/kg)			
SATURATION PROFILE								
Vapor Saturation	Vapor Frac Flow	dKr/dSv	dKr/dSI	Total Mobility	dFv/dSv	lambda	Mass Inside	Enthalpy Inside
1.0000						0.000000		
1.0000						0.008362		
0.9568	0.999986	1.0000	0.0056	44.192244	0.000986	0.008362	0.070520	109896.100936
0.9554	0.999985	1.0000	0.0060	44.127471	0.001053	0.008932	0.026712	6637.799000
0.9540	0.999983	1.0000	0.0063	44.062702	0.001123	0.009522	0.028345	6871.204397
0.9526	0.999981	1.0000	0.0067	43.997938	0.001195	0.010132	0.030031	7106.018903
0.9512	0.999980	1.0000	0.0071	43.933177	0.001269	0.010763	0.031770	7342.252548
0.9498	0.999978	1.0000	0.0076	43.868421	0.001346	0.011414	0.033564	7579.915436
0.9484	0.999976	1.0000	0.0080	43.803670	0.001425	0.012085	0.035411	7819.017744
0.9470	0.999974	1.0000	0.0084	43.738923	0.001507	0.012777	0.037314	8059.569725
0.9456	0.999972	1.0000	0.0089	43.674181	0.001591	0.013490	0.039272	8301.581705
0.9442	0.999969	1.0000	0.0093	43.609444	0.001677	0.014223	0.041285	8545.064089
0.9428	0.999967	1.0000	0.0098	43.544712	0.001766	0.014978	0.043355	8790.027356
0.9414	0.999964	1.0000	0.0103	43.479985	0.001858	0.015753	0.045482	9036.482063
0.9400	0.999962	1.0000	0.0108	43.415264	0.001952	0.016550	0.047666	9284.438844
0.9386	0.999959	1.0000	0.0113	43.350548	0.002048	0.017368	0.049907	9533.908413
0.9372	0.999956	1.0000	0.0118	43.285837	0.002147	0.018207	0.052207	9784.901562
0.9358	0.999953	1.0000	0.0124	43.221133	0.002249	0.019068	0.054565	10037.429162
0.9344	0.999950	1.0000	0.0129	43.156434	0.002353	0.019951	0.056983	10291.502166
0.9330	0.999946	1.0000	0.0135	43.091741	0.002459	0.020856	0.059460	10547.131606
0.9316	0.999943	1.0000	0.0141	43.027054	0.002569	0.021783	0.061998	10804.328597
0.9302	0.999939	1.0000	0.0146	42.962373	0.002680	0.022731	0.064597	11063.104337
0.9287	0.999935	1.0000	0.0152	42.897699	0.002795	0.023702	0.067257	11323.470105
0.9273	0.999931	1.0000	0.0158	42.833031	0.002912	0.024696	0.069979	11585.437265
0.9259	0.999927	1.0000	0.0165	42.768370	0.003032	0.025711	0.072763	11849.017264
0.9245	0.999923	1.0000	0.0171	42.703715	0.003154	0.026750	0.075610	12114.221636
0.9231	0.999918	1.0000	0.0177	42.639068	0.003279	0.027811	0.078521	12381.061998
0.9217	0.999914	1.0000	0.0184	42.574427	0.003407	0.028895	0.081495	12649.550058
0.9203	0.999909	1.0000	0.0190	42.509793	0.003538	0.030003	0.084535	12919.697605
0.9189	0.999904	1.0000	0.0197	42.445167	0.003671	0.031133	0.087639	13191.516521
0.9175	0.999898	1.0000	0.0204	42.380548	0.003807	0.032287	0.090809	13465.018775
0.9161	0.999893	1.0000	0.0211	42.315937	0.003946	0.033464	0.094046	13740.216423
0.9147	0.999887	1.0000	0.0218	42.251333	0.004088	0.034665	0.097350	14017.121614
0.9133	0.999881	1.0000	0.0225	42.186737	0.004232	0.035890	0.100721	14295.746588
0.9119	0.999875	1.0000	0.0233	42.122148	0.004379	0.037138	0.104160	14576.103673
0.9105	0.999869	1.0000	0.0240	42.057568	0.004529	0.038411	0.107667	14858.205293
0.9091	0.999863	1.0000	0.0248	41.992996	0.004682	0.039708	0.111244	15142.063964
0.9077	0.999856	1.0000	0.0256	41.928432	0.004838	0.041029	0.114891	15427.692294
0.9063	0.999849	1.0000	0.0263	41.863876	0.004997	0.042374	0.118609	15715.102987
0.9049	0.999842	1.0000	0.0271	41.799329	0.005158	0.043744	0.122397	16004.308844
0.9035	0.999835	1.0000	0.0279	41.734791	0.005323	0.045140	0.126258	16295.322759
0.9021	0.999827	1.0000	0.0288	41.670261	0.005490	0.046560	0.130190	16588.157725
0.9007	0.999819	1.0000	0.0296	41.605741	0.005661	0.048005	0.134196	16882.826832
0.8993	0.999811	1.0000	0.0304	41.541229	0.005834	0.049475	0.138276	17179.343269
0.8979	0.999803	1.0000	0.0313	41.476726	0.006010	0.050971	0.142429	17477.720325
0.8965	0.999794	1.0000	0.0322	41.412233	0.006190	0.052492	0.146658	17777.971386
0.8951	0.999785	1.0000	0.0330	41.347749	0.006372	0.054039	0.150962	18080.109944
0.8937	0.999776	1.0000	0.0339	41.283275	0.006558	0.055612	0.155343	18384.149588
0.8923	0.999767	1.0000	0.0348	41.218810	0.006746	0.057211	0.159800	18690.104014
0.8908	0.999757	1.0000	0.0357	41.154355	0.006938	0.058836	0.164335	18997.987018
0.8894	0.999748	1.0000	0.0367	41.089910	0.007133	0.060487	0.168949	19307.812503
0.8880	0.999737	1.0000	0.0376	41.025475	0.007330	0.062165	0.173641	19619.594476
0.8866	0.999727	1.0000	0.0386	40.961050	0.007531	0.063870	0.178414	19933.347051
0.0000						0.063870		
0.0000						1.000000		

Spreadsheet for Calculation of Stream-Water Saturation Profiles

Injection Temperature 550 °K		Initial Temperature 350 °K		Matrix Heat Capacity 1.0000 (kJ/kg)				
TRAILING SHOCK CALCULATIONS								
Saturation	OF	Wave V	Flow V	Shock V	f _v	dK _{rv} /dS _v	dKr/dS _i	
0.7500	2.94E-01	0.320776	0.699604	0.026967	0.996549	1.0000	0.1875	
0.875	6.70E-02	0.077468	0.831097	0.010486	0.999629	1.0000	0.0469	
0.9375	9.55E-03	0.017994	0.847359	0.008448	0.999957	1.0000	0.0117	
0.96875	-4.08E-03	0.004307	0.847835	0.008388	0.999995	1.0000	0.0029	
0.953125	1.54E-03	0.009907	0.848020	0.008365	0.999982	1.0000	0.0066	
0.9609375	-1.56E-03	0.006805	0.848016	0.008365	0.999990	1.0000	0.0046	
0.95703125	-8.22E-05	0.008280	0.848043	0.008362	0.999986	1.0000	0.0055	
0.955078125	7.12E-04	0.009074	0.848038	0.008363	0.999984	1.0000	0.0061	
0.9560546875	3.10E-04	0.008672	0.848042	0.008362	0.999985	1.0000	0.0058	
0.9565429688	1.13E-04	0.008475	0.848043	0.008362	0.999986	1.0000	0.0057	
0.9567871094	1.50E-05	0.008377	0.848043	0.008362	0.999986	1.0000	0.0056	
0.9569091797	-3.37E-05	0.008328	0.848043	0.008362	0.999986	1.0000	0.0056	
0.9568481445	-9.38E-06	0.008353	0.848043	0.008362	0.999986	1.0000	0.0056	
0.956817627	2.80E-06	0.008365	0.848043	0.008362	0.999986	1.0000	0.0056	
0.9568328857	-3.29E-06	0.008359	0.848043	0.008362	0.999986	1.0000	0.0056	
0.9568252563	-2.47E-07	0.008362	0.848043	0.008362	0.999986	1.0000	0.0056	
0.9568214417	1.28E-06	0.008363	0.848043	0.008362	0.999986	1.0000	0.0056	
0.956823349	5.14E-07	0.008362	0.848043	0.008362	0.999986	1.0000	0.0056	
0.9568243027	1.33E-07	0.008362	0.848043	0.008362	0.999986	1.0000	0.0056	
0.9568247795	-5.68E-08	0.008362	0.848043	0.008362	0.999986	1.0000	0.0056	
0.9568245411	3.83E-08	0.008362	0.848043	0.008362	0.999986	1.0000	0.0056	
0.9568246603	-9.23E-09	0.008362	0.848043	0.008362	0.999986	1.0000	0.0056	
0.9568246007	1.46E-08	0.008362	0.848043	0.008362	0.999986	1.0000	0.0056	
0.9568246305	2.67E-09	0.008362	0.848043	0.008362	0.999986	1.0000	0.0056	
0.9568246454	-3.28E-09	0.008362	0.848043	0.008362	0.999986	1.0000	0.0056	
0.9568246379	-3.07E-10	0.008362	0.848043	0.008362	0.999986	1.0000	0.0056	
Saturation	Total Mob	dF _v /dS _v	G	F	Gamma	Theta	High	Low
0.75	34.759228	0.045851	220.095758	12.870589	1.1794E+07	30550.407113	1	0.5
0.875	40.427490	0.009321	115.033000	10.281953	1.1701E+07	28275.535543	1	0.75
0.9375	43.300978	0.002124	62.501620	10.006619	1.1635E+07	28033.574650	1	0.875
0.96875	44.742642	0.000508	36.235931	9.974642	1.1632E+07	28005.473055	1	0.9375
0.953125	44.021547	0.001168	49.368776	9.985337	1.1643E+07	28014.871837	0.96875	0.9375
0.9609375	44.382039	0.000802	42.802353	9.978906	1.1638E+07	28009.220503	0.96875	0.953125
0.95703125	44.201778	0.000976	46.085564	9.981821	1.1641E+07	28011.782338	0.9609375	0.953125
0.955078125	44.111658	0.001070	47.727170	9.983500	1.1642E+07	28013.257853	0.95703125	0.953125
0.9560546875	44.156717	0.001023	46.906367	9.982642	1.1641E+07	28012.503198	0.95703125	0.955078125
0.9565429688	44.179247	0.000999	46.495966	9.982227	1.1641E+07	28012.138595	0.95703125	0.9560546875
0.9567871094	44.190513	0.000988	46.290765	9.982023	1.1641E+07	28011.959430	0.95703125	0.95654296875
0.9569091797	44.196145	0.000982	46.188165	9.981922	1.1641E+07	28011.870625	0.95703125	0.95678710938
0.9568481445	44.193329	0.000985	46.239465	9.981972	1.1641E+07	28011.914963	0.95690917969	0.95678710938
0.956817627	44.191921	0.000986	46.265115	9.981997	1.1641E+07	28011.937180	0.95684814453	0.95678710938
0.9568328857	44.192625	0.000986	46.252290	9.981985	1.1641E+07	28011.926067	0.95684814453	0.95681762695
0.9568252563	44.192273	0.000986	46.258702	9.981991	1.1641E+07	28011.931623	0.95683288574	0.95681762695
0.9568214417	44.192097	0.000986	46.261909	9.981994	1.1641E+07	28011.934401	0.95682525635	0.95681762695
0.956823349	44.192185	0.000986	46.260306	9.981993	1.1641E+07	28011.933012	0.95682525635	0.95682144165
0.9568243027	44.192229	0.000986	46.259504	9.981992	1.1641E+07	28011.932317	0.95682525635	0.956823349
0.9568247795	44.192251	0.000986	46.259103	9.981992	1.1641E+07	28011.931970	0.95682525635	0.95682430267
0.9568245411	44.192240	0.000986	46.259304	9.981992	1.1641E+07	28011.932144	0.95682477951	0.95682430267
0.9568246603	44.192245	0.000986	46.259203	9.981992	1.1641E+07	28011.932057	0.95682477951	0.95682454109
0.9568246007	44.192243	0.000986	46.259253	9.981992	1.1641E+07	28011.932100	0.9568246603	0.95682454109
0.9568246305	44.192244	0.000986	46.259228	9.981992	1.1641E+07	28011.932079	0.9568246603	0.9568246007
0.9568246454	44.192245	0.000986	46.259216	9.981992	1.1641E+07	28011.932068	0.9568246603	0.9568246305
0.9568246379	44.192244	0.000986	46.259222	9.981992	1.1641E+07	28011.932073	0.9568246454	0.9568246305

Spreadsheet for Calculation of Stream-Water Saturation Profiles

Injection Temperature 550 °K Initial Temperature 350 °K Matrix Heat Capacity 1.0000 (kJ/kg)

LEADING SHOCK CALCULATIONS

Saturation	OF	Wave V	Flow V	Shock V	f _v	dK _{rv} /dS _v	dK _r /dS ₁
0.7500	3.22E-01	0.388836	0.016333	0.066405	0.996549	1.0000	0.1875
0.875	1.52E-02	0.079047	0.014575	0.063882	0.999629	1.0000	0.0469
0.9375	-4.60E-02	0.018009	0.014696	0.064055	0.999957	1.0000	0.0117
0.90625	-2.15E-02	0.042411	0.014588	0.063901	0.999849	1.0000	0.0264
0.890625	-4.78E-03	0.059094	0.014567	0.063871	0.999756	1.0000	0.0359
0.8828125	4.78E-03	0.068648	0.014567	0.063871	0.999697	1.0000	0.0412
0.88671875	-1.03E-04	0.063767	0.014566	0.063870	0.999728	1.0000	0.0385
0.884765625	2.31E-03	0.066181	0.014567	0.063870	0.999713	1.0000	0.0398
0.8857421875	1.10E-03	0.064968	0.014566	0.063870	0.999720	1.0000	0.0392
0.8862304688	4.96E-04	0.064366	0.014566	0.063870	0.999724	1.0000	0.0388
0.8864746094	1.96E-04	0.064066	0.014566	0.063870	0.999726	1.0000	0.0387
0.8865966797	4.69E-05	0.063917	0.014566	0.063870	0.999727	1.0000	0.0386
0.8866577148	-2.78E-05	0.063842	0.014566	0.063870	0.999727	1.0000	0.0385
0.8866271973	9.50E-06	0.063879	0.014566	0.063870	0.999727	1.0000	0.0386
0.8866424561	-9.18E-06	0.063861	0.014566	0.063870	0.999727	1.0000	0.0385
0.8866348267	1.61E-07	0.063870	0.014566	0.063870	0.999727	1.0000	0.0386
0.8866386414	-4.51E-06	0.063865	0.014566	0.063870	0.999727	1.0000	0.0386
0.886636734	-2.17E-06	0.063868	0.014566	0.063870	0.999727	1.0000	0.0386
0.8866357803	-1.01E-06	0.063869	0.014566	0.063870	0.999727	1.0000	0.0386
0.8866353035	-4.23E-07	0.063869	0.014566	0.063870	0.999727	1.0000	0.0386
0.8866350651	-1.31E-07	0.063870	0.014566	0.063870	0.999727	1.0000	0.0386
0.8866349459	1.49E-08	0.063870	0.014566	0.063870	0.999727	1.0000	0.0386
0.8866350055	-5.80E-08	0.063870	0.014566	0.063870	0.999727	1.0000	0.0386
0.8866349757	-2.15E-08	0.063870	0.014566	0.063870	0.999727	1.0000	0.0386
0.8866349608	-3.30E-09	0.063870	0.014566	0.063870	0.999727	1.0000	0.0386
0.8866349533	5.82E-09	0.063870	0.014566	0.063870	0.999727	1.0000	0.0386

Saturation	Total Mob	dF _v /dS _v	G	F	Gamma	Theta	High	Low
0.75	34.759228	0.045851	220.095758	12.870589	1.1794E+07	30550.407113	1	0.5
0.875	40.427490	0.009321	115.033000	10.281953	1.1701E+07	28275.535543	1	0.75
0.9375	43.300978	0.002124	62.501620	10.006619	1.1655E+07	28033.574650	1	0.875
0.90625	41.862126	0.005001	88.767310	10.097238	1.1678E+07	28113.209409	0.9375	0.875
0.890625	41.144193	0.006968	101.900155	10.175426	1.1690E+07	28181.920650	0.90625	0.875
0.8828125	40.785677	0.008095	108.466577	10.224828	1.1695E+07	28225.334700	0.890625	0.875
0.88671875	40.964895	0.007519	105.183366	10.199203	1.1693E+07	28202.815133	0.890625	0.8828125
0.884765625	40.875276	0.007804	106.824972	10.211779	1.1694E+07	28213.867353	0.88671875	0.8828125
0.8857421875	40.920083	0.007661	106.004169	10.205432	1.1693E+07	28208.289909	0.88671875	0.884765625
0.8862304688	40.942489	0.007590	105.593767	10.202303	1.1693E+07	28205.539756	0.88671875	0.8857421875
0.8864746094	40.953692	0.007555	105.388567	10.200749	1.1693E+07	28204.174262	0.88671875	0.8862304688
0.8865966797	40.959294	0.007537	105.285966	10.199975	1.1693E+07	28203.493903	0.88671875	0.8864746094
0.8866577148	40.962095	0.007528	105.234666	10.199589	1.1693E+07	28203.154319	0.88671875	0.8865966797
0.8866271973	40.960694	0.007533	105.260316	10.199782	1.1693E+07	28203.324062	0.8866577148	0.8865966797
0.8866424561	40.961394	0.007530	105.247491	10.199685	1.1693E+07	28203.239178	0.8866577148	0.8866271973
0.8866348267	40.961044	0.007531	105.253904	10.199733	1.1693E+07	28203.281617	0.8866424561	0.8866271973
0.8866386414	40.961219	0.007531	105.250698	10.199709	1.1693E+07	28203.260397	0.8866424561	0.8866348267
0.886636734	40.961132	0.007531	105.252301	10.199721	1.1693E+07	28203.271006	0.8866386414	0.8866348267
0.8866357803	40.961088	0.007531	105.253102	10.199727	1.1693E+07	28203.276312	0.886636734	0.8866348267
0.8866353035	40.961066	0.007531	105.253503	10.199730	1.1693E+07	28203.278964	0.8866357803	0.8866348267
0.8866350651	40.961055	0.007531	105.253703	10.199732	1.1693E+07	28203.280290	0.8866350651	0.8866348267
0.8866349459	40.961050	0.007531	105.253804	10.199733	1.1693E+07	28203.280954	0.8866350651	0.8866348267
0.8866350055	40.961052	0.007531	105.253753	10.199732	1.1693E+07	28203.280622	0.8866350651	0.8866349459
0.8866349757	40.961051	0.007531	105.253779	10.199732	1.1693E+07	28203.280788	0.8866350055	0.8866349459
0.8866349608	40.961050	0.007531	105.253791	10.199733	1.1693E+07	28203.280871	0.8866349757	0.8866349459
0.8866349533	40.961050	0.007531	105.253797	10.199733	1.1693E+07	28203.280912	0.8866349608	0.8866349459

Spreadsheet for Calculation of Stream-Water Saturation Profiles

Injection Temperature
600 °K

Initial Temperature
350 °K

Matrix Heat Capacity
1.0000 (kJ/kg)

MATRIX PROPERTIES

Porosity	Cp Matrix	Density	Rho * Cp
0.10	1.00	2650.00	2650.0000
Nw	Ng	Swl	Denom
3.00	1.00	0.00	1.000000

SATURATION CONDITIONS

Tsaturation = 485.57

	Volumes (m3/kg)	Enthalpies (kJ/kg)	Densities (kg/m3)	Viscosities (cp)	Saturation Step
Liquid	0.001176	901.41	850.4723	0.1303	0.0014037451
Vapor	0.100298	2808.52	9.970241	0.0217	

BOUNDARY CONDITIONS

	Temperature	Velocity	Heat Capacity	Wave Velocity	Density	Enthalpy
Injection	600	1.000000	2.34	0.007420	7.566513	3084.04
Initial	350	0.013070	4.15	0.018946	975.3174	319.98
	G	F	Gamma	Theta		
Injection	600	7.57	14333335.44	23335.44		
Initial	350	975.32	8659580.72	312080.72		

SHOCK CONDITIONS

	Initial Guess		Vapor Saturation	Objective Function	Two-Phase Wave Velocity	Upstream Flow Velocity	Shock Velocity	Vapor Frac Flow
Trailing	Sv-Hi	Sv-Low	0.9568	3.1784E-10	0.0075	0.760925	0.0075	1.0000
Leading	1	0.5	0.8866	5.2186E-09	0.0573	0.013070	0.0573	0.9997
	dKrv/dSv	dKrl/dSl	Total Mobility	dFv/dSv	G	F'	Gamma	Theta'
Trailing	1.0000	0.0056	44.1921	0.0010	46.2613	9.9820	1.1641E+07	28011.9338
Leading	1.0000	0.0386	40.9610	0.0075	105.2538	10.1997	1.1693E+07	28203.2809

MATERIAL BALANCES

	Mass	Inside	Initial	Injected	Produced	Balance	Error
Mass	92.350805	97.531740	7.566513	12.747437	0.0000	0.0000%	
Enthalpy	885220.4196	865958.0720	23335.4376	4078.9074	-5.8174	0.0007%	

Spreadsheet for Calculation of Stream-Water Saturation Profiles

Injection Temperature 600 °K		Initial Temperature 350 °K		Matrix Heat Capacity 1.0000 (kJ/kg)				
SATURATION PROFILE								
Vapor Saturation	Vapor Frac Flow	dKrv/dSv	dKr/dSI	Total Mobility	dFv/dSv	lambda	Mass Inside	Enthalpy Inside
1.0000						0.000000		
1.0000						0.007504		
0.9568	0.999986	1.0000	0.0056	44.192132	0.000986	0.007504	0.056777	107553.776798
0.9554	0.999985	1.0000	0.0060	44.127361	0.001053	0.008015	0.023969	5956.062891
0.9540	0.999983	1.0000	0.0063	44.062595	0.001123	0.008545	0.025435	6165.478665
0.9526	0.999981	1.0000	0.0067	43.997832	0.001195	0.009092	0.026948	6376.158678
0.9512	0.999980	1.0000	0.0071	43.933074	0.001269	0.009658	0.028508	6588.111928
0.9498	0.999978	1.0000	0.0076	43.868320	0.001346	0.010242	0.030117	6801.347478
0.9484	0.999976	1.0000	0.0080	43.803571	0.001425	0.010845	0.031775	7015.874461
0.9470	0.999974	1.0000	0.0084	43.738827	0.001507	0.011465	0.033482	7231.702073
0.9456	0.999972	1.0000	0.0089	43.674087	0.001591	0.012105	0.035239	7448.839580
0.9442	0.999969	1.0000	0.0093	43.609352	0.001677	0.012763	0.037046	7667.296316
0.9428	0.999967	1.0000	0.0098	43.544622	0.001766	0.013440	0.038903	7887.081683
0.9414	0.999964	1.0000	0.0103	43.479898	0.001858	0.014136	0.040811	8108.205151
0.9400	0.999962	1.0000	0.0108	43.415179	0.001952	0.014851	0.042770	8330.676261
0.9386	0.999959	1.0000	0.0113	43.350465	0.002048	0.015585	0.044781	8554.504626
0.9372	0.999956	1.0000	0.0118	43.285757	0.002147	0.016338	0.046845	8779.699927
0.9358	0.999953	1.0000	0.0124	43.221054	0.002249	0.017111	0.048961	9006.271918
0.9344	0.999950	1.0000	0.0129	43.156358	0.002353	0.017903	0.051130	9234.230424
0.9330	0.999946	1.0000	0.0135	43.091667	0.002459	0.018714	0.053353	9463.585344
0.9316	0.999943	1.0000	0.0141	43.026982	0.002569	0.019546	0.055630	9694.346650
0.9302	0.999939	1.0000	0.0146	42.962304	0.002681	0.020397	0.057962	9926.524386
0.9287	0.999935	1.0000	0.0152	42.897632	0.002795	0.021268	0.060348	10160.128673
0.9273	0.999931	1.0000	0.0158	42.832966	0.002912	0.022160	0.062790	10395.169706
0.9259	0.999927	1.0000	0.0165	42.768307	0.003032	0.023071	0.065288	10631.657755
0.9245	0.999923	1.0000	0.0171	42.703655	0.003154	0.024003	0.067843	10869.603167
0.9231	0.999918	1.0000	0.0177	42.639010	0.003280	0.024955	0.070454	11109.016365
0.9217	0.999914	1.0000	0.0184	42.574371	0.003407	0.025928	0.073123	11349.907852
0.9203	0.999909	1.0000	0.0190	42.509740	0.003538	0.026921	0.075850	11592.288206
0.9189	0.999904	1.0000	0.0197	42.445116	0.003671	0.027936	0.078636	11836.168085
0.9175	0.999898	1.0000	0.0204	42.380499	0.003807	0.028971	0.081480	12081.558228
0.9161	0.999893	1.0000	0.0211	42.315890	0.003946	0.030027	0.084384	12328.469452
0.9147	0.999887	1.0000	0.0218	42.251288	0.004088	0.031105	0.087348	12576.912656
0.9133	0.999881	1.0000	0.0225	42.186694	0.004232	0.032204	0.090373	12826.898819
0.9119	0.999875	1.0000	0.0233	42.122108	0.004379	0.033324	0.093458	13078.439004
0.9105	0.999869	1.0000	0.0240	42.057530	0.004529	0.034466	0.096606	13331.544357
0.9091	0.999863	1.0000	0.0248	41.992960	0.004682	0.035629	0.099815	13586.226104
0.9077	0.999856	1.0000	0.0256	41.928398	0.004838	0.036814	0.103087	13842.495559
0.9063	0.999849	1.0000	0.0263	41.863845	0.004997	0.038022	0.106422	14100.364119
0.9049	0.999842	1.0000	0.0271	41.799300	0.005158	0.039251	0.109822	14359.843267
0.9035	0.999835	1.0000	0.0279	41.734764	0.005323	0.040503	0.113285	14620.944573
0.9021	0.999827	1.0000	0.0288	41.670237	0.005490	0.041777	0.116814	14883.679692
0.9007	0.999819	1.0000	0.0296	41.605718	0.005661	0.043074	0.120408	15148.060369
0.8993	0.999811	1.0000	0.0304	41.541209	0.005834	0.044393	0.124068	15414.098435
0.8979	0.999803	1.0000	0.0313	41.476708	0.006010	0.045735	0.127794	15681.805812
0.8965	0.999794	1.0000	0.0322	41.412217	0.006190	0.047100	0.131588	15951.194512
0.8951	0.999785	1.0000	0.0330	41.347736	0.006372	0.048488	0.135450	16222.276637
0.8937	0.999776	1.0000	0.0339	41.283263	0.006558	0.049899	0.139381	16495.064379
0.8922	0.999767	1.0000	0.0348	41.218801	0.006746	0.051334	0.143380	16769.570025
0.8908	0.999757	1.0000	0.0357	41.154348	0.006938	0.052792	0.147449	17045.805953
0.8894	0.999748	1.0000	0.0367	41.089905	0.007133	0.054274	0.151588	17323.784635
0.8880	0.999737	1.0000	0.0376	41.025473	0.007330	0.055779	0.155798	17603.518638
0.8866	0.999727	1.0000	0.0386	40.961050	0.007531	0.057309	0.160080	17885.020624
0.0000						0.057309		
0.0000						1.000000		

Spreadsheet for Calculation of Stream-Water Saturation Profiles

Injection Temperature 600 °K		Initial Temperature 350 °K		Matrix Heat Capacity 1.0000 (kJ/kg)				
TRAILING SHOCK CALCULATIONS								
Saturation	OF	Wave V	Flow V	Shock V	f _v	dK _{rv} /dS _v	dK _{rl} /dS _l	
0.7500	2.65E-01	0.282922	0.617047	0.017656	0.996549	1.0000	0.1875	
0.875	6.08E-02	0.069435	0.744925	0.008433	0.999629	1.0000	0.0469	
0.9375	8.60E-03	0.016146	0.760295	0.007548	0.999957	1.0000	0.0117	
0.96875	-3.65E-03	0.003865	0.760735	0.007517	0.999995	1.0000	0.0029	
0.953125	1.38E-03	0.008890	0.760904	0.007505	0.999982	1.0000	0.0066	
0.9609375	-1.40E-03	0.006106	0.760901	0.007505	0.999990	1.0000	0.0046	
0.95703125	-7.47E-05	0.007429	0.760925	0.007504	0.999986	1.0000	0.0055	
0.955078125	6.38E-04	0.008142	0.760920	0.007504	0.999984	1.0000	0.0061	
0.9560546875	2.77E-04	0.007781	0.760924	0.007504	0.999985	1.0000	0.0058	
0.9565429688	1.00E-04	0.007604	0.760925	0.007504	0.999986	1.0000	0.0057	
0.9567871094	1.26E-05	0.007516	0.760925	0.007504	0.999986	1.0000	0.0056	
0.9569091797	-3.11E-05	0.007473	0.760925	0.007504	0.999986	1.0000	0.0056	
0.9568481445	-9.28E-06	0.007494	0.760925	0.007504	0.999986	1.0000	0.0056	
0.956817627	1.64E-06	0.007505	0.760925	0.007504	0.999986	1.0000	0.0056	
0.9568328857	-3.82E-06	0.007500	0.760925	0.007504	0.999986	1.0000	0.0056	
0.9568252563	-1.09E-06	0.007503	0.760925	0.007504	0.999986	1.0000	0.0056	
0.9568214417	2.75E-07	0.007504	0.760925	0.007504	0.999986	1.0000	0.0056	
0.956823349	-4.08E-07	0.007503	0.760925	0.007504	0.999986	1.0000	0.0056	
0.9568223953	-6.64E-08	0.007504	0.760925	0.007504	0.999986	1.0000	0.0056	
0.9568219185	1.04E-07	0.007504	0.760925	0.007504	0.999986	1.0000	0.0056	
0.9568221569	1.90E-08	0.007504	0.760925	0.007504	0.999986	1.0000	0.0056	
0.9568222761	-2.37E-08	0.007504	0.760925	0.007504	0.999986	1.0000	0.0056	
0.9568222165	-2.35E-09	0.007504	0.760925	0.007504	0.999986	1.0000	0.0056	
0.9568221867	8.32E-09	0.007504	0.760925	0.007504	0.999986	1.0000	0.0056	
0.9568222016	2.99E-09	0.007504	0.760925	0.007504	0.999986	1.0000	0.0056	
0.9568222091	3.18E-10	0.007504	0.760925	0.007504	0.999986	1.0000	0.0056	
Saturation	Total Mob	dF _v /dS _v	G	F	Gamma	Theta	High	Low
0.75	34.759228	0.045851	220.095758	12.870589	1.1794E+07	30550.407113	1	0.5
0.875	40.427490	0.009321	115.033000	10.281953	1.1701E+07	28275.535543	1	0.75
0.9375	43.300978	0.002124	62.501620	10.006619	1.1655E+07	28033.574650	1	0.875
0.96875	44.742642	0.000508	36.235931	9.974642	1.1632E+07	28005.473055	1	0.9375
0.953125	44.021547	0.001168	49.368776	9.985337	1.1643E+07	28014.871837	0.96875	0.9375
0.9609375	44.382039	0.000802	42.802353	9.978906	1.1638E+07	28009.220503	0.96875	0.953125
0.95703125	44.201778	0.000976	46.085564	9.981821	1.1641E+07	28011.782338	0.9609375	0.953125
0.955078125	44.111658	0.001070	47.727170	9.983500	1.1642E+07	28013.257853	0.95703125	0.953125
0.9560546875	44.156717	0.001023	46.906367	9.982642	1.1641E+07	28012.503198	0.95703125	0.9560546875
0.9565429688	44.179247	0.000999	46.495966	9.982227	1.1641E+07	28012.138595	0.95703125	0.9560546875
0.9567871094	44.190513	0.000988	46.290765	9.982023	1.1641E+07	28011.959430	0.95703125	0.95654296875
0.9569091797	44.196145	0.000982	46.188165	9.981922	1.1641E+07	28011.870625	0.95703125	0.95678710938
0.9568481445	44.193329	0.000985	46.239465	9.981972	1.1641E+07	28011.914963	0.95690917969	0.95678710938
0.956817627	44.191921	0.000986	46.265115	9.981997	1.1641E+07	28011.937180	0.95684814453	0.95678710938
0.9568328857	44.192625	0.000986	46.252290	9.981985	1.1641E+07	28011.926067	0.95684814453	0.95681762695
0.9568252563	44.192273	0.000986	46.258702	9.981991	1.1641E+07	28011.931623	0.95683288574	0.95681762695
0.9568214417	44.192097	0.000986	46.261909	9.981994	1.1641E+07	28011.934401	0.95682525635	0.95681762695
0.956823349	44.192185	0.000986	46.260306	9.981993	1.1641E+07	28011.933012	0.95682525635	0.95682144165
0.9568223953	44.192141	0.000986	46.261107	9.981994	1.1641E+07	28011.933706	0.956823349	0.95682144165
0.9568219185	44.192119	0.000986	46.261508	9.981994	1.1641E+07	28011.934054	0.95682239532	0.95682144165
0.9568221569	44.192130	0.000986	46.261307	9.981994	1.1641E+07	28011.933880	0.95682239532	0.95682191849
0.9568222761	44.192135	0.000986	46.261207	9.981994	1.1641E+07	28011.933793	0.95682239532	0.95682215691
0.9568222165	44.192133	0.000986	46.261257	9.981994	1.1641E+07	28011.933837	0.95682227612	0.95682215691
0.9568221867	44.192131	0.000986	46.261282	9.981994	1.1641E+07	28011.933858	0.95682221651	0.95682215691
0.9568222016	44.192132	0.000986	46.261270	9.981994	1.1641E+07	28011.933848	0.95682221651	0.95682218671
0.9568222091	44.192132	0.000986	46.261264	9.981994	1.1641E+07	28011.933842	0.95682221651	0.95682220161

Spreadsheet for Calculation of Stream-Water Saturation Profiles

Injection Temperature
600 °K

Initial Temperature
350 °K

Matrix Heat Capacity
1.0000 (kJ/kg)

LEADING SHOCK CALCULATIONS

Saturation	OP	Wave V	Flow V	Shock V	f_v	dK_{rv}/dS_v	dK_r/dS_l
0.7500	2.89E-01	0.348892	0.014455	0.059583	0.996549	1.0000	0.1875
0.875	1.36E-02	0.070927	0.013078	0.057320	0.999629	1.0000	0.0469
0.9375	-4.13E-02	0.016159	0.013186	0.057475	0.999957	1.0000	0.0117
0.90625	-1.93E-02	0.038054	0.013089	0.057336	0.999849	1.0000	0.0264
0.890625	-4.29E-03	0.053024	0.013071	0.057310	0.999756	1.0000	0.0359
0.8828125	4.29E-03	0.061596	0.013071	0.057310	0.999697	1.0000	0.0412
0.88671875	-9.20E-05	0.057217	0.013070	0.057309	0.999728	1.0000	0.0385
0.884765625	2.07E-03	0.059383	0.013070	0.057309	0.999713	1.0000	0.0398
0.8857421875	9.85E-04	0.058294	0.013070	0.057309	0.999720	1.0000	0.0392
0.8862304688	4.45E-04	0.057754	0.013070	0.057309	0.999724	1.0000	0.0388
0.8864746094	1.76E-04	0.057485	0.013070	0.057309	0.999726	1.0000	0.0387
0.8865966797	4.20E-05	0.057351	0.013070	0.057309	0.999727	1.0000	0.0386
0.8866577148	-2.50E-05	0.057284	0.013070	0.057309	0.999727	1.0000	0.0385
0.8866271973	8.52E-06	0.057317	0.013070	0.057309	0.999727	1.0000	0.0386
0.8866424561	-8.23E-06	0.057300	0.013070	0.057309	0.999727	1.0000	0.0385
0.8866348267	1.44E-07	0.057309	0.013070	0.057309	0.999727	1.0000	0.0386
0.8866386414	-4.04E-06	0.057304	0.013070	0.057309	0.999727	1.0000	0.0386
0.886636734	-1.95E-06	0.057307	0.013070	0.057309	0.999727	1.0000	0.0386
0.8866357803	-9.03E-07	0.057308	0.013070	0.057309	0.999727	1.0000	0.0386
0.8866353035	-3.79E-07	0.057308	0.013070	0.057309	0.999727	1.0000	0.0386
0.8866350651	-1.18E-07	0.057308	0.013070	0.057309	0.999727	1.0000	0.0386
0.8866349459	1.34E-08	0.057309	0.013070	0.057309	0.999727	1.0000	0.0386
0.8866350055	-5.21E-08	0.057308	0.013070	0.057309	0.999727	1.0000	0.0386
0.8866349757	-1.93E-08	0.057309	0.013070	0.057309	0.999727	1.0000	0.0386
0.8866349608	-2.96E-09	0.057309	0.013070	0.057309	0.999727	1.0000	0.0386
0.8866349533	5.22E-09	0.057309	0.013070	0.057309	0.999727	1.0000	0.0386

Saturation	Total Mob	dP_v/dS_v	G	F	Gamma	Theta	High	Low
0.75	34.759228	0.045851	220.095758	12.870589	1.1794E+07	30550.407113	1	0.5
0.875	40.427490	0.009321	115.033000	10.281953	1.1701E+07	28275.535543	1	0.75
0.9375	43.300978	0.002124	62.501620	10.006619	1.1655E+07	28033.574650	1	0.875
0.90625	41.862126	0.005001	88.767310	10.097238	1.1678E+07	28113.209409	0.9375	0.875
0.890625	41.144193	0.006968	101.900155	10.175426	1.1690E+07	28181.920650	0.90625	0.875
0.8828125	40.785677	0.008095	108.466577	10.224828	1.1695E+07	28225.334700	0.890625	0.875
0.88671875	40.964895	0.007519	105.183366	10.199203	1.1693E+07	28202.815133	0.890625	0.8828125
0.884765625	40.875276	0.007804	106.824972	10.211779	1.1694E+07	28213.867353	0.88671875	0.8828125
0.8857421875	40.920083	0.007661	106.004169	10.205432	1.1693E+07	28208.289909	0.88671875	0.884765625
0.8862304688	40.942489	0.007590	105.593767	10.202303	1.1693E+07	28205.539756	0.88671875	0.8857421875
0.8864746094	40.953692	0.007555	105.388567	10.200749	1.1693E+07	28204.174262	0.88671875	0.8862304688
0.8865966797	40.959294	0.007537	105.285966	10.199975	1.1693E+07	28203.493903	0.88671875	0.88647460938
0.8866577148	40.962095	0.007528	105.234666	10.199589	1.1693E+07	28203.154319	0.88671875	0.88659667969
0.8866271973	40.960694	0.007533	105.260316	10.199782	1.1693E+07	28203.324062	0.88665771484	0.88659667969
0.8866424561	40.961394	0.007530	105.247491	10.199685	1.1693E+07	28203.239178	0.88665771484	0.88662719727
0.8866348267	40.961044	0.007531	105.253904	10.199733	1.1693E+07	28203.281617	0.88664245605	0.88662719727
0.8866386414	40.961219	0.007531	105.250698	10.199709	1.1693E+07	28203.260397	0.88664245605	0.88663482666
0.886636734	40.961132	0.007531	105.252301	10.199721	1.1693E+07	28203.271006	0.88663864136	0.88663482666
0.8866357803	40.961088	0.007531	105.253102	10.199727	1.1693E+07	28203.276312	0.88663673401	0.88663482666
0.8866353035	40.961066	0.007531	105.253503	10.199730	1.1693E+07	28203.278964	0.88663578033	0.88663482666
0.8866350651	40.961055	0.007531	105.253703	10.199732	1.1693E+07	28203.280290	0.8866353035	0.88663482666
0.8866349459	40.961050	0.007531	105.253804	10.199733	1.1693E+07	28203.280954	0.88663506508	0.88663482666
0.8866350055	40.961052	0.007531	105.253753	10.199732	1.1693E+07	28203.280622	0.88663506508	0.88663494587
0.8866349757	40.961051	0.007531	105.253779	10.199732	1.1693E+07	28203.280788	0.88663500547	0.88663494587
0.8866349608	40.961050	0.007531	105.253791	10.199733	1.1693E+07	28203.280871	0.88663497567	0.88663494587
0.8866349533	40.961050	0.007531	105.253797	10.199733	1.1693E+07	28203.280912	0.88663496077	0.88663494587

Spreadsheet for Calculation of Stream-Water Saturation Profiles

Injection Temperature
650 °K

Initial Temperature
350 °K

Matrix Heat Capacity
1.0000 (kJ/kg)

MATRIX PROPERTIES

Porosity	Cp Matrix	Density	Rho * Cp
0.10	1.00	2650.00	2650.0000
Nw	Ng	Swi	Denom
3.00	1.00	0.00	1.000000

SATURATION CONDITIONS

Tsaturation = 485.57

	Volumes (m3/kg)	Enthalpies (kJ/kg)	Densities (kg/m3)	Viscosities (cp)	Saturation Step
Liquid	0.001176	901.41	850.4723	0.1303	0.0014063597
Vapor	0.100298	2808.52	9.970241	0.0217	

BOUNDARY CONDITIONS

	Temperature	Velocity	Heat Capacity	Wave Velocity	Density	Enthalpy
Injection	650	1.000000	2.30	0.006622	6.882648	3199.91
Initial	350	0.011889	4.15	0.017234	975.3174	319.98
	G	F	Gamma	Theta		
Injection	650	6.88	6.88	15524523.87	22023.87	
Initial	350	975.32	975.32	8659580.72	312080.72	

SHOCK CONDITIONS

	Initial Guess		Vapor Saturation	Objective Function	Two-Phase Wave Velocity	Upstream Flow Velocity	Shock Velocity	Vapor Frac Flow
Trailing	Sv-Hi	Sv-Low	0.9570	1.4356E-09	0.0068	0.692182	0.0068	1.0000
Leading	1	0.5	0.8866	4.7472E-09	0.0521	0.011889	0.0521	0.9997
	dKrv/dSv	dKrl/dSl	Total Mobility	dFv/dSv	G	F'	Gamma	Theta'
Trailing	1.0000	0.0056	44.1982	0.0010	46.1514	9.9819	1.1641E+07	28011.8389
Leading	1.0000	0.0386	40.9610	0.0075	105.2538	10.1997	1.1693E+07	28203.2809

MATERIAL BALANCES

	Inside	Initial	Injected	Produced	Balance	Error
Mass	92.818555	97.531740	6.882648	11.595824	0.0000	0.0000%
Enthalpy	884276.8231	865958.0720	22023.8721	3710.4157	-5.2947	0.0006%

Spreadsheet for Calculation of Stream-Water Saturation Profiles

Injection Temperature 650 °K		Initial Temperature 350 °K				Matrix Heat Capacity 1.0000 (kJ/kg)		
SATURATION PROFILE								
Vapor Saturation	Vapor Frac Flow	dKrv/dSv	dKrl/dSl	Total Mobility	dFv/dSv	lambda	Mass Inside	Enthalpy Inside
1.0000						0.000000		
1.0000						0.006783		
0.9570	0.999986	1.0000	0.0056	44.198164	0.000980	0.006783	0.046687	105308.165674
0.9555	0.999985	1.0000	0.0059	44.133273	0.001047	0.007248	0.021724	5410.540844
0.9541	0.999983	1.0000	0.0063	44.068385	0.001117	0.007729	0.023058	5601.643180
0.9527	0.999982	1.0000	0.0067	44.003501	0.001189	0.008227	0.024435	5793.901239
0.9513	0.999980	1.0000	0.0071	43.938622	0.001263	0.008741	0.025856	5987.323262
0.9499	0.999978	1.0000	0.0075	43.873748	0.001340	0.009272	0.027322	6181.917552
0.9485	0.999976	1.0000	0.0080	43.808877	0.001419	0.009819	0.028832	6377.692471
0.9471	0.999974	1.0000	0.0084	43.744012	0.001500	0.010384	0.030386	6574.656444
0.9457	0.999972	1.0000	0.0088	43.679151	0.001584	0.010965	0.031987	6772.817956
0.9443	0.999970	1.0000	0.0093	43.614295	0.001671	0.011564	0.033633	6972.185556
0.9429	0.999967	1.0000	0.0098	43.549445	0.001760	0.012179	0.035325	7172.767856
0.9415	0.999965	1.0000	0.0103	43.484599	0.001851	0.012812	0.037063	7374.573531
0.9401	0.999962	1.0000	0.0108	43.419759	0.001945	0.013462	0.038849	7577.611320
0.9387	0.999959	1.0000	0.0113	43.354924	0.002041	0.014130	0.040682	7781.890027
0.9373	0.999956	1.0000	0.0118	43.290095	0.002140	0.014815	0.042563	7987.418520
0.9359	0.999953	1.0000	0.0123	43.225272	0.002242	0.015518	0.044492	8194.205734
0.9345	0.999950	1.0000	0.0129	43.160454	0.002346	0.016239	0.046469	8402.260668
0.9330	0.999947	1.0000	0.0134	43.095643	0.002453	0.016978	0.048496	8611.592391
0.9316	0.999943	1.0000	0.0140	43.030837	0.002562	0.017734	0.050572	8822.210036
0.9302	0.999939	1.0000	0.0146	42.966038	0.002674	0.018509	0.052697	9034.122805
0.9288	0.999935	1.0000	0.0152	42.901245	0.002789	0.019302	0.054874	9247.339969
0.9274	0.999931	1.0000	0.0158	42.836459	0.002906	0.020113	0.057100	9461.870866
0.9260	0.999927	1.0000	0.0164	42.771679	0.003026	0.020943	0.059379	9677.724906
0.9246	0.999923	1.0000	0.0171	42.706906	0.003148	0.021791	0.061708	9894.911566
0.9232	0.999918	1.0000	0.0177	42.642140	0.003273	0.022658	0.064090	10113.440397
0.9218	0.999914	1.0000	0.0183	42.577381	0.003401	0.023544	0.066524	10333.321018
0.9204	0.999909	1.0000	0.0190	42.512629	0.003532	0.024448	0.069012	10554.563121
0.9190	0.999904	1.0000	0.0197	42.447884	0.003666	0.025372	0.071553	10777.176472
0.9176	0.999899	1.0000	0.0204	42.383147	0.003802	0.026315	0.074148	11001.170907
0.9162	0.999893	1.0000	0.0211	42.318417	0.003941	0.027277	0.076797	11226.556337
0.9148	0.999887	1.0000	0.0218	42.253694	0.004082	0.028258	0.079501	11453.342748
0.9134	0.999882	1.0000	0.0225	42.188980	0.004227	0.029259	0.082260	11681.540198
0.9119	0.999876	1.0000	0.0233	42.124273	0.004374	0.030279	0.085076	11911.158824
0.9105	0.999869	1.0000	0.0240	42.059575	0.004525	0.031319	0.087947	12142.208835
0.9091	0.999863	1.0000	0.0248	41.994884	0.004678	0.032379	0.090876	12374.700521
0.9077	0.999856	1.0000	0.0255	41.930202	0.004834	0.033458	0.093862	12608.644246
0.9063	0.999849	1.0000	0.0263	41.865528	0.004993	0.034558	0.096906	12844.050453
0.9049	0.999842	1.0000	0.0271	41.800863	0.005154	0.035678	0.100008	13080.929663
0.9035	0.999835	1.0000	0.0279	41.736207	0.005319	0.036818	0.103169	13319.292477
0.9021	0.999827	1.0000	0.0288	41.671559	0.005487	0.037979	0.106389	13559.149576
0.9007	0.999819	1.0000	0.0296	41.606920	0.005657	0.039160	0.109669	13800.511719
0.8993	0.999811	1.0000	0.0304	41.542290	0.005831	0.040362	0.113010	14043.389750
0.8979	0.999803	1.0000	0.0313	41.477669	0.006008	0.041585	0.116412	14287.794593
0.8965	0.999794	1.0000	0.0321	41.413058	0.006187	0.042828	0.119875	14533.737253
0.8951	0.999786	1.0000	0.0330	41.348456	0.006370	0.044093	0.123400	14781.228821
0.8937	0.999776	1.0000	0.0339	41.283864	0.006556	0.045379	0.126988	15030.280471
0.8923	0.999767	1.0000	0.0348	41.219281	0.006745	0.046686	0.130639	15280.903459
0.8909	0.999757	1.0000	0.0357	41.154708	0.006937	0.048015	0.134354	15533.109131
0.8894	0.999748	1.0000	0.0367	41.090145	0.007132	0.049365	0.138133	15786.908915
0.8880	0.999737	1.0000	0.0376	41.025593	0.007330	0.050737	0.141977	16042.314328
0.8866	0.999727	1.0000	0.0386	40.961050	0.007531	0.052131	0.145886	16299.336973
0.0000						0.052131		
0.0000						1.000000		

Spreadsheet for Calculation of Stream-Water Saturation Profiles

Injection Temperature Initial Temperature Matrix Heat Capacity
 650 °K 350 °K 1.0000 (kJ/kg)

TRAILING SHOCK CALCULATIONS

Saturation	OF	Wave V	Flow V	Shock V	Iv	dKrv/dSv	dKrl/dSl		
0.7500	2.42E-01	0.255386	0.556992	0.013421	0.996549	1.0000	0.1875		
0.875	5.56E-02	0.063132	0.677295	0.007514	0.999629	1.0000	0.0469		
0.9375	7.87E-03	0.014687	0.691596	0.006812	0.999957	1.0000	0.0117		
0.96875	-3.28E-03	0.003516	0.692013	0.006792	0.999995	1.0000	0.0029		
0.953125	1.30E-03	0.008087	0.692162	0.006784	0.999982	1.0000	0.0066		
0.9609375	-1.23E-03	0.005554	0.692162	0.006784	0.999990	1.0000	0.0046		
0.95703125	-2.54E-05	0.006758	0.692182	0.006783	0.999986	1.0000	0.0055		
0.955078125	6.23E-04	0.007406	0.692178	0.006784	0.999984	1.0000	0.0061		
0.9560546875	2.95E-04	0.007078	0.692181	0.006783	0.999985	1.0000	0.0058		
0.9565429688	1.34E-04	0.006917	0.692182	0.006783	0.999986	1.0000	0.0057		
0.9567871094	5.40E-05	0.006837	0.692182	0.006783	0.999986	1.0000	0.0056		
0.9569091797	1.42E-05	0.006798	0.692182	0.006783	0.999986	1.0000	0.0056		
0.9569702148	-5.61E-06	0.006778	0.692182	0.006783	0.999986	1.0000	0.0056		
0.9569396973	4.30E-06	0.006788	0.692182	0.006783	0.999986	1.0000	0.0056		
0.9569549561	-6.54E-07	0.006783	0.692182	0.006783	0.999986	1.0000	0.0056		
0.9569473267	1.82E-06	0.006785	0.692182	0.006783	0.999986	1.0000	0.0056		
0.9569511414	5.84E-07	0.006784	0.692182	0.006783	0.999986	1.0000	0.0056		
0.9569530487	-3.48E-08	0.006783	0.692182	0.006783	0.999986	1.0000	0.0056		
0.956952095	2.75E-07	0.006784	0.692182	0.006783	0.999986	1.0000	0.0056		
0.9569525719	1.20E-07	0.006783	0.692182	0.006783	0.999986	1.0000	0.0056		
0.9569528103	4.26E-08	0.006783	0.692182	0.006783	0.999986	1.0000	0.0056		
0.9569529295	3.85E-09	0.006783	0.692182	0.006783	0.999986	1.0000	0.0056		
0.9569529891	-1.55E-08	0.006783	0.692182	0.006783	0.999986	1.0000	0.0056		
0.9569529593	-5.82E-09	0.006783	0.692182	0.006783	0.999986	1.0000	0.0056		
0.9569529444	-9.83E-10	0.006783	0.692182	0.006783	0.999986	1.0000	0.0056		
0.9569529369	1.44E-09	0.006783	0.692182	0.006783	0.999986	1.0000	0.0056		

Saturation	Total Mob	dFv/dSv	G	F	Gamma	Theta	High	Low
0.75	34.759228	0.045851	220.095758	12.870589	1.1794E+07	30550.407113	1	0.5
0.875	40.427490	0.009321	115.033000	10.281953	1.1701E+07	28275.535543	1	0.75
0.9375	43.300978	0.002124	62.501620	10.006619	1.1635E+07	28033.574650	1	0.875
0.96875	44.742642	0.000508	36.235931	9.974642	1.1632E+07	28005.473055	1	0.9375
0.953125	44.021547	0.001168	49.368776	9.985337	1.1643E+07	28014.871837	0.96875	0.9375
0.9609375	44.382039	0.000802	42.802353	9.978906	1.1638E+07	28009.220503	0.96875	0.953125
0.95703125	44.201778	0.000976	46.085564	9.981821	1.1641E+07	28011.782338	0.9609375	0.953125
0.955078125	44.111658	0.001070	47.727170	9.983500	1.1642E+07	28013.257853	0.95703125	0.953125
0.9560546875	44.156717	0.001023	46.906367	9.982642	1.1641E+07	28012.503198	0.95703125	0.955078125
0.9565429688	44.179247	0.000999	46.495966	9.982227	1.1641E+07	28012.138595	0.95703125	0.9560546875
0.9567871094	44.190513	0.000988	46.290765	9.982023	1.1641E+07	28011.959430	0.95703125	0.95654296875
0.9569091797	44.196145	0.000982	46.188165	9.981922	1.1641E+07	28011.870625	0.95703125	0.95678710938
0.9569702148	44.198962	0.000979	46.136864	9.981871	1.1641E+07	28011.826417	0.95703125	0.95690917969
0.9569396973	44.197553	0.000981	46.162515	9.981897	1.1641E+07	28011.848505	0.95697021484	0.95690917969
0.9569549561	44.198258	0.000980	46.149690	9.981884	1.1641E+07	28011.837457	0.95697021484	0.95693969727
0.9569473267	44.197905	0.000980	46.156102	9.981890	1.1641E+07	28011.842980	0.95695495605	0.95693969727
0.9569511414	44.198082	0.000980	46.152896	9.981887	1.1641E+07	28011.840218	0.95695495605	0.95694732666
0.9569530487	44.198170	0.000980	46.151293	9.981886	1.1641E+07	28011.838838	0.95695495605	0.95695114136
0.956952095	44.198126	0.000980	46.152094	9.981886	1.1641E+07	28011.839528	0.95695304871	0.95695114136
0.9569525719	44.198148	0.000980	46.151693	9.981886	1.1641E+07	28011.839183	0.95695304871	0.95695209503
0.9569528103	44.198159	0.000980	46.151493	9.981886	1.1641E+07	28011.839010	0.95695304871	0.95695257187
0.9569529295	44.198164	0.000980	46.151393	9.981886	1.1641E+07	28011.838924	0.95695304871	0.95695281029
0.9569529891	44.198167	0.000980	46.151343	9.981886	1.1641E+07	28011.838881	0.95695304871	0.9569529295
0.9569529593	44.198165	0.000980	46.151368	9.981886	1.1641E+07	28011.838902	0.9569529891	0.9569529295
0.9569529444	44.198165	0.000980	46.151380	9.981886	1.1641E+07	28011.838913	0.9569529593	0.9569529295
0.9569529369	44.198164	0.000980	46.151387	9.981886	1.1641E+07	28011.838919	0.9569529444	0.9569529295

Spreadsheet for Calculation of Stream-Water Saturation Profiles

Injection Temperature 650 °K Initial Temperature 350 °K Matrix Heat Capacity 1.0000 (kJ/kg)

LEADING SHOCK CALCULATIONS

Saturation	OF	Wave V	Flow V	Shock V	f _v	dK _{rv} /dS _v	dK _{rl} /dS _l
0.7500	2.63E-01	0.317373	0.013331	0.054201	0.996549	1.0000	0.1875
0.875	1.24E-02	0.064519	0.011896	0.052141	0.999629	1.0000	0.0469
0.9375	-3.76E-02	0.014699	0.011995	0.052283	0.999957	1.0000	0.0117
0.90625	-1.75E-02	0.034616	0.011907	0.052157	0.999849	1.0000	0.0264
0.890625	-3.90E-03	0.048233	0.011890	0.052132	0.999756	1.0000	0.0359
0.8828125	3.90E-03	0.056031	0.011890	0.052132	0.999697	1.0000	0.0412
0.88671875	-8.37E-05	0.052048	0.011889	0.052131	0.999728	1.0000	0.0385
0.884765625	1.89E-03	0.054018	0.011889	0.052131	0.999713	1.0000	0.0398
0.8857421875	8.96E-04	0.053027	0.011889	0.052131	0.999720	1.0000	0.0392
0.8862304688	4.05E-04	0.052536	0.011889	0.052131	0.999724	1.0000	0.0388
0.8864746094	1.60E-04	0.052292	0.011889	0.052131	0.999726	1.0000	0.0387
0.8865966797	3.82E-05	0.052169	0.011889	0.052131	0.999727	1.0000	0.0386
0.8866577148	-2.27E-05	0.052108	0.011889	0.052131	0.999727	1.0000	0.0385
0.8866271973	7.75E-06	0.052139	0.011889	0.052131	0.999727	1.0000	0.0386
0.8866424561	-7.49E-06	0.052124	0.011889	0.052131	0.999727	1.0000	0.0385
0.8866348267	1.31E-07	0.052131	0.011889	0.052131	0.999727	1.0000	0.0386
0.8866386414	-3.68E-06	0.052128	0.011889	0.052131	0.999727	1.0000	0.0386
0.886636734	-1.77E-06	0.052129	0.011889	0.052131	0.999727	1.0000	0.0386
0.8866357803	-8.21E-07	0.052130	0.011889	0.052131	0.999727	1.0000	0.0386
0.8866353035	-3.45E-07	0.052131	0.011889	0.052131	0.999727	1.0000	0.0386
0.8866350651	-1.07E-07	0.052131	0.011889	0.052131	0.999727	1.0000	0.0386
0.8866349459	1.22E-08	0.052131	0.011889	0.052131	0.999727	1.0000	0.0386
0.8866350055	-4.74E-08	0.052131	0.011889	0.052131	0.999727	1.0000	0.0386
0.8866349757	-1.76E-08	0.052131	0.011889	0.052131	0.999727	1.0000	0.0386
0.8866349608	-2.70E-09	0.052131	0.011889	0.052131	0.999727	1.0000	0.0386
0.8866349533	4.75E-09	0.052131	0.011889	0.052131	0.999727	1.0000	0.0386

Saturation	Total Mob	dF _v /dS _v	G	F	Gamma	Theta	High	Low
0.75	34.759228	0.045851	220.095758	12.870589	1.1794E+07	30550.407113	1	0.5
0.875	40.427490	0.009321	115.033000	10.281953	1.1701E+07	28275.535543	1	0.75
0.9375	43.300978	0.002124	62.501620	10.006619	1.1655E+07	28033.574650	1	0.875
0.90625	41.862126	0.005001	88.767310	10.097238	1.1678E+07	28113.209409	0.9375	0.875
0.890625	41.144193	0.006968	101.900155	10.175426	1.1690E+07	28181.920650	0.90625	0.875
0.8828125	40.785677	0.008095	108.466577	10.224828	1.1695E+07	28225.334700	0.890625	0.875
0.88671875	40.964895	0.007519	105.183366	10.199203	1.1693E+07	28202.815133	0.890625	0.8828125
0.884765625	40.875276	0.007804	106.824972	10.211779	1.1694E+07	28213.867353	0.88671875	0.8828125
0.8857421875	40.920083	0.007661	106.004169	10.205432	1.1693E+07	28208.289909	0.88671875	0.884765625
0.8862304688	40.942489	0.007590	105.593767	10.202303	1.1693E+07	28205.539756	0.88671875	0.8857421875
0.8864746094	40.953692	0.007555	105.388567	10.200749	1.1693E+07	28204.174262	0.88671875	0.88623046875
0.8865966797	40.959294	0.007537	105.285966	10.199975	1.1693E+07	28203.493903	0.88671875	0.88647460938
0.8866577148	40.962095	0.007528	105.234666	10.199589	1.1693E+07	28203.154319	0.88671875	0.88659667969
0.8866271973	40.960694	0.007533	105.260316	10.199782	1.1693E+07	28203.324062	0.88665771484	0.88659667969
0.8866424561	40.961394	0.007530	105.247491	10.199685	1.1693E+07	28203.239178	0.88665771484	0.88662719727
0.8866348267	40.961044	0.007531	105.253904	10.199733	1.1693E+07	28203.281617	0.88664245605	0.88662719727
0.8866386414	40.961219	0.007531	105.250698	10.199709	1.1693E+07	28203.260397	0.88664245605	0.88663482666
0.886636734	40.961132	0.007531	105.252301	10.199721	1.1693E+07	28203.271006	0.88663864136	0.88663482666
0.8866357803	40.961088	0.007531	105.253102	10.199727	1.1693E+07	28203.276312	0.88663673401	0.88663482666
0.8866353035	40.961066	0.007531	105.253503	10.199730	1.1693E+07	28203.278964	0.88663578033	0.88663482666
0.8866350651	40.961055	0.007531	105.253703	10.199732	1.1693E+07	28203.280290	0.8866353035	0.88663482666
0.8866349459	40.961050	0.007531	105.253804	10.199733	1.1693E+07	28203.280954	0.88663506508	0.88663482666
0.8866350055	40.961052	0.007531	105.253753	10.199732	1.1693E+07	28203.280622	0.88663506508	0.88663494587
0.8866349757	40.961051	0.007531	105.253779	10.199732	1.1693E+07	28203.280788	0.88663500547	0.88663494587
0.8866349608	40.961050	0.007531	105.253791	10.199733	1.1693E+07	28203.280871	0.88663497567	0.88663494587
0.8866349533	40.961050	0.007531	105.253797	10.199733	1.1693E+07	28203.280912	0.88663496077	0.88663494587

Spreadsheet for Calculation of Stream-Water Saturation Profiles

Injection Temperature
700 °K

Initial Temperature
350 °K

Matrix Heat Capacity
1.0000 (kJ/kg)

MATRIX PROPERTIES

Porosity	Cp Matrix	Density	Rho * Cp
0.10	1.00	2650.00	2650.0000
Nw	Ng	Swi	Denom
3.00	1.00	0.00	1.000000

SATURATION CONDITIONS

Tsaturation = 485.57

	Volumes (m3/kg)	Enthalpies (kJ/kg)	Densities (kg/m3)	Viscosities (cp)	Saturation Step
Liquid	0.001176	901.41	850.4723	0.1303	0.0014093366
Vapor	0.100298	2808.52	9.970241	0.0217	

BOUNDARY CONDITIONS

	Temperature	Velocity	Heat Capacity	Wave Velocity	Density	Enthalpy
Injection	700	1.000000	2.26	0.006003	6.327955	3313.87
Initial	350	0.010931	4.15	0.015846	975.3174	319.98
	G	F	Gamma	Theta		
Injection	700	6.33	6.33	16715970.02	20970.02	
Initial	350	975.32	975.32	8659580.72	312080.72	

SHOCK CONDITIONS

	Initial Guess		Vapor Saturation	Objective Function	Two-Phase Wave Velocity	Upstream Flow Velocity	Shock Velocity	Vapor Frac Flow
Trailing	Sv-Hi	Sv-Low	0.9571	-6.2479E-10	0.0062	0.636414	0.0062	1.0000
Leading	1	0.5	0.8866	4.3647E-09	0.0479	0.010931	0.0479	0.9997
	dKrv/dSv	dKrl/dSl	Total Mobility	dFv/dSv	G	F'	Gamma	Theta'
Trailing	1.0000	0.0055	44.2050	0.0010	46.0263	9.9818	1.1641E+07	28011.7316
Leading	1.0000	0.0386	40.9610	0.0075	105.2538	10.1997	1.1693E+07	28203.2809

MATERIAL BALANCES

	Inside	Initial	Injected	Produced	Balance	Error
Mass	93.198119	97.531740	6.327955	10.661567	0.0000	0.0000%
Enthalpy	883521.4881	865958.0720	20970.0198	3411.4735	-4.8698	0.0005%

Spreadsheet for Calculation of Stream-Water Saturation Profiles

Injection Temperature 700 °K		Initial Temperature 350 °K		Matrix Heat Capacity 1.0000 (kJ/kg)				
SATURATION PROFILE								
Vapor Saturation	Vapor Frac Flow	dKrv/dSv	dKr/dSI	Total Mobility	dFv/dSv	lambda	Mass Inside	Enthalpy Inside
1.0000						0.000000		
1.0000						0.006192		
0.9571	0.999986	1.0000	0.0055	44.205033	0.000973	0.006192	0.039186	103513.160498
0.9557	0.999985	1.0000	0.0059	44.140003	0.001040	0.006619	0.019889	4966.764438
0.9543	0.999983	1.0000	0.0063	44.074978	0.001109	0.007061	0.021117	5143.104365
0.9529	0.999982	1.0000	0.0067	44.009956	0.001181	0.007518	0.022384	5320.512883
0.9515	0.999980	1.0000	0.0071	43.944939	0.001255	0.007990	0.023693	5498.997628
0.9501	0.999978	1.0000	0.0075	43.879927	0.001332	0.008478	0.025042	5678.566292
0.9486	0.999976	1.0000	0.0079	43.814919	0.001411	0.008981	0.026432	5859.226625
0.9472	0.999974	1.0000	0.0084	43.749916	0.001493	0.009499	0.027864	6040.986431
0.9458	0.999972	1.0000	0.0088	43.684917	0.001577	0.010034	0.029337	6223.853575
0.9444	0.999970	1.0000	0.0093	43.619924	0.001663	0.010584	0.030853	6407.835977
0.9430	0.999967	1.0000	0.0097	43.554936	0.001752	0.011149	0.032412	6592.941617
0.9416	0.999965	1.0000	0.0102	43.489952	0.001843	0.011731	0.034014	6779.178535
0.9402	0.999962	1.0000	0.0107	43.424975	0.001937	0.012329	0.035659	6966.554828
0.9388	0.999959	1.0000	0.0112	43.360002	0.002034	0.012943	0.037348	7155.078655
0.9374	0.999956	1.0000	0.0118	43.295035	0.002133	0.013573	0.039081	7344.758234
0.9360	0.999953	1.0000	0.0123	43.230074	0.002234	0.014220	0.040858	7535.601844
0.9346	0.999950	1.0000	0.0129	43.165119	0.002338	0.014883	0.042681	7727.617827
0.9331	0.999947	1.0000	0.0134	43.100170	0.002445	0.015562	0.044549	7920.814585
0.9317	0.999943	1.0000	0.0140	43.035227	0.002555	0.016258	0.046462	8115.200582
0.9303	0.999940	1.0000	0.0146	42.970290	0.002667	0.016971	0.048422	8310.784349
0.9289	0.999936	1.0000	0.0152	42.905360	0.002781	0.017700	0.050428	8507.574474
0.9275	0.999932	1.0000	0.0158	42.840436	0.002899	0.018447	0.052482	8705.579616
0.9261	0.999928	1.0000	0.0164	42.775518	0.003018	0.019210	0.054582	8904.808492
0.9247	0.999923	1.0000	0.0170	42.710608	0.003141	0.019991	0.056730	9105.269888
0.9233	0.999919	1.0000	0.0177	42.645704	0.003266	0.020788	0.058927	9306.972656
0.9219	0.999914	1.0000	0.0183	42.580808	0.003395	0.021604	0.061172	9509.925710
0.9205	0.999909	1.0000	0.0190	42.515918	0.003525	0.022436	0.063466	9714.138035
0.9190	0.999904	1.0000	0.0197	42.451036	0.003659	0.023286	0.065809	9919.618680
0.9176	0.999899	1.0000	0.0203	42.386161	0.003795	0.024154	0.068203	10126.376765
0.9162	0.999893	1.0000	0.0211	42.321294	0.003934	0.025039	0.070647	10334.421476
0.9148	0.999888	1.0000	0.0218	42.256434	0.004076	0.025943	0.073141	10543.762067
0.9134	0.999882	1.0000	0.0225	42.191582	0.004221	0.026864	0.075687	10754.407863
0.9120	0.999876	1.0000	0.0232	42.126739	0.004369	0.027803	0.078284	10966.368260
0.9106	0.999870	1.0000	0.0240	42.061903	0.004519	0.028761	0.080934	11179.652723
0.9092	0.999863	1.0000	0.0247	41.997075	0.004673	0.029737	0.083636	11394.270788
0.9078	0.999856	1.0000	0.0255	41.932256	0.004829	0.030731	0.086391	11610.232063
0.9064	0.999849	1.0000	0.0263	41.867445	0.004988	0.031743	0.089200	11827.546229
0.9050	0.999842	1.0000	0.0271	41.802642	0.005150	0.032775	0.092062	12046.223040
0.9035	0.999835	1.0000	0.0279	41.737849	0.005315	0.033825	0.094980	12266.272322
0.9021	0.999827	1.0000	0.0287	41.673064	0.005483	0.034894	0.097952	12487.703978
0.9007	0.999820	1.0000	0.0296	41.608288	0.005654	0.035982	0.100979	12710.527982
0.8993	0.999811	1.0000	0.0304	41.543521	0.005828	0.037089	0.104062	12934.754388
0.8979	0.999803	1.0000	0.0313	41.478764	0.006005	0.038215	0.107202	13160.393321
0.8965	0.999794	1.0000	0.0321	41.414015	0.006185	0.039361	0.110399	13387.454987
0.8951	0.999786	1.0000	0.0330	41.349277	0.006368	0.040526	0.113653	13615.949667
0.8937	0.999777	1.0000	0.0339	41.284547	0.006554	0.041710	0.116965	13845.887720
0.8923	0.999767	1.0000	0.0348	41.219828	0.006743	0.042915	0.120336	14077.279584
0.8909	0.999758	1.0000	0.0357	41.155118	0.006936	0.044139	0.123765	14310.135778
0.8895	0.999748	1.0000	0.0367	41.090419	0.007131	0.045383	0.127254	14544.466897
0.8880	0.999737	1.0000	0.0376	41.025729	0.007330	0.046647	0.130803	14780.283620
0.8866	0.999727	1.0000	0.0386	40.961050	0.007531	0.047931	0.134412	15017.596707
0.0000						0.047931		
0.0000						1.000000		

Spreadsheet for Calculation of Stream-Water Saturation Profiles

Injection Temperature 700 °K		Initial Temperature 350 °K		Matrix Heat Capacity 1.0000 (kJ/kg)				
TRAILING SHOCK CALCULATIONS								
Saturation	OF	Wave V	Flow V	Shock V	fv	dKrv/dSv	dKr/dSI	
0.7500	2.23E-01	0.233775	0.509859	0.010957	0.996549	1.0000	0.1875	
0.875	5.13E-02	0.058028	0.622542	0.006715	0.999629	1.0000	0.0469	
0.9375	7.29E-03	0.013503	0.635865	0.006213	0.999957	1.0000	0.0117	
0.96875	-2.97E-03	0.003233	0.636263	0.006198	0.999995	1.0000	0.0029	
0.953125	1.24E-03	0.007435	0.636394	0.006193	0.999982	1.0000	0.0066	
0.9609375	-1.09E-03	0.005107	0.636397	0.006193	0.999990	1.0000	0.0046	
0.95703125	2.10E-05	0.006213	0.636414	0.006192	0.999986	1.0000	0.0055	
0.958984375	-5.47E-04	0.005646	0.636410	0.006193	0.999988	1.0000	0.0050	
0.9580078125	-2.66E-04	0.005926	0.636413	0.006193	0.999987	1.0000	0.0053	
0.9575195313	-1.24E-04	0.006069	0.636414	0.006192	0.999987	1.0000	0.0054	
0.9572753906	-5.15E-05	0.006141	0.636414	0.006192	0.999986	1.0000	0.0055	
0.9571533203	-1.53E-05	0.006177	0.636414	0.006192	0.999986	1.0000	0.0055	
0.9570922852	2.82E-06	0.006195	0.636414	0.006192	0.999986	1.0000	0.0055	
0.9571228027	-6.25E-06	0.006186	0.636414	0.006192	0.999986	1.0000	0.0055	
0.9571075439	-1.71E-06	0.006191	0.636414	0.006192	0.999986	1.0000	0.0055	
0.9570999146	5.56E-07	0.006193	0.636414	0.006192	0.999986	1.0000	0.0055	
0.9571037292	-5.79E-07	0.006192	0.636414	0.006192	0.999986	1.0000	0.0055	
0.9571018219	-1.17E-08	0.006192	0.636414	0.006192	0.999986	1.0000	0.0055	
0.9571008682	2.72E-07	0.006193	0.636414	0.006192	0.999986	1.0000	0.0055	
0.9571013451	1.30E-07	0.006193	0.636414	0.006192	0.999986	1.0000	0.0055	
0.9571015835	5.92E-08	0.006193	0.636414	0.006192	0.999986	1.0000	0.0055	
0.9571017027	2.37E-08	0.006192	0.636414	0.006192	0.999986	1.0000	0.0055	
0.9571017623	6.02E-09	0.006192	0.636414	0.006192	0.999986	1.0000	0.0055	
0.9571017921	-2.84E-09	0.006192	0.636414	0.006192	0.999986	1.0000	0.0055	
0.9571017772	1.59E-09	0.006192	0.636414	0.006192	0.999986	1.0000	0.0055	
0.9571017846	-6.25E-10	0.006192	0.636414	0.006192	0.999986	1.0000	0.0055	
Saturation	Total Mob	dPv/dSv	G	F	Gamma	Theta	High	Low
0.75	34.759228	0.045851	220.095758	12.870589	1.1794E+07	30550.407113	1	0.5
0.875	40.427490	0.009321	115.033000	10.281953	1.1701E+07	28275.535543	1	0.75
0.9375	43.300978	0.002124	62.501620	10.006619	1.1655E+07	28033.574650	1	0.875
0.96875	44.742642	0.000508	36.235931	9.974642	1.1632E+07	28005.473055	1	0.9375
0.953125	44.021547	0.001168	49.368776	9.985337	1.1643E+07	28014.871837	0.96875	0.9375
0.9609375	44.382039	0.000802	42.802353	9.978906	1.1638E+07	28009.220503	0.96875	0.953125
0.95703125	44.201778	0.000976	46.085564	9.981821	1.1641E+07	28011.782338	0.9609375	0.953125
0.958984375	44.291905	0.000887	44.443959	9.980292	1.1639E+07	28010.438726	0.9609375	0.95703125
0.9580078125	44.246841	0.000931	45.264762	9.981039	1.1640E+07	28011.094453	0.958984375	0.95703125
0.9575195313	44.224309	0.000954	45.675163	9.981425	1.1640E+07	28011.434324	0.9580078125	0.95703125
0.9572753906	44.213043	0.000965	45.880364	9.981622	1.1640E+07	28011.607307	0.95751953125	0.95703125
0.9571533203	44.207411	0.000971	45.982964	9.981721	1.1640E+07	28011.694566	0.95727539063	0.95703125
0.9570922852	44.204594	0.000973	46.034264	9.981771	1.1641E+07	28011.738388	0.95715332031	0.95703125
0.9571228027	44.206003	0.000972	46.008614	9.981746	1.1641E+07	28011.716461	0.95715332031	0.95709228516
0.9571075439	44.205298	0.000973	46.021439	9.981759	1.1641E+07	28011.727420	0.95712280273	0.95709228516
0.9570999146	44.204946	0.000973	46.027852	9.981765	1.1641E+07	28011.732903	0.95710754395	0.95709228516
0.9571037292	44.205122	0.000973	46.024645	9.981762	1.1641E+07	28011.730161	0.95710754395	0.95709991455
0.9571018219	44.205034	0.000973	46.026248	9.981763	1.1641E+07	28011.731532	0.95710372925	0.95709991455
0.9571008682	44.204990	0.000973	46.027050	9.981764	1.1641E+07	28011.732217	0.9571018219	0.95709991455
0.9571013451	44.205012	0.000973	46.026649	9.981764	1.1641E+07	28011.731875	0.9571018219	0.95710086823
0.9571015835	44.205023	0.000973	46.026449	9.981764	1.1641E+07	28011.731703	0.9571018219	0.95710134506
0.9571017027	44.205029	0.000973	46.026349	9.981764	1.1641E+07	28011.731618	0.9571018219	0.95710158348
0.9571017623	44.205032	0.000973	46.026299	9.981764	1.1641E+07	28011.731575	0.9571018219	0.95710170269
0.9571017921	44.205033	0.000973	46.026274	9.981763	1.1641E+07	28011.731553	0.9571018219	0.95710176229
0.9571017772	44.205032	0.000973	46.026286	9.981764	1.1641E+07	28011.731564	0.9571017921	0.95710176229
0.9571017846	44.205033	0.000973	46.026280	9.981764	1.1641E+07	28011.731559	0.9571017921	0.9571017772

Spreadsheet for Calculation of Stream-Water Saturation Profiles

Injection Temperature 700 °K Initial Temperature 350 °K Matrix Heat Capacity 1.0000 (kJ/kg)

LEADING SHOCK CALCULATIONS

Saturation	OF	Wave V	Flow V	Shock V	f _v	dKr _v /dS _v	dKr/dS _l
0.7500	2.42E-01	0.291802	0.012257	0.049834	0.996549	1.0000	0.1875
0.875	1.14E-02	0.059321	0.010938	0.047940	0.999629	1.0000	0.0469
0.9375	-3.46E-02	0.013515	0.011029	0.048071	0.999957	1.0000	0.0117
0.90625	-1.61E-02	0.031827	0.010948	0.047954	0.999849	1.0000	0.0264
0.890625	-3.58E-03	0.044347	0.010932	0.047932	0.999756	1.0000	0.0359
0.8828125	3.58E-03	0.051517	0.010932	0.047932	0.999697	1.0000	0.0412
0.88671875	-7.69E-05	0.047854	0.010931	0.047931	0.999728	1.0000	0.0385
0.884765625	1.73E-03	0.049666	0.010932	0.047931	0.999713	1.0000	0.0398
0.8857421875	8.24E-04	0.048755	0.010931	0.047931	0.999720	1.0000	0.0392
0.8862304688	3.72E-04	0.048303	0.010931	0.047931	0.999724	1.0000	0.0388
0.8864746094	1.47E-04	0.048078	0.010931	0.047931	0.999726	1.0000	0.0387
0.8865966797	3.52E-05	0.047966	0.010931	0.047931	0.999727	1.0000	0.0386
0.8866577148	-2.09E-05	0.047910	0.010931	0.047931	0.999727	1.0000	0.0385
0.8866271973	7.13E-06	0.047938	0.010931	0.047931	0.999727	1.0000	0.0386
0.8866424561	-6.89E-06	0.047924	0.010931	0.047931	0.999727	1.0000	0.0385
0.8866348267	1.21E-07	0.047931	0.010931	0.047931	0.999727	1.0000	0.0386
0.8866386414	-3.38E-06	0.047928	0.010931	0.047931	0.999727	1.0000	0.0386
0.886636734	-1.63E-06	0.047929	0.010931	0.047931	0.999727	1.0000	0.0386
0.8866357803	-7.55E-07	0.047930	0.010931	0.047931	0.999727	1.0000	0.0386
0.8866353035	-3.17E-07	0.047931	0.010931	0.047931	0.999727	1.0000	0.0386
0.8866350651	-9.83E-08	0.047931	0.010931	0.047931	0.999727	1.0000	0.0386
0.8866349459	1.12E-08	0.047931	0.010931	0.047931	0.999727	1.0000	0.0386
0.8866350055	-4.35E-08	0.047931	0.010931	0.047931	0.999727	1.0000	0.0386
0.8866349757	-1.62E-08	0.047931	0.010931	0.047931	0.999727	1.0000	0.0386
0.8866349608	-2.48E-09	0.047931	0.010931	0.047931	0.999727	1.0000	0.0386
0.8866349533	4.36E-09	0.047931	0.010931	0.047931	0.999727	1.0000	0.0386

Saturation	Total Mob	dF _v /dS _v	G	F	Gamma	Theta	High	Low
0.75	34.759228	0.045851	220.095758	12.870589	1.1794E+07	30550.407113	1	0.5
0.875	40.427490	0.009321	115.033000	10.281953	1.1701E+07	28275.535543	1	0.75
0.9375	43.300978	0.002124	62.501620	10.006619	1.1655E+07	28033.574650	1	0.875
0.90625	41.862126	0.005001	88.767310	10.097238	1.1678E+07	28113.209409	0.9375	0.875
0.890625	41.144193	0.006968	101.900155	10.175426	1.1690E+07	28181.920650	0.90625	0.875
0.8828125	40.785677	0.008095	108.466577	10.224828	1.1695E+07	28225.334700	0.890625	0.875
0.88671875	40.964895	0.007519	105.183366	10.199203	1.1693E+07	28202.815133	0.890625	0.8828125
0.884765625	40.875276	0.007804	106.824972	10.211779	1.1694E+07	28213.867353	0.88671875	0.8828125
0.8857421875	40.920083	0.007661	106.004169	10.205432	1.1693E+07	28208.289909	0.88671875	0.884765625
0.8862304688	40.942489	0.007590	105.593767	10.202303	1.1693E+07	28205.539756	0.88671875	0.8857421875
0.8864746094	40.953692	0.007555	105.388567	10.200749	1.1693E+07	28204.174262	0.88671875	0.8862304688
0.8865966797	40.959294	0.007537	105.285966	10.199975	1.1693E+07	28203.493903	0.88671875	0.88647460938
0.8866577148	40.962095	0.007528	105.234666	10.199589	1.1693E+07	28203.154319	0.88671875	0.88659667969
0.8866271973	40.960694	0.007533	105.260316	10.199782	1.1693E+07	28203.324062	0.88665771484	0.88659667969
0.8866424561	40.961394	0.007530	105.247491	10.199685	1.1693E+07	28203.239178	0.88665771484	0.88662719727
0.8866348267	40.961044	0.007531	105.253904	10.199733	1.1693E+07	28203.281617	0.88664245605	0.88662719727
0.8866386414	40.961219	0.007531	105.250698	10.199709	1.1693E+07	28203.260397	0.88664245605	0.88663482666
0.886636734	40.961132	0.007531	105.252301	10.199721	1.1693E+07	28203.271006	0.88663864136	0.88663482666
0.8866357803	40.961088	0.007531	105.253102	10.199727	1.1693E+07	28203.276312	0.88663673401	0.88663482666
0.8866353035	40.961066	0.007531	105.253503	10.199730	1.1693E+07	28203.278964	0.88663578033	0.88663482666
0.8866350651	40.961055	0.007531	105.253703	10.199732	1.1693E+07	28203.280290	0.8866353035	0.88663482666
0.8866349459	40.961050	0.007531	105.253804	10.199733	1.1693E+07	28203.280954	0.88663506508	0.88663482666
0.8866350055	40.961052	0.007531	105.253753	10.199732	1.1693E+07	28203.280622	0.88663506508	0.88663494587
0.8866349757	40.961051	0.007531	105.253779	10.199732	1.1693E+07	28203.280788	0.88663500547	0.88663494587
0.8866349608	40.961050	0.007531	105.253791	10.199733	1.1693E+07	28203.280871	0.88663497567	0.88663494587
0.8866349533	40.961050	0.007531	105.253797	10.199733	1.1693E+07	28203.280912	0.88663496077	0.88663494587

Spreadsheet for Calculation of Stream-Water Saturation Profiles

Injection Temperature
750 °K

Initial Temperature
350 °K

Matrix Heat Capacity
1.0000 (kJ/kg)

MATRIX PROPERTIES

Porosity	Cp Matrix	Density	Rho * Cp
0.10	1.00	2650.00	2650.0000
Nw	Ng	Swi	Denom
3.00	1.00	0.00	1.000000

SATURATION CONDITIONS

Testuration = 485.57

	Volumes (m3/kg)	Enthalpies (kJ/kg)	Densities (kg/m3)	Viscosities (cp)	Saturation Step
Liquid	0.001176	901.41	850.4723	0.1303	0.0014120916
Vapor	0.100298	2808.52	9.970241	0.0217	

BOUNDARY CONDITIONS

	Temperature	Velocity	Heat Capacity	Wave Velocity	Density	Enthalpy
Injection	750	1.000000	2.24	0.005516	5.867544	3426.50
Initial	350	0.010136	4.15	0.014693	975.3174	319.98
	G	F	Gamma	Theta		
Injection	750	5.87	5.87	17907605.13	20105.13	
Initial	350	975.32	975.32	8659580.72	312080.72	

SHOCK CONDITIONS

	Initial Guess		Vapor Saturation	Objective Function	Two-Phase Wave Velocity	Upstream Flow Velocity	Shock Velocity	Vapor Frac Flow
Trailing	Sv-Hi	Sv-Low	0.9572	1.9290E-09	0.0057	0.590121	0.0057	1.0000
Landing	1	0.5	0.8866	4.0472E-09	0.0444	0.010136	0.0444	0.9997
	dKrv/dSv	dKrl/dSI	Total Mobility	dFv/dSv	G	F'	Gamma	Theta'
Trailing	1.0000	0.0055	44.2114	0.0010	45.9105	9.9817	1.1640E+07	28011.6329
Landing	1.0000	0.0386	40.9610	0.0075	105.2538	10.1997	1.1693E+07	28203.2809

MATERIAL BALANCES

	Inside	Initial	Injected	Produced	Balance	Error
Mass	93.513236	97.531740	5.867544	9.886039	0.0000	0.0000%
Enthalpy	882904.3953	865958.0720	20105.1252	3163.3211	-4.5192	0.0005%

Spreadsheet for Calculation of Stream-Water Saturation Profiles

Injection Temperature 750 °K		Initial Temperature 350 °K				Matrix Heat Capacity 1.0000 (kJ/kg)		
SATURATION PROFILE								
Vapor Saturation	Vapor Frac Flow	dKr/dSv	dKr/dSI	Total Mobility	dFv/dSv	lambda	Mass Inside	Enthalpy Inside
1.0000						0.000000		
1.0000						0.005704		
0.9572	0.999986	1.0000	0.0055	44.211389	0.000967	0.005704	0.033469	102146.953984
0.9558	0.999985	1.0000	0.0059	44.146232	0.001034	0.006099	0.018370	4598.682045
0.9544	0.999984	1.0000	0.0062	44.081079	0.001103	0.006508	0.019509	4762.739893
0.9530	0.999982	1.0000	0.0066	44.015930	0.001175	0.006931	0.020686	4927.793751
0.9516	0.999980	1.0000	0.0070	43.950786	0.001249	0.007369	0.021900	5093.850752
0.9502	0.999978	1.0000	0.0074	43.885646	0.001325	0.007821	0.023153	5260.918078
0.9488	0.999976	1.0000	0.0079	43.820510	0.001404	0.008287	0.024443	5429.002967
0.9474	0.999974	1.0000	0.0083	43.755379	0.001486	0.008767	0.025773	5598.112708
0.9459	0.999972	1.0000	0.0088	43.690254	0.001570	0.009263	0.027141	5768.254645
0.9445	0.999970	1.0000	0.0092	43.625133	0.001656	0.009772	0.028549	5939.436177
0.9431	0.999968	1.0000	0.0097	43.560017	0.001745	0.010297	0.029997	6111.664757
0.9417	0.999965	1.0000	0.0102	43.494906	0.001836	0.010836	0.031485	6284.947892
0.9403	0.999962	1.0000	0.0107	43.429801	0.001930	0.011391	0.033013	6459.293147
0.9389	0.999960	1.0000	0.0112	43.364701	0.002027	0.011960	0.034582	6634.708140
0.9375	0.999957	1.0000	0.0117	43.299607	0.002126	0.012544	0.036193	6811.200548
0.9361	0.999954	1.0000	0.0123	43.234519	0.002227	0.013144	0.037845	6988.778106
0.9346	0.999950	1.0000	0.0128	43.169436	0.002331	0.013759	0.039538	7167.448602
0.9332	0.999947	1.0000	0.0134	43.104360	0.002438	0.014389	0.041274	7347.219886
0.9318	0.999943	1.0000	0.0139	43.039289	0.002548	0.015035	0.043053	7528.099865
0.9304	0.999940	1.0000	0.0145	42.974225	0.002660	0.015696	0.044874	7710.096505
0.9290	0.999936	1.0000	0.0151	42.909167	0.002774	0.016373	0.046739	7893.217830
0.9276	0.999932	1.0000	0.0157	42.844116	0.002892	0.017065	0.048648	8077.471928
0.9262	0.999928	1.0000	0.0164	42.779071	0.003012	0.017774	0.050601	8262.866942
0.9248	0.999923	1.0000	0.0170	42.714034	0.003135	0.018498	0.052598	8449.411079
0.9233	0.999919	1.0000	0.0176	42.649003	0.003260	0.019238	0.054640	8637.112607
0.9219	0.999914	1.0000	0.0183	42.583979	0.003388	0.019995	0.056728	8825.979855
0.9205	0.999909	1.0000	0.0189	42.518962	0.003519	0.020767	0.058861	9016.021216
0.9191	0.999904	1.0000	0.0196	42.453953	0.003653	0.021556	0.061041	9207.245144
0.9177	0.999899	1.0000	0.0203	42.388951	0.003789	0.022362	0.063267	9399.660157
0.9163	0.999894	1.0000	0.0210	42.323957	0.003929	0.023184	0.065539	9593.274838
0.9149	0.999888	1.0000	0.0217	42.258970	0.004071	0.024022	0.067860	9788.097833
0.9135	0.999882	1.0000	0.0225	42.193991	0.004216	0.024878	0.070228	9984.137854
0.9121	0.999876	1.0000	0.0232	42.129020	0.004363	0.025750	0.072644	10181.403677
0.9106	0.999870	1.0000	0.0240	42.064057	0.004514	0.026639	0.075108	10379.904147
0.9092	0.999863	1.0000	0.0247	41.999102	0.004668	0.027545	0.077622	10579.648172
0.9078	0.999857	1.0000	0.0255	41.934156	0.004824	0.028468	0.080185	10780.644731
0.9064	0.999850	1.0000	0.0263	41.869218	0.004983	0.029409	0.082798	10982.902867
0.9050	0.999843	1.0000	0.0271	41.804289	0.005146	0.030366	0.085462	11186.431693
0.9036	0.999835	1.0000	0.0279	41.739369	0.005311	0.031341	0.088176	11391.240392
0.9022	0.999828	1.0000	0.0287	41.674457	0.005479	0.032334	0.090941	11597.338214
0.9008	0.999820	1.0000	0.0295	41.609554	0.005650	0.033345	0.093759	11804.734482
0.8993	0.999812	1.0000	0.0304	41.544661	0.005825	0.034373	0.096628	12013.438587
0.8979	0.999803	1.0000	0.0313	41.479776	0.006002	0.035419	0.099550	12223.459991
0.8965	0.999795	1.0000	0.0321	41.414901	0.006182	0.036483	0.102525	12434.808231
0.8951	0.999786	1.0000	0.0330	41.350036	0.006366	0.037565	0.105553	12647.492913
0.8937	0.999777	1.0000	0.0339	41.285180	0.006552	0.038666	0.108636	12861.523717
0.8923	0.999767	1.0000	0.0348	41.220334	0.006742	0.039784	0.111773	13076.910398
0.8909	0.999758	1.0000	0.0357	41.155498	0.006934	0.040921	0.114965	13293.662783
0.8895	0.999748	1.0000	0.0367	41.090672	0.007130	0.042077	0.118212	13511.790775
0.8880	0.999737	1.0000	0.0376	41.025856	0.007329	0.043251	0.121515	13731.304353
0.8866	0.999727	1.0000	0.0386	40.961050	0.007531	0.044445	0.124875	13952.213571
0.0000						0.044445		
0.0000						1.000000		

Spreadsheet for Calculation of Stream-Water Saturation Profiles

Injection Temperature 750 °K Initial Temperature 350 °K Matrix Heat Capacity 1.0000 (kJ/kg)

TRAILING SHOCK CALCULATIONS

Saturation	OF	Wave V	Flow V	Shock V	f _v	dK _{rv} /dS _v	dK _r /dS _i
0.7500	2.07E-01	0.216148	0.471414	0.009328	0.996549	1.0000	0.1875
0.875	4.77E-02	0.053796	0.577141	0.006100	0.999629	1.0000	0.0469
0.9375	6.80E-03	0.012521	0.589604	0.005720	0.999957	1.0000	0.0117
0.96875	-2.71E-03	0.002997	0.589984	0.005708	0.999995	1.0000	0.0029
0.953125	1.19E-03	0.006894	0.590101	0.005705	0.999982	1.0000	0.0066
0.9609375	-9.69E-04	0.004736	0.590106	0.005705	0.999990	1.0000	0.0046
0.95703125	5.74E-05	0.005761	0.590121	0.005704	0.999986	1.0000	0.0055
0.958984375	-4.69E-04	0.005235	0.590118	0.005704	0.999988	1.0000	0.0050
0.9580078125	-2.09E-04	0.005495	0.590121	0.005704	0.999987	1.0000	0.0053
0.9575195313	-7.67E-05	0.005627	0.590121	0.005704	0.999987	1.0000	0.0054
0.9572753906	-9.85E-06	0.005694	0.590121	0.005704	0.999986	1.0000	0.0055
0.9571533203	2.37E-05	0.005728	0.590121	0.005704	0.999986	1.0000	0.0055
0.9572143555	6.92E-06	0.005711	0.590121	0.005704	0.999986	1.0000	0.0055
0.957244873	-1.47E-06	0.005703	0.590121	0.005704	0.999986	1.0000	0.0055
0.9572296143	2.73E-06	0.005707	0.590121	0.005704	0.999986	1.0000	0.0055
0.9572372437	6.30E-07	0.005705	0.590121	0.005704	0.999986	1.0000	0.0055
0.9572410583	-4.18E-07	0.005704	0.590121	0.005704	0.999986	1.0000	0.0055
0.957239151	1.06E-07	0.005704	0.590121	0.005704	0.999986	1.0000	0.0055
0.9572401047	-1.56E-07	0.005704	0.590121	0.005704	0.999986	1.0000	0.0055
0.9572396278	-2.47E-08	0.005704	0.590121	0.005704	0.999986	1.0000	0.0055
0.9572393894	4.08E-08	0.005704	0.590121	0.005704	0.999986	1.0000	0.0055
0.9572395086	8.07E-09	0.005704	0.590121	0.005704	0.999986	1.0000	0.0055
0.9572395682	-8.31E-09	0.005704	0.590121	0.005704	0.999986	1.0000	0.0055
0.9572395384	-1.18E-10	0.005704	0.590121	0.005704	0.999986	1.0000	0.0055
0.9572395235	3.98E-09	0.005704	0.590121	0.005704	0.999986	1.0000	0.0055
0.957239531	1.93E-09	0.005704	0.590121	0.005704	0.999986	1.0000	0.0055

Saturation	Total Mob	dF _v /dS _v	G	F	Gamma	Theta	High	Low
0.75	34.759228	0.045851	220.095758	12.870589	1.1794E+07	30550.407113	1	0.5
0.875	40.427490	0.009321	115.033000	10.281953	1.1701E+07	28275.535543	1	0.75
0.9375	43.300978	0.002124	62.501620	10.006619	1.1655E+07	28033.574650	1	0.875
0.96875	44.742642	0.000508	36.235931	9.974642	1.1632E+07	28005.473055	1	0.9375
0.953125	44.021547	0.001168	49.368776	9.985337	1.1643E+07	28014.871837	0.96875	0.9375
0.9609375	44.382039	0.000802	42.802353	9.978906	1.1638E+07	28009.220503	0.96875	0.953125
0.95703125	44.201778	0.000976	46.085564	9.981821	1.1641E+07	28011.782338	0.9609375	0.953125
0.958984375	44.291905	0.000887	44.443959	9.980292	1.1639E+07	28010.438726	0.9609375	0.95703125
0.9580078125	44.246841	0.000931	45.264762	9.981039	1.1640E+07	28011.094453	0.958984375	0.95703125
0.9575195313	44.224309	0.000954	45.675163	9.981425	1.1640E+07	28011.434324	0.9580078125	0.95703125
0.9572753906	44.213043	0.000965	45.880364	9.981622	1.1640E+07	28011.607307	0.95751953125	0.95703125
0.9571533203	44.207411	0.000971	45.982964	9.981721	1.1640E+07	28011.694566	0.95727539063	0.95703125
0.9572143555	44.210227	0.000968	45.931664	9.981672	1.1640E+07	28011.650872	0.95727539063	0.95715332031
0.957244873	44.211635	0.000966	45.906014	9.981647	1.1640E+07	28011.629074	0.95727539063	0.95721435547
0.9572296143	44.210931	0.000967	45.918839	9.981659	1.1640E+07	28011.639969	0.95724487305	0.95721435547
0.9572372437	44.211283	0.000967	45.912426	9.981653	1.1640E+07	28011.634520	0.95724487305	0.95722961426
0.9572410583	44.211459	0.000967	45.909220	9.981650	1.1640E+07	28011.631797	0.95724487305	0.95723724365
0.957239151	44.211371	0.000967	45.910823	9.981652	1.1640E+07	28011.633158	0.95724105835	0.95723724365
0.9572401047	44.211415	0.000967	45.910022	9.981651	1.1640E+07	28011.632478	0.95724105835	0.957239151
0.9572396278	44.211393	0.000967	45.910422	9.981651	1.1640E+07	28011.632818	0.95724010468	0.957239151
0.9572393894	44.211382	0.000967	45.910623	9.981651	1.1640E+07	28011.632988	0.95723962784	0.957239151
0.9572395086	44.211388	0.000967	45.910522	9.981651	1.1640E+07	28011.632903	0.95723962784	0.95723938942
0.9572395682	44.211390	0.000967	45.910472	9.981651	1.1640E+07	28011.632861	0.95723962784	0.95723950863
0.9572395384	44.211389	0.000967	45.910497	9.981651	1.1640E+07	28011.632882	0.95723956823	0.95723950863
0.9572395235	44.211388	0.000967	45.910510	9.981651	1.1640E+07	28011.632893	0.95723953843	0.95723950863
0.957239531	44.211389	0.000967	45.910504	9.981651	1.1640E+07	28011.632887	0.95723953843	0.95723952353

Spreadsheet for Calculation of Stream-Water Saturation Profiles

Injection Temperature 750 °K Initial Temperature 350 °K Matrix Heat Capacity 1.0000 (kJ/kg)

LEADING SHOCK CALCULATIONS

Saturation	OF	Wave V	Flow V	Shock V	f _v	dK _{rv} /dS _v	dK _r /dS ₁
0.7500	2.24E-01	0.270577	0.011366	0.046209	0.996549	1.0000	0.1875
0.875	1.06E-02	0.055006	0.010142	0.044453	0.999629	1.0000	0.0469
0.9375	-3.20E-02	0.012532	0.010226	0.044574	0.999957	1.0000	0.0117
0.90625	-1.50E-02	0.029512	0.010151	0.044466	0.999849	1.0000	0.0264
0.890625	-3.32E-03	0.041122	0.010137	0.044446	0.999756	1.0000	0.0359
0.8828125	3.32E-03	0.047770	0.010137	0.044445	0.999697	1.0000	0.0412
0.88671875	-7.13E-05	0.044373	0.010136	0.044445	0.999728	1.0000	0.0385
0.884765625	1.61E-03	0.046053	0.010136	0.044445	0.999713	1.0000	0.0398
0.8857421875	7.64E-04	0.045209	0.010136	0.044445	0.999720	1.0000	0.0392
0.8862304688	3.45E-04	0.044790	0.010136	0.044445	0.999724	1.0000	0.0388
0.8864746094	1.37E-04	0.044581	0.010136	0.044445	0.999726	1.0000	0.0387
0.8865966797	3.26E-05	0.044477	0.010136	0.044445	0.999727	1.0000	0.0386
0.8866577148	-1.94E-05	0.044425	0.010136	0.044445	0.999727	1.0000	0.0385
0.8866271973	6.61E-06	0.044451	0.010136	0.044445	0.999727	1.0000	0.0386
0.8866424561	-6.39E-06	0.044438	0.010136	0.044445	0.999727	1.0000	0.0385
0.8866348267	1.12E-07	0.044445	0.010136	0.044445	0.999727	1.0000	0.0386
0.8866386414	-3.14E-06	0.044441	0.010136	0.044445	0.999727	1.0000	0.0386
0.886636734	-1.51E-06	0.044443	0.010136	0.044445	0.999727	1.0000	0.0386
0.8866357803	-7.00E-07	0.044444	0.010136	0.044445	0.999727	1.0000	0.0386
0.8866353035	-2.94E-07	0.044444	0.010136	0.044445	0.999727	1.0000	0.0386
0.8866350651	-9.11E-08	0.044444	0.010136	0.044445	0.999727	1.0000	0.0386
0.8866349459	1.04E-08	0.044445	0.010136	0.044445	0.999727	1.0000	0.0386
0.8866350055	-4.04E-08	0.044445	0.010136	0.044445	0.999727	1.0000	0.0386
0.8866349757	-1.50E-08	0.044445	0.010136	0.044445	0.999727	1.0000	0.0386
0.8866349608	-2.30E-09	0.044445	0.010136	0.044445	0.999727	1.0000	0.0386
0.8866349533	4.05E-09	0.044445	0.010136	0.044445	0.999727	1.0000	0.0386

Saturation	Total Mob	dF _v /dS _v	G	F	Gamma	Theta	High	Low
0.75	34.759228	0.045851	220.095758	12.870589	1.1794E+07	30550.407113	1	0.5
0.875	40.427490	0.009321	115.033000	10.281953	1.1701E+07	28275.535543	1	0.75
0.9375	43.300978	0.002124	62.501620	10.006619	1.1655E+07	28033.574650	1	0.875
0.90625	41.862126	0.005001	88.767310	10.097238	1.1678E+07	28113.209409	0.9375	0.875
0.890625	41.144193	0.006968	101.900155	10.175426	1.1690E+07	28181.920650	0.90625	0.875
0.8828125	40.785677	0.008095	108.466577	10.224828	1.1695E+07	28225.334700	0.890625	0.875
0.88671875	40.964895	0.007519	105.183366	10.199203	1.1693E+07	28202.815133	0.890625	0.8828125
0.884765625	40.875276	0.007804	106.824972	10.211779	1.1694E+07	28213.867353	0.88671875	0.8828125
0.8857421875	40.920083	0.007661	106.004169	10.205432	1.1693E+07	28208.289909	0.88671875	0.884765625
0.8862304688	40.942489	0.007590	105.593767	10.202303	1.1693E+07	28205.539756	0.88671875	0.8857421875
0.8864746094	40.953692	0.007555	105.388567	10.200749	1.1693E+07	28204.174262	0.88671875	0.88623046875
0.8865966797	40.959294	0.007537	105.285966	10.199975	1.1693E+07	28203.493903	0.88671875	0.88647460938
0.8866577148	40.962095	0.007528	105.234666	10.199589	1.1693E+07	28203.154319	0.88671875	0.88659667969
0.8866271973	40.960694	0.007533	105.260316	10.199782	1.1693E+07	28203.324062	0.8865771484	0.88659667969
0.8866424561	40.961394	0.007530	105.247491	10.199685	1.1693E+07	28203.239178	0.8865771484	0.88662719727
0.8866348267	40.961044	0.007531	105.253904	10.199733	1.1693E+07	28203.281617	0.88664245605	0.88662719727
0.8866386414	40.961219	0.007531	105.252301	10.199709	1.1693E+07	28203.260397	0.88664245605	0.88663482666
0.886636734	40.961132	0.007531	105.252301	10.199721	1.1693E+07	28203.271006	0.88663864136	0.88663482666
0.8866357803	40.961088	0.007531	105.253102	10.199727	1.1693E+07	28203.276312	0.88663673401	0.88663482666
0.8866353035	40.961066	0.007531	105.253503	10.199730	1.1693E+07	28203.278964	0.88663578033	0.88663482666
0.8866350651	40.961055	0.007531	105.253703	10.199732	1.1693E+07	28203.280290	0.8866353035	0.88663482666
0.8866349459	40.961050	0.007531	105.253804	10.199733	1.1693E+07	28203.280954	0.88663506508	0.88663482666
0.8866350055	40.961052	0.007531	105.253753	10.199732	1.1693E+07	28203.280622	0.88663506508	0.88663494587
0.8866349757	40.961051	0.007531	105.253779	10.199732	1.1693E+07	28203.280788	0.88663500547	0.88663494587
0.8866349608	40.961050	0.007531	105.253791	10.199733	1.1693E+07	28203.280871	0.88663497567	0.88663494587
0.8866349533	40.961050	0.007531	105.253797	10.199733	1.1693E+07	28203.280912	0.88663496077	0.88663494587

Spreadsheet for Calculation of Stream-Water Saturation Profiles

Injection Temperature
800 °K

Initial Temperature
350 °K

Matrix Heat Capacity
1.0000 (kJ/kg)

MATRIX PROPERTIES

Porosity	Cp Matrix	Density	Rho * Cp
0.10	1.00	2650.00	2650.0000
Nw	Ng	Swi	Denom
3.00	1.00	0.00	1.000000

SATURATION CONDITIONS

Tsaturation = 485.57

	Volumes (m3/kg)	Enthalpies (kJ/kg)	Densities (kg/m3)	Viscosities (cp)	Saturation Step
Liquid	0.001176	901.41	850.4723	0.1303	0.0014144045
Vapor	0.100298	2808.52	9.970241	0.0217	

BOUNDARY CONDITIONS

	Temperature	Velocity	Heat Capacity	Wave Velocity	Density	Enthalpy
Injection	800	1.000000	2.23	0.005129	5.477862	3538.38
Initial	350	0.009463	4.15	0.013717	975.3174	319.98
	G	F	Gamma	Theta		
Injection	800	5.48	5.48	19099382.75	19382.75	
Initial	350	975.32	975.32	8659580.72	312080.72	

SHOCK CONDITIONS

	Initial Guess		Vapor Saturation	Objective Function	Two-Phase Wave Velocity	Upstream Flow Velocity	Shock Velocity	Vapor Frac Flow
Trailing	Sv-Hi	Sv-Low	0.9574	7.6573E-10	0.0053	0.550938	0.0053	1.0000
Leading	1	0.5	0.8866	3.7785E-09	0.0415	0.009463	0.0415	0.9997
	dKrv/dSv	dKrl/dSl	Total Mobility	dFv/dSv	G	F'	Gamma	Theta'
Trailing	1.0000	0.0055	44.2167	0.0010	45.8133	9.9816	1.1640E+07	28011.5505
Leading	1.0000	0.0386	40.9610	0.0075	105.2538	10.1997	1.1693E+07	28203.2809

MATERIAL BALANCES

	Inside	Initial	Injected	Produced	Balance	Error
Mass	93.779969	97.531740	5.477862	9.229625	0.0000	0.0000%
Enthalpy	882391.7623	865958.0720	19382.7528	2953.2827	-4.2202	0.0005%

Spreadsheet for Calculation of Stream-Water Saturation Profiles

Injection Temperature 800 °K		Initial Temperature 350 °K				Matrix Heat Capacity 1.0000 (kJ/kg)		
SATURATION PROFILE								
Vapor Saturation	Vapor Frac Flow	dKrv/dSv	dKrV/dSI	Total Mobility	dFv/dSv	lambda	Mass Inside	Enthalpy Inside
1.0000						0.000000		
1.0000						0.005296		
0.9574	0.999987	1.0000	0.0055	44.216725	0.000961	0.005296	0.029009	101145.435953
0.9559	0.999985	1.0000	0.0058	44.151461	0.001028	0.005664	0.017094	4287.972705
0.9545	0.999984	1.0000	0.0062	44.086201	0.001097	0.006046	0.018158	4441.565010
0.9531	0.999982	1.0000	0.0066	44.020945	0.001169	0.006440	0.019257	4596.091240
0.9517	0.999980	1.0000	0.0070	43.955694	0.001243	0.006848	0.020392	4751.558093
0.9503	0.999979	1.0000	0.0074	43.890447	0.001320	0.007270	0.021562	4907.972315
0.9489	0.999977	1.0000	0.0078	43.825204	0.001398	0.007705	0.022768	5065.340704
0.9475	0.999975	1.0000	0.0083	43.759967	0.001480	0.008153	0.024011	5223.670106
0.9460	0.999972	1.0000	0.0087	43.694734	0.001564	0.008615	0.025290	5382.967419
0.9446	0.999970	1.0000	0.0092	43.629506	0.001650	0.009091	0.026607	5543.239592
0.9432	0.999968	1.0000	0.0097	43.564283	0.001739	0.009581	0.027960	5704.493625
0.9418	0.999965	1.0000	0.0102	43.499065	0.001830	0.010084	0.029351	5866.736570
0.9404	0.999963	1.0000	0.0107	43.433853	0.001924	0.010602	0.030781	6029.975532
0.9390	0.999960	1.0000	0.0112	43.368646	0.002021	0.011133	0.032248	6194.217667
0.9376	0.999957	1.0000	0.0117	43.303445	0.002120	0.011679	0.033754	6359.470186
0.9361	0.999954	1.0000	0.0122	43.238250	0.002221	0.012239	0.035299	6525.740353
0.9347	0.999951	1.0000	0.0128	43.173060	0.002326	0.012813	0.036883	6693.035486
0.9333	0.999947	1.0000	0.0133	43.107877	0.002432	0.013401	0.038507	6861.362957
0.9319	0.999944	1.0000	0.0139	43.042700	0.002542	0.014004	0.040170	7030.730194
0.9305	0.999940	1.0000	0.0145	42.977529	0.002654	0.014622	0.041875	7201.144680
0.9291	0.999936	1.0000	0.0151	42.912364	0.002769	0.015254	0.043619	7372.613953
0.9277	0.999932	1.0000	0.0157	42.847206	0.002886	0.015901	0.045405	7545.145608
0.9262	0.999928	1.0000	0.0163	42.782054	0.003006	0.016563	0.047232	7718.747298
0.9248	0.999924	1.0000	0.0170	42.716910	0.003129	0.017239	0.049101	7893.426731
0.9234	0.999919	1.0000	0.0176	42.651772	0.003255	0.017931	0.051012	8069.191675
0.9220	0.999914	1.0000	0.0183	42.586641	0.003383	0.018638	0.052966	8246.049553
0.9206	0.999910	1.0000	0.0189	42.521518	0.003514	0.019360	0.054962	8424.009450
0.9192	0.999905	1.0000	0.0196	42.456402	0.003648	0.020097	0.057002	8603.078109
0.9178	0.999899	1.0000	0.0203	42.391293	0.003784	0.020850	0.059085	8783.263932
0.9163	0.999894	1.0000	0.0210	42.326192	0.003924	0.021618	0.061212	8964.574981
0.9149	0.999888	1.0000	0.0217	42.261099	0.004066	0.022402	0.063384	9147.019381
0.9135	0.999882	1.0000	0.0224	42.196013	0.004211	0.023201	0.065601	9330.605315
0.9121	0.999876	1.0000	0.0232	42.130935	0.004359	0.024016	0.067862	9515.341030
0.9107	0.999870	1.0000	0.0239	42.065866	0.004510	0.024847	0.070169	9701.234834
0.9093	0.999863	1.0000	0.0247	42.000805	0.004664	0.025694	0.072523	9888.295099
0.9079	0.999857	1.0000	0.0255	41.935752	0.004820	0.026557	0.074922	10076.530257
0.9064	0.999850	1.0000	0.0263	41.870707	0.004980	0.027436	0.077369	10265.948807
0.9050	0.999843	1.0000	0.0271	41.805672	0.005142	0.028331	0.079862	10456.559312
0.9036	0.999835	1.0000	0.0279	41.740645	0.005308	0.029242	0.082404	10648.370398
0.9022	0.999828	1.0000	0.0287	41.675626	0.005476	0.030170	0.084993	10841.390758
0.9008	0.999820	1.0000	0.0295	41.610617	0.005648	0.031115	0.087631	11035.629150
0.8994	0.999812	1.0000	0.0304	41.545617	0.005822	0.032076	0.090318	11231.094399
0.8980	0.999803	1.0000	0.0312	41.480626	0.006000	0.033054	0.093054	11427.795396
0.8965	0.999795	1.0000	0.0321	41.415645	0.006180	0.034049	0.095840	11625.741101
0.8951	0.999786	1.0000	0.0330	41.350673	0.006364	0.035061	0.098676	11824.940541
0.8937	0.999777	1.0000	0.0339	41.285711	0.006551	0.036090	0.101562	12025.402813
0.8923	0.999767	1.0000	0.0348	41.220759	0.006740	0.037136	0.104500	12227.137080
0.8909	0.999758	1.0000	0.0357	41.155816	0.006933	0.038199	0.107490	12430.152580
0.8895	0.999748	1.0000	0.0367	41.090884	0.007130	0.039280	0.110531	12634.458616
0.8880	0.999737	1.0000	0.0376	41.025962	0.007329	0.040378	0.113625	12840.064567
0.8866	0.999727	1.0000	0.0386	40.961050	0.007531	0.041494	0.116772	13046.979879
0.0000						0.041494		
0.0000						1.000000		

Spreadsheet for Calculation of Stream-Water Saturation Profiles

Injection Temperature 800 °K		Initial Temperature 350 °K		Matrix Heat Capacity 1.0000 (kJ/kg)				
TRAILING SHOCK CALCULATIONS								
Saturation	OF	Wave V	Flow V	Shock V	fv	dKrv/dSv	dKr/dSI	
0.7500	1.93E-01	0.201389	0.439224	0.008164	0.996549	1.0000	0.1875	
0.875	4.46E-02	0.050217	0.538741	0.005609	0.999629	1.0000	0.0469	
0.9375	6.38E-03	0.011689	0.550449	0.005308	0.999957	1.0000	0.0117	
0.96875	-2.50E-03	0.002798	0.550813	0.005299	0.999995	1.0000	0.0029	
0.953125	1.14E-03	0.006436	0.550919	0.005296	0.999982	1.0000	0.0066	
0.9609375	-8.75E-04	0.004421	0.550925	0.005296	0.999990	1.0000	0.0046	
0.95703125	8.32E-05	0.005379	0.550938	0.005296	0.999986	1.0000	0.0055	
0.958984375	-4.08E-04	0.004888	0.550936	0.005296	0.999988	1.0000	0.0050	
0.9580078125	-1.66E-04	0.005130	0.550938	0.005296	0.999987	1.0000	0.0053	
0.9575195313	-4.20E-05	0.005254	0.550938	0.005296	0.999987	1.0000	0.0054	
0.9572753906	2.04E-05	0.005316	0.550938	0.005296	0.999986	1.0000	0.0055	
0.9573974609	-1.08E-05	0.005285	0.550938	0.005296	0.999987	1.0000	0.0054	
0.9573364258	4.80E-06	0.005301	0.550938	0.005296	0.999987	1.0000	0.0055	
0.9573669434	-3.01E-06	0.005293	0.550938	0.005296	0.999987	1.0000	0.0055	
0.9573516846	8.95E-07	0.005297	0.550938	0.005296	0.999987	1.0000	0.0055	
0.957359314	-1.06E-06	0.005295	0.550938	0.005296	0.999987	1.0000	0.0055	
0.9573554993	-8.12E-08	0.005296	0.550938	0.005296	0.999987	1.0000	0.0055	
0.9573535919	4.07E-07	0.005296	0.550938	0.005296	0.999987	1.0000	0.0055	
0.9573545456	1.63E-07	0.005296	0.550938	0.005296	0.999987	1.0000	0.0055	
0.9573550224	4.08E-08	0.005296	0.550938	0.005296	0.999987	1.0000	0.0055	
0.9573552608	-2.02E-08	0.005296	0.550938	0.005296	0.999987	1.0000	0.0055	
0.9573551416	1.03E-08	0.005296	0.550938	0.005296	0.999987	1.0000	0.0055	
0.9573552012	-4.95E-09	0.005296	0.550938	0.005296	0.999987	1.0000	0.0055	
0.9573551714	2.67E-09	0.005296	0.550938	0.005296	0.999987	1.0000	0.0055	
0.9573551863	-1.14E-09	0.005296	0.550938	0.005296	0.999987	1.0000	0.0055	
0.9573551789	7.66E-10	0.005296	0.550938	0.005296	0.999987	1.0000	0.0055	
Saturation	Total Mob	dPv/dSv	G	F	Gamma	Theta	High	Low
0.75	34.759228	0.045851	220.095758	12.870589	1.1794E+07	30550.407113	1	0.5
0.875	40.427490	0.009321	115.033000	10.281953	1.1701E+07	28275.535543	1	0.75
0.9375	43.300978	0.002124	62.501620	10.006619	1.1655E+07	28033.574650	1	0.875
0.96875	44.742642	0.000508	36.235931	9.974642	1.1632E+07	28005.473055	1	0.9375
0.953125	44.021547	0.001168	49.368776	9.985337	1.1643E+07	28014.871837	0.96875	0.9375
0.9609375	44.382039	0.000802	42.802353	9.978906	1.1638E+07	28009.220503	0.96875	0.953125
0.95703125	44.201778	0.000976	46.085564	9.981821	1.1641E+07	28011.782338	0.9609375	0.953125
0.958984375	44.291905	0.000887	44.443959	9.980292	1.1639E+07	28010.438726	0.9609375	0.95703125
0.9580078125	44.246841	0.000931	45.264762	9.981039	1.1640E+07	28011.094453	0.958984375	0.95703125
0.9575195313	44.224309	0.000954	45.675163	9.981425	1.1640E+07	28011.434324	0.9580078125	0.95703125
0.9572753906	44.213043	0.000965	45.880364	9.981622	1.1640E+07	28011.607307	0.95751953125	0.95703125
0.9573974609	44.218676	0.000959	45.777763	9.981523	1.1640E+07	28011.520561	0.95751953125	0.95727539063
0.9573364258	44.215860	0.000962	45.829063	9.981573	1.1640E+07	28011.563870	0.95739746094	0.95727539063
0.9573669434	44.217268	0.000961	45.803413	9.981548	1.1640E+07	28011.542199	0.95739746094	0.95733642578
0.9573516846	44.216564	0.000961	45.816238	9.981560	1.1640E+07	28011.553031	0.95736694336	0.95733642578
0.957359314	44.216916	0.000961	45.809826	9.981554	1.1640E+07	28011.547614	0.95736694336	0.95735168457
0.9573554993	44.216740	0.000961	45.813032	9.981557	1.1640E+07	28011.550322	0.95735931396	0.95735168457
0.9573535919	44.216652	0.000961	45.814635	9.981559	1.1640E+07	28011.551676	0.95735549927	0.95735168457
0.9573545456	44.216696	0.000961	45.813834	9.981558	1.1640E+07	28011.550999	0.95735549927	0.95735359192
0.9573550224	44.216718	0.000961	45.813433	9.981558	1.1640E+07	28011.550661	0.95735549927	0.95735454559
0.9573552608	44.216729	0.000961	45.813233	9.981557	1.1640E+07	28011.550491	0.95735549927	0.95735502243
0.9573551416	44.216723	0.000961	45.813333	9.981558	1.1640E+07	28011.550576	0.95735526085	0.95735502243
0.9573552012	44.216726	0.000961	45.813283	9.981558	1.1640E+07	28011.550534	0.95735526085	0.95735514164
0.9573551714	44.216725	0.000961	45.813308	9.981558	1.1640E+07	28011.550555	0.95735520124	0.95735514164
0.9573551863	44.216726	0.000961	45.813295	9.981558	1.1640E+07	28011.550544	0.95735520124	0.95735517144
0.9573551789	44.216725	0.000961	45.813301	9.981558	1.1640E+07	28011.550549	0.95735518634	0.95735517144

Spreadsheet for Calculation of Stream-Water Saturation Profiles

Injection Temperature 800 °K Initial Temperature 350 °K Matrix Heat Capacity 1.0000 (kJ/kg)

LEADING SHOCK CALCULATIONS

Saturation	OF	Wave V	Flow V	Shock V	fv	dKrv/dSv	dKr/dSI
0.7500	2.09E-01	0.252611	0.010611	0.043141	0.996549	1.0000	0.1875
0.875	9.85E-03	0.051354	0.009469	0.041501	0.999629	1.0000	0.0469
0.9375	-2.99E-02	0.011700	0.009547	0.041614	0.999957	1.0000	0.0117
0.90625	-1.40E-02	0.027553	0.009477	0.041514	0.999849	1.0000	0.0264
0.890625	-3.10E-03	0.038391	0.009464	0.041494	0.999756	1.0000	0.0359
0.8828125	3.10E-03	0.044598	0.009464	0.041494	0.999697	1.0000	0.0412
0.88671875	-6.66E-05	0.041427	0.009463	0.041494	0.999728	1.0000	0.0385
0.884765625	1.50E-03	0.042995	0.009463	0.041494	0.999713	1.0000	0.0398
0.8857421875	7.13E-04	0.042207	0.009463	0.041494	0.999720	1.0000	0.0392
0.8862304688	3.22E-04	0.041816	0.009463	0.041494	0.999724	1.0000	0.0388
0.8864746094	1.28E-04	0.041621	0.009463	0.041494	0.999726	1.0000	0.0387
0.8865966797	3.04E-05	0.041524	0.009463	0.041494	0.999727	1.0000	0.0386
0.8866577148	-1.81E-05	0.041475	0.009463	0.041494	0.999727	1.0000	0.0385
0.8866271973	6.17E-06	0.041500	0.009463	0.041494	0.999727	1.0000	0.0386
0.8866424561	-5.96E-06	0.041488	0.009463	0.041494	0.999727	1.0000	0.0385
0.8866348267	1.04E-07	0.041494	0.009463	0.041494	0.999727	1.0000	0.0386
0.8866386414	-2.93E-06	0.041491	0.009463	0.041494	0.999727	1.0000	0.0386
0.886636734	-1.41E-06	0.041492	0.009463	0.041494	0.999727	1.0000	0.0386
0.8866357803	-6.54E-07	0.041493	0.009463	0.041494	0.999727	1.0000	0.0386
0.8866353035	-2.75E-07	0.041493	0.009463	0.041494	0.999727	1.0000	0.0386
0.8866350651	-8.51E-08	0.041493	0.009463	0.041494	0.999727	1.0000	0.0386
0.8866349459	9.70E-09	0.041494	0.009463	0.041494	0.999727	1.0000	0.0386
0.8866350055	-3.77E-08	0.041493	0.009463	0.041494	0.999727	1.0000	0.0386
0.8866349757	-1.40E-08	0.041494	0.009463	0.041494	0.999727	1.0000	0.0386
0.8866349608	-2.15E-09	0.041494	0.009463	0.041494	0.999727	1.0000	0.0386
0.8866349533	3.78E-09	0.041494	0.009463	0.041494	0.999727	1.0000	0.0386

Saturation	Total Mob	dFv/dSv	G	F	Gamma	Theta	High	Low
0.75	34.759228	0.045851	220.095758	12.870589	1.1794E+07	30550.407113	1	0.5
0.875	40.427490	0.009321	115.033000	10.281953	1.1701E+07	28275.535543	1	0.75
0.9375	43.300978	0.002124	62.501620	10.006619	1.1655E+07	28033.574650	1	0.875
0.90625	41.862126	0.005001	88.767310	10.097238	1.1678E+07	28113.209409	0.9375	0.875
0.890625	41.144193	0.006968	101.900155	10.175426	1.1690E+07	28181.920650	0.90625	0.875
0.8828125	40.785677	0.008095	108.466577	10.224828	1.1695E+07	28225.334700	0.890625	0.875
0.88671875	40.964895	0.007519	105.183366	10.199203	1.1693E+07	28202.815133	0.890625	0.8828125
0.884765625	40.875276	0.007804	106.824972	10.211779	1.1694E+07	28213.867353	0.88671875	0.8828125
0.8857421875	40.920083	0.007661	106.004169	10.205432	1.1693E+07	28208.289909	0.88671875	0.884765625
0.8862304688	40.942489	0.007590	105.593767	10.202303	1.1693E+07	28205.539756	0.88671875	0.8857421875
0.8864746094	40.953692	0.007555	105.388567	10.200749	1.1693E+07	28204.174262	0.88671875	0.8862304688
0.8865966797	40.959294	0.007537	105.285966	10.199975	1.1693E+07	28203.493903	0.88671875	0.8864746094
0.8866577148	40.962095	0.007528	105.234666	10.199589	1.1693E+07	28203.154319	0.88671875	0.8865966797
0.8866271973	40.960694	0.007533	105.260316	10.199782	1.1693E+07	28203.324062	0.8866577148	0.8865966797
0.8866424561	40.961394	0.007530	105.247491	10.199685	1.1693E+07	28203.239178	0.8866577148	0.8866271973
0.8866348267	40.961044	0.007531	105.253904	10.199733	1.1693E+07	28203.281617	0.8866424561	0.8866271973
0.8866386414	40.961219	0.007531	105.250698	10.199709	1.1693E+07	28203.260397	0.8866424561	0.8866348267
0.886636734	40.961132	0.007531	105.252301	10.199721	1.1693E+07	28203.271006	0.8866386414	0.8866348267
0.8866357803	40.961088	0.007531	105.253102	10.199727	1.1693E+07	28203.276312	0.886636734	0.8866348267
0.8866353035	40.961066	0.007531	105.253503	10.199730	1.1693E+07	28203.278964	0.8866357803	0.8866348267
0.8866350651	40.961055	0.007531	105.253703	10.199732	1.1693E+07	28203.280290	0.8866353035	0.8866348267
0.8866349459	40.961050	0.007531	105.253804	10.199733	1.1693E+07	28203.280954	0.8866350651	0.8866348267
0.8866350055	40.961052	0.007531	105.253753	10.199732	1.1693E+07	28203.280622	0.8866350651	0.8866349459
0.8866349757	40.961051	0.007531	105.253779	10.199732	1.1693E+07	28203.280788	0.8866350055	0.8866349459
0.8866349608	40.961050	0.007531	105.253791	10.199733	1.1693E+07	28203.280871	0.8866349757	0.8866349459
0.8866349533	40.961050	0.007531	105.253797	10.199733	1.1693E+07	28203.280912	0.8866349608	0.8866349459

Spreadsheet for Calculation of Stream-Water Saturation Profiles

Injection Temperature
850 °K

Initial Temperature
350 °K

Matrix Heat Capacity
1.0000 (kJ/kg)

MATRIX PROPERTIES

Porosity	Cp Matrix	Density	Rho * Cp
0.10	1.00	2650.00	2650.0000
Nw	Ng	Swi	Denom
3.00	1.00	0.00	1.000000

SATURATION CONDITIONS

Tsaturation = 485.57

	Volumes (m3/kg)	Enthalpies (kJ/kg)	Densities (kg/m3)	Viscosities (cp)	Saturation Step
Liquid	0.001176	901.41	850.4723	0.1303	0.0014161715
Vapor	0.100298	2808.52	9.970241	0.0217	

BOUNDARY CONDITIONS

	Temperature	Velocity	Heat Capacity	Wave Velocity	Density	Enthalpy
Injection	850	1.000000	2.24	0.004820	5.142437	3650.10
Initial	350	0.008884	4.15	0.012878	975.3174	319.98
	G	F	Gamma	Theta		
Injection	850	5.14	5.14	20291270.40	18770.40	
Initial	350	975.32	975.32	8659580.72	312080.72	

SHOCK CONDITIONS

	Initial Guess		Vapor Saturation	Objective Function	Two-Phase Wave Velocity	Upstream Flow Velocity	Shock Velocity	Vapor Frac Flow
Trailing	Sv-Hi	Sv-Low	0.9574	1.4180E-09	0.0050	0.517211	0.0050	1.0000
Leading	1	0.5	0.8866	3.5472E-09	0.0390	0.008884	0.0390	0.9997
	dKr/dSv	dKr/dSI	Total Mobility	dPv/dSv	G	F'	Gamma	Theta'
Trailing	1.0000	0.0054	44.2208	0.0010	45.7390	9.9815	1.1640E+07	28011.4880
Leading	1.0000	0.0386	40.9610	0.0075	105.2538	10.1997	1.1693E+07	28203.2809

MATERIAL BALANCES

	Mass	Inside	Initial	Injected	Produced	Balance	Error
Mass	94.009565	97.531740	97.531740	5.142437	8.664605	0.0000	0.0000%
Enthalpy	881959.9444	865958.0720	865958.0720	18770.3970	2772.4883	-3.9637	0.0004%

Spreadsheet for Calculation of Stream-Water Saturation Profiles

Injection Temperature 850 °K		Initial Temperature 350 °K				Matrix Heat Capacity 1.0000 (kJ/kg)		
SATURATION PROFILE								
Vapor Saturation	Vapor Frac Flow	dKrv/dSv	dKr/dSI	Total Mobility	dFv/dSv	lambda	Mass Inside	Enthalpy Inside
1.0000						0.000000		
1.0000						0.004950		
0.9574	0.999987	1.0000	0.0054	44.220802	0.000957	0.004950	0.025457	100449.039107
0.9560	0.999985	1.0000	0.0058	44.155456	0.001024	0.005296	0.016006	4021.601074
0.9546	0.999984	1.0000	0.0062	44.090114	0.001093	0.005654	0.017006	4166.097638
0.9532	0.999982	1.0000	0.0066	44.024777	0.001165	0.006024	0.018039	4311.473863
0.9518	0.999980	1.0000	0.0070	43.959444	0.001239	0.006407	0.019104	4457.736065
0.9504	0.999979	1.0000	0.0074	43.894115	0.001315	0.006802	0.020204	4604.890608
0.9489	0.999977	1.0000	0.0078	43.828790	0.001394	0.007210	0.021337	4752.943901
0.9475	0.999975	1.0000	0.0083	43.763471	0.001475	0.007631	0.022505	4901.902401
0.9461	0.999973	1.0000	0.0087	43.698156	0.001559	0.008065	0.023707	5051.772614
0.9447	0.999970	1.0000	0.0092	43.632847	0.001646	0.008511	0.024944	5202.561093
0.9433	0.999968	1.0000	0.0097	43.567542	0.001734	0.008971	0.026216	5354.274440
0.9419	0.999965	1.0000	0.0101	43.502243	0.001826	0.009444	0.027524	5506.919307
0.9404	0.999963	1.0000	0.0106	43.436949	0.001920	0.009929	0.028867	5660.502392
0.9390	0.999960	1.0000	0.0112	43.371660	0.002016	0.010428	0.030246	5815.030448
0.9376	0.999957	1.0000	0.0117	43.306378	0.002115	0.010940	0.031662	5970.510273
0.9362	0.999954	1.0000	0.0122	43.241100	0.002217	0.011466	0.033114	6126.948720
0.9348	0.999951	1.0000	0.0128	43.175829	0.002321	0.012005	0.034603	6284.352689
0.9334	0.999947	1.0000	0.0133	43.110564	0.002428	0.012558	0.036130	6442.729136
0.9320	0.999944	1.0000	0.0139	43.045305	0.002537	0.013124	0.037694	6602.085065
0.9305	0.999940	1.0000	0.0145	42.980052	0.002650	0.013704	0.039296	6762.427534
0.9291	0.999936	1.0000	0.0151	42.914806	0.002764	0.014298	0.040937	6923.763653
0.9277	0.999932	1.0000	0.0157	42.849566	0.002882	0.014905	0.042616	7086.100587
0.9263	0.999928	1.0000	0.0163	42.784333	0.003002	0.015527	0.044334	7249.445553
0.9249	0.999924	1.0000	0.0169	42.719107	0.003125	0.016162	0.046092	7413.805821
0.9235	0.999919	1.0000	0.0176	42.653888	0.003251	0.016812	0.047889	7579.188718
0.9220	0.999915	1.0000	0.0182	42.588676	0.003379	0.017476	0.049726	7745.601625
0.9206	0.999910	1.0000	0.0189	42.523470	0.003510	0.018154	0.051604	7913.051979
0.9192	0.999905	1.0000	0.0196	42.458273	0.003644	0.018847	0.053522	8081.547270
0.9178	0.999899	1.0000	0.0203	42.393083	0.003781	0.019554	0.055482	8251.095048
0.9164	0.999894	1.0000	0.0210	42.327900	0.003920	0.020275	0.057483	8421.702919
0.9150	0.999888	1.0000	0.0217	42.262725	0.004062	0.021012	0.059525	8593.378544
0.9135	0.999882	1.0000	0.0224	42.197558	0.004208	0.021763	0.061610	8766.129644
0.9121	0.999876	1.0000	0.0232	42.132399	0.004356	0.022528	0.063738	8939.963998
0.9107	0.999870	1.0000	0.0239	42.067248	0.004507	0.023309	0.065908	9114.889444
0.9093	0.999864	1.0000	0.0247	42.002105	0.004661	0.024105	0.068122	9290.913876
0.9079	0.999857	1.0000	0.0255	41.936971	0.004817	0.024915	0.070380	9468.045253
0.9065	0.999850	1.0000	0.0262	41.871845	0.004977	0.025741	0.072681	9646.291590
0.9050	0.999843	1.0000	0.0270	41.806728	0.005140	0.026583	0.075027	9825.660965
0.9036	0.999835	1.0000	0.0279	41.741619	0.005305	0.027439	0.077418	10006.161515
0.9022	0.999828	1.0000	0.0287	41.676520	0.005474	0.028311	0.079854	10187.801442
0.9008	0.999820	1.0000	0.0295	41.611429	0.005645	0.029199	0.082336	10370.589006
0.8994	0.999812	1.0000	0.0304	41.546348	0.005820	0.030102	0.084864	10554.532534
0.8980	0.999803	1.0000	0.0312	41.481276	0.005998	0.031021	0.087439	10739.640414
0.8965	0.999795	1.0000	0.0321	41.416213	0.006179	0.031956	0.090060	10925.921098
0.8951	0.999786	1.0000	0.0330	41.351160	0.006362	0.032907	0.092729	11113.383102
0.8937	0.999777	1.0000	0.0339	41.286117	0.006549	0.033874	0.095445	11302.035008
0.8923	0.999767	1.0000	0.0348	41.221083	0.006739	0.034857	0.098210	11491.885463
0.8909	0.999758	1.0000	0.0357	41.156060	0.006933	0.035857	0.101023	11682.943179
0.8895	0.999748	1.0000	0.0367	41.091046	0.007129	0.036872	0.103885	11875.216936
0.8881	0.999737	1.0000	0.0376	41.026043	0.007329	0.037905	0.106797	12068.715580
0.8866	0.999727	1.0000	0.0386	40.961050	0.007531	0.038953	0.109759	12263.448026
0.0000						0.038953		
0.0000						1.000000		

Spreadsheet for Calculation of Stream-Water Saturation Profiles

Injection Temperature 850 °K		Initial Temperature 350 °K		Matrix Heat Capacity 1.0000 (kJ/kg)				
TRAILING SHOCK CALCULATIONS								
Saturation	OF	Wave V	Flow V	Shock V	fv	dKrv/dSv	dKr/dSI	
0.7500	1.81E-01	0.188777	0.411719	0.007287	0.996549	1.0000	0.1875	
0.875	4.19E-02	0.047137	0.505705	0.005205	0.999629	1.0000	0.0469	
0.9375	6.01E-03	0.010974	0.516747	0.004961	0.999957	1.0000	0.0117	
0.96875	-2.33E-03	0.002627	0.517095	0.004953	0.999995	1.0000	0.0029	
0.953125	1.09E-03	0.006042	0.517192	0.004951	0.999982	1.0000	0.0066	
0.9609375	-8.00E-04	0.004150	0.517199	0.004951	0.999990	1.0000	0.0046	
0.95703125	9.93E-05	0.005050	0.517211	0.004950	0.999986	1.0000	0.0055	
0.958984375	-3.62E-04	0.004588	0.517209	0.004950	0.999988	1.0000	0.0050	
0.9580078125	-1.34E-04	0.004816	0.517211	0.004950	0.999987	1.0000	0.0053	
0.9575195313	-1.82E-05	0.004932	0.517211	0.004950	0.999987	1.0000	0.0054	
0.9572753906	4.04E-05	0.004991	0.517211	0.004950	0.999986	1.0000	0.0055	
0.9573974609	1.10E-05	0.004961	0.517211	0.004950	0.999987	1.0000	0.0054	
0.9574584961	-3.58E-06	0.004947	0.517211	0.004950	0.999987	1.0000	0.0054	
0.9574279785	3.73E-06	0.004954	0.517211	0.004950	0.999987	1.0000	0.0054	
0.9574432373	7.10E-08	0.004950	0.517211	0.004950	0.999987	1.0000	0.0054	
0.9574508667	-1.76E-06	0.004949	0.517211	0.004950	0.999987	1.0000	0.0054	
0.957447052	-8.43E-07	0.004950	0.517211	0.004950	0.999987	1.0000	0.0054	
0.9574451447	-3.86E-07	0.004950	0.517211	0.004950	0.999987	1.0000	0.0054	
0.957444191	-1.57E-07	0.004950	0.517211	0.004950	0.999987	1.0000	0.0054	
0.9574437141	-4.32E-08	0.004950	0.517211	0.004950	0.999987	1.0000	0.0054	
0.9574434757	1.39E-08	0.004950	0.517211	0.004950	0.999987	1.0000	0.0054	
0.9574435949	-1.46E-08	0.004950	0.517211	0.004950	0.999987	1.0000	0.0054	
0.9574435353	-3.67E-10	0.004950	0.517211	0.004950	0.999987	1.0000	0.0054	
0.9574435055	6.77E-09	0.004950	0.517211	0.004950	0.999987	1.0000	0.0054	
0.9574435204	3.20E-09	0.004950	0.517211	0.004950	0.999987	1.0000	0.0054	
0.9574435279	1.42E-09	0.004950	0.517211	0.004950	0.999987	1.0000	0.0054	
Saturation	Total Mob	dFv/dSv	G	F	Gamma	Theta	High	Low
0.75	34.759228	0.045851	220.095758	12.870589	1.1794E+07	30550.407113	1	0.5
0.875	40.427490	0.009321	115.033000	10.281953	1.1701E+07	28275.535543	1	0.75
0.9375	43.300978	0.002124	62.501620	10.006619	1.1655E+07	28033.574650	1	0.875
0.96875	44.742642	0.000508	36.235931	9.974642	1.1632E+07	28005.473055	1	0.9375
0.953125	44.021547	0.001168	49.368776	9.985337	1.1643E+07	28014.871837	0.96875	0.9375
0.9609375	44.382039	0.000802	42.802353	9.978906	1.1638E+07	28009.220503	0.96875	0.953125
0.95703125	44.201778	0.000976	46.085564	9.981821	1.1641E+07	28011.782338	0.9609375	0.953125
0.958984375	44.291905	0.000887	44.443959	9.980292	1.1639E+07	28010.438726	0.9609375	0.95703125
0.9580078125	44.246841	0.000931	45.264762	9.981039	1.1640E+07	28011.094453	0.958984375	0.95703125
0.9575195313	44.224309	0.000954	45.675163	9.981425	1.1640E+07	28011.434324	0.9580078125	0.95703125
0.9572753906	44.213043	0.000965	45.880364	9.981622	1.1640E+07	28011.607307	0.95751953125	0.95703125
0.9573974609	44.218676	0.000959	45.777763	9.981523	1.1640E+07	28011.520561	0.95751953125	0.95727539063
0.9574584961	44.221493	0.000956	45.726463	9.981474	1.1640E+07	28011.477379	0.95751953125	0.95739746094
0.9574279785	44.220084	0.000958	45.752113	9.981499	1.1640E+07	28011.498954	0.95745849609	0.95739746094
0.9574432373	44.220789	0.000957	45.739288	9.981487	1.1640E+07	28011.488162	0.95745849609	0.95742797852
0.9574508667	44.221141	0.000957	45.732876	9.981480	1.1640E+07	28011.482770	0.95745849609	0.9574432373
0.957447052	44.220965	0.000957	45.736082	9.981483	1.1640E+07	28011.485466	0.9574508667	0.9574432373
0.9574451447	44.220877	0.000957	45.737685	9.981485	1.1640E+07	28011.486814	0.957447052	0.9574432373
0.957444191	44.220833	0.000957	45.738487	9.981486	1.1640E+07	28011.487488	0.95744514465	0.9574432373
0.9574437141	44.220811	0.000957	45.738887	9.981486	1.1640E+07	28011.487825	0.95744419098	0.9574432373
0.9574434757	44.220800	0.000957	45.739088	9.981486	1.1640E+07	28011.487994	0.95744371414	0.9574432373
0.9574435949	44.220805	0.000957	45.738988	9.981486	1.1640E+07	28011.487909	0.95744371414	0.95744347572
0.9574435353	44.220802	0.000957	45.739038	9.981486	1.1640E+07	28011.487952	0.95744359493	0.95744347572
0.9574435055	44.220801	0.000957	45.739063	9.981486	1.1640E+07	28011.487973	0.95744353533	0.95744347572
0.9574435204	44.220802	0.000957	45.739050	9.981486	1.1640E+07	28011.487962	0.95744353533	0.95744350553
0.9574435279	44.220802	0.000957	45.739044	9.981486	1.1640E+07	28011.487957	0.95744353533	0.95744352043

Spreadsheet for Calculation of Stream-Water Saturation Profiles

Injection Temperature 850 °K Initial Temperature 350 °K Matrix Heat Capacity 1.0000 (kJ/kg)

LEADING SHOCK CALCULATIONS

Saturation	OF	Wave V	Flow V	Shock V	fv	dKrv/dSv	dKr/dSi
0.7500	1.97E-01	0.237146	0.009961	0.040500	0.996549	1.0000	0.1875
0.875	9.25E-03	0.048210	0.008889	0.038961	0.999629	1.0000	0.0469
0.9375	-2.81E-02	0.010983	0.008963	0.039067	0.999957	1.0000	0.0117
0.90625	-1.31E-02	0.025866	0.008897	0.038972	0.999849	1.0000	0.0264
0.890625	-2.91E-03	0.036041	0.008884	0.038954	0.999756	1.0000	0.0359
0.8828125	2.91E-03	0.041868	0.008884	0.038954	0.999697	1.0000	0.0412
0.88671875	-6.25E-05	0.038891	0.008884	0.038953	0.999728	1.0000	0.0385
0.884765625	1.41E-03	0.040363	0.008884	0.038954	0.999713	1.0000	0.0398
0.8857421875	6.70E-04	0.039623	0.008884	0.038953	0.999720	1.0000	0.0392
0.8862304688	3.03E-04	0.039256	0.008884	0.038953	0.999724	1.0000	0.0388
0.8864746094	1.20E-04	0.039073	0.008884	0.038953	0.999726	1.0000	0.0387
0.8865966797	2.86E-05	0.038982	0.008884	0.038953	0.999727	1.0000	0.0386
0.8866577148	-1.70E-05	0.038936	0.008884	0.038953	0.999727	1.0000	0.0385
0.8866271973	5.79E-06	0.038959	0.008884	0.038953	0.999727	1.0000	0.0386
0.8866424561	-5.60E-06	0.038948	0.008884	0.038953	0.999727	1.0000	0.0385
0.8866348267	9.81E-08	0.038953	0.008884	0.038953	0.999727	1.0000	0.0386
0.8866386414	-2.75E-06	0.038951	0.008884	0.038953	0.999727	1.0000	0.0386
0.886636734	-1.33E-06	0.038952	0.008884	0.038953	0.999727	1.0000	0.0386
0.8866357803	-6.14E-07	0.038953	0.008884	0.038953	0.999727	1.0000	0.0386
0.8866353035	-2.58E-07	0.038953	0.008884	0.038953	0.999727	1.0000	0.0386
0.8866350651	-7.99E-08	0.038953	0.008884	0.038953	0.999727	1.0000	0.0386
0.8866349459	9.11E-09	0.038953	0.008884	0.038953	0.999727	1.0000	0.0386
0.8866350055	-3.54E-08	0.038953	0.008884	0.038953	0.999727	1.0000	0.0386
0.8866349757	-1.31E-08	0.038953	0.008884	0.038953	0.999727	1.0000	0.0386
0.8866349608	-2.01E-09	0.038953	0.008884	0.038953	0.999727	1.0000	0.0386
0.8866349533	3.55E-09	0.038953	0.008884	0.038953	0.999727	1.0000	0.0386

Saturation	Total Mob	dFv/dSv	G	F	Gamma	Theta	High	Low
0.75	34.759228	0.045851	220.095758	12.870589	1.1794E+07	30550.407113	1	0.5
0.875	40.427490	0.009321	115.033000	10.281953	1.1701E+07	28275.535543	1	0.75
0.9375	43.300978	0.002124	62.501620	10.006619	1.1655E+07	28033.574650	1	0.875
0.90625	41.862126	0.005001	88.767310	10.097238	1.1678E+07	28113.209409	0.9375	0.875
0.890625	41.144193	0.006968	101.900155	10.175426	1.1690E+07	28181.920650	0.90625	0.875
0.8828125	40.785677	0.008095	108.466577	10.224828	1.1695E+07	28225.944700	0.890625	0.875
0.88671875	40.964895	0.007519	105.183366	10.199203	1.1693E+07	28202.815133	0.890625	0.8828125
0.884765625	40.875276	0.007804	106.824972	10.211779	1.1694E+07	28213.867353	0.88671875	0.8828125
0.8857421875	40.920083	0.007661	106.004169	10.205432	1.1693E+07	28208.289909	0.88671875	0.884765625
0.8862304688	40.942489	0.007590	105.593767	10.202303	1.1693E+07	28205.539756	0.88671875	0.8857421875
0.8864746094	40.953692	0.007555	105.388567	10.200749	1.1693E+07	28204.174262	0.88671875	0.88623046875
0.8865966797	40.959294	0.007537	105.285966	10.199975	1.1693E+07	28203.493903	0.88671875	0.88647460938
0.8866577148	40.962095	0.007528	105.234666	10.199589	1.1693E+07	28203.154319	0.88671875	0.88659667969
0.8866271973	40.960694	0.007533	105.260316	10.199782	1.1693E+07	28203.324062	0.88665771484	0.88659667969
0.8866424561	40.961394	0.007530	105.247491	10.199685	1.1693E+07	28203.239178	0.88665771484	0.88662719727
0.8866348267	40.961044	0.007531	105.253904	10.199733	1.1693E+07	28203.281617	0.88664245605	0.88662719727
0.8866386414	40.961219	0.007531	105.250698	10.199709	1.1693E+07	28203.260397	0.88664245605	0.88663482666
0.886636734	40.961132	0.007531	105.252301	10.199721	1.1693E+07	28203.271006	0.88663864136	0.88663482666
0.8866357803	40.961088	0.007531	105.253102	10.199727	1.1693E+07	28203.276312	0.88663673401	0.88663482666
0.8866353035	40.961066	0.007531	105.253503	10.199730	1.1693E+07	28203.278964	0.88663578033	0.88663482666
0.8866350651	40.961055	0.007531	105.253703	10.199732	1.1693E+07	28203.280290	0.88663506508	0.88663482666
0.8866349459	40.961050	0.007531	105.253804	10.199733	1.1693E+07	28203.280954	0.88663506508	0.88663482666
0.8866350055	40.961052	0.007531	105.253753	10.199732	1.1693E+07	28203.280622	0.88663506508	0.88663494587
0.8866349757	40.961051	0.007531	105.253779	10.199732	1.1693E+07	28203.280788	0.88663500547	0.88663494587
0.8866349608	40.961050	0.007531	105.253791	10.199733	1.1693E+07	28203.280871	0.88663497567	0.88663494587
0.8866349533	40.961050	0.007531	105.253797	10.199733	1.1693E+07	28203.280912	0.88663496077	0.88663494587

Spreadsheet for Calculation of Stream-Water Saturation Profiles

Injection Temperature
900 °K

Initial Temperature
350 °K

Matrix Heat Capacity
1.0000 (kJ/kg)

MATRIX PROPERTIES

Porosity	Cp Matrix	Density	Rho * Cp
0.10	1.00	2650.00	2650.0000
Nw	Ng	Swl	Denom
3.00	1.00	0.00	1.000000

SATURATION CONDITIONS

Tsaturation = 485.57

	Volumes (m3/kg)	Enthalpies (kJ/kg)	Densities (kg/m3)	Viscosities (cp)	Saturation Step
Liquid	0.001176	901.41	850.4723	0.1303	0.0014173371
Vapor	0.100298	2808.52	9.970241	0.0217	

BOUNDARY CONDITIONS

	Temperature	Velocity	Heat Capacity	Wave Velocity	Density	Enthalpy
Injection	900	1.000000	2.25	0.004575	4.849406	3762.24
Initial	350	0.008378	4.15	0.012144	975.3174	319.98
	G	F	Gamma	Theta		
Injection	900	4.85	4.85	21483244.61	18244.61	
Initial	350	975.32	975.32	8659580.72	312080.72	

SHOCK CONDITIONS

	Initial Guess Sv-HI	Sv-Low	Vapor Saturation	Objective Function	Two-Phase Wave Velocity	Upstream Flow Velocity	Shock Velocity	Vapor Frac Flow
Trailing	1	0.5	0.9575	2.3802E-10	0.0047	0.487747	0.0047	1.0000
Leading	1	0.5	0.8866	3.3451E-09	0.0367	0.008378	0.0367	0.9997
	dKrv/dSv	dKrl/dSl	Total Mobility	dFv/dSv	G	F'	Gamma	Theta'
Trailing	1.0000	0.0054	44.2235	0.0010	45.6901	9.9814	1.1640E+07	28011.4468
Leading	1.0000	0.0386	40.9610	0.0075	105.2538	10.1997	1.1693E+07	28203.2809

MATERIAL BALANCES

	Inside Mass	Initial	Injected	Produced	Balance	Error
Mass	94.210129	97.531740	4.849406	8.171010	0.0000	0.0000%
Enthalpy	881591.8742	865958.0720	18244.6130	2614.5485	-3.7377	0.0004%

Spreadsheet for Calculation of Stream-Water Saturation Profiles

Injection Temperature 900 °K		Initial Temperature 350 °K				Matrix Heat Capacity 1.0000 (kJ/kg)		
SATURATION PROFILE								
Vapor Saturation	Vapor Frac Flow	dKr/dSv	dKr/dSI	Total Mobility	dFv/dSv	lambda	Mass Inside	Enthalpy Inside
1.0000						0.000000		
1.0000						0.004655		
0.9575	0.999987	1.0000	0.0054	44.223491	0.000954	0.004655	0.022575	100008.669898
0.9561	0.999985	1.0000	0.0058	44.158091	0.001021	0.004981	0.015069	3790.086155
0.9547	0.999984	1.0000	0.0062	44.092696	0.001090	0.005318	0.016012	3926.542222
0.9532	0.999982	1.0000	0.0066	44.027304	0.001162	0.005667	0.016986	4063.829651
0.9518	0.999980	1.0000	0.0070	43.961917	0.001236	0.006028	0.017992	4201.954416
0.9504	0.999979	1.0000	0.0074	43.896534	0.001312	0.006401	0.019029	4340.922537
0.9490	0.999977	1.0000	0.0078	43.831156	0.001391	0.006785	0.020099	4480.740075
0.9476	0.999975	1.0000	0.0082	43.765783	0.001473	0.007182	0.021200	4621.413139
0.9462	0.999973	1.0000	0.0087	43.700414	0.001556	0.007591	0.022335	4762.947882
0.9447	0.999970	1.0000	0.0092	43.635050	0.001643	0.008012	0.023502	4905.350503
0.9433	0.999968	1.0000	0.0096	43.569692	0.001732	0.008445	0.024703	5048.627246
0.9419	0.999965	1.0000	0.0101	43.504339	0.001823	0.008891	0.025936	5192.784404
0.9405	0.999963	1.0000	0.0106	43.438991	0.001917	0.009349	0.027204	5337.828313
0.9391	0.999960	1.0000	0.0111	43.373648	0.002013	0.009820	0.028506	5483.765359
0.9377	0.999957	1.0000	0.0117	43.308312	0.002112	0.010303	0.029842	5630.601975
0.9362	0.999954	1.0000	0.0122	43.242981	0.002214	0.010798	0.031213	5778.344641
0.9348	0.999951	1.0000	0.0127	43.177656	0.002318	0.011307	0.032619	5926.999886
0.9334	0.999947	1.0000	0.0133	43.112337	0.002425	0.011828	0.034060	6076.574289
0.9320	0.999944	1.0000	0.0139	43.047024	0.002535	0.012362	0.035536	6227.074474
0.9306	0.999940	1.0000	0.0145	42.981717	0.002647	0.012909	0.037049	6378.507120
0.9292	0.999936	1.0000	0.0151	42.916417	0.002762	0.013469	0.038597	6530.878952
0.9277	0.999932	1.0000	0.0157	42.851123	0.002879	0.014042	0.040183	6684.196746
0.9263	0.999928	1.0000	0.0163	42.785837	0.002999	0.014629	0.041805	6838.467331
0.9249	0.999924	1.0000	0.0169	42.720556	0.003122	0.015228	0.043464	6993.697584
0.9235	0.999919	1.0000	0.0176	42.655283	0.003248	0.015841	0.045161	7149.894436
0.9221	0.999915	1.0000	0.0182	42.590017	0.003376	0.016467	0.046895	7307.064869
0.9207	0.999910	1.0000	0.0189	42.524758	0.003507	0.017107	0.048668	7465.215918
0.9192	0.999905	1.0000	0.0196	42.459507	0.003641	0.017761	0.050479	7624.354670
0.9178	0.999899	1.0000	0.0203	42.394263	0.003778	0.018428	0.052330	7784.488267
0.9164	0.999894	1.0000	0.0210	42.329026	0.003918	0.019108	0.054219	7945.623902
0.9150	0.999888	1.0000	0.0217	42.263798	0.004060	0.019803	0.056148	8107.768825
0.9136	0.999883	1.0000	0.0224	42.198577	0.004205	0.020512	0.058116	8270.930339
0.9121	0.999876	1.0000	0.0232	42.133364	0.004354	0.021234	0.060125	8435.115803
0.9107	0.999870	1.0000	0.0239	42.068159	0.004505	0.021971	0.062175	8600.332633
0.9093	0.999864	1.0000	0.0247	42.002963	0.004658	0.022722	0.064266	8766.588297
0.9079	0.999857	1.0000	0.0254	41.937775	0.004815	0.023487	0.066397	8933.890323
0.9065	0.999850	1.0000	0.0262	41.872595	0.004975	0.024266	0.068571	9102.246294
0.9051	0.999843	1.0000	0.0270	41.807424	0.005138	0.025060	0.070787	9271.663854
0.9036	0.999835	1.0000	0.0279	41.742262	0.005304	0.025868	0.073045	9442.150699
0.9022	0.999828	1.0000	0.0287	41.677109	0.005472	0.026691	0.075345	9613.714590
0.9008	0.999820	1.0000	0.0295	41.611965	0.005644	0.027529	0.077689	9786.363341
0.8994	0.999812	1.0000	0.0304	41.546830	0.005819	0.028381	0.080077	9960.104830
0.8980	0.999803	1.0000	0.0312	41.481704	0.005997	0.029249	0.082508	10134.946993
0.8966	0.999795	1.0000	0.0321	41.416588	0.006178	0.030131	0.084984	10310.897825
0.8951	0.999786	1.0000	0.0330	41.351481	0.006362	0.031028	0.087505	10487.965385
0.8937	0.999777	1.0000	0.0339	41.286385	0.006549	0.031941	0.090070	10666.157791
0.8923	0.999767	1.0000	0.0348	41.221297	0.006739	0.032869	0.092682	10845.483225
0.8909	0.999758	1.0000	0.0357	41.156220	0.006932	0.033812	0.095339	11025.949928
0.8895	0.999748	1.0000	0.0367	41.091153	0.007129	0.034770	0.098042	11207.566209
0.8881	0.999737	1.0000	0.0376	41.026096	0.007328	0.035745	0.100793	11390.340436
0.8866	0.999727	1.0000	0.0386	40.961050	0.007531	0.036734	0.103590	11574.281043
0.0000						0.036734		
0.0000						1.000000		

Spreadsheet for Calculation of Stream-Water Saturation Profiles

Injection Temperature 900 °K		Initial Temperature 350 °K		Matrix Heat Capacity 1.0000 (kJ/kg)				
TRAILING SHOCK CALCULATIONS								
Saturation	OF	Wave V	Flow V	Shock V	fv	dKrv/dSv	dKr/dSI	
0.7500	1.71E-01	0.177820	0.387822	0.006601	0.996549	1.0000	0.1875	
0.875	3.96E-02	0.044449	0.476858	0.004867	0.999629	1.0000	0.0469	
0.9375	5.68E-03	0.010348	0.487307	0.004664	0.999957	1.0000	0.0117	
0.96875	-2.18E-03	0.002477	0.487639	0.004657	0.999995	1.0000	0.0029	
0.953125	1.04E-03	0.005698	0.487728	0.004656	0.999982	1.0000	0.0066	
0.9609375	-7.41E-04	0.003914	0.487736	0.004655	0.999990	1.0000	0.0046	
0.95703125	1.07E-04	0.004762	0.487747	0.004655	0.999986	1.0000	0.0055	
0.958984375	-3.28E-04	0.004327	0.487745	0.004655	0.999988	1.0000	0.0050	
0.9580078125	-1.13E-04	0.004542	0.487747	0.004655	0.999987	1.0000	0.0053	
0.9575195313	-4.00E-06	0.004651	0.487747	0.004655	0.999987	1.0000	0.0054	
0.9572753906	5.12E-05	0.004706	0.487747	0.004655	0.999986	1.0000	0.0055	
0.9573974609	2.36E-05	0.004679	0.487747	0.004655	0.999987	1.0000	0.0054	
0.9574584961	9.78E-06	0.004665	0.487747	0.004655	0.999987	1.0000	0.0054	
0.9574890137	2.89E-06	0.004658	0.487747	0.004655	0.999987	1.0000	0.0054	
0.9575042725	-5.56E-07	0.004655	0.487747	0.004655	0.999987	1.0000	0.0054	
0.9574966431	1.17E-06	0.004656	0.487747	0.004655	0.999987	1.0000	0.0054	
0.9575004578	3.04E-07	0.004655	0.487747	0.004655	0.999987	1.0000	0.0054	
0.9575023651	-1.26E-07	0.004655	0.487747	0.004655	0.999987	1.0000	0.0054	
0.9575014114	8.93E-08	0.004655	0.487747	0.004655	0.999987	1.0000	0.0054	
0.9575018883	-1.83E-08	0.004655	0.487747	0.004655	0.999987	1.0000	0.0054	
0.9575016499	3.55E-08	0.004655	0.487747	0.004655	0.999987	1.0000	0.0054	
0.9575017691	8.64E-09	0.004655	0.487747	0.004655	0.999987	1.0000	0.0054	
0.9575018287	-4.80E-09	0.004655	0.487747	0.004655	0.999987	1.0000	0.0054	
0.9575017989	1.92E-09	0.004655	0.487747	0.004655	0.999987	1.0000	0.0054	
0.9575018138	-1.44E-09	0.004655	0.487747	0.004655	0.999987	1.0000	0.0054	
0.9575018063	2.38E-10	0.004655	0.487747	0.004655	0.999987	1.0000	0.0054	
Saturation	Total Mob	dFv/dSv	G	F	Gamma	Theta	High	Low
0.75	34.759228	0.045851	220.095758	12.870589	1.1794E+07	30550.407113	1	0.5
0.875	40.427490	0.009321	115.033000	10.281953	1.1701E+07	28275.535543	1	0.75
0.9375	43.300978	0.002124	62.501620	10.006619	1.1655E+07	28033.574650	1	0.875
0.96875	44.742642	0.000508	36.235931	9.974642	1.1632E+07	28005.473055	1	0.9375
0.953125	44.021547	0.001168	49.368776	9.985337	1.1643E+07	28014.871837	0.96875	0.9375
0.9609375	44.382039	0.000802	42.802353	9.978906	1.1638E+07	28009.220503	0.96875	0.953125
0.95703125	44.201778	0.000976	46.085564	9.981821	1.1641E+07	28011.782338	0.9609375	0.953125
0.958984375	44.291905	0.000887	44.443959	9.980292	1.1639E+07	28010.438726	0.9609375	0.95703125
0.9580078125	44.246841	0.000931	45.264762	9.981039	1.1640E+07	28011.094453	0.958984375	0.95703125
0.9575195313	44.224309	0.000954	45.675163	9.981425	1.1640E+07	28011.434324	0.9580078125	0.95703125
0.9572753906	44.213043	0.000965	45.880364	9.981622	1.1640E+07	28011.607307	0.95751953125	0.95703125
0.9573974609	44.218676	0.000959	45.777763	9.981523	1.1640E+07	28011.520561	0.95751953125	0.95727539063
0.9574584961	44.221493	0.000956	45.726463	9.981474	1.1640E+07	28011.477379	0.95751953125	0.95739746094
0.9574890137	44.222901	0.000955	45.700813	9.981450	1.1640E+07	28011.455836	0.95751953125	0.95745849609
0.9575042725	44.223605	0.000954	45.687988	9.981438	1.1640E+07	28011.445076	0.95751953125	0.95748901367
0.9574966431	44.223253	0.000955	45.694400	9.981444	1.1640E+07	28011.450455	0.95750427246	0.95748901367
0.9575004578	44.223429	0.000954	45.691194	9.981441	1.1640E+07	28011.447765	0.95750427246	0.95749664307
0.9575023651	44.223517	0.000954	45.689591	9.981439	1.1640E+07	28011.446421	0.95750427246	0.95750045776
0.9575014114	44.223473	0.000954	45.690393	9.981440	1.1640E+07	28011.447093	0.95750236511	0.95750045776
0.9575018883	44.223495	0.000954	45.689992	9.981439	1.1640E+07	28011.446757	0.95750236511	0.95750141144
0.9575016499	44.223484	0.000954	45.690192	9.981440	1.1640E+07	28011.446925	0.95750188828	0.95750141144
0.9575017691	44.223489	0.000954	45.690092	9.981440	1.1640E+07	28011.446841	0.95750188828	0.95750164986
0.9575018287	44.223492	0.000954	45.690042	9.981439	1.1640E+07	28011.446799	0.95750188828	0.95750176907
0.9575017989	44.223491	0.000954	45.690067	9.981439	1.1640E+07	28011.446820	0.95750182867	0.95750176907
0.9575018138	44.223492	0.000954	45.690054	9.981439	1.1640E+07	28011.446809	0.95750182867	0.95750179887
0.9575018063	44.223491	0.000954	45.690061	9.981439	1.1640E+07	28011.446815	0.95750181377	0.95750179887

Spreadsheet for Calculation of Stream-Water Saturation Profiles

Injection Temperature 900 °K		Initial Temperature 350 °K		Matrix Heat Capacity 1.0000 (kJ/kg)			
LEADING SHOCK CALCULATIONS							
Saturation	OF	Wave V	Flow V	Shock V	f _v	dK _{rv} /dS _v	dK _r /dS _i
0.7500	1.85E-01	0.223637	0.009394	0.038193	0.996549	1.0000	0.1875
0.875	8.72E-03	0.045464	0.008383	0.036741	0.999629	1.0000	0.0469
0.9375	-2.65E-02	0.010358	0.008452	0.036841	0.999957	1.0000	0.0117
0.90625	-1.24E-02	0.024392	0.008390	0.036752	0.999849	1.0000	0.0264
0.890625	-2.75E-03	0.033988	0.008378	0.036735	0.999756	1.0000	0.0359
0.8828125	2.75E-03	0.039482	0.008378	0.036735	0.999697	1.0000	0.0412
0.88671875	-5.90E-05	0.036675	0.008378	0.036734	0.999728	1.0000	0.0385
0.884765625	1.33E-03	0.038064	0.008378	0.036735	0.999713	1.0000	0.0398
0.8857421875	6.31E-04	0.037366	0.008378	0.036734	0.999720	1.0000	0.0392
0.8862304688	2.85E-04	0.037020	0.008378	0.036734	0.999724	1.0000	0.0388
0.8864746094	1.13E-04	0.036847	0.008378	0.036734	0.999726	1.0000	0.0387
0.8865966797	2.69E-05	0.036761	0.008378	0.036734	0.999727	1.0000	0.0386
0.8866577148	-1.60E-05	0.036718	0.008378	0.036734	0.999727	1.0000	0.0385
0.8866271973	5.46E-06	0.036740	0.008378	0.036734	0.999727	1.0000	0.0386
0.8866424561	-5.28E-06	0.036729	0.008378	0.036734	0.999727	1.0000	0.0385
0.8866348267	9.25E-08	0.036734	0.008378	0.036734	0.999727	1.0000	0.0386
0.8866386414	-2.59E-06	0.036732	0.008378	0.036734	0.999727	1.0000	0.0386
0.886636734	-1.25E-06	0.036733	0.008378	0.036734	0.999727	1.0000	0.0386
0.8866357803	-5.79E-07	0.036734	0.008378	0.036734	0.999727	1.0000	0.0386
0.8866353035	-2.43E-07	0.036734	0.008378	0.036734	0.999727	1.0000	0.0386
0.8866350651	-7.53E-08	0.036734	0.008378	0.036734	0.999727	1.0000	0.0386
0.8866349459	8.59E-09	0.036734	0.008378	0.036734	0.999727	1.0000	0.0386
0.8866350055	-3.34E-08	0.036734	0.008378	0.036734	0.999727	1.0000	0.0386
0.8866349757	-1.24E-08	0.036734	0.008378	0.036734	0.999727	1.0000	0.0386
0.8866349608	-1.90E-09	0.036734	0.008378	0.036734	0.999727	1.0000	0.0386
0.8866349533	3.35E-09	0.036734	0.008378	0.036734	0.999727	1.0000	0.0386

Saturation	Total Mob	dF _v /dS _v	G	F	Gamma	Theta	High	Low
0.75	34.759228	0.045851	220.095758	12.870589	1.1794E+07	30550.407113	1	0.5
0.875	40.427490	0.009321	115.033000	10.281953	1.1701E+07	28275.535543	1	0.75
0.9375	43.300978	0.002124	62.501620	10.006619	1.1655E+07	28033.574650	1	0.875
0.90625	41.862126	0.005001	88.767310	10.097238	1.1678E+07	28113.209409	0.9375	0.875
0.890625	41.144193	0.006968	101.900155	10.175426	1.1690E+07	28181.920650	0.90625	0.875
0.8828125	40.785677	0.008095	108.466577	10.224828	1.1695E+07	28225.334700	0.890625	0.875
0.88671875	40.964895	0.007519	105.183366	10.199203	1.1693E+07	28202.815133	0.890625	0.8828125
0.884765625	40.875276	0.007804	106.824972	10.211779	1.1694E+07	28213.867353	0.88671875	0.8828125
0.8857421875	40.920083	0.007661	106.004169	10.205432	1.1693E+07	28208.289909	0.88671875	0.884765625
0.8862304688	40.942489	0.007590	105.593767	10.202303	1.1693E+07	28205.539756	0.88671875	0.8857421875
0.8864746094	40.953692	0.007555	105.388567	10.200749	1.1693E+07	28204.174262	0.88671875	0.8862304688
0.8865966797	40.959294	0.007537	105.285966	10.199975	1.1693E+07	28203.493903	0.88671875	0.88647460938
0.8866577148	40.962095	0.007528	105.234666	10.199589	1.1693E+07	28203.154319	0.88671875	0.88659667969
0.8866271973	40.960694	0.007533	105.260316	10.199782	1.1693E+07	28203.324062	0.88665771484	0.88659667969
0.8866424561	40.961394	0.007530	105.247491	10.199685	1.1693E+07	28203.239178	0.88665771484	0.88662719727
0.8866348267	40.961044	0.007531	105.253904	10.199733	1.1693E+07	28203.281617	0.88664245605	0.88662719727
0.8866386414	40.961219	0.007531	105.250698	10.199709	1.1693E+07	28203.260397	0.88664245605	0.88663482666
0.886636734	40.961132	0.007531	105.252301	10.199721	1.1693E+07	28203.271006	0.88663864136	0.88663482666
0.8866357803	40.961088	0.007531	105.253102	10.199727	1.1693E+07	28203.276312	0.88663673401	0.88663482666
0.8866353035	40.961066	0.007531	105.253503	10.199730	1.1693E+07	28203.278964	0.88663578033	0.88663482666
0.8866350651	40.961055	0.007531	105.253703	10.199732	1.1693E+07	28203.280290	0.8866353035	0.88663482666
0.8866349459	40.961050	0.007531	105.253804	10.199733	1.1693E+07	28203.280954	0.88663506508	0.88663482666
0.8866350055	40.961052	0.007531	105.253753	10.199732	1.1693E+07	28203.280622	0.88663506508	0.88663494587
0.8866349757	40.961051	0.007531	105.253779	10.199732	1.1693E+07	28203.280788	0.88663500547	0.88663494587
0.8866349608	40.961050	0.007531	105.253791	10.199733	1.1693E+07	28203.280871	0.88663497567	0.88663494587
0.8866349533	40.961050	0.007531	105.253797	10.199733	1.1693E+07	28203.280912	0.88663496077	0.88663494587

Spreadsheet for Calculation of Stream-Water Saturation Profiles

Injection Temperature
950 °K

Initial Temperature
350 °K

Matrix Heat Capacity
1.0000 (kJ/kg)

MATRIX PROPERTIES

Porosity	Cp Matrix	Density	Rho * Cp
0.10	1.00	2650.00	2650.0000
Nw	Ng	Swl	Denom
3.00	1.00	0.00	1.000000

SATURATION CONDITIONS

Tsaturation = 485.57

	Volumes (m3/kg)	Enthalpies (kJ/kg)	Densities (kg/m3)	Viscosities (cp)	Saturation Step
Liquid	0.001176	901.41	850.4723	0.1303	0.0014178684
Vapor	0.100298	2808.52	9.970241	0.0217	

BOUNDARY CONDITIONS

	Temperature	Velocity	Heat Capacity	Wave Velocity	Density	Enthalpy
Injection	950	1.000000	2.28	0.004380	4.590016	3875.38
Initial	350	0.007930	4.15	0.011495	975.3174	319.98
		G	F	Gamma	Theta	
Injection	950	4.59	4.59	22675288.06	17788.06	
Initial	350	975.32	975.32	8659580.72	312080.72	

SHOCK CONDITIONS

	Initial Guess		Vapor Saturation	Objective Function	Two-Phase Wave Velocity	Upstream Flow Velocity	Shock Velocity	Vapor Frac Flow
Trailing	Sv-Hi	Sv-Low	0.9575	7.7304E-10	0.0044	0.461667	0.0044	1.0000
Leading	1	0.5	0.8866	3.1662E-09	0.0348	0.007930	0.0348	0.9997
	dKrv/dSv	dKrl/dSl	Total Mobility	dFv/dSv	G	F'	Gamma	Theta'
Trailing	1.0000	0.0054	44.2247	0.0010	45.6677	9.9814	1.1640E+07	28011.4281
Leading	1.0000	0.0386	40.9610	0.0075	105.2538	10.1997	1.1693E+07	28203.2809

MATERIAL BALANCES

	Inside	Initial	Injected	Produced	Balance	Error
Mass	94.387645	97.531740	4.590016	7.734104	0.0000	0.0000%
Enthalpy	881274.9209	865958.0720	17788.0580	2474.7480	-3.5388	0.0004%

Spreadsheet for Calculation of Stream-Water Saturation Profiles

Injection Temperature 950 °K		Initial Temperature 350 °K				Matrix Heat Capacity 1.0000 (kJ/kg)		
SATURATION PROFILE								
Vapor Saturation	Vapor Frac Flow	dKrv/dSv	dKr/dSI	Total Mobility	dFv/dSv	lambda	Mass Inside	Enthalpy Inside
1.0000						0.000000		
1.0000						0.004401		
0.9575	0.999987	1.0000	0.0054	44.224717	0.000953	0.004401	0.020199	99785.059391
0.9561	0.999985	1.0000	0.0058	44.159293	0.001020	0.004709	0.014253	3586.383941
0.9547	0.999984	1.0000	0.0062	44.093872	0.001089	0.005028	0.015145	3715.626122
0.9533	0.999982	1.0000	0.0065	44.028456	0.001161	0.005358	0.016067	3845.655996
0.9519	0.999981	1.0000	0.0070	43.963045	0.001235	0.005700	0.017019	3976.479224
0.9504	0.999979	1.0000	0.0074	43.897637	0.001311	0.006052	0.018002	4108.101511
0.9490	0.999977	1.0000	0.0078	43.832234	0.001390	0.006416	0.019014	4240.528603
0.9476	0.999975	1.0000	0.0082	43.766836	0.001471	0.006792	0.020057	4373.766291
0.9462	0.999973	1.0000	0.0087	43.701443	0.001555	0.007179	0.021131	4507.820405
0.9448	0.999970	1.0000	0.0092	43.636055	0.001641	0.007577	0.022236	4642.698822
0.9433	0.999968	1.0000	0.0096	43.570672	0.001730	0.007988	0.023373	4778.401461
0.9419	0.999965	1.0000	0.0101	43.505294	0.001822	0.008409	0.024541	4914.940284
0.9405	0.999963	1.0000	0.0106	43.439922	0.001915	0.008843	0.025742	5052.319300
0.9391	0.999960	1.0000	0.0111	43.374555	0.002012	0.009288	0.026974	5190.544560
0.9377	0.999957	1.0000	0.0117	43.309194	0.002111	0.009746	0.028239	5329.622161
0.9363	0.999954	1.0000	0.0122	43.243838	0.002213	0.010215	0.029537	5469.558246
0.9348	0.999951	1.0000	0.0127	43.178488	0.002317	0.010696	0.030869	5610.359005
0.9334	0.999947	1.0000	0.0133	43.113145	0.002424	0.011190	0.032233	5752.030670
0.9320	0.999944	1.0000	0.0139	43.047807	0.002533	0.011695	0.033631	5894.579524
0.9306	0.999940	1.0000	0.0145	42.982476	0.002645	0.012213	0.035064	6038.011895
0.9292	0.999936	1.0000	0.0151	42.917151	0.002760	0.012743	0.036530	6182.334158
0.9278	0.999932	1.0000	0.0157	42.851833	0.002878	0.013286	0.038031	6327.552736
0.9263	0.999928	1.0000	0.0163	42.786522	0.002998	0.013841	0.039568	6473.674102
0.9249	0.999924	1.0000	0.0169	42.721217	0.003121	0.014408	0.041139	6620.704775
0.9235	0.999919	1.0000	0.0176	42.655920	0.003247	0.014988	0.042746	6768.651324
0.9221	0.999915	1.0000	0.0182	42.590629	0.003375	0.015581	0.044389	6917.520367
0.9207	0.999910	1.0000	0.0189	42.525346	0.003506	0.016187	0.046068	7067.318573
0.9192	0.999905	1.0000	0.0196	42.460070	0.003640	0.016806	0.047783	7218.052659
0.9178	0.999900	1.0000	0.0203	42.394801	0.003777	0.017437	0.049535	7369.729394
0.9164	0.999894	1.0000	0.0210	42.329540	0.003917	0.018082	0.051324	7522.355599
0.9150	0.999888	1.0000	0.0217	42.264287	0.004059	0.018739	0.053151	7675.938143
0.9136	0.999883	1.0000	0.0224	42.199041	0.004204	0.019410	0.055016	7830.483951
0.9122	0.999877	1.0000	0.0231	42.133804	0.004353	0.020094	0.056919	7985.999998
0.9107	0.999870	1.0000	0.0239	42.068575	0.004504	0.020791	0.058860	8142.493312
0.9093	0.999864	1.0000	0.0247	42.003354	0.004658	0.021502	0.060840	8299.970973
0.9079	0.999857	1.0000	0.0254	41.938141	0.004814	0.022227	0.062859	8458.440117
0.9065	0.999850	1.0000	0.0262	41.872937	0.004974	0.022965	0.064917	8617.907933
0.9051	0.999843	1.0000	0.0270	41.807742	0.005137	0.023716	0.067016	8778.381664
0.9036	0.999836	1.0000	0.0279	41.742555	0.005303	0.024481	0.069155	8939.868609
0.9022	0.999828	1.0000	0.0287	41.677378	0.005472	0.025261	0.071334	9102.376120
0.9008	0.999820	1.0000	0.0295	41.612209	0.005643	0.026054	0.073554	9265.911609
0.8994	0.999812	1.0000	0.0304	41.547050	0.005818	0.026861	0.075815	9430.482540
0.8980	0.999803	1.0000	0.0312	41.481900	0.005996	0.027682	0.078118	9596.096437
0.8966	0.999795	1.0000	0.0321	41.416759	0.006177	0.028518	0.080464	9762.760879
0.8951	0.999786	1.0000	0.0330	41.351628	0.006361	0.029367	0.082851	9930.483505
0.8937	0.999777	1.0000	0.0339	41.286507	0.006548	0.030231	0.085281	10099.272010
0.8923	0.999767	1.0000	0.0348	41.221395	0.006739	0.031110	0.087755	10269.134150
0.8909	0.999758	1.0000	0.0357	41.156293	0.006932	0.032003	0.090272	10440.077739
0.8895	0.999748	1.0000	0.0367	41.091202	0.007129	0.032911	0.092832	10612.110651
0.8881	0.999737	1.0000	0.0376	41.026121	0.007328	0.033833	0.095437	10785.240818
0.8866	0.999727	1.0000	0.0386	40.961050	0.007531	0.034770	0.098087	10959.476238
0.0000						0.034770		
0.0000						1.000000		

Spreadsheet for Calculation of Stream-Water Saturation Profiles

Injection Temperature 950 °K		Initial Temperature 350 °K		Matrix Heat Capacity 1.0000 (kJ/kg)				
TRAILING SHOCK CALCULATIONS								
Saturation	OF	Wave V	Flow V	Shock V	f _v	dK _{rv} /dS _v	dK _r /dS _i	
0.7500	1.62E-01	0.168162	0.366758	0.006050	0.996549	1.0000	0.1875	
0.875	3.75E-02	0.042069	0.451335	0.004580	0.999629	1.0000	0.0469	
0.9375	5.39E-03	0.009795	0.461249	0.004408	0.999957	1.0000	0.0117	
0.96875	-2.06E-03	0.002345	0.461565	0.004402	0.999995	1.0000	0.0029	
0.953125	9.93E-04	0.005393	0.461649	0.004401	0.999982	1.0000	0.0066	
0.9609375	-6.96E-04	0.003705	0.461657	0.004401	0.999990	1.0000	0.0046	
0.95703125	1.07E-04	0.004507	0.461667	0.004401	0.999986	1.0000	0.0055	
0.958984375	-3.05E-04	0.004096	0.461665	0.004401	0.999988	1.0000	0.0050	
0.9580078125	-1.02E-04	0.004299	0.461667	0.004401	0.999987	1.0000	0.0053	
0.9575195313	1.89E-06	0.004402	0.461667	0.004401	0.999987	1.0000	0.0054	
0.9577636719	-5.01E-05	0.004351	0.461667	0.004401	0.999987	1.0000	0.0054	
0.9576416016	-2.41E-05	0.004376	0.461667	0.004401	0.999987	1.0000	0.0054	
0.9575805664	-1.11E-05	0.004389	0.461667	0.004401	0.999987	1.0000	0.0054	
0.9575500488	-4.62E-06	0.004396	0.461667	0.004401	0.999987	1.0000	0.0054	
0.95753479	-1.37E-06	0.004399	0.461667	0.004401	0.999987	1.0000	0.0054	
0.9575271606	2.60E-07	0.004401	0.461667	0.004401	0.999987	1.0000	0.0054	
0.9575309753	-5.54E-07	0.004400	0.461667	0.004401	0.999987	1.0000	0.0054	
0.957529068	-1.47E-07	0.004400	0.461667	0.004401	0.999987	1.0000	0.0054	
0.9575281143	5.64E-08	0.004401	0.461667	0.004401	0.999987	1.0000	0.0054	
0.9575285912	-4.53E-08	0.004401	0.461667	0.004401	0.999987	1.0000	0.0054	
0.9575283527	5.54E-09	0.004401	0.461667	0.004401	0.999987	1.0000	0.0054	
0.9575284719	-1.99E-08	0.004401	0.461667	0.004401	0.999987	1.0000	0.0054	
0.9575284123	-7.18E-09	0.004401	0.461667	0.004401	0.999987	1.0000	0.0054	
0.9575283825	-8.17E-09	0.004401	0.461667	0.004401	0.999987	1.0000	0.0054	
0.9575283676	2.36E-09	0.004401	0.461667	0.004401	0.999987	1.0000	0.0054	
0.9575283751	7.73E-10	0.004401	0.461667	0.004401	0.999987	1.0000	0.0054	
Saturation	Total Mob	dF _v /dS _v	G	F	Gamma	Theta	High	Low
0.75	34.759228	0.045851	220.095758	12.870589	1.1794E+07	30550.407113	1	0.5
0.875	40.427490	0.009321	115.033000	10.281953	1.1701E+07	28275.535543	1	0.75
0.9375	43.300978	0.002124	62.501620	10.006619	1.1655E+07	28033.574650	1	0.875
0.96875	44.742642	0.000508	36.235931	9.974642	1.1632E+07	28005.473055	1	0.9375
0.953125	44.021547	0.001168	49.368776	9.985337	1.1643E+07	28014.871837	0.96875	0.9375
0.9609375	44.382039	0.000802	42.802353	9.978906	1.1638E+07	28009.220503	0.96875	0.953125
0.95703125	44.201778	0.000976	46.085564	9.981821	1.1641E+07	28011.782338	0.9609375	0.953125
0.958984375	44.291905	0.000887	44.443959	9.980292	1.1639E+07	28010.438726	0.9609375	0.95703125
0.9580078125	44.246841	0.000931	45.264762	9.981039	1.1640E+07	28011.094453	0.958984375	0.95703125
0.9575195313	44.224309	0.000954	45.675163	9.981425	1.1640E+07	28011.434324	0.9580078125	0.95703125
0.9577636719	44.235575	0.000942	45.469962	9.981231	1.1640E+07	28011.263377	0.9580078125	0.95751953125
0.9576416016	44.229942	0.000948	45.572563	9.981328	1.1640E+07	28011.348597	0.95776367188	0.95751953125
0.9575805664	44.227125	0.000951	45.623863	9.981376	1.1640E+07	28011.391397	0.95764160156	0.95751953125
0.9575500488	44.225717	0.000952	45.649513	9.981401	1.1640E+07	28011.412845	0.95758056641	0.95751953125
0.95753479	44.225013	0.000953	45.662338	9.981413	1.1640E+07	28011.423581	0.95755004883	0.95751953125
0.9575271606	44.224661	0.000953	45.668750	9.981419	1.1640E+07	28011.428952	0.95753479004	0.95751953125
0.9575309753	44.224837	0.000953	45.665544	9.981416	1.1640E+07	28011.426266	0.95753479004	0.95752716064
0.957529068	44.224749	0.000953	45.667147	9.981418	1.1640E+07	28011.427609	0.95753097534	0.95752716064
0.9575281143	44.224705	0.000953	45.667949	9.981418	1.1640E+07	28011.428280	0.95752906799	0.95752716064
0.9575285912	44.224727	0.000953	45.667548	9.981418	1.1640E+07	28011.427944	0.95752906799	0.95752811432
0.9575283527	44.224716	0.000953	45.667748	9.981418	1.1640E+07	28011.428112	0.95752859116	0.95752811432
0.9575284719	44.224722	0.000953	45.667648	9.981418	1.1640E+07	28011.428028	0.95752859116	0.95752835274
0.9575284123	44.224719	0.000953	45.667698	9.981418	1.1640E+07	28011.428070	0.95752847195	0.95752835274
0.9575283825	44.224718	0.000953	45.667723	9.981418	1.1640E+07	28011.428091	0.95752841234	0.95752835274
0.9575283676	44.224717	0.000953	45.667736	9.981418	1.1640E+07	28011.428102	0.95752838254	0.95752835274
0.9575283751	44.224717	0.000953	45.667730	9.981418	1.1640E+07	28011.428097	0.95752838254	0.95752836764

Spreadsheet for Calculation of Stream-Water Saturation Profiles

Injection Temperature 950 °K		Initial Temperature 350 °K		Matrix Heat Capacity 1.0000 (kJ/kg)				
LEADING SHOCK CALCULATIONS								
Saturation	OF	Wave V	Flow V	Shock V	f _v	dKrv/dSv	dKr/dSI	
0.7500	1.76E-01	0.211679	0.008892	0.036150	0.996549	1.0000	0.1875	
0.875	8.26E-03	0.043033	0.007934	0.034777	0.999629	1.0000	0.0469	
0.9375	-2.51E-02	0.009804	0.008000	0.034871	0.999957	1.0000	0.0117	
0.90625	-1.17E-02	0.023088	0.007942	0.034787	0.999849	1.0000	0.0264	
0.890625	-2.60E-03	0.032170	0.007930	0.034771	0.999756	1.0000	0.0359	
0.8828125	2.60E-03	0.037371	0.007930	0.034771	0.999697	1.0000	0.0412	
0.88671875	-5.58E-05	0.034714	0.007930	0.034770	0.999728	1.0000	0.0385	
0.884765625	1.26E-03	0.036029	0.007930	0.034770	0.999713	1.0000	0.0398	
0.8857421875	5.98E-04	0.035368	0.007930	0.034770	0.999720	1.0000	0.0392	
0.8862304688	2.70E-04	0.035040	0.007930	0.034770	0.999724	1.0000	0.0388	
0.8864746094	1.07E-04	0.034877	0.007930	0.034770	0.999726	1.0000	0.0387	
0.8865966797	2.55E-05	0.034796	0.007930	0.034770	0.999727	1.0000	0.0386	
0.8866577148	-1.52E-05	0.034755	0.007930	0.034770	0.999727	1.0000	0.0385	
0.8866271973	5.17E-06	0.034775	0.007930	0.034770	0.999727	1.0000	0.0386	
0.8866424561	-5.00E-06	0.034765	0.007930	0.034770	0.999727	1.0000	0.0385	
0.8866348267	8.76E-08	0.034770	0.007930	0.034770	0.999727	1.0000	0.0386	
0.8866386414	-2.45E-06	0.034768	0.007930	0.034770	0.999727	1.0000	0.0386	
0.886636734	-1.18E-06	0.034769	0.007930	0.034770	0.999727	1.0000	0.0386	
0.8866357803	-5.48E-07	0.034770	0.007930	0.034770	0.999727	1.0000	0.0386	
0.8866353035	-2.30E-07	0.034770	0.007930	0.034770	0.999727	1.0000	0.0386	
0.8866350651	-7.13E-08	0.034770	0.007930	0.034770	0.999727	1.0000	0.0386	
0.8866349459	8.13E-09	0.034770	0.007930	0.034770	0.999727	1.0000	0.0386	
0.8866350055	-3.16E-08	0.034770	0.007930	0.034770	0.999727	1.0000	0.0386	
0.8866349757	-1.17E-08	0.034770	0.007930	0.034770	0.999727	1.0000	0.0386	
0.8866349608	-1.80E-09	0.034770	0.007930	0.034770	0.999727	1.0000	0.0386	
0.8866349533	3.17E-09	0.034770	0.007930	0.034770	0.999727	1.0000	0.0386	
Saturation	Total Mob	dFv/dSv	G	F	Gamma	Theta	High	Low
0.75	34.759228	0.045851	220.095758	12.870589	1.1794E+07	30550.407113	1	0.5
0.875	40.427490	0.009321	115.033000	10.281953	1.1701E+07	28275.535543	1	0.75
0.9375	43.300978	0.002124	62.501620	10.006619	1.1655E+07	28033.574650	1	0.875
0.90625	41.862126	0.005001	88.767310	10.097238	1.1678E+07	28113.209409	0.9375	0.875
0.890625	41.144193	0.006968	101.900155	10.175426	1.1690E+07	28181.920650	0.90625	0.875
0.8828125	40.785677	0.008095	108.466577	10.224828	1.1695E+07	28225.334700	0.890625	0.875
0.88671875	40.964895	0.007519	105.183366	10.199203	1.1693E+07	28202.815133	0.890625	0.8828125
0.884765625	40.875276	0.007804	106.824972	10.211779	1.1694E+07	28213.867353	0.88671875	0.8828125
0.8857421875	40.920083	0.007661	106.004169	10.205432	1.1693E+07	28208.289909	0.88671875	0.884765625
0.8862304688	40.942489	0.007590	105.593767	10.202303	1.1693E+07	28205.539756	0.88671875	0.8857421875
0.8864746094	40.953692	0.007555	105.388567	10.200749	1.1693E+07	28204.174262	0.88671875	0.8862304688
0.8865966797	40.959294	0.007537	105.285966	10.199975	1.1693E+07	28203.493903	0.88671875	0.88647460938
0.8866577148	40.962095	0.007528	105.234666	10.199589	1.1693E+07	28203.154319	0.88671875	0.88659667969
0.8866271973	40.960694	0.007533	105.260316	10.199782	1.1693E+07	28203.324062	0.88665771484	0.88659667969
0.8866424561	40.961394	0.007530	105.247491	10.199685	1.1693E+07	28203.239178	0.88665771484	0.88662719727
0.8866348267	40.961044	0.007531	105.253904	10.199727	1.1693E+07	28203.281617	0.88664245605	0.88662719727
0.8866386414	40.961219	0.007531	105.250698	10.199709	1.1693E+07	28203.260397	0.88664245605	0.88663482666
0.886636734	40.961132	0.007531	105.252301	10.199721	1.1693E+07	28203.271006	0.88663864136	0.88663482666
0.8866357803	40.961088	0.007531	105.253102	10.199727	1.1693E+07	28203.276312	0.88663673401	0.88663482666
0.8866353035	40.961066	0.007531	105.253503	10.199730	1.1693E+07	28203.278964	0.88663578033	0.88663482666
0.8866350651	40.961055	0.007531	105.253703	10.199732	1.1693E+07	28203.280290	0.8866353035	0.88663482666
0.8866349459	40.961050	0.007531	105.253804	10.199733	1.1693E+07	28203.280954	0.88663506508	0.88663482666
0.8866350055	40.961052	0.007531	105.253753	10.199732	1.1693E+07	28203.280622	0.88663506508	0.88663494587
0.8866349757	40.961051	0.007531	105.253779	10.199732	1.1693E+07	28203.280788	0.88663500547	0.88663494587
0.8866349608	40.961050	0.007531	105.253791	10.199733	1.1693E+07	28203.280871	0.88663497567	0.88663494587
0.8866349533	40.961050	0.007531	105.253797	10.199733	1.1693E+07	28203.280912	0.88663496077	0.88663494587

Spreadsheet for Calculation of Stream-Water Saturation Profiles

Injection Temperature
1000 °K

Initial Temperature
350 °K

Matrix Heat Capacity
1.0000 (kJ/kg)

MATRIX PROPERTIES

Porosity	Cp Matrix	Density	Rho * Cp
0.10	1.00	2650.00	2650.0000
Nw	Ng	Swl	Denom
3.00	1.00	0.00	1.000000

SATURATION CONDITIONS

Tsaturation = 485.57

	Volumes (m3/kg)	Enthalpies (kJ/kg)	Densities (kg/m3)	Viscosities (cp)	Saturation Step
Liquid	0.001176	901.41	850.4723	0.1303	0.0014177462
Vapor	0.100298	2808.52	9.970241	0.0217	

BOUNDARY CONDITIONS

	Temperature	Velocity	Heat Capacity	Wave Velocity	Density	Enthalpy
Injection	1000	1.000000	2.31	0.004227	4.357678	3990.11
Initial	350	0.007529	4.15	0.010913	975.3174	319.98
	G	F	Gamma	Theta		
Injection	1000	4.36	4.36	23867387.62	17387.62	
Initial	350	975.32	975.32	8659580.72	312080.72	

SHOCK CONDITIONS

	Initial Guess Sv-Hi	Initial Guess Sv-Low	Vapor Saturation	Objective Function	Two-Phase Wave Velocity	Upstream Flow Velocity	Shock Velocity	Vapor Frac Flow
Trailing	1	0.5	0.9575	1.0026E-09	0.0042	0.438309	0.0042	1.0000
Leading	1	0.5	0.8866	3.0060E-09	0.0330	0.007529	0.0330	0.9997
	dKr/dSv	dKr/dSI	Total Mobility	dFv/dSv	G	F'	Gamma	Theta'
Trailing	1.0000	0.0054	44.2244	0.0010	45.6729	9.9814	1.1640E+07	28011.4324
Leading	1.0000	0.0386	40.9610	0.0075	105.2538	10.1997	1.1693E+07	28203.2809

MATERIAL BALANCES

	Mass	Inside	Initial	Injected	Produced	Balance	Error
Mass	94.546621	880999.5190	97.531740	4.357678	7.342791	0.0000	0.0000%
Enthalpy	880999.5190	880999.5190	865958.0720	17387.6229	2349.5360	-3.3601	0.0004%

Spreadsheet for Calculation of Stream-Water Saturation Profiles

Injection Temperature 1000 °K		Initial Temperature 350 °K				Matrix Heat Capacity 1.0000 (kJ/kg)		
SATURATION PROFILE								
Vapor Saturation	Vapor Frac Flow	dKr/dSv	dKr/dSI	Total Mobility	dFv/dSv	lambda	Mass Inside	Enthalpy Inside
1.0000						0.000000		
1.0000						0.004179		
0.9575	0.999987	1.0000	0.0054	44.224435	0.000953	0.004179	0.018212	99746.431124
0.9561	0.999985	1.0000	0.0058	44.159017	0.001020	0.004472	0.013534	3405.156115
0.9547	0.999984	1.0000	0.0062	44.093602	0.001089	0.004775	0.014381	3527.841176
0.9533	0.999982	1.0000	0.0066	44.028191	0.001161	0.005088	0.015257	3651.273903
0.9519	0.999981	1.0000	0.0070	43.962785	0.001235	0.005413	0.016161	3775.459671
0.9504	0.999979	1.0000	0.0074	43.897384	0.001311	0.005747	0.017093	3900.403895
0.9490	0.999977	1.0000	0.0078	43.831987	0.001390	0.006093	0.018054	4026.112029
0.9476	0.999975	1.0000	0.0082	43.766594	0.001471	0.006450	0.019044	4152.589567
0.9462	0.999973	1.0000	0.0087	43.701207	0.001555	0.006817	0.020064	4279.842044
0.9448	0.999970	1.0000	0.0092	43.635824	0.001642	0.007195	0.021113	4407.875038
0.9433	0.999968	1.0000	0.0096	43.570447	0.001730	0.007585	0.022192	4536.694166
0.9419	0.999965	1.0000	0.0101	43.505075	0.001822	0.007985	0.023301	4666.305087
0.9405	0.999963	1.0000	0.0106	43.439708	0.001916	0.008397	0.024441	4796.713504
0.9391	0.999960	1.0000	0.0111	43.374346	0.002012	0.008820	0.025611	4927.925160
0.9377	0.999957	1.0000	0.0117	43.308991	0.002111	0.009254	0.026812	5059.945842
0.9363	0.999954	1.0000	0.0122	43.243641	0.002213	0.009699	0.028044	5192.781380
0.9348	0.999951	1.0000	0.0127	43.178297	0.002317	0.010156	0.029308	5326.437647
0.9334	0.999947	1.0000	0.0133	43.112959	0.002424	0.010625	0.030603	5460.920562
0.9320	0.999944	1.0000	0.0139	43.047627	0.002534	0.011105	0.031931	5596.236084
0.9306	0.999940	1.0000	0.0145	42.982302	0.002646	0.011596	0.033290	5732.390222
0.9292	0.999936	1.0000	0.0151	42.916983	0.002761	0.012100	0.034683	5869.389025
0.9277	0.999932	1.0000	0.0157	42.851670	0.002878	0.012615	0.036108	6007.238590
0.9263	0.999928	1.0000	0.0163	42.786364	0.002998	0.013142	0.037566	6145.945058
0.9249	0.999924	1.0000	0.0169	42.721065	0.003121	0.013680	0.039058	6285.514619
0.9235	0.999919	1.0000	0.0176	42.655773	0.003247	0.014231	0.040583	6425.953506
0.9221	0.999915	1.0000	0.0182	42.590488	0.003375	0.014794	0.042143	6567.268001
0.9207	0.999910	1.0000	0.0189	42.525211	0.003506	0.015369	0.043736	6709.464433
0.9192	0.999905	1.0000	0.0196	42.459940	0.003640	0.015956	0.045365	6852.549177
0.9178	0.999900	1.0000	0.0203	42.394677	0.003777	0.016556	0.047028	6996.528658
0.9164	0.999894	1.0000	0.0210	42.329422	0.003917	0.017168	0.048727	7141.409349
0.9150	0.999888	1.0000	0.0217	42.264174	0.004059	0.017792	0.050461	7287.197770
0.9136	0.999883	1.0000	0.0224	42.198935	0.004205	0.018429	0.052231	7433.900493
0.9122	0.999876	1.0000	0.0232	42.133703	0.004353	0.019078	0.054037	7581.524138
0.9107	0.999870	1.0000	0.0239	42.068479	0.004504	0.019740	0.055880	7730.075374
0.9093	0.999864	1.0000	0.0247	42.003264	0.004658	0.020415	0.057759	7879.560923
0.9079	0.999857	1.0000	0.0254	41.938057	0.004815	0.021103	0.059676	8029.987556
0.9065	0.999850	1.0000	0.0262	41.872859	0.004974	0.021803	0.061630	8181.362096
0.9051	0.999843	1.0000	0.0270	41.807669	0.005137	0.022517	0.063622	8333.691418
0.9036	0.999835	1.0000	0.0279	41.742488	0.005303	0.023244	0.065652	8486.982449
0.9022	0.999828	1.0000	0.0287	41.677316	0.005472	0.023983	0.067721	8641.242167
0.9008	0.999820	1.0000	0.0295	41.612153	0.005644	0.024736	0.069828	8796.477605
0.8994	0.999812	1.0000	0.0304	41.546999	0.005818	0.025502	0.071975	8952.695849
0.8980	0.999803	1.0000	0.0312	41.481855	0.005996	0.026282	0.074161	9109.904039
0.8966	0.999795	1.0000	0.0321	41.416720	0.006177	0.027075	0.076387	9268.109369
0.8951	0.999786	1.0000	0.0330	41.351594	0.006361	0.027882	0.078654	9427.319087
0.8937	0.999777	1.0000	0.0339	41.286479	0.006548	0.028702	0.080960	9587.540499
0.8923	0.999767	1.0000	0.0348	41.221373	0.006739	0.029536	0.083308	9748.780963
0.8909	0.999758	1.0000	0.0357	41.156277	0.006932	0.030384	0.085698	9911.047897
0.8895	0.999748	1.0000	0.0367	41.091191	0.007129	0.031246	0.088128	10074.348773
0.8881	0.999737	1.0000	0.0376	41.026115	0.007328	0.032121	0.090601	10238.691122
0.8866	0.999727	1.0000	0.0386	40.961050	0.007531	0.033011	0.093117	10404.082531
0.0000						0.033011		
0.0000						1.000000		

Spreadsheet for Calculation of Stream-Water Saturation Profiles

Injection Temperature Initial Temperature Matrix Heat Capacity
1000 °K 350 °K 1.0000 (kJ/kg)

TRAILING SHOCK CALCULATIONS

Saturation	OF	Wave V	Flow V	Shock V	f _v	dKrv/dSv	dKr/dSI
0.7500	1.54E-01	0.159542	0.347958	0.005597	0.996549	1.0000	0.1875
0.875	3.56E-02	0.039939	0.428483	0.004333	0.999629	1.0000	0.0469
0.9375	5.11E-03	0.009299	0.437912	0.004185	0.999957	1.0000	0.0117
0.96875	-1.95E-03	0.002226	0.438212	0.004181	0.999995	1.0000	0.0029
0.953125	9.41E-04	0.005121	0.438292	0.004179	0.999982	1.0000	0.0066
0.9609375	-6.62E-04	0.003517	0.438299	0.004179	0.999990	1.0000	0.0046
0.95703125	1.00E-04	0.004279	0.438309	0.004179	0.999986	1.0000	0.0055
0.958984375	-2.91E-04	0.003888	0.438307	0.004179	0.999988	1.0000	0.0050
0.9580078125	-9.78E-05	0.004081	0.438309	0.004179	0.999987	1.0000	0.0053
0.9575195313	5.55E-07	0.004180	0.438309	0.004179	0.999987	1.0000	0.0054
0.9577636719	-4.88E-05	0.004130	0.438309	0.004179	0.999987	1.0000	0.0054
0.9576416016	-2.41E-05	0.004155	0.438309	0.004179	0.999987	1.0000	0.0054
0.9575805664	-1.18E-05	0.004167	0.438309	0.004179	0.999987	1.0000	0.0054
0.9575500488	-5.63E-06	0.004174	0.438309	0.004179	0.999987	1.0000	0.0054
0.95753479	-2.54E-06	0.004177	0.438309	0.004179	0.999987	1.0000	0.0054
0.9575271606	-9.91E-07	0.004178	0.438309	0.004179	0.999987	1.0000	0.0054
0.9575233459	-2.18E-07	0.004179	0.438309	0.004179	0.999987	1.0000	0.0054
0.9575214386	1.69E-07	0.004179	0.438309	0.004179	0.999987	1.0000	0.0054
0.9575223923	-2.47E-08	0.004179	0.438309	0.004179	0.999987	1.0000	0.0054
0.9575219154	7.20E-08	0.004179	0.438309	0.004179	0.999987	1.0000	0.0054
0.9575221539	2.36E-08	0.004179	0.438309	0.004179	0.999987	1.0000	0.0054
0.9575222731	-5.07E-10	0.004179	0.438309	0.004179	0.999987	1.0000	0.0054
0.9575222135	1.16E-08	0.004179	0.438309	0.004179	0.999987	1.0000	0.0054
0.9575222433	5.53E-09	0.004179	0.438309	0.004179	0.999987	1.0000	0.0054
0.9575222582	2.51E-09	0.004179	0.438309	0.004179	0.999987	1.0000	0.0054
0.9575222656	1.00E-09	0.004179	0.438309	0.004179	0.999987	1.0000	0.0054

Saturation	Total Mob	dFv/dSv	G	F	Gamma	Theta	High	Low
0.75	34.759228	0.045851	220.095758	12.870589	1.1794E+07	30550.407113	1	0.5
0.875	40.427490	0.009321	115.033000	10.281953	1.1701E+07	28275.535543	1	0.75
0.9375	43.300978	0.002124	62.501620	10.006619	1.1655E+07	28033.574650	1	0.875
0.96875	44.742642	0.000508	36.235931	9.974642	1.1632E+07	28005.473055	1	0.9375
0.953125	44.021547	0.001168	49.368776	9.985337	1.1643E+07	28014.871837	0.96875	0.9375
0.9609375	44.382039	0.000802	42.802353	9.978906	1.1638E+07	28009.220503	0.96875	0.953125
0.95703125	44.201778	0.000976	46.085564	9.981821	1.1641E+07	28011.782338	0.9609375	0.953125
0.958984375	44.291905	0.000887	44.443959	9.980292	1.1639E+07	28010.438726	0.9609375	0.95703125
0.9580078125	44.246841	0.000931	45.264762	9.981039	1.1640E+07	28011.094453	0.958984375	0.95703125
0.9575195313	44.224309	0.000954	45.675163	9.981425	1.1640E+07	28011.434324	0.9580078125	0.95703125
0.9577636719	44.235575	0.000942	45.469962	9.981231	1.1640E+07	28011.263377	0.9580078125	0.95751953125
0.9576416016	44.229942	0.000948	45.572563	9.981328	1.1640E+07	28011.348597	0.95776367188	0.95751953125
0.9575805664	44.227125	0.000951	45.623863	9.981376	1.1640E+07	28011.391397	0.95764160156	0.95751953125
0.9575500488	44.225717	0.000952	45.649513	9.981401	1.1640E+07	28011.412845	0.95758056641	0.95751953125
0.95753479	44.225013	0.000953	45.662338	9.981413	1.1640E+07	28011.423581	0.95755004883	0.95751953125
0.9575271606	44.224661	0.000953	45.668750	9.981419	1.1640E+07	28011.428952	0.95753479004	0.95751953125
0.9575233459	44.224485	0.000953	45.671957	9.981422	1.1640E+07	28011.431638	0.95752716064	0.95751953125
0.9575214386	44.224397	0.000954	45.673560	9.981424	1.1640E+07	28011.432981	0.95752334595	0.95751953125
0.9575223923	44.224441	0.000953	45.672758	9.981423	1.1640E+07	28011.432309	0.95752334595	0.9575214386
0.9575219154	44.224419	0.000953	45.673159	9.981423	1.1640E+07	28011.432645	0.95752239227	0.9575214386
0.9575221539	44.224430	0.000953	45.672959	9.981423	1.1640E+07	28011.432477	0.95752239227	0.95752191544
0.9575222731	44.224436	0.000953	45.672858	9.981423	1.1640E+07	28011.432393	0.95752239227	0.95752215385
0.9575222135	44.224433	0.000953	45.672909	9.981423	1.1640E+07	28011.432435	0.95752227306	0.95752215385
0.9575222433	44.224434	0.000953	45.672883	9.981423	1.1640E+07	28011.432414	0.95752227306	0.95752221346
0.9575222582	44.224435	0.000953	45.672871	9.981423	1.1640E+07	28011.432404	0.95752227306	0.95752224326
0.9575222656	44.224435	0.000953	45.672865	9.981423	1.1640E+07	28011.432399	0.95752227306	0.95752225816

Spreadsheet for Calculation of Stream-Water Saturation Profiles

Injection Temperature Initial Temperature Matrix Heat Capacity
1000 °K 350 °K 1.0000 (kJ/kg)

LEADING SHOCK CALCULATIONS

Saturation	OF	Wave V	Flow V	Shock V	fv	dKrv/dSv	dKrl/dSl
0.7500	1.67E-01	0.200969	0.008442	0.034321	0.996549	1.0000	0.1875
0.875	7.84E-03	0.040855	0.007533	0.033017	0.999629	1.0000	0.0469
0.9375	-2.38E-02	0.009308	0.007596	0.033107	0.999957	1.0000	0.0117
0.90625	-1.11E-02	0.021920	0.007540	0.033027	0.999849	1.0000	0.0264
0.890625	-2.47E-03	0.030543	0.007529	0.033012	0.999756	1.0000	0.0359
0.8828125	2.47E-03	0.035480	0.007529	0.033012	0.999697	1.0000	0.0412
0.88671875	-3.30E-05	0.032958	0.007529	0.033011	0.999728	1.0000	0.0385
0.884765625	1.19E-03	0.034206	0.007529	0.033011	0.999713	1.0000	0.0398
0.8857421875	5.67E-04	0.033578	0.007529	0.033011	0.999720	1.0000	0.0392
0.8862304688	2.56E-04	0.033267	0.007529	0.033011	0.999724	1.0000	0.0388
0.8864746094	1.02E-04	0.033112	0.007529	0.033011	0.999726	1.0000	0.0387
0.8865966797	2.42E-05	0.033035	0.007529	0.033011	0.999727	1.0000	0.0386
0.8866577148	-1.44E-05	0.032997	0.007529	0.033011	0.999727	1.0000	0.0385
0.8866271973	4.91E-06	0.033016	0.007529	0.033011	0.999727	1.0000	0.0386
0.8866424561	-4.74E-06	0.033006	0.007529	0.033011	0.999727	1.0000	0.0385
0.8866348267	8.31E-08	0.033011	0.007529	0.033011	0.999727	1.0000	0.0386
0.8866386414	-2.33E-06	0.033009	0.007529	0.033011	0.999727	1.0000	0.0386
0.886636734	-1.12E-06	0.033010	0.007529	0.033011	0.999727	1.0000	0.0386
0.8866357803	-5.20E-07	0.033010	0.007529	0.033011	0.999727	1.0000	0.0386
0.8866353035	-2.18E-07	0.033011	0.007529	0.033011	0.999727	1.0000	0.0386
0.8866350651	-6.77E-08	0.033011	0.007529	0.033011	0.999727	1.0000	0.0386
0.8866349459	7.72E-09	0.033011	0.007529	0.033011	0.999727	1.0000	0.0386
0.8866350055	-3.00E-08	0.033011	0.007529	0.033011	0.999727	1.0000	0.0386
0.8866349757	-1.11E-08	0.033011	0.007529	0.033011	0.999727	1.0000	0.0386
0.8866349608	-1.71E-09	0.033011	0.007529	0.033011	0.999727	1.0000	0.0386
0.8866349533	3.01E-09	0.033011	0.007529	0.033011	0.999727	1.0000	0.0386

Saturation	Total Mob	dFv/dSv	G	F	Gamma	Theta	High	Low
0.75	34.759228	0.045851	220.095758	12.870589	1.1794E+07	30550.407113	1	0.5
0.875	40.427490	0.009321	115.033000	10.281953	1.1701E+07	28275.535543	1	0.75
0.9375	43.300978	0.002124	62.501620	10.006619	1.1655E+07	28033.574650	1	0.875
0.90625	41.862126	0.005001	88.767310	10.097238	1.1678E+07	28113.209409	0.9375	0.875
0.890625	41.144193	0.006968	101.900155	10.175426	1.1690E+07	28181.920650	0.90625	0.875
0.8828125	40.785677	0.008095	108.466577	10.224828	1.1695E+07	28225.334700	0.890625	0.875
0.88671875	40.964895	0.007519	105.183366	10.199203	1.1693E+07	28202.815133	0.890625	0.8828125
0.884765625	40.875276	0.007804	106.824972	10.211779	1.1694E+07	28213.867353	0.88671875	0.8828125
0.8857421875	40.920083	0.007661	106.004169	10.205432	1.1693E+07	28208.289909	0.88671875	0.884765625
0.8862304688	40.942489	0.007590	105.593767	10.202303	1.1693E+07	28205.539756	0.88671875	0.8857421875
0.8864746094	40.953692	0.007555	105.388567	10.200749	1.1693E+07	28204.174262	0.88671875	0.88623046875
0.8865966797	40.959294	0.007537	105.285966	10.199975	1.1693E+07	28203.493903	0.88671875	0.88647460938
0.8866577148	40.962095	0.007528	105.234666	10.199589	1.1693E+07	28203.154319	0.88671875	0.88659667969
0.8866271973	40.960694	0.007533	105.260316	10.199782	1.1693E+07	28203.324062	0.88665771484	0.88659667969
0.8866424561	40.961394	0.007530	105.247491	10.199685	1.1693E+07	28203.239178	0.88665771484	0.88662719727
0.8866348267	40.961044	0.007531	105.253904	10.199733	1.1693E+07	28203.281617	0.88664245605	0.88662719727
0.8866386414	40.961219	0.007531	105.250698	10.199709	1.1693E+07	28203.260397	0.88664245605	0.88663482666
0.886636734	40.961132	0.007531	105.252301	10.199721	1.1693E+07	28203.271006	0.88663864136	0.88663482666
0.8866357803	40.961088	0.007531	105.253102	10.199727	1.1693E+07	28203.276312	0.88663673401	0.88663482666
0.8866353035	40.961066	0.007531	105.253503	10.199730	1.1693E+07	28203.278964	0.88663578033	0.88663482666
0.8866350651	40.961055	0.007531	105.253703	10.199732	1.1693E+07	28203.280290	0.8866353035	0.88663482666
0.8866349459	40.961050	0.007531	105.253804	10.199733	1.1693E+07	28203.280954	0.88663506508	0.88663482666
0.8866350055	40.961052	0.007531	105.253753	10.199732	1.1693E+07	28203.280622	0.88663506508	0.88663494587
0.8866349757	40.961051	0.007531	105.253779	10.199732	1.1693E+07	28203.280788	0.88663500547	0.88663494587
0.8866349608	40.961050	0.007531	105.253791	10.199733	1.1693E+07	28203.280871	0.88663497567	0.88663494587
0.8866349533	40.961050	0.007531	105.253797	10.199733	1.1693E+07	28203.280912	0.88663496077	0.88663494587

D.3 Changes in Initial Temperature

The next eight worksheets examine the effect of initial temperature. The initial temperature is entered in cell B23. The section contains worksheets with the injection temperature ranging from 300--475 K, in 25 K intervals.

Spreadsheet for Calculation of Stream-Water Saturation Profiles

Injection Temperature
650 °K

Initial Temperature
300 °K

Matrix Heat Capacity
1.0000 (kJ/kg)

MATRIX PROPERTIES

Porosity	Cp Matrix	Density	Rho * Cp
0.10	1.00	2650.00	2650.0000
Nw	Ng	Swl	Denom
3.00	1.00	0.00	1.000000

SATURATION CONDITIONS

Tsaturation = 485.57

	Volumes (m3/kg)	Enthalpies (kJ/kg)	Densities (kg/m3)	Viscosities (cp)	Saturation Step
Liquid	0.001176	901.41	850.4723	0.1303	0.0011764038
Vapor	0.100298	2808.52	9.970241	0.0217	

BOUNDARY CONDITIONS

	Temperature	Velocity	Heat Capacity	Wave Velocity	Density	Enthalpy
Injection	650	1.000000	2.30	0.006622	6.882648	3199.91
Initial	300	0.010726	4.16	0.015992	1004.6293	112.70
	G	F	Gamma	Theta		
Injection	650	6.88	6.88	15524523.87	22023.87	
Initial	300	1004.63	1004.63	7268218.71	113218.71	

SHOCK CONDITIONS

	Initial Guess Sv-Hi	Initial Guess Sv-Low	Vapor Saturation	Objective Function	Two-Phase Wave Velocity	Upstream Flow Velocity	Shock Velocity	Vapor Frac Flow
Trailing	1	0.5	0.9570	1.4356E-09	0.0068	0.692182	0.0068	1.0000
Leading	1	0.5	0.8981	4.0467E-09	0.0414	0.010726	0.0414	0.9998
	dKrv/dSv	dKrl/dSl	Total Mobility	dFv/dSv	G	F'	Gamma	Theta'
Trailing	1.0000	0.0056	44.1982	0.0010	46.1514	9.9819	1.1641E+07	28011.8389
Leading	1.0000	0.0311	41.4890	0.0060	95.5899	10.1346	1.1684E+07	28146.0687

MATERIAL BALANCES

	Inside	Initial	Injected	Produced	Balance	Error
Mass	96.569994	100.462933	6.882648	10.775582	0.0000	0.0000%
Enthalpy	747635.0622	726821.8712	22023.8721	1214.3758	-3.6947	0.0005%

Spreadsheet for Calculation of Stream-Water Saturation Profiles

Injection Temperature 650 °K		Initial Temperature 300 °K				Matrix Heat Capacity 1.0000 (kJ/kg)			
SATURATION PROFILE									
Vapor Saturation	Vapor Frac Flow	dKrv/dSv	dKr/dSI	Total Mobility	dFv/dSv	lambda	Mass Inside	Enthalpy Inside	
1.0000						0.000000			
1.0000						0.006783			
0.9570	0.999986	1.0000	0.0056	44.198164	0.000980	0.006783	0.046687	105308.165674	
0.9558	0.999985	1.0000	0.0059	44.143883	0.001036	0.007171	0.018082	4512.817923	
0.9546	0.999984	1.0000	0.0062	44.089604	0.001094	0.007570	0.019010	4646.402924	
0.9534	0.999982	1.0000	0.0065	44.035329	0.001153	0.007981	0.019964	4780.663193	
0.9522	0.999981	1.0000	0.0068	43.981056	0.001214	0.008403	0.020944	4915.602756	
0.9511	0.999980	1.0000	0.0072	43.926786	0.001277	0.008837	0.021949	5051.225662	
0.9499	0.999978	1.0000	0.0075	43.872519	0.001341	0.009282	0.022980	5187.535987	
0.9487	0.999976	1.0000	0.0079	43.818256	0.001407	0.009739	0.024037	5324.537830	
0.9475	0.999975	1.0000	0.0083	43.763996	0.001475	0.010208	0.025120	5462.235316	
0.9464	0.999973	1.0000	0.0086	43.709739	0.001544	0.010689	0.026230	5600.632596	
0.9452	0.999971	1.0000	0.0090	43.655486	0.001615	0.011182	0.027367	5739.733845	
0.9440	0.999969	1.0000	0.0094	43.601236	0.001688	0.011686	0.028530	5879.543266	
0.9428	0.999967	1.0000	0.0098	43.546989	0.001763	0.012203	0.029721	6020.065085	
0.9417	0.999965	1.0000	0.0102	43.492747	0.001839	0.012732	0.030938	6161.303557	
0.9405	0.999963	1.0000	0.0106	43.438508	0.001918	0.013273	0.032184	6303.262960	
0.9393	0.999960	1.0000	0.0111	43.384273	0.001997	0.013826	0.033457	6445.947603	
0.9381	0.999958	1.0000	0.0115	43.330041	0.002079	0.014391	0.034757	6589.361816	
0.9370	0.999956	1.0000	0.0119	43.275814	0.002163	0.014969	0.036086	6733.509960	
0.9358	0.999953	1.0000	0.0124	43.221591	0.002248	0.015559	0.037443	6878.396422	
0.9346	0.999950	1.0000	0.0128	43.167371	0.002335	0.016161	0.038829	7024.025615	
0.9334	0.999947	1.0000	0.0133	43.113156	0.002424	0.016776	0.040243	7170.401980	
0.9322	0.999945	1.0000	0.0138	43.058945	0.002514	0.017404	0.041686	7317.529986	
0.9311	0.999942	1.0000	0.0143	43.004739	0.002607	0.018044	0.043159	7465.414130	
0.9299	0.999938	1.0000	0.0147	42.950537	0.002701	0.018697	0.044660	7614.058934	
0.9287	0.999935	1.0000	0.0152	42.896339	0.002797	0.019363	0.046192	7763.468952	
0.9275	0.999932	1.0000	0.0158	42.842146	0.002895	0.020041	0.047752	7913.648764	
0.9264	0.999928	1.0000	0.0163	42.787958	0.002995	0.020733	0.049343	8064.602979	
0.9252	0.999925	1.0000	0.0168	42.733774	0.003097	0.021437	0.050964	8216.336234	
0.9240	0.999921	1.0000	0.0173	42.679595	0.003201	0.022155	0.052616	8368.853197	
0.9228	0.999917	1.0000	0.0179	42.625421	0.003306	0.022885	0.054298	8522.158563	
0.9217	0.999913	1.0000	0.0184	42.571251	0.003414	0.023629	0.056011	8676.257057	
0.9205	0.999909	1.0000	0.0190	42.517087	0.003523	0.024386	0.057755	8831.153433	
0.9193	0.999905	1.0000	0.0195	42.462928	0.003634	0.025156	0.059530	8986.852475	
0.9181	0.999901	1.0000	0.0201	42.408774	0.003747	0.025939	0.061337	9143.358996	
0.9170	0.999896	1.0000	0.0207	42.354625	0.003863	0.026736	0.063175	9300.677842	
0.9158	0.999892	1.0000	0.0213	42.300481	0.003980	0.027547	0.065046	9458.813886	
0.9146	0.999887	1.0000	0.0219	42.246343	0.004099	0.028371	0.066949	9617.772033	
0.9134	0.999882	1.0000	0.0225	42.192210	0.004220	0.029208	0.068884	9777.557218	
0.9122	0.999877	1.0000	0.0231	42.138083	0.004343	0.030059	0.070852	9938.174408	
0.9111	0.999872	1.0000	0.0237	42.083962	0.004468	0.030924	0.072853	10099.628600	
0.9099	0.999866	1.0000	0.0244	42.029846	0.004595	0.031803	0.074887	10261.924822	
0.9087	0.999861	1.0000	0.0250	41.975735	0.004724	0.032696	0.076955	10425.068137	
0.9075	0.999855	1.0000	0.0256	41.921631	0.004855	0.033603	0.079056	10589.063634	
0.9064	0.999849	1.0000	0.0263	41.867533	0.004988	0.034524	0.081191	10753.916439	
0.9052	0.999844	1.0000	0.0270	41.813440	0.005123	0.035459	0.083360	10919.631709	
0.9040	0.999837	1.0000	0.0276	41.759354	0.005260	0.036408	0.085564	11086.214631	
0.9028	0.999831	1.0000	0.0283	41.705273	0.005399	0.037371	0.087802	11253.670427	
0.9017	0.999825	1.0000	0.0290	41.651199	0.005540	0.038349	0.090076	11422.004352	
0.9005	0.999818	1.0000	0.0297	41.597131	0.005684	0.039341	0.092384	11591.221693	
0.8993	0.999811	1.0000	0.0304	41.543070	0.005829	0.040347	0.094728	11761.327771	
0.8981	0.999804	1.0000	0.0311	41.489014	0.005977	0.041369	0.097108	11932.327941	
0.0000						0.041369			
0.0000						1.000000			

Spreadsheet for Calculation of Stream-Water Saturation Profiles

Injection Temperature 650 °K Initial Temperature 300 °K Matrix Heat Capacity 1.0000 (kJ/kg)

TRAILING SHOCK CALCULATIONS

Saturation	OF	Wave V	Flow V	Shock V	fv	dKrv/dSv	dKr/dSI
0.7500	2.42E-01	0.255386	0.556992	0.013421	0.996549	1.0000	0.1875
0.875	5.56E-02	0.063132	0.677295	0.007514	0.999629	1.0000	0.0469
0.9375	7.87E-03	0.014687	0.691596	0.006812	0.999957	1.0000	0.0117
0.96875	-3.28E-03	0.003516	0.692013	0.006792	0.999995	1.0000	0.0029
0.953125	1.30E-03	0.008087	0.692162	0.006784	0.999982	1.0000	0.0066
0.9609375	-1.23E-03	0.005554	0.692162	0.006784	0.999990	1.0000	0.0046
0.95703125	-2.54E-05	0.006758	0.692182	0.006783	0.999986	1.0000	0.0055
0.955078125	6.23E-04	0.007406	0.692178	0.006784	0.999984	1.0000	0.0061
0.9560546875	2.95E-04	0.007078	0.692181	0.006783	0.999985	1.0000	0.0058
0.9565429688	1.34E-04	0.006917	0.692182	0.006783	0.999986	1.0000	0.0057
0.9567871094	5.40E-05	0.006837	0.692182	0.006783	0.999986	1.0000	0.0056
0.9569091797	1.42E-05	0.006798	0.692182	0.006783	0.999986	1.0000	0.0056
0.9569702148	-5.61E-06	0.006778	0.692182	0.006783	0.999986	1.0000	0.0056
0.9569396973	4.30E-06	0.006788	0.692182	0.006783	0.999986	1.0000	0.0056
0.9569549561	-6.54E-07	0.006783	0.692182	0.006783	0.999986	1.0000	0.0056
0.9569473267	1.82E-06	0.006785	0.692182	0.006783	0.999986	1.0000	0.0056
0.9569511414	5.84E-07	0.006784	0.692182	0.006783	0.999986	1.0000	0.0056
0.9569530487	-3.48E-08	0.006783	0.692182	0.006783	0.999986	1.0000	0.0056
0.956952095	2.75E-07	0.006784	0.692182	0.006783	0.999986	1.0000	0.0056
0.9569525719	1.20E-07	0.006783	0.692182	0.006783	0.999986	1.0000	0.0056
0.9569528103	4.26E-08	0.006783	0.692182	0.006783	0.999986	1.0000	0.0056
0.9569529295	3.85E-09	0.006783	0.692182	0.006783	0.999986	1.0000	0.0056
0.9569529891	-1.55E-08	0.006783	0.692182	0.006783	0.999986	1.0000	0.0056
0.9569529593	-5.82E-09	0.006783	0.692182	0.006783	0.999986	1.0000	0.0056
0.9569529444	-9.83E-10	0.006783	0.692182	0.006783	0.999986	1.0000	0.0056
0.9569529369	1.44E-09	0.006783	0.692182	0.006783	0.999986	1.0000	0.0056

Saturation	Total Mob	dFv/dSv	G	F	Gamma	Theta	High	Low
0.75	34.759228	0.045851	220.095758	12.870589	1.1794E+07	30550.407113	1	0.5
0.875	40.427490	0.009321	115.033000	10.281953	1.1701E+07	28275.535543	1	0.75
0.9375	43.300978	0.002124	62.501620	10.006619	1.1655E+07	28033.574650	1	0.875
0.96875	44.742642	0.000508	36.235931	9.974642	1.1632E+07	28005.473055	1	0.9375
0.953125	44.021547	0.001168	49.368776	9.985337	1.1643E+07	28014.871837	0.96875	0.9375
0.9609375	44.382039	0.000802	42.802353	9.978906	1.1638E+07	28009.220503	0.96875	0.953125
0.95703125	44.201778	0.000976	46.085564	9.981821	1.1641E+07	28011.782338	0.9609375	0.953125
0.955078125	44.111658	0.001070	47.727170	9.983500	1.1642E+07	28013.257853	0.95703125	0.953125
0.9560546875	44.156717	0.001023	46.906367	9.982642	1.1641E+07	28012.503198	0.95703125	0.955078125
0.9565429688	44.179247	0.000999	46.495966	9.982227	1.1641E+07	28012.138595	0.95703125	0.9560546875
0.9567871094	44.190513	0.000988	46.290765	9.982023	1.1641E+07	28011.959430	0.95703125	0.95654296875
0.9569091797	44.196145	0.000982	46.188165	9.981922	1.1641E+07	28011.870625	0.95703125	0.95678710938
0.9569702148	44.198962	0.000979	46.136864	9.981871	1.1641E+07	28011.826417	0.95703125	0.95690917969
0.9569396973	44.197553	0.000981	46.162515	9.981897	1.1641E+07	28011.848505	0.95697021484	0.95690917969
0.9569549561	44.198258	0.000980	46.149690	9.981884	1.1641E+07	28011.837457	0.95697021484	0.95693969727
0.9569473267	44.197905	0.000980	46.156102	9.981890	1.1641E+07	28011.842980	0.95695495605	0.95693969727
0.9569511414	44.198082	0.000980	46.152896	9.981887	1.1641E+07	28011.840218	0.95695495605	0.95694732666
0.9569530487	44.198170	0.000980	46.151293	9.981886	1.1641E+07	28011.838838	0.95695495605	0.95695114136
0.956952095	44.198126	0.000980	46.152094	9.981886	1.1641E+07	28011.839528	0.95695304871	0.95695114136
0.9569525719	44.198148	0.000980	46.151693	9.981886	1.1641E+07	28011.839183	0.95695304871	0.95695209503
0.9569528103	44.198159	0.000980	46.151493	9.981886	1.1641E+07	28011.839010	0.95695304871	0.95695257187
0.9569529295	44.198164	0.000980	46.151393	9.981886	1.1641E+07	28011.838924	0.95695304871	0.95695281029
0.9569529891	44.198167	0.000980	46.151343	9.981886	1.1641E+07	28011.838881	0.95695304871	0.9569529295
0.9569529593	44.198165	0.000980	46.151368	9.981886	1.1641E+07	28011.838902	0.9569529891	0.9569529295
0.9569529444	44.198165	0.000980	46.151380	9.981886	1.1641E+07	28011.838913	0.9569529593	0.9569529295
0.9569529369	44.198164	0.000980	46.151387	9.981886	1.1641E+07	28011.838919	0.9569529444	0.9569529295

Spreadsheet for Calculation of Stream-Water Saturation Profiles

Injection Temperature 650 °K		Initial Temperature 300 °K		Matrix Heat Capacity 1.0000 (kJ/kg)				
LEADING SHOCK CALCULATIONS								
Saturation	OP	Wave V	Flow V	Shock V	f_v	dK_{rv}/dS_v	dK_{rl}/dS_l	
0.7500	2.74E-01	0.317373	0.012277	0.043658	0.996549	1.0000	0.1875	
0.875	2.31E-02	0.064519	0.010751	0.041405	0.999629	1.0000	0.0469	
0.9375	-2.68E-02	0.014699	0.010782	0.041451	0.999957	1.0000	0.0117	
0.90625	-6.76E-03	0.034616	0.010729	0.041373	0.999849	1.0000	0.0264	
0.890625	6.86E-03	0.048233	0.010728	0.041372	0.999756	1.0000	0.0359	
0.8984375	-2.66E-04	0.041103	0.010726	0.041369	0.999806	1.0000	0.0309	
0.89453125	3.22E-03	0.044586	0.010726	0.041369	0.999782	1.0000	0.0334	
0.896484375	1.46E-03	0.042824	0.010726	0.041369	0.999794	1.0000	0.0321	
0.8974609375	5.90E-04	0.041958	0.010726	0.041369	0.999800	1.0000	0.0315	
0.8979492188	1.61E-04	0.041529	0.010726	0.041369	0.999803	1.0000	0.0312	
0.8981933594	-5.30E-05	0.041316	0.010726	0.041369	0.999805	1.0000	0.0311	
0.8980712891	5.38E-05	0.041422	0.010726	0.041369	0.999804	1.0000	0.0312	
0.8981323242	3.75E-07	0.041369	0.010726	0.041369	0.999804	1.0000	0.0311	
0.8981628418	-2.63E-05	0.041342	0.010726	0.041369	0.999805	1.0000	0.0311	
0.898147583	-1.30E-05	0.041356	0.010726	0.041369	0.999805	1.0000	0.0311	
0.8981399536	-6.29E-06	0.041362	0.010726	0.041369	0.999804	1.0000	0.0311	
0.8981361389	-2.96E-06	0.041366	0.010726	0.041369	0.999804	1.0000	0.0311	
0.8981342316	-1.29E-06	0.041367	0.010726	0.041369	0.999804	1.0000	0.0311	
0.8981332779	-4.58E-07	0.041368	0.010726	0.041369	0.999804	1.0000	0.0311	
0.8981328011	-4.15E-08	0.041369	0.010726	0.041369	0.999804	1.0000	0.0311	
0.8981325626	1.67E-07	0.041369	0.010726	0.041369	0.999804	1.0000	0.0311	
0.8981326818	6.27E-08	0.041369	0.010726	0.041369	0.999804	1.0000	0.0311	
0.8981327415	1.06E-08	0.041369	0.010726	0.041369	0.999804	1.0000	0.0311	
0.8981327713	-1.55E-08	0.041369	0.010726	0.041369	0.999804	1.0000	0.0311	
0.8981327564	-2.47E-09	0.041369	0.010726	0.041369	0.999804	1.0000	0.0311	
0.8981327489	4.05E-09	0.041369	0.010726	0.041369	0.999804	1.0000	0.0311	
Saturation	Total Mob	dF_v/dS_v	G	F	Gamma	Theta	High	Low
0.75	34.759228	0.045851	220.095758	12.870589	1.1794E+07	30550.407113	1	0.5
0.875	40.427490	0.009321	115.033000	10.281953	1.1701E+07	28275.535543	1	0.75
0.9375	43.300978	0.002124	62.501620	10.006619	1.1655E+07	28033.574650	1	0.875
0.90625	41.862126	0.005001	88.767310	10.097238	1.1678E+07	28113.209409	0.9375	0.875
0.890625	41.144193	0.006968	101.900155	10.175426	1.1690E+07	28181.920650	0.90625	0.875
0.8984375	41.503017	0.005938	95.333732	10.133103	1.1684E+07	28144.727756	0.90625	0.890625
0.89453125	41.323568	0.006441	98.616944	10.153419	1.1687E+07	28162.581158	0.8984375	0.890625
0.896484375	41.413283	0.006187	96.975338	10.143055	1.1685E+07	28153.472957	0.8984375	0.89453125
0.8974609375	41.458148	0.006062	96.154535	10.138028	1.1685E+07	28149.055510	0.8984375	0.896484375
0.8979492188	41.480582	0.006000	95.744134	10.135553	1.1684E+07	28146.880487	0.8984375	0.8974609375
0.8981933594	41.491799	0.005969	95.538933	10.134325	1.1684E+07	28145.801343	0.8984375	0.89794921875
0.8980712891	41.486191	0.005984	95.641533	10.134938	1.1684E+07	28146.340220	0.89819335938	0.89794921875
0.8981323242	41.488995	0.005977	95.590233	10.134631	1.1684E+07	28146.070608	0.89819335938	0.89807128906
0.8981628418	41.490397	0.005973	95.564583	10.134478	1.1684E+07	28145.935932	0.89819335938	0.89813232422
0.898147583	41.489696	0.005975	95.577408	10.134555	1.1684E+07	28146.003259	0.8981628418	0.89813232422
0.8981399536	41.489345	0.005976	95.583821	10.134593	1.1684E+07	28146.036931	0.89814758301	0.89813232422
0.8981361389	41.489170	0.005976	95.587027	10.134612	1.1684E+07	28146.053768	0.89813995361	0.89813232422
0.8981342316	41.489082	0.005976	95.588630	10.134622	1.1684E+07	28146.062188	0.89813613892	0.89813232422
0.8981332779	41.489039	0.005976	95.589432	10.134627	1.1684E+07	28146.066398	0.89813423157	0.89813232422
0.8981328011	41.489017	0.005977	95.589833	10.134629	1.1684E+07	28146.068503	0.89813327789	0.89813232422
0.8981325626	41.489006	0.005977	95.590033	10.134630	1.1684E+07	28146.069555	0.89813280106	0.89813232422
0.8981326818	41.489011	0.005977	95.589933	10.134630	1.1684E+07	28146.069029	0.89813280106	0.89813256264
0.8981327415	41.489014	0.005977	95.589883	10.134629	1.1684E+07	28146.068766	0.89813280106	0.89813268185
0.8981327713	41.489015	0.005977	95.589858	10.134629	1.1684E+07	28146.068634	0.89813280106	0.89813274145
0.8981327564	41.489015	0.005977	95.589870	10.134629	1.1684E+07	28146.068700	0.89813277125	0.89813274145
0.8981327489	41.489014	0.005977	95.589876	10.134629	1.1684E+07	28146.068733	0.89813275635	0.89813274145

Spreadsheet for Calculation of Stream-Water Saturation Profiles

Injection Temperature
650 °K

Initial Temperature
325 °K

Matrix Heat Capacity
1.0000 (kJ/kg)

MATRIX PROPERTIES

Porosity	Cp Matrix	Density	Rho * Cp
0.10	1.00	2650.00	2650.0000
Nw	Ng	Swl	Denom
3.00	1.00	0.00	1.000000

SATURATION CONDITIONS

Tsaturation = 485.57

	Volumes (m3/kg)	Enthalpies (kJ/kg)	Densities (kg/m3)	Viscosities (cp)	Saturation Step
Liquid	0.001176	901.41	850.4723	0.1303	0.0012773478
Vapor	0.100298	2808.52	9.970241	0.0217	

BOUNDARY CONDITIONS

	Temperature	Velocity	Heat Capacity	Wave Velocity	Density	Enthalpy
Injection	650	1.000000	2.30	0.006622	6.882648	3199.91
Initial	325	0.011229	4.14	0.016483	990.6532	216.43
	G	F	Gamma	Theta		
Injection	650	6.88	6.88	15524523.87	22023.87	
Initial	325	990.65	990.65	7965654.57	214404.57	

SHOCK CONDITIONS

	Initial Guess		Vapor Saturation	Objective Function	Two-Phase Wave Velocity	Upstream Flow Velocity	Shock Velocity	Vapor Frac Flow
	Sv-Hi	Sv-Low						
Trailing	1	0.5	0.9570	1.4356E-09	0.0068	0.692182	0.0068	1.0000
Leading	1	0.5	0.8931	3.0084E-09	0.0459	0.011229	0.0459	0.9998
	dKrv/dSv	dKrl/dSl	Total Mobility	dFv/dSv	G	F'	Gamma	Theta'
Trailing	1.0000	0.0056	44.1982	0.0010	46.1514	9.9819	1.1641E+07	28011.8389
Leading	1.0000	0.0343	41.2572	0.0066	99.8321	10.1614	1.1688E+07	28169.5618

MATERIAL BALANCES

	Inside	Initial	Injected	Produced	Balance	Error
Mass	94.824078	99.065316	6.882648	11.123879	0.0000	0.0000%
Enthalpy	816186.1657	796565.4571	22023.8721	2407.5132	-4.3497	0.0005%

Spreadsheet for Calculation of Stream-Water Saturation Profiles

Injection Temperature 650 °K		Initial Temperature 325 °K				Matrix Heat Capacity 1.0000 (kJ/kg)		
SATURATION PROFILE								
Vapor Saturation	Vapor Frac Flow	dKrv/dSv	dKrI/dSI	Total Mobility	dFv/dSv	lambda	Mass Inside	Enthalpy Inside
1.0000						0.000000		
1.0000						0.006783		
0.9570	0.999986	1.0000	0.0056	44.198164	0.000980	0.006783	0.046687	105308.165674
0.9557	0.999985	1.0000	0.0059	44.139225	0.001041	0.007205	0.019676	4906.263740
0.9544	0.999983	1.0000	0.0062	44.080290	0.001104	0.007640	0.020773	5063.825641
0.9531	0.999982	1.0000	0.0066	44.021357	0.001169	0.008088	0.021903	5222.252643
0.9518	0.999980	1.0000	0.0070	43.962428	0.001235	0.008550	0.023065	5381.550348
0.9506	0.999979	1.0000	0.0073	43.903503	0.001304	0.009026	0.024261	5541.724393
0.9493	0.999977	1.0000	0.0077	43.844582	0.001375	0.009516	0.025490	5702.780456
0.9480	0.999975	1.0000	0.0081	43.785664	0.001448	0.010019	0.026752	5864.724249
0.9467	0.999973	1.0000	0.0085	43.726750	0.001522	0.010537	0.028048	6027.561524
0.9455	0.999971	1.0000	0.0089	43.667841	0.001599	0.011068	0.029378	6191.298073
0.9442	0.999969	1.0000	0.0093	43.608935	0.001678	0.011614	0.030743	6355.939723
0.9429	0.999967	1.0000	0.0098	43.550034	0.001759	0.012174	0.032142	6521.492342
0.9416	0.999965	1.0000	0.0102	43.491136	0.001842	0.012748	0.033576	6687.961839
0.9403	0.999962	1.0000	0.0107	43.432244	0.001927	0.013336	0.035045	6855.354160
0.9391	0.999960	1.0000	0.0111	43.373355	0.002014	0.013939	0.036549	7023.675291
0.9378	0.999957	1.0000	0.0116	43.314472	0.002103	0.014556	0.038089	7192.931260
0.9365	0.999955	1.0000	0.0121	43.255593	0.002194	0.015187	0.039666	7363.128134
0.9352	0.999952	1.0000	0.0126	43.196718	0.002288	0.015834	0.041278	7534.272021
0.9340	0.999949	1.0000	0.0131	43.137849	0.002383	0.016495	0.042927	7706.369069
0.9327	0.999946	1.0000	0.0136	43.078985	0.002481	0.017171	0.044613	7879.425471
0.9314	0.999942	1.0000	0.0141	43.020125	0.002580	0.017861	0.046336	8053.447458
0.9301	0.999939	1.0000	0.0146	42.961271	0.002682	0.018567	0.048097	8228.441303
0.9289	0.999936	1.0000	0.0152	42.902422	0.002786	0.019288	0.049895	8404.413324
0.9276	0.999932	1.0000	0.0157	42.843578	0.002893	0.020023	0.051731	8581.369880
0.9263	0.999928	1.0000	0.0163	42.784740	0.003001	0.020774	0.053606	8759.317372
0.9250	0.999924	1.0000	0.0169	42.725908	0.003112	0.021541	0.055519	8938.262247
0.9237	0.999920	1.0000	0.0174	42.667081	0.003225	0.022322	0.057472	9118.210992
0.9225	0.999916	1.0000	0.0180	42.608259	0.003340	0.023119	0.059463	9299.170141
0.9212	0.999912	1.0000	0.0186	42.549444	0.003457	0.023932	0.061494	9481.146270
0.9199	0.999907	1.0000	0.0192	42.490634	0.003577	0.024760	0.063565	9664.146001
0.9186	0.999903	1.0000	0.0199	42.431831	0.003699	0.025604	0.065676	9848.176001
0.9174	0.999898	1.0000	0.0205	42.373034	0.003823	0.026464	0.067828	10033.242980
0.9161	0.999893	1.0000	0.0211	42.314242	0.003950	0.027339	0.070020	10219.335397
0.9148	0.999888	1.0000	0.0218	42.255457	0.004079	0.028231	0.072254	10406.514954
0.9135	0.999882	1.0000	0.0224	42.196679	0.004210	0.029138	0.074529	10594.733661
0.9122	0.999877	1.0000	0.0231	42.137907	0.004343	0.030062	0.076846	10784.016533
0.9110	0.999871	1.0000	0.0238	42.079142	0.004479	0.031002	0.079205	10974.370693
0.9097	0.999865	1.0000	0.0245	42.020383	0.004617	0.031958	0.081607	11165.803072
0.9084	0.999859	1.0000	0.0252	41.961631	0.004758	0.032931	0.084052	11358.320707
0.9071	0.999853	1.0000	0.0259	41.902886	0.004900	0.033920	0.086539	11551.930684
0.9059	0.999847	1.0000	0.0266	41.844148	0.005046	0.034926	0.089070	11746.640138
0.9046	0.999840	1.0000	0.0273	41.785417	0.005194	0.035948	0.091646	11942.456250
0.9033	0.999834	1.0000	0.0281	41.726693	0.005344	0.036988	0.094265	12139.386254
0.9020	0.999827	1.0000	0.0288	41.667977	0.005496	0.038044	0.096929	12337.437430
0.9007	0.999820	1.0000	0.0296	41.609268	0.005651	0.039117	0.099637	12536.617110
0.8995	0.999812	1.0000	0.0303	41.550566	0.005809	0.040207	0.102392	12736.932676
0.8982	0.999805	1.0000	0.0311	41.491872	0.005969	0.041314	0.105191	12938.391559
0.8969	0.999797	1.0000	0.0319	41.433185	0.006131	0.042439	0.108037	13141.001243
0.8956	0.999789	1.0000	0.0327	41.374507	0.006296	0.043581	0.110929	13344.769261
0.8944	0.999781	1.0000	0.0335	41.315836	0.006464	0.044740	0.113868	13549.703201
0.8931	0.999773	1.0000	0.0343	41.257173	0.006634	0.045917	0.116854	13755.810700
0.0000						0.045917		
0.0000						1.000000		

Spreadsheet for Calculation of Stream-Water Saturation Profiles

Injection Temperature 650 °K Initial Temperature 325 °K Matrix Heat Capacity 1.0000 (kJ/kg)

TRAILING SHOCK CALCULATIONS

Saturation	OF	Wave V	Flow V	Shock V	fv	dKrv/dSv	dKr/dSi
0.7500	2.42E-01	0.255386	0.556992	0.013421	0.996549	1.0000	0.1875
0.875	5.56E-02	0.063132	0.677295	0.007514	0.999629	1.0000	0.0469
0.9375	7.87E-03	0.014687	0.691596	0.006812	0.999957	1.0000	0.0117
0.96875	-3.28E-03	0.003516	0.692013	0.006792	0.999995	1.0000	0.0029
0.953125	1.30E-03	0.008087	0.692162	0.006784	0.999982	1.0000	0.0066
0.9609375	-1.23E-03	0.005554	0.692162	0.006784	0.999990	1.0000	0.0046
0.95703125	-2.54E-05	0.006758	0.692182	0.006783	0.999986	1.0000	0.0055
0.955078125	6.23E-04	0.007406	0.692178	0.006784	0.999984	1.0000	0.0061
0.9560546875	2.95E-04	0.007078	0.692181	0.006783	0.999985	1.0000	0.0058
0.9565429688	1.34E-04	0.006917	0.692182	0.006783	0.999986	1.0000	0.0057
0.9567871094	5.40E-05	0.006837	0.692182	0.006783	0.999986	1.0000	0.0056
0.9569091797	1.42E-05	0.006798	0.692182	0.006783	0.999986	1.0000	0.0056
0.9569702148	-5.61E-06	0.006778	0.692182	0.006783	0.999986	1.0000	0.0056
0.9569396973	4.30E-06	0.006788	0.692182	0.006783	0.999986	1.0000	0.0056
0.9569549561	-6.54E-07	0.006783	0.692182	0.006783	0.999986	1.0000	0.0056
0.9569473267	1.82E-06	0.006785	0.692182	0.006783	0.999986	1.0000	0.0056
0.9569511414	5.84E-07	0.006784	0.692182	0.006783	0.999986	1.0000	0.0056
0.9569530487	-3.48E-08	0.006783	0.692182	0.006783	0.999986	1.0000	0.0056
0.956952095	2.75E-07	0.006784	0.692182	0.006783	0.999986	1.0000	0.0056
0.9569525719	1.20E-07	0.006783	0.692182	0.006783	0.999986	1.0000	0.0056
0.9569528103	4.26E-08	0.006783	0.692182	0.006783	0.999986	1.0000	0.0056
0.9569529295	3.85E-09	0.006783	0.692182	0.006783	0.999986	1.0000	0.0056
0.9569529891	-1.55E-08	0.006783	0.692182	0.006783	0.999986	1.0000	0.0056
0.9569529593	-5.82E-09	0.006783	0.692182	0.006783	0.999986	1.0000	0.0056
0.9569529444	-9.83E-10	0.006783	0.692182	0.006783	0.999986	1.0000	0.0056
0.9569529369	1.44E-09	0.006783	0.692182	0.006783	0.999986	1.0000	0.0056

Saturation	Total Mob	dFv/dSv	G	F	Gamma	Theta	High	Low
0.75	34.759228	0.045851	220.095758	12.870589	1.1794E+07	30550.407113	1	0.5
0.875	40.427490	0.009321	115.033000	10.261953	1.1701E+07	28275.535543	1	0.75
0.9375	43.300978	0.002124	62.501620	10.006619	1.1655E+07	28033.574650	1	0.875
0.96875	44.742642	0.000508	36.235931	9.974642	1.1632E+07	28005.473055	1	0.9375
0.953125	44.021547	0.001168	49.368776	9.983337	1.1643E+07	28014.871837	0.96875	0.9375
0.9609375	44.382039	0.000802	42.802353	9.978906	1.1638E+07	28009.220503	0.96875	0.953125
0.95703125	44.201778	0.000976	46.085564	9.981821	1.1641E+07	28011.782338	0.9609375	0.953125
0.955078125	44.111658	0.001070	47.727170	9.983500	1.1642E+07	28013.257853	0.95703125	0.953125
0.9560546875	44.156717	0.001023	46.906367	9.982642	1.1641E+07	28012.503198	0.95703125	0.955078125
0.9565429688	44.179247	0.000999	46.495966	9.982227	1.1641E+07	28012.138595	0.95703125	0.9560546875
0.9567871094	44.190513	0.000988	46.290765	9.982023	1.1641E+07	28011.959430	0.95703125	0.95654296875
0.9569091797	44.196145	0.000982	46.188165	9.981922	1.1641E+07	28011.870625	0.95703125	0.95678710938
0.9569702148	44.198962	0.000979	46.136864	9.981871	1.1641E+07	28011.826417	0.95703125	0.95690917969
0.9569396973	44.197553	0.000981	46.162515	9.981897	1.1641E+07	28011.848505	0.95697021484	0.95690917969
0.9569549561	44.198258	0.000980	46.149690	9.981884	1.1641E+07	28011.837457	0.95697021484	0.95693969727
0.9569473267	44.197905	0.000980	46.156102	9.981890	1.1641E+07	28011.842980	0.95695495605	0.95693969727
0.9569511414	44.198082	0.000980	46.152896	9.981887	1.1641E+07	28011.840218	0.95695495605	0.95694732666
0.9569530487	44.198170	0.000980	46.151293	9.981886	1.1641E+07	28011.838838	0.95695495605	0.95695114136
0.956952095	44.198126	0.000980	46.152094	9.981886	1.1641E+07	28011.839528	0.95695304871	0.95695114136
0.9569525719	44.198148	0.000980	46.151693	9.981886	1.1641E+07	28011.839183	0.95695304871	0.95695209503
0.9569528103	44.198159	0.000980	46.151493	9.981886	1.1641E+07	28011.839010	0.95695304871	0.95695257187
0.9569529295	44.198164	0.000980	46.151393	9.981886	1.1641E+07	28011.838924	0.95695304871	0.95695281029
0.9569529891	44.198167	0.000980	46.151343	9.981886	1.1641E+07	28011.838881	0.95695304871	0.9569529295
0.9569529593	44.198165	0.000980	46.151368	9.981886	1.1641E+07	28011.838902	0.9569529891	0.9569529295
0.9569529444	44.198165	0.000980	46.151380	9.981886	1.1641E+07	28011.838913	0.9569529593	0.9569529295
0.9569529369	44.198164	0.000980	46.151387	9.981886	1.1641E+07	28011.838919	0.9569529444	0.9569529295

Spreadsheet for Calculation of Stream-Water Saturation Profiles

Injection Temperature 650 °K		Initial Temperature 325 °K				Matrix Heat Capacity 1.0000 (kJ/kg)	
LEADING SHOCK CALCULATIONS							
Saturation	OF	Wave V	Flow V	Shock V	f _v	dKr _v /dS _v	dKr _i /dS _i
0.7500	2.69E-01	0.317373	0.012735	0.048111	0.996549	1.0000	0.1875
0.875	1.86E-02	0.064519	0.011245	0.045940	0.999629	1.0000	0.0469
0.9375	-3.13E-02	0.014699	0.011304	0.046026	0.999957	1.0000	0.0117
0.90625	-1.13E-02	0.034616	0.011236	0.045928	0.999849	1.0000	0.0264
0.890625	2.32E-03	0.048233	0.011229	0.045917	0.999756	1.0000	0.0359
0.8984375	-4.82E-03	0.041103	0.011230	0.045919	0.999806	1.0000	0.0309
0.89453125	-1.33E-03	0.044586	0.011229	0.045917	0.999782	1.0000	0.0334
0.892578125	4.72E-04	0.046389	0.011229	0.045917	0.999769	1.0000	0.0346
0.8935546875	-4.34E-04	0.045483	0.011229	0.045917	0.999776	1.0000	0.0340
0.8930664063	1.78E-05	0.045935	0.011229	0.045917	0.999772	1.0000	0.0343
0.8933105469	-2.09E-04	0.045708	0.011229	0.045917	0.999774	1.0000	0.0341
0.8931884766	-9.55E-05	0.045821	0.011229	0.045917	0.999773	1.0000	0.0342
0.8931274414	-3.89E-05	0.045878	0.011229	0.045917	0.999773	1.0000	0.0343
0.8930969238	-1.06E-05	0.045906	0.011229	0.045917	0.999773	1.0000	0.0343
0.893081665	3.61E-06	0.045920	0.011229	0.045917	0.999773	1.0000	0.0343
0.8930892944	-3.48E-06	0.045913	0.011229	0.045917	0.999773	1.0000	0.0343
0.8930854797	6.52E-08	0.045917	0.011229	0.045917	0.999773	1.0000	0.0343
0.8930873871	-1.71E-06	0.045915	0.011229	0.045917	0.999773	1.0000	0.0343
0.8930864334	-8.20E-07	0.045916	0.011229	0.045917	0.999773	1.0000	0.0343
0.8930859566	-3.77E-07	0.045916	0.011229	0.045917	0.999773	1.0000	0.0343
0.8930857182	-1.56E-07	0.045917	0.011229	0.045917	0.999773	1.0000	0.0343
0.8930855989	-4.54E-08	0.045917	0.011229	0.045917	0.999773	1.0000	0.0343
0.8930855393	9.92E-09	0.045917	0.011229	0.045917	0.999773	1.0000	0.0343
0.8930855691	-1.77E-08	0.045917	0.011229	0.045917	0.999773	1.0000	0.0343
0.8930855542	-3.91E-09	0.045917	0.011229	0.045917	0.999773	1.0000	0.0343
0.8930855468	3.01E-09	0.045917	0.011229	0.045917	0.999773	1.0000	0.0343

Saturation	Total Mob	dF _v /dS _v	G	F	Gamma	Theta	High	Low
0.75	34.759228	0.045851	220.095758	12.870589	1.1794E+07	30550.407113	1	0.5
0.875	40.427490	0.009321	115.033000	10.281953	1.1701E+07	28275.535543	1	0.75
0.9375	43.300978	0.002124	62.501620	10.006619	1.1655E+07	28033.574650	1	0.875
0.90625	41.862126	0.005001	88.767310	10.097238	1.1678E+07	28113.209409	0.9375	0.875
0.890625	41.144193	0.006968	101.900155	10.175426	1.1690E+07	28181.920650	0.90625	0.875
0.8984375	41.503017	0.005938	95.333732	10.133103	1.1684E+07	28144.727756	0.90625	0.890625
0.89453125	41.323568	0.006441	98.616944	10.153419	1.1687E+07	28162.581158	0.8984375	0.890625
0.892578125	41.233871	0.006702	100.258549	10.164206	1.1688E+07	28172.060864	0.89453125	0.890625
0.8935546875	41.278717	0.006571	99.437746	10.158759	1.1687E+07	28167.274039	0.89453125	0.892578125
0.8930664063	41.256294	0.006636	99.848148	10.161469	1.1688E+07	28169.655641	0.8935546875	0.892578125
0.8933105469	41.267505	0.006603	99.642947	10.160111	1.1688E+07	28168.461896	0.8935546875	0.89306640625
0.8931884766	41.261899	0.006620	99.745547	10.160789	1.1688E+07	28169.058032	0.89331054688	0.89306640625
0.8931274414	41.259097	0.006628	99.796848	10.161129	1.1688E+07	28169.356652	0.89318847656	0.89306640625
0.8930969238	41.257695	0.006632	99.822498	10.161299	1.1688E+07	28169.506101	0.89312744141	0.89306640625
0.893081665	41.256994	0.006634	99.835323	10.161384	1.1688E+07	28169.580859	0.89309692383	0.89306640625
0.8930892944	41.257345	0.006633	99.828910	10.161342	1.1688E+07	28169.543477	0.89309692383	0.89308166504
0.8930854797	41.257170	0.006634	99.832117	10.161363	1.1688E+07	28169.562168	0.89308929443	0.89308166504
0.8930873871	41.257257	0.006633	99.830513	10.161352	1.1688E+07	28169.552822	0.89308929443	0.89308547974
0.8930864334	41.257213	0.006634	99.831315	10.161358	1.1688E+07	28169.557495	0.89308738708	0.89308547974
0.8930859566	41.257191	0.006634	99.831716	10.161360	1.1688E+07	28169.559831	0.89308643341	0.89308547974
0.8930857182	41.257181	0.006634	99.831916	10.161362	1.1688E+07	28169.560999	0.89308595657	0.89308547974
0.8930855989	41.257175	0.006634	99.832016	10.161362	1.1688E+07	28169.561583	0.89308571815	0.89308547974
0.8930855393	41.257172	0.006634	99.832066	10.161363	1.1688E+07	28169.561876	0.89308559895	0.89308547974
0.8930855691	41.257174	0.006634	99.832041	10.161363	1.1688E+07	28169.561730	0.89308559895	0.89308553934
0.8930855542	41.257173	0.006634	99.832054	10.161363	1.1688E+07	28169.561803	0.89308556914	0.89308553934
0.8930855468	41.257173	0.006634	99.832060	10.161363	1.1688E+07	28169.561839	0.89308555424	0.89308553934

Spreadsheet for Calculation of Stream-Water Saturation Profiles

Injection Temperature 650 °K Initial Temperature 350 °K Matrix Heat Capacity 1.0000 (kJ/kg)

MATRIX PROPERTIES

<i>Porosity</i>	<i>Cp Matrix</i>	<i>Density</i>	<i>Rho * Cp</i>
0.10	1.00	2650.00	2650.0000
<i>Nw</i>	<i>Ng</i>	<i>Swi</i>	<i>Denom</i>
3.00	1.00	0.00	1.000000

SATURATION CONDITIONS

Tsaturation = 485.57

	<i>Volumes</i>	<i>Enthalpies</i>	<i>Densities</i>	<i>Viscosities</i>	<i>Saturation</i>
	(m3/kg)	(kJ/kg)	(kg/m3)	(cp)	Step
Liquid	0.001176	901.41	850.4723	0.1303	0.0014063597
Vapor	0.100298	2808.52	9.970241	0.0217	

BOUNDARY CONDITIONS

	<i>Temperature</i>	<i>Velocity</i>	<i>Heat Capacity</i>	<i>Wave Velocity</i>	<i>Density</i>	<i>Enthalpy</i>
Injection	650	1.000000	2.30	0.006622	6.882648	3199.91
Initial	350	0.011889	4.15	0.017234	975.3174	319.98
		<i>G</i>	<i>F</i>	<i>Gamma</i>	<i>Theta</i>	
Injection	650	6.88	6.88	15524523.87	22023.87	
Initial	350	975.32	975.32	8659580.72	312080.72	

SHOCK CONDITIONS

	<i>Initial Guess</i>	<i>Vapor Saturation</i>	<i>Objective Function</i>	<i>Two-Phase Wave Velocity</i>	<i>Upstream Flow Velocity</i>	<i>Shock Velocity</i>	<i>Vapor Frac Flow</i>
	<i>Sv-Hi</i>	<i>Sv-Low</i>					
Trailing	1	0.5	0.9570	1.4356E-09	0.0068	0.692182	1.0000
Leading	1	0.5	0.8866	4.7472E-09	0.0521	0.011889	0.9997
	<i>dKr/dSv</i>	<i>dKrl/dSl</i>	<i>Total Mobility</i>	<i>dPv/dSv</i>	<i>G</i>	<i>F'</i>	<i>Gamma</i>
							<i>Theta'</i>
Trailing	1.0000	0.0056	44.1982	0.0010	46.1514	9.9819	1.1641E+07
Leading	1.0000	0.0386	40.9610	0.0075	105.2538	10.1997	1.1693E+07

MATERIAL BALANCES

	<i>Inside</i>	<i>Initial</i>	<i>Injected</i>	<i>Produced</i>	<i>Balance</i>	<i>Error</i>
Mass	92.818555	97.531740	6.882648	11.595824	0.0000	0.0000%
Enthalpy	884276.8231	865958.0720	22023.8721	3710.4157	-5.2947	0.0006%

Spreadsheet for Calculation of Stream-Water Saturation Profiles

Injection Temperature 650 °K		Initial Temperature 350 °K				Matrix Heat Capacity 1.0000 (kJ/kg)		
SATURATION PROFILE								
Vapor Saturation	Vapor Frac Flow	dKr/dSv	dKr/dSI	Total Mobility	dFv/dSv	lambda	Mass Inside	Enthalpy Inside
1.0000						0.000000		
1.0000						0.006783		
0.9570	0.999986	1.0000	0.0056	44.198164	0.000980	0.006783	0.046687	105308.165674
0.9555	0.999985	1.0000	0.0059	44.133273	0.001047	0.007248	0.021724	5410.540844
0.9541	0.999983	1.0000	0.0063	44.068385	0.001117	0.007729	0.023058	5601.643180
0.9527	0.999982	1.0000	0.0067	44.003501	0.001189	0.008227	0.024435	5793.901239
0.9513	0.999980	1.0000	0.0071	43.938622	0.001263	0.008741	0.025856	5987.323262
0.9499	0.999978	1.0000	0.0075	43.873748	0.001340	0.009272	0.027322	6181.917552
0.9485	0.999976	1.0000	0.0080	43.808877	0.001419	0.009819	0.028832	6377.692471
0.9471	0.999974	1.0000	0.0084	43.744012	0.001500	0.010384	0.030386	6574.656444
0.9457	0.999972	1.0000	0.0088	43.679151	0.001584	0.010965	0.031987	6772.817956
0.9443	0.999970	1.0000	0.0093	43.614295	0.001671	0.011564	0.033633	6972.185556
0.9429	0.999967	1.0000	0.0098	43.549445	0.001760	0.012179	0.035325	7172.767856
0.9415	0.999965	1.0000	0.0103	43.484599	0.001851	0.012812	0.037063	7374.573531
0.9401	0.999962	1.0000	0.0108	43.419759	0.001945	0.013462	0.038849	7577.611320
0.9387	0.999959	1.0000	0.0113	43.354924	0.002041	0.014130	0.040682	7781.890027
0.9373	0.999956	1.0000	0.0118	43.290095	0.002140	0.014815	0.042563	7987.418520
0.9359	0.999953	1.0000	0.0123	43.225272	0.002242	0.015518	0.044492	8194.205734
0.9345	0.999950	1.0000	0.0129	43.160454	0.002346	0.016239	0.046469	8402.260668
0.9330	0.999947	1.0000	0.0134	43.095643	0.002453	0.016978	0.048496	8611.592391
0.9316	0.999943	1.0000	0.0140	43.030837	0.002562	0.017734	0.050572	8822.210036
0.9302	0.999939	1.0000	0.0146	42.966038	0.002674	0.018509	0.052697	9034.122805
0.9288	0.999935	1.0000	0.0152	42.901245	0.002789	0.019302	0.054874	9247.339969
0.9274	0.999931	1.0000	0.0158	42.836459	0.002906	0.020113	0.057100	9461.870866
0.9260	0.999927	1.0000	0.0164	42.771679	0.003026	0.020943	0.059379	9677.724906
0.9246	0.999923	1.0000	0.0171	42.706906	0.003148	0.021791	0.061708	9894.911566
0.9232	0.999918	1.0000	0.0177	42.642140	0.003273	0.022658	0.064090	10113.440397
0.9218	0.999914	1.0000	0.0183	42.577381	0.003401	0.023544	0.066524	10333.321018
0.9204	0.999909	1.0000	0.0190	42.512629	0.003532	0.024448	0.069012	10554.563121
0.9190	0.999904	1.0000	0.0197	42.447884	0.003666	0.025372	0.071553	10777.176472
0.9176	0.999899	1.0000	0.0204	42.383147	0.003802	0.026315	0.074148	11001.170907
0.9162	0.999893	1.0000	0.0211	42.318417	0.003941	0.027277	0.076797	11226.563337
0.9148	0.999887	1.0000	0.0218	42.253694	0.004082	0.028258	0.079501	11453.342748
0.9134	0.999882	1.0000	0.0225	42.188980	0.004227	0.029259	0.082260	11681.540198
0.9119	0.999876	1.0000	0.0233	42.124273	0.004374	0.030279	0.085076	11911.158824
0.9105	0.999869	1.0000	0.0240	42.059575	0.004525	0.031319	0.087947	12142.208835
0.9091	0.999863	1.0000	0.0248	41.994884	0.004678	0.032379	0.090876	12374.700521
0.9077	0.999856	1.0000	0.0255	41.930202	0.004834	0.033458	0.093862	12608.644246
0.9063	0.999849	1.0000	0.0263	41.865528	0.004993	0.034558	0.096906	12844.050453
0.9049	0.999842	1.0000	0.0271	41.800863	0.005154	0.035678	0.100008	13080.929663
0.9035	0.999835	1.0000	0.0279	41.736207	0.005319	0.036818	0.103169	13319.292477
0.9021	0.999827	1.0000	0.0288	41.671559	0.005487	0.037979	0.106389	13559.149576
0.9007	0.999819	1.0000	0.0296	41.606920	0.005657	0.039160	0.109669	13800.511719
0.8993	0.999811	1.0000	0.0304	41.542290	0.005831	0.040362	0.113010	14043.389750
0.8979	0.999803	1.0000	0.0313	41.477669	0.006008	0.041585	0.116412	14287.794593
0.8965	0.999794	1.0000	0.0321	41.413058	0.006187	0.042828	0.119875	14533.737253
0.8951	0.999786	1.0000	0.0330	41.348456	0.006370	0.044093	0.123400	14781.228821
0.8937	0.999776	1.0000	0.0339	41.283864	0.006556	0.045379	0.126988	15030.280471
0.8923	0.999767	1.0000	0.0348	41.219281	0.006745	0.046686	0.130639	15280.903459
0.8909	0.999757	1.0000	0.0357	41.154708	0.006937	0.048015	0.134354	15533.109131
0.8894	0.999748	1.0000	0.0367	41.090145	0.007132	0.049365	0.138133	15786.908915
0.8880	0.999737	1.0000	0.0376	41.025593	0.007330	0.050737	0.141977	16042.314328
0.8866	0.999727	1.0000	0.0386	40.961050	0.007531	0.052131	0.145886	16299.336973
0.0000						0.052131		
0.0000						1.000000		

Spreadsheet for Calculation of Stream-Water Saturation Profiles

Injection Temperature 650 °K		Initial Temperature 350 °K		Matrix Heat Capacity 1.0000 (kJ/kg)				
TRAILING SHOCK CALCULATIONS								
Saturation	OF	Wave V	Flow V	Shock V	fv	dKrv/dSv	dKr/dSi	
0.7500	2.42E-01	0.255386	0.556992	0.013421	0.996549	1.0000	0.1875	
0.875	5.56E-02	0.063132	0.677295	0.007514	0.999629	1.0000	0.0469	
0.9375	7.87E-03	0.014687	0.691596	0.006812	0.999957	1.0000	0.0117	
0.96875	-3.28E-03	0.003516	0.692013	0.006792	0.999995	1.0000	0.0029	
0.953125	1.30E-03	0.008087	0.692162	0.006784	0.999982	1.0000	0.0066	
0.9609375	-1.23E-03	0.005554	0.692162	0.006784	0.999990	1.0000	0.0046	
0.95703125	-2.54E-05	0.006758	0.692182	0.006783	0.999986	1.0000	0.0055	
0.955078125	6.23E-04	0.007406	0.692178	0.006784	0.999984	1.0000	0.0061	
0.9560546875	2.95E-04	0.007078	0.692181	0.006783	0.999985	1.0000	0.0058	
0.9565429688	1.34E-04	0.006917	0.692182	0.006783	0.999986	1.0000	0.0057	
0.9567871094	5.40E-05	0.006837	0.692182	0.006783	0.999986	1.0000	0.0056	
0.9569091797	1.42E-05	0.006798	0.692182	0.006783	0.999986	1.0000	0.0056	
0.9569702148	-5.61E-06	0.006778	0.692182	0.006783	0.999986	1.0000	0.0056	
0.9569396973	4.30E-06	0.006788	0.692182	0.006783	0.999986	1.0000	0.0056	
0.9569549561	-6.54E-07	0.006783	0.692182	0.006783	0.999986	1.0000	0.0056	
0.9569473267	1.82E-06	0.006785	0.692182	0.006783	0.999986	1.0000	0.0056	
0.9569511414	5.84E-07	0.006784	0.692182	0.006783	0.999986	1.0000	0.0056	
0.9569530487	-3.48E-08	0.006783	0.692182	0.006783	0.999986	1.0000	0.0056	
0.956952095	2.75E-07	0.006784	0.692182	0.006783	0.999986	1.0000	0.0056	
0.9569525719	1.20E-07	0.006783	0.692182	0.006783	0.999986	1.0000	0.0056	
0.9569528103	4.26E-08	0.006783	0.692182	0.006783	0.999986	1.0000	0.0056	
0.9569529295	3.85E-09	0.006783	0.692182	0.006783	0.999986	1.0000	0.0056	
0.9569529891	-1.55E-08	0.006783	0.692182	0.006783	0.999986	1.0000	0.0056	
0.9569529593	-5.82E-09	0.006783	0.692182	0.006783	0.999986	1.0000	0.0056	
0.9569529444	-9.83E-10	0.006783	0.692182	0.006783	0.999986	1.0000	0.0056	
0.9569529369	1.44E-09	0.006783	0.692182	0.006783	0.999986	1.0000	0.0056	
Saturation	Total Mob	dFv/dSv	G	F	Gamma	Theta	High	Low
0.75	34.759228	0.045851	220.095758	12.870589	1.1794E+07	30550.407113	1	0.5
0.875	40.427490	0.009321	115.033000	10.281953	1.1701E+07	28275.535543	1	0.75
0.9375	43.300978	0.002124	62.501620	10.006619	1.1655E+07	28033.574650	1	0.875
0.96875	44.742642	0.000508	36.235931	9.974642	1.1632E+07	28005.473055	1	0.9375
0.953125	44.021547	0.001168	49.368776	9.985337	1.1643E+07	28014.871837	0.96875	0.9375
0.9609375	44.382039	0.000802	42.802353	9.978906	1.1638E+07	28009.220503	0.96875	0.953125
0.95703125	44.201778	0.000976	46.085564	9.981821	1.1641E+07	28011.782338	0.9609375	0.953125
0.955078125	44.111658	0.001070	47.727170	9.983500	1.1642E+07	28013.257853	0.95703125	0.953125
0.9560546875	44.156717	0.001023	46.906367	9.982642	1.1641E+07	28012.503198	0.95703125	0.955078125
0.9565429688	44.179247	0.000999	46.495966	9.982227	1.1641E+07	28012.138595	0.95703125	0.9560546875
0.9567871094	44.190513	0.000988	46.290765	9.982023	1.1641E+07	28011.959430	0.95703125	0.95654296875
0.9569091797	44.196145	0.000982	46.188165	9.981922	1.1641E+07	28011.870625	0.95703125	0.95678710938
0.9569702148	44.198962	0.000979	46.136864	9.981871	1.1641E+07	28011.826417	0.95703125	0.95690917969
0.9569396973	44.197553	0.000981	46.162515	9.981897	1.1641E+07	28011.848505	0.95697021484	0.95690917969
0.9569549561	44.198258	0.000980	46.149690	9.981884	1.1641E+07	28011.837457	0.95697021484	0.95693969727
0.9569473267	44.197905	0.000980	46.156102	9.981890	1.1641E+07	28011.842980	0.95695495605	0.95693969727
0.9569511414	44.198082	0.000980	46.152896	9.981887	1.1641E+07	28011.840218	0.95695495605	0.95694732666
0.9569530487	44.198170	0.000980	46.151293	9.981886	1.1641E+07	28011.838838	0.95695495605	0.95695114136
0.956952095	44.198126	0.000980	46.152094	9.981886	1.1641E+07	28011.839528	0.95695304871	0.95695114136
0.9569525719	44.198148	0.000980	46.151693	9.981886	1.1641E+07	28011.839183	0.95695304871	0.95695209503
0.9569528103	44.198159	0.000980	46.151493	9.981886	1.1641E+07	28011.839010	0.95695304871	0.95695257187
0.9569529295	44.198164	0.000980	46.151393	9.981886	1.1641E+07	28011.838924	0.95695304871	0.95695281029
0.9569529891	44.198167	0.000980	46.151343	9.981886	1.1641E+07	28011.838801	0.95695304871	0.9569529295
0.9569529593	44.198165	0.000980	46.151368	9.981886	1.1641E+07	28011.838902	0.9569529891	0.9569529295
0.9569529444	44.198165	0.000980	46.151380	9.981886	1.1641E+07	28011.838913	0.9569529593	0.9569529295
0.9569529369	44.198164	0.000980	46.151387	9.981886	1.1641E+07	28011.838919	0.9569529444	0.9569529295

Spreadsheet for Calculation of Stream-Water Saturation Profiles

Injection Temperature 650 °K Initial Temperature 350 °K Matrix Heat Capacity 1.0000 (kJ/kg)

LEADING SHOCK CALCULATIONS

Table with columns: Saturation, OP, Wave V, Flow V, Shock V, fv, dKrv/dSv, dKr/dSI, Saturation, Total Mob, dFv/dSv, G, F, Gamma, Theta, High, Low. It contains two data series, one for leading shock calculations and one for mobility and other parameters.

Spreadsheet for Calculation of Stream-Water Saturation Profiles

Injection Temperature
650 °K

Initial Temperature
375 °K

Matrix Heat Capacity
1.0000 (kJ/kg)

MATRIX PROPERTIES

Porosity	Cp Matrix	Density	Rho * Cp
0.10	1.00	2650.00	2650.0000
Nw	Ng	Swi	Denom
3.00	1.00	0.00	1.000000

SATURATION CONDITIONS

Tsaturation = 485.57

	Volumes (m3/kg)	Enthalpies (kJ/kg)	Densities (kg/m3)	Viscosities (cp)	Saturation Step
Liquid	0.001176	901.41	850.4723	0.1303	0.0015779915
Vapor	0.100298	2808.52	9.970241	0.0217	

BOUNDARY CONDITIONS

	Temperature	Velocity	Heat Capacity	Wave Velocity	Density	Enthalpy
Injection	650	1.000000	2.30	0.006622	6.882648	3199.91
Initial	375	0.012806	4.17	0.018375	958.0702	423.88
	G	F	Gamma	Theta		
Injection	650	6.88	6.88	15524523.87	22023.87	
Initial	375	958.07	958.07	9349861.31	406111.31	

SHOCK CONDITIONS

	Initial Sv-Hi	Guess Sv-Low	Vapor Saturation	Objective Function	Two-Phase Wave Velocity	Upstream Flow Velocity	Shock Velocity	Vapor Frac Flow
Trailing	1	0.5	0.9570	1.4356E-09	0.0068	0.692182	0.0068	1.0000
Leading	1	0.5	0.8781	1.2943E-09	0.0611	0.012806	0.0611	0.9997
	dKr/dSv	dKri/dSi	Total Mobility	dFv/dSv	G	F'	Gamma	Theta'
Trailing	1.0000	0.0056	44.1982	0.0010	46.1514	9.9819	1.1641E+07	28011.8389
Leading	1.0000	0.0446	40.5674	0.0088	112.4666	10.2587	1.1699E+07	28255.0707

MATERIAL BALANCES

	Mass	Inside	Initial	Injected	Produced	Balance	Error
Mass	90.420616	95.807021	95.807021	6.882648	12.269040	0.0000	0.0000%
Enthalpy	951816.0963	934986.1305	934986.1305	22023.8721	5200.6583	-6.7520	0.0007%

Spreadsheet for Calculation of Stream-Water Saturation Profiles

Injection Temperature 650 °K		Initial Temperature 375 °K				Matrix Heat Capacity 1.0000 (kJ/kg)		
SATURATION PROFILE								
Vapor Saturation	Vapor Frac Flow	dKrv/dSv	dKrI/dSI	Total Mobility	dFv/dSv	lambda	Mass Inside	Enthalpy Inside
1.0000						0.000000		
1.0000						0.006783		
0.9570	0.999986	1.0000	0.0056	44.198164	0.000980	0.006783	0.046687	105308.165674
0.9554	0.999985	1.0000	0.0060	44.125354	0.001055	0.007306	0.024465	6083.902275
0.9538	0.999983	1.0000	0.0064	44.052548	0.001134	0.007849	0.026151	6324.672234
0.9522	0.999981	1.0000	0.0068	43.979747	0.001215	0.008413	0.027898	6567.076916
0.9506	0.999979	1.0000	0.0073	43.906953	0.001300	0.008998	0.029708	6811.129407
0.9491	0.999977	1.0000	0.0078	43.834163	0.001387	0.009604	0.031580	7056.842901
0.9475	0.999975	1.0000	0.0083	43.761380	0.001478	0.010231	0.033516	7304.230701
0.9459	0.999972	1.0000	0.0088	43.688602	0.001572	0.010879	0.035515	7553.306219
0.9443	0.999970	1.0000	0.0093	43.615831	0.001669	0.011549	0.037579	7804.082978
0.9428	0.999967	1.0000	0.0098	43.543066	0.001768	0.012241	0.039708	8056.574612
0.9412	0.999964	1.0000	0.0104	43.470308	0.001871	0.012954	0.041903	8310.794870
0.9396	0.999961	1.0000	0.0109	43.397557	0.001978	0.013689	0.044164	8566.757614
0.9380	0.999958	1.0000	0.0115	43.324812	0.002087	0.014446	0.046492	8824.476820
0.9364	0.999954	1.0000	0.0121	43.252075	0.002200	0.015226	0.048888	9083.966580
0.9349	0.999951	1.0000	0.0127	43.179344	0.002315	0.016027	0.051352	9345.241104
0.9333	0.999947	1.0000	0.0134	43.106622	0.002435	0.016851	0.053885	9608.314720
0.9317	0.999943	1.0000	0.0140	43.033907	0.002557	0.017698	0.056488	9873.201875
0.9301	0.999939	1.0000	0.0146	42.961199	0.002682	0.018568	0.059162	10139.917134
0.9285	0.999935	1.0000	0.0153	42.888500	0.002811	0.019460	0.061906	10408.475188
0.9270	0.999930	1.0000	0.0160	42.815809	0.002944	0.020376	0.064722	10678.890847
0.9254	0.999925	1.0000	0.0167	42.743127	0.003079	0.021315	0.067611	10951.179045
0.9238	0.999920	1.0000	0.0174	42.670453	0.003218	0.022277	0.070573	11225.354841
0.9222	0.999915	1.0000	0.0181	42.597787	0.003361	0.023263	0.073609	11501.433422
0.9207	0.999910	1.0000	0.0189	42.525131	0.003507	0.024272	0.076719	11779.430099
0.9191	0.999904	1.0000	0.0196	42.452483	0.003656	0.025306	0.079905	12059.360313
0.9175	0.999898	1.0000	0.0204	42.379845	0.003809	0.026363	0.083167	12341.239634
0.9159	0.999892	1.0000	0.0212	42.307217	0.003965	0.027445	0.086506	12625.083763
0.9143	0.999886	1.0000	0.0220	42.234598	0.004125	0.028551	0.089922	12910.908531
0.9128	0.999879	1.0000	0.0228	42.161989	0.004288	0.029682	0.093417	13198.729905
0.9112	0.999872	1.0000	0.0237	42.089390	0.004455	0.030837	0.096991	13488.563984
0.9096	0.999865	1.0000	0.0245	42.016801	0.004626	0.032017	0.100645	13780.427004
0.9080	0.999858	1.0000	0.0254	41.944222	0.004800	0.033222	0.104380	14074.335336
0.9065	0.999850	1.0000	0.0263	41.871654	0.004977	0.034453	0.108196	14370.305492
0.9049	0.999842	1.0000	0.0271	41.799097	0.005159	0.035709	0.112094	14668.354120
0.9033	0.999834	1.0000	0.0281	41.726551	0.005344	0.036990	0.116076	14968.498011
0.9017	0.999825	1.0000	0.0290	41.654015	0.005533	0.038297	0.120142	15270.754097
0.9001	0.999816	1.0000	0.0299	41.581491	0.005725	0.039631	0.124292	15575.139453
0.8986	0.999807	1.0000	0.0309	41.508979	0.005922	0.040990	0.128528	15881.671300
0.8970	0.999797	1.0000	0.0318	41.436478	0.006122	0.042375	0.132850	16190.367003
0.8954	0.999788	1.0000	0.0328	41.363989	0.006326	0.043787	0.137260	16501.244076
0.8938	0.999778	1.0000	0.0338	41.291512	0.006534	0.045226	0.141758	16814.320181
0.8923	0.999767	1.0000	0.0348	41.219047	0.006745	0.046691	0.146345	17129.613130
0.8907	0.999756	1.0000	0.0359	41.146594	0.006961	0.048184	0.151022	17447.140886
0.8891	0.999745	1.0000	0.0369	41.074154	0.007181	0.049703	0.155790	17766.921567
0.8875	0.999734	1.0000	0.0380	41.001727	0.007404	0.051250	0.160650	18088.973443
0.8859	0.999722	1.0000	0.0390	40.929312	0.007632	0.052825	0.165602	18413.314940
0.8844	0.999709	1.0000	0.0401	40.856911	0.007863	0.054427	0.170648	18739.964643
0.8828	0.999697	1.0000	0.0412	40.784523	0.008099	0.056057	0.175788	19068.941294
0.8812	0.999684	1.0000	0.0423	40.712148	0.008338	0.057716	0.181024	19400.263796
0.8796	0.999671	1.0000	0.0435	40.639787	0.008582	0.059403	0.186356	19733.951214
0.8781	0.999657	1.0000	0.0446	40.567440	0.008830	0.061118	0.191786	20070.022776
0.0000						0.061118		
0.0000						1.000000		

Spreadsheet for Calculation of Stream-Water Saturation Profiles

Injection Temperature 650 °K		Initial Temperature 375 °K		Matrix Heat Capacity 1.0000 (kJ/kg)				
TRAILING SHOCK CALCULATIONS								
Saturation	OF	Wave V	Flow V	Shock V	f _v	dK _{rv} /dS _v	dK _{rl} /dS _l	
0.7500	2.42E-01	0.255386	0.556992	0.013421	0.996549	1.0000	0.1875	
0.875	5.56E-02	0.063132	0.677295	0.007514	0.999629	1.0000	0.0469	
0.9375	7.87E-03	0.014687	0.691596	0.006812	0.999957	1.0000	0.0117	
0.96875	-3.28E-03	0.003516	0.692013	0.006792	0.999995	1.0000	0.0029	
0.953125	1.30E-03	0.008087	0.692162	0.006784	0.999982	1.0000	0.0066	
0.9609375	-1.23E-03	0.005554	0.692162	0.006784	0.999990	1.0000	0.0046	
0.95703125	-2.54E-05	0.006758	0.692182	0.006783	0.999986	1.0000	0.0055	
0.955078125	6.23E-04	0.007406	0.692178	0.006784	0.999984	1.0000	0.0061	
0.9560546875	2.95E-04	0.007078	0.692181	0.006783	0.999985	1.0000	0.0058	
0.9565429688	1.34E-04	0.006917	0.692182	0.006783	0.999986	1.0000	0.0057	
0.9567871094	5.40E-05	0.006837	0.692182	0.006783	0.999986	1.0000	0.0056	
0.9569091797	1.42E-05	0.006798	0.692182	0.006783	0.999986	1.0000	0.0056	
0.9569702148	-5.61E-06	0.006778	0.692182	0.006783	0.999986	1.0000	0.0056	
0.9569396973	4.30E-06	0.006788	0.692182	0.006783	0.999986	1.0000	0.0056	
0.9569549561	-6.54E-07	0.006783	0.692182	0.006783	0.999986	1.0000	0.0056	
0.9569473267	1.82E-06	0.006785	0.692182	0.006783	0.999986	1.0000	0.0056	
0.9569511414	5.84E-07	0.006784	0.692182	0.006783	0.999986	1.0000	0.0056	
0.9569530487	-3.48E-08	0.006783	0.692182	0.006783	0.999986	1.0000	0.0056	
0.956952095	2.75E-07	0.006784	0.692182	0.006783	0.999986	1.0000	0.0056	
0.9569525719	1.20E-07	0.006783	0.692182	0.006783	0.999986	1.0000	0.0056	
0.9569528103	4.26E-08	0.006783	0.692182	0.006783	0.999986	1.0000	0.0056	
0.9569529295	3.85E-09	0.006783	0.692182	0.006783	0.999986	1.0000	0.0056	
0.9569529891	-1.55E-08	0.006783	0.692182	0.006783	0.999986	1.0000	0.0056	
0.9569529593	-5.82E-09	0.006783	0.692182	0.006783	0.999986	1.0000	0.0056	
0.9569529444	-9.83E-10	0.006783	0.692182	0.006783	0.999986	1.0000	0.0056	
0.9569529369	1.44E-09	0.006783	0.692182	0.006783	0.999986	1.0000	0.0056	
Saturation	Total Mob	dF _v /dS _v	G	F	Gamma	Theta	High	Low
0.75	34.759228	0.045851	220.095758	12.870589	1.1794E+07	30550.407113	1	0.5
0.875	40.427490	0.009321	115.033000	10.281953	1.1701E+07	28275.535543	1	0.75
0.9375	43.300978	0.002124	62.501620	10.006619	1.1655E+07	28033.574650	1	0.875
0.96875	44.742642	0.000508	36.235931	9.974642	1.1632E+07	28005.473055	1	0.9375
0.953125	44.021547	0.001168	49.368776	9.985337	1.1643E+07	28014.871837	0.96875	0.9375
0.9609375	44.382039	0.000802	42.802353	9.978906	1.1638E+07	28009.220503	0.96875	0.953125
0.95703125	44.201778	0.000976	46.085564	9.981821	1.1641E+07	28011.782338	0.9609375	0.953125
0.955078125	44.111658	0.001070	47.727170	9.983500	1.1642E+07	28013.257853	0.95703125	0.953125
0.9560546875	44.156717	0.001023	46.906367	9.982642	1.1641E+07	28012.503198	0.95703125	0.955078125
0.9565429688	44.179247	0.000999	46.495966	9.982227	1.1641E+07	28012.138595	0.95703125	0.9560546875
0.9567871094	44.190513	0.000988	46.290765	9.982023	1.1641E+07	28011.959430	0.95703125	0.95654296875
0.9569091797	44.196145	0.000982	46.188165	9.981922	1.1641E+07	28011.870625	0.95703125	0.95678710938
0.9569702148	44.198962	0.000979	46.136864	9.981871	1.1641E+07	28011.826417	0.95703125	0.95690917969
0.9569396973	44.197553	0.000981	46.162515	9.981897	1.1641E+07	28011.848505	0.95697021484	0.95690917969
0.9569549561	44.198258	0.000980	46.149690	9.981884	1.1641E+07	28011.837457	0.95697021484	0.95693969727
0.9569473267	44.197905	0.000980	46.156102	9.981890	1.1641E+07	28011.842980	0.95695495605	0.95693969727
0.9569511414	44.198082	0.000980	46.152896	9.981887	1.1641E+07	28011.840218	0.95695495605	0.95694732666
0.9569530487	44.198170	0.000980	46.151293	9.981886	1.1641E+07	28011.838838	0.95695495605	0.95695114136
0.956952095	44.198126	0.000980	46.152094	9.981886	1.1641E+07	28011.839528	0.95695304871	0.95695114136
0.9569525719	44.198148	0.000980	46.151693	9.981886	1.1641E+07	28011.839183	0.95695304871	0.95695209503
0.9569528103	44.198159	0.000980	46.151493	9.981886	1.1641E+07	28011.839010	0.95695304871	0.95695257187
0.9569529295	44.198164	0.000980	46.151393	9.981886	1.1641E+07	28011.838924	0.95695304871	0.95695281029
0.9569529891	44.198167	0.000980	46.151343	9.981886	1.1641E+07	28011.838881	0.95695304871	0.9569529295
0.9569529593	44.198165	0.000980	46.151368	9.981886	1.1641E+07	28011.838902	0.9569529891	0.9569529295
0.9569529444	44.198165	0.000980	46.151380	9.981886	1.1641E+07	28011.838913	0.9569529593	0.9569529295
0.9569529369	44.198164	0.000980	46.151387	9.981886	1.1641E+07	28011.838919	0.9569529444	0.9569529295

Spreadsheet for Calculation of Stream-Water Saturation Profiles

Injection Temperature 650 °K		Initial Temperature 375 °K				Matrix Heat Capacity 1.0000 (kJ/kg)		
LEADING SHOCK CALCULATIONS								
Saturation	OF	Wave V	Flow V	Shock V	f _v	dK _{rv} /dS _v	dKr/dS _l	
0.7500	2.54E-01	0.317373	0.014153	0.063016	0.996549	1.0000	0.1875	
0.875	3.40E-03	0.064519	0.012807	0.061119	0.999629	1.0000	0.0469	
0.9375	-4.66E-02	0.014699	0.012963	0.061340	0.999957	1.0000	0.0117	
0.90625	-2.66E-02	0.034616	0.012846	0.061174	0.999849	1.0000	0.0264	
0.890625	-1.29E-02	0.048233	0.012814	0.061130	0.999756	1.0000	0.0359	
0.8828125	-5.09E-03	0.056031	0.012807	0.061120	0.999697	1.0000	0.0412	
0.87890625	-9.31E-04	0.060187	0.012806	0.061118	0.999664	1.0000	0.0440	
0.876953125	1.21E-03	0.062331	0.012806	0.061118	0.999647	1.0000	0.0454	
0.8779296875	1.36E-04	0.061254	0.012806	0.061118	0.999656	1.0000	0.0447	
0.8784179688	-3.99E-04	0.060719	0.012806	0.061118	0.999660	1.0000	0.0443	
0.8781738281	-1.32E-04	0.060986	0.012806	0.061118	0.999658	1.0000	0.0445	
0.8780517578	1.76E-06	0.061120	0.012806	0.061118	0.999657	1.0000	0.0446	
0.878112793	-6.51E-05	0.061053	0.012806	0.061118	0.999657	1.0000	0.0446	
0.8780822754	-3.17E-05	0.061086	0.012806	0.061118	0.999657	1.0000	0.0446	
0.8780670166	-1.50E-05	0.061103	0.012806	0.061118	0.999657	1.0000	0.0446	
0.8780593872	-6.61E-06	0.061112	0.012806	0.061118	0.999657	1.0000	0.0446	
0.8780555725	-2.42E-06	0.061116	0.012806	0.061118	0.999657	1.0000	0.0446	
0.8780536652	-3.34E-07	0.061118	0.012806	0.061118	0.999657	1.0000	0.0446	
0.8780527115	7.12E-07	0.061119	0.012806	0.061118	0.999657	1.0000	0.0446	
0.8780531883	1.89E-07	0.061118	0.012806	0.061118	0.999657	1.0000	0.0446	
0.8780534267	-7.22E-08	0.061118	0.012806	0.061118	0.999657	1.0000	0.0446	
0.8780533075	5.85E-08	0.061118	0.012806	0.061118	0.999657	1.0000	0.0446	
0.8780533671	-6.87E-09	0.061118	0.012806	0.061118	0.999657	1.0000	0.0446	
0.8780533373	2.58E-08	0.061118	0.012806	0.061118	0.999657	1.0000	0.0446	
0.8780533522	9.46E-09	0.061118	0.012806	0.061118	0.999657	1.0000	0.0446	
0.8780533597	1.29E-09	0.061118	0.012806	0.061118	0.999657	1.0000	0.0446	

Saturation	Total Mob	dFv/dSv	G	F	Gamma	Theta	High	Low
0.75	34.759228	0.045851	220.095758	12.870589	1.1794E+07	30550.407113	1	0.5
0.875	40.427490	0.009321	115.033000	10.281953	1.1701E+07	28275.535543	1	0.75
0.9375	43.300978	0.002124	62.501620	10.006619	1.1655E+07	28033.574650	1	0.875
0.90625	41.862126	0.005001	88.767310	10.097238	1.1678E+07	28113.209409	0.9375	0.875
0.890625	41.144193	0.006968	101.900155	10.175426	1.1690E+07	28181.920650	0.90625	0.875
0.8828125	40.785677	0.008095	108.466577	10.224828	1.1695E+07	28225.334700	0.890625	0.875
0.87890625	40.606541	0.008695	111.749788	10.252384	1.1698E+07	28249.550656	0.8828125	0.875
0.876953125	40.517005	0.009005	113.391394	10.266912	1.1700E+07	28262.317400	0.87890625	0.875
0.8779296875	40.561770	0.008849	112.570591	10.259584	1.1699E+07	28255.878179	0.87890625	0.876953125
0.8784179688	40.584155	0.008772	112.160190	10.255968	1.1699E+07	28252.700527	0.87890625	0.8779296875
0.8781738281	40.572963	0.008811	112.365391	10.257772	1.1699E+07	28254.285872	0.87841796875	0.8779296875
0.8780517578	40.567367	0.008830	112.467991	10.258677	1.1699E+07	28255.081154	0.87817382813	0.8779296875
0.878112793	40.570165	0.008820	112.416691	10.258225	1.1699E+07	28254.683295	0.87817382813	0.87805175781
0.8780822754	40.568766	0.008825	112.442341	10.258451	1.1699E+07	28254.882170	0.87811279297	0.87805175781
0.8780670166	40.568066	0.008828	112.455166	10.258564	1.1699E+07	28254.981648	0.87808227539	0.87805175781
0.8780593872	40.567716	0.008829	112.461578	10.258621	1.1699E+07	28255.031398	0.8780670166	0.87805175781
0.8780555725	40.567541	0.008829	112.464785	10.258649	1.1699E+07	28255.056275	0.87805938721	0.87805175781
0.8780536652	40.567454	0.008830	112.466388	10.258663	1.1699E+07	28255.068714	0.87805557251	0.87805175781
0.8780527115	40.567410	0.008830	112.467189	10.258670	1.1699E+07	28255.074934	0.87805366516	0.87805175781
0.8780531883	40.567432	0.008830	112.466789	10.258667	1.1699E+07	28255.071824	0.87805366516	0.87805271149
0.8780534267	40.567443	0.008830	112.466588	10.258665	1.1699E+07	28255.070269	0.87805366516	0.87805318832
0.8780533075	40.567438	0.008830	112.466688	10.258666	1.1699E+07	28255.071047	0.87805342674	0.87805318832
0.8780533671	40.567440	0.008830	112.466638	10.258665	1.1699E+07	28255.070658	0.87805342674	0.87805330753
0.8780533373	40.567439	0.008830	112.466663	10.258666	1.1699E+07	28255.070852	0.87805336714	0.87805330753
0.8780533522	40.567440	0.008830	112.466651	10.258666	1.1699E+07	28255.070755	0.87805336714	0.87805333734
0.8780533597	40.567440	0.008830	112.466645	10.258666	1.1699E+07	28255.070707	0.87805336714	0.87805335224

Spreadsheet for Calculation of Stream-Water Saturation Profiles

Injection Temperature
650 °K

Initial Temperature
400 °K

Matrix Heat Capacity
1.0000 (kJ/kg)

MATRIX PROPERTIES

Porosity	Cp Matrix	Density	Rho * Cp
0.10	1.00	2650.00	2650.0000
Nw	Ng	Swi	Denom
3.00	1.00	0.00	1.000000

SATURATION CONDITIONS

Testation = 485.57

	Volumes (m3/kg)	Enthalpies (kJ/kg)	Densities (kg/m3)	Viscosities (cp)	Saturation Step
Liquid	0.001176	901.41	850.4723	0.1303	0.0018203139
Vapor	0.100298	2808.52	9.970241	0.0217	

BOUNDARY CONDITIONS

	Temperature	Velocity	Heat Capacity	Wave Velocity	Density	Enthalpy
Injection	650	1.000000	2.30	0.006622	6.882648	3199.91
Initial	400	0.014183	4.22	0.020184	938.4701	528.68
	G	F	Gamma	Theta		
Injection	650	6.88	6.88	15524523.87	22023.87	
Initial	400	938.47	938.47	10036150.40	496150.40	

SHOCK CONDITIONS

	Initial Guess		Vapor Saturation	Objective Function	Two-Phase Wave Velocity	Upstream Flow Velocity	Shock Velocity	Vapor Frac Flow
	Sv-Hi	Sv-Low						
Trailing	1	0.5	0.9570	1.4356E-09	0.0068	0.692182	0.0068	1.0000
Leading	1	0.5	0.8659	-4.2045E-09	0.0753	0.014183	0.0753	0.9995
	dKrv/dSv	dKrl/dSl	Total Mobility	dPv/dSv	G	F'	Gamma	Theta'
Trailing	1.0000	0.0056	44.1982	0.0010	46.1514	9.9819	1.1641E+07	28011.8389
Leading	1.0000	0.0539	40.0124	0.0109	122.6503	10.3588	1.1708E+07	28343.0467

MATERIAL BALANCES

	Inside	Initial	Injected	Produced	Balance	Error
Mass	87.419438	93.847014	6.882648	13.310204	0.0000	0.0000%
Enthalpy	1018611.3195	1003615.0395	22023.8721	7036.8385	-9.2464	0.0009%

Spreadsheet for Calculation of Stream-Water Saturation Profiles

Injection Temperature 650 °K		Initial Temperature 400 °K				Matrix Heat Capacity 1.0000 (kJ/kg)		
SATURATION PROFILE								
Vapor Saturation	Vapor Frac Flow	dKr/dSv	dKr/dSI	Total Mobility	dPv/dSv	lambda	Mass Inside	Enthalpy Inside
1.0000						0.000000		
1.0000						0.006783		
0.9570	0.999986	1.0000	0.0056	44.198164	0.000980	0.006783	0.046687	105308.165674
0.9551	0.999984	1.0000	0.0060	44.114173	0.001067	0.007388	0.028369	7039.452627
0.9533	0.999982	1.0000	0.0065	44.030188	0.001159	0.008020	0.030625	7360.180838
0.9515	0.999980	1.0000	0.0071	43.946211	0.001254	0.008680	0.032976	7683.423065
0.9497	0.999978	1.0000	0.0076	43.862241	0.001353	0.009368	0.035422	8009.202536
0.9479	0.999975	1.0000	0.0082	43.778278	0.001457	0.010084	0.037965	8337.542705
0.9460	0.999972	1.0000	0.0087	43.694324	0.001564	0.010828	0.040606	8668.467246
0.9442	0.999969	1.0000	0.0093	43.610378	0.001676	0.011600	0.043345	9002.000061
0.9424	0.999966	1.0000	0.0100	43.526440	0.001792	0.012402	0.046185	9338.165279
0.9406	0.999963	1.0000	0.0106	43.442511	0.001912	0.013232	0.049126	9676.987258
0.9387	0.999959	1.0000	0.0113	43.358591	0.002036	0.014092	0.052168	10018.490593
0.9369	0.999955	1.0000	0.0119	43.274681	0.002164	0.014981	0.055315	10362.700110
0.9351	0.999951	1.0000	0.0126	43.190780	0.002297	0.015900	0.058566	10709.640876
0.9333	0.999947	1.0000	0.0134	43.106889	0.002434	0.016848	0.061922	11059.338195
0.9315	0.999943	1.0000	0.0141	43.023008	0.002575	0.017827	0.065386	11411.817619
0.9296	0.999938	1.0000	0.0148	42.939138	0.002721	0.018836	0.068957	11767.104940
0.9278	0.999933	1.0000	0.0156	42.855278	0.002871	0.019876	0.072638	12125.226201
0.9260	0.999927	1.0000	0.0164	42.771429	0.003026	0.020946	0.076430	12486.207692
0.9242	0.999922	1.0000	0.0172	42.687592	0.003185	0.022048	0.080333	12850.075972
0.9224	0.999916	1.0000	0.0181	42.603766	0.003349	0.023181	0.084350	13216.857832
0.9205	0.999909	1.0000	0.0189	42.519952	0.003517	0.024345	0.088481	13586.580336
0.9187	0.999903	1.0000	0.0198	42.436151	0.003690	0.025541	0.092727	13959.270809
0.9169	0.999896	1.0000	0.0207	42.352361	0.003867	0.026770	0.097091	14334.956838
0.9151	0.999889	1.0000	0.0216	42.268585	0.004050	0.028030	0.101573	14713.666278
0.9133	0.999881	1.0000	0.0226	42.184821	0.004236	0.029323	0.106175	15095.427255
0.9114	0.999873	1.0000	0.0235	42.101071	0.004428	0.030649	0.110897	15480.268165
0.9096	0.999865	1.0000	0.0245	42.017334	0.004624	0.032008	0.115743	15868.217682
0.9078	0.999857	1.0000	0.0255	41.933610	0.004825	0.033401	0.120712	16259.304760
0.9060	0.999848	1.0000	0.0265	41.849901	0.005031	0.034827	0.125806	16653.558633
0.9042	0.999838	1.0000	0.0276	41.766207	0.005242	0.036287	0.131027	17051.008820
0.9023	0.999828	1.0000	0.0286	41.682527	0.005458	0.037781	0.136375	17451.685127
0.9005	0.999818	1.0000	0.0297	41.598861	0.005679	0.039309	0.141854	17855.617654
0.8987	0.999808	1.0000	0.0308	41.515211	0.005905	0.040872	0.147463	18262.836792
0.8969	0.999797	1.0000	0.0319	41.431577	0.006136	0.042470	0.153206	18673.373231
0.8951	0.999785	1.0000	0.0330	41.347958	0.006372	0.044103	0.159082	19087.257961
0.8932	0.999774	1.0000	0.0342	41.264355	0.006613	0.045772	0.165093	19504.522276
0.8914	0.999761	1.0000	0.0354	41.180769	0.006859	0.047476	0.171242	19925.197776
0.8896	0.999749	1.0000	0.0366	41.097199	0.007110	0.049217	0.177530	20349.316372
0.8878	0.999735	1.0000	0.0378	41.013646	0.007367	0.050994	0.183957	20776.910290
0.8860	0.999722	1.0000	0.0390	40.930110	0.007629	0.052807	0.190527	21208.012071
0.8841	0.999708	1.0000	0.0403	40.846591	0.007896	0.054658	0.197240	21642.654577
0.8823	0.999693	1.0000	0.0415	40.763090	0.008169	0.056546	0.204099	22080.870995
0.8805	0.999678	1.0000	0.0428	40.679607	0.008447	0.058471	0.211104	22522.694838
0.8787	0.999662	1.0000	0.0442	40.596143	0.008731	0.060434	0.218258	22968.159952
0.8769	0.999646	1.0000	0.0455	40.512696	0.009020	0.062435	0.225562	23417.300515
0.8750	0.999629	1.0000	0.0468	40.429269	0.009315	0.064475	0.233018	23870.151046
0.8732	0.999612	1.0000	0.0482	40.345861	0.009615	0.066554	0.240627	24326.746404
0.8714	0.999594	1.0000	0.0496	40.262472	0.009921	0.068672	0.248392	24787.121795
0.8696	0.999576	1.0000	0.0510	40.179102	0.010233	0.070829	0.256315	25251.312774
0.8678	0.999557	1.0000	0.0525	40.095753	0.010550	0.073025	0.264396	25719.355248
0.8659	0.999538	1.0000	0.0539	40.012424	0.010873	0.075262	0.272638	26191.285484
0.0000						0.075262		
0.0000						1.000000		

Spreadsheet for Calculation of Stream-Water Saturation Profiles

Injection Temperature 650 °K Initial Temperature 400 °K Matrix Heat Capacity 1.0000 (kJ/kg)

TRAILING SHOCK CALCULATIONS

Saturation	OF	Wave V	Flow V	Shock V	f_v	dK_{rv}/dS_v	dK_{rl}/dS_l		
0.7500	2.42E-01	0.255386	0.556992	0.013421	0.996549	1.0000	0.1875		
0.875	5.56E-02	0.063132	0.677295	0.007514	0.999629	1.0000	0.0469		
0.9375	7.87E-03	0.014687	0.691596	0.006812	0.999957	1.0000	0.0117		
0.96875	-3.28E-03	0.003516	0.692013	0.006792	0.999995	1.0000	0.0029		
0.953125	1.30E-03	0.008087	0.692162	0.006784	0.999982	1.0000	0.0066		
0.9609375	-1.23E-03	0.005554	0.692162	0.006784	0.999990	1.0000	0.0046		
0.95703125	-2.54E-05	0.006758	0.692182	0.006783	0.999986	1.0000	0.0055		
0.955078125	6.23E-04	0.007406	0.692178	0.006784	0.999984	1.0000	0.0061		
0.9560546875	2.95E-04	0.007078	0.692181	0.006783	0.999985	1.0000	0.0058		
0.9565429688	1.34E-04	0.006917	0.692182	0.006783	0.999986	1.0000	0.0057		
0.9567871094	5.40E-05	0.006837	0.692182	0.006783	0.999986	1.0000	0.0056		
0.9569091797	1.42E-05	0.006798	0.692182	0.006783	0.999986	1.0000	0.0056		
0.9569702148	-5.61E-06	0.006778	0.692182	0.006783	0.999986	1.0000	0.0056		
0.9569396973	4.30E-06	0.006788	0.692182	0.006783	0.999986	1.0000	0.0056		
0.9569549561	-6.54E-07	0.006783	0.692182	0.006783	0.999986	1.0000	0.0056		
0.9569473267	1.82E-06	0.006785	0.692182	0.006783	0.999986	1.0000	0.0056		
0.9569511414	5.84E-07	0.006784	0.692182	0.006783	0.999986	1.0000	0.0056		
0.9569530487	-3.48E-08	0.006783	0.692182	0.006783	0.999986	1.0000	0.0056		
0.956952095	2.75E-07	0.006784	0.692182	0.006783	0.999986	1.0000	0.0056		
0.9569525719	1.20E-07	0.006783	0.692182	0.006783	0.999986	1.0000	0.0056		
0.9569528103	4.26E-08	0.006783	0.692182	0.006783	0.999986	1.0000	0.0056		
0.9569529295	3.85E-09	0.006783	0.692182	0.006783	0.999986	1.0000	0.0056		
0.9569529891	-1.55E-08	0.006783	0.692182	0.006783	0.999986	1.0000	0.0056		
0.9569529593	-5.82E-09	0.006783	0.692182	0.006783	0.999986	1.0000	0.0056		
0.9569529444	-9.83E-10	0.006783	0.692182	0.006783	0.999986	1.0000	0.0056		
0.9569529369	1.44E-09	0.006783	0.692182	0.006783	0.999986	1.0000	0.0056		

Saturation	Total Mob	dF_v/dS_v	G	F	Gamma	Theta	High	Low
0.75	34.759228	0.045851	220.095758	12.870589	1.1794E+07	30550.407113	1	0.5
0.875	40.427490	0.009321	115.033000	10.281953	1.1701E+07	28275.535543	1	0.75
0.9375	43.300978	0.002124	62.501620	10.006619	1.1655E+07	28033.574650	1	0.875
0.96875	44.742642	0.000508	36.235931	9.974642	1.1632E+07	28005.473055	1	0.9375
0.953125	44.021547	0.001168	49.368776	9.985337	1.1643E+07	28014.871837	0.96875	0.9375
0.9609375	44.382039	0.000802	42.802353	9.978906	1.1638E+07	28009.220503	0.96875	0.953125
0.95703125	44.201778	0.000976	46.085564	9.981821	1.1641E+07	28011.782338	0.9609375	0.953125
0.955078125	44.111658	0.001070	47.727170	9.983500	1.1642E+07	28013.257853	0.95703125	0.953125
0.9560546875	44.156717	0.001023	46.906367	9.982642	1.1641E+07	28012.503198	0.95703125	0.955078125
0.9565429688	44.179247	0.000999	46.495966	9.982227	1.1641E+07	28012.138595	0.95703125	0.9560546875
0.9567871094	44.190513	0.000988	46.290765	9.982023	1.1641E+07	28011.959430	0.95703125	0.95654296875
0.9569091797	44.196145	0.000982	46.188165	9.981922	1.1641E+07	28011.870625	0.95703125	0.95678710938
0.9569702148	44.198962	0.000979	46.136864	9.981871	1.1641E+07	28011.826417	0.95703125	0.95690917969
0.9569396973	44.197553	0.000981	46.162515	9.981897	1.1641E+07	28011.848505	0.95697021484	0.95690917969
0.9569549561	44.198258	0.000980	46.149690	9.981884	1.1641E+07	28011.837457	0.95697021484	0.95693969727
0.9569473267	44.197905	0.000980	46.156102	9.981890	1.1641E+07	28011.842980	0.95695495605	0.95693969727
0.9569511414	44.198082	0.000980	46.152896	9.981887	1.1641E+07	28011.840218	0.95695495605	0.95694732666
0.9569530487	44.198170	0.000980	46.151293	9.981886	1.1641E+07	28011.838838	0.95695495605	0.95695114136
0.956952095	44.198126	0.000980	46.152094	9.981886	1.1641E+07	28011.839528	0.95695304871	0.95695114136
0.9569525719	44.198148	0.000980	46.151693	9.981886	1.1641E+07	28011.839183	0.95695304871	0.95695209503
0.9569528103	44.198159	0.000980	46.151493	9.981886	1.1641E+07	28011.839010	0.95695304871	0.95695257187
0.9569529295	44.198164	0.000980	46.151393	9.981886	1.1641E+07	28011.838924	0.95695304871	0.95695281029
0.9569529891	44.198167	0.000980	46.151343	9.981886	1.1641E+07	28011.838881	0.95695304871	0.9569529295
0.9569529593	44.198165	0.000980	46.151368	9.981886	1.1641E+07	28011.838902	0.9569529891	0.9569529295
0.9569529444	44.198165	0.000980	46.151380	9.981886	1.1641E+07	28011.838913	0.9569529593	0.9569529295
0.9569529369	44.198164	0.000980	46.151387	9.981886	1.1641E+07	28011.838919	0.9569529444	0.9569529295

Spreadsheet for Calculation of Stream-Water Saturation Profiles

Injection Temperature 650 °K		Initial Temperature 400 °K			Matrix Heat Capacity 1.0000 (kJ/kg)		
LEADING SHOCK CALCULATIONS							
Saturation	OF	Wave V	Flow V	Shock V	f_v	dK_{rv}/dS_v	dK_{rl}/dS_l
0.7500	2.40E-01	0.317373	0.015380	0.076909	0.996549	1.0000	0.1875
0.875	-1.07E-02	0.064519	0.014188	0.075269	0.999629	1.0000	0.0469
0.8125	8.48E-02	0.160394	0.014395	0.075554	0.998653	1.0000	0.1055
0.84375	3.06E-02	0.105872	0.014216	0.075308	0.999249	1.0000	0.0732
0.859375	8.40E-03	0.083664	0.014186	0.075266	0.999462	1.0000	0.0593
0.8671875	-1.54E-03	0.073722	0.014183	0.075262	0.999551	1.0000	0.0529
0.86328125	3.34E-03	0.078598	0.014183	0.075263	0.999508	1.0000	0.0561
0.865234375	8.74E-04	0.076137	0.014183	0.075262	0.999530	1.0000	0.0545
0.8662109375	-3.39E-04	0.074923	0.014183	0.075262	0.999541	1.0000	0.0537
0.8657226563	2.66E-04	0.075529	0.014183	0.075262	0.999535	1.0000	0.0541
0.8659667969	-3.66E-05	0.075226	0.014183	0.075262	0.999538	1.0000	0.0539
0.8658447266	1.15E-04	0.075377	0.014183	0.075262	0.999537	1.0000	0.0540
0.8659057617	3.90E-05	0.075301	0.014183	0.075262	0.999537	1.0000	0.0539
0.8659362793	1.19E-06	0.075263	0.014183	0.075262	0.999538	1.0000	0.0539
0.8659515381	-1.77E-05	0.075244	0.014183	0.075262	0.999538	1.0000	0.0539
0.8659439087	-8.27E-06	0.075254	0.014183	0.075262	0.999538	1.0000	0.0539
0.865940094	-3.54E-06	0.075259	0.014183	0.075262	0.999538	1.0000	0.0539
0.8659381866	-1.18E-06	0.075261	0.014183	0.075262	0.999538	1.0000	0.0539
0.865937233	5.03E-09	0.075262	0.014183	0.075262	0.999538	1.0000	0.0539
0.8659377098	-5.86E-07	0.075262	0.014183	0.075262	0.999538	1.0000	0.0539
0.8659374714	-2.91E-07	0.075262	0.014183	0.075262	0.999538	1.0000	0.0539
0.8659373522	-1.43E-07	0.075262	0.014183	0.075262	0.999538	1.0000	0.0539
0.8659372926	-6.89E-08	0.075262	0.014183	0.075262	0.999538	1.0000	0.0539
0.8659372628	-3.19E-08	0.075262	0.014183	0.075262	0.999538	1.0000	0.0539
0.8659372479	-1.34E-08	0.075262	0.014183	0.075262	0.999538	1.0000	0.0539
0.8659372404	-4.20E-09	0.075262	0.014183	0.075262	0.999538	1.0000	0.0539

Saturation	Total Mob	dF_v/dS_v	G	F	Gamma	Theta	High	Low
0.75	34.759228	0.045851	220.095758	12.870589	1.1794E+07	30550.407113	1	0.5
0.875	40.427490	0.009321	115.033000	10.281953	1.1701E+07	28275.535543	1	0.75
0.8125	37.576492	0.023172	167.564379	11.102088	1.1747E+07	28996.263468	0.875	0.75
0.84375	38.998477	0.015295	141.298689	10.601362	1.1724E+07	28556.229528	0.875	0.8125
0.859375	39.712193	0.012087	128.165845	10.422059	1.1713E+07	28398.659931	0.875	0.84375
0.8671875	40.069655	0.010651	121.599422	10.347467	1.1707E+07	28333.108609	0.875	0.859375
0.86328125	39.890876	0.011355	124.882633	10.383584	1.1710E+07	28364.848284	0.8671875	0.859375
0.865234375	39.980254	0.011000	123.241028	10.365236	1.1708E+07	28348.724340	0.8671875	0.86328125
0.8662109375	40.024952	0.010824	122.420225	10.356280	1.1708E+07	28340.853555	0.8671875	0.865234375
0.8657226563	40.002602	0.010912	122.830626	10.360740	1.1708E+07	28344.773142	0.8662109375	0.865234375
0.8659667969	40.013777	0.010868	122.625426	10.358506	1.1708E+07	28342.809407	0.8662109375	0.86572265625
0.8658447266	40.008189	0.010890	122.728026	10.359622	1.1708E+07	28343.790288	0.86596679688	0.86572265625
0.8659057617	40.010983	0.010879	122.676726	10.359064	1.1708E+07	28343.299601	0.86596679688	0.86584472656
0.8659362793	40.012380	0.010873	122.651076	10.358785	1.1708E+07	28343.054442	0.86596679688	0.86590576172
0.8659515381	40.013078	0.010871	122.638251	10.358645	1.1708E+07	28342.931909	0.86596679688	0.8659362793
0.8659439087	40.012729	0.010872	122.644663	10.358715	1.1708E+07	28342.993172	0.86595153809	0.8659362793
0.865940094	40.012554	0.010873	122.647869	10.358750	1.1708E+07	28343.023806	0.86594390869	0.8659362793
0.8659381866	40.012467	0.010873	122.649473	10.358767	1.1708E+07	28343.039124	0.86594009399	0.8659362793
0.865937233	40.012423	0.010873	122.650274	10.358776	1.1708E+07	28343.046783	0.86593818665	0.8659362793
0.8659377098	40.012445	0.010873	122.649873	10.358771	1.1708E+07	28343.042953	0.86593818665	0.86593723297
0.8659374714	40.012434	0.010873	122.650074	10.358774	1.1708E+07	28343.044868	0.86593770981	0.86593723297
0.8659373522	40.012429	0.010873	122.650174	10.358775	1.1708E+07	28343.045825	0.86593747139	0.86593723297
0.8659372926	40.012426	0.010873	122.650224	10.358775	1.1708E+07	28343.046304	0.86593735218	0.86593723297
0.8659372628	40.012425	0.010873	122.650249	10.358776	1.1708E+07	28343.046543	0.86593729258	0.86593723297
0.8659372479	40.012424	0.010873	122.650262	10.358776	1.1708E+07	28343.046663	0.86593726277	0.86593723297
0.8659372404	40.012424	0.010873	122.650268	10.358776	1.1708E+07	28343.046723	0.86593724787	0.86593723297

Spreadsheet for Calculation of Stream-Water Saturation Profiles

Injection Temperature
650 °K

Initial Temperature
425 °K

Matrix Heat Capacity
1.0000 (kJ/kg)

MATRIX PROPERTIES

Porosity	Cp Matrix	Density	Rho * Cp
0.10	1.00	2650.00	2650.0000
Nw	Ng	Swl	Denom
3.00	1.00	0.00	1.000000

SATURATION CONDITIONS

Tsaturation = 485.57

	Volumes (m3/kg)	Enthalpies (kJ/kg)	Densities (kg/m3)	Viscosities (cp)	Saturation Step
Liquid	0.001176	901.41	850.4723	0.1303	0.0021968707
Vapor	0.100298	2808.52	9.970241	0.0217	

BOUNDARY CONDITIONS

	Temperature	Velocity	Heat Capacity	Wave Velocity	Density	Enthalpy
Injection	650	1.000000	2.30	0.006622	6.882648	3199.91
Initial	425	0.016536	4.28	0.023370	916.2032	634.90
	G	F	Gamma	Theta		
Injection	650	6.88	6.88	15524523.87	22023.87	
Initial	425	916.20	916.20	10717946.32	581696.32	

SHOCK CONDITIONS

	Initial Guess Sv-Hi	Initial Guess Sv-Low	Vapor Saturation	Objective Function	Two-Phase Wave Velocity	Upstream Flow Velocity	Shock Velocity	Vapor Frac Flow
Trailing	1	0.5	0.9570	1.4356E-09	0.0068	0.692182	0.0068	1.0000
Leading	1	0.5	0.8471	8.5479E-09	0.1008	0.016536	0.1008	0.9993
	dKr/dSv	dKr/dSl	Total Mobility	dPv/dSv	G	F'	Gamma	Theta'
Trailing	1.0000	0.0056	44.1982	0.0010	46.1514	9.9819	1.1641E+07	22011.8389
Leading	1.0000	0.0701	39.1518	0.0146	138.4751	10.5592	1.1722E+07	28519.1850

MATERIAL BALANCES

	Inside	Initial	Injected	Produced	Balance	Error
Mass	83.352360	91.620322	6.882648	15.150571	0.0000	0.0000%
Enthalpy	1084213.7253	1071794.6324	22023.8721	9619.0792	-14.3000	0.0013%

Spreadsheet for Calculation of Stream-Water Saturation Profiles

Injection Temperature 650 °K			Initial Temperature 425 °K			Matrix Heat Capacity 1.0000 (kJ/kg)		
SATURATION PROFILE								
Vapor Saturation	Vapor Frac Flow	dKrv/dSv	dKr/dSi	Total Mobility	dFv/dSv	lambda	Mass Inside	Enthalpy Inside
1.0000						0.000000		
1.0000						0.006783		
0.9570	0.999986	1.0000	0.0056	44.198164	0.000980	0.006783	0.046687	105308.165674
0.9548	0.999984	1.0000	0.0061	44.096799	0.001086	0.007517	0.034514	8535.609228
0.9526	0.999981	1.0000	0.0068	43.995444	0.001198	0.008290	0.037828	9003.512125
0.9504	0.999979	1.0000	0.0074	43.894099	0.001315	0.009103	0.041310	9475.846860
0.9482	0.999976	1.0000	0.0081	43.792765	0.001439	0.009958	0.044960	9952.662911
0.9460	0.999972	1.0000	0.0088	43.691443	0.001568	0.010854	0.048782	10434.010322
0.9438	0.999969	1.0000	0.0095	43.590132	0.001703	0.011791	0.052777	10919.939716
0.9416	0.999965	1.0000	0.0102	43.488835	0.001845	0.012770	0.056948	11410.502299
0.9394	0.999961	1.0000	0.0110	43.387550	0.001993	0.013792	0.061298	11905.749868
0.9372	0.999956	1.0000	0.0118	43.286279	0.002146	0.014856	0.065829	12405.734818
0.9350	0.999951	1.0000	0.0127	43.185021	0.002306	0.015964	0.070542	12910.510149
0.9328	0.999946	1.0000	0.0136	43.083778	0.002473	0.017115	0.075442	13420.129478
0.9306	0.999940	1.0000	0.0145	42.982551	0.002645	0.018310	0.080530	13934.647041
0.9284	0.999934	1.0000	0.0154	42.881338	0.002824	0.019549	0.085809	14454.117705
0.9262	0.999928	1.0000	0.0163	42.780141	0.003010	0.020834	0.091281	14978.596974
0.9240	0.999921	1.0000	0.0173	42.678961	0.003202	0.022163	0.096949	15508.140998
0.9218	0.999914	1.0000	0.0183	42.577798	0.003401	0.023538	0.102817	16042.806583
0.9196	0.999906	1.0000	0.0194	42.476652	0.003606	0.024959	0.108886	16582.651195
0.9174	0.999898	1.0000	0.0205	42.375524	0.003818	0.026427	0.115159	17127.732973
0.9152	0.999889	1.0000	0.0216	42.274414	0.004037	0.027942	0.121639	17678.110736
0.9130	0.999880	1.0000	0.0227	42.173324	0.004262	0.029504	0.128329	18233.843991
0.9108	0.999871	1.0000	0.0239	42.072252	0.004495	0.031113	0.135233	18794.992942
0.9086	0.999860	1.0000	0.0250	41.971200	0.004735	0.032772	0.142351	19361.618501
0.9064	0.999850	1.0000	0.0263	41.870169	0.004981	0.034478	0.149689	19933.782295
0.9042	0.999839	1.0000	0.0275	41.769158	0.005235	0.036235	0.157249	20511.546676
0.9020	0.999827	1.0000	0.0288	41.668169	0.005496	0.038040	0.165033	21094.974729
0.8998	0.999814	1.0000	0.0301	41.567202	0.005764	0.039896	0.173045	21684.130286
0.8976	0.999801	1.0000	0.0314	41.466257	0.006039	0.041803	0.181288	22279.077930
0.8954	0.999788	1.0000	0.0328	41.365334	0.006322	0.043761	0.189766	22879.883008
0.8932	0.999774	1.0000	0.0342	41.264435	0.006612	0.045770	0.198481	23486.611641
0.8910	0.999759	1.0000	0.0356	41.163559	0.006910	0.047832	0.207436	24099.330734
0.8888	0.999743	1.0000	0.0371	41.062708	0.007216	0.049946	0.216636	24718.107983
0.8867	0.999727	1.0000	0.0385	40.961882	0.007529	0.052113	0.226084	25343.011890
0.8845	0.999710	1.0000	0.0401	40.861080	0.007850	0.054334	0.235782	25974.111772
0.8823	0.999693	1.0000	0.0416	40.760304	0.008178	0.056609	0.245734	26611.477770
0.8801	0.999674	1.0000	0.0432	40.659555	0.008515	0.058939	0.255945	27255.180861
0.8779	0.999655	1.0000	0.0448	40.558832	0.008860	0.061324	0.266417	27905.292869
0.8757	0.999635	1.0000	0.0464	40.458136	0.009212	0.063765	0.277154	28561.886477
0.8735	0.999615	1.0000	0.0480	40.357468	0.009573	0.066262	0.288160	29225.035237
0.8713	0.999593	1.0000	0.0497	40.256828	0.009942	0.068816	0.299438	29894.813581
0.8691	0.999571	1.0000	0.0514	40.156217	0.010319	0.071428	0.310993	30571.296833
0.8669	0.999548	1.0000	0.0532	40.055635	0.010705	0.074097	0.322828	31254.561223
0.8647	0.999524	1.0000	0.0549	39.955082	0.011099	0.076825	0.334947	31944.683896
0.8625	0.999499	1.0000	0.0567	39.854560	0.011502	0.079612	0.347353	32641.742925
0.8603	0.999473	1.0000	0.0586	39.754068	0.011913	0.082459	0.360052	33345.817325
0.8581	0.999447	1.0000	0.0604	39.653607	0.012333	0.085366	0.373047	34056.987060
0.8559	0.999419	1.0000	0.0623	39.553177	0.012762	0.088334	0.386343	34775.333065
0.8537	0.999391	1.0000	0.0642	39.452780	0.013199	0.091364	0.399942	35500.937249
0.8515	0.999361	1.0000	0.0662	39.352415	0.013646	0.094456	0.413851	36233.882513
0.8493	0.999331	1.0000	0.0681	39.252083	0.014102	0.097610	0.428072	36974.252765
0.8471	0.999299	1.0000	0.0701	39.151785	0.014567	0.100828	0.442610	37722.132929
0.0000						0.100828		
0.0000						1.000000		

Spreadsheet for Calculation of Stream-Water Saturation Profiles

Injection Temperature 650 °K		Initial Temperature 425 °K		Matrix Heat Capacity 1.0000 (kJ/kg)				
TRAILING SHOCK CALCULATIONS								
Saturation	OP	Wave V	Flow V	Shock V	fv	dKr/dSv	dKr/dSI	
0.7500	2.42E-01	0.255386	0.556992	0.013421	0.996549	1.0000	0.1875	
0.875	5.56E-02	0.063132	0.677295	0.007514	0.999629	1.0000	0.0469	
0.9375	7.87E-03	0.014687	0.691596	0.006812	0.999957	1.0000	0.0117	
0.96875	-3.28E-03	0.003516	0.692013	0.006792	0.999995	1.0000	0.0029	
0.953125	1.30E-03	0.008087	0.692162	0.006784	0.999982	1.0000	0.0066	
0.9609375	-1.23E-03	0.005554	0.692162	0.006784	0.999990	1.0000	0.0046	
0.95703125	-2.54E-05	0.006758	0.692182	0.006783	0.999986	1.0000	0.0055	
0.955078125	6.23E-04	0.007406	0.692178	0.006784	0.999984	1.0000	0.0061	
0.9560546875	2.95E-04	0.007078	0.692181	0.006783	0.999985	1.0000	0.0058	
0.9565429688	1.34E-04	0.006917	0.692182	0.006783	0.999986	1.0000	0.0057	
0.9567871094	5.40E-05	0.006837	0.692182	0.006783	0.999986	1.0000	0.0056	
0.9569091797	1.42E-05	0.006798	0.692182	0.006783	0.999986	1.0000	0.0056	
0.9569702148	-5.61E-06	0.006778	0.692182	0.006783	0.999986	1.0000	0.0056	
0.9569396973	4.30E-06	0.006788	0.692182	0.006783	0.999986	1.0000	0.0056	
0.9569549561	-6.54E-07	0.006783	0.692182	0.006783	0.999986	1.0000	0.0056	
0.9569473267	1.82E-06	0.006785	0.692182	0.006783	0.999986	1.0000	0.0056	
0.9569511414	5.84E-07	0.006784	0.692182	0.006783	0.999986	1.0000	0.0056	
0.9569530487	-3.48E-08	0.006783	0.692182	0.006783	0.999986	1.0000	0.0056	
0.956952095	2.75E-07	0.006784	0.692182	0.006783	0.999986	1.0000	0.0056	
0.9569525719	1.20E-07	0.006783	0.692182	0.006783	0.999986	1.0000	0.0056	
0.9569528103	4.26E-08	0.006783	0.692182	0.006783	0.999986	1.0000	0.0056	
0.9569529295	3.85E-09	0.006783	0.692182	0.006783	0.999986	1.0000	0.0056	
0.9569529891	-1.55E-08	0.006783	0.692182	0.006783	0.999986	1.0000	0.0056	
0.9569529593	-5.82E-09	0.006783	0.692182	0.006783	0.999986	1.0000	0.0056	
0.9569529444	-9.83E-10	0.006783	0.692182	0.006783	0.999986	1.0000	0.0056	
0.9569529369	1.44E-09	0.006783	0.692182	0.006783	0.999986	1.0000	0.0056	
Saturation	Total Mob	dFv/dSv	G	F	Gamma	Theta	High	Low
0.75	34.759228	0.045851	220.095758	12.870589	1.1794E+07	30550.407113	1	0.5
0.875	40.427490	0.009321	115.033000	10.281953	1.1701E+07	28275.535543	1	0.75
0.9375	43.300978	0.002124	62.501620	10.006619	1.1655E+07	28033.574650	1	0.875
0.96875	44.742642	0.000508	36.235931	9.974642	1.1632E+07	28005.473055	1	0.9375
0.953125	44.021547	0.001168	49.368776	9.985337	1.1643E+07	28014.871837	0.96875	0.9375
0.9609375	44.382039	0.000802	42.802353	9.978906	1.1638E+07	28009.220503	0.96875	0.953125
0.95703125	44.201778	0.000976	46.085564	9.981821	1.1641E+07	28011.782338	0.9609375	0.953125
0.955078125	44.111658	0.001070	47.727170	9.983500	1.1642E+07	28013.257853	0.95703125	0.953125
0.9560546875	44.156717	0.001023	46.906367	9.982642	1.1641E+07	28012.503198	0.95703125	0.955078125
0.9565429688	44.179247	0.000999	46.495966	9.982227	1.1641E+07	28012.138595	0.95703125	0.9560546875
0.9567871094	44.190513	0.000988	46.290765	9.982023	1.1641E+07	28011.959430	0.95703125	0.95654296875
0.9569091797	44.196145	0.000982	46.188165	9.981922	1.1641E+07	28011.870625	0.95703125	0.95678710938
0.9569702148	44.198962	0.000979	46.136864	9.981871	1.1641E+07	28011.826417	0.95703125	0.95690917969
0.9569396973	44.197553	0.000981	46.162515	9.981897	1.1641E+07	28011.848505	0.95697021484	0.95690917969
0.9569549561	44.198258	0.000980	46.149690	9.981884	1.1641E+07	28011.837457	0.95697021484	0.95693969727
0.9569473267	44.197905	0.000980	46.156102	9.981890	1.1641E+07	28011.842980	0.95695495605	0.95694732666
0.9569511414	44.198082	0.000980	46.152896	9.981887	1.1641E+07	28011.840218	0.95695495605	0.95694732666
0.9569530487	44.198170	0.000980	46.151293	9.981886	1.1641E+07	28011.838838	0.95695495605	0.95695114136
0.956952095	44.198126	0.000980	46.152094	9.981886	1.1641E+07	28011.839528	0.95695304871	0.95695114136
0.9569525719	44.198148	0.000980	46.151693	9.981886	1.1641E+07	28011.839183	0.95695304871	0.95695209503
0.9569528103	44.198159	0.000980	46.151493	9.981886	1.1641E+07	28011.839010	0.95695304871	0.95695257187
0.9569529295	44.198164	0.000980	46.151393	9.981886	1.1641E+07	28011.838924	0.95695304871	0.95695281029
0.9569529891	44.198167	0.000980	46.151343	9.981886	1.1641E+07	28011.838881	0.95695304871	0.9569529295
0.9569529593	44.198165	0.000980	46.151368	9.981886	1.1641E+07	28011.838902	0.9569529891	0.9569529295
0.9569529444	44.198165	0.000980	46.151380	9.981886	1.1641E+07	28011.838913	0.9569529593	0.9569529295
0.9569529369	44.198164	0.000980	46.151387	9.981886	1.1641E+07	28011.838919	0.9569529444	0.9569529295

Spreadsheet for Calculation of Stream-Water Saturation Profiles

Injection Temperature 650 °K Initial Temperature 425 °K Matrix Heat Capacity 1.0000 (kJ/kg)

LEADING SHOCK CALCULATIONS

Saturation	OF	Wave V	Flow V	Shock V	fv	dKrv/dSv	dKr/dsI
0.7500	2.15E-01	0.317373	0.017479	0.102077	0.996549	1.0000	0.1875
0.875	-3.64E-02	0.064519	0.016591	0.100901	0.999629	1.0000	0.0469
0.8125	5.94E-02	0.160394	0.016637	0.100962	0.998653	1.0000	0.1055
0.84375	5.04E-03	0.105872	0.016537	0.100829	0.999249	1.0000	0.0732
0.859375	-1.72E-02	0.083664	0.016547	0.100843	0.999462	1.0000	0.0593
0.8515625	-6.46E-03	0.094371	0.016538	0.100830	0.999362	1.0000	0.0661
0.84765625	-8.07E-04	0.100021	0.016536	0.100828	0.999307	1.0000	0.0696
0.845703125	2.09E-03	0.102921	0.016536	0.100828	0.999279	1.0000	0.0714
0.8466796875	6.37E-04	0.101465	0.016536	0.100828	0.999293	1.0000	0.0705
0.8471679688	-8.66E-05	0.100741	0.016536	0.100828	0.999300	1.0000	0.0701
0.8469238281	2.75E-04	0.101103	0.016536	0.100828	0.999297	1.0000	0.0703
0.8470458984	9.40E-05	0.100922	0.016536	0.100828	0.999298	1.0000	0.0702
0.8471069336	3.66E-06	0.100832	0.016536	0.100828	0.999299	1.0000	0.0701
0.8471374512	-4.15E-05	0.100786	0.016536	0.100828	0.999300	1.0000	0.0701
0.8471221924	-1.89E-05	0.100809	0.016536	0.100828	0.999299	1.0000	0.0701
0.847114563	-7.63E-06	0.100820	0.016536	0.100828	0.999299	1.0000	0.0701
0.8471107483	-1.99E-06	0.100826	0.016536	0.100828	0.999299	1.0000	0.0701
0.8471088409	8.35E-07	0.100829	0.016536	0.100828	0.999299	1.0000	0.0701
0.8471097946	-5.76E-07	0.100827	0.016536	0.100828	0.999299	1.0000	0.0701
0.8471093178	1.30E-07	0.100828	0.016536	0.100828	0.999299	1.0000	0.0701
0.8471095562	-2.23E-07	0.100828	0.016536	0.100828	0.999299	1.0000	0.0701
0.847109437	-4.66E-08	0.100828	0.016536	0.100828	0.999299	1.0000	0.0701
0.8471093774	4.16E-08	0.100828	0.016536	0.100828	0.999299	1.0000	0.0701
0.8471094072	-2.47E-09	0.100828	0.016536	0.100828	0.999299	1.0000	0.0701
0.8471093923	1.96E-08	0.100828	0.016536	0.100828	0.999299	1.0000	0.0701
0.8471093997	8.55E-09	0.100828	0.016536	0.100828	0.999299	1.0000	0.0701

Saturation	Total Mob	dFv/dSv	G	F	Gamma	Theta	High	Low
0.75	34.759228	0.045851	220.095758	12.870589	1.1794E+07	30550.407113	1	0.5
0.875	40.427490	0.009321	115.033000	10.281953	1.1701E+07	28275.535543	1	0.75
0.8125	37.576492	0.023172	167.564379	11.102088	1.1747E+07	28996.263468	0.875	0.75
0.84375	38.998477	0.015295	141.298489	10.601362	1.1724E+07	28556.229528	0.875	0.8125
0.859375	39.712193	0.012087	128.165845	10.422059	1.1713E+07	28398.659931	0.875	0.84375
0.8515625	39.355127	0.013634	134.732267	10.506445	1.1718E+07	28472.816977	0.859375	0.84375
0.84765625	39.176748	0.014450	138.015478	10.552540	1.1721E+07	28513.324807	0.8515625	0.84375
0.845703125	39.087599	0.014869	139.657084	10.576604	1.1723E+07	28534.472287	0.84765625	0.84375
0.8466796875	39.132170	0.014659	138.836281	10.564486	1.1722E+07	28523.822989	0.84765625	0.845703125
0.8471679688	39.154459	0.014554	138.425880	10.558491	1.1722E+07	28518.555091	0.84765625	0.8466796875
0.8469238281	39.143314	0.014606	138.631080	10.561483	1.1722E+07	28521.184328	0.84716796875	0.84692382813
0.8470458984	39.148886	0.014580	138.528480	10.559986	1.1722E+07	28519.868533	0.84716796875	0.84704589844
0.8471069336	39.151672	0.014567	138.477180	10.559238	1.1722E+07	28519.211518	0.84716796875	0.84710693359
0.8471374512	39.153066	0.014561	138.451530	10.558865	1.1722E+07	28518.883231	0.84716796875	0.84710693359
0.8471221924	39.152369	0.014564	138.464355	10.559052	1.1722E+07	28519.047356	0.84713745117	0.84710693359
0.847114563	39.152021	0.014566	138.470767	10.559145	1.1722E+07	28519.129432	0.84712219238	0.84710693359
0.8471107483	39.151847	0.014566	138.473973	10.559192	1.1722E+07	28519.170474	0.84711456299	0.84710693359
0.8471088409	39.151760	0.014567	138.475577	10.559215	1.1722E+07	28519.190996	0.84711074829	0.84710693359
0.8471097946	39.151803	0.014567	138.474775	10.559203	1.1722E+07	28519.180735	0.84711074829	0.84710884094
0.8471093178	39.151781	0.014567	138.475176	10.559209	1.1722E+07	28519.185865	0.84710979462	0.84710884094
0.8471095562	39.151792	0.014567	138.474975	10.559206	1.1722E+07	28519.183300	0.84710979462	0.84710931778
0.847109437	39.151787	0.014567	138.475076	10.559208	1.1722E+07	28519.184583	0.8471095562	0.84710931778
0.8471093774	39.151784	0.014567	138.475126	10.559208	1.1722E+07	28519.185224	0.84710943699	0.84710931778
0.8471094072	39.151785	0.014567	138.475101	10.559208	1.1722E+07	28519.184903	0.84710943699	0.84710937738
0.8471093923	39.151785	0.014567	138.475113	10.559208	1.1722E+07	28519.185064	0.84710940719	0.84710937738
0.8471093997	39.151785	0.014567	138.475107	10.559208	1.1722E+07	28519.184983	0.84710940719	0.84710939229

Spreadsheet for Calculation of Stream-Water Saturation Profiles

Injection Temperature
650 °K

Initial Temperature
450 °K

Matrix Heat Capacity
1.0000 (kJ/kg)

MATRIX PROPERTIES

Porosity	Cp Matrix	Density	Rho * Cp
0.10	1.00	2650.00	2650.0000
Nw	Ng	Swl	Denom
3.00	1.00	0.00	1.000000

SATURATION CONDITIONS

Tsaturation = 485.57

	Volumes (m3/kg)	Enthalpies (kJ/kg)	Densities (kg/m3)	Viscosities (cp)	Saturation Step
Liquid	0.001176	901.41	850.4723	0.1303	0.0028981477
Vapor	0.100298	2808.52	9.970241	0.0217	

BOUNDARY CONDITIONS

	Temperature	Velocity	Heat Capacity	Wave Velocity	Density	Enthalpy
Injection	650	1.000000	2.30	0.006622	6.882648	3199.91
Initial	450	0.021720	4.37	0.030506	891.0974	743.08
	G	F	Gamma	Theta		
Injection	650	6.88	6.88	15524523.87	22023.87	
Initial	450	891.10	891.10	11394652.55	662152.55	

SHOCK CONDITIONS

	Initial Guess		Vapor Saturation	Objective Function	Two-Phase Wave Velocity	Upstream Flow Velocity	Shock Velocity	Vapor Frac Flow
Trailing	Sv-Hi	Sv-Low	0.9570	1.4356E-09	0.0068	0.692182	0.0068	1.0000
Leading	1	0.5	0.8120	1.5598E-09	0.1613	0.021720	0.1613	0.9986
	dKrv/dSv	dKrl/dSl	Total Mobility	dFv/dSv	G	F'	Gamma	Theta'
Trailing	1.0000	0.0056	44.1982	0.0010	46.1514	9.9819	1.1641E+07	28011.8389
Leading	1.0000	0.1060	37.5559	0.0233	167.9463	11.1110	1.1748E+07	29004.0634

MATERIAL BALANCES

	Inside	Initial	Injected	Produced	Balance	Error
Mass	76.637490	89.109742	6.882648	19.354803	0.0001	0.0001%
Enthalpy	1147135.5437	1139465.2553	22023.8721	14382.0777	-28.4941	0.0025%

Spreadsheet for Calculation of Stream-Water Saturation Profiles

Injection Temperature 650 °K		Initial Temperature 450 °K				Matrix Heat Capacity 1.0000 (kJ/kg)		
SATURATION PROFILE								
Vapor Saturation	Vapor Frac Flow	dKrv/dSv	dKr/dSi	Total Mobility	dFv/dSv	lambda	Mass Inside	Enthalpy Inside
1.0000						0.000000		
1.0000						0.006783		
0.9570	0.999986	1.0000	0.0056	44.198164	0.000980	0.006783	0.046687	105308.165674
0.9541	0.999983	1.0000	0.0063	44.064444	0.001121	0.007759	0.046215	11358.614465
0.9512	0.999980	1.0000	0.0072	43.930740	0.001272	0.008805	0.052076	12175.378329
0.9483	0.999976	1.0000	0.0080	43.797056	0.001433	0.009921	0.058322	13002.371478
0.9454	0.999971	1.0000	0.0090	43.663392	0.001605	0.011109	0.064961	13839.744867
0.9425	0.999966	1.0000	0.0099	43.529749	0.001787	0.012370	0.071998	14687.651745
0.9396	0.999961	1.0000	0.0110	43.396128	0.001980	0.013704	0.079442	15546.247699
0.9367	0.999955	1.0000	0.0120	43.262531	0.002183	0.015112	0.087300	16415.690688
0.9338	0.999948	1.0000	0.0132	43.128958	0.002398	0.016596	0.095580	17296.141087
0.9309	0.999941	1.0000	0.0143	42.995411	0.002623	0.018156	0.104288	18187.761725
0.9280	0.999933	1.0000	0.0156	42.861891	0.002859	0.019793	0.113432	19090.717929
0.9251	0.999924	1.0000	0.0168	42.728398	0.003107	0.021508	0.123021	20005.177563
0.9222	0.999915	1.0000	0.0182	42.594934	0.003366	0.023302	0.133063	20931.311076
0.9193	0.999905	1.0000	0.0195	42.461501	0.003637	0.025176	0.143565	21869.291542
0.9164	0.999894	1.0000	0.0210	42.328098	0.003920	0.027131	0.154537	22819.294704
0.9135	0.999882	1.0000	0.0225	42.194728	0.004214	0.029169	0.165986	23781.499023
0.9106	0.999870	1.0000	0.0240	42.061392	0.004520	0.031289	0.177921	24756.085723
0.9077	0.999856	1.0000	0.0256	41.928090	0.004839	0.033494	0.190351	25743.238838
0.9048	0.999841	1.0000	0.0272	41.794824	0.005170	0.035784	0.203285	26743.145256
0.9019	0.999826	1.0000	0.0289	41.661595	0.005513	0.038160	0.216733	27755.994778
0.8990	0.999809	1.0000	0.0306	41.528403	0.005869	0.040623	0.230703	28781.980156
0.8961	0.999792	1.0000	0.0324	41.395251	0.006238	0.043175	0.245205	29821.297154
0.8932	0.999773	1.0000	0.0342	41.262139	0.006619	0.045816	0.260249	30874.144591
0.8903	0.999754	1.0000	0.0361	41.129068	0.007014	0.048549	0.275845	31940.724401
0.8874	0.999733	1.0000	0.0380	40.996040	0.007422	0.051373	0.292002	33021.241683
0.8845	0.999711	1.0000	0.0400	40.863055	0.007843	0.054290	0.308732	34115.904754
0.8816	0.999687	1.0000	0.0421	40.730115	0.008278	0.057302	0.326044	35224.925210
0.8787	0.999663	1.0000	0.0441	40.597220	0.008727	0.060409	0.343950	36348.517976
0.8758	0.999637	1.0000	0.0463	40.464373	0.009190	0.063612	0.362460	37486.901372
0.8729	0.999609	1.0000	0.0485	40.331574	0.009667	0.066914	0.381585	38640.297162
0.8700	0.999581	1.0000	0.0507	40.198824	0.010158	0.070315	0.401336	39808.930623
0.8671	0.999550	1.0000	0.0530	40.066124	0.010664	0.073816	0.421726	40993.030601
0.8642	0.999519	1.0000	0.0553	39.933475	0.011185	0.077419	0.442765	42192.829574
0.8613	0.999486	1.0000	0.0577	39.800879	0.011720	0.081126	0.464466	43408.563716
0.8584	0.999451	1.0000	0.0601	39.668337	0.012271	0.084936	0.486841	44640.472962
0.8555	0.999414	1.0000	0.0626	39.535849	0.012837	0.088853	0.509903	45888.801074
0.8526	0.999376	1.0000	0.0652	39.403418	0.013418	0.092877	0.533663	47153.795706
0.8497	0.999337	1.0000	0.0678	39.271043	0.014015	0.097009	0.558135	48435.708473
0.8468	0.999295	1.0000	0.0704	39.138727	0.014628	0.101252	0.583333	49734.795025
0.8439	0.999252	1.0000	0.0731	39.006470	0.015257	0.105606	0.609268	51051.315111
0.8410	0.999207	1.0000	0.0758	38.874273	0.015902	0.110073	0.635956	52385.532655
0.8381	0.999160	1.0000	0.0786	38.742137	0.016564	0.114654	0.663410	53737.715831
0.8352	0.999111	1.0000	0.0814	38.610065	0.017243	0.119351	0.691644	55108.137134
0.8323	0.999060	1.0000	0.0843	38.478056	0.017938	0.124166	0.720673	56497.073461
0.8294	0.999007	1.0000	0.0873	38.346112	0.018651	0.129100	0.750512	57904.806187
0.8265	0.998952	1.0000	0.0903	38.214233	0.019381	0.134155	0.781174	59331.621243
0.8236	0.998894	1.0000	0.0933	38.082422	0.020129	0.139331	0.812677	60777.809198
0.8207	0.998835	1.0000	0.0964	37.950680	0.020895	0.144632	0.845034	62243.665344
0.8178	0.998773	1.0000	0.0995	37.819006	0.021679	0.150058	0.878263	63729.489777
0.8149	0.998709	1.0000	0.1027	37.687403	0.022481	0.155612	0.912379	65235.587483
0.8120	0.998643	1.0000	0.1060	37.555872	0.023302	0.161294	0.947400	66762.268427
0.0000						0.161294		
0.0000						1.000000		

Spreadsheet for Calculation of Stream-Water Saturation Profiles

Injection Temperature 650 °K		Initial Temperature 450 °K		Matrix Heat Capacity 1.0000 (kJ/kg)				
TRAILING SHOCK CALCULATIONS								
Saturation	OF	Wave V	Flow V	Shock V	f _v	dK _{rv} /dS _v	dK _r /dS _l	
0.7500	2.42E-01	0.255386	0.556992	0.013421	0.996549	1.0000	0.1875	
0.875	5.56E-02	0.063132	0.677295	0.007514	0.999629	1.0000	0.0469	
0.9375	7.87E-03	0.014687	0.691596	0.006812	0.999957	1.0000	0.0117	
0.96875	-3.28E-03	0.003516	0.692013	0.006792	0.999995	1.0000	0.0029	
0.953125	1.30E-03	0.008087	0.692162	0.006784	0.999982	1.0000	0.0066	
0.9609375	-1.23E-03	0.005554	0.692162	0.006784	0.999990	1.0000	0.0046	
0.95703125	-2.54E-05	0.006758	0.692182	0.006783	0.999986	1.0000	0.0055	
0.955078125	6.23E-04	0.007406	0.692178	0.006784	0.999984	1.0000	0.0061	
0.9560546875	2.95E-04	0.007078	0.692181	0.006783	0.999985	1.0000	0.0058	
0.9565429688	1.34E-04	0.006917	0.692182	0.006783	0.999986	1.0000	0.0057	
0.9567871094	5.40E-05	0.006837	0.692182	0.006783	0.999986	1.0000	0.0056	
0.9569091797	1.42E-05	0.006798	0.692182	0.006783	0.999986	1.0000	0.0056	
0.9569702148	-3.61E-06	0.006778	0.692182	0.006783	0.999986	1.0000	0.0056	
0.9569396973	4.30E-06	0.006788	0.692182	0.006783	0.999986	1.0000	0.0056	
0.9569549561	-6.54E-07	0.006783	0.692182	0.006783	0.999986	1.0000	0.0056	
0.9569473267	1.82E-06	0.006785	0.692182	0.006783	0.999986	1.0000	0.0056	
0.9569511414	5.84E-07	0.006784	0.692182	0.006783	0.999986	1.0000	0.0056	
0.9569530487	-3.48E-08	0.006783	0.692182	0.006783	0.999986	1.0000	0.0056	
0.956952095	2.75E-07	0.006784	0.692182	0.006783	0.999986	1.0000	0.0056	
0.9569525719	1.20E-07	0.006783	0.692182	0.006783	0.999986	1.0000	0.0056	
0.9569528103	4.26E-08	0.006783	0.692182	0.006783	0.999986	1.0000	0.0056	
0.9569529295	3.85E-09	0.006783	0.692182	0.006783	0.999986	1.0000	0.0056	
0.9569529891	-1.55E-08	0.006783	0.692182	0.006783	0.999986	1.0000	0.0056	
0.9569529593	-5.82E-09	0.006783	0.692182	0.006783	0.999986	1.0000	0.0056	
0.9569529444	-9.83E-10	0.006783	0.692182	0.006783	0.999986	1.0000	0.0056	
0.9569529369	1.44E-09	0.006783	0.692182	0.006783	0.999986	1.0000	0.0056	
Saturation	Total Mob	dF _v /dS _v	G	F	Gamma	Theta	High	Low
0.75	34.759228	0.045851	220.095758	12.870589	1.1794E+07	30550.407113	1	0.5
0.875	40.427490	0.009321	115.033000	10.281953	1.1701E+07	28275.535543	1	0.75
0.9375	43.300978	0.002124	62.501620	10.006619	1.1655E+07	28033.574650	1	0.875
0.96875	44.742642	0.000508	36.235931	9.974642	1.1632E+07	28005.473055	1	0.9375
0.953125	44.021547	0.001168	49.368776	9.985337	1.1643E+07	28014.871837	0.96875	0.9375
0.9609375	44.382039	0.000802	42.802353	9.978906	1.1638E+07	28009.220503	0.96875	0.953125
0.95703125	44.201778	0.000976	46.085564	9.981821	1.1641E+07	28011.782338	0.9609375	0.953125
0.955078125	44.111658	0.001070	47.727170	9.983500	1.1642E+07	28013.257853	0.95703125	0.953125
0.9560546875	44.156717	0.001023	46.906367	9.982642	1.1641E+07	28012.503198	0.95703125	0.955078125
0.9565429688	44.179247	0.000999	46.495966	9.982227	1.1641E+07	28012.138595	0.95703125	0.9560546875
0.9567871094	44.190513	0.000988	46.290765	9.982023	1.1641E+07	28011.959430	0.95703125	0.95654296875
0.9569091797	44.196145	0.000982	46.188165	9.981922	1.1641E+07	28011.870625	0.95703125	0.95678710938
0.9569702148	44.198962	0.000979	46.136864	9.981871	1.1641E+07	28011.826417	0.95703125	0.95690917969
0.9569396973	44.197553	0.000981	46.162515	9.981897	1.1641E+07	28011.848505	0.95697021484	0.95690917969
0.9569549561	44.198258	0.000980	46.149690	9.981884	1.1641E+07	28011.837457	0.95697021484	0.95693969727
0.9569473267	44.197905	0.000980	46.156102	9.981890	1.1641E+07	28011.842980	0.95695495605	0.95693969727
0.9569511414	44.198082	0.000980	46.152896	9.981887	1.1641E+07	28011.840218	0.95695495605	0.95694732666
0.9569530487	44.198170	0.000980	46.151293	9.981886	1.1641E+07	28011.838838	0.95695495605	0.95695114136
0.956952095	44.198126	0.000980	46.152094	9.981886	1.1641E+07	28011.839528	0.95695304871	0.95695114136
0.9569525719	44.198148	0.000980	46.151693	9.981886	1.1641E+07	28011.839183	0.95695304871	0.95695209503
0.9569528103	44.198159	0.000980	46.151493	9.981886	1.1641E+07	28011.839010	0.95695304871	0.95695257187
0.9569529295	44.198164	0.000980	46.151393	9.981886	1.1641E+07	28011.838924	0.95695304871	0.95695281029
0.9569529891	44.198167	0.000980	46.151343	9.981886	1.1641E+07	28011.838881	0.95695304871	0.9569529295
0.9569529593	44.198165	0.000980	46.151368	9.981886	1.1641E+07	28011.838902	0.9569529891	0.9569529295
0.9569529444	44.198165	0.000980	46.151380	9.981886	1.1641E+07	28011.838913	0.9569529593	0.9569529295
0.9569529369	44.198164	0.000980	46.151387	9.981886	1.1641E+07	28011.838919	0.9569529444	0.9569529295

Spreadsheet for Calculation of Stream-Water Saturation Profiles

Injection Temperature 650 °K Initial Temperature 450 °K Matrix Heat Capacity 1.0000 (kJ/kg)

LEADING SHOCK CALCULATIONS

Saturation	OF	Wave V	Flow V	Shock V	fv	dKrv/dSv	dKr/dSi
0.7500	1.56E-01	0.317373	0.022186	0.161864	0.996549	1.0000	0.1875
0.875	-9.72E-02	0.064519	0.022071	0.161724	0.999629	1.0000	0.0469
0.8125	-9.00E-04	0.160394	0.021720	0.161294	0.998653	1.0000	0.1055
0.78125	6.87E-02	0.230103	0.021826	0.161424	0.997778	1.0000	0.1436
0.796875	3.19E-02	0.193211	0.021745	0.161324	0.998255	1.0000	0.1238
0.8046875	1.50E-02	0.176312	0.021726	0.161301	0.998463	1.0000	0.1144
0.80859375	6.94E-03	0.168232	0.021721	0.161295	0.998561	1.0000	0.1099
0.810546875	2.99E-03	0.164283	0.021720	0.161294	0.998608	1.0000	0.1077
0.8115234375	1.04E-03	0.162331	0.021720	0.161294	0.998631	1.0000	0.1066
0.8120117188	6.71E-05	0.161361	0.021720	0.161294	0.998642	1.0000	0.1060
0.8122558594	-4.17E-04	0.160877	0.021720	0.161294	0.998648	1.0000	0.1057
0.8121337891	-1.75E-04	0.161119	0.021720	0.161294	0.998645	1.0000	0.1059
0.8120727539	-5.39E-05	0.161240	0.021720	0.161294	0.998643	1.0000	0.1059
0.8120422363	6.58E-06	0.161301	0.021720	0.161294	0.998643	1.0000	0.1060
0.8120574951	-2.37E-05	0.161270	0.021720	0.161294	0.998643	1.0000	0.1060
0.8120498657	-8.55E-06	0.161285	0.021720	0.161294	0.998643	1.0000	0.1060
0.812046051	-9.88E-07	0.161293	0.021720	0.161294	0.998643	1.0000	0.1060
0.8120441437	2.79E-06	0.161297	0.021720	0.161294	0.998643	1.0000	0.1060
0.8120450974	9.03E-07	0.161295	0.021720	0.161294	0.998643	1.0000	0.1060
0.8120455742	-4.28E-08	0.161294	0.021720	0.161294	0.998643	1.0000	0.1060
0.8120453358	4.30E-07	0.161294	0.021720	0.161294	0.998643	1.0000	0.1060
0.812045455	1.94E-07	0.161294	0.021720	0.161294	0.998643	1.0000	0.1060
0.8120455146	7.54E-08	0.161294	0.021720	0.161294	0.998643	1.0000	0.1060
0.8120455444	1.63E-08	0.161294	0.021720	0.161294	0.998643	1.0000	0.1060
0.8120455593	-1.32E-08	0.161294	0.021720	0.161294	0.998643	1.0000	0.1060
0.8120455518	1.56E-09	0.161294	0.021720	0.161294	0.998643	1.0000	0.1060

Saturation	Total Mob	dFv/dSv	G	F	Gamma	Theta	High	Low
0.75	34.759228	0.045851	220.095758	12.870589	1.1794E+07	30550.407113	1	0.5
0.875	40.427490	0.009321	115.033000	10.281953	1.1701E+07	28275.535543	1	0.75
0.8125	37.576492	0.023172	167.564379	11.102088	1.1747E+07	28996.263468	0.875	0.75
0.78125	36.162941	0.033243	193.830069	11.837827	1.1770E+07	29642.824736	0.8125	0.75
0.796875	36.868574	0.027913	180.697224	11.436916	1.1759E+07	29290.507675	0.8125	0.78125
0.8046875	37.222259	0.025472	174.130801	11.261721	1.1753E+07	29136.547240	0.8125	0.796875
0.80859375	37.399308	0.024305	170.847590	11.180017	1.1750E+07	29064.746716	0.8125	0.8046875
0.810546875	37.487883	0.023734	169.205985	11.140588	1.1749E+07	29030.096701	0.8125	0.80859375
0.8115234375	37.532184	0.023452	168.385182	11.121223	1.1748E+07	29013.078764	0.8125	0.810546875
0.8120117188	37.554337	0.023312	167.974780	11.111627	1.1748E+07	29004.645883	0.8125	0.8115234375
0.8122558594	37.565414	0.023242	167.769580	11.106850	1.1748E+07	29000.448379	0.8125	0.81201171875
0.8121337891	37.559875	0.023277	167.872180	11.109237	1.1748E+07	29002.545555	0.81225585938	0.81201171875
0.8120727539	37.557106	0.023294	167.923480	11.110431	1.1748E+07	29003.595325	0.81213378906	0.81201171875
0.8120422363	37.555721	0.023303	167.949130	11.111029	1.1748E+07	29004.120505	0.81207275391	0.81201171875
0.8120574951	37.556414	0.023299	167.936305	11.110730	1.1748E+07	29003.857890	0.81207275391	0.81204223633
0.8120498657	37.556068	0.023301	167.942718	11.110880	1.1748E+07	29003.989192	0.81205749512	0.81204223633
0.812046051	37.555895	0.023302	167.945924	11.110954	1.1748E+07	29004.054847	0.81204986572	0.81204223633
0.8120441437	37.555808	0.023303	167.947527	11.110992	1.1748E+07	29004.087676	0.81204605103	0.81204223633
0.8120450974	37.555851	0.023302	167.946726	11.110973	1.1748E+07	29004.071261	0.81204605103	0.81204414368
0.8120455742	37.555873	0.023302	167.946325	11.110964	1.1748E+07	29004.063054	0.81204605103	0.81204509735
0.8120453358	37.555862	0.023302	167.946525	11.110968	1.1748E+07	29004.067158	0.81204557419	0.81204509735
0.812045455	37.555868	0.023302	167.946425	11.110966	1.1748E+07	29004.065106	0.81204557419	0.81204533577
0.8120455146	37.555870	0.023302	167.946375	11.110965	1.1748E+07	29004.064080	0.81204557419	0.81204545498
0.8120455444	37.555872	0.023302	167.946350	11.110964	1.1748E+07	29004.063567	0.81204557419	0.81204551458
0.8120455593	37.555872	0.023302	167.946337	11.110964	1.1748E+07	29004.063311	0.81204557419	0.81204554439
0.8120455518	37.555872	0.023302	167.946344	11.110964	1.1748E+07	29004.063439	0.81204555929	0.81204554439

Spreadsheet for Calculation of Stream-Water Saturation Profiles

Injection Temperature
650 °K

Initial Temperature
475 °K

Matrix Heat Capacity
1.0000 (kJ/kg)

MATRIX PROPERTIES

Porosity	Cp Matrix	Density	Rho * Cp
0.10	1.00	2650.00	2650.0000
Nw	Ng	Swl	Denom
3.00	1.00	0.00	1.000000

SATURATION CONDITIONS

Tsaturation = 485.57

	Volumes (m3/kg)	Enthalpies (kJ/kg)	Densities (kg/m3)	Viscosities (cp)	Saturation Step
Liquid	0.001176	901.41	850.4723	0.1303	0.0050828201
Vapor	0.100298	2808.52	9.970241	0.0217	

BOUNDARY CONDITIONS

	Temperature	Velocity	Heat Capacity	Wave Velocity	Density	Enthalpy
Injection	650	1.000000	2.30	0.006622	6.882648	3199.91
Initial	475	0.046322	4.48	0.064671	863.1310	853.74
	G	F	Gamma	Theta		
Injection	650	6.88	6.88	15524523.87	22023.87	
Initial	475	863.13	863.13	12065642.90	736892.90	

SHOCK CONDITIONS

	Initial Guess		Vapor Saturation	Objective Function	Two-Phase Wave Velocity	Upstream Flow Velocity	Shock Velocity	Vapor Frac Flow
	Sv-Hi	Sv-Low						
Trailing	1	0.5	0.9570	1.4356E-09	0.0068	0.692182	0.0068	1.0000
Leading	1	0.5	0.7028	-5.4916E-09	0.4888	0.046322	0.4888	0.9938
	dKr/dSv	dKr/dSl	Total Mobility	dFv/dSv	G	F'	Gamma	Theta'
Trailing	1.0000	0.0056	44.1982	0.0010	46.1514	9.9819	1.1641E+07	28011.8389
Leading	1.0000	0.2650	32.6614	0.0706	259.7574	15.1554	1.1828E+07	32558.2584

MATERIAL BALANCES

	Inside Mass	Initial	Injected	Produced	Balance	Error
Mass	53.213192	86.313097	6.882648	39.981852	0.0007	0.0008%
Enthalpy	1194593.1371	1206564.2904	22023.8721	34134.2668	-139.2414	0.0113%

Spreadsheet for Calculation of Stream-Water Saturation Profiles

Injection Temperature 650 °K			Initial Temperature 475 °K			Matrix Heat Capacity 1.0000 (kJ/kg)		
SATURATION PROFILE								
Vapor Saturation	Vapor Frac Flow	dKrv/dSv	dKr/dSI	Total Mobility	dFv/dSv	lambda	Mass Inside	Enthalpy Inside
1.0000						0.000000		
1.0000						0.006783		
0.9570	0.999986	1.0000	0.0056	44.198164	0.000980	0.006783	0.046687	105308.165674
0.9519	0.999981	1.0000	0.0069	43.963654	0.001234	0.008541	0.084854	20460.207161
0.9468	0.999974	1.0000	0.0085	43.729201	0.001519	0.010515	0.103776	22996.220295
0.9417	0.999965	1.0000	0.0102	43.494812	0.001836	0.012711	0.124818	25588.340310
0.9366	0.999955	1.0000	0.0121	43.260492	0.002186	0.015134	0.148049	28238.028402
0.9315	0.999943	1.0000	0.0141	43.026247	0.002570	0.017789	0.173538	30946.785096
0.9265	0.999929	1.0000	0.0162	42.792084	0.002988	0.020680	0.201356	33716.151411
0.9214	0.999912	1.0000	0.0185	42.558008	0.003440	0.023813	0.231579	36547.710077
0.9163	0.999894	1.0000	0.0210	42.324026	0.003929	0.027192	0.264282	39443.086781
0.9112	0.999872	1.0000	0.0237	42.090143	0.004453	0.030825	0.299546	42403.951455
0.9061	0.999848	1.0000	0.0264	41.856366	0.005015	0.034715	0.337452	45432.019610
0.9010	0.999821	1.0000	0.0294	41.622701	0.005616	0.038870	0.378086	48529.053708
0.8960	0.999791	1.0000	0.0325	41.389153	0.006255	0.043294	0.421535	51696.864582
0.8909	0.999758	1.0000	0.0357	41.155730	0.006934	0.047994	0.467889	54937.312902
0.8858	0.999721	1.0000	0.0391	40.922436	0.007653	0.052976	0.517243	58252.310690
0.8807	0.999680	1.0000	0.0427	40.689278	0.008415	0.058246	0.569694	61643.822877
0.8756	0.999635	1.0000	0.0464	40.456262	0.009219	0.063811	0.625341	65113.868926
0.8705	0.999586	1.0000	0.0503	40.223394	0.010066	0.069678	0.684288	68664.524494
0.8655	0.999533	1.0000	0.0543	39.990680	0.010958	0.075853	0.746642	72297.923157
0.8604	0.999474	1.0000	0.0585	39.758126	0.011896	0.082343	0.812514	76016.258189
0.8553	0.999412	1.0000	0.0628	39.525738	0.012880	0.089156	0.882018	79821.784403
0.8502	0.999343	1.0000	0.0673	39.293523	0.013912	0.096300	0.955273	83716.820051
0.8451	0.999270	1.0000	0.0720	39.061485	0.014993	0.103781	1.032400	87703.748788
0.8400	0.999191	1.0000	0.0768	38.829632	0.016124	0.111607	1.113527	91785.021700
0.8350	0.999106	1.0000	0.0817	38.597970	0.017306	0.119787	1.198783	95963.159403
0.8299	0.999015	1.0000	0.0868	38.366503	0.018540	0.128330	1.288304	100240.754214
0.8248	0.998917	1.0000	0.0921	38.135239	0.019827	0.137242	1.382229	104620.472389
0.8197	0.998813	1.0000	0.0975	37.904184	0.021170	0.146533	1.480704	109105.056440
0.8146	0.998702	1.0000	0.1031	37.673343	0.022568	0.156213	1.583876	113697.327534
0.8096	0.998584	1.0000	0.1088	37.442723	0.024024	0.166289	1.691901	118400.187969
0.8045	0.998458	1.0000	0.1147	37.212329	0.025538	0.176772	1.804938	123216.623732
0.7994	0.998324	1.0000	0.1207	36.982168	0.027113	0.187671	1.923151	128149.707155
0.7943	0.998182	1.0000	0.1269	36.752246	0.028749	0.198996	2.046713	133202.599648
0.7892	0.998032	1.0000	0.1333	36.522568	0.030448	0.210758	2.175799	138378.554536
0.7841	0.997872	1.0000	0.1398	36.293142	0.032212	0.222966	2.310591	143680.919988
0.7791	0.997704	1.0000	0.1465	36.063972	0.034042	0.235631	2.451279	149113.142050
0.7740	0.997526	1.0000	0.1533	35.835065	0.035939	0.248765	2.598057	154678.767782
0.7689	0.997339	1.0000	0.1602	35.606427	0.037906	0.262379	2.751127	160381.448504
0.7638	0.997141	1.0000	0.1674	35.378064	0.039944	0.276484	2.910699	166224.943149
0.7587	0.996933	1.0000	0.1746	35.149982	0.042054	0.291093	3.076988	172213.121744
0.7536	0.996713	1.0000	0.1821	34.922187	0.044239	0.306217	3.250216	178349.969002
0.7486	0.996483	1.0000	0.1897	34.694685	0.046501	0.321870	3.430617	184639.588043
0.7435	0.996240	1.0000	0.1974	34.467483	0.048840	0.338064	3.618427	191086.204248
0.7384	0.995986	1.0000	0.2053	34.240586	0.051260	0.354812	3.813896	197694.169244
0.7333	0.995719	1.0000	0.2134	34.014000	0.053762	0.372129	4.017277	204467.965031
0.7282	0.995439	1.0000	0.2216	33.787731	0.056348	0.390028	4.228837	211412.208257
0.7231	0.995146	1.0000	0.2299	33.561786	0.059020	0.408524	4.448848	218531.654640
0.7181	0.994839	1.0000	0.2385	33.336170	0.061780	0.427631	4.677595	225831.203546
0.7130	0.994518	1.0000	0.2471	33.110890	0.064631	0.447365	4.915369	233315.902736
0.7079	0.994182	1.0000	0.2560	32.885951	0.067575	0.467742	5.162475	240990.953276
0.7028	0.993831	1.0000	0.2650	32.661360	0.070614	0.488778	5.419227	248861.714624
0.0000						0.488778		
0.0000						1.000000		

Spreadsheet for Calculation of Stream-Water Saturation Profiles

Injection Temperature 650 °K Initial Temperature 475 °K Matrix Heat Capacity 1.0000 (kJ/kg)

TRAILING SHOCK CALCULATIONS

Saturation	OP	Wave V	Flow V	Shock V	f_v	dK_{rv}/dS_v	dK_r/dS_l
0.7500	2.42E-01	0.255386	0.556992	0.013421	0.996549	1.0000	0.1875
0.875	5.56E-02	0.063132	0.677295	0.007514	0.999629	1.0000	0.0469
0.9375	7.87E-03	0.014687	0.691596	0.006812	0.999957	1.0000	0.0117
0.96875	-3.28E-03	0.003516	0.692013	0.006792	0.999995	1.0000	0.0029
0.953125	1.30E-03	0.008087	0.692162	0.006784	0.999982	1.0000	0.0066
0.9609375	-1.23E-03	0.005554	0.692162	0.006784	0.999990	1.0000	0.0046
0.95703125	-2.54E-05	0.006758	0.692182	0.006783	0.999986	1.0000	0.0055
0.955078125	6.23E-04	0.007406	0.692178	0.006784	0.999984	1.0000	0.0061
0.9560546875	2.95E-04	0.007078	0.692181	0.006783	0.999985	1.0000	0.0058
0.9565429688	1.34E-04	0.006917	0.692182	0.006783	0.999986	1.0000	0.0057
0.9567871094	5.40E-05	0.006837	0.692182	0.006783	0.999986	1.0000	0.0056
0.9569091797	1.42E-05	0.006798	0.692182	0.006783	0.999986	1.0000	0.0056
0.9569702148	-5.61E-06	0.006778	0.692182	0.006783	0.999986	1.0000	0.0056
0.9569396973	4.30E-06	0.006788	0.692182	0.006783	0.999986	1.0000	0.0056
0.9569549561	-6.54E-07	0.006783	0.692182	0.006783	0.999986	1.0000	0.0056
0.9569473267	1.82E-06	0.006785	0.692182	0.006783	0.999986	1.0000	0.0056
0.9569511414	5.84E-07	0.006784	0.692182	0.006783	0.999986	1.0000	0.0056
0.9569530487	-3.48E-08	0.006783	0.692182	0.006783	0.999986	1.0000	0.0056
0.956952095	2.75E-07	0.006784	0.692182	0.006783	0.999986	1.0000	0.0056
0.9569525719	1.20E-07	0.006783	0.692182	0.006783	0.999986	1.0000	0.0056
0.9569528103	4.26E-08	0.006783	0.692182	0.006783	0.999986	1.0000	0.0056
0.9569529295	3.85E-09	0.006783	0.692182	0.006783	0.999986	1.0000	0.0056
0.9569529891	-1.55E-08	0.006783	0.692182	0.006783	0.999986	1.0000	0.0056
0.9569529593	-5.82E-09	0.006783	0.692182	0.006783	0.999986	1.0000	0.0056
0.9569529444	-9.83E-10	0.006783	0.692182	0.006783	0.999986	1.0000	0.0056
0.9569529369	1.44E-09	0.006783	0.692182	0.006783	0.999986	1.0000	0.0056

Saturation	Total Mob	dP_v/dS_v	G	F	Gamma	Theta	High	Low
0.75	34.759228	0.045851	220.095758	12.870589	1.1794E+07	30550.407113	1	0.5
0.875	40.427490	0.009321	115.033000	10.281953	1.1701E+07	28275.535543	1	0.75
0.9375	43.300978	0.002124	62.501620	10.006619	1.1655E+07	28033.574650	1	0.875
0.96875	44.742642	0.000508	36.235931	9.974642	1.1632E+07	28005.473055	1	0.9375
0.953125	44.021547	0.001168	49.368776	9.983337	1.1643E+07	28014.871837	0.96875	0.9375
0.9609375	44.382039	0.000802	42.802353	9.978906	1.1638E+07	28009.220503	0.96875	0.953125
0.95703125	44.201778	0.000976	46.085564	9.981821	1.1641E+07	28011.782338	0.9609375	0.953125
0.955078125	44.111658	0.001070	47.727170	9.983500	1.1642E+07	28013.257853	0.95703125	0.953125
0.9560546875	44.156717	0.001023	46.906367	9.982642	1.1641E+07	28012.503198	0.95703125	0.955078125
0.9565429688	44.179247	0.000999	46.495966	9.982227	1.1641E+07	28012.138595	0.95703125	0.9560546875
0.9567871094	44.190513	0.000988	46.290765	9.982023	1.1641E+07	28011.959430	0.95703125	0.95654296875
0.9569091797	44.196145	0.000982	46.188165	9.981922	1.1641E+07	28011.870625	0.95703125	0.95678710938
0.9569702148	44.198962	0.000979	46.136864	9.981871	1.1641E+07	28011.826417	0.95703125	0.95690917969
0.9569396973	44.197553	0.000981	46.162515	9.981897	1.1641E+07	28011.848505	0.95697021484	0.95690917969
0.9569549561	44.198258	0.000980	46.149690	9.981884	1.1641E+07	28011.837457	0.95697021484	0.95693969727
0.9569473267	44.197905	0.000980	46.156102	9.981890	1.1641E+07	28011.842980	0.95695495605	0.95693969727
0.9569511414	44.198082	0.000980	46.152896	9.981887	1.1641E+07	28011.840218	0.95695495605	0.95694732666
0.9569530487	44.198170	0.000980	46.151293	9.981886	1.1641E+07	28011.838838	0.95695495605	0.95695114136
0.956952095	44.198126	0.000980	46.152094	9.981886	1.1641E+07	28011.839528	0.95695304871	0.95695114136
0.9569525719	44.198148	0.000980	46.151693	9.981886	1.1641E+07	28011.839183	0.95695304871	0.95695209503
0.9569528103	44.198159	0.000980	46.151493	9.981886	1.1641E+07	28011.839010	0.95695304871	0.95695257187
0.9569529295	44.198164	0.000980	46.151393	9.981886	1.1641E+07	28011.838924	0.95695304871	0.95695281029
0.9569529891	44.198167	0.000980	46.151343	9.981886	1.1641E+07	28011.838881	0.95695304871	0.9569529295
0.9569529593	44.198165	0.000980	46.151368	9.981886	1.1641E+07	28011.838902	0.9569529891	0.9569529295
0.9569529444	44.198165	0.000980	46.151380	9.981886	1.1641E+07	28011.838913	0.9569529593	0.9569529295
0.9569529369	44.198164	0.000980	46.151387	9.981886	1.1641E+07	28011.838919	0.9569529444	0.9569529295

Spreadsheet for Calculation of Stream-Water Saturation Profiles

Injection Temperature 650 °K		Initial Temperature 475 °K			Matrix Heat Capacity 1.0000 (kJ/kg)		
LEADING SHOCK CALCULATIONS							
Saturation	OP	Wave V	Flow V	Shock V	f _v	dK _{rv} /dS _v	dK _{rl} /dS _l
0.7500	-1.72E-01	0.317373	0.046760	0.489101	0.996549	1.0000	0.1875
0.625	4.16E-01	0.906281	0.047852	0.489907	0.986170	1.0000	0.4219
0.6875	6.75E-02	0.556298	0.046374	0.488816	0.992676	1.0000	0.2930
0.71875	-6.38E-02	0.425002	0.046375	0.488817	0.994882	1.0000	0.2373
0.703125	-1.32E-03	0.487463	0.046322	0.488778	0.993853	1.0000	0.2644
0.6953125	3.23E-02	0.521053	0.046334	0.488787	0.993284	1.0000	0.2785
0.69921875	1.53E-02	0.504055	0.046325	0.488780	0.993573	1.0000	0.2714
0.701171875	6.93E-03	0.495709	0.046322	0.488778	0.993714	1.0000	0.2679
0.7021484375	2.80E-03	0.491573	0.046322	0.488778	0.993784	1.0000	0.2661
0.7026367188	7.37E-04	0.489515	0.046322	0.488778	0.993819	1.0000	0.2653
0.7028808594	-2.90E-04	0.488488	0.046322	0.488778	0.993836	1.0000	0.2648
0.7027587891	2.23E-04	0.489001	0.046322	0.488778	0.993827	1.0000	0.2651
0.7028198242	-3.32E-05	0.488745	0.046322	0.488778	0.993831	1.0000	0.2649
0.7027893066	9.51E-05	0.488873	0.046322	0.488778	0.993829	1.0000	0.2650
0.7028045654	3.10E-05	0.488809	0.046322	0.488778	0.993830	1.0000	0.2650
0.7028121948	-1.10E-06	0.488777	0.046322	0.488778	0.993831	1.0000	0.2650
0.7028083801	1.49E-05	0.488793	0.046322	0.488778	0.993831	1.0000	0.2650
0.7028102875	6.92E-06	0.488785	0.046322	0.488778	0.993831	1.0000	0.2650
0.7028112411	2.91E-06	0.488781	0.046322	0.488778	0.993831	1.0000	0.2650
0.702811718	9.03E-07	0.488779	0.046322	0.488778	0.993831	1.0000	0.2650
0.7028119564	-9.95E-08	0.488778	0.046322	0.488778	0.993831	1.0000	0.2650
0.7028118372	4.02E-07	0.488778	0.046322	0.488778	0.993831	1.0000	0.2650
0.7028118968	1.51E-07	0.488778	0.046322	0.488778	0.993831	1.0000	0.2650
0.7028119266	2.58E-08	0.488778	0.046322	0.488778	0.993831	1.0000	0.2650
0.7028119415	-3.68E-08	0.488778	0.046322	0.488778	0.993831	1.0000	0.2650
0.7028119341	-5.49E-09	0.488778	0.046322	0.488778	0.993831	1.0000	0.2650

Saturation	Total Mob	dF _v /dS _v	G	F	Gamma	Theta	High	Low
0.75	34.759228	0.045851	220.095758	12.870589	1.1794E+07	30550.407113	1	0.5
0.625	29.270883	0.130931	325.158517	21.594311	1.1886E+07	38216.739851	0.75	0.5
0.6875	31.986944	0.080369	272.627138	16.125943	1.1840E+07	33411.184085	0.75	0.625
0.71875	33.366761	0.061400	246.361448	14.272175	1.1817E+07	31782.109202	0.75	0.6875
0.703125	32.675183	0.070424	259.494293	15.136820	1.1828E+07	32541.951705	0.71875	0.6875
0.6953125	32.330635	0.075277	266.060715	15.615059	1.1834E+07	32962.223587	0.703125	0.6875
0.69921875	32.502803	0.072821	262.777504	15.371956	1.1831E+07	32748.587401	0.703125	0.6953125
0.701171875	32.588967	0.071615	261.135898	15.253405	1.1830E+07	32644.405041	0.703125	0.69921875
0.7021484375	32.632068	0.071018	260.315096	15.194868	1.1829E+07	32592.963553	0.703125	0.701171875
0.7026367188	32.653624	0.070721	259.904694	15.165783	1.1828E+07	32567.404087	0.703125	0.7021484375
0.7028808594	32.664403	0.070572	259.699494	15.151286	1.1828E+07	32554.664530	0.703125	0.70263671875
0.7027587891	32.659014	0.070646	259.802094	15.158531	1.1828E+07	32561.030965	0.70288085938	0.70263671875
0.7028198242	32.661708	0.070609	259.750794	15.154908	1.1828E+07	32557.846912	0.70288085938	0.70275878906
0.7027893066	32.660361	0.070628	259.776444	15.156719	1.1828E+07	32559.438729	0.70281982422	0.70275878906
0.7028045654	32.661035	0.070619	259.763619	15.155813	1.1828E+07	32558.642768	0.70281982422	0.70278930664
0.7028121948	32.661372	0.070614	259.757206	15.155361	1.1828E+07	32558.244827	0.70281982422	0.70280456543
0.7028083801	32.661203	0.070616	259.760412	15.155587	1.1828E+07	32558.443794	0.70281219482	0.70280456543
0.7028102875	32.661287	0.070615	259.758809	15.155474	1.1828E+07	32558.344310	0.70281219482	0.70280838013
0.7028112411	32.661329	0.070614	259.758008	15.155417	1.1828E+07	32558.294568	0.70281219482	0.70281028748
0.702811718	32.661350	0.070614	259.757607	15.155389	1.1828E+07	32558.269698	0.70281219482	0.70281124115
0.7028119564	32.661361	0.070614	259.757407	15.155375	1.1828E+07	32558.257262	0.70281219482	0.70281171799
0.7028118372	32.661356	0.070614	259.757507	15.155382	1.1828E+07	32558.263480	0.70281195641	0.70281171799
0.7028118968	32.661358	0.070614	259.757457	15.155378	1.1828E+07	32558.260371	0.70281195641	0.7028118372
0.7028119266	32.661360	0.070614	259.757432	15.155377	1.1828E+07	32558.258817	0.70281195641	0.7028118968
0.7028119415	32.661360	0.070614	259.757419	15.155376	1.1828E+07	32558.258040	0.70281195641	0.7028119266
0.7028119341	32.661360	0.070614	259.757425	15.155376	1.1828E+07	32558.258428	0.7028119415	0.7028119266

D4. . Changes in Matrix Heat Capacity

The final seven worksheets examine the effect of matrix heat capacity. The matrix heat capacity is entered in cell B23. The section contains worksheets with the matrix heat capacity ranging from between 0-1 (kJ/kg-K).

Spreadsheet for Calculation of Stream-Water Saturation Profiles

Injection Temperature
650 °K

Initial Temperature
300 °K

Matrix Heat Capacity
0.0400 (kJ/kg)

MATRIX PROPERTIES

Porosity	Cp Matrix	Density	Rho * Cp
0.10	0.04	2650.00	106.0000
Nw	Ng	Swi	Denom
3.00	1.00	0.00	1.000000

SATURATION CONDITIONS

Tsaturation = 485.57

	Volumes (m3/kg)	Enthalpies (kJ/kg)	Densities (kg/m3)	Viscosities (cp)	Saturation Step
Liquid	0.001176	901.41	850.4723	0.1303	0.0034412763
Vapor	0.100298	2808.52	9.970241	0.0217	

BOUNDARY CONDITIONS

	Temperature	Velocity	Heat Capacity	Wave Velocity	Density	Enthalpy
Injection	650	1.000000	2.30	0.162970	6.882648	3199.91
Initial	300	0.055466	4.16	0.451575	1004.6293	112.70
	G	F	Gamma	Theta		
Injection	650	6.88	6.88	642123.87	22023.87	
Initial	300	1004.63	1004.63	399418.71	113218.71	

SHOCK CONDITIONS

	Initial Guess		Vapor Saturation	Objective Function	Two-Phase Wave Velocity	Upstream Flow Velocity	Shock Velocity	Vapor Frac Flow
Trailing	Sv-Hi	Sv-Low	0.8632	-1.8451E-09	0.0866	0.761219	0.0866	0.9995
Leading	1	0.5	0.6911	-3.4809E-08	0.5936	0.055466	0.5936	0.9930
	dKrv/dSv	dKrl/dSl	Total Mobility	dFv/dSv	G	F'	Gamma	Theta'
Trailing	1.0000	0.0562	39.8865	0.0114	124.9622	10.3845	5.9229E+05	28365.6429
Leading	1.0000	0.2862	32.1462	0.0780	269.5822	15.8849	7.1938E+05	33199.3395

MATERIAL BALANCES

	Inside	Initial	Injected	Produced	Balance	Error
Mass	51.622698	100.462933	6.882648	55.722590	0.0003	0.0003%
Enthalpy	55852.4441	39941.8712	22023.8721	6279.7688	-166.4695	0.2686%

Spreadsheet for Calculation of Stream-Water Saturation Profiles

Injection Temperature 650 °K		Initial Temperature 300 °K			Matrix Heat Capacity 0.0400 (kJ/kg)			
SATURATION PROFILE								
Vapor Saturation	Vapor Frac Flow	dKrv/dSv	dKr/dSi	Total Mobility	dFv/dSv	lambda	Mass Inside	Enthalpy Inside
1.0000						0.000000		
1.0000						0.086570		
0.8632	0.999507	1.0000	0.0562	39.886544	0.011373	0.086570	0.595832	55588.783670
0.8597	0.999467	1.0000	0.0590	39.729128	0.012016	0.091471	0.619488	2918.204472
0.8563	0.999424	1.0000	0.0619	39.571787	0.012682	0.096535	0.654755	3028.456739
0.8529	0.999380	1.0000	0.0649	39.414525	0.013369	0.101764	0.691302	3141.074679
0.8494	0.999332	1.0000	0.0680	39.257344	0.014078	0.107162	0.729154	3256.105120
0.8460	0.999283	1.0000	0.0712	39.100244	0.014809	0.112730	0.768342	3373.595870
0.8425	0.999230	1.0000	0.0744	38.943229	0.015564	0.118473	0.808895	3493.595740
0.8391	0.999176	1.0000	0.0777	38.786299	0.016341	0.124391	0.850842	3616.154566
0.8357	0.999118	1.0000	0.0810	38.629457	0.017142	0.130488	0.894214	3741.323230
0.8322	0.999058	1.0000	0.0845	38.472705	0.017967	0.136768	0.939043	3869.153685
0.8288	0.998994	1.0000	0.0880	38.316044	0.018816	0.143232	0.985361	3999.698978
0.8253	0.998928	1.0000	0.0915	38.159477	0.019690	0.149883	1.033200	4133.013274
0.8219	0.998859	1.0000	0.0952	38.003005	0.020589	0.156725	1.082595	4269.151883
0.8184	0.998786	1.0000	0.0989	37.846630	0.021513	0.163761	1.133579	4408.171284
0.8150	0.998711	1.0000	0.1027	37.690355	0.022463	0.170993	1.186188	4550.129152
0.8116	0.998632	1.0000	0.1065	37.534180	0.023439	0.178426	1.240458	4695.084384
0.8081	0.998549	1.0000	0.1104	37.378107	0.024443	0.186061	1.296425	4843.097125
0.8047	0.998463	1.0000	0.1144	37.222140	0.025473	0.193902	1.354127	4994.228801
0.8012	0.998374	1.0000	0.1185	37.066279	0.026530	0.201953	1.413603	5148.542144
0.7978	0.998281	1.0000	0.1227	36.910526	0.027616	0.210217	1.474892	5306.101222
0.7944	0.998184	1.0000	0.1269	36.754884	0.028730	0.218698	1.538035	5466.971469
0.7909	0.998083	1.0000	0.1311	36.599354	0.029873	0.227398	1.603071	5631.219719
0.7875	0.997978	1.0000	0.1355	36.443938	0.031045	0.236322	1.670045	5798.914232
0.7840	0.997869	1.0000	0.1399	36.288638	0.032247	0.245472	1.738998	5970.124733
0.7806	0.997756	1.0000	0.1444	36.133456	0.033480	0.254854	1.809975	6144.922442
0.7772	0.997639	1.0000	0.1490	35.978393	0.034743	0.264469	1.883020	6323.380105
0.7737	0.997517	1.0000	0.1536	35.823452	0.036037	0.274323	1.958181	6505.572037
0.7703	0.997391	1.0000	0.1583	35.668634	0.037364	0.284420	2.035505	6691.574149
0.7668	0.997260	1.0000	0.1631	35.513942	0.038722	0.294762	2.115039	6881.463992
0.7634	0.997124	1.0000	0.1680	35.359376	0.040114	0.305355	2.196833	7075.320788
0.7599	0.996984	1.0000	0.1729	35.204940	0.041539	0.316201	2.280937	7273.225475
0.7565	0.996838	1.0000	0.1779	35.050635	0.042998	0.327306	2.367404	7475.260741
0.7531	0.996688	1.0000	0.1829	34.896463	0.044491	0.338674	2.456287	7681.511067
0.7496	0.996532	1.0000	0.1881	34.742425	0.046020	0.350309	2.547639	7892.062770
0.7462	0.996371	1.0000	0.1933	34.588524	0.047584	0.362216	2.641516	8107.004042
0.7427	0.996204	1.0000	0.1985	34.434761	0.049184	0.374398	2.737974	8326.424993
0.7393	0.996032	1.0000	0.2039	34.281139	0.050821	0.386861	2.837073	8550.417702
0.7359	0.995855	1.0000	0.2093	34.127659	0.052496	0.399609	2.938870	8779.076255
0.7324	0.995671	1.0000	0.2148	33.974322	0.054209	0.412647	3.043427	9012.496795
0.7290	0.995482	1.0000	0.2204	33.821132	0.055960	0.425980	3.150807	9250.777572
0.7255	0.995286	1.0000	0.2260	33.668090	0.057751	0.439612	3.261072	9494.018988
0.7221	0.995084	1.0000	0.2317	33.515197	0.059582	0.453549	3.374287	9742.323651
0.7187	0.994876	1.0000	0.2375	33.362456	0.061454	0.467797	3.490521	9995.796425
0.7152	0.994661	1.0000	0.2433	33.209869	0.063367	0.482359	3.609839	10254.544482
0.7118	0.994440	1.0000	0.2492	33.057436	0.065322	0.497242	3.732314	10518.677358
0.7083	0.994211	1.0000	0.2552	32.905161	0.067320	0.512450	3.858015	10788.307008
0.7049	0.993976	1.0000	0.2613	32.753046	0.069361	0.527990	3.987016	11063.547865
0.7014	0.993734	1.0000	0.2674	32.601091	0.071447	0.543867	4.119392	11344.516892
0.6980	0.993484	1.0000	0.2736	32.449298	0.073578	0.560087	4.255220	11631.333650
0.6946	0.993227	1.0000	0.2799	32.297671	0.075754	0.576655	4.394577	11924.120355
0.6911	0.992963	1.0000	0.2862	32.146210	0.077977	0.593577	4.537545	12223.001941
0.0000						0.593577		
0.0000						1.000000		

Spreadsheet for Calculation of Stream-Water Saturation Profiles

Injection Temperature 650 °K		Initial Temperature 300 °K			Matrix Heat Capacity 0.0400 (kJ/kg)			
TRAILING SHOCK CALCULATIONS								
Saturation	OF	Wave V	Flow V	Shock V	f _v	dKrv/dSv	dKr/dSI	
0.7500	2.16E-01	0.336643	0.734211	0.120400	0.996549	1.0000	0.1875	
0.875	-1.61E-02	0.070923	0.760887	0.086986	0.999629	1.0000	0.0469	
0.8125	8.14E-02	0.175075	0.755537	0.093687	0.998653	1.0000	0.1055	
0.84375	2.86E-02	0.116300	0.760356	0.087650	0.999249	1.0000	0.0732	
0.859375	5.39E-03	0.092004	0.761185	0.086613	0.999462	1.0000	0.0593	
0.8671875	-5.55E-03	0.081070	0.761181	0.086617	0.999551	1.0000	0.0529	
0.86328125	-1.33E-04	0.086438	0.761219	0.086570	0.999508	1.0000	0.0561	
0.861328125	2.62E-03	0.089196	0.761210	0.086580	0.999486	1.0000	0.0577	
0.8623046875	1.24E-03	0.087810	0.761217	0.086572	0.999497	1.0000	0.0569	
0.8627929688	5.52E-04	0.087122	0.761218	0.086571	0.999503	1.0000	0.0565	
0.8630371094	2.09E-04	0.086780	0.761219	0.086570	0.999505	1.0000	0.0563	
0.8631591797	3.84E-05	0.086609	0.761219	0.086570	0.999507	1.0000	0.0562	
0.8632202148	-4.71E-05	0.086523	0.761219	0.086570	0.999508	1.0000	0.0561	
0.8631896973	-4.37E-06	0.086566	0.761219	0.086570	0.999507	1.0000	0.0562	
0.8631744385	1.70E-05	0.086587	0.761219	0.086570	0.999507	1.0000	0.0562	
0.8631820679	6.31E-06	0.086577	0.761219	0.086570	0.999507	1.0000	0.0562	
0.8631858826	9.69E-07	0.086571	0.761219	0.086570	0.999507	1.0000	0.0562	
0.8631877899	-1.70E-06	0.086568	0.761219	0.086570	0.999507	1.0000	0.0562	
0.8631868362	-3.67E-07	0.086570	0.761219	0.086570	0.999507	1.0000	0.0562	
0.8631863594	3.01E-07	0.086570	0.761219	0.086570	0.999507	1.0000	0.0562	
0.8631865978	-3.32E-08	0.086570	0.761219	0.086570	0.999507	1.0000	0.0562	
0.8631864786	1.34E-07	0.086570	0.761219	0.086570	0.999507	1.0000	0.0562	
0.8631865382	5.03E-08	0.086570	0.761219	0.086570	0.999507	1.0000	0.0562	
0.863186568	8.59E-09	0.086570	0.761219	0.086570	0.999507	1.0000	0.0562	
0.8631865829	-1.23E-08	0.086570	0.761219	0.086570	0.999507	1.0000	0.0562	
0.8631865755	-1.85E-09	0.086570	0.761219	0.086570	0.999507	1.0000	0.0562	
Saturation	Total Mob	dFv/dSv	G	F	Gamma	Theta	High	Low
0.75	34.759228	0.045851	220.095758	12.870589	6.7589E+05	30550.407113	1	0.5
0.875	40.427490	0.009321	115.033000	10.281953	5.8356E+05	28275.535543	1	0.75
0.8125	37.576492	0.023172	167.564379	11.102088	6.2973E+05	28996.263468	0.875	0.75
0.84375	38.998477	0.015295	141.298689	10.601362	6.0665E+05	28556.229528	0.875	0.8125
0.859375	39.712193	0.012087	128.165845	10.422059	5.9510E+05	28398.659931	0.875	0.84375
0.8671875	40.069655	0.010651	121.599422	10.347467	5.8933E+05	28333.108609	0.875	0.859375
0.86328125	39.890876	0.011355	124.882633	10.383584	5.9222E+05	28364.848284	0.8671875	0.859375
0.861328125	39.801522	0.011718	126.524239	10.402522	5.9366E+05	28381.490199	0.86328125	0.859375
0.8623046875	39.846196	0.011536	125.703436	10.392979	5.9294E+05	28373.103881	0.86328125	0.861328125
0.8627929688	39.868535	0.011445	125.293035	10.388263	5.9258E+05	28368.959819	0.86328125	0.8623046875
0.8630371094	39.879706	0.011400	125.087834	10.385919	5.9240E+05	28366.899995	0.86328125	0.86279296875
0.8631591797	39.885291	0.011378	124.985234	10.384751	5.9231E+05	28365.873127	0.86328125	0.86303710938
0.8632202148	39.888083	0.011366	124.933933	10.384167	5.9226E+05	28365.360452	0.86328125	0.86315917969
0.8631896973	39.886687	0.011372	124.959584	10.384459	5.9229E+05	28365.616726	0.86322021484	0.86315917969
0.8631744385	39.885989	0.011375	124.972409	10.384605	5.9230E+05	28365.744911	0.86318969727	0.86315917969
0.8631820679	39.886338	0.011379	124.965996	10.384532	5.9229E+05	28365.680814	0.86318969727	0.86317443848
0.8631858826	39.886513	0.011373	124.962790	10.384495	5.9229E+05	28365.648769	0.86318969727	0.86318206787
0.8631877899	39.886600	0.011372	124.961187	10.384477	5.9229E+05	28365.632747	0.86318969727	0.86318588257
0.8631868362	39.886556	0.011373	124.961988	10.384486	5.9229E+05	28365.640758	0.86318778992	0.86318588257
0.8631863594	39.886534	0.011373	124.962389	10.384491	5.9229E+05	28365.644764	0.86318683624	0.86318588257
0.8631865978	39.886545	0.011373	124.962189	10.384488	5.9229E+05	28365.642761	0.86318683624	0.86318635941
0.8631864786	39.886540	0.011373	124.962289	10.384490	5.9229E+05	28365.643762	0.86318659782	0.86318635941
0.8631865382	39.886543	0.011373	124.962239	10.384489	5.9229E+05	28365.643262	0.86318659782	0.86318647861
0.863186568	39.886544	0.011373	124.962214	10.384489	5.9229E+05	28365.643011	0.86318659782	0.86318653822
0.8631865829	39.886545	0.011373	124.962201	10.384489	5.9229E+05	28365.642886	0.86318659782	0.86318656802
0.8631865755	39.886544	0.011373	124.962207	10.384489	5.9229E+05	28365.642949	0.86318658292	0.86318656802

Spreadsheet for Calculation of Stream-Water Saturation Profiles

Injection Temperature 650 °K Initial Temperature 300 °K Matrix Heat Capacity 0.0400 (kJ/kg)

LEADING SHOCK CALCULATIONS

Saturation	OF	Wave V	Flow V	Shock V	f _v	dKr/dSv	dKr/dSI
0.7500	-2.58E-01	0.349026	0.057160	0.607075	0.996549	1.0000	0.1875
0.625	3.85E-01	0.996671	0.057727	0.611591	0.986170	1.0000	0.4219
0.6875	1.82E-02	0.611782	0.055472	0.593629	0.992676	1.0000	0.2930
0.71875	-1.29E-01	0.467391	0.055842	0.596576	0.994882	1.0000	0.2373
0.703125	-5.81E-02	0.536081	0.055537	0.594147	0.993853	1.0000	0.2644
0.6953125	-2.06E-02	0.573021	0.055475	0.593647	0.993284	1.0000	0.2785
0.69140625	-1.41E-03	0.592170	0.055466	0.593578	0.992985	1.0000	0.2857
0.689453125	8.33E-03	0.601917	0.055467	0.593588	0.992832	1.0000	0.2893
0.6904296875	3.45E-03	0.597029	0.055466	0.593579	0.992909	1.0000	0.2875
0.6909179688	1.02E-03	0.594596	0.055466	0.593577	0.992947	1.0000	0.2866
0.6911621094	-1.96E-04	0.593382	0.055466	0.593577	0.992966	1.0000	0.2861
0.6910400391	4.11E-04	0.593988	0.055466	0.593577	0.992957	1.0000	0.2864
0.6911010742	1.08E-04	0.593685	0.055466	0.593577	0.992961	1.0000	0.2863
0.6911315918	-4.39E-05	0.593533	0.055466	0.593577	0.992964	1.0000	0.2862
0.691116333	3.19E-05	0.593609	0.055466	0.593577	0.992962	1.0000	0.2862
0.6911239624	-6.00E-06	0.593571	0.055466	0.593577	0.992963	1.0000	0.2862
0.6911201477	1.30E-06	0.593590	0.055466	0.593577	0.992963	1.0000	0.2862
0.6911220551	3.48E-06	0.593581	0.055466	0.593577	0.992963	1.0000	0.2862
0.6911230087	-1.26E-06	0.593576	0.055466	0.593577	0.992963	1.0000	0.2862
0.6911225319	1.11E-06	0.593578	0.055466	0.593577	0.992963	1.0000	0.2862
0.6911227703	-7.18E-08	0.593577	0.055466	0.593577	0.992963	1.0000	0.2862
0.6911226511	5.21E-07	0.593578	0.055466	0.593577	0.992963	1.0000	0.2862
0.6911227107	2.24E-07	0.593577	0.055466	0.593577	0.992963	1.0000	0.2862
0.6911227405	7.63E-08	0.593577	0.055466	0.593577	0.992963	1.0000	0.2862
0.6911227554	2.22E-09	0.593577	0.055466	0.593577	0.992963	1.0000	0.2862
0.6911227629	-3.48E-08	0.593577	0.055466	0.593577	0.992963	1.0000	0.2862

Saturation	Total Mob	dFv/dSv	G	F	Gamma	Theta	High	Low
0.75	34.759228	0.045851	220.095758	12.870589	6.7589E+05	30550.407113	1	0.5
0.625	29.270883	0.130931	325.158517	21.594311	7.6822E+05	38216.739851	0.75	0.5
0.6875	31.986944	0.080369	272.627138	16.125943	7.2206E+05	33411.184085	0.75	0.625
0.71875	33.366761	0.061400	246.361448	14.272175	6.9897E+05	31782.109202	0.75	0.6875
0.703125	32.675183	0.070424	259.494293	15.136820	7.1052E+05	32541.951705	0.71875	0.6875
0.6953125	32.330635	0.075277	266.060715	15.615059	7.1629E+05	32962.223587	0.703125	0.6875
0.69140625	32.158681	0.077792	269.343926	15.866321	7.1917E+05	33183.031099	0.6953125	0.6875
0.689453125	32.072785	0.079073	270.985532	15.995075	7.2061E+05	33296.178392	0.69140625	0.6875
0.6904296875	32.115726	0.078431	270.164729	15.930435	7.1989E+05	33239.373831	0.69140625	0.689453125
0.6909179688	32.137202	0.078111	269.754328	15.898313	7.1953E+05	33211.144908	0.69140625	0.6904296875
0.6911621094	32.147941	0.077952	269.549127	15.882301	7.1935E+05	33197.073636	0.69140625	0.69091796875
0.6910400391	32.142571	0.078031	269.651727	15.890303	7.1944E+05	33204.105678	0.69116210938	0.69091796875
0.6911010742	32.145256	0.077991	269.600427	15.886301	7.1940E+05	33200.588759	0.69116210938	0.69104003906
0.6911315918	32.146599	0.077971	269.574777	15.884300	7.1937E+05	33198.830973	0.69116210938	0.69110107422
0.691116333	32.145927	0.077981	269.587602	15.885300	7.1938E+05	33199.709810	0.6911315918	0.69110107422
0.6911239624	32.146263	0.077976	269.581190	15.884800	7.1938E+05	33199.270377	0.6911315918	0.69111633301
0.6911201477	32.146095	0.077979	269.584396	15.885050	7.1938E+05	33199.490090	0.6911239624	0.69111633301
0.6911220551	32.146179	0.077978	269.582793	15.884925	7.1938E+05	33199.380233	0.6911239624	0.69112014771
0.6911230087	32.146221	0.077977	269.581991	15.884863	7.1938E+05	33199.325305	0.6911239624	0.69112205505
0.6911225319	32.146200	0.077977	269.582392	15.884894	7.1938E+05	33199.352769	0.69112300873	0.69112253189
0.6911227703	32.146211	0.077977	269.582192	15.884879	7.1938E+05	33199.339037	0.69112300873	0.69112253189
0.6911226511	32.146205	0.077977	269.582292	15.884886	7.1938E+05	33199.345903	0.69112277031	0.69112253189
0.6911227107	32.146208	0.077977	269.582242	15.884882	7.1938E+05	33199.342470	0.69112277031	0.6911226511
0.6911227405	32.146209	0.077977	269.582217	15.884881	7.1938E+05	33199.340753	0.69112277031	0.6911227107
0.6911227554	32.146210	0.077977	269.582204	15.884880	7.1938E+05	33199.339895	0.69112277031	0.69112274051
0.6911227629	32.146210	0.077977	269.582198	15.884879	7.1938E+05	33199.339466	0.69112277031	0.69112275541

Spreadsheet for Calculation of Stream-Water Saturation Profiles

Injection Temperature
650 °K

Initial Temperature
300 °K

Matrix Heat Capacity
0.2000 (kJ/kg)

MATRIX PROPERTIES

Porosity	Cp Matrix	Density	Rho * Cp
0.10	0.20	2650.00	530.0000
Nw	Ng	Swi	Denom
3.00	1.00	0.00	1.000000

SATURATION CONDITIONS
Tsaturation = 485.57

	Volumes (m3/kg)	Enthalpies (kJ/kg)	Densities (kg/m3)	Viscosities (cp)	Saturation Step
Liquid	0.001176	901.41	850.4723	0.1303	0.0022453558
Vapor	0.100298	2808.52	9.970241	0.0217	

BOUNDARY CONDITIONS

	Temperature	Velocity	Heat Capacity	Wave Velocity	Density	Enthalpy
Injection	650	1.000000	2.30	0.033025	6.882648	3199.91
Initial	300	0.023600	4.16	0.110208	1004.6293	112.70

	G	F	Gamma	Theta	
Injection	650	6.88	6.88	3122523.87	22023.87
Initial	300	1004.63	1004.63	1544218.71	113218.71

SHOCK CONDITIONS

	Initial Guess		Vapor Saturation	Objective Function	Two-Phase Wave Velocity	Upstream Flow Velocity	Shock Velocity	Vapor Frac Flow
	Sv-Hi	Sv-Low						
Trailing	1	0.5	0.9125	-1.2549E-09	0.0305	0.706498	0.0305	0.9999
Leading	1	0.5	0.8002	-6.9074E-09	0.1897	0.023600	0.1897	0.9983

	dKrv/dSv	dKrl/dSl	Total Mobility	dFv/dSv	G	F'	Gamma	Theta'
Trailing	1.0000	0.0230	42.1491	0.0043	83.5243	10.0728	2.4088E+06	28091.7631
Leading	1.0000	0.1197	37.0199	0.0269	177.8856	11.3599	2.4917E+06	29222.8569

MATERIAL BALANCES

	Inside	Initial	Injected	Produced	Balance	Error
Mass	83.636756	100.462933	6.882648	23.708774	0.0001	0.0000%
Enthalpy	173807.5362	154421.8712	22023.8721	2671.9077	-33.7006	0.0191%

Spreadsheet for Calculation of Stream-Water Saturation Profiles

Injection Temperature 650 °K		Initial Temperature 300 °K				Matrix Heat Capacity 0.2000 (kJ/kg)		
SATURATION PROFILE								
Vapor Saturation	Vapor Frac Flow	dKrv/dSv	dKr/dSI	Total Mobility	dFv/dSv	lambda	Mass Inside	Enthalpy Inside
1.0000						0.000000		
1.0000						0.030504		
0.9125	0.999878	1.0000	0.0230	42.149052	0.004318	0.030504	0.209947	95248.933937
0.9102	0.999868	1.0000	0.0242	42.045755	0.004557	0.032196	0.142920	4079.181063
0.9080	0.999857	1.0000	0.0254	41.942478	0.004804	0.033939	0.150571	4206.588211
0.9058	0.999846	1.0000	0.0266	41.839223	0.005058	0.035735	0.158462	4335.385193
0.9035	0.999835	1.0000	0.0279	41.735990	0.005320	0.037584	0.166595	4465.588443
0.9013	0.999823	1.0000	0.0292	41.632780	0.005589	0.039485	0.174974	4597.214601
0.8990	0.999810	1.0000	0.0306	41.529592	0.005866	0.041440	0.183603	4730.280514
0.8968	0.999796	1.0000	0.0320	41.426428	0.006150	0.043450	0.192485	4864.803237
0.8945	0.999782	1.0000	0.0334	41.323288	0.006442	0.045514	0.201623	5000.800041
0.8923	0.999767	1.0000	0.0348	41.220172	0.006742	0.047633	0.211022	5138.288410
0.8900	0.999752	1.0000	0.0363	41.117081	0.007050	0.049809	0.220685	5277.286049
0.8878	0.999736	1.0000	0.0378	41.014016	0.007366	0.052040	0.230615	5417.810882
0.8855	0.999719	1.0000	0.0393	40.910977	0.007690	0.054329	0.240817	5559.881060
0.8833	0.999701	1.0000	0.0409	40.807964	0.008022	0.056675	0.251294	5703.514961
0.8811	0.999683	1.0000	0.0424	40.704979	0.008362	0.059079	0.262050	5848.731192
0.8788	0.999663	1.0000	0.0441	40.602021	0.008711	0.061542	0.273089	5995.548596
0.8766	0.999643	1.0000	0.0457	40.499091	0.009068	0.064064	0.284416	6143.986254
0.8743	0.999623	1.0000	0.0474	40.396190	0.009433	0.066645	0.296034	6294.063485
0.8721	0.999601	1.0000	0.0491	40.293318	0.009807	0.069287	0.307947	6445.799852
0.8698	0.999579	1.0000	0.0508	40.190476	0.010190	0.071991	0.320159	6599.215167
0.8676	0.999555	1.0000	0.0526	40.087664	0.010581	0.074755	0.332676	6754.329490
0.8653	0.999531	1.0000	0.0544	39.984883	0.010981	0.077582	0.345501	6911.163137
0.8631	0.999506	1.0000	0.0562	39.882133	0.011390	0.080472	0.358638	7069.736679
0.8608	0.999480	1.0000	0.0581	39.779415	0.011808	0.083426	0.372092	7230.070951
0.8586	0.999453	1.0000	0.0600	39.676729	0.012235	0.086443	0.385868	7392.187049
0.8564	0.999425	1.0000	0.0619	39.574076	0.012672	0.089526	0.399969	7556.106339
0.8541	0.999396	1.0000	0.0639	39.471456	0.013117	0.092674	0.414402	7721.850459
0.8519	0.999366	1.0000	0.0658	39.368871	0.013572	0.095887	0.429170	7889.441322
0.8496	0.999335	1.0000	0.0678	39.266319	0.014037	0.099168	0.444278	8058.901121
0.8474	0.999303	1.0000	0.0699	39.163803	0.014510	0.102516	0.459731	8230.252332
0.8451	0.999270	1.0000	0.0720	39.061322	0.014994	0.105932	0.475534	8403.517717
0.8429	0.999236	1.0000	0.0741	38.958877	0.015487	0.109418	0.491692	8578.720331
0.8406	0.999200	1.0000	0.0762	38.856468	0.015990	0.112972	0.508211	8755.883523
0.8384	0.999164	1.0000	0.0784	38.754097	0.016504	0.116597	0.525094	8935.030942
0.8361	0.999126	1.0000	0.0805	38.651763	0.017027	0.120293	0.542348	9116.186540
0.8339	0.999087	1.0000	0.0828	38.549467	0.017560	0.124060	0.559978	9299.374578
0.8317	0.999047	1.0000	0.0850	38.447210	0.018103	0.127900	0.577989	9484.619626
0.8294	0.999006	1.0000	0.0873	38.344991	0.018657	0.131813	0.596387	9671.946575
0.8272	0.998964	1.0000	0.0896	38.242813	0.019222	0.135800	0.615177	9861.380632
0.8249	0.998920	1.0000	0.0920	38.140674	0.019797	0.139862	0.634365	10052.947332
0.8227	0.998875	1.0000	0.0943	38.038576	0.020382	0.143999	0.653956	10246.672541
0.8204	0.998828	1.0000	0.0967	37.936520	0.020978	0.148213	0.673956	10442.582455
0.8182	0.998781	1.0000	0.0992	37.834505	0.021586	0.152503	0.694372	10640.703615
0.8159	0.998731	1.0000	0.1016	37.732532	0.022204	0.156871	0.715209	10841.062901
0.8137	0.998681	1.0000	0.1041	37.630602	0.022833	0.161318	0.736473	11043.687544
0.8114	0.998629	1.0000	0.1067	37.528715	0.023474	0.165844	0.758171	11248.605129
0.8092	0.998575	1.0000	0.1092	37.426872	0.024126	0.170451	0.780308	11455.843599
0.8070	0.998520	1.0000	0.1118	37.325073	0.024790	0.175138	0.802891	11665.431261
0.8047	0.998464	1.0000	0.1144	37.223319	0.025465	0.179908	0.825927	11877.396791
0.8025	0.998406	1.0000	0.1171	37.121611	0.026152	0.184760	0.849421	12091.769239
0.8002	0.998347	1.0000	0.1197	37.019948	0.026850	0.189696	0.873381	12308.578034
0.0000						0.189696		
0.0000						1.000000		

Spreadsheet for Calculation of Stream-Water Saturation Profiles

Injection Temperature 650 °K		Initial Temperature 300 °K			Matrix Heat Capacity 0.2000 (kJ/kg)			
TRAILING SHOCK CALCULATIONS								
Saturation	OF	Wave V	Flow V	Shock V	fv	dKrv/dSv	dKri/dSi	
0.7500	2.33E-01	0.284467	0.620417	0.051708	0.996549	1.0000	0.1875	
0.875	3.40E-02	0.065482	0.702510	0.031486	0.999629	1.0000	0.0469	
0.9375	-1.59E-02	0.014971	0.704973	0.030879	0.999957	1.0000	0.0117	
0.90625	4.80E-03	0.035327	0.706395	0.030529	0.999849	1.0000	0.0264	
0.921875	-6.59E-03	0.023971	0.706274	0.030559	0.999914	1.0000	0.0183	
0.9140625	-1.16E-03	0.029348	0.706491	0.030505	0.999885	1.0000	0.0222	
0.91015625	1.75E-03	0.032261	0.706484	0.030507	0.999868	1.0000	0.0242	
0.912109375	2.82E-04	0.030786	0.706497	0.030504	0.999876	1.0000	0.0232	
0.9130859375	-4.42E-04	0.030062	0.706497	0.030504	0.999881	1.0000	0.0227	
0.9125976563	-8.13E-05	0.030423	0.706498	0.030504	0.999878	1.0000	0.0229	
0.9123535156	9.99E-05	0.030604	0.706498	0.030504	0.999877	1.0000	0.0230	
0.9124755859	9.21E-06	0.030513	0.706498	0.030504	0.999878	1.0000	0.0230	
0.9125366211	-3.61E-05	0.030468	0.706498	0.030504	0.999878	1.0000	0.0229	
0.9125061035	-1.34E-05	0.030490	0.706498	0.030504	0.999878	1.0000	0.0230	
0.9124908447	-2.12E-06	0.030502	0.706498	0.030504	0.999878	1.0000	0.0230	
0.9124832153	3.54E-06	0.030507	0.706498	0.030504	0.999878	1.0000	0.0230	
0.91248703	7.12E-07	0.030505	0.706498	0.030504	0.999878	1.0000	0.0230	
0.9124889374	-7.03E-07	0.030503	0.706498	0.030504	0.999878	1.0000	0.0230	
0.9124879837	4.27E-09	0.030504	0.706498	0.030504	0.999878	1.0000	0.0230	
0.9124884605	-3.50E-07	0.030503	0.706498	0.030504	0.999878	1.0000	0.0230	
0.9124882221	-1.73E-07	0.030504	0.706498	0.030504	0.999878	1.0000	0.0230	
0.9124881029	-8.42E-08	0.030504	0.706498	0.030504	0.999878	1.0000	0.0230	
0.9124880433	-4.00E-08	0.030504	0.706498	0.030504	0.999878	1.0000	0.0230	
0.9124880135	-1.78E-08	0.030504	0.706498	0.030504	0.999878	1.0000	0.0230	
0.9124879986	-6.78E-09	0.030504	0.706498	0.030504	0.999878	1.0000	0.0230	
0.9124879912	-1.25E-09	0.030504	0.706498	0.030504	0.999878	1.0000	0.0230	
Saturation	Total Mob	dFv/dSv	G	F	Gamma	Theta	High	Low
0.75	34.759228	0.045851	220.095758	12.870589	2.5288E+06	30550.407113	1	0.5
0.875	40.427490	0.009321	115.033000	10.281953	2.4365E+06	28275.535543	1	0.75
0.9375	43.300978	0.002124	62.501620	10.006619	2.3903E+06	28033.574650	1	0.875
0.90625	41.862126	0.005001	88.767310	10.097238	2.4134E+06	28113.209409	0.9375	0.875
0.921875	42.581113	0.003394	75.634465	10.042494	2.4019E+06	28065.100645	0.9375	0.90625
0.9140625	42.221499	0.004154	82.200888	10.067228	2.4076E+06	28086.837287	0.921875	0.90625
0.91015625	42.041781	0.004566	85.484099	10.081538	2.4105E+06	28099.412396	0.9140625	0.90625
0.912109375	42.131632	0.004357	83.842493	10.074214	2.4091E+06	28092.976085	0.9140625	0.91015625
0.9130859375	42.176563	0.004255	83.021690	10.070679	2.4084E+06	28089.869991	0.9140625	0.912109375
0.9125976563	42.154097	0.004306	83.432092	10.072436	2.4087E+06	28091.413802	0.9130859375	0.912109375
0.9123535156	42.142865	0.004332	83.637292	10.073322	2.4089E+06	28092.192627	0.91259765625	0.912109375
0.9124755859	42.148481	0.004319	83.534692	10.072878	2.4088E+06	28091.802636	0.91259765625	0.91235351563
0.9125366211	42.151289	0.004313	83.483392	10.072657	2.4088E+06	28091.608075	0.91259765625	0.91247558594
0.9125061035	42.149885	0.004316	83.509042	10.072768	2.4088E+06	28091.705320	0.91253662109	0.91247558594
0.9124908447	42.149183	0.004317	83.521867	10.072823	2.4088E+06	28091.753969	0.91250610352	0.91247558594
0.9124832153	42.148832	0.004318	83.528280	10.072851	2.4088E+06	28091.778300	0.91249084473	0.91247558594
0.91248703	42.149007	0.004318	83.525073	10.072837	2.4088E+06	28091.766134	0.91249084473	0.91248321533
0.9124889374	42.149095	0.004318	83.523470	10.072830	2.4088E+06	28091.760051	0.91249084473	0.91248703003
0.9124879837	42.149051	0.004318	83.524272	10.072833	2.4088E+06	28091.763093	0.91248893738	0.91248703003
0.9124884605	42.149073	0.004318	83.523871	10.072832	2.4088E+06	28091.761572	0.91248893738	0.9124879837
0.9124882221	42.149062	0.004318	83.524071	10.072833	2.4088E+06	28091.762332	0.91248846054	0.9124879837
0.9124881029	42.149057	0.004318	83.524172	10.072833	2.4088E+06	28091.762713	0.91248822212	0.9124879837
0.9124880433	42.149054	0.004318	83.524222	10.072833	2.4088E+06	28091.762903	0.91248810291	0.9124879837
0.9124880135	42.149053	0.004318	83.524247	10.072833	2.4088E+06	28091.762998	0.91248804331	0.9124879837
0.9124879986	42.149052	0.004318	83.524259	10.072833	2.4088E+06	28091.763045	0.91248801351	0.9124879837
0.9124879912	42.149052	0.004318	83.524266	10.072833	2.4088E+06	28091.763069	0.9124879986	0.9124879837

Spreadsheet for Calculation of Stream-Water Saturation Profiles

Injection Temperature 650 °K Initial Temperature 300 °K Matrix Heat Capacity 0.2000 (kJ/kg)

LEADING SHOCK CALCULATIONS

Saturation	OF	Wave V	Flow V	Shock V	f _v	dKrv/dSv	dKr/dSI
0.7500	1.32E-01	0.323936	0.024013	0.191599	0.996549	1.0000	0.1875
0.875	-1.27E-01	0.065854	0.024323	0.193020	0.999629	1.0000	0.0469
0.8125	-2.61E-02	0.163712	0.023622	0.189797	0.998653	1.0000	0.1055
0.78125	4.49E-02	0.234862	0.023655	0.189952	0.997778	1.0000	0.1436
0.796875	7.50E-03	0.197207	0.023601	0.189704	0.998255	1.0000	0.1238
0.8046875	-9.75E-03	0.179958	0.023602	0.189710	0.998463	1.0000	0.1144
0.80078125	-1.24E-03	0.188455	0.023600	0.189696	0.998362	1.0000	0.1191
0.798828125	3.10E-03	0.192799	0.023600	0.189697	0.998309	1.0000	0.1214
0.7998046875	9.23E-04	0.190619	0.023600	0.189696	0.998335	1.0000	0.1202
0.8002929688	-1.61E-04	0.189535	0.023600	0.189696	0.998349	1.0000	0.1196
0.8000488281	3.80E-04	0.190076	0.023600	0.189696	0.998342	1.0000	0.1199
0.8001708984	1.09E-04	0.189805	0.023600	0.189696	0.998345	1.0000	0.1198
0.8002319336	-2.60E-05	0.189670	0.023600	0.189696	0.998347	1.0000	0.1197
0.800201416	4.16E-05	0.189738	0.023600	0.189696	0.998346	1.0000	0.1198
0.8002166748	7.81E-06	0.189704	0.023600	0.189696	0.998346	1.0000	0.1197
0.8002243042	-9.11E-06	0.189687	0.023600	0.189696	0.998347	1.0000	0.1197
0.8002204895	-6.51E-07	0.189695	0.023600	0.189696	0.998347	1.0000	0.1197
0.8002185822	3.58E-06	0.189700	0.023600	0.189696	0.998347	1.0000	0.1197
0.8002195358	1.46E-06	0.189698	0.023600	0.189696	0.998347	1.0000	0.1197
0.8002200127	4.06E-07	0.189696	0.023600	0.189696	0.998347	1.0000	0.1197
0.8002202511	-1.23E-07	0.189696	0.023600	0.189696	0.998347	1.0000	0.1197
0.8002201319	1.42E-07	0.189696	0.023600	0.189696	0.998347	1.0000	0.1197
0.8002201915	9.61E-09	0.189696	0.023600	0.189696	0.998347	1.0000	0.1197
0.8002202213	-5.65E-08	0.189696	0.023600	0.189696	0.998347	1.0000	0.1197
0.8002202064	-2.34E-08	0.189696	0.023600	0.189696	0.998347	1.0000	0.1197
0.8002201989	-6.91E-09	0.189696	0.023600	0.189696	0.998347	1.0000	0.1197

Saturation	Total Mob	dPv/dSv	G	F	Gamma	Theta	High	Low
0.75	34.759228	0.045851	220.095758	12.870589	2.5288E+06	30550.407113	1	0.5
0.875	40.427490	0.009321	115.039000	10.281953	2.4365E+06	28275.535543	1	0.75
0.8125	37.576492	0.023172	167.564379	11.102088	2.4827E+06	28996.263468	0.875	0.75
0.78125	36.162941	0.033243	193.830069	11.837827	2.5057E+06	29642.824736	0.8125	0.75
0.796875	36.868574	0.027913	180.697224	11.436916	2.4942E+06	29290.507675	0.8125	0.78125
0.8046875	37.222259	0.025472	174.130801	11.261721	2.4884E+06	29136.547240	0.8125	0.796875
0.80078125	37.045346	0.026675	177.414013	11.347315	2.4913E+06	29211.766467	0.8046875	0.796875
0.798828125	36.956943	0.027289	179.055618	11.391607	2.4928E+06	29250.690295	0.80078125	0.796875
0.7998046875	37.001140	0.026981	178.234815	11.369335	2.4920E+06	29231.117508	0.80078125	0.798828125
0.8002929688	37.023242	0.026827	177.824414	11.358293	2.4917E+06	29221.414371	0.80078125	0.7998046875
0.8000488281	37.012191	0.026904	178.029615	11.363806	2.4919E+06	29226.259023	0.80029296875	0.7998046875
0.8001708984	37.017717	0.026866	177.927014	11.361048	2.4918E+06	29223.834969	0.80029296875	0.80004882813
0.8002319336	37.020479	0.026847	177.875714	11.359670	2.4917E+06	29222.624239	0.80029296875	0.80017089844
0.800201416	37.019098	0.026856	177.901364	11.360359	2.4917E+06	29223.229496	0.80023193359	0.80017089844
0.8002166748	37.019789	0.026851	177.888539	11.360014	2.4917E+06	29222.926840	0.80023193359	0.80020141602
0.8002243042	37.020134	0.026849	177.882127	11.359842	2.4917E+06	29222.775533	0.80023193359	0.8002166748
0.8002204895	37.019961	0.026850	177.885333	11.359928	2.4917E+06	29222.851185	0.8002243042	0.8002166748
0.8002185822	37.019875	0.026851	177.886936	11.359971	2.4917E+06	29222.889012	0.8002204895	0.8002166748
0.8002195358	37.019918	0.026850	177.886435	11.359950	2.4917E+06	29222.870099	0.8002204895	0.80021858215
0.8002200127	37.019940	0.026850	177.885734	11.359939	2.4917E+06	29222.860642	0.8002204895	0.80021953583
0.8002202511	37.019951	0.026850	177.885533	11.359934	2.4917E+06	29222.855913	0.8002204895	0.80022001266
0.8002201319	37.019945	0.026850	177.885634	11.359936	2.4917E+06	29222.858278	0.80022025108	0.80022013187
0.8002201915	37.019948	0.026850	177.885583	11.359935	2.4917E+06	29222.857095	0.80022025108	0.80022019148
0.8002202213	37.019949	0.026850	177.885558	11.359934	2.4917E+06	29222.856504	0.80022022128	0.80022019148
0.8002202064	37.019949	0.026850	177.885571	11.359935	2.4917E+06	29222.856800	0.80022022128	0.80022019148
0.8002201989	37.019948	0.026850	177.885577	11.359935	2.4917E+06	29222.856948	0.80022020638	0.80022019148

Spreadsheet for Calculation of Stream-Water Saturation Profiles

Injection Temperature
650 °K

Initial Temperature
300 °K

Matrix Heat Capacity
1.0000 (kJ/kg)

MATRIX PROPERTIES

Porosity	Cp Matrix	Density	Rho * Cp
0.10	1.00	2650.00	2650.0000
Nw	Ng	Swi	Denom
3.00	1.00	0.00	1.000000

SATURATION CONDITIONS

Tsaturation = 485.57

	Volumes (m3/kg)	Enthalpies (kJ/kg)	Densities (kg/m3)	Viscosities (cp)	Saturation Step
Liquid	0.001176	901.41	850.4723	0.1303	0.0011764038
Vapor	0.100298	2808.52	9.970241	0.0217	

BOUNDARY CONDITIONS

	Temperature	Velocity	Heat Capacity	Wave Velocity	Density	Enthalpy
Injection	650	1.000000	2.30	0.006622	6.882648	3199.91
Initial	300	0.010726	4.16	0.015992	1004.6293	112.70
	G	F	Gamma	Theta		
Injection	650	6.88	6.88	15524523.87	22023.87	
Initial	300	1004.63	1004.63	7268218.71	113218.71	

SHOCK CONDITIONS

	Initial Guess		Vapor Saturation	Objective Function	Two-Phase Wave Velocity	Upstream Flow Velocity	Shock Velocity	Vapor Frac Flow
	Sv-Hi	Sv-Low						
Trailing	1	0.5	0.9570	1.4356E-09	0.0068	0.692182	0.0068	1.0000
Leading	1	0.5	0.8981	4.0467E-09	0.0414	0.010726	0.0414	0.9998
	dKr/dSv	dKrl/dSl	Total Mobility	dFv/dSv	G	F'	Gamma	Theta'
Trailing	1.0000	0.0056	44.1982	0.0010	46.1514	9.9819	1.1641E+07	28011.8389
Leading	1.0000	0.0311	41.4890	0.0060	95.5899	10.1346	1.1684E+07	28146.0687

MATERIAL BALANCES

	Inside	Initial	Injected	Produced	Balance	Error
Mass	96.569994	100.462933	6.882648	10.775582	0.0000	0.0000%
Enthalpy	747635.0622	726821.8712	22023.8721	1214.3758	-3.6947	0.0005%

Spreadsheet for Calculation of Stream-Water Saturation Profiles

Injection Temperature 650 °K Initial Temperature 300 °K Matrix Heat Capacity 1.0000 (kJ/kg)

SATURATION PROFILE

Vapor Saturation	Vapor Frac Flow	dKr/dSv	dKr/dSI	Total Mobility	dFv/dSv	lambda	Mass Inside	Enthalpy Inside
1.0000						0.000000		
1.0000						0.006783		
0.9570	0.999986	1.0000	0.0056	44.198164	0.000980	0.006783	0.046687	105308.165674
0.9558	0.999985	1.0000	0.0059	44.143883	0.001036	0.007171	0.018082	4512.817923
0.9546	0.999984	1.0000	0.0062	44.089604	0.001094	0.007570	0.019010	4646.402924
0.9534	0.999982	1.0000	0.0065	44.035329	0.001153	0.007981	0.019964	4780.663193
0.9522	0.999981	1.0000	0.0068	43.981056	0.001214	0.008403	0.020944	4915.602756
0.9511	0.999980	1.0000	0.0072	43.926786	0.001277	0.008837	0.021949	5051.225662
0.9499	0.999978	1.0000	0.0075	43.872519	0.001341	0.009282	0.022980	5187.535987
0.9487	0.999976	1.0000	0.0079	43.818256	0.001407	0.009739	0.024037	5324.537830
0.9475	0.999975	1.0000	0.0083	43.763996	0.001475	0.010208	0.025120	5462.235316
0.9464	0.999973	1.0000	0.0086	43.709739	0.001544	0.010689	0.026230	5600.632596
0.9452	0.999971	1.0000	0.0090	43.655486	0.001615	0.011182	0.027367	5739.733845
0.9440	0.999969	1.0000	0.0094	43.601236	0.001688	0.011686	0.028530	5879.543266
0.9428	0.999967	1.0000	0.0098	43.546989	0.001763	0.012203	0.029721	6020.065085
0.9417	0.999965	1.0000	0.0102	43.492747	0.001839	0.012732	0.030938	6161.303557
0.9405	0.999963	1.0000	0.0106	43.438508	0.001918	0.013273	0.032184	6303.262960
0.9393	0.999960	1.0000	0.0111	43.384273	0.001997	0.013826	0.033457	6445.947603
0.9381	0.999958	1.0000	0.0115	43.330041	0.002079	0.014391	0.034757	6589.361816
0.9370	0.999956	1.0000	0.0119	43.275814	0.002163	0.014969	0.036086	6733.509960
0.9358	0.999953	1.0000	0.0124	43.221591	0.002248	0.015559	0.037443	6878.396422
0.9346	0.999950	1.0000	0.0128	43.167371	0.002335	0.016161	0.038829	7024.025615
0.9334	0.999947	1.0000	0.0133	43.113156	0.002424	0.016776	0.040243	7170.401980
0.9322	0.999945	1.0000	0.0138	43.058945	0.002514	0.017404	0.041686	7317.529986
0.9311	0.999942	1.0000	0.0143	43.004739	0.002607	0.018044	0.043159	7465.414130
0.9299	0.999938	1.0000	0.0147	42.950537	0.002701	0.018697	0.044660	7614.058934
0.9287	0.999935	1.0000	0.0152	42.896339	0.002797	0.019363	0.046192	7763.468952
0.9275	0.999932	1.0000	0.0158	42.842146	0.002895	0.020041	0.047752	7913.648764
0.9264	0.999928	1.0000	0.0163	42.787958	0.002995	0.020733	0.049343	8064.602979
0.9252	0.999925	1.0000	0.0168	42.733774	0.003097	0.021437	0.050964	8216.336234
0.9240	0.999921	1.0000	0.0173	42.679595	0.003201	0.022155	0.052616	8368.853197
0.9228	0.999917	1.0000	0.0179	42.625421	0.003306	0.022885	0.054298	8522.158563
0.9217	0.999913	1.0000	0.0184	42.571251	0.003414	0.023629	0.056011	8676.257057
0.9205	0.999909	1.0000	0.0190	42.517087	0.003523	0.024386	0.057755	8831.153433
0.9193	0.999905	1.0000	0.0195	42.462928	0.003634	0.025156	0.059530	8986.852475
0.9181	0.999901	1.0000	0.0201	42.408774	0.003747	0.025939	0.061337	9143.358996
0.9170	0.999896	1.0000	0.0207	42.354625	0.003863	0.026736	0.063175	9300.677842
0.9158	0.999892	1.0000	0.0213	42.300481	0.003980	0.027547	0.065046	9458.813886
0.9146	0.999887	1.0000	0.0219	42.246343	0.004099	0.028371	0.066949	9617.772033
0.9134	0.999882	1.0000	0.0225	42.192210	0.004220	0.029208	0.068884	9777.557218
0.9122	0.999877	1.0000	0.0231	42.138083	0.004343	0.030059	0.070852	9938.174408
0.9111	0.999872	1.0000	0.0237	42.083962	0.004468	0.030924	0.072853	10099.628600
0.9099	0.999866	1.0000	0.0244	42.029846	0.004595	0.031803	0.074887	10261.924822
0.9087	0.999861	1.0000	0.0250	41.975735	0.004724	0.032696	0.076955	10425.068137
0.9075	0.999855	1.0000	0.0256	41.921631	0.004855	0.033603	0.079056	10589.063634
0.9064	0.999849	1.0000	0.0263	41.867533	0.004988	0.034524	0.081191	10753.916439
0.9052	0.999844	1.0000	0.0270	41.813440	0.005123	0.035459	0.083360	10919.631709
0.9040	0.999837	1.0000	0.0276	41.759354	0.005260	0.036408	0.085564	11086.214631
0.9028	0.999831	1.0000	0.0283	41.705273	0.005399	0.037371	0.087802	11253.670427
0.9017	0.999825	1.0000	0.0290	41.651199	0.005540	0.038349	0.090076	11422.004352
0.9005	0.999818	1.0000	0.0297	41.597131	0.005684	0.039341	0.092384	11591.221693
0.8993	0.999811	1.0000	0.0304	41.543070	0.005829	0.040347	0.094728	11761.327771
0.8981	0.999804	1.0000	0.0311	41.489014	0.005977	0.041369	0.097108	11932.327941
0.0000						0.041369		
0.0000						1.000000		

Spreadsheet for Calculation of Stream-Water Saturation Profiles

Injection Temperature 650 °K		Initial Temperature 300 °K			Matrix Heat Capacity 1.0000 (kJ/kg)			
TRAILING SHOCK CALCULATIONS								
Saturation	OF	Wave V	Flow V	Shock V	fv	dKrv/dSv	dKr/dSI	
0.7500	2.42E-01	0.255386	0.556992	0.013421	0.996549	1.0000	0.1875	
0.875	5.54E-02	0.063132	0.677295	0.007514	0.999629	1.0000	0.0469	
0.9375	7.87E-03	0.014687	0.691596	0.006812	0.999957	1.0000	0.0117	
0.96875	-3.28E-03	0.003516	0.692013	0.006792	0.999995	1.0000	0.0029	
0.953125	1.30E-03	0.008087	0.692162	0.006784	0.999982	1.0000	0.0066	
0.9609375	-1.23E-03	0.005554	0.692162	0.006784	0.999990	1.0000	0.0046	
0.95703125	-2.54E-05	0.006758	0.692182	0.006783	0.999986	1.0000	0.0055	
0.955078125	6.23E-04	0.007406	0.692178	0.006784	0.999984	1.0000	0.0061	
0.9560546875	2.95E-04	0.007078	0.692181	0.006783	0.999985	1.0000	0.0058	
0.9565429688	1.34E-04	0.006917	0.692182	0.006783	0.999986	1.0000	0.0057	
0.9567871094	5.40E-05	0.006837	0.692182	0.006783	0.999986	1.0000	0.0056	
0.9569091797	1.42E-05	0.006798	0.692182	0.006783	0.999986	1.0000	0.0056	
0.9569702148	-5.61E-06	0.006778	0.692182	0.006783	0.999986	1.0000	0.0056	
0.9569396973	4.30E-06	0.006788	0.692182	0.006783	0.999986	1.0000	0.0056	
0.9569549561	-6.54E-07	0.006783	0.692182	0.006783	0.999986	1.0000	0.0056	
0.9569473267	1.82E-06	0.006785	0.692182	0.006783	0.999986	1.0000	0.0056	
0.9569511414	5.84E-07	0.006784	0.692182	0.006783	0.999986	1.0000	0.0056	
0.9569530487	-3.48E-08	0.006783	0.692182	0.006783	0.999986	1.0000	0.0056	
0.956952095	2.75E-07	0.006784	0.692182	0.006783	0.999986	1.0000	0.0056	
0.9569525719	1.20E-07	0.006783	0.692182	0.006783	0.999986	1.0000	0.0056	
0.9569528103	4.26E-08	0.006783	0.692182	0.006783	0.999986	1.0000	0.0056	
0.9569529295	3.85E-09	0.006783	0.692182	0.006783	0.999986	1.0000	0.0056	
0.9569529891	-1.55E-08	0.006783	0.692182	0.006783	0.999986	1.0000	0.0056	
0.9569529593	-5.82E-09	0.006783	0.692182	0.006783	0.999986	1.0000	0.0056	
0.9569529444	-9.83E-10	0.006783	0.692182	0.006783	0.999986	1.0000	0.0056	
0.9569529369	1.44E-09	0.006783	0.692182	0.006783	0.999986	1.0000	0.0056	
Saturation	Total Mob	dFv/dSv	G	F	Gamma	Theta	High	Low
0.75	34.759228	0.045851	220.095758	12.870589	1.1794E+07	30550.407113	1	0.5
0.875	40.427490	0.009321	115.033000	10.281953	1.1701E+07	28275.535543	1	0.75
0.9375	43.300978	0.002124	62.501620	10.006619	1.1655E+07	28033.574650	1	0.875
0.96875	44.742642	0.000508	36.235931	9.974642	1.1632E+07	28005.473055	1	0.9375
0.953125	44.021547	0.001168	49.368776	9.985337	1.1643E+07	28014.871837	0.96875	0.9375
0.9609375	44.382039	0.000802	42.802353	9.978906	1.1638E+07	28009.220503	0.96875	0.953125
0.95703125	44.201778	0.000976	46.085564	9.981821	1.1641E+07	28011.782338	0.9609375	0.953125
0.955078125	44.111658	0.001070	47.727170	9.983500	1.1642E+07	28013.257853	0.95703125	0.953125
0.9560546875	44.156717	0.001023	46.906367	9.982642	1.1641E+07	28012.503198	0.95703125	0.955078125
0.9565429688	44.179247	0.000999	46.495966	9.982227	1.1641E+07	28012.138595	0.95703125	0.9560546875
0.9567871094	44.190513	0.000988	46.290765	9.982023	1.1641E+07	28011.959430	0.95703125	0.95654296875
0.9569091797	44.196145	0.000982	46.188165	9.981922	1.1641E+07	28011.870625	0.95703125	0.95678710938
0.9569702148	44.198962	0.000979	46.136864	9.981871	1.1641E+07	28011.826417	0.95703125	0.95690917969
0.9569396973	44.197553	0.000981	46.162515	9.981897	1.1641E+07	28011.848505	0.95697021484	0.95690917969
0.9569549561	44.198258	0.000980	46.149690	9.981884	1.1641E+07	28011.837457	0.95697021484	0.95693969727
0.9569473267	44.197905	0.000980	46.156102	9.981890	1.1641E+07	28011.842980	0.95695495605	0.95693969727
0.9569511414	44.198082	0.000980	46.152896	9.981887	1.1641E+07	28011.840218	0.95695495605	0.95694732666
0.9569530487	44.198170	0.000980	46.151293	9.981886	1.1641E+07	28011.838838	0.95695495605	0.95695114136
0.956952095	44.198126	0.000980	46.152094	9.981886	1.1641E+07	28011.839528	0.95695304871	0.95695114136
0.9569525719	44.198148	0.000980	46.151693	9.981886	1.1641E+07	28011.839183	0.95695304871	0.95695209503
0.9569528103	44.198159	0.000980	46.151493	9.981886	1.1641E+07	28011.839010	0.95695304871	0.95695257187
0.9569529295	44.198164	0.000980	46.151393	9.981886	1.1641E+07	28011.838924	0.95695304871	0.95695281029
0.9569529891	44.198167	0.000980	46.151343	9.981886	1.1641E+07	28011.838881	0.95695304871	0.9569529295
0.9569529593	44.198165	0.000980	46.151368	9.981886	1.1641E+07	28011.838902	0.9569529891	0.9569529295
0.9569529444	44.198165	0.000980	46.151380	9.981886	1.1641E+07	28011.838913	0.9569529593	0.9569529295
0.9569529369	44.198164	0.000980	46.151387	9.981886	1.1641E+07	28011.838919	0.9569529444	0.9569529295

Spreadsheet for Calculation of Stream-Water Saturation Profiles

Injection Temperature 650 °K Initial Temperature 300 °K Matrix Heat Capacity 1.0000 (kJ/kg)

LEADING SHOCK CALCULATIONS

Saturation	OF	Wave V	Flow V	Shock V	f_v	dK_{rv}/dS_v	dK_r/dS_l
0.7500	2.74E-01	0.317373	0.012277	0.043658	0.996549	1.0000	0.1875
0.875	2.31E-02	0.064519	0.010751	0.041405	0.999629	1.0000	0.0469
0.9375	-2.68E-02	0.014699	0.010782	0.041451	0.999957	1.0000	0.0117
0.90625	-6.76E-03	0.034616	0.010729	0.041373	0.999849	1.0000	0.0264
0.890625	6.86E-03	0.048233	0.010728	0.041372	0.999756	1.0000	0.0359
0.8984375	-2.66E-04	0.041103	0.010726	0.041369	0.999806	1.0000	0.0309
0.89453125	3.22E-03	0.044586	0.010726	0.041369	0.999782	1.0000	0.0334
0.896484375	1.46E-03	0.042824	0.010726	0.041369	0.999794	1.0000	0.0321
0.8974609375	5.90E-04	0.041958	0.010726	0.041369	0.999800	1.0000	0.0315
0.8979492188	1.61E-04	0.041529	0.010726	0.041369	0.999803	1.0000	0.0312
0.8981933594	-5.30E-05	0.041316	0.010726	0.041369	0.999805	1.0000	0.0311
0.8980712891	5.38E-05	0.041422	0.010726	0.041369	0.999804	1.0000	0.0312
0.8981323242	3.75E-07	0.041369	0.010726	0.041369	0.999804	1.0000	0.0311
0.8981628418	-2.63E-05	0.041342	0.010726	0.041369	0.999805	1.0000	0.0311
0.898147583	-1.30E-05	0.041356	0.010726	0.041369	0.999805	1.0000	0.0311
0.8981399536	-6.29E-06	0.041362	0.010726	0.041369	0.999804	1.0000	0.0311
0.8981361389	-2.96E-06	0.041366	0.010726	0.041369	0.999804	1.0000	0.0311
0.8981342316	-1.29E-06	0.041367	0.010726	0.041369	0.999804	1.0000	0.0311
0.8981332779	-4.58E-07	0.041368	0.010726	0.041369	0.999804	1.0000	0.0311
0.8981328011	-4.15E-08	0.041369	0.010726	0.041369	0.999804	1.0000	0.0311
0.8981325626	1.67E-07	0.041369	0.010726	0.041369	0.999804	1.0000	0.0311
0.8981326818	6.27E-08	0.041369	0.010726	0.041369	0.999804	1.0000	0.0311
0.8981327415	1.06E-08	0.041369	0.010726	0.041369	0.999804	1.0000	0.0311
0.8981327713	-1.55E-08	0.041369	0.010726	0.041369	0.999804	1.0000	0.0311
0.8981327564	-2.47E-09	0.041369	0.010726	0.041369	0.999804	1.0000	0.0311
0.8981327489	4.05E-09	0.041369	0.010726	0.041369	0.999804	1.0000	0.0311

Saturation	Total Mob	dF_v/dS_v	G	F	Gamma	Theta	High	Low
0.75	34.759228	0.045851	220.095758	12.870589	1.1794E+07	30550.407113	1	0.5
0.875	40.427490	0.009321	115.033000	10.281953	1.1701E+07	28275.535543	1	0.75
0.9375	43.300978	0.002124	62.501620	10.006619	1.1655E+07	28033.574650	1	0.875
0.90625	41.862126	0.005001	88.767310	10.097238	1.1678E+07	28113.209409	0.9375	0.875
0.890625	41.144193	0.006968	101.900155	10.175426	1.1690E+07	28181.920650	0.90625	0.875
0.8984375	41.503017	0.005938	95.333732	10.133103	1.1684E+07	28144.727756	0.90625	0.890625
0.89453125	41.323568	0.006441	98.616944	10.153419	1.1687E+07	28162.581158	0.8984375	0.890625
0.896484375	41.413283	0.006187	96.975338	10.143055	1.1685E+07	28153.472957	0.8984375	0.89453125
0.8974609375	41.458148	0.006062	96.154535	10.138028	1.1685E+07	28149.055510	0.8984375	0.896484375
0.8979492188	41.480582	0.006000	95.744134	10.135553	1.1684E+07	28146.880487	0.8984375	0.8974609375
0.8981933594	41.491799	0.005969	95.538933	10.134325	1.1684E+07	28145.801343	0.8984375	0.89794921875
0.8980712891	41.486191	0.005984	95.641533	10.134938	1.1684E+07	28146.340220	0.89819335938	0.89794921875
0.8981323242	41.488995	0.005977	95.590233	10.134631	1.1684E+07	28146.070608	0.89819335938	0.89807128906
0.8981628418	41.490397	0.005973	95.564583	10.134478	1.1684E+07	28145.935932	0.89819335938	0.89813232422
0.898147583	41.489696	0.005975	95.577408	10.134555	1.1684E+07	28146.003259	0.8981628418	0.89813232422
0.8981399536	41.489345	0.005976	95.583821	10.134593	1.1684E+07	28146.036931	0.89814758301	0.89813232422
0.8981361389	41.489170	0.005976	95.587027	10.134612	1.1684E+07	28146.053768	0.89813995361	0.89813232422
0.8981342316	41.489082	0.005976	95.588630	10.134622	1.1684E+07	28146.062188	0.89813613892	0.89813232422
0.8981332779	41.489039	0.005976	95.589432	10.134627	1.1684E+07	28146.066398	0.89813423157	0.89813232422
0.8981328011	41.489017	0.005977	95.589833	10.134629	1.1684E+07	28146.068503	0.89813327789	0.89813232422
0.8981325626	41.489006	0.005977	95.590033	10.134630	1.1684E+07	28146.069555	0.89813280106	0.89813232422
0.8981326818	41.489011	0.005977	95.589933	10.134630	1.1684E+07	28146.069029	0.89813280106	0.89813256264
0.8981327415	41.489014	0.005977	95.589883	10.134629	1.1684E+07	28146.068766	0.89813280106	0.89813268185
0.8981327713	41.489015	0.005977	95.589858	10.134629	1.1684E+07	28146.068634	0.89813280106	0.89813274145
0.8981327564	41.489015	0.005977	95.589870	10.134629	1.1684E+07	28146.068700	0.89813277125	0.89813274145
0.8981327489	41.489014	0.005977	95.589876	10.134629	1.1684E+07	28146.068733	0.89813275635	0.89813274145

Spreadsheet for Calculation of Stream-Water Saturation Profiles

Injection Temperature
650 °K

Initial Temperature
300 °K

Matrix Heat Capacity
5.0000 (kJ/kg)

MATRIX PROPERTIES

Porosity	Cp Matrix	Density	Rho * Cp
0.10	5.00	2650.00	13250.0000
Nw	Ng	Swi	Denom
3.00	1.00	0.00	1.000000

SATURATION CONDITIONS

Tsaturation = 485.57

	Volumes (m3/kg)	Enthalpies (kJ/kg)	Densities (kg/m3)	Viscosities (cp)	Saturation Step
Liquid	0.001176	901.41	850.4723	0.1303	0.0005603138
Vapor	0.100298	2808.52	9.970241	0.0217	

BOUNDARY CONDITIONS

	Temperature	Velocity	Heat Capacity	Wave Velocity	Density	Enthalpy
Injection	650	1.000000	2.30	0.001325	6.882648	3199.91
Initial	300	0.007659	4.16	0.002593	1004.6293	112.70
	G	F	Gamma	Theta		
Injection	650	6.88	6.88	77534523.87	22023.87	
Initial	300	1004.63	1004.63	35888218.71	113218.71	

SHOCK CONDITIONS

	Initial Guess		Vapor Saturation	Objective Function	Two-Phase Wave Velocity	Upstream Flow Velocity	Shock Velocity	Vapor Frac Flow
Trailing	1	0.5	0.9803	-7.4421E-10	0.0014	0.690514	0.0014	1.0000
Leading	1	0.5	0.9523	-5.6620E-10	0.0084	0.007659	0.0084	1.0000
	dKrv/dSv	dKrl/dSl	Total Mobility	dFv/dSv	G	F'	Gamma	Theta'
Trailing	1.0000	0.0012	45.2759	0.0002	26.5277	9.9713	5.7947E+07	28002.5631
Leading	1.0000	0.0068	43.9828	0.0012	50.0750	9.9862	5.7967E+07	28015.6104

MATERIAL BALANCES

	Inside	Initial	Injected	Produced	Balance	Error
Mass	99.651123	100.462933	6.882648	7.694459	0.0000	0.0000%
Enthalpy	3609978.9454	3588821.8712	22023.8721	867.1424	-0.3445	0.0000%

Spreadsheet for Calculation of Stream-Water Saturation Profiles

Injection Temperature 650 °K		Initial Temperature 300 °K		Matrix Heat Capacity 5.0000 (kJ/kg)				
SATURATION PROFILE								
Vapor Saturation	Vapor Frac Flow	dKr/dSv	dKr/dSI	Total Mobility	dPv/dSv	lambda	Mass Inside	Enthalpy Inside
1.0000						0.000000		
1.0000						0.001372		
0.9803	0.999999	1.0000	0.0012	45.275934	0.000199	0.001372	0.009444	106387.959165
0.9797	0.999999	1.0000	0.0012	45.250061	0.000210	0.001452	0.002148	4651.756898
0.9792	0.999998	1.0000	0.0013	45.224188	0.000222	0.001535	0.002250	4787.753799
0.9786	0.999998	1.0000	0.0014	45.198315	0.000235	0.001620	0.002354	4924.063840
0.9781	0.999998	1.0000	0.0014	45.172443	0.000247	0.001707	0.002461	5060.687899
0.9775	0.999998	1.0000	0.0015	45.146571	0.000260	0.001797	0.002569	5197.626860
0.9769	0.999998	1.0000	0.0016	45.120699	0.000274	0.001889	0.002681	5334.881609
0.9764	0.999998	1.0000	0.0017	45.094827	0.000287	0.001984	0.002794	5472.453033
0.9758	0.999998	1.0000	0.0018	45.068956	0.000301	0.002080	0.002910	5610.342022
0.9753	0.999997	1.0000	0.0018	45.043085	0.000316	0.002180	0.003029	5748.549470
0.9747	0.999997	1.0000	0.0019	45.017215	0.000330	0.002281	0.003149	5887.076272
0.9741	0.999997	1.0000	0.0020	44.991345	0.000345	0.002385	0.003273	6025.923327
0.9736	0.999997	1.0000	0.0021	44.965475	0.000361	0.002491	0.003398	6165.091534
0.9730	0.999997	1.0000	0.0022	44.939606	0.000377	0.002600	0.003526	6304.581797
0.9725	0.999996	1.0000	0.0023	44.913737	0.000393	0.002711	0.003657	6444.395022
0.9719	0.999996	1.0000	0.0024	44.887869	0.000409	0.002825	0.003790	6584.532118
0.9713	0.999996	1.0000	0.0025	44.862001	0.000426	0.002941	0.003925	6724.993994
0.9708	0.999996	1.0000	0.0026	44.836133	0.000443	0.003060	0.004063	6865.781566
0.9702	0.999995	1.0000	0.0027	44.810266	0.000461	0.003181	0.004204	7006.895748
0.9697	0.999995	1.0000	0.0028	44.784399	0.000478	0.003304	0.004347	7148.337461
0.9691	0.999995	1.0000	0.0029	44.758532	0.000497	0.003430	0.004492	7290.107625
0.9685	0.999995	1.0000	0.0030	44.732666	0.000515	0.003558	0.004640	7432.207164
0.9680	0.999994	1.0000	0.0031	44.706801	0.000534	0.003689	0.004790	7574.637005
0.9674	0.999994	1.0000	0.0032	44.680936	0.000553	0.003822	0.004943	7717.398079
0.9669	0.999994	1.0000	0.0033	44.655071	0.000573	0.003957	0.005099	7860.491315
0.9663	0.999993	1.0000	0.0034	44.629207	0.000593	0.004095	0.005257	8003.917650
0.9657	0.999993	1.0000	0.0035	44.603344	0.000613	0.004236	0.005417	8147.678021
0.9652	0.999993	1.0000	0.0036	44.577481	0.000634	0.004379	0.005581	8291.773368
0.9646	0.999992	1.0000	0.0038	44.551618	0.000655	0.004525	0.005746	8436.204634
0.9641	0.999992	1.0000	0.0039	44.525756	0.000677	0.004673	0.005915	8580.972764
0.9635	0.999992	1.0000	0.0040	44.499894	0.000699	0.004823	0.006086	8726.078707
0.9629	0.999991	1.0000	0.0041	44.474033	0.000721	0.004976	0.006259	8871.523413
0.9624	0.999991	1.0000	0.0042	44.448173	0.000743	0.005132	0.006435	9017.307836
0.9618	0.999990	1.0000	0.0044	44.422313	0.000766	0.005290	0.006614	9163.432933
0.9612	0.999990	1.0000	0.0045	44.396454	0.000789	0.005451	0.006795	9309.899662
0.9607	0.999989	1.0000	0.0046	44.370595	0.000813	0.005614	0.006979	9456.708987
0.9601	0.999989	1.0000	0.0048	44.344736	0.000837	0.005779	0.007166	9603.861871
0.9596	0.999989	1.0000	0.0049	44.318879	0.000861	0.005948	0.007355	9751.359281
0.9590	0.999988	1.0000	0.0050	44.293022	0.000886	0.006119	0.007547	9899.202190
0.9584	0.999988	1.0000	0.0052	44.267165	0.000911	0.006292	0.007741	10047.391568
0.9579	0.999987	1.0000	0.0053	44.241309	0.000937	0.006468	0.007938	10195.928393
0.9573	0.999987	1.0000	0.0055	44.215454	0.000963	0.006646	0.008138	10344.813642
0.9568	0.999986	1.0000	0.0056	44.189599	0.000989	0.006827	0.008341	10494.048298
0.9562	0.999985	1.0000	0.0058	44.163745	0.001015	0.007011	0.008546	10643.633345
0.9556	0.999985	1.0000	0.0059	44.137892	0.001042	0.007197	0.008754	10793.569770
0.9551	0.999984	1.0000	0.0061	44.112039	0.001070	0.007386	0.008965	10943.858563
0.9545	0.999984	1.0000	0.0062	44.086187	0.001097	0.007577	0.009179	11094.500716
0.9540	0.999983	1.0000	0.0064	44.060335	0.001125	0.007771	0.009395	11245.497227
0.9534	0.999982	1.0000	0.0065	44.034485	0.001154	0.007968	0.009614	11396.849092
0.9528	0.999982	1.0000	0.0067	44.008634	0.001183	0.008167	0.009835	11548.557315
0.9523	0.999981	1.0000	0.0068	43.982785	0.001212	0.008369	0.010060	11700.622898
0.0000						0.008369		
0.0000						1.000000		

Spreadsheet for Calculation of Stream-Water Saturation Profiles

Injection Temperature 650 °K		Initial Temperature 300 °K		Matrix Heat Capacity 5.0000 (kJ/kg)				
TRAILING SHOCK CALCULATIONS								
Saturation	OF	Wave V	Flow V	Shock V	f _v	dKrv/dSv	dKr/dSI	
0.7500	2.45E-01	0.247360	0.539486	0.002854	0.996549	1.0000	0.1875	
0.875	6.10E-02	0.062548	0.671036	0.001563	0.999629	1.0000	0.0469	
0.9375	1.32E-02	0.014623	0.688583	0.001391	0.999957	1.0000	0.0117	
0.96875	2.13E-03	0.003508	0.690419	0.001373	0.999995	1.0000	0.0029	
0.984375	-5.14E-04	0.000858	0.690505	0.001372	0.999999	1.0000	0.0007	
0.9765625	5.80E-04	0.001952	0.690505	0.001372	0.999998	1.0000	0.0016	
0.98046875	-2.36E-05	0.001348	0.690514	0.001372	0.999999	1.0000	0.0011	
0.978515625	2.64E-04	0.001636	0.690512	0.001372	0.999998	1.0000	0.0014	
0.9794921875	1.17E-04	0.001489	0.690514	0.001372	0.999999	1.0000	0.0013	
0.9799804688	4.56E-05	0.001418	0.690514	0.001372	0.999999	1.0000	0.0012	
0.9802246094	1.07E-05	0.001383	0.690514	0.001372	0.999999	1.0000	0.0012	
0.9803466797	-6.51E-06	0.001366	0.690514	0.001372	0.999999	1.0000	0.0012	
0.9802856445	2.10E-06	0.001374	0.690514	0.001372	0.999999	1.0000	0.0012	
0.9803161621	-2.21E-06	0.001370	0.690514	0.001372	0.999999	1.0000	0.0012	
0.9803009033	-5.86E-08	0.001372	0.690514	0.001372	0.999999	1.0000	0.0012	
0.9802932739	1.02E-06	0.001373	0.690514	0.001372	0.999999	1.0000	0.0012	
0.9802970886	4.80E-07	0.001373	0.690514	0.001372	0.999999	1.0000	0.0012	
0.980298996	2.11E-07	0.001372	0.690514	0.001372	0.999999	1.0000	0.0012	
0.9802999496	7.60E-08	0.001372	0.690514	0.001372	0.999999	1.0000	0.0012	
0.9803004265	8.72E-09	0.001372	0.690514	0.001372	0.999999	1.0000	0.0012	
0.9803006649	-2.49E-08	0.001372	0.690514	0.001372	0.999999	1.0000	0.0012	
0.9803005457	-8.11E-09	0.001372	0.690514	0.001372	0.999999	1.0000	0.0012	
0.9803004861	3.08E-10	0.001372	0.690514	0.001372	0.999999	1.0000	0.0012	
0.9803005159	-3.90E-09	0.001372	0.690514	0.001372	0.999999	1.0000	0.0012	
0.980300501	-1.80E-09	0.001372	0.690514	0.001372	0.999999	1.0000	0.0012	
0.9803004935	-7.44E-10	0.001372	0.690514	0.001372	0.999999	1.0000	0.0012	
Saturation	Total Mob	dFv/dSv	G	F	Gamma	Theta	High	Low
0.75	34.759228	0.045851	220.095758	12.870589	5.8117E+07	30550.407113	1	0.5
0.875	40.427490	0.009321	115.033000	10.281953	5.8025E+07	28275.535543	1	0.75
0.9375	43.300978	0.002124	62.501620	10.006619	5.7978E+07	28033.574650	1	0.875
0.96875	44.742642	0.000508	36.235931	9.974642	5.7955E+07	28005.473055	1	0.9375
0.984375	45.464089	0.000124	23.103086	9.970782	5.7944E+07	28002.081444	1	0.96875
0.9765625	45.103332	0.000283	29.669508	9.972083	5.7950E+07	28003.224190	0.984375	0.96875
0.98046875	45.283704	0.000195	26.386297	9.971303	5.7947E+07	28002.538594	0.984375	0.9765625
0.978515625	45.193516	0.000237	28.027903	9.971657	5.7948E+07	28002.849861	0.98046875	0.9765625
0.9794921875	45.238610	0.000216	27.207100	9.971471	5.7947E+07	28002.686718	0.98046875	0.978515625
0.9799804688	45.261157	0.000205	26.796698	9.971385	5.7947E+07	28002.610825	0.98046875	0.9794921875
0.9802246094	45.272430	0.000200	26.591498	9.971343	5.7947E+07	28002.574258	0.98046875	0.97998046875
0.9803466797	45.278067	0.000198	26.488897	9.971323	5.7947E+07	28002.556313	0.98046875	0.98022460938
0.9802856445	45.275249	0.000199	26.540198	9.971333	5.7947E+07	28002.565257	0.98034667969	0.98022460938
0.9803161621	45.276658	0.000198	26.514547	9.971328	5.7947E+07	28002.560778	0.98034667969	0.98028564453
0.9803009033	45.275953	0.000199	26.527373	9.971330	5.7947E+07	28002.563016	0.98031616211	0.98028564453
0.9802932739	45.275601	0.000199	26.533785	9.971332	5.7947E+07	28002.564136	0.98030090332	0.98028564453
0.9802970886	45.275777	0.000199	26.530579	9.971331	5.7947E+07	28002.563576	0.98030090332	0.98029327393
0.980298996	45.275865	0.000199	26.528976	9.971331	5.7947E+07	28002.563296	0.98030090332	0.98029708862
0.9802999496	45.275909	0.000199	26.528174	9.971331	5.7947E+07	28002.563156	0.98030090332	0.98029899597
0.9803004265	45.275931	0.000199	26.527773	9.971330	5.7947E+07	28002.563086	0.98030090332	0.98029994965
0.9803006649	45.275942	0.000199	26.527573	9.971330	5.7947E+07	28002.563051	0.98030090332	0.98030042648
0.9803005457	45.275937	0.000199	26.527673	9.971330	5.7947E+07	28002.563069	0.9803006649	0.98030042648
0.9803004861	45.275934	0.000199	26.527723	9.971330	5.7947E+07	28002.563077	0.98030054569	0.98030042648
0.9803005159	45.275935	0.000199	26.527698	9.971330	5.7947E+07	28002.563073	0.98030054569	0.98030048609
0.980300501	45.275935	0.000199	26.527711	9.971330	5.7947E+07	28002.563075	0.98030051589	0.98030048609
0.9803004935	45.275934	0.000199	26.527717	9.971330	5.7947E+07	28002.563076	0.98030050099	0.98030048609

Spreadsheet for Calculation of Stream-Water Saturation Profiles

Injection Temperature 650 °K Initial Temperature 300 °K Matrix Heat Capacity 5.0000 (kJ/kg)

LEADING SHOCK CALCULATIONS

Saturation	OF	Wave V	Flow V	Shock V	fv	dKrv/dSv	dKr/dSi
0.7500	3.08E-01	0.316608	0.009549	0.009004	0.996549	1.0000	0.1875
0.875	5.59E-02	0.064364	0.007813	0.008421	0.999629	1.0000	0.0469
0.9375	6.29E-03	0.014664	0.007663	0.008370	0.999957	1.0000	0.0117
0.96875	-4.86E-03	0.003508	0.007663	0.008370	0.999995	1.0000	0.0029
0.953125	-3.02E-04	0.008067	0.007659	0.008369	0.999982	1.0000	0.0066
0.9453125	2.73E-03	0.011102	0.007660	0.008369	0.999971	1.0000	0.0090
0.94921875	1.15E-03	0.009520	0.007659	0.008369	0.999977	1.0000	0.0077
0.951171875	4.09E-04	0.008778	0.007659	0.008369	0.999980	1.0000	0.0072
0.9521484375	4.95E-05	0.008418	0.007659	0.008369	0.999981	1.0000	0.0069
0.9526367188	-1.27E-04	0.008242	0.007659	0.008369	0.999981	1.0000	0.0067
0.9523925781	-3.90E-05	0.008330	0.007659	0.008369	0.999981	1.0000	0.0068
0.9522705078	5.18E-06	0.008374	0.007659	0.008369	0.999981	1.0000	0.0068
0.952331543	-1.69E-05	0.008352	0.007659	0.008369	0.999981	1.0000	0.0068
0.9523010254	-5.88E-06	0.008363	0.007659	0.008369	0.999981	1.0000	0.0068
0.9522857666	-3.49E-07	0.008369	0.007659	0.008369	0.999981	1.0000	0.0068
0.9522781372	2.42E-06	0.008371	0.007659	0.008369	0.999981	1.0000	0.0068
0.9522819519	1.03E-06	0.008370	0.007659	0.008369	0.999981	1.0000	0.0068
0.9522838593	3.43E-07	0.008369	0.007659	0.008369	0.999981	1.0000	0.0068
0.9522848129	-3.27E-09	0.008369	0.007659	0.008369	0.999981	1.0000	0.0068
0.9522843361	1.70E-07	0.008369	0.007659	0.008369	0.999981	1.0000	0.0068
0.9522845745	8.32E-08	0.008369	0.007659	0.008369	0.999981	1.0000	0.0068
0.9522846937	4.00E-08	0.008369	0.007659	0.008369	0.999981	1.0000	0.0068
0.9522847533	1.83E-08	0.008369	0.007659	0.008369	0.999981	1.0000	0.0068
0.9522847831	7.54E-09	0.008369	0.007659	0.008369	0.999981	1.0000	0.0068
0.952284798	2.14E-09	0.008369	0.007659	0.008369	0.999981	1.0000	0.0068
0.9522848055	-5.66E-10	0.008369	0.007659	0.008369	0.999981	1.0000	0.0068

Saturation	Total Mob	dFv/dSv	G	F	Gamma	Theta	High	Low
0.75	34.759228	0.045851	220.095758	12.870589	5.8117E+07	30550.407113	1	0.5
0.875	40.427490	0.009321	115.033000	10.281953	5.8025E+07	28275.535543	1	0.75
0.9375	43.300978	0.002124	62.501620	10.006619	5.7978E+07	28033.574650	1	0.875
0.96875	44.742642	0.000508	36.235931	9.974642	5.7955E+07	28005.473055	1	0.9375
0.953125	44.021547	0.001168	49.368776	9.985337	5.7967E+07	28014.871837	0.96875	0.9375
0.9453125	43.661186	0.001608	55.935198	9.994411	5.7973E+07	28022.845709	0.953125	0.9375
0.94921875	43.841348	0.001379	52.651987	9.989513	5.7970E+07	28018.541754	0.953125	0.9453125
0.951171875	43.931443	0.001271	51.010381	9.987339	5.7968E+07	28016.630913	0.953125	0.94921875
0.9521484375	43.976494	0.001219	50.189578	9.986317	5.7968E+07	28015.732823	0.953125	0.951171875
0.9526367188	43.999020	0.001194	49.779177	9.985822	5.7967E+07	28015.297744	0.953125	0.9521484375
0.9523925781	43.987757	0.001206	49.984378	9.986068	5.7967E+07	28015.514131	0.95263671875	0.9521484375
0.9522705078	43.982125	0.001213	50.086978	9.986192	5.7967E+07	28015.623188	0.95239257813	0.9521484375
0.952331543	43.984941	0.001210	50.035678	9.986130	5.7967E+07	28015.568587	0.95239257813	0.95227050781
0.9523010254	43.983533	0.001211	50.061328	9.986161	5.7967E+07	28015.595869	0.95233154297	0.95227050781
0.9522857666	43.982829	0.001212	50.074153	9.986176	5.7967E+07	28015.609524	0.95230102539	0.95227050781
0.9522781372	43.982477	0.001212	50.080565	9.986184	5.7967E+07	28015.616355	0.9522857666	0.95227050781
0.9522819519	43.982653	0.001212	50.077359	9.986180	5.7967E+07	28015.612939	0.9522857666	0.95227813721
0.9522838593	43.982741	0.001212	50.075756	9.986178	5.7967E+07	28015.611232	0.9522857666	0.9522819519
0.9522848129	43.982785	0.001212	50.074954	9.986177	5.7967E+07	28015.610378	0.9522857666	0.95228385925
0.9522843361	43.982763	0.001212	50.075355	9.986178	5.7967E+07	28015.610805	0.95228481293	0.95228385925
0.9522845745	43.982774	0.001212	50.075155	9.986178	5.7967E+07	28015.610591	0.95228481293	0.95228433609
0.9522846937	43.982780	0.001212	50.075055	9.986177	5.7967E+07	28015.610484	0.95228481293	0.95228457451
0.9522847533	43.982783	0.001212	50.075005	9.986177	5.7967E+07	28015.610431	0.95228481293	0.95228469372
0.9522847831	43.982784	0.001212	50.074980	9.986177	5.7967E+07	28015.610404	0.95228481293	0.95228475332
0.952284798	43.982785	0.001212	50.074967	9.986177	5.7967E+07	28015.610391	0.95228481293	0.95228478312
0.9522848055	43.982785	0.001212	50.074961	9.986177	5.7967E+07	28015.610384	0.95228481293	0.95228479803

Spreadsheet for Calculation of Stream-Water Saturation Profiles

Injection Temperature 650 °K	Initial Temperature 300 °K	Matrix Heat Capacity 25.0000 (kJ/kg)
---------------------------------	-------------------------------	---

MATRIX PROPERTIES

<i>Porosity</i>	<i>Cp Matrix</i>	<i>Density</i>	<i>Rho * Cp</i>
0.10	25.00	2650.00	66250.0000
<i>Nw</i>	<i>Ng</i>	<i>Swl</i>	<i>Denom</i>
3.00	1.00	0.00	1.000000

SATURATION CONDITIONS

Tsaturation = 485.57

	<i>Volumes</i>	<i>Enthalpies</i>	<i>Densities</i>	<i>Viscosities</i>	<i>Saturation</i>
	<i>(m3/kg)</i>	<i>(kJ/kg)</i>	<i>(kg/m3)</i>	<i>(cp)</i>	<i>Step</i>
Liquid	0.001176	901.41	850.4723	0.1303	0.000257321
Vapor	0.100298	2808.52	9.970241	0.0217	

BOUNDARY CONDITIONS

	<i>Temperature</i>	<i>Velocity</i>	<i>Heat Capacity</i>	<i>Wave Velocity</i>	<i>Density</i>	<i>Enthalpy</i>
Injection	650	1.000000	2.30	0.000265	6.882648	3199.91
Initial	300	0.007015	4.16	0.000488	1004.6293	112.70
	<i>G</i>	<i>F</i>	<i>Gamma</i>	<i>Theta</i>		
Injection	650	6.88	6.88	387584523.87	22023.87	
Initial	300	1004.63	1004.63	178988218.71	113218.71	

SHOCK CONDITIONS

	<i>Initial Guess</i>	<i>Vapor</i>	<i>Objective</i>	<i>Two-Phase</i>	<i>Upstream</i>	<i>Shock</i>	<i>Vapor</i>
	<i>Sv-HI</i>	<i>Sv-Low</i>	<i>Saturation</i>	<i>Wave Function</i>	<i>Flow Velocity</i>	<i>Velocity</i>	<i>Frac Flow</i>
Trailing	1	0.5	0.9911	-3.3901E-10	0.0003	0.690341	0.0003
Leading	1	0.5	0.9783	-4.2991E-11	0.0017	0.007015	0.0017
	<i>dKr/dSv</i>	<i>dKrl/dSl</i>	<i>Total Mobility</i>	<i>dPv/dSv</i>	<i>G</i>	<i>F'</i>	<i>Gamma</i>
Trailing	1.0000	0.0002	45.7756	0.0000	17.4345	9.9703	2.8956E+08
Leading	1.0000	0.0014	45.1814	0.0002	28.2485	9.9717	2.8957E+08
							<i>Theta'</i>
							28001.6925
							28002.8964

MATERIAL BALANCES

	<i>Inside</i>	<i>Initial</i>	<i>Injected</i>	<i>Produced</i>	<i>Balance</i>	<i>Error</i>
Mass	100.298015	100.462933	6.882648	7.047566	0.0000	0.0000%
Enthalpy	17920051.5315	17898821.8712	22023.8721	794.2396	-0.0278	0.0000%

Spreadsheet for Calculation of Stream-Water Saturation Profiles

Injection Temperature
650 °K

Initial Temperature
300 °K

Matrix Heat Capacity:
25.0000 (kJ/kg)

SATURATION PROFILE

Vapor Saturation	Vapor Frac Flow	dKrv/dSv	dKr/dSI	Total Mobility	dFv/dSv	lambda	Mass Inside	Enthalpy Inside
1.0000						0.000000		
1.0000						0.000275		
0.9911	1.000000	1.0000	0.0002	45.775554	0.000040	0.000275	0.001891	106480.881543
0.9909	1.000000	1.0000	0.0003	45.763670	0.000042	0.000291	0.000285	4705.924436
0.9906	1.000000	1.0000	0.0003	45.751786	0.000045	0.000308	0.000297	4842.857546
0.9903	1.000000	1.0000	0.0003	45.739902	0.000047	0.000325	0.000309	4979.933142
0.9901	1.000000	1.0000	0.0003	45.728018	0.000050	0.000343	0.000321	5117.151406
0.9898	1.000000	1.0000	0.0003	45.716134	0.000052	0.000361	0.000334	5254.512523
0.9896	1.000000	1.0000	0.0003	45.704250	0.000055	0.000379	0.000347	5392.016676
0.9893	1.000000	1.0000	0.0003	45.692366	0.000058	0.000398	0.000360	5529.664050
0.9891	1.000000	1.0000	0.0004	45.680482	0.000061	0.000418	0.000373	5667.454829
0.9888	1.000000	1.0000	0.0004	45.668598	0.000063	0.000438	0.000386	5805.389199
0.9885	1.000000	1.0000	0.0004	45.656715	0.000066	0.000459	0.000400	5943.467343
0.9883	1.000000	1.0000	0.0004	45.644831	0.000069	0.000480	0.000414	6081.689447
0.9880	1.000000	1.0000	0.0004	45.632947	0.000073	0.000501	0.000428	6220.055697
0.9878	1.000000	1.0000	0.0004	45.621063	0.000076	0.000523	0.000442	6358.566278
0.9875	1.000000	1.0000	0.0005	45.609180	0.000079	0.000545	0.000457	6497.221375
0.9873	1.000000	1.0000	0.0005	45.597296	0.000082	0.000568	0.000471	6636.021177
0.9870	1.000000	1.0000	0.0005	45.585413	0.000086	0.000592	0.000486	6774.965868
0.9867	1.000000	1.0000	0.0005	45.573529	0.000089	0.000616	0.000502	6914.055635
0.9865	1.000000	1.0000	0.0005	45.561646	0.000093	0.000640	0.000517	7053.290665
0.9862	1.000000	1.0000	0.0006	45.549762	0.000096	0.000665	0.000532	7192.671146
0.9860	1.000000	1.0000	0.0006	45.537879	0.000100	0.000690	0.000548	7332.197264
0.9857	1.000000	1.0000	0.0006	45.525995	0.000104	0.000716	0.000564	7471.869208
0.9855	0.999999	1.0000	0.0006	45.514112	0.000108	0.000742	0.000581	7611.687164
0.9852	0.999999	1.0000	0.0007	45.502229	0.000111	0.000769	0.000597	7751.651322
0.9849	0.999999	1.0000	0.0007	45.490345	0.000115	0.000796	0.000614	7891.761870
0.9847	0.999999	1.0000	0.0007	45.478462	0.000119	0.000824	0.000631	8032.018996
0.9844	0.999999	1.0000	0.0007	45.466579	0.000123	0.000852	0.000648	8172.422887
0.9842	0.999999	1.0000	0.0008	45.454696	0.000128	0.000881	0.000665	8312.973737
0.9839	0.999999	1.0000	0.0008	45.442813	0.000132	0.000910	0.000683	8453.671731
0.9837	0.999999	1.0000	0.0008	45.430930	0.000136	0.000940	0.000700	8594.517059
0.9834	0.999999	1.0000	0.0008	45.419047	0.000141	0.000970	0.000718	8735.509913
0.9831	0.999999	1.0000	0.0009	45.407164	0.000145	0.001001	0.000737	8876.650482
0.9829	0.999999	1.0000	0.0009	45.395281	0.000149	0.001032	0.000755	9017.938955
0.9826	0.999999	1.0000	0.0009	45.383399	0.000154	0.001063	0.000774	9159.375525
0.9824	0.999999	1.0000	0.0009	45.371516	0.000159	0.001096	0.000793	9300.960381
0.9821	0.999999	1.0000	0.0010	45.359633	0.000163	0.001128	0.000812	9442.693714
0.9819	0.999999	1.0000	0.0010	45.347750	0.000168	0.001161	0.000831	9584.575716
0.9816	0.999999	1.0000	0.0010	45.335868	0.000173	0.001195	0.000851	9726.606579
0.9813	0.999999	1.0000	0.0010	45.323985	0.000178	0.001229	0.000871	9868.786494
0.9811	0.999999	1.0000	0.0011	45.312103	0.000183	0.001264	0.000891	10011.115653
0.9808	0.999999	1.0000	0.0011	45.300221	0.000188	0.001299	0.000911	10153.594249
0.9806	0.999999	1.0000	0.0011	45.288338	0.000193	0.001334	0.000931	10296.222474
0.9803	0.999999	1.0000	0.0012	45.276456	0.000198	0.001370	0.000952	10439.000521
0.9801	0.999999	1.0000	0.0012	45.264574	0.000204	0.001407	0.000973	10581.928583
0.9798	0.999999	1.0000	0.0012	45.252692	0.000209	0.001444	0.000994	10725.006853
0.9795	0.999999	1.0000	0.0013	45.240809	0.000215	0.001481	0.001016	10868.235525
0.9793	0.999998	1.0000	0.0013	45.228927	0.000220	0.001519	0.001037	11011.614793
0.9790	0.999998	1.0000	0.0013	45.217045	0.000226	0.001558	0.001059	11155.144850
0.9788	0.999998	1.0000	0.0014	45.205163	0.000231	0.001597	0.001081	11298.825891
0.9785	0.999998	1.0000	0.0014	45.193282	0.000237	0.001636	0.001103	11442.658111
0.9783	0.999998	1.0000	0.0014	45.181400	0.000243	0.001676	0.001126	11586.641705
0.0000						0.001676		
0.0000						1.000000		

Spreadsheet for Calculation of Stream-Water Saturation Profiles

Injection Temperature 650 °K Initial Temperature 300 °K Matrix Heat Capacity 25.0000 (kJ/kg)

TRAILING SHOCK CALCULATIONS

Saturation	OF	Wave V	Flow V	Shock V	fv	dKrv/dSv	dKrVdSI
0.7500	2.45E-01	0.245631	0.535716	0.000578	0.996549	1.0000	0.1875
0.875	6.21E-02	0.062426	0.669723	0.000315	0.999629	1.0000	0.0469
0.9375	1.43E-02	0.014610	0.687965	0.000279	0.999957	1.0000	0.0117
0.96875	3.23E-03	0.003506	0.690096	0.000275	0.999995	1.0000	0.0029
0.984375	5.83E-04	0.000858	0.690326	0.000275	0.999999	1.0000	0.0007
0.9921875	-6.24E-05	0.000212	0.690341	0.000275	1.000000	1.0000	0.0002
0.98828125	2.05E-04	0.000480	0.690339	0.000275	1.000000	1.0000	0.0004
0.990234375	5.79E-05	0.000333	0.690341	0.000275	1.000000	1.0000	0.0003
0.9912109375	-3.68E-06	0.000269	0.690341	0.000275	1.000000	1.0000	0.0002
0.9907226563	2.52E-05	0.000300	0.690341	0.000275	1.000000	1.0000	0.0003
0.9909667969	9.57E-06	0.000284	0.690341	0.000275	1.000000	1.0000	0.0002
0.9910888672	1.90E-06	0.000277	0.690341	0.000275	1.000000	1.0000	0.0002
0.9911499023	-1.90E-06	0.000273	0.690341	0.000275	1.000000	1.0000	0.0002
0.9911193848	-7.29E-09	0.000275	0.690341	0.000275	1.000000	1.0000	0.0002
0.991104126	9.43E-07	0.000276	0.690341	0.000275	1.000000	1.0000	0.0002
0.9911117554	4.68E-07	0.000275	0.690341	0.000275	1.000000	1.0000	0.0002
0.9911155701	2.30E-07	0.000275	0.690341	0.000275	1.000000	1.0000	0.0002
0.9911174774	1.11E-07	0.000275	0.690341	0.000275	1.000000	1.0000	0.0002
0.9911184311	5.21E-08	0.000275	0.690341	0.000275	1.000000	1.0000	0.0002
0.9911189079	2.24E-08	0.000275	0.690341	0.000275	1.000000	1.0000	0.0002
0.9911191463	7.54E-09	0.000275	0.690341	0.000275	1.000000	1.0000	0.0002
0.9911192656	1.25E-10	0.000275	0.690341	0.000275	1.000000	1.0000	0.0002
0.9911193252	-3.59E-09	0.000275	0.690341	0.000275	1.000000	1.0000	0.0002
0.9911192954	-1.73E-09	0.000275	0.690341	0.000275	1.000000	1.0000	0.0002
0.9911192805	-8.03E-10	0.000275	0.690341	0.000275	1.000000	1.0000	0.0002
0.991119273	-3.39E-10	0.000275	0.690341	0.000275	1.000000	1.0000	0.0002

Saturation	Total Mob	dFv/dSv	G	F	Gamma	Theta	High	Low
0.75	34.759228	0.045851	220.095758	12.870589	2.8973E+08	30550.407113	1	0.5
0.875	40.427490	0.009321	115.033000	10.281953	2.8964E+08	28275.535543	1	0.75
0.9375	43.300978	0.002124	62.501620	10.006619	2.8960E+08	28033.574650	1	0.875
0.96875	44.742642	0.000508	36.235931	9.974642	2.8957E+08	28005.473055	1	0.9375
0.984375	45.464089	0.000124	23.103086	9.970782	2.8956E+08	28002.081444	1	0.96875
0.9921875	45.824889	0.000031	16.536663	9.970308	2.8955E+08	28001.664696	1	0.984375
0.98828125	45.644485	0.000070	19.819875	9.970469	2.8956E+08	28001.805609	0.9921875	0.984375
0.990234375	45.734686	0.000048	18.178269	9.970372	2.8956E+08	28001.721158	0.9921875	0.98828125
0.9912109375	45.779787	0.000039	17.357466	9.970337	2.8956E+08	28001.689785	0.9921875	0.990234375
0.9907226563	45.757237	0.000043	17.767868	9.970354	2.8956E+08	28001.704641	0.9912109375	0.990234375
0.9909667969	45.768512	0.000041	17.562667	9.970345	2.8956E+08	28001.697011	0.9912109375	0.9907226563
0.9910888672	45.774150	0.000040	17.460067	9.970341	2.8956E+08	28001.693348	0.9912109375	0.9909667969
0.9911499023	45.776969	0.000040	17.408766	9.970339	2.8956E+08	28001.691554	0.9912109375	0.9910888672
0.9911193848	45.775559	0.000040	17.434416	9.970340	2.8956E+08	28001.692448	0.9911499023	0.9910888672
0.991104126	45.774854	0.000040	17.447242	9.970340	2.8956E+08	28001.692897	0.9911193847	0.9910888672
0.9911117554	45.775207	0.000040	17.440829	9.970340	2.8956E+08	28001.692672	0.9911193847	0.991104126
0.9911155701	45.775383	0.000040	17.437623	9.970340	2.8956E+08	28001.692560	0.9911193847	0.9911155701
0.9911174774	45.775471	0.000040	17.436020	9.970340	2.8956E+08	28001.692504	0.9911193847	0.9911155701
0.9911184311	45.775515	0.000040	17.435218	9.970340	2.8956E+08	28001.692476	0.9911193847	0.9911174774
0.9911189079	45.775537	0.000040	17.434817	9.970340	2.8956E+08	28001.692462	0.9911193847	0.9911184311
0.9911191463	45.775548	0.000040	17.434617	9.970340	2.8956E+08	28001.692455	0.9911193847	0.9911189079
0.9911192656	45.775554	0.000040	17.434517	9.970340	2.8956E+08	28001.692451	0.9911193847	0.9911191463
0.9911193252	45.775556	0.000040	17.434467	9.970340	2.8956E+08	28001.692450	0.9911193847	0.9911192656
0.9911192954	45.775555	0.000040	17.434492	9.970340	2.8956E+08	28001.692450	0.9911193252	0.9911192656
0.9911192805	45.775554	0.000040	17.434504	9.970340	2.8956E+08	28001.692451	0.9911192954	0.9911192656
0.991119273	45.775554	0.000040	17.434510	9.970340	2.8956E+08	28001.692451	0.9911192805	0.9911192656

Spreadsheet for Calculation of Stream-Water Saturation Profiles

Injection Temperature 650 °K Initial Temperature 300 °K Matrix Heat Capacity 25.0000 (kJ/kg)

LEADING SHOCK CALCULATIONS

Saturation	OF	Wave V	Flow V	Shock V	f _v	dK _{rv} /dS _v	dK _r /dS _i
0.7500	3.15E-01	0.316528	0.008986	0.001813	0.996549	1.0000	0.1875
0.875	6.27E-02	0.064348	0.007215	0.001690	0.999629	1.0000	0.0469
0.9375	1.30E-02	0.014660	0.007033	0.001678	0.999957	1.0000	0.0117
0.96875	1.83E-03	0.003507	0.007016	0.001676	0.999995	1.0000	0.0029
0.984375	-8.18E-04	0.000858	0.007015	0.001676	0.999999	1.0000	0.0007
0.9765625	2.75E-04	0.001952	0.007015	0.001676	0.999998	1.0000	0.0016
0.98046875	-3.28E-04	0.001348	0.007015	0.001676	0.999999	1.0000	0.0011
0.978515625	-4.08E-05	0.001636	0.007015	0.001676	0.999998	1.0000	0.0014
0.9775390625	1.14E-04	0.001790	0.007015	0.001676	0.999998	1.0000	0.0015
0.9780273438	3.55E-05	0.001712	0.007015	0.001676	0.999998	1.0000	0.0014
0.9782714844	-2.86E-06	0.001674	0.007015	0.001676	0.999998	1.0000	0.0014
0.9781494141	1.63E-05	0.001693	0.007015	0.001676	0.999998	1.0000	0.0014
0.9782104492	6.70E-06	0.001683	0.007015	0.001676	0.999998	1.0000	0.0014
0.9782409668	1.92E-06	0.001678	0.007015	0.001676	0.999998	1.0000	0.0014
0.9782562256	-4.70E-07	0.001676	0.007015	0.001676	0.999998	1.0000	0.0014
0.9782485962	7.24E-07	0.001677	0.007015	0.001676	0.999998	1.0000	0.0014
0.9782524109	1.27E-07	0.001677	0.007015	0.001676	0.999998	1.0000	0.0014
0.9782543182	-1.71E-07	0.001676	0.007015	0.001676	0.999998	1.0000	0.0014
0.9782533646	-2.22E-08	0.001676	0.007015	0.001676	0.999998	1.0000	0.0014
0.9782528877	5.24E-08	0.001676	0.007015	0.001676	0.999998	1.0000	0.0014
0.9782531261	1.51E-08	0.001676	0.007015	0.001676	0.999998	1.0000	0.0014
0.9782532454	-3.54E-09	0.001676	0.007015	0.001676	0.999998	1.0000	0.0014
0.9782531857	5.79E-09	0.001676	0.007015	0.001676	0.999998	1.0000	0.0014
0.9782532156	1.12E-09	0.001676	0.007015	0.001676	0.999998	1.0000	0.0014
0.9782532305	-1.21E-09	0.001676	0.007015	0.001676	0.999998	1.0000	0.0014
0.978253223	-4.30E-11	0.001676	0.007015	0.001676	0.999998	1.0000	0.0014

Saturation	Total Mob	dF _v /dS _v	G	F	Gamma	Theta	High	Low
0.75	34.759228	0.045851	220.095758	12.870589	2.8973E+08	30550.407113	1	0.5
0.875	40.427490	0.009321	115.033000	10.281953	2.8964E+08	28275.535543	1	0.75
0.9375	43.300978	0.002124	62.501620	10.006619	2.8960E+08	28033.574650	1	0.875
0.96875	44.742642	0.000508	36.235931	9.974642	2.8957E+08	28005.473055	1	0.9375
0.984375	45.464089	0.000124	23.103086	9.970782	2.8956E+08	28002.081444	1	0.96875
0.9765625	45.103332	0.000283	29.669508	9.972083	2.8957E+08	28003.224190	0.984375	0.96875
0.98046875	45.283704	0.000195	26.346297	9.971303	2.8956E+08	28002.538594	0.984375	0.9765625
0.978515625	45.193516	0.000237	28.027903	9.971657	2.8956E+08	28002.849861	0.98046875	0.9765625
0.9775390625	45.148424	0.000259	28.848705	9.971860	2.8957E+08	28003.028768	0.978515625	0.9765625
0.9780273438	45.170970	0.000248	28.438304	9.971736	2.8957E+08	28002.937297	0.978515625	0.9775390625
0.9782714844	45.182243	0.000242	28.233103	9.971706	2.8957E+08	28002.893081	0.978515625	0.97802734375
0.9781494141	45.176606	0.000245	28.335704	9.971731	2.8957E+08	28002.915063	0.97827148438	0.97802734375
0.9782104492	45.179425	0.000244	28.284404	9.971718	2.8957E+08	28002.904041	0.97827148438	0.97814941406
0.9782409668	45.180834	0.000243	28.258753	9.971712	2.8957E+08	28002.898553	0.97827148438	0.97821044922
0.9782562256	45.181538	0.000243	28.245928	9.971709	2.8957E+08	28002.895815	0.97827148438	0.9782409668
0.9782485962	45.181186	0.000243	28.252341	9.971711	2.8957E+08	28002.897183	0.97825622559	0.9782409668
0.9782524109	45.181362	0.000243	28.249135	9.971710	2.8957E+08	28002.896499	0.97825622559	0.97824859619
0.9782543182	45.181450	0.000243	28.247532	9.971709	2.8957E+08	28002.896157	0.97825622559	0.97825241089
0.9782533646	45.181406	0.000243	28.248333	9.971710	2.8957E+08	28002.896328	0.97825431824	0.97825241089
0.9782528877	45.181384	0.000243	28.248734	9.971710	2.8957E+08	28002.896413	0.97825336456	0.97825241089
0.9782531261	45.181395	0.000243	28.248533	9.971710	2.8957E+08	28002.896371	0.97825336456	0.97825288773
0.9782532454	45.181401	0.000243	28.248433	9.971710	2.8957E+08	28002.896349	0.97825336456	0.97825312614
0.9782531857	45.181398	0.000243	28.248483	9.971710	2.8957E+08	28002.896360	0.97825324535	0.97825312614
0.9782532156	45.181399	0.000243	28.248458	9.971710	2.8957E+08	28002.896355	0.97825324535	0.97825318575
0.9782532305	45.181400	0.000243	28.248446	9.971710	2.8957E+08	28002.896352	0.97825324535	0.97825321555
0.978253223	45.181400	0.000243	28.248452	9.971710	2.8957E+08	28002.896353	0.97825323045	0.97825321555

APPENDIX E COMPUTER PROGRAMS

This appendix contains the source code for the programs to do the path integration and to calculate the shock conditions. All the programs are written in the C programming language and were implemented using the BSD 4.3 Unix compiler. The eigenvalue routines were from the IMSL library and were linked to the C code.

Each problem has its own set of source code. The techniques used to trace the composition paths and the shock conditions are similar for the steam-oil-water problem in §4.2 and the CO₂-oil-water problem in §4.3. This results in a large amount of overlap between the two sets of source code, but time constraints dictated the large amount of duplication.

E.1 STEAM-OIL-WATER CODE

The code for the steam-oil-water problem is divided into a main library of programs that calculate the properties of each composition point. These properties are the phase saturations, the phase densities, the phase viscosities and the relative permeabilities. Using these properties, the eigenvalues and eigenvectors are calculated and reported.

Each individual composition point is represented by a C structure that holds all the information about a composition point. These composition points are stored in a two-way linked list so the user can traverse the list in any direction. This makes backtracking along a path relatively simple.

There are two main programs used to calculate the steam-oil-water solutions. The first of these, *tracepath* integrates from a given initial composition along a user specified path. A simplified flow chart for *tracepath* is shown in Figure E.1.

The program integrates along the path selected by the user. The integration continues along this path until a path switch is detected or the path reached the edge of the current hodograph space. Path switches are detected by taking the dot product of the all the current eigenvectors with the previous path eigenvector. If the current eigenvector nearest in direction to the previous eigenvector is along a different path, a path switch is indicated and the user is alerted.

The results of the integration are written to a file named "path.pts." This file contains all the information needed to construct the saturation, temperature and flow velocity profiles. Each line of the file represents one composition point with the following information:

1. The path eigenvalue. This represents the velocity of the composition point and is used to determine the location of the composition point at a given time.
2. The composition point. This is given by the temperature, flow velocity, steam saturation, oil saturation, and water saturation in that order.
3. The two eigenvalues at the composition point. The small eigenvalue is listed followed by the large eigenvalue.

The second program is called *jump*. This program is used to find the discontinuities in the final solution. The program uses a Newton-Raphson iteration to calculate the composition point that matches the downstream conditions, given an upstream composition point. The Rankine-Hugoniot conditions across the shock require that the shock velocity can be calculated using a material balance on the water, oil, or enthalpy components, and that these three velocities be equal. This condition was given in Eq. 2.35.

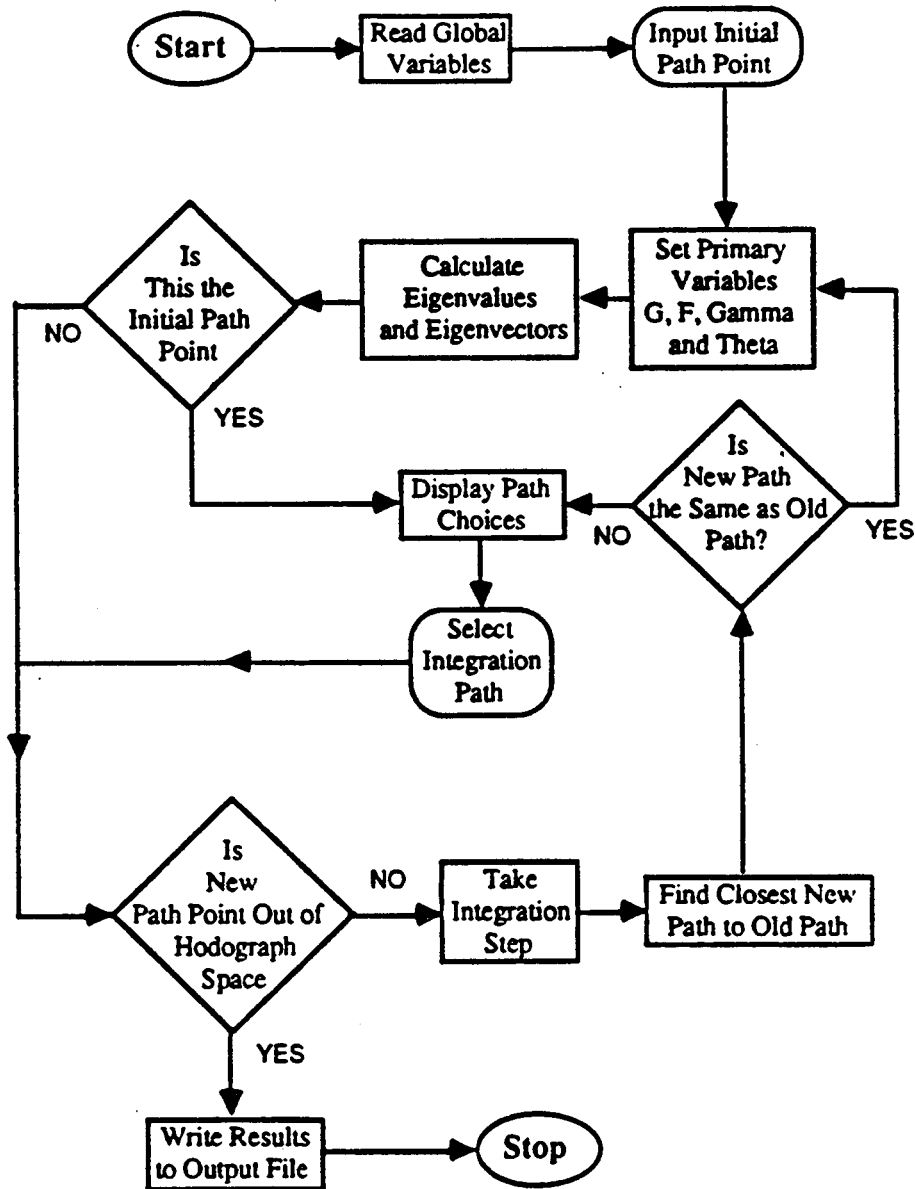


Figure E.1: Basic Flow Chart for the tracepath Program that performs the path integration for the steam-oil-water problem.

The program begins by requesting the upstream composition point. The primary variables and eigenvalues are calculated for this point. Then the user is asked for the kind of shock to be found, intermediate discontinuity or genuine shock. If an intermediate discontinuity is required, the direction of the shock is specified next by telling the program to match the eigenvalue of the upstream of downstream point. Once the direction of the intermediate discontinuity is selected, the actual eigenvalue to match (small or large) is requested.

Selecting the genuine shock gives no specific shock velocity as with an intermediate discontinuity. The shock velocity may be set, by giving a value to the next prompt, or left indeterminate by entering a question mark (?).

Finally, an initial guess of the downstream composition point is entered. The initial guess is required regardless of the type of shock. The range of convergence for these problems is small and if the initial guess is not excellent, the system will fail to converge.

The program begins searching for the downstream composition point that connects to the upstream point via the specified shock. The first step is to calculate the flow velocity of the downstream composition point. This is done by equating the Rankine-Hugoniot conditions for the oil component and the enthalpy component. This results in the following equation for the downstream velocity,

$$u^{dn} = u^{up} \frac{\Theta^{up}(G_o^{up} - G_o^{dn}) - F_o^{up}(\Gamma_o^{up} - \Gamma_o^{dn})}{\Theta^{dn}(G_o^{up} - G_o^{dn}) - F_o^{dn}(\Gamma_o^{up} - \Gamma_o^{dn})} \quad (E.1)$$

Solving for the downstream flow velocity by Eq. E.1 forces the shock velocities of the oil and enthalpy components to be equal.

Depending on the specification of the shock velocity, the program searches for the roots of one or two objective functions. \mathcal{F}_1 matches the shock velocity of the water component to the oil component and \mathcal{F}_2 matches the shock velocity of the water component to either the given velocity in the case of a genuine shock or the specified eigenvalue in the case of the intermediate discontinuity. The solution is found when both these functions are zero.

$$\mathcal{F}_1 = \Lambda_w - \Lambda_o = 0 \quad (E.2)$$

and

$$\mathcal{F}_2 = \begin{cases} \Lambda_w - \lambda & \text{for intermediate discontinuity} \\ \Lambda_{given} & \text{for specified genuine shock} \\ 0 & \text{for unspecified genuine shock} \end{cases} \quad (E.3)$$

Convergence tolerance is set to 10^{-8} for both functions. The derivatives are calculated by forward difference using a step of 0.001 for saturation and 1.0 for temperature. These derivatives overshoot the solution when the initial guess is far from a root. To remedy this, an under relaxation factor of 0.3 is applied when the absolute values of either \mathcal{F}_1 or \mathcal{F}_2 is greater than 10^{-4} . The flow cart for jump is given in Figure E.2.

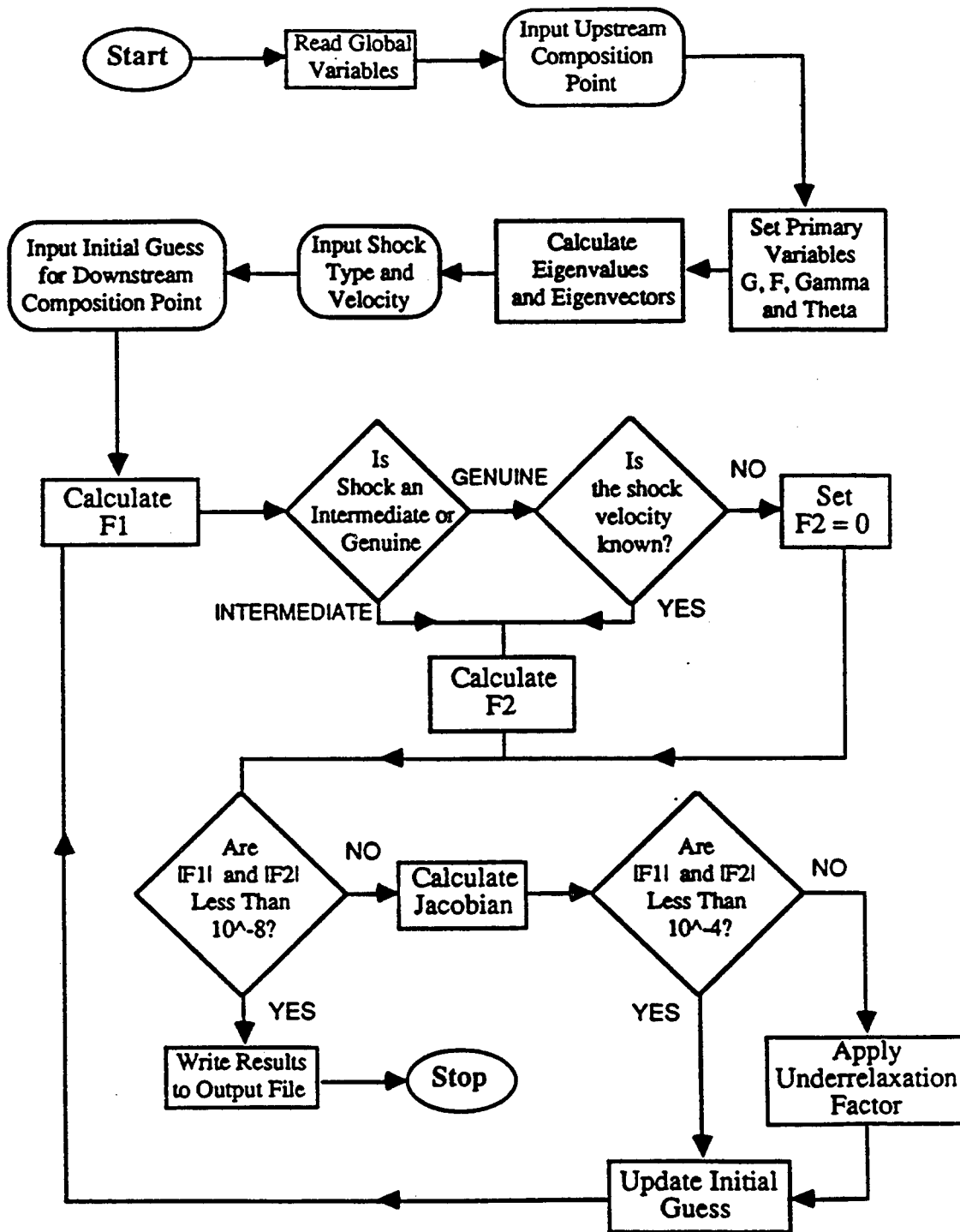


Figure E.2: Basic Flow Chart for the jump Program that calculates the shock conditions for the steam-oil-water problem.